



BINDING SERVICES
Tel +44 (0)29 2087 4949
Fax +44 (0)29 20371921
e-mail bindery@cardiff.ac.uk



HYDRO-GEOCHEMICAL MODELLING OF AN UNLINED
LANDFILL SITE

EMMA CORINNE PARIS

A THESIS IN PART FULFILMENT OF THE DOCTOR OF
PHILOSOPHY DEGREE SCHEME

SCHOOL OF EARTH, OCEAN AND PLANETARY SCIENCES
CARDIFF UNIVERSITY

2005

UMI Number: U584718

All rights reserved

INFORMATION TO ALL USERS

The quality of this reproduction is dependent upon the quality of the copy submitted.

In the unlikely event that the author did not send a complete manuscript and there are missing pages, these will be noted. Also, if material had to be removed, a note will indicate the deletion.



UMI U584718

Published by ProQuest LLC 2013. Copyright in the Dissertation held by the Author.
Microform Edition © ProQuest LLC.

All rights reserved. This work is protected against
unauthorized copying under Title 17, United States Code.



ProQuest LLC
789 East Eisenhower Parkway
P.O. Box 1346
Ann Arbor, MI 48106-1346

SUMMARY

This project reports results of a hydro-geochemical study of leachate production at the Silent Valley landfill, Blaenau Gwent, South Wales, UK.

Silent Valley landfill site is an active unlined landfill in South Wales. It lies on interbedded sandstones and mudstones of the Rhondda Beds, which are overlain by a mixture of boulder clay, head deposits and made ground. The annual rainfall recorded in the area is approximately 1250 mm.

Resistivity surveys were performed across part of the site to help improve the understanding of the internal structure of the landfill. Instrumentation to measure leachate discharge, conductivity and meteorological inputs installed at the Silent Valley landfill site are described and relationships between the rainfall and discharge data are analysed. Regression analysis is used to model the discharge of leachate from the measured meteorological data.

Water balance analysis has demonstrated that groundwater is entering the site. The leachate generated on site is collected by a series of drains that feed into the Settlement Tank, which then discharges to foul sewer. The discharge through the Settlement Tank shows a rapid response to rainfall events with dilution effects indicated by conductivity readings and chemical analysis. The volume of discharge from the Settlement Tank is shown to have a long-term upward trend.

A preliminary study was undertaken to investigate the use of neural networks to model the discharge in the Settlement Tank. Feedforward backpropagation neural networks were constructed using the measured meteorological data to produce predictions of daily discharge for the Settlement Tank.

Ion Chromatography analysis was performed on the leachate to complement the historical leachate analysis data. Element concentration was correlated with conductivity data and variations related to discharge measurements. Since monitoring began in 1993, many of the leachate constituents have shown an increase in concentration.

ACKNOWLEDGEMENTS

I would especially like to express my thanks to my supervisors, Professor Charles Harris and Dr Simon Wakefield, for the support, encouragement, guidance and advice that they have provided throughout this research project.

I am grateful for the funding of this project by Blaenau Gwent County Borough Council and Silent Valley Waste Services. Within those organisations, I would particularly like to thank Mark Saunders, Christian Cadwallader and Clive Rogers of Blaenau Gwent County Borough Council, and Noel Chard of Silent Valley Waste Services for their input, particularly the provision of data. I am also grateful to Steve Conner of Silent Valley Waste Services for collecting daily leachate samples over an eighteen month period.

I would like to thank Jon Russill and Jon Thomas of TerraDat, both for advice and for the loan of resistivity equipment.

Within Cardiff University, I am grateful to Ian Bulter and Tony Oldroyd for geochemical advice and support whilst using IC equipment, and to my fellow research student Andrew George for his assistance with some of the site surveys.

I am also grateful to Dr Hasan Al-Madfai of the University of Glamorgan for a number of useful discussions about the statistical analysis of the data, and to my father, Stuart Paris, for advice and assistance with the application of artificial neural networks.

Finally, thanks to my husband Simon Cole, to my parents Stuart and Susan Paris and to my sister Victoria, for their love, support and encouragement.

TABLE OF CONTENTS

	Page
DECLARATION AND STATEMENTS	
SUMMARY	
ACKNOWLEDGEMENTS	
TABLE OF CONTENTS	i
LIST OF FIGURES	xiii
LIST OF TABLES	xxiv
ABBREVIATIONS	xxx
<hr/>	
CHAPTER 1 - INTRODUCTION	1
1.1 AIMS & OBJECTIVES	2
1.2 RESEARCH CONTEXT	2
1.3 THESIS OUTLINE	3
<hr/>	
CHAPTER 2 – RESEARCH CONTEXT	5
2.1 LANDFILLS	6
2.1.1 What is a Landfill?	6
2.1.2 Landfill Types	7
2.1.2.1 “Dilute and Disperse” Sites	7
2.1.2.2 Engineered “Containment” Sites	7
2.1.2.3 “Flushing Bioreactor” Site	8
2.1.3 Site Selection	8

2.1.4	Landfill Design Stages	9
2.1.5	Landfill Design Components	11
2.1.5.1	Liner Systems	12
2.1.5.1.1	<i>Single Liner System</i>	13
2.1.5.1.2	<i>Composite Liner System</i>	13
2.1.5.1.3	<i>Double Liner System</i>	14
2.1.5.1.4	<i>Multiple Liner System</i>	14
2.1.5.2	Liner Materials	14
2.1.5.2.1	<i>Clay Liners</i>	15
2.1.5.2.2	<i>Geomembranes</i>	15
2.1.5.2.3	<i>Geosynthetic Clay Liners</i>	16
2.1.5.2.4	<i>Geotextile, Geonets & Geogrids</i>	18
2.1.5.3	Leachate Collection and Removal System	19
2.1.5.4	Gas Collection and Control System	19
2.1.5.5	Final Cover System	20
2.1.5.5.1	<i>Surface Layer</i>	21
2.1.5.5.2	<i>Protection Layer</i>	21
2.1.5.5.3	<i>Drainage Layer</i>	22
2.1.5.5.4	<i>Hydraulic/Gas Barrier Layer</i>	23
2.1.5.5.5	<i>Gas Collection Layer</i>	23
2.1.5.5.6	<i>Foundation Layer</i>	23
2.1.6	Landfill Monitoring	24
2.1.6.1	Leachate, Groundwater and Surface Water Monitoring	25
2.1.6.2	Landfill Gas Monitoring	26
2.2	REVIEW OF LANDFILL REGULATION	28
2.2.1	Legal Framework	28
2.2.1.1	Control of Pollution Act 1974	28
2.2.1.2	Framework Directive on Waste	28
2.2.1.3	Dangerous Substances Directive (76/464/EEC)	29
2.2.1.4	Groundwater Directive (80/68/EEC)	29
2.2.1.5	Town and Country Planning Act 1990	29
2.2.1.6	Environmental Protection Act 1990	30
2.2.1.7	Water Resources Act 1991	31
2.2.1.8	Waste Management Licensing Regulations 1994	31
2.2.1.9	Environment Act 1995	31
2.2.1.10	Special Waste Regulations 1996	32
2.2.1.11	Landfill Tax Regulations 1996	32
2.2.1.12	Integrated Pollution Prevention Control	33
2.2.1.13	Pollution Prevention Control (PPC)	34
2.2.1.14	Landfill Directive (99/31/EC)	34
2.2.1.15	Landfill (England and Wales) Regulations 2002	37
2.2.2	Environment Agency	38
2.2.3	Consented Discharges from Landfill Sites	39

2.2.3.1	List I and II Substances	39
2.2.3.2	Discharge to Sewer	40
2.2.4	International Context	40
2.3	LANDFILLS IN WALES	42
2.3.1	Waste Management Facilities	43
2.3.2	Waste Disposal	44
2.3.3	Waste Production	44
2.3.3.1	Municipal Solid Waste	44
2.3.3.2	Industrial and Commercial Waste	45
2.3.3.3	Special Waste	47
2.3.4	Remaining Landfill Capacity	48
2.4	REVIEW OF NATURE AND EVOLUTION OF MIXED WASTE LANDFILLS	50
2.4.1	Waste	50
2.4.2	Leachate	53
2.4.2.1	Leachate Generation	53
2.4.2.2	Leachate Composition	54
2.4.2.3	Environmental Effects of Leachate	62
2.4.2.3.1	<i>Surface Waters</i>	62
2.4.2.3.2	<i>Groundwater</i>	62
2.4.2.4	Leachate Management	63
2.4.3	Landfill Gas	65
2.4.3.1	Landfill Gas Generation	65
2.4.3.2	Landfill Gas Composition	68
2.4.3.3	Landfill Gas Production	70
2.4.3.3.1	<i>Quantity</i>	70
2.4.3.3.2	<i>Production Rate</i>	70
2.4.3.3.3	<i>Landfill Gas Yields</i>	70
2.4.3.3.4	<i>Landfill Gas Generation Time</i>	73
2.4.3.3.5	<i>Estimating Landfill Gas Quantity</i>	73
2.4.3.3.5.1	<i>Simple Approximation</i>	73
2.4.3.3.5.2	<i>First Order Decay Model</i>	74
2.4.3.3.5.3	<i>Pump Test</i>	75
2.4.3.3.6	<i>Landfill Gas Properties</i>	75
2.4.3.3.6.1	<i>Major Constituents</i>	75
2.4.3.3.6.2	<i>Minor Constituents</i>	76
2.4.3.3.6.3	<i>Density</i>	76
2.4.3.4	Environmental Effects of Landfill Gas	77
2.4.3.4.1	<i>Atmospheric Pollution</i>	77
2.4.3.4.2	<i>Soil Pollution</i>	77
2.4.3.4.3	<i>Damage to Health</i>	78
2.4.3.4.4	<i>Flammability</i>	79
2.4.3.4.5	<i>Toxicity</i>	79

	2.4.3.4.6 <i>Corrosive Properties</i>	80
2.5	HYDROLOGY / HYDROGEOLOGY OF LANDFILLS	81
2.5.1	Water Balance	81
2.5.1.1	Precipitation	82
2.5.1.2	Infiltration	82
2.5.1.3	Run-Off	82
	2.5.1.3.1 <i>Rational Method</i>	83
	2.5.1.3.2 <i>Infiltration Curve Method</i>	84
2.5.1.4	Evaporation	84
2.5.1.5	Evapotranspiration	86
2.5.2	Water Balance Analysis on a Landfill Cap	87
2.5.2.1	Computer Analysis	87
2.5.2.2	Hand Analysis	87
2.5.2.2.1	Row A: Average Monthly Temperature	89
2.5.2.2.2	Row B: Monthly Heat Index (H_m)	89
2.5.2.2.3	Row C: Unadjusted Daily Potential Evapotranspiration (UPET)	89
2.5.2.2.4	Row D: Monthly Duration of Sunlight (N)	90
2.5.2.2.5	Row E: Potential Evapotranspiration (PET)	90
2.5.2.2.6	Row F: Precipitation (P)	90
2.5.2.2.7	Row G: Runoff Coefficient (C)	90
2.5.2.2.8	Row H: Runoff (R)	91
2.5.2.2.9	Row I: Infiltration (IN)	91
2.5.2.2.10	Row J: Infiltration minus Potential Evapotranspiration (IN-PET)	91
2.5.2.2.11	Row K: Accumulated Water Loss (WL)	92
2.5.2.2.12	Row L: Water Stored in Root Zone (WS)	92
2.5.2.2.13	Row M: Change in Water Storage (CWS)	92
2.5.2.2.14	Row N: Actual Evapotranspiration (AET)	92
2.5.2.2.15	Row O: Percolation (PERC)	93
2.5.2.2.16	Row P: Check foe Calculations (CK)	93
2.5.2.2.17	Row Q: Percolation Rate (FLUX)	93
2.6	RESEARCH BY THE WASTE MANAGEMENT INFORMATION BUREAU (WMIB)	94
2.6.1	Valley Landfills with Groundwater Ingress	94
<hr/>		
CHAPTER 3 – DESK STUDY		96
<hr/>		
3.1	SITE DESCRIPTION	97
3.1.1	Site Location	97
3.1.2	Site Access	98
3.1.3	Site of Special Scientific Interest (SSSI)	99
3.2	GEOLOGY	100
3.2.1	Solid Geology	100
<hr/>		

3.2.1.1	Llynfi Beds	100
3.2.1.2	Rhondda Beds	100
3.2.1.3	Brithdir Beds	103
3.2.1.4	Hughes Beds	103
3.2.2	Superficial Deposits	104
3.2.2.1	Boulder Clay & Head Deposits	104
3.3	HYDROLOGY	106
3.3.1	Surface Water	106
3.3.1.1	Surface Water Catchment	106
3.3.1.2	General Quality Assessment of the Ebbw Fawr	106
3.3.1.2.1	<i>Chemistry</i>	107
3.3.1.2.2	<i>Biology</i>	108
3.3.1.2.3	<i>Nutrients</i>	110
3.3.1.2.4	<i>Aesthetics</i>	111
3.3.2	Rainfall	118
3.4	HYDROGEOLOGY	120
3.4.1	Regional Hydrogeology	120
3.4.2	Site Hydrogeology	121
3.4.3	Analysis of Groundwater Flows	125
3.5	SITE HISTORY	131
3.6	PRESENT SITE CONDITIONS	142
3.6.1	Site Layout	142
3.6.2	Ground Conditions	144
3.6.2.1	Superficial Deposits	144
3.6.2.1.1	<i>Made Ground</i>	144
3.6.2.1.1.1	<i>Landfill</i>	144
3.6.2.1.1.2	<i>Steelworks Waste</i>	145
3.6.2.1.2	<i>Landslip Deposits</i>	146
3.6.2.2	Geological Structure	147
3.6.2.3	Stability	148
3.6.2.3.1	<i>Phase 1A</i>	148
3.6.2.3.2	<i>Phase 2</i>	150
3.6.2.4	Economic Geology	152
3.6.2.4.1	<i>Coal</i>	152
3.6.2.4.2	<i>Iron Ore</i>	152
3.6.2.4.3	<i>Mineral Extraction</i>	152
3.6.3	Topography & Morphology	154
3.6.4	Site Operation	167
3.6.4.1	Waste	169
3.6.4.2	Leachate Management	171
3.6.4.2.1	<i>Drainage</i>	174
3.6.4.3	Gas Management	178
3.6.4.4	Monitoring	178

CHAPTER 4 – INTERNAL STRUCTURE	179
4.1 BOREHOLE AND TRIAL PIT DATA	180
4.1.1 Blaenau Gwent Borough Council	180
4.1.2 Golder Associates	182
4.1.2.1 1992 Site Investigation	182
4.1.2.1.1 Trial Pits	182
4.1.2.1.2 Boreholes	184
4.1.2.2 1993 Site Investigation	185
4.1.2.2.1 Trial Pits and Hand Auger	185
4.1.2.2.2 Trial Trenches	186
4.1.2.2.3 Boreholes	188
4.1.3 Sir Alexander Gibb & Partners	190
4.1.3.1 Trial Pits	190
4.1.3.2 Boreholes	190
4.1.4 Exploration Associates	191
4.1.4.1 Trial Pits	191
4.1.4.2 Boreholes	191
4.2 RESISTIVITY SURVEYING	193
4.2.1 Electrical Resistivity	193
4.2.2 Resistivity Survey	194
4.2.2.1 Electrode Configurations	195
4.2.2.1.1 Wenner Array	196
4.2.2.1.2 Schlumberger Array	196
4.2.2.1.3 Wenner-Schlumberger Array	197
4.2.2.2 Resistivity Surveying Equipment	200
4.2.2.3 Data Processing	200
4.2.2.4 Limitations of Resistivity Surveying	201
4.2.2.5 Interpretation of Resistivity Data	201
4.2.2.5.1 Inversion method	202
4.2.2.5.2 RES2DINV Program	202
4.2.2.6 The use of Resistivity on Landfill Sites	205
4.2.3 Resistivity Surveys Undertaken at Silent Valley	206
4.2.3.1 Summer 2000 Survey	206
4.2.3.1.1 Survey Line 1	208
4.2.3.1.2 Survey Line 2	209
4.2.3.1.3 Survey Line 3	209
4.2.3.1.4 Survey Line 4	210
4.2.3.2 Summer 2001 Survey	212
4.2.3.2.1 Survey Line 1	212
4.2.3.2.2 Survey Line 2	214
4.2.3.3 Monthly Surveys	216
4.2.3.3.1 Survey Lines	216
4.2.3.3.2 Data Analysis	218

	4.2.3.3.3 Results	218
	4.2.3.4 3D Survey	227
	4.2.3.5 Time-Lapse Resistivity	237
	4.2.3.5.1 Theory	237
	4.2.3.5.2 Results	239
	4.2.3.6 General Interpretative Model based on Geophysics	249
4.3	CONCEPTUAL SITE MODEL	250
<hr/>		
	CHAPTER 5 – HYDRO-METROLOGY	257
5.1	INSTRUMENTATION	258
5.1.1	Weather Station	258
5.1.1.1	Outside Temperature	258
5.1.1.2	Rainfall	259
5.1.1.3	Wind	260
5.1.1.3.1	Wind Speed/Direction	260
5.1.1.3.2	Wind Chill	262
5.1.1.4	Humidity	263
5.1.1.5	TH Index	263
5.1.1.6	Dew Point	264
5.1.1.7	Pressure	265
5.1.2	Flow Monitoring	266
5.1.2.1	Settlement Tank	271
5.1.2.2	BSC Pipe (LP1)	274
5.1.2.3	Flume	275
5.1.2.4	Nant Merddog	275
5.1.2.5	LP2A in Sump	277
5.1.3	Real Time Data Retrieval	279
5.2	RAINFALL DATA	282
5.2.1	MORECS	282
5.2.2	Silent Valley Waste Services (SWVS)	284
5.2.3	Raingauge – Remote Link	285
5.3	ANALYSIS OF RAINFALL DATA	286
5.3.1	Rainfall Record	286
5.3.1.1	Silent Valley Waste Services Data	386
5.3.1.2	Met Office Data	289
5.3.1.2.1	Potential Evaporation (PE)	289
5.3.1.2.2	Actual Evaporation (AE)	290
5.3.1.2.3	Effective Rainfall (ER)	290
5.3.2	Comparison of Met Office and Silent Valley Data	292
5.4	FLOW DATA	294
5.4.1	BSC Pipe	295
5.4.2	Settlement Tank	298

5.5	ANALYSIS OF FLOW DATA	302
5.5.1	BSC Pipe	302
5.5.1.1	Discharge	302
5.5.1.2	Discharge and Rainfall	302
5.5.1.3	Lag Time	308
5.5.1.4	Regression Analysis	310
5.5.1.4.1	<i>Simple, Two-Variable Regression</i>	313
5.5.1.4.1.1	<i>Discharge and Rainfall</i>	313
5.5.1.4.1.2	<i>Discharge and Effective Rainfall</i>	316
5.5.1.4.1.3	<i>Discharge and Temperature</i>	317
5.5.1.4.1.4	<i>Discharge and Average Wind Speed</i>	317
5.5.1.4.1.5	<i>Discharge and Pressure</i>	318
5.5.1.4.1.6	<i>Summary</i>	319
5.5.1.4.2	<i>Multiple Regression</i>	322
5.5.1.4.2.1	<i>Simultaneous Multiple Regression</i>	322
5.5.1.4.2.2	<i>Stepwise Multiple Regression</i>	326
5.5.1.4.2.3	<i>Summary</i>	330
5.5.2	Settlement Tank	331
5.5.2.1	Discharge	331
5.5.2.2	Discharge and Rainfall	331
5.5.2.3	Lag Time	336
5.5.2.4	Regression Analysis	339
5.5.2.4.1	<i>Simple, Two-Variable Regression</i>	341
5.5.2.4.1.1	<i>Discharge and Rainfall</i>	342
5.5.2.4.1.2	<i>Discharge and Effective Rainfall</i>	343
5.5.2.4.1.3	<i>Discharge and Temperature</i>	344
5.5.2.4.1.4	<i>Discharge and Average Wind Speed</i>	346
5.5.2.4.1.5	<i>Discharge and Pressure</i>	346
5.5.2.4.1.6	<i>Summary</i>	347
5.5.2.4.2	<i>Multiple Regression</i>	350
5.5.2.4.2.1	<i>Simultaneous Multiple Regression – Unadjusted Discharge</i>	351
5.5.2.4.2.2	<i>Simultaneous Multiple Regression – Trend removed from Discharge</i>	355
5.5.2.4.2.3	<i>Stepwise Multiple Regression – Unadjusted Discharge</i>	359
5.5.2.4.2.4	<i>Stepwise Multiple Regression – Trend removed from Discharge</i>	363
5.5.2.4.2.5	<i>Summary</i>	367
5.5.2.4.3	<i>Seasonal Data</i>	369
5.5.2.4.3.1	<i>Simple, Two-Variable Regression</i>	369
5.5.2.4.3.2	<i>Multiple Regression</i>	370
5.5.3	Summary	372
5.5.3.1	BSC Pipe	372

	5.5.3.2 Settlement Tank	373
	5.5.3.3 Seasonal Data	374
5.6	WATER BALANCE	376
5.6.1	Water Balance across site	376
	5.6.1.1 Water Catchment area as 106 ha	376
	5.6.1.2 Water Catchment is landfill area (20.1 ha)	377
	5.6.1.3 Calculation of Catchment Area to account for all Rainfall Input	377
	5.6.1.4 Water Catchment area estimated as 25 ha	378
5.6.2	Water Balance on capped Southern Slope	380
	5.6.2.1 Row A: Average Monthly Temperature	380
	5.6.2.2 Row B: Monthly Heat Index (H_m)	382
	5.6.2.3 Row C: Unadjusted Daily Potential Evapotranspiration (UPET)	383
	5.6.2.4 Row D: Monthly Duration of Sunlight (N)	383
	5.6.2.5 Row E: Potential Evapotranspiration (PET)	383
	5.6.2.6 Row F: Precipitation (P)	384
	5.6.2.7 Row G: Runoff Coefficient (C)	385
	5.6.2.8 Row H: Runoff (R)	386
	5.6.2.9 Row I: Infiltration (IN)	386
	5.6.2.10 Row J: Infiltration minus Potential Evapotranspiration (IN-PET)	386
	5.6.2.11 Row K: Accumulated Water Loss (WL)	386
	5.6.2.12 Row L: Water Stored in Root Zone (WS)	387
	5.6.2.13 Row M: Change in Water Storage (CWS)	387
	5.6.2.14 Row N: Actual Evapotranspiration (AET)	388
	5.6.2.15 Row O: Percolation (PERC)	388
	5.6.2.16 Row P: Check for Calculations (CK)	388
	5.6.2.17 Row Q: Percolation Rate (FLUX)	388
	5.6.2.18 Summary	388
<hr/> CHAPTER 6 – LEACHATE COMPOSITION		390
6.1	LEACHATE ANALYSIS - PRE PROJECT	391
6.1.1	Past Studies	391
6.1.2	Historical Data	392
	6.1.2.1 pH	393
	6.1.2.2 Temperature	393
	6.1.2.3 Electrical Conductivity	393
	6.1.2.4 Ammoniacal Nitrogen	394
	6.1.2.5 Alkalinity	394
	6.1.2.6 Chemical Oxygen Demand (COD)	395
	6.1.2.7 Biochemical Oxygen Demand (BOD)	395
	6.1.2.8 BOD/COD Ratio	396

	6.1.2.9 Total Organic Carbon (TOC)	396
	6.1.2.10 Metals	397
6.2	LEACHATE ANALYSIS - CURRENT STUDY	406
	6.2.1 Sampling Strategy	406
	6.2.2 Ion chromatography (IC)	407
	6.2.2.1 Dionex DX-80	407
	6.2.2.1.1 <i>Stages of Analysis</i>	407
	6.2.2.1.2 <i>Flow path through the DX-80</i>	409
	6.2.2.1.3 <i>Calibration</i>	411
	6.2.2.2 Sample Preparation	411
	6.2.2.3 Detection Limits	412
	6.2.2.4 Precision	413
	6.2.2.5 Errors	413
	6.2.2.6 Frozen/Chilled Samples	414
	6.2.3 Results	416
	6.2.3.1 BSC Pipe (LP1)	416
	6.2.3.1.1 <i>Fluoride</i>	416
	6.2.3.1.2 <i>Chloride</i>	416
	6.2.3.1.3 <i>Bromide</i>	417
	6.2.3.1.4 <i>Nitrate</i>	417
	6.2.3.1.5 <i>Sulphate</i>	417
	6.2.3.2 Settlement Tank	423
	6.2.3.2.1 <i>Fluoride</i>	423
	6.2.3.2.2 <i>Chloride</i>	423
	6.2.3.2.3 <i>Bromide</i>	423
	6.2.3.2.4 <i>Nitrate</i>	424
	6.2.3.2.5 <i>Sulphate</i>	424
6.3	CONDUCTIVITY MONITORING	428
	6.3.1 Conductivity Monitors	428
	6.3.2 Results	430
	6.3.2.1 BSC Pipe (LP1)	430
	6.3.2.2 Settlement Tank	432
6.4	ANALYSIS OF GEOCHEMICAL DATA	435
	6.4.1 BSC Pipe (LP1)	435
	6.4.2 Settlement Tank	440
6.5	SUMMARY	447
CHAPTER 7 - THE USE OF ARTIFICIAL NEURAL NETWORKS TO PREDICT DISCHARGE AT SILENT VALLEY		451
7.1	ARTIFICIAL NEURAL NETWORKS (ANN)	452
	7.1.1 The Multi-Layer Perceptrons (MLP)	453
	7.1.2 Applications of ANNs as Forecasting Tools	455

7.1.2.1	Rainfall-Runoff Modelling	455
7.1.2.2	River Flow Forecasting	456
7.1.2.3	Rainfall-Runoff Model for Real-Time Flash-Flood Forecasting	456
7.2	BUILDING A MODEL	458
7.2.1	Step 1: Variable Selection	458
7.2.2	Step 2: Data Collection	459
7.2.3	Step 3: Data Pre-Processing	459
7.2.4	Step 4: Training, Testing and Validation Sets	460
7.2.5	Step 5: Neural Network Paradigms	460
7.2.5.1	Number of Input Nodes	460
7.2.5.2	Number of Hidden Layers	461
7.2.5.3	Number of Hidden Nodes	461
7.2.5.4	Number of Output Nodes	462
7.2.5.5	Transfer Functions	462
7.2.6	Step 6: Evaluation Criteria	463
7.2.7	Step 7: Neural Network Training	463
7.2.7.1	Number of Training Iterations	463
7.2.7.2	Learning Rate and Momentum	464
7.2.8	Step 8: Implementation	465
7.3	SILENT VALLEY MODEL	466
7.3.1	Network Architecture and Training	466
7.3.2	The Data	467
7.3.3	Results	469
7.4	SUMMARY	475

CHAPTER 8 – DISCUSSION	476
-------------------------------	------------

8.1	INTRODUCTION	476
8.2	WATER BALANCE ANALYSIS	477
8.3	BSC PIPE DISCHARGE	478
8.4	SETTLEMENT TANK DISCHARGE	479
8.5	BSC PIPE LEACHATE GEOCHEMISTRY	482
8.6	SETTLEMENT TANK LEACHATE GEOCHEMISTRY	485
8.7	FORECASTING USING ANNS	486

CHAPTER 9 – CONCLUSIONS AND RECOMMENDATIONS	489
--	------------

9.1	CONCLUSIONS	490
9.2	RECOMMENDATIONS	496

REFERENCE LIST	497
-----------------------	------------

APPENDICES	503	
Appendix A	Mean possible monthly duration of sunlight in the Northern Hemisphere	504
Appendix B	Resistivity Sections	506
Appendix C	Pearson's level of significance	529
Appendix D	Discharge Data	CD
Appendix E	Weather Data	CD
Appendix F	Leachate Data	CD

LIST OF FIGURES

	Page
Figure 2.1	Schematic diagram of a municipal solid waste landfill containment system. 11
Figure 2.2	Four types of geosynthetic clay liner. 18
Figure 2.3	Typical layers of final cover systems for municipal solid waste. 21
Figure 2.4	Map showing how data from unitary authorities have been grouped together into seven sub-regions for Wales. 42
Figure 2.5	Chart showing waste form and method of disposal or recovery. 47
Figure 2.6	Chart showing waste form and method of management used for special waste. 48
Figure 2.7	Major stages of waste degradation. 55
Figure 2.8	Graph showing changes in composition of leachate with time. 56
Figure 2.9	Graph showing changes in composition of landfill gas. 67
Figure 2.10	Potential pathways of water movement on a landfill site. 81
Figure 3.1	Map showing the location of Silent Valley landfill site. 97
Figure 3.2	Geological map of area surrounding Silent Valley landfill site. 101
Figure 3.3	Geological map of area surrounding Silent Valley landfill site. 102
Figure 3.4	Classification under the General Quality Assessment scheme (GQA) for river chemistry in 2002. 113
Figure 3.5	Classification under the General Quality Assessment scheme (GQA) for river biology in 2002. 114
Figure 3.6	Classification under the General Quality Assessment scheme (GQA) for river phosphate in 2002. 115

Figure 3.7	Classification under the General Quality Assessment scheme (GQA) for river nitrate in 2002.	116
Figure 3.8	Classification under the General Quality Assessment scheme (GQA) for river aesthetics in 2000.	117
Figure 3.9	Monthly rainfall data for Silent Valley landfill site.	118
Figure 3.10	Hydrogeological map of Silent Valley and surrounding area.	122
Figure 3.11	Groundwater vulnerability map of area surrounding Silent Valley landfill site.	123
Figure 3.12	Estimated recharge area for calculation of flow through the equivalent layer.	127
Figure 3.13	Estimated surface water catchment area.	130
Figure 3.14	Map taken from the 1880 1:2500 Monmouthshire map.	135
Figure 3.15	Map taken from the 1901 1:10,560 Monmouthshire map.	136
Figure 3.16	Map taken from the 1920 1:2500 Monmouthshire map.	137
Figure 3.17	Oblique aerial photograph showing the twin Maclane cones at Cwm Merddog taken on 26th October 1948.	138
Figure 3.18	Aerial photograph showing the twin Maclane cones at Cwm Merddog taken on 12th May 1951.	139
Figure 3.19	1969 map of area around Silent Valley landfill site.	140
Figure 3.20	Georeferenced photograph of Silent Valley taken in 2000.	141
Figure 3.21	Photograph (taken 2000) showing the layout of Silent Valley landfill site.	143
Figure 3.22	Photograph showing layering within the slag deposits taken June 2001	145
Figure 3.23	Map of Phase 2.	151
Figure 3.24	Map showing the location of the following cross-sections.	156
Figure 3.25	Contours of the site based on photogrammetric work of 1955 aerial photographs.	163
Figure 3.26	Contours of the site based on photogrammetric work of 1983 aerial photographs.	164
Figure 3.27a	3D surface of Silent Valley landfill site, Ebbw Vale and Cwm using a georeferenced air photograph taken in 2000.	165
Figure 3.27b	3D surface of Silent Valley landfill site using a georeferenced air photograph taken in 2000.	166

Figure 3.28	Location of the approximate base area of Phase 1A landfill cells 1 to 5.	168
Figure 3.29	The proportions of different waste categories that entered Silent Valley landfill site between July 1999 and June 2000. The values indicate the waste volume to the nearest tonne.	170
Figure 3.30	The proportions of different waste categories that entered Silent Valley landfill site between April 2003 and March 2004. The values indicate the waste volume to the nearest tonne.	171
Figure 3.31	Map showing the location of monitoring points at Silent Valley landfill.	173
Figure 3.32	Drainage map of Silent Valley.	176
Figure 3.33	2004 drainage map of Silent Valley.	177
Figure 4.1	Map showing the location of the boreholes and trial pits.	181
Figure 4.2	Wenner electrode configuration.	196
Figure 4.3	Schlumberger electrode configuration.	197
Figure 4.4	The steps used by the (a) Wenner and the (b) Wenner-Schlumberger arrays to increase the depth of investigation.	198
Figure 4.5	Schematic showing the arrangement of data points in the pseudosections for the (a) Wenner and the (b) Wenner-Schlumberger arrays.	199
Figure 4.6	An example of a field data set with a few bad data points.	204
Figure 4.7	Map showing the locations of the Summer 2000 and 2001 resistivity surveys.	207
Figure 4.8	Line 1 of the summer 2000 resistivity survey.	208
Figure 4.9	Line 2 of the summer 2000 resistivity survey.	209
Figure 4.10	Line 3 of the summer 2000 resistivity survey.	210
Figure 4.11	Line 4 of the summer 2000 resistivity survey.	211
Figure 4.12	Line 1 of the summer 2001 resistivity survey.	213
Figure 4.13	Line 2 of the summer 2001 resistivity survey.	215
Figure 4.14	Photo (taken June 2001) showing the area where seepage is evident at the surface.	215
Figure 4.15	Map showing location of survey lines 1 and 2.	217
Figure 4.16	Resistivity profiles for survey Line 1 between December 2001 and November 2002.	219-221

Figure 4.17	Resistivity profiles for survey Line 2 between December 2001 and November 2002.	222-225
Figure 4.18	Rainfall recorded at Silent Valley by Silent Valley Waste Services.	226
Figure 4.19	The arrangement of the electrodes for a 3D survey.	227
Figure 4.20	Map showing the location of the resistivity survey lines.	228
Figure 4.21	Resistivity survey lines for June 2002.	231
Figure 4.22	Resistivity modelled on surfaces at increasing depth, based on integration of five 2D resistivity tomography models.	232-236
Figure 4.23	Time-lapse data for time series 10 for the initial data set (December 2001), a subsequent data set (October 2002) and the percentage change in resistivity between them.	239
Figure 4.24	Profiles of Line 1 showing the percentage change in resistivity between December 2001 and surveys done between January and November 2002.	241-243
Figure 4.25	Time-lapse data for time series 10 for the preceding data set (September 2002), a data set (October 2002) and the percentage change in resistivity between them.	244
Figure 4.26	Profiles of Line 1 showing the percentage change in resistivity between months.	246-248
Figure 4.27	Cross-section across northling 206950.	252
Figure 4.28	Cross-section running south-south-east north-north-west between 318670 206600 and 318552 207290.	253
Figure 4.29	Conceptual Site Model across northling 206950.	255
Figure 4.30	Conceptual Site Model running south-south-east north-north-west between 318670 206600 and 318552 207290.	256
Figure 5.1	Graph showing the average daily temperature recorded at Silent Valley between October 1998 and June 2004.	259
Figure 5.2	Windrose for wind recorded at Silent Valley in 2003.	261
Figure 5.3	Windrose for wind recorded at Sennybridge in 2003.	262
Figure 5.4	Photograph showing the WJ460 box.	266
Figure 5.5	Schematic showing the location of the leachate sampling points, the sump and lagoon (Settlement Tank).	270
Figure 5.6	Photograph of the Settlement Tank at Silent Valley Landfill site. Photograph taken looking south.	272

Figure 5.7	Photograph of the Settlement Tank rectangular weir at Silent Valley Landfill site.	273
Figure 5.8	Photograph showing the BSC Pipe (LP1).	274
Figure 5.9	Graph showing total daily rainfall and discharge over the crump weir in the Nant Merddog between 1 October and 31 December 2001.	276
Figure 5.10	Graph showing the relationship between daily rainfall and discharge over the crump weir in the Nant Merddog between 1 October and 31 December 2001.	276
Figure 5.11	Photograph showing the V-notch weir measuring LP2A.	277
Figure 5.12	Graph showing typical flow data for the Settlement Tank downloaded directly from the datalogger and from the remote download.	281
Figure 5.13	A map showing the location of the 40 km squares and their associated reference number.	283
Figure 5.14	Raingauge installed at the base of the landfill by the sump and flow monitoring data loggers (approximately 310 mAOD).	285
Figure 5.15	Graph showing the monthly rainfall totals recorded at Silent Valley by Silent Valley Waste Services.	287
Figure 5.16	Graph showing monthly Potential Evaporation values for Cwm.	289
Figure 5.17	Graph showing monthly Actual Evaporation values for Cwm.	290
Figure 5.18	Graph showing monthly Actual Evaporation and Effective Rainfall recorded at Cwm by the Met Office.	291
Figure 5.19	Rainfall data collected on site by Silent Valley waste Services and at Cwm by the Met Office between January and December 2003.	292
Figure 5.20	Graph showing the correlation of rainfall recorded at Silent Valley and Cwm.	293
Figure 5.21	Graph showing total daily discharge over the weir in the BSC Pipe between February 1994 and July 2004.	296
Figure 5.22	Graph showing total daily discharge (suspect data removed) over the weir in the BSC Pipe between February 1994 and July 2004.	297
Figure 5.23	Graph showing total daily discharge over the weir in the Settlement Tank between December 1993 and July 2004.	299
Figure 5.24	Graph showing total weekly Settlement Tank discharge and rainfall between October 1998 and June 2004.	300

Figure 5.25	(a) Graph showing the discharge data with trend, (b) graph showing the discharge data with the trend removed.	301
Figure 5.26	Graph showing discharge through the BSC Pipe and rainfall between 28 November 2003 and 22 June 2004.	305
Figure 5.27	Graph showing discharge through the BSC Pipe and Effective Rainfall between 28 November 2003 and 31 May 2004	306
Figure 5.28	Cumulative graph showing discharge through the BSC Pipe, rainfall and Effective Rainfall between 9 May 2003 and 31 May 2004.	307
Figure 5.29	Chart showing the cross-correlation for daily discharge in the BSC Pipe with Rainfall between 21 October 1998 and 23 June 2004.	308
Figure 5.30	Chart showing the cross-correlation for daily discharge in the BSC Pipe with Effective Rainfall between 21 October 1998 and 23 June 2004.	309
Figure 5.31	Scale of correlation.	310
Figure 5.32	Graph showing the distribution of daily BSC Pipe discharge and a normal curve with the same mean and variance as the data.	311
Figure 5.33	Graph showing the distribution of the natural logarithms of the daily BSC Pipe discharge and a normal curve with the same mean and variance as the data.	312
Figure 5.34	Graph showing the relationship between daily rainfall and daily discharge (October 1998 to June 2004).	314
Figure 5.35	Graph showing the relationship between daily rainfall and daily discharge recorded 5 days ago (lag time) (October 1998 to June 2004).	315
Figure 5.36	Graph showing the relationship between daily rainfall and the natural logarithms of daily discharge recorded 5 days ago (lag time) (October 1998 to June 2004).	315
Figure 5.37	Graph showing the relationship between daily effective rainfall and daily discharge (April 2000 to June 2004).	316
Figure 5.38	Graph showing the relationship between average daily temperature and daily discharge (October 1998 to June 2004).	317
Figure 5.39	Graph showing the relationship between average daily wind speed and daily discharge (October 1998 to June 2004).	318
Figure 5.40	Graph showing the relationship between average daily pressure and daily discharge (October 1998 to June 2004).	319
Figure 5.41	Graph showing the recorded and predicted discharge through the BSC Pipe using simultaneous regression.	325

Figure 5.42	Graph showing the recorded against the predicted discharge through the BSC Pipe using simultaneous regression.	325
Figure 5.43	Graph showing the recorded and predicted discharge through the BSC Pipe using stepwise regression.	329
Figure 5.44	Graph showing the recorded against the predicted discharge through the Settlement Tank using stepwise regression.	329
Figure 5.45	Graph showing discharge through the Settlement Tank and rainfall between 28 November 2003 and 22 June 2004.	333
Figure 5.46	Graph showing discharge through the Settlement Tank and effective rainfall between 28 November 2003 and 31 May 2004.	334
Figure 5.47	Cumulative graph showing discharge through the Settlement Tank, rainfall and Effective Rainfall between 9 May 2003 and 31 May 2004.	335
Figure 5.48	Chart showing the cross-correlation for daily discharge in the Settlement Tank with Rainfall between 21 October 1998 and 23 June 2004.	336
Figure 5.49	Chart showing the cross-correlation for daily discharge in the Settlement Tank with Effective Rainfall between 21 October 1998 and 23 June 2004.	337
Figure 5.50	Chart showing the cross-correlation between half hourly discharge in the Settlement Tank and Rainfall between 28 November 2003 and 24 June 2004.	339
Figure 5.51	Graph showing discharge through the Settlement Tank and rainfall between 4am on 20 December 2003 and 1am on 21 December 2003.	338
Figure 5.52	Graph showing the distribution of daily Settlement Tank discharge and a normal curve with the same mean and variance as the data.	340
Figure 5.53	Graph showing the distribution of the natural logarithms of the daily Settlement Tank discharge and a normal curve with the same mean and variance as the data.	341
Figure 5.54	Graph showing the relationship between average daily rainfall and daily discharge (October 1998 to June 2004).	342
Figure 5.55	Graph showing the relationship between average daily rainfall and natural logarithms of daily discharge (October 1998 to June 2004).	343
Figure 5.56	Graph showing the relationship between average daily effective rainfall and daily discharge (October 1998 to June 2004).	344
Figure 5.57	Graph showing the relationship between average daily temperature and daily discharge (October 1998 to June 2004).	345

Figure 5.58	Graph showing the relationship between temperature and flow through the Settlement Tank.	345
Figure 5.59	Graph showing the relationship between average daily wind speed and daily discharge (October 1998 to June 2004).	346
Figure 5.60	Graph showing the relationship between average daily pressure and daily discharge (October 1998 to June 2004).	347
Figure 5.61	Graph showing the recorded (unadjusted) and predicted discharge through the Settlement Tank using simultaneous regression.	353
Figure 5.62	Graph showing the recorded (unadjusted) against the predicted discharge through the Settlement Tank using simultaneous regression.	354
Figure 5.63	Graph showing the recorded (trend removed) and predicted discharge through the Settlement Tank using simultaneous regression.	357
Figure 5.64	Graph showing the recorded (trend removed) against the predicted discharge through the Settlement Tank using simultaneous regression.	358
Figure 5.65	Graph showing the recorded (unadjusted) and predicted discharge through the Settlement Tank using stepwise regression.	362
Figure 5.66	Graph showing the recorded (unadjusted) against the predicted discharge through the Settlement Tank using stepwise regression.	362
Figure 5.67	Graph showing the recorded (trend removed) and predicted discharge through the Settlement Tank using stepwise regression.	366
Figure 5.68	Graph showing the recorded (trend removed) against the predicted discharge through the Settlement Tank using stepwise regression.	366
Figure 5.69	Graph showing the average, minimum and maximum monthly temperatures recorded at Silent Valley between October 1998 and June 2004.	382
Figure 5.70	Graph showing the average, minimum and maximum monthly rainfall recorded at Cwm by the Met Office between April 2000 and May 2004.	385
Figure 6.1	Graph showing the pH recorded for LP1 between July 1993 and May 2004.	399
Figure 6.2	Graph showing the temperature recorded for LP1 between July 1993 and May 2004.	400
Figure 6.3	Graph showing the conductivity recorded for LP1 between July 1993 and May 2004.	400

Figure 6.4	Graph showing the ammoniacal nitrogen recorded for LP1 between July 1993 and May 2004.	401
Figure 6.5	Graph showing the alkalinity recorded for LP1 between July 1993 and May 2004.	401
Figure 6.6	Graph showing the Chemical Oxygen Demand (COD) recorded for LP1 between July 1993 and May 2004.	402
Figure 6.7	Graph showing the Biochemical Oxygen Demand (BOD) recorded for LP1 between July 1993 and May 2004.	402
Figure 6.8	Graph showing the BOD/COD ratio recorded for LP1 between July 1993 and May 2004.	403
Figure 6.9	Graph showing the Total Organic Carbon (TOC) recorded for LP1 between July 1993 and May 2004.	403
Figure 6.10	Graph showing the concentrations of calcium, sodium, potassium and magnesium recorded for LP1 between July 1993 and May 2004.	404
Figure 6.11	Graph showing the concentrations of iron, manganese, cadmium, chromium, copper, nickel, lead and zinc recorded for LP1 between July 1993 and May 2004.	405
Figure 6.12	Ion analysis process.	409
Figure 6.13	Schematic of the flow through the DX-80.	410
Figure 6.14	Graph showing fluoride concentrations measured in LP1 between 22 June 2002 and 7 July 2004.	418
Figure 6.15	Graph showing chloride concentrations measured in LP1 between 22 June 2002 and 7 July 2004.	419
Figure 6.16	Graph showing chloride concentrations measured in LP1 between July 1993 and July 2004.	419
Figure 6.17	Graph showing bromide concentrations measured in LP1 between 22 June 2002 and 7 July 2004.	420
Figure 6.18	Graph showing nitrate concentrations measured in LP1 between 22 June 2002 and 7 July 2004.	420
Figure 6.19	Graph showing nitrate concentrations measured in LP1 between July 1993 and July 2004.	421
Figure 6.20	Graph showing sulphate concentrations measured in LP1 between 22 June 2002 and 7 July 2004.	421
Figure 6.21	Graph showing sulphate concentrations measured in LP1 between July 1993 and July 2004.	422

Figure 6.22	Graph showing fluoride concentrations measured in the Settlement Tank between 22 June 2002 and 7 July 2004.	425
Figure 6.23	Graph showing chloride concentrations measured in the Settlement Tank between 22 June 2002 and 7 July 2004.	425
Figure 6.24	Graph showing bromide concentrations measured in the Settlement Tank between 22 June 2002 and 7 July 2004.	426
Figure 6.25	Graph showing nitrate concentrations measured in the Settlement Tank between 22 June 2002 and 7 July 2004.	426
Figure 6.26	Graph showing sulphate concentrations measured in the Settlement Tank between 22 June 2002 and 7 July 2004.	427
Figure 6.27	Graph showing how average daily conductivity varies for LP1 between January 2003 and June 2004.	430
Figure 6.28	Graph showing average daily conductivity and discharge for the BSC Pipe (LP1) between January 2003 and June 2004.	431
Figure 6.29	Graph showing discharge for the BSC Pipe (LP1) against average daily conductivity between January 2003 and June 2004.	431
Figure 6.30	Graph showing how average daily conductivity varies for the Settlement Tank between January 2003 and June 2004.	433
Figure 6.31	Graph showing average daily conductivity and discharge for the Settlement Tank between January 2003 and June 2004.	433
Figure 6.32	Graph showing discharge for the Settlement Tank against average daily conductivity between January 2003 and June 2004.	434
Figure 6.33	Graph showing discharge for the Settlement Tank against average daily conductivity between 8 September 2003 and June 2004.	434
Figure 6.34	Graph showing fluoride concentration for the BSC Pipe (LP1) against average daily conductivity between January 2003 and June 2004.	436
Figure 6.35	Graph showing chloride concentration for the BSC Pipe (LP1) against average daily conductivity between January 2003 and June 2004.	436
Figure 6.36	Graph showing bromide concentration for the BSC Pipe (LP1) against average daily conductivity between January 2003 and June 2004.	437
Figure 6.37	Graph showing nitrate concentration for the BSC Pipe (LP1) against average daily conductivity between January 2003 and June 2004.	437

Figure 6.38	Graph showing sulphate concentration for the BSC Pipe (LP1) against average daily conductivity between January 2003 and June 2004.	438
Figure 6.39	Graph showing discharge through the BSC Pipe (LP1) against the IC results.	438
Figure 6.40	Graph showing fluoride concentration for the Settlement Tank against average daily conductivity between January 2003 and June 2004.	442
Figure 6.41	Graph showing chloride concentration for the Settlement Tank against average daily conductivity between January 2003 and June 2004.	442
Figure 6.42	Graph showing bromide concentration for the Settlement Tank against average daily conductivity between January 2003 and June 2004.	443
Figure 6.43	Graph showing nitrate concentration for the Settlement Tank against average daily conductivity between January 2003 and June 2004.	443
Figure 6.44	Graph showing sulphate concentration for the Settlement Tank against average daily conductivity between January 2003 and June 2004.	444
Figure 6.45	Graph showing discharge through the Settlement Tank against the chloride, nitrate and sulphate IC results.	444
Figure 6.46	Graph showing discharge through the Settlement Tank against the fluoride and bromide IC results.	445
Figure 7.1	A simple Multi-Layered Perception network	453
Figure 7.2	Graph showing the training Mean Squared Error of a model using the normalised data.	472
Figure 7.3	Graph showing the observed discharge in the Settlement Tank with predicted discharge using neural networks, simultaneous regression analysis and stepwise regression analysis between 2 August and 9 October 2001.	473
Figure 7.4	Graph showing the observed discharge in the Settlement Tank with predicted discharge using neural networks, simultaneous regression analysis and stepwise regression analysis between 11 April and 18 May 2004.	474
Figure 8.1	Graph showing the observed concentrations of chloride, bromide, nitrate and sulphate in the Settlement Tank with the predicted concentrations based on the predicted discharge using neural networks between 11 April and 18 May 2004.	488

LIST OF TABLES

		Page
Table 2.1	Summary of licensed waste management facilities operating in Wales in March 1999.	43
Table 2.2	Amount (000s tonnes) and collection method of municipal solid waste produced in Wales.	45
Table 2.3	Amount (000s tonnes) and composition of industrial and commercial waste produced in Wales for 1998-99.	46
Table 2.4	Voidspace deposits and remaining capacity at landfill sites licensed for biodegradable waste.	49
Table 2.5	Summary of composition of acetogenic leachates sampled from large landfills with a high waste input rate, relatively dry (35 samples in all).	60
Table 2.6	Summary of composition of methanogenic leachates sampled from large landfills with a high waste input rate, relatively dry (29 samples in all).	61
Table 2.7	Typical landfill gas composition values.	69
Table 2.8	Composition and methane potential of municipal refuse by chemical constituent.	69
Table 2.9	Typical data on the elementary composition of the biodegradable fraction of MSW, expressed as percentage of dry weight.	71
Table 2.10	Landfill gas yields and generation rates that have been reported in the literature.	72
Table 2.11	Suggested values for first order decay model variables.	75
Table 2.12	Values of c for the evaluation of the hydrological balance around a landfill site.	84
Table 2.13	Saturation humidity of air (g/m^3).	85

Table 2.14	Spreadsheet used for water balance analysis.	88
Table 2.15	Suggested runoff coefficients.	91
Table 2.16	Summary of leachate quality in 1995 at valley landfills with groundwater ingress.	95
Table 3.1	Summary of laboratory results (BGBC and Golder Associates) and NRA guidelines for landfill lining material.	105
Table 3.2	Table showing the General Quality Assessment scheme grades for chemistry.	108
Table 3.3	Table showing the General Quality Assessment scheme grades for biology.	109
Table 3.4	Table showing the General Quality Assessment scheme grades for phosphate.	110
Table 3.5	Table showing the General Quality Assessment scheme grades for nitrate.	111
Table 3.6	The annual permitted wastes that Silent Valley landfill site can receive.	169
Table 4.1	Summary of borehole logs data for Blaenau Gwent Borough Council site investigation.	180
Table 4.2	A summary of the trial pit logs from the 1992 Golder Associates site investigation.	183
Table 4.3	Summary of borehole logs data for 1992 Golder Associates site investigation.	184
Table 4.4	Summary of trial pit and hand auger data for 1993 Golder Associates site investigation.	187
Table 4.5	Summary of borehole logs data for 1993 Golder Associates site investigation.	189
Table 4.6	Summary of trial pit logs for Sir Alexander Gibb & Partners site investigation.	190
Table 4.7	Summary of borehole logs for Sir Alexander Gibb & Partners site investigation.	191
Table 4.8	Summary of trial pit logs for Exploration Associates site investigation.	192
Table 4.9	Summary of borehole logs for Exploration Associates site investigation.	192
Table 4.10	Resistivities of common geologic materials.	194

Table 4.11	Comparison of Wenner and Schlumberger electrode arrays.	195
Table 5.1	Table showing the specification of the WJ460.	267
Table 5.2	Table showing the specification of the ultra-sonic device.	268
Table 5.3	Weir configurations at Silent Valley landfill site.	269
Table 5.4	Table showing typical flow data for the Settlement Tank downloaded directly from the datalogger and from the remote download.	280
Table 5.5	Minimum and maximum amounts of rainfall recorded at Silent Valley for different time periods between October 1998 and June 2004.	288
Table 5.6	Discharge (m ³) recorded through the BSC Pipe between October 1998 and July 2004 for different time scales.	304
Table 5.7	Table of correlations for the BSC Pipe discharge and meteorological data.	321
Table 5.8	Table of correlations for simultaneous multiple regression for discharge through the BSC Pipe.	323
Table 5.9	Table giving the value of <i>R</i> for simultaneous multiple regression for discharge through the BSC Pipe.	323
Table 5.10	The regression equation and associated statistics for simultaneous multiple regression for discharge through the BSC Pipe.	324
Table 5.11	List of variables entered into the stepwise multiple regression for discharge through the BSC Pipe.	326
Table 5.12	Value of <i>R</i> and associated statistics for each model in the stepwise multiple regression for discharge through the BSC Pipe	326
Table 5.13	The regression coefficients for the single variable (Model 1) and the two variables (Model 2) remaining in the stepwise regression analysis.	327
Table 5.14	The variables excluded from the stepwise regression analysis.	328
Table 5.15	Discharge (m ³) recorded in the Settlement Tank between October 1998 and July 2004 for different time scales.	332
Table 5.16	Table of correlations for the Settlement Tank discharge and meteorological data.	349
Table 5.17	Table of correlations for simultaneous multiple regression for discharge (unadjusted) through the Settlement Tank	351
Table 5.18	Table giving the value of <i>R</i> for simultaneous multiple regression for discharge (unadjusted) through the Settlement Tank.	352

Table 5.19	The regression equation and associated statistics for simultaneous multiple regression for discharge (unadjusted) through the Settlement Tank.	352
Table 5.20	Table of correlations for simultaneous multiple regression for discharge (trend removed) through the Settlement Tank.	355
Table 5.21	Table giving the value of R for simultaneous multiple regression for discharge (trend removed) through the Settlement Tank.	356
Table 5.22	The regression equation and associated statistics for simultaneous multiple regression for discharge (trend removed) through the Settlement Tank.	356
Table 5.23	List of variables entered into the stepwise multiple regression for discharge (unadjusted) through the Settlement Tank.	359
Table 5.24	Value of R and associated statistics for each model in the stepwise multiple regression for discharge (unadjusted) through the Settlement Tank.	360
Table 5.25	The regression coefficients for the single variable (Model 1), the two variables (Model 2) and the three variables (Model 3) remaining in the stepwise regression analysis for the unadjusted discharge.	360
Table 5.26	The variables excluded from the stepwise regression analysis for the unadjusted discharge.	361
Table 5.27	List of variables entered into the stepwise multiple regression for discharge (trend removed) through the Settlement Tank.	363
Table 5.28	Value of R and associated statistics for each model in the stepwise multiple regression for discharge (trend removed) through the Settlement Tank.	363
Table 5.29	The regression coefficients for the single variable (Model 1) and the two variables (Model 2) remaining in the stepwise regression analysis for the discharge with the trend removed.	364
Table 5.30	The variables excluded from the stepwise regression analysis for the discharge with the trend removed.	365
Table 5.31	Summary of multiple regression analysis models for the Settlement Tank.	367
Table 5.32	Table showing the correlations for the Settlement Tank discharge and meteorological data for all the year, Summer (April to September) and Winter (October to March).	370
Table 5.33	Table showing value of R and associated statistics for each simultaneous and stepwise multiple regression for discharge through the Settlement Tank using all the data, winter data and summer data.	371

Table 5.34	Spreadsheet used to analyse the annual water balance on the Southern Slope landfill cap at Silent Valley landfill site using monthly averages.	381
Table 5.35	Table showing average monthly temperatures recorded at Silent Valley between October 1998 and June 2004.	380
Table 5.36	Table showing average monthly rainfall recorded at Cwm by the Met Office between April 2000 and May 2004.	384
Table 5.37	Suggested Volumetric Water contents of various soils.	387
Table 5.38	Table showing analysis results of the annual water balance on the southern Slope at Silent Valley landfill.	389
Table 6.1	Chemical analysis results for metals in LP1 between July 1993 to May 2004.	397
Table 6.2	Standard concentrations for a four-level anion calibration.	411
Table 6.3	Detection limits of the anions analysed using IC.	412
Table 6.4	Precision for anions analysed using IC.	413
Table 6.5	Results of analysis of samples that were analysed after being refrigerated over night and after being frozen and thawed.	415
Table 6.6	Minimum, maximum, mean and standard deviation of determinands in LP1 analysed using IC.	418
Table 6.7	Minimum, maximum, mean and standard deviation of determinands in the Settlement Tank discharge analysed using IC.	424
Table 6.8	Table showing the specification of the E53 Analyser and 3700E-Series Electrodeless Conductivity Sensor.	429
Table 6.9	Table of correlations for the BSC Pipe (LP1) discharge and geochemical data.	439
Table 6.10	Table of correlations for the Settlement Tank discharge and geochemical data.	446
Table 6.11	Long-term trends for determinands measured in LP1.	448
Table 6.12	Changes in concentration of leachate parameters with age of the waste.	448
Table 7.1	Steps in designing a neural network forecasting model.	458
Table 7.2	Root Mean Square Errors for the predicted discharge over each period.	470
Table 8.1	Table showing present and predicted levels of constituents within LP1 based on trends seen between 1993 and the present.	482

Table 8.2	Dutch guidelines on water standards compared with LP1.	484
-----------	--	-----

ABBREVIATIONS

2D	two dimensional
3D	three dimensional
AE	actual evaporation
AET	actual evapotranspiration
ANN	Artificial Neural Networks
AOD	above Ordnance Datum
ARMA	auto-regressive moving average
BAT	best available technique
BES	bentonite enhanced soils
BGBC	Blaenau Gwent Borough Council
BH	borehole
BOD	biochemical oxygen demand
BP	backpropagation
BS	British Standard
BSC	British Steel culvert
CCF	cross-correlation function
CCL	compacted clay liner
CCTV	closed-circuit television
COD	chemical oxygen demand
COPA	Control of Pollution Act
CSM	Conceptual Site Model
CSPE	chlorosulfonated polyethylene
CST	constant separation traversing

Abbreviations

DoE	Department of the Environment
EA	Environment Agency
EC	European Community
EEC	European Economic Community
EPA	Environmental Protection Act
EPA	Environmental Protection Agency (US)
ER	Effective Rainfall
EU	European Union
FML	flexible membrane line
fPP	flexible polypropylene
FSM	Functional Series Models
GCL	geosynthetic clay liners
GCS	groundwater collection system
GM	geomembrane
GQA	General Quality Assessment
HDPE	high density polyethylene
HELP	Hydraulic Evaluation of Landfill Performance
HSE	Health and Safety Executive
HWL	hazardous waste list
IC	Ion Chromatography
IP	induced polarisation
IPC	Integrated Pollution Control
IPPC	Integrated Pollution Prevention and Control
ISO	International Organization for Standardization
LAPC	Local Air Pollution Control
LAWDC	Local Authority Waste Disposal Company
LC	Liquid Chromatography
LCS	leachate collection system
LDR	Land Disposal Restrictions (in US)
LEL	lower explosive limit
LFG	landfill gas
LLDPE	linear low-density polyethylene
LPM	linear perturbation model

Abbreviations

mbgl	meters below ground level
MLP	multi-layer perceptrons
MORECS	Meteorological Office Rainfall and Evaporation Calculation System
MSE	mean squared error
mst	mudstone
MSW	municipal solid waste
NNLPM	nearest neighbour linear perturbation model
NRA	National Rivers Authority
NRSC	National Remote Sensing Centre
OS	Ordnance Survey
PE	potential evaporation
PET	potential evapotranspiration
PPC	Pollution Prevention and Control
PVC	polyvinyl chloride
RBF	radial basis function
RCRA	Resource Conservation and Recovery Act (in US)
RH	relative humidity
RIVPACS	River Invertebrate Prediction and Classification System
RMS	root mean square
RMSE	root mean squared error
SEPA	Scottish Environment Protection Agency
SLM	simple linear model
SSSI	Site of Special Scientific Interest
sst	sandstone
STP	standard temperature and pressure
SVWS	Silent Valley Waste Services
SWMA	Strategic Waste Management Assessment
TBP-NN	temporal back propagation neural network
TDS	total dissolved solids
TH	temperature-humidity
TOC	total organic carbon
TP	trial pit
UEL	upper explosive limit

Abbreviations

UPET	unadjusted daily potential evapotranspiration
USDA-SCS	United States Department of Agriculture and Soil Conservation Service
VES	Vertical Electrical Sounding
VLDPE	very low density polyethylene
WDA	waste disposal authority
WMIB	Waste Management Information Bureau
WMP	Waste Management Paper
wmst	weathered mudstone

CHAPTER 1

INTRODUCTION

Understanding the generation, character, long-term evolution and control of leachate discharges from unlined landfills still provides an important scientific and engineering challenge, requiring integration of hydrogeological and geochemical modelling.

Rainfall causes infiltration of water into the landfilled waste and also the generation of leachate. Prediction of the volume of leachate that can be generated from a landfill is generally based on water budget principals. This research will perform water budget analysis for Silent Valley landfill site and take it a step further to identify trends in the discharge in relation to meteorological variables in an attempt to produce a forecasting tool. Coupled to this hydrological study, variation in selected geochemical characteristics of the leachate produced by and discharged from the site are analysed in an attempt to improve the understanding of this complex hydro-geochemical system.

1.1 AIMS & OBJECTIVES

The aims of this study are to examine the relationships between the meteorological data collected for the site and the discharge through the BSC Pipe and Settlement Tank and to investigate the geochemical evolution of the leachate. Water balance analysis will be performed for the Silent Valley using rainfall, Effective Rainfall and discharge data for the site. The study aims to develop a hydro-geochemical model of leachate system, to allow prediction of volumes and quality.

It is hoped that the research outcomes will provide a firm basis for the management of Silent Valley landfill site. It is also anticipated that research techniques employed at this case study site can be used at other landfill sites where similar or more extensive temporal monitoring data are available.

1.2 CONTEXT OF RESEARCH

Silent Valley Landfill site (National Grid Reference SO 185 075) has been in operation as a landfill site since 1981. Before accepting municipal waste it received large quantities of waste from the iron and steel works at Ebbw Vale. The site is currently licensed to accept household waste.

Much of the area surrounding the site is a Local Nature Reserve, with part of it designated as a Site of Special Scientific Interest (SSSI).

The site is located on the interbedded sandstones and mudstones of the Rhondda Beds of the Lower Pennant Measures. The solid geology is overlain by a mixture of boulder clay, head deposits and made ground.

The site is unlined and works on a dilute and disperse principal (Section 2.1.2.1). The clay rich deposits covering the valley floor act a relatively impermeable layer. The thickness of the clay, where present, varies across the site from 0.2 m to in excess of 3.5 m. Over most of the site the clay is a silty clay with a measured permeability of 2.85×10^{-9} to 8.9×10^{-10} m/s. The head deposits on site have a measured permeability of 2.35×10^{-9} to 7.18×10^{-9} m/s (Golder Associates, 1993c). Both the materials met the National Rivers Authority (NRA) guideline of $<1 \times 10^{-8}$ m/s for an acceptable lining material (Golder Associates, 1993b; Table 3.1).

The operational site can be divided into two areas. Phase I (20.1 ha) is active at present and Phase II (13.5 ha) is the proposed area for future development. Phase I is located to the south of the site. The southern face was filled, in an uncontrolled manner, during the early 1980s while Blaenau Gwent Borough Council ran the site. Phase IA is the present day active phase, which is working northward from this face. It is being run by Silent Valley Waste Services (SVWS) and is being infilled using the area method.

The leachate is collected through the drainage network at the base of the landfill and flows into a sump. The leachate and contaminated water is then pumped into the Settlement Tank. Water is discharged from here to foul sewer.

1.3 THESIS OUTLINE

Following the introduction, Chapter 2 reviews landfill practice in the United Kingdom, the legal framework surrounding landfills, leachate and landfill gas, and the hydrology/hydrogeology of landfill sites.

Silent Valley landfill site is described in Chapter 3. Descriptions of the site, the geology, hydrology, hydrogeology, site history and the present site operating conditions are given.

Chapter 4 reviews the site investigations and resistivity surveys that have been performed at Silent Valley landfill site to help improve the understanding of the internal structure of the landfill. The chapter concludes by using the information presented in Chapters 3 and 4 to produce a Conceptual Site Model of the landfill site.

The hydro-metrology of the site is examined in Chapter 5. The flow and meteorological instrumentation installed at the Silent Valley landfill site are described and relationships between the rainfall and flow data are analysed. Water balance analysis is performed across the site for catchment areas given in previous consultancy reports and the current catchment area within the drainage network surrounding the site. This is used to identify if groundwater is entering the site or if leachate is entering the groundwater. Regression analysis is used to model the discharge of leachate from the measured meteorological data.

Chapter 6 presents results of an investigation of leachate geochemistry. Historical leachate analysis results of the basal drainage pipe where it emerges from the base of the landfill are discussed over the period from 1993 to the present. Details of the Ion Chromatography (IC) analysis performed on leachate exiting this pipe (LP1) and the Settlement Tank beyond, from which leachate is discharged to sewer, are given. These results are compared with the conductivity measurements from two installed sensors.

In Chapter 7 artificial neural networks are used to predict leachate discharges. Artificial neural networks have the advantage that they can be used where the form of the relationship between the variables involved is unknown. Feedforward backpropagation neural networks were constructed for Silent Valley¹ to produce a forecast of daily discharge for the Settlement Tank.

In Chapter 8, results of monitoring, regression-based modelling and the application of neural network analysis are discussed in the context of the landfill system, and an assessment is made of the significance and limitations of the results described.

Chapter 9 presents the main conclusions and recommendations arising from the study.

¹ Neural networks for Silent Valley landfill were built by Stuart Paris using data supplied by the author.

CHAPTER 2

RESEARCH CONTEXT

Since wastes have been produced the routes for its disposal have been landfilling, recycling and combustion. We produce around 400 million tonnes of waste in England and Wales each year. Industry, commerce and households produce 106 million tonnes of this waste. The remainder is made up of construction and demolition wastes, agricultural wastes, mining wastes, sewage sludge and dredged spoils (DoE, 2000).

Landfills play an important role in the disposal of waste. Most waste produced in England and Wales goes to landfill. Around 54% of commercial and industrial waste, and 83% of municipal waste is managed in this way (DoE, 2000). The quality of landfill design, according to technical, social and economic development, has improved dramatically over the last few decades.

This chapter reviews current landfill practice in the United Kingdom, the legal framework surrounding landfills, leachate and landfill gas, and the hydrology/hydrogeology of landfill sites.

2.1 LANDFILLS

In the past landfills were not engineered to the extent that they are today. An engineered landfill is a controlled method of waste disposal. The site of the landfill must be geologically, hydrologically, and environmentally suitable.

The most important requirement of a landfill is that it does not pollute or degrade its environment. This is achieved by careful siting and by proper design/construction.

2.1.1 WHAT IS A LANDFILL?

Article 2(g) of the Landfill Directive (99/31/EC) gives a definition of a landfill as “*a waste disposal site for the deposit of the waste onto or into land (i.e. underground), including:*

- *internal waste disposal sites (i.e. landfill where a producer of waste is carrying out its own waste disposal at the place of production), and*
- *a permanent site (i.e. more than one year) which is used for the temporary storage of waste,*

but excluding:

- *facilities where waste is unloaded in order to permit its preparation for further transport for recovery, treatment or disposal elsewhere, and*
- *storage of waste prior to recovery or treatment for a period less than three years as a general rule, or*
- *storage of waste prior to disposal for a period less than one year”.*

2.1.2 LANDFILL TYPES

The principles of landfill practice used have changed considerably since the 1970s. The various changes in design philosophy have developed in response to an increased understanding of landfill leachate, its behaviour and the risk to water.

2.1.2.1 “Dilute and Disperse” Sites

Sites constructed before the mid 1980s were commonly dilute and disperse sites, where there is little or no engineering of the site boundary. The leachate and the landfill gas produced during the lifetime of the landfill is released to the surrounding environment. The movement of leachate is allowed so that the leachate is diluted, reduced in toxicity and dispersed.

In 1980, the introduction of the EC Groundwater Directive (80/68/EEC) (see Section 2.2.1.4) caused a reassessment of the dilute and disperse principal.

Silent Valley landfill was designed on the dilute and disperse principal.

2.1.2.2 Engineered “Containment” Sites

Engineered containment sites developed extensively in the UK since the early 1980s. The majority of UK landfills are now designed as containment landfills. A liner material contains the leachate within the landfill site boundary. The degradation processes take place within the landfill mass until stabilisation is complete. The leachate and landfill gas are collected and treated.

Phase II of Silent Valley Landfill will be designed as a containment landfill.

2.1.2.3 “Flushing Bioreactor” Site

The design and development of the flushing bioreactor landfill site in the UK is driven by the strategy of sustainable waste management. The strategy requires that waste should be dealt with by the present generation and not be left for future generations to deal with. The aim is to maximise waste degradation by the recirculation of water and/or leachate in order to stabilise waste degradation within one generation (i.e. 30 to 50 years). Although several sites within England and Wales operate leachate recirculation, no sites of this type had been constructed by the end of the 1990s (Environment Agency, 2001).

2.1.3 SITE SELECTION

Some of the factors that must be considered when siting a landfill include:

1. proximity to waste generators
 - transport costs
2. availability of transportation systems for moving waste to the site
 - transport costs
 - road network
3. available land area
 - site ownership
 - rights of way
 - proximity to property
 - void space available
4. site access
 - road networks
5. site conditions and topography
6. climatic conditions
 - rain
 - wind (on very windy days tipping may not be possible)
7. surface water hydrology

- potential for flooding
8. geology and hydrogeology
 - geological structure (e.g. folds, faults, fractures)
 - history of mining activity
 - slope stability
 - minerals availability and suitability for use on site (e.g. daily cover)
 - movement and utilisation of groundwater in the vicinity
 9. proximity of airports
 - bird strike
 10. land use
 - present and in the future
 11. impacts on the local community
 - visual
 - noise
 - odour/air quality
 - traffic
 12. ultimate use for completed landfill.

The research reported in this thesis relates to factors 6 to 8 for the Silent Valley landfill in the south Wales valleys. The significance of climatic inputs and geological conditions in this unlined landfill are investigated in detail with particular reference to leachate management and control.

2.1.4 LANDFILL DESIGN STAGES

Landfill design should follow a staged approach, which can be broadly divided into three key stages:

- Conceptual stage

The designer will be principally concerned with the feasibility and viability of the site, which will result in a notional model for the development of the site, giving

approximate volumes, possible design features and proposals for afteruse and setting out the principal aspects for clarification or investigation of subsequent stages.

- Main design stage

At this stage a detailed site investigation and assessment of environmental issues should be carried out. This should lead to a design for the overall construction, operation and restoration of the site.

- Construction design stage

When the site progresses to construction, the main design should be developed into a fully documented construction design with sufficient detail, specification and contract documentation to permit construction. The construction design is likely to be carried out on a number of occasions during the site's life and should be periodically reviewed (DoE, 1995).

Design objectives for a landfill must run consistently through the design, preparation, operation, restoration and aftercare stages. Key objectives for all sites include:

- Environmental protection

The requirements of environmental protection should be determined by risk assessment.

- Physical acceptability

The site must be acceptable in relation to its former use and in the context of the surrounding land use.

- Longevity

- Appropriateness

The design must be appropriate to the location, waste type, receptors at risk, intended method of operation and proposed restoration and afteruse.

- Cost effectiveness

2.1.5 LANDFILL DESIGN COMPONENTS

In modern landfill design, the landfill envelope is the most important consideration. It encapsulates the waste and isolates it from the surrounding environment. It should prevent escape of leachate, limit rainfall infiltration, and handle gas generation. The main components of the envelope are the liner system, leachate collection and removal system, gas collection and control system, and final cover system (Fig. 2.1).

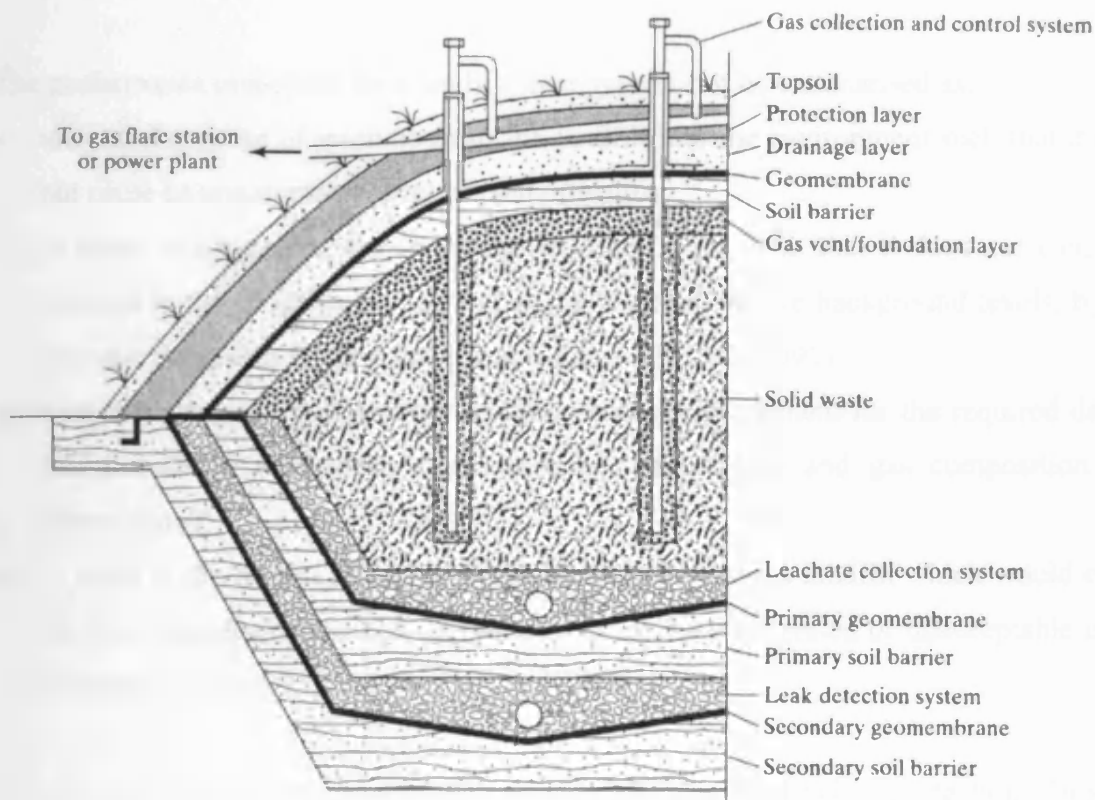


Figure 2.1 Schematic diagram of a municipal solid waste landfill containment system. From Qian *et al* (2002).

2.1.5.1 Liner Systems

The liner system is placed on the bottom and up the sides of the landfill. The selection of a liner system is determined on a site specific basis, with the initial selection process involving a risk assessment.

The protection of groundwater from unacceptable impact from landfill leachates is one of the principal objectives of modern landfills, and is increasingly satisfied by the provision of high specification low permeability liners which assist the management of landfill leachate.

The performance objectives for a landfill liner system can be summarised as:

- to control seepage of leachate from the landfill into the environment such that it does not cause an unacceptable level of contamination
- to assist in controlling the migration of landfill gas such that it does not cause an increase in the concentration of soil gases, over and above background levels, by the amounts defined in Waste Management Paper 27 (DoE, 1991)
- to retain consistent performance in its operating environment for the required design life and to be compatible with the expected leachate and gas composition and temperature
- to assist in the control of any groundwater ingress into the landfill which would cause an unmanageable increase in the volume of leachate generated or unacceptable uplift pressures (DoE, 1995).

A liner system should not rely on the provision of only one level of protection. In some circumstances the ground conditions under the site may provide some protection in terms of naturally low permeability, or attenuation/dilution of any seepage from the site. The level of protection required will be based on risk assessment.

Liner systems should, in addition to the property of low permeability, be robust, durable, and resistant to chemical attack, puncture and rupture.

A landfill liner system may comprise a combination of barriers and fluid collection layers, plus mineral or synthetic components acting as separation or protection. Landfill liners are typically overlain by a leachate collection system (LCS) with appropriate separation/protection layer and where necessary can be underlain by a groundwater collection system (GCS), again with an appropriate separation/protection layer. The drainage layers use either granular materials with geotextiles, or geonets.

Appropriate liner protection must be provided. Mineral liners are susceptible to erosion, weathering, desiccation and penetration. Geomembranes are susceptible to puncture and stress. A variety of granular materials and geotextiles can be used.

2.1.5.1.1 Single Liner System

The single liner system has a single primary barrier. It is typically only used in low vulnerability situations. It is commonly made from clay, bentonite enhanced soil or hydraulic asphalt (commonly used in dam construction).

2.1.5.1.2 Composite Liner System

Composite liners generally comprise of two or more barriers placed in contact with each other. It combines the advantages of two different materials with different physical and hydraulic properties. The performance of these barriers in combination is greater than the sum of the individual components.

Typically, a primary geomembrane (flexible membrane line – FML) is placed above a secondary low permeability cohesive mineral barrier. The FML is placed in contact with the mineral liner to ensure that any flaws in the geomembrane will not lead to lateral migration along the interface between the two components.

2.1.5.1.3 Double Liner System

The double liner system includes primary and secondary barriers with an intermediate high-permeability drainage layer to monitor and remove liquids or gasses from between the barriers. In its most basic form, where geomembranes are used for the barriers, the double liner system is generally inferior to the composite liner in terms of performance and robustness.

2.1.5.1.4 Multiple Liner System

A multiple liner system represents a combination of the above. An inter-barrier drainage layer allows the monitoring and removal of any fluids that may seep from the landfill, as in the double liner system. A composite liner is used for the primary or secondary barriers or both. This system combines the containment ability and robustness of a composite liner with the monitoring and recoverability that a double liner system offers.

2.1.5.2 Liner Materials

Clay (natural and reworked) or bentonite enhanced soils (BES) are commonly used in landfill engineering. Five major types of geosynthetic products that are used in landfill engineering are (Qian *et al*, 2002):

- geomembranes
- geosynthetic clay liners
- geonets
- geotextiles
- geogrids

2.1.5.2.1 Clay Liners

Where suitable low permeability clay materials are available, either on-site or locally, these generally provide the lowest cost lining material. A typical specification is that the material should be placed and compacted in layers to form a homogeneous layer with a total thickness no less than 1000 mm with a hydraulic conductivity no greater than 1×10^{-9} m/s (Qian *et al*, 2002).

Where naturally occurring soils do not contain enough clay to achieve the desired permeability, bentonite can be added to improve their permeability. Bentonite enhanced soils (BES) work by the swelling of the bentonite particles on hydration, which forces the hydrated bentonite around the soil particles to produce a synthetic clay. The maximum coefficient of permeability of BEH is frequently specified as 1×10^{-10} m/s (Qian *et al*, 2002).

2.1.5.2.2 Geomembranes

Geomembranes (also known as flexible membrane liner or FML) are relatively thin sheets of flexible thermoplastic or thermoset polymeric materials. They are manufactured and prefabricated at a factory and transported to site. They are placed directly on the subgrade or another geosynthetic material and seamed.

Geomembranes are made of one or more polymers along with a variety of other ingredients such as carbon black, pigments, fillers, plasticizers, processing aids, crosslinking chemicals, antidegradants and biocides. The polymers used include a wide range of plastics and rubbers differing in properties such as chemical resistance and tensile strength. The polymeric materials may be categorised as follows:

- Semicrystalline thermoplastic
such as high density polyethylene (HDPE), linear low-density polyethylene (LLDPE), very low density polyethylene (VLDPE), and flexible polypropylene (fPP)
- Thermoplastics

such as polyvinyl chloride (PVC)

- Thermoplastic elastomers

such as chlorosulfonated polyethylene (CSPE) (Qian *et al*, 2002).

The recommended minimum thickness for all geomembranes is 0.75 mm, with the exception of HDPE, which should be at least 1.5 mm to allow for extrusion seaming (Qian *et al*, 2002).

For an intact geomembrane the transfer of moisture across the membrane occurs by diffusion and the rates are extremely low. Diffusion values related to permeability values range from 0.5×10^{-10} cm/s to 0.5×10^{-13} cm/s (Qian *et al*, 2002). This is 10^3 to 10^6 times lower in permeability than required for a clay liner.

Both HDPE and LLDPE can be made with textured surfaces. They can be made on one or both sides of the geomembrane. The textured surface greatly improves slope stability by increasing interface friction between the geomembrane and soils, geotextiles and other geosynthetics. HDPE is the most widely used geomembrane in waste management. It is the most chemically resistant of all geomembranes, has a very low permeability, has excellent resistance to ultraviolet degradation and is available in many thicknesses and as smooth and textured styles. It can be used for landfill liners (primary and secondary), landfill caps, lagoon liners, wastewater treatment facilities etc.

2.1.5.2.3 Geosynthetic Clay Liners

Geosynthetic clay liners (GCL) are a combination of bentonite with geotextiles. At present there are four types:

1. Geotextile-encased, adhesive-bonded GCL (Fig. 2.2a)

A non-reinforced GCL with two light woven or nonwoven geotextiles encapsulating a bentonite layer.

2. Geotextile-encased, stitch-bonded GCL (Fig. 2.2b)

A layer of bentonite is encapsulated between two woven or nonwoven geotextiles that are stitched together with parallel rows of stitches. The stitch-bonding of the encapsulating geotextiles increases the internal strength.

3. Geotextile-encased, needle-punched GCL (Fig. 2.2c)

A layer of bentonite is encapsulated between two woven or nonwoven geotextiles that are needle-punched together. The internal matrix of bentonite and needle-punched fibres provides high internal shear strength.

4. Geomembrane-supported, adhesive-bonded GCL (Fig. 2.2d)

This is a bentonite-geomembrane composite GCL. The geomembrane can be any type (usually HDPE or LLDPE), of any thickness, and either rough or textured. It can be installed with the geomembrane side facing up or down.

Geosynthetic clay liners are manufactured in continuous sheets. They are installed by unrolling and overlapping the edges, which self-seal when the bentonite hydrates.

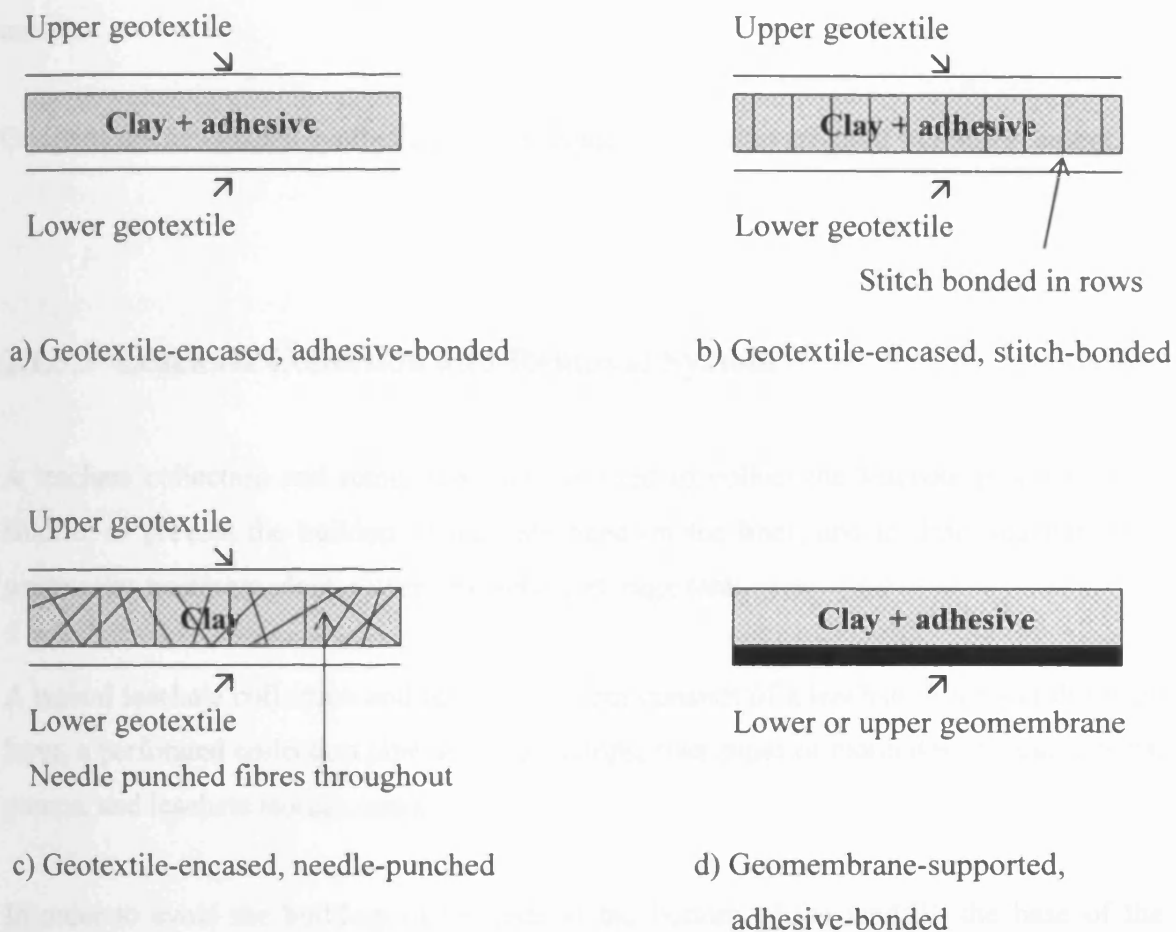


Figure 2.2 Four types of geosynthetic clay liner. After Qian *et al* (2002).

2.1.5.2.4 Geotextile, Geonets & Geogrids

Geotextiles consist of polymeric fibres made into woven or unwoven textile sheets. The primary functions of geotextiles are separation, reinforcement, filtration, and drainage.

Geonets are formed from polyethylene and are unitised sets of repeating parallel ribs positioned in layers such that liquid can be transmitted within their open spaces. Geonets are used almost exclusively for their drainage capability. They are always covered with a geomembrane or geotextile on their upper and lower surfaces because if they were in

direct contact with the soil, soil particles would fill the apertures of the geonet rendering it useless.

Geogrids are net-shaped synthetic polymer-coated fibres that are used in reinforcement.

2.1.5.3 Leachate Collection and Removal System

A leachate collection and removal system is used to collect the leachate produced in a landfill, to prevent the buildup of leachate head on the liner, and to drain leachate to a wastewater treatment plant, sewer or leachate storage tank.

A typical leachate collection and removal system consists of a leachate filter and drainage layer, a perforated collection pipe network, sumps, riser pipes or manholes, cleanout ports, pumps, and leachate storage tanks.

In order to avoid the build-up of leachate at the bottom of the landfill, the base of the landfill should be graded so that the leachate can flow under gravity to low points for collection.

2.1.5.4 Gas Collection and Control System

The gas collection and control system is used to collect the landfill gas, which can either be used to produce energy or flared under controlled conditions. There are different systems that can be used to collect landfill gas:

- Passive gas collection system
- Active gas collection system

Passive gas collection systems allow gas to be released without the use of mechanical devices. Trenches and perforated pipes can be used to intercept the migration of gas

through the soil and vent it to the atmosphere. Passive gas collection systems are relatively inexpensive and require little maintenance. However, due to the shallow construction of these vents, the effectiveness of the vent for collecting gas is limited.

Most active gas collection systems use negative pressure and apply a vacuum to pull gas out of the landfill via vertical extraction wells, horizontal extraction trenches, or venting layer beneath the cover barrier system. The gas collected must be treated before releasing to the atmosphere and this is commonly done through gas flaring or gas processing and energy recovery.

2.1.5.5 Final Cover System

The capping system is the final component in the construction of the landform, comprising of engineering and restoration layers.

The objectives of the engineering cap are to:

- contain the wastes
- manage leachate production by controlling the ingress of rain and surface water into the underlying waste
- prevent uncontrolled escape of landfill gas or the entry of air into the wastes
- provide protection for the emplaced wastes
- accommodate the environmental control measures (DoE, 1995).

The objective of the restoration layers is to enable the planned afteruse of the site.

The usual components within a final cover system are the surface or erosion control layer, protection layer, drainage layer, hydraulic barrier layer, gas collection layer (as required) and foundation layer (Fig. 2.3).

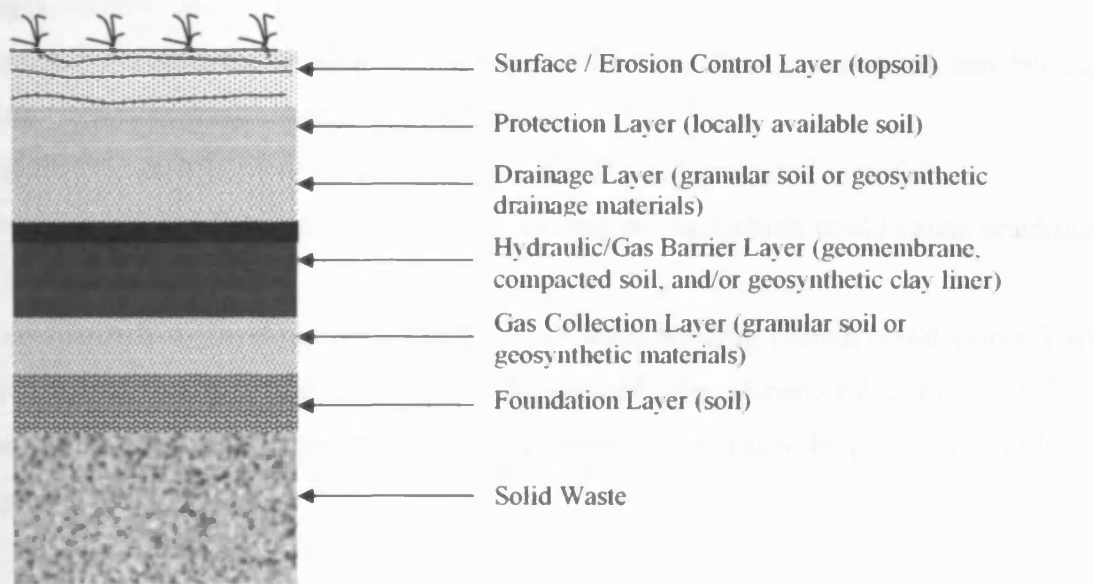


Figure 2.3 Typical layers of final cover systems for municipal solid waste (not to scale). After Qian *et al* (2002).

2.1.5.5.1 Surface Layer

Topsoil is commonly used for the surface layer. When vegetated it helps minimise erosion and promote transpiration of water back to the atmosphere. Vegetation also creates a leaf cover above the soil to reduce rainfall impact and decrease wind velocity on the soil surface. The minimum thickness of soil used is 150 mm.

2.1.5.5.2 Protection Layer

The protection layer lies directly beneath the surface layer, and in some cases is combined with it into a single “cover soil”. Locally available soil is most commonly used. The protection layer serves one or more of the following functions:

- store water that has infiltrated into the cover until it is later removed by evapotranspiration
- physically separate the underlying drainage and barrier layer components and buried waste from burrowing animals and plant roots
- minimise the possibility of human intrusion into the contaminated material
- protect underlying layers from excessive wetting/drying (which could cause cracking of fine-grained soils)
- protect underlying layers in the surface barrier from freezing (which could cause frost heave of underlying soils or cracking of fine-grained soils) (Koerner & Daniel, 1997).

The required thickness of the protection layer depends on what is to be protected and how much protection is needed.

2.1.5.5.3 Drainage Layer

Water that penetrates through the cover soil may be removed from the cover system using a drainage layer. It serves three principal functions:

- reduces head of liquid on the underlying barrier layer, thereby minimising the amount of water percolation into underlying layers, waste, or contaminated soil
- drains water from the overlying soil, allowing it to absorb and retain additional water
- eliminates pore water pressures at the interface to the underlying barrier layer (Koerner & Daniel, 1997).

The materials used in a drainage layer are sand or gravel, or geosynthetic materials. If constructed using granular materials, the layer should have a minimum thickness of 300 mm. Whether constructed out of granular or geosynthetic materials, the hydraulic conductivity of the drainage material should be no less than 1×10^{-2} cm/sec (hydraulic transmissivity no less than 3×10^{-5} m²/sec) at time of installation (Koerner & Daniel, 1997).

The drainage layer should be designed, constructed, and operated to function without excessive clogging over the lifetime of the facility.

2.1.5.5.4 Hydraulic/Gas Barrier Layer

The barrier layer is generally viewed as the most critical component of an engineered final cover system. It minimises percolation of water through the cover system directly by blocking water and indirectly by promoting storage or drainage of water in the overlying layers, where water is eventually removed by runoff, evapotranspiration, or internal drainage. The barrier layer also prevents landfill gases from escaping into the atmosphere, forcing it to migrate beneath it and so the barrier layer must be used in conjunction with an effective landfill gas venting or collection system to control lateral gas migration.

Site-specific and waste-specific conditions dictate the type and configuration of materials used as a barrier layer. The main materials used are:

- geomembranes (GMs)
- geosynthetic clay liners (GCLs)
- compacted clay liners (CCLs).

2.1.5.5.5 Gas Collection Layer

The gas collection layer may be constructed of sand, gravel, geonet, geotextile, geocomposite, or other gas-transmitting material. If natural soils are used, the layer should be a minimum of 300 mm thick. Gas is captured and flows into periodically-spaced collection pipes or vents. More details are given in section 2.1.5.4.

2.1.5.5.6 Foundation Layer

Depending on the type of waste being covered, the foundation layer can be the last lift of daily soil cover, a temporary soil cover, or a previously placed soil cover which does not meet regulatory standards.

2.1.6 LANDFILL MONITORING

Monitoring is a long-term commitment accompanying the development, operation and post-closure management of a landfill. Reasons for monitoring a landfill are:

- to meet the requirements of legislation
- to demonstrate that the landfill is performing as designed
- to provide reassurance that leachate controls are preventing pollution of the environment (by reference to a pre-established baseline)
- to indicate where further investigation is required and, where risks are unacceptable, the need for measures to prevent, reduce or remove pollution by leachate
- to identify where a site no longer presents a significant risk of pollution or harm to human health (to enable an application for surrender of a landfill permit).

Guidance on monitoring can be found in:

- Waste Management Papers (WMP) published by the Department of the Environment
 - WMP 4 Licensing of Waste Management Facilities, 1994
 - WMP 26A Landfill Completion, 1998
 - WMP 26B Landfill Design, Construction and Operational Practice (DoE, 1995)
 - WMP 26D Landfill Monitoring, 1996
 - WMP 27 Monitoring of Landfill Gas (DoE, 1991)
- Environment Agency documents
 - Regulation 15 Guidance, 1999
 - National Sampling Procedures Manual, 1998
 - Guidance on Monitoring of Landfill Leachate, Groundwater and Surface Water, 2001 (EA, 2001)
- National and international standards
 - Standing Committee of Analysts, 1996
 - ISO 5667: Water Quality Sampling

2.1.6.1 Leachate, Groundwater and Surface Water Monitoring

All water monitoring should be fit for the purpose of detecting any significant leakage or overspill of leachate. Effective water monitoring will provide early warning of water pollution and should allow corrective action to be taken in good time.

Monitoring of leachate, groundwater and surface water is undertaken to:

- define baseline water quality and physical conditions in surrounding groundwater and surface water
- allow assessment of compliance with site licence conditions
- provide confirmation that landfill engineering measures are controlling leachate as designed
- provide information about the processes occurring within the landfill site
- provide information on the state and rate of stabilisation of the waste body for comparison to the design lifetime of containment and monitoring systems
- provide an early warning of any departure from design conditions
- provide an early warning of breach of regulatory standards
- provide information to enable decisions on the management of the site to be taken
- to provide information to support an application for the certificate of completion (Environment Agency, 2001).

Typically the leachate level in a landfill site is measured once a week. Chemical analysis of the leachate composition is typically done monthly. A typical suite of determinands would include (North West Waste Disposal Officers, 1991):

- pH
- COD and or BOD/TOC
- Chloride
- Nitrite
- Sulphide
- Chromium
- Lead
- Zinc
- Conductivity
- Ammonia
- Nitrate
- Sulphate
- Cadmium
- Copper
- Nickel

The actual suite of determinands should be tailored to address the working controls and risks posed by the individual site. The leachate monitoring at Silent Valley will be discussed in Chapter 6.

2.1.6.2 Landfill Gas Monitoring

A monitoring programme's aim is to provide information to assess whether gas generation from wastes is likely to give rise to risk to public health or the environment, or a nuisance.

For sites without control measures, monitoring should be targeted at measuring for changes in gas evolution and migration patterns.

The frequency of monitoring required will be site specific, and will depend on:

- the age of the site
- the type and mix of waste
- the possible hazard or nuisance from gas escaping from the site
- the results of previous monitoring
- the control measures that have been or are to be installed
- the development surrounding the site
- the geology.

Site monitoring frequencies should be varied under certain conditions. They should be increased when:

- increases in gas quantity or changes in gas quality are found during routine off-site monitoring
- control systems are changed by landfill operations
- capping of part or all of the site takes place
- pumping of leachate ceases or starts or leachate levels rise within the wastes
- variations in weather occur when gas migration pathways can be changed significantly (eg when ground freezing is widespread)
- building development on or adjacent to the site takes place. Additional monitoring points may also be necessary if this occurs.

Waste Management Paper No. 27 (DoE, 1991) recommends that monitoring should continue until:

- the maximum concentration of flammable gas from biodegradation within the landfill remains less than 1% by volume (20/5 LEL) and the concentration of carbon dioxide from biodegradation within the landfill site remains less than 1.5% by volume measured in any monitoring point within the wastes over a 24 month period taken on at least four separate occasions, including two occasions when atmospheric pressure was falling and was below 1000 mb
- an examination of the waste using an appropriate statistical sampling method provides a 95% level of confidence that the biodegradable matter has been used up.

The monitoring strategy should be kept under regular review and subject to specialist appraisal. Waste Management Paper No. 27 (DoE, 1991) recommends that the interval of such assessment should not exceed 12 months.

2.2 REVIEW OF LANDFILL REGULATION

The UK's legislative regime concerning waste has evolved over many years. As a result, there are numerous Acts of Parliament that set out a regulatory system for waste management in the UK.

2.2.1 LEGAL FRAMEWORK

2.2.1.1 Control of Pollution Act 1974

The Control of Pollution Act 1974 (COPA 1974) covered waste on land (Part I), the pollution of water (Part II), noise (Part III), and pollution of the atmosphere (Part IV).

Part I (waste on land) of the Act introduced a system of licensing under which a waste disposal licence was required from the waste disposal authority (WDA) for the deposit of household, industrial or commercial waste, referred to generically as “controlled waste”.

2.2.1.2 Framework Directive on Waste

The Framework Directive on Waste 75/442 (later amended by Directive 91/156/EEC) established a general framework of controls for waste management. In accordance with the EC's general policies, it aimed to encourage the recovery of waste and its management at the point of production. The Directive also requires Member States of the EU to produce a National Waste Strategy setting out their policies on the disposal and recovery of waste.

2.2.1.3 Dangerous Substances Directive (76/464/EEC)

The Directive covered discharges to inland surface waters, territorial waters, inland coastal waters and ground water.

The Directive was the response to the need for general and simultaneous action by the Member States to protect the aquatic environment of the Community from pollution, particularly that caused by certain persistent, toxic and bioaccumulable substances. Two lists of substances, List I and List II, were established and listed in the Annex (see Section 2.2.3.1).

2.2.1.4 Groundwater Directive (80/68/EEC)

In 1980 the protection of groundwater was taken out of 76/464/EEC to be regulated under the separate Council Directive 80/68/EEC (Groundwater Directive) on the protection of groundwater against pollution caused by certain dangerous substances.

Transposition of the EC Groundwater Directive (80/68/EEC) was completed by the Groundwater Regulations 1998 (SI 1998 No. 2746) in England, Wales and Scotland.

2.2.1.5 Town and Country Planning Act 1990

The Town and Country Planning Act 1990 requires that all development, operational or a material change of use, requires planning permission.

2.2.1.6 Environmental Protection Act 1990

The Environmental Protection Act seeks *"to re-enact the provisions of the Control of Pollution Act 1974 relating to waste on land with modifications as respects the functions of the regulatory and other authorities concerned in the collection and disposal of waste and to make further provision in relation to such waste"*.

Part I of the Environmental Protection Act (EPA) 1990 deals with Integrated Pollution Control (IPC) and Local Air Pollution Control (LAPC).

Part II (waste on land) of the Environmental Protection Act (EPA) 1990 deals with:

- duty of care
- waste management licences
- collection, disposal or treatment of controlled waste
- Special waste and non-controlled waste
- Publicity
- Supervision and enforcement

Virtually all of Part I of COPA 1974 was repealed and replaced by Part II of EAP 1990. The waste on land provisions of Part II of EPA were brought into force progressively between 1991 and 1994.

The powers for a waste disposal authority to undertake waste disposal through its own operational landfill and other sites were removed by section 32 of EPA 1990.

The main changes by EAP 1990 to COPA 1974 were:

- The separation of regulatory and operational functions of the waste disposal authorities
- The extension of control to all types of handling of waste
- The imposition of a duty of care on all persons who produce, handle or dispose of waste
- Tighter control on transfer and surrender of licences
- The imposition of fees for applications for, and the subsistence of licences
- A requirement that a licence holder should be "fit and proper".

2.2.1.7 Water Resources Act 1991

Under the Water Resources Act 1991, the Environment Agency has the duty to monitor and protect controlled waters. Section 85 says that it is an offence to cause or knowingly permit pollution of controlled waters without appropriate authorisation. Section 88(1)(c) provides a defence if the discharge is made as a result of compliance with a waste management or disposal licence.

2.2.1.8 Waste Management Licensing Regulations 1994

The Waste Management Licensing Regulations 1994 (SI 1994 No. 1056) bring into force the waste management licensing system under Part II of the Environmental Protection Act 1990. It also implements the Framework Directive on Waste (91/156/EEC) by requiring that Waste Regulation Authorities take the Directive into account when drawing up their waste management plans.

2.2.1.9 Environment Act 1995

The Environment Act 1995 provides *“for the establishment of a body corporate to be known as the Environment Agency and a body corporate to be known as the Scottish Environment Protection Agency; to provide for the transfer of functions, property, rights and liabilities to those bodies and for the conferring of other functions on them”*.

The main provisions of the Environment Act 1995 are as follows:

- The creation of Environment Agencies
- The new contaminated land regime
- Protection of the Aquatic Environment
- Air quality management
- Producer responsibility

Part I of the Act sets up two new Environmental Agencies namely the Environment Agency (EA) (England and Wales), and the Scottish Environment Protection Agency (SEPA). The agencies encompass:

- The National Rivers Authority (England and Wales)
- The River Purification Authority (Scotland)
- The Waste Regulation Authorities
- Her Majesties Inspectorate of Pollution

The new contaminated land regime (Section 57) amends Part II of the Environmental Protection Act 1990 by introducing new provisions as regards contaminated land.

Section 93 of the Environment Act 1995 provides for the introduction of Regulation to impose obligations on the producers of materials or products to recycle, recover or re-use those products or materials.

2.2.1.10 Special Waste Regulations 1996

The Special Waste Regulations 1996 (SI 1996 No. 9727) came into force on 1 September 1996. The regulations were primarily introduced in order to transpose the Hazardous Waste Directive (91/689/EEC) into British law.

2.2.1.11 Landfill Tax Regulations 1996

The landfill tax became effective on 1st October 1996 and is levied on waste deposited in landfills. The objectives of the tax are to encourage waste producers to minimise the volume of waste generated, reduce the amount deposited in landfills and to encourage recycling.

Landfill operators are liable for the tax on all consignments of wastes accepted for landfill disposal. All landfill operators will add the cost of the tax on to any waste disposal charges to be paid by the customers or taxpayers.

Levies of £7 per tonne were introduced for active waste and £2 per tonne for inactive waste. The standard rate for active waste was raised to £10 per tonne from April 1999. In the March 1999 budget, the Chancellor announced that the standard rate would be subject to a landfill tax escalator of £1 per tonne per year for at least five years, reaching £15 per tonne in 2004. In the 2003 Budget the Government announced that the rate would increase to £18 per tonne in 2005-06 and by at least £3 per tonne in the years thereafter on the way to a medium-to-long-term rate of £35 per tonne. The lower rate, which applies to inactive waste disposed of to landfill, remains at £2 per tonne.

The tax is collected by HM Customs & Excise on a quarterly basis, but one fifth of the tax value may be reclaimed and donated to Environmental Bodies for projects satisfying set objectives. The scheme is overseen by ENTRUST.

2.2.1.12 Integrated Pollution Prevention and Control

The Integrated Pollution Prevention and Control (IPPC) Directive is about minimising pollution from various point sources throughout the European Union. All installations covered by Annex I of the Directive are required to obtain an authorisation (permit) from the authorities in the EU countries. Unless they have a permit, they are not allowed to operate. The permits must be based on the concept of Best Available Techniques (BAT), which is defined in Article 2 of the Directive.

The fifteen EU Member States had until the end of October 1999 to adjust their national legislation in line with the Directive. As from October 1999 the Directive applies to all new installations, as well as existing installations that intend to carry out changes that may have significant negative effects on human beings or the environment. As mentioned

above, the Directive does not immediately apply to other existing installations. These have been granted an additional 8 years of grace.

The IPPC Directive is designed to prevent, reduce and eliminate pollution at source through the efficient use of natural resources. It is intended to help industrial operators move towards greater environmental sustainability.

2.2.1.13 Pollution Prevention and Control (PPC)

The Pollution Prevention and Control Act 1999 and the subsequent Pollution Prevention Control (England and Wales) Regulations 2000 provide the replacement of Part 1 of the Environmental Protection Act 1990.

The Pollution Prevention and Control (PPC) Regulations 2000 are the UK enactment of the European Commission Directive 96/61 of Integrated Pollution Prevention and Control (IPPC), and the successor to the old Integrated Pollution Control (IPC) regulations.

2.2.1.14 Landfill Directive (99/31/EC)

The EC Landfill Directive (99/31/EC) was adopted in July 1999 and should have been implemented by 16 July 2001. The Directive aims *“by way of stringent operational and technical requirements on the waste and landfills, to provide for measures, procedures and guidance to prevent or reduce as far as possible negative effects on the environment, as well as any resulting risk to human health, from landfilling of waste, during the whole life-cycle of the landfill”* (Article 1).

The Directive requires that all landfills are classed as one of the following:

- landfill for hazardous waste

'hazardous waste' means any waste which is covered by Article 1(4) of Council Directive 91/689/EEC (Article 2, paragraph (c)).

The list identifying hazardous wastes is called the Hazardous Waste List (HWL) and is subject to constant review. The latest HWL is dictated by European Directive 2000/532/EC.

- landfill for non-hazardous waste

'non-hazardous waste means waste which is not covered by [Article 2] paragraph (c) (Article 2, paragraph (d)).

- landfill for inert waste. (Article 4)

'inert waste' means waste that does not undergo any significant physical, chemical or biological transformations. Inert waste will not dissolve, burn or otherwise physically or chemically react, biodegrade or adversely affect other matter with which it comes into contact in a way likely to give rise to environmental pollution or harm to human health. The total leachability and pollutant content of the waste and the ecotoxicity of the leachate must be insignificant and, in particular, do not endanger the quality or any surface water and/ or groundwater. (Article 2, paragraph (e))

It also states that the following wastes will not be accepted in a landfill:

- liquid waste;
- waste which is explosive, corrosive, oxidising, highly flammable or flammable;
- hospital or other clinical waste or infectious waste
- whole tyres (from 2003) and shredded tyres (from 2006)
- any other type of waste which does not fulfil the acceptance criteria determined in accordance with Annex II (Article 5).

Article 5 states that Member States shall set up a national strategy for the implementation of the reduction of biodegradable waste going to landfill by means of in particular, recycling, composting, biogas production or materials/energy recovery. The strategy must ensure that:

- by 2006 the amount of biodegradable municipal waste going to landfill must be reduced to 75% of the total amount (by weight) of biodegradable waste produced in 1995;

- by 2009 the amount of biodegradable municipal waste going to landfill must be reduced to 50% of the total amount (by weight) of biodegradable waste produced in 1995;
- by 2016 the amount of biodegradable municipal waste going to landfill must be reduced to 35% of the total amount (by weight) of biodegradable waste produced in 1995;

Member States that in 1995 put more than 80% of their collected municipal waste to landfill can postpone the attainment of the above targets by a period not exceeding four years. Because the UK is so dependent on landfill, it has been allowed the extra four years to meet the targets, giving the UK targets to reduce the biodegradable municipal waste going to landfill to:

- 75% of biodegradable waste produced in 1995 by 2010;
- 50% of biodegradable waste produced in 1995 by 2013;
- 35% of biodegradable waste produced in 1995 by 2020.

Article 6 specifies that:

- only waste that has been treated to reduce the quantity of the waste or the hazards to human health or the environment may be landfilled;
- only hazardous waste that fulfils the criteria set out in accordance with Annex II can be assigned to a hazardous landfill;
- landfill of non-hazardous waste may be used for:
 - municipal waste;
 - non-hazardous waste in accordance with criteria set out in Annex II;
 - stable, non-reactive hazardous wastes (e.g. solidifies, vitrified) which fulfil criteria in Annex II.
- inert waste landfill sites shall be used only for inert waste.

The Directive also covers landfill permits, waste acceptance procedures, control and monitoring procedures in the operational phase, closure and after-care procedures, procedures for existing landfills and the functions and activities of a Committee.

Annex I lays down general requirements for all classes of landfills covering:

- location;
- water control and leachate management;
- protection of soil and water;
- gas control;
- nuisances and hazards;
- stability;
- barriers.

Annex II covers waste acceptance criteria and procedures. It describes:

- general principals for acceptance of waste at various types of landfills;
- the general characterisation and testing of waste procedures based on a three-level hierarchy;
- guidelines for the acceptance of waste at the three major classes of landfill;
- sampling of waste.

Annex III outlines the control and monitoring procedures in operation and after-care phases. It details the:

- collection of meteorological data;
- monitoring leachate, surface water and gas;
- protection of groundwater through sampling, monitoring and setting trigger levels;
- landfill body topography.

2.2.1.15 Landfill (England and Wales) Regulations 2002

The Landfill Directive (99/31/EC) was adopted by the European Union in 1999 and was brought into force in the UK on 15 June 2002 as the Landfill (England and Wales) Regulations 2002.

Landfill sites “closed” before 16 July 2001 are not affected by the Landfill Regulations and can continue to be subject to their licence until the Environment Agency accepts its

surrender under Part II of the EPA 1990. Sites closed between 16 July 2001 and 16 July 2002 will need to meet the Landfill Regulation requirements on closure.

All new landfill sites (permitted after 16 July 2001) must comply with the full requirements of the Landfill Directive.

Existing landfills (granted a permit before July 2001) that wished to continue operating after 16 July 2002 were required to submit a “Conditioning Plan” to the Environment Agency by 16 July 2002. This set out how the landfill intended to comply with the Regulations. The site would have decided whether it was going to operate as a hazardous, non-hazardous or inert site. Following submission, the plans were assessed and prioritised against a standard set of criteria by the Environment Agency’s Conditioning Plan Assessment Centre. Once the Environment Agency had assessed the plans it informed operators of the date (between 2003 and 2006) by which they need to apply for a PPC permit. These sites have a transitional period within which to comply with the requirements of the Directive, with the precise timing depending upon the agreed conditioning plan. Full compliance with the regulations must be by 31 March 2007 (Schedule 4).

2.2.2 ENVIRONMENT AGENCY

The Environment Agency took over responsibility, in England and Wales, of waste management administration from the waste regulation authorities in April 1996. The Scottish Environment Protection Agency (SEPA) took responsibility for Scotland. The Environment Agency has responsibility for the main regulatory functions in relation to waste management including the administration, supervision and enforcement of licensed activities. It is also responsible for the system of licensing waste carriers, special waste provisions, and the operation and enforcement of the duty of care.

2.2.3 CONSENTED DISCHARGES FROM LANDFILL SITES

The discharge to controlled waters of potentially polluting waters from landfill operations should be controlled by the terms of a discharge consent or other authorisation issued by the Environment Agency under the Water Resources Act 1991. All discharges are evaluated in relation to the quality of the effluent and receiving water.

2.2.3.1 List I and II Substances

“List I” substances were selected mainly on the basis of their toxicity, persistence, and bioaccumulation, with the exception of those which are biologically harmless or which are rapidly converted into substances which are biologically harmless.

“List II” substances have a deleterious effect on the aquatic environment, which can, however, be confined to a given area and which depend on the characteristics and location of the water into which they are discharged.

The Dangerous Substances Directive stated that pollution through the discharge of the various dangerous substances within List I must be eliminated, and that it is necessary to reduce water pollution caused by the substances within List II. Any discharge of these substances should be subject to prior authorisation which specifies emission standards.

Under the Groundwater Directive, implemented by Regulation 15, List I substances should not be discharged directly to the saturated zone, and the release of List II substances should be controlled so that there is no pollution to groundwater. Similar controls on discharges to surface waters are provided for within the EC Dangerous Substances Directive for List I (“Black List”) and List II (“Grey List”) substances.

2.2.3.2 Discharge to Sewer

The discharge of leachate to foul sewer requires authorisation by way of a Trade Effluent Consent or Agreement. The appropriate water utility may grant these. Discharges of specific “Red List” substances to sewer can not be authorised without prior approval of the Environment Agency. Most “Red List” substances are also List I substances.

Silent Valley landfill has a consent to discharge to foul sewer. The leachate is then treated by Welsh Water.

2.2.4 INTERNATIONAL CONTEXT

In the United States, under the Resource Conservation and Recovery Act (RCRA), landfills that accept MSW are primarily regulated by state, tribal, and local governments. The Environmental Protection Agency (EPA), however, has established national standards that these landfills must meet in order to stay open. EPA regulates how hazardous wastes are managed and disposed under a program known as the Land Disposal Restrictions (LDR) program. The number of landfills in the United States is steadily decreasing with numbers falling from 8,000 in 1988 to 1,767 in 2002 (figures from EAP website <http://www.epa.gov/epaoswer/non-hw/muncpl/facts.htm>). The capacity, however, has remained relatively constant with new landfills much larger than those in the past.

In both the United States and European Union current legislation demands that landfill sites are engineered to minimise ingress or egress of groundwater and leachate. The precise engineering strategy may vary, but increasingly landfill sites are isolated from the surrounding environment by artificial barriers, lining systems and caps. However, in many countries there remains a large number of residual unlined landfills with the potential to generate leachate for many decades to come. The case study presented in this dissertation provides a detailed analysis of leachate generation in a still active unlined landfill and develops methodologies to model leachate quality and volume. It is hoped

that methodologies and approaches developed here may be adopted elsewhere in order that the potential environmental effects of unlined landfills (active and closed) may be better predicted and understood.

2.3 LANDFILLS IN WALES

In 2000 the Environment Agency produced ten Strategic Waste Management Assessment (SWMA) reports, with nine covering the planning regions of England and a single report for Wales. The Strategic Waste Management Assessment reports provide local information about the amounts and types of wastes produced and how that waste is managed. The following information in this section comes from this report.

The report divides Wales into seven sub-regions (Fig. 2.4) because some of the key datasets cannot be broken down to local authority level with sufficient confidence. Blaenau Gwent is in sub-region South Wales-East.

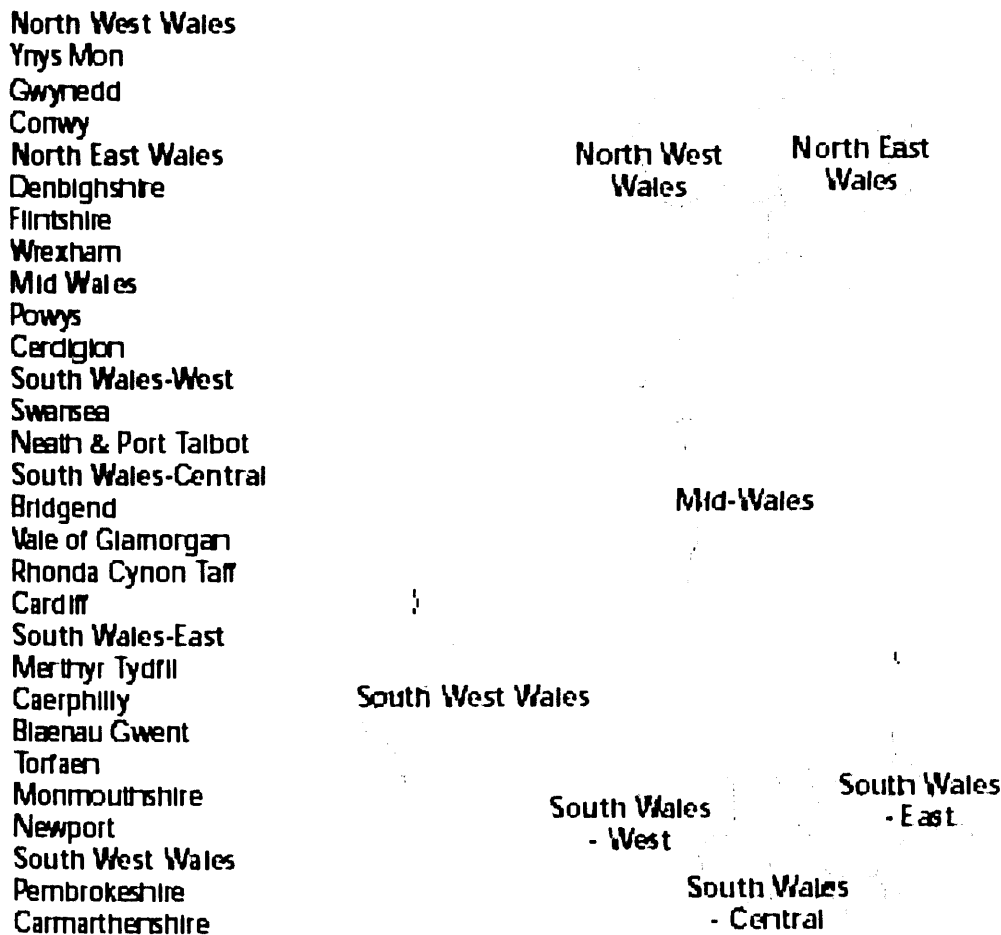


Figure 2.4 Map showing how data from unitary authorities have been grouped together into seven sub-regions for Wales. From Environment Agency (2000).

2.3.1 WASTE MANAGEMENT FACILITIES

As of March 1999 there were 351 licensed waste management facilities operating in Wales (Table 2.1). Half of these are located in the three sub-regions in south Wales. Excluding the 63 civic amenity sites, the remaining facilities are divided almost equally between landfills, treatment plants and transfer stations. Three quarters of the treatment facilities are metal recycling sites, the remainder are physical/chemical and biological treatment sites. More than half the open-gate landfill sites receive only inert and construction and demolition wastes and only nine are licensed for any special wastes other than asbestos.

	Landfills	Treatment	Transfer Stations	Civic Amenity Sites	TOTAL
North West Wales	15	3	9	12	39
North East Wales	11	15	27	14	67
Mid Wales	10	1	5	5	21
South West Wales	17	9	8	11	45
South Wales-West	12	10	14	13	49
South Wales-Central	14	9	17	19	59
South Wales-East	19	16	16	20	71
TOTAL	98	63	96	94	351

Table 2.1 Summary of licensed waste management facilities operating in Wales in March 1999. After Environment Agency (2000).

Around 16% of the waste managed in Wales received treatment of some sort. More than 80% of this originated from commerce or industry. Some of the waste which is being treated will be recovered for re-use or recycling but much of it goes on to final disposal at a landfill site after treatment. 1 million tonnes of waste was handled by licensed waste transfer facilities. Around a quarter of the municipal, industrial and commercial, and special wastes which were consigned to landfill was subject to transfer before disposal (on the assumption that imports/exports of such waste to and from Wales are negligible).

2.3.2 WASTE DISPOSAL

Some 7.0 million tonnes of waste were handled, treated or disposed of at licensed waste management sites in Wales in 1998-99. The 1998-99 dataset is the most up-to-date complete information available at present. Of the 4.4 million tonnes that were landfilled approximately 25% (1 million tonnes) was classified as inert and construction/demolition waste, 35% (1.5 million tonnes) as industrial and commercial waste and 35% (1.5 million tonnes) as municipal waste. Special waste accounted for 5% (0.2 million tonnes) of waste disposed to landfill in Wales.

The waste stream received at Silent Valley will be discussed in Section 3.6.4.1.

2.3.3 WASTE PRODUCTION

2.3.3.1 Municipal Solid Waste

Municipal waste typically accounts for 15% of the 'controlled' waste produced in an area. In Wales, around 955,700 tonnes (about two-thirds) of the municipal waste produced is collected from households by the local authority refuse collection, and 230,200 tonnes (about 16%) is taken by the public to civic amenity sites (Table 2.2). Other household collections, such as bulky waste, green waste, or a separate collection of recyclables amounts to 69,500 tonnes (around 5% of total).

In Wales 95% of all municipal solid waste goes to landfill, with around 5% going for recycling. No municipal waste is moved to England for disposal.

Sub-region	Collections				TOTAL
	Refuse Collection Vehicles	Other Household	Civic Amenity	Non Household	
North West Wales	108.6	15.8	11.2	13.0	148.6
North East Wales	110.8	6.7	50.7	17.7	185.9
Mid Wales	61.6	2.1	6.5	15.2	85.4
South West Wales	89.9	2.0	28.1	12.4	132.4
South Wales-West	112.6	5.5	34.1	47.5	199.7
South Wales-Central	270.6	20.1	50.3	36.1	377.1
South Wales-East	201.6	17.3	49.3	78.4	346.6
TOTAL	955.7	69.5	230.2	220.3	1475.7

Table 2.2 Amount (000s tonnes) and collection method of municipal solid waste produced in Wales. After Environment Agency (2000).

2.3.3.2 Industrial and Commercial Waste

Wales produced around 6 million tonnes of industrial and commercial waste in 1998/99 (Table 2.3). More than 80% came from industrial activities and less than 20% was produced by the commercial sector.

The proportion of waste produced by the industrial sector is higher than the national average because of the very large tonnage of minerals waste and residues (2.6 million tonnes; 53% of all the waste produced by industry in Wales) produced in the iron and steel and electricity generating industries. Around 11.5% of the region's industrial waste is classified as 'general industrial', and a further 7.5% is classed as 'other general and biodegradable'. 'Metals and scrap equipment' and 'chemical and other' wastes together account for around 15%, while 'paper and card' accounts for 3%, and 'food' just over 2%. 'Inert' and 'construction and demolition' each account for around 2.6%.

The commercial sector produces less than 20% of the region's waste and its waste is much less varied, more than 75% being reported as 'general commercial'. Most of the remainder (around 9.5%) is 'paper & card' and 'other general and biodegradable' waste at 7%.

Waste Type	Industry	Commerce	TOTAL	% England & Wales
Inert/C&D	129	9	138	5.8%
Paper & card	150	106	256	4.9%
Food	105	18	123	4.8%
General industrial & commercial	572	853	1,425	5.0%
Other general & biodegradable	370	80	450	5.1%
Metals & scrap equipment	393	22	415	8.7%
Contaminated general	198	33	231	5.8%
Mineral wastes & residues	2,654	1	2,655	20.7%
Chemical & other	418	19	437	7.4%
TOTAL	4,989	1,141	6,130	8.2%

Table 2.3 Amount (000s tonnes) and composition of industrial and commercial waste produced in Wales for 1998-99. After Environment Agency (2000).

The National Waste Production Survey indicated that 6% of industrial waste and 3% of commercial waste produced in 1998-99 in Wales was 'special'.

The waste management methods used for both industrial and commercial waste are predominantly land disposal (landfill) and recycling and re-use. The industrial sector also makes significant use of treatment in managing its wastes.

The form in which the waste is produced has a significant impact on the method of recovery or disposal adopted. In Wales, nearly 5.5 million tonnes was solid, around 215,000 tonnes was liquid, with only 175,000 tonnes sludge and 134,000 tonnes mixed (Fig. 2.5). Solid waste was predominantly disposed of to landfill or recycled/re-used (showing again the influence of the 'mineral wastes and residues' waste stream) whereas liquid waste was much more likely to receive some form of treatment.

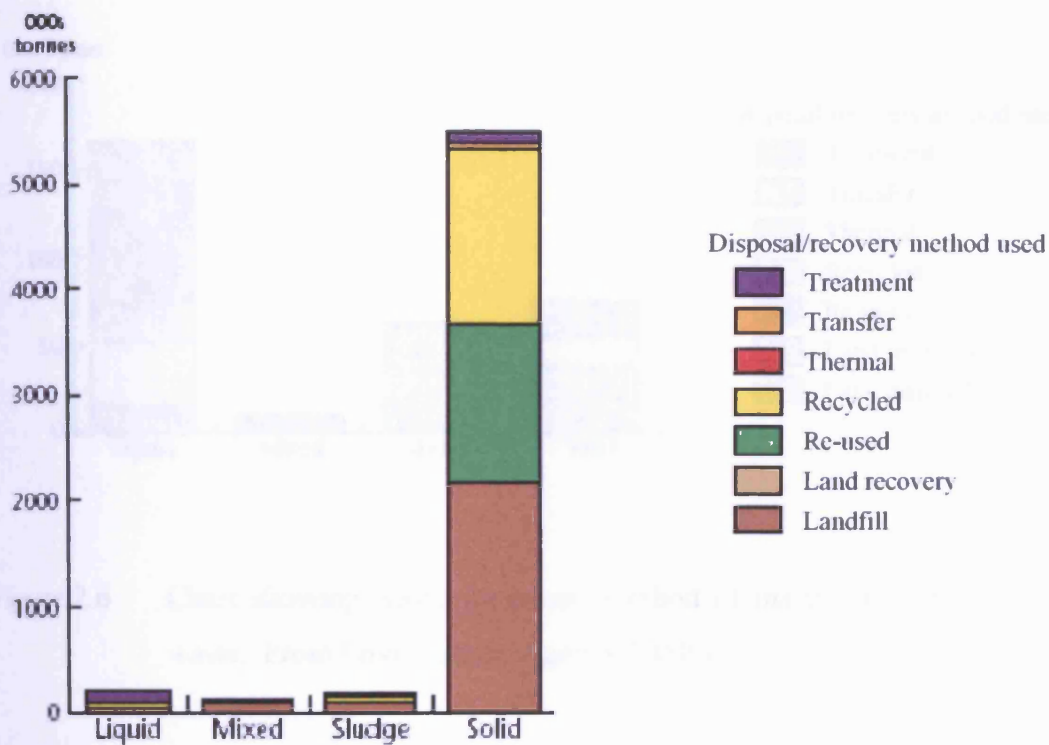


Figure 2.5 Chart showing waste form and method of disposal or recovery. From Environment Agency (2000).

2.3.3.3 Special Waste

Overall, Wales produced 8.5% of the total special waste for England and Wales. Production of special waste in Wales was dominated by the three sub-regions in the south which between them produced three-quarters of the special waste.

The physical form of special waste is different from other wastes, where solids predominate. For special waste liquids form 50%, sludges a further 20%, with solids just one quarter of the total (Fig. 2.6).

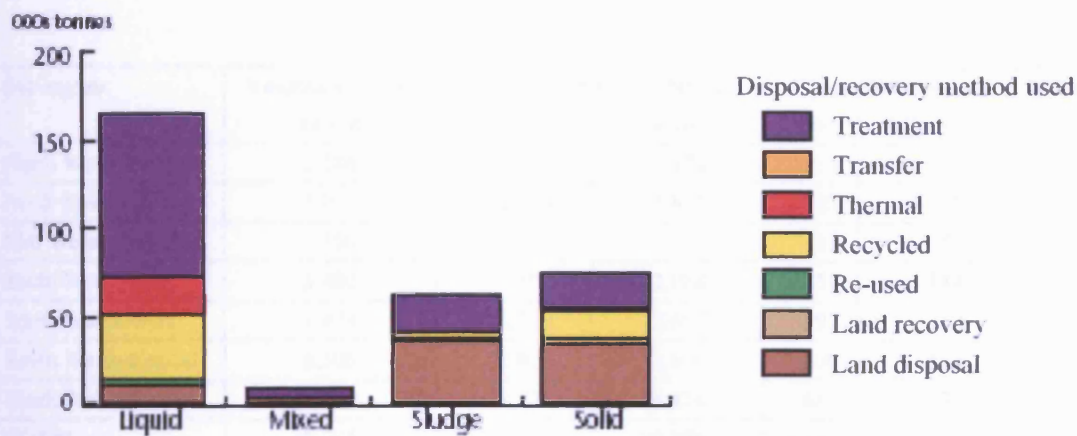


Figure 2.6 Chart showing waste form and method of management used for special waste. From Environment Agency (2000).

A substantial proportion (almost 100,000 tonnes of liquids and more than 40,000 tonnes of solids and sludges) of special wastes were treated. Only a small proportion (12,000 tonnes) of liquid special wastes were landfilled and overall only one quarter of all forms was disposed of to landfill. Almost 20% of special waste was recycled and just less than 10% was subject to thermal treatment (mostly liquids).

2.3.4 REMAINING LANDFILL CAPACITY

Estimates of voidspace and the operational life for landfills licensed for household, industrial and commercial waste (including those that take special waste) for each sub-region of Wales are shown in table 2.4.

Wales has around 34 million m³ of disposal capacity for biodegradable waste with the largest remaining voidspace in South Wales-East, South Wales-Central and North West Wales.

Sub-region	Voidspace 1/4/99 (000s m ³)	Capacity 1998-99 (000s m ³)		Inputs (000s tonnes)		Life expectancy years
		cap/cover	waste	all	degradable	
North West Wales	5,286	2,114	3,172	361	239	11
North East Wales	3,059	1,224	1,835	703	480	3.2
Mid Wales	350	140	210	91	57	3.1
South West Wales	3,480	1,392	2,088	252	184	9.5
South Wales-West	4,429	1,772	2,657	597	452	4.9
South Wales-Central	6,500	2,600	3,900	800	532	6.1
South Wales-East	10,690	4,276	6,414	881	699	7.6
TOTAL	33,794	13,518	20,276	3,685	2643	6.4

Table 2.4 Voidspace deposits and remaining capacity at landfill sites licensed for biodegradable waste. After Environment Agency (2000).

2.4 REVIEW OF NATURE AND EVOLUTION OF MIXED WASTE LANDFILLS

2.4.1 WASTE

Section 75(2) of the Environmental Protection Act 1990 gives the definition of “waste” to include:

- “(a) any substance which constitutes a scrap material or an effluent or other unwanted surplus substance arising from the application of any process; and*
- (b) any substance or article which requires to be disposed of as being broken, worn out, contaminated or otherwise spoiled;*

but does not include a substance which is an explosive within the meaning of the [1875 c. 17.] Explosives Act 1875.”

It also states (section 75(3)) that *“any thing which is discarded or otherwise dealt with as if it were waste shall be presumed to be waste unless the contrary is proved”*. Thus, material will still be classed as waste even where it has value to other persons, such as recyclers, as it is the original holder's intention to discard that is relevant.

A definition for "Controlled waste" is given (section 75(4)) as meaning *“household, industrial and commercial waste or any such waste”* where,

- *“household waste” means waste from:*
 - (a) domestic property, that is to say, a building or self-contained part of a building which is used wholly for the purposes of living accommodation;*
 - (b) a caravan (as defined in section 29(1) of the [1960 c. 62.] Caravan Sites and Control of Development Act 1960) which usually and for the time being is situated on a caravan site (within the meaning of that Act);*
 - (c) a residential home;*
 - (d) premises forming part of a university or school or other educational establishment;*
 - (e) premises forming part of a hospital or nursing home. (Section 75(5))*
- *“industrial waste” means waste from any of the following premises:*

- (a) any factory (within the meaning of the [1961 c. 34.] Factories Act 1961);*
 - (b) any premises used for the purposes of, or in connection with, the provision to the public of transport services by land, water or air;*
 - (c) any premises used for the purposes of, or in connection with, the supply to the public of gas, water or electricity or the provision of sewerage services; or*
 - (d) any premises used for the purposes of, or in connection with, the provision to the public of postal or telecommunications services. (Section 75(6))*
- *"commercial waste" means waste from premises used wholly or mainly for the purposes of a trade or business or the purposes of sport, recreation or entertainment excluding:*
 - (a) household waste;*
 - (b) industrial waste;*
 - (c) waste from any mine or quarry and waste from premises used for agriculture within the meaning of the [1947 c. 48.] Agriculture Act 1947 or, in Scotland, the [1948 c. 45.] Agriculture (Scotland) Act 1948; and*
 - (d) waste of any other description prescribed by regulations made by the Secretary of State for the purposes of this paragraph." (Section 75(7))*

"Special waste" is controlled waste of any kind that *"is or may be so dangerous or difficult to treat, keep or dispose of that special provision is required for dealing with it"* (Section 62(1)).

In 1994 the Department of the Environment (DoE) announced its intention to repeal the existing definition of "waste" and to replace it with the definition which appears in the Framework Directive (75/442/EEC as amended by 91/156/EEC), so that *"waste shall mean any substance or object in the categories set out in Annex I which holder discards or intends is required to discard"*.

In the Waste Management Licensing Regulations 1994 (SI 1994 No. 1056) "waste" means "Directive waste" (reg 1(3)). *"Directive waste" means any substance or object in the categories set out in Part II of Schedule 4 which the producer or the person in possession of it discards or intends or is required to discard but with the exception of anything excluded from the scope of the Directive by Article 2 of the Directive."*

“For the purposes of all the provisions of Part I of the Act [EPA 1990], waste which is not Directive waste shall not be treated as household waste, industrial waste or commercial waste” (reg 22(3)).

The Landfill (England and Wales) Regulations 2002 use “waste” to mean “controlled waste” as given in section 75(4) of the Environmental Protection Act 1990. Other expressions used have the same meaning as in the Landfill Directive (99/31/EC).

2.4.2 LEACHATE

Landfill leachate is comprised of the soluble components of waste and the soluble intermediates and products of waste degradation which enter as it percolates through the waste body (Westlake, 1995).

Leachate may vary in colour from light brown to red (ochreous precipitates of iron hydroxide) to black (sulphide precipitation). It commonly has a sweetish or sickly odour (due to organic esters) but this may be masked by the rotten egg smell if sulphides are present. Some leachates exhibit an iridescent sheen on their surface (North West Disposal Officers, 1991).

2.4.2.1 Leachate Generation

The amount of leachate generated is dependent upon a number of factors which can be summarised as follows:

- Water availability

Factors affecting water availability include precipitation, surface run-off, groundwater intrusion, irrigation, liquid waste disposal and refuse decomposition.

- Landfill surface conditions

Surface conditions that may affect leachate generation include vegetation, cover material (density, permeability, moisture content etc.), surface topography and local meteorological conditions.

- Refuse state

The refuse state will affect the "field capacity" of the waste. The field capacity is defined as the maximum moisture content which a soil or a solid material can retain in a gravitational field without producing continuous downward percolation. The water content of the waste will be affected by the water content at emplacement, infiltration during landfill development, the waste composition and waste density.

- Conditions of surrounding strata

The condition of surrounding strata includes the ground characteristics and the level of the water table.

Measurements of each of the above can be used in the water balance equation (DoE, 1995) to assess likely leachate generation volumes.

$$L_o = [ER + LIW + IRA] - [LTP + aW + DL] \quad (1)$$

where: L_o = free leachate retained

ER = effective rainfall

LIW = liquid industrial waste

IRA = infiltration through restored and capped area

LTP = discharge of leachate off-site

a = unit absorptive capacity of wastes

W = weight of absorptive waste

DL = designed seepage

Parameters listed above may be measured on site or values typical for the region and the waste stream may be derived from published literature.

2.4.2.2 Leachate Composition

The composition of leachate depends on the stage of degradation and the type of waste within the landfill (Fig. 2.7). Degradation of the organic fraction of waste materials within a landfill may be divided into a five stage process (Fig. 2.8). Each stage of the process has an impact on the characteristics of the intermediate and final breakdown products and the quality and rate of leachate and landfill gas generation.

The first and fifth stage occur under aerobic conditions (in the presence of oxygen) whilst the remaining stages take place under predominantly anaerobic conditions (in the absence of oxygen). The following summary of the stages is adapted from Waste Management Paper 26B (DoE, 1995).

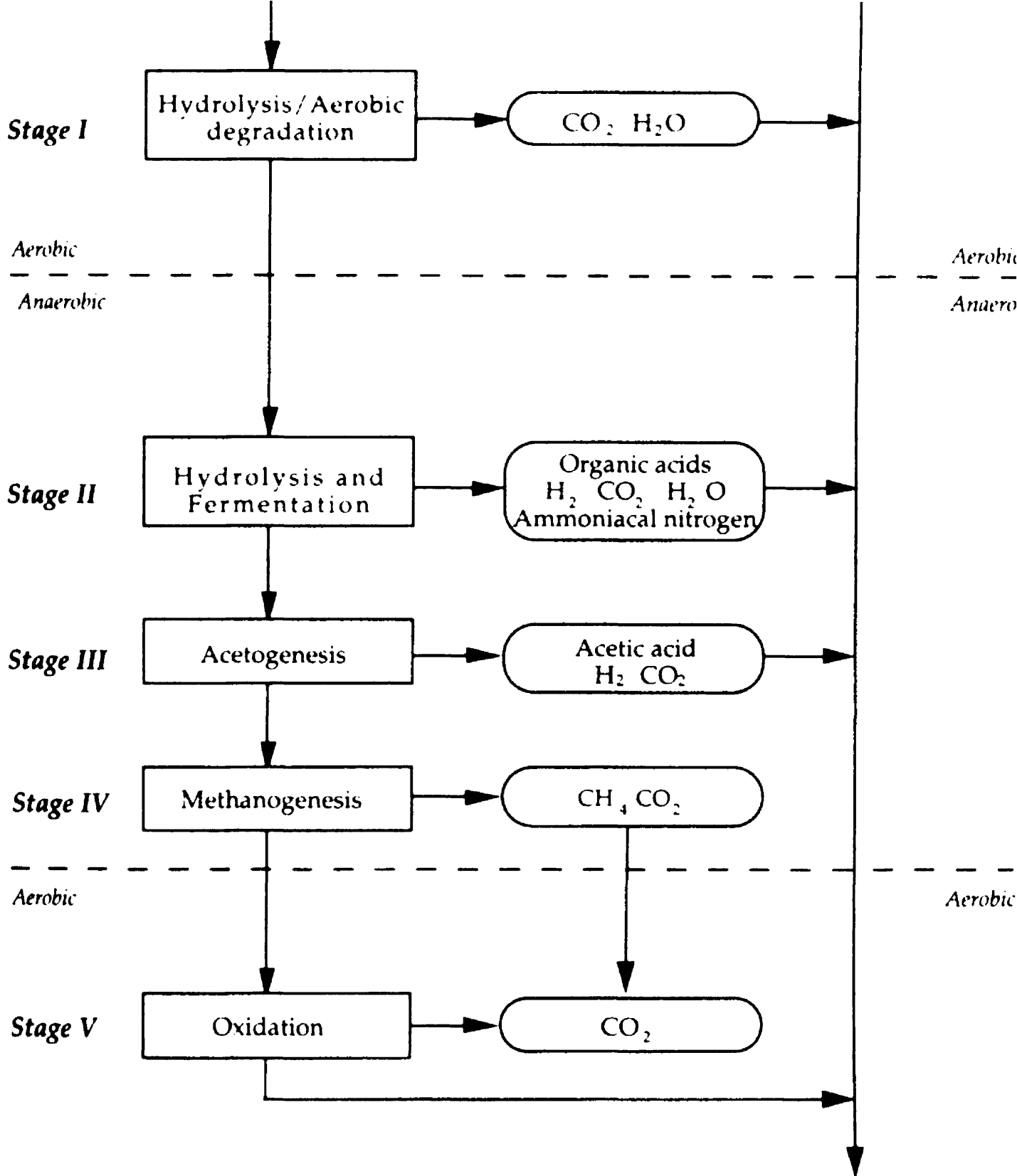


Figure 2.7 Major stages of waste degradation. From WMP26B (DoE, 1995).

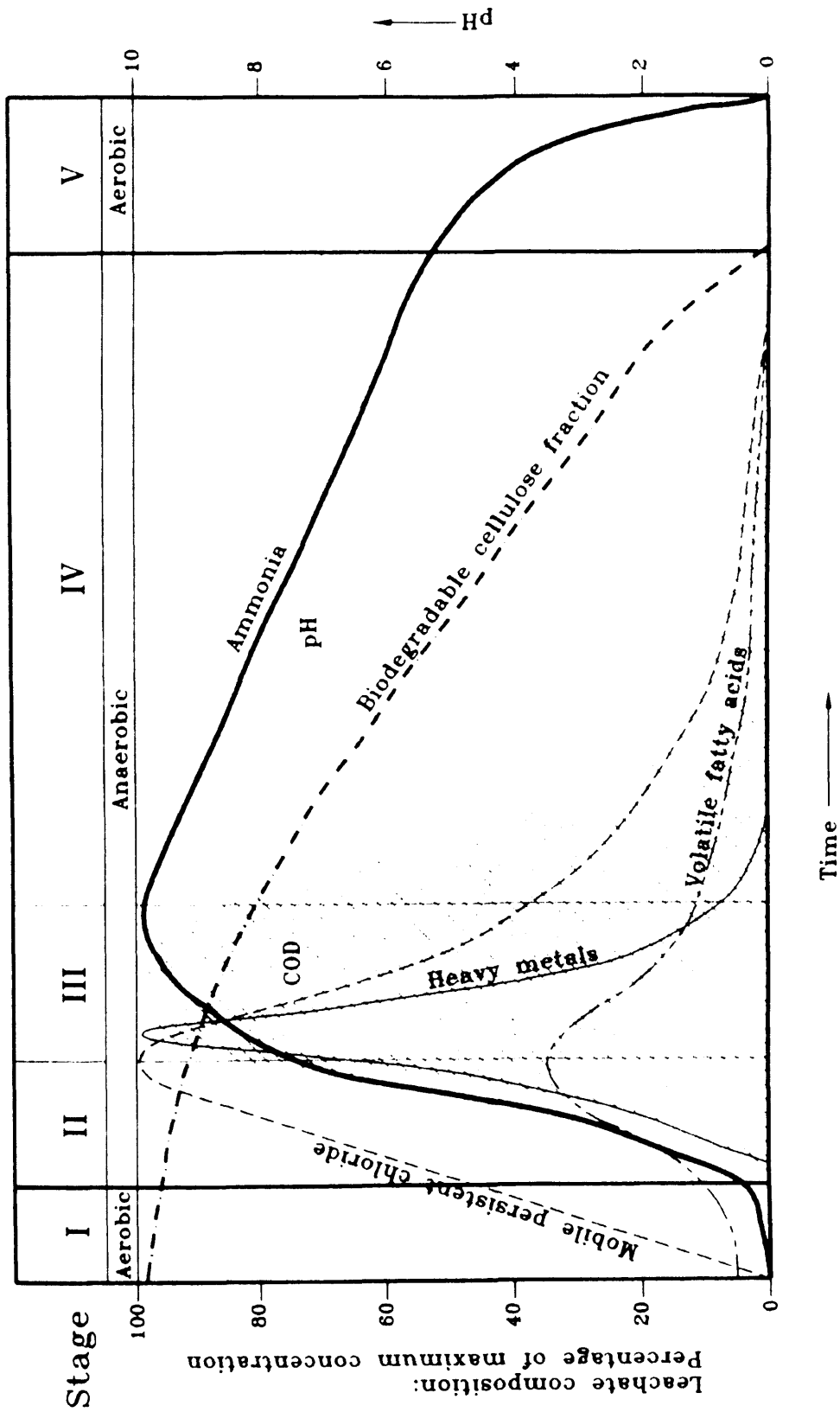


Figure 2.8 Graph showing changes in composition of leachate with time. From WMP26B (DoE, 1995).

Stage I – Hydrolysis/Aerobic Degradation

This first stage occurs both during and for a period after waste placement. A proportion of the organic fraction of waste is metabolised by aerobic micro-organisms present in the waste. The micro-organisms convert readily degradable carbohydrates to simple sugars such as glucose, carbon dioxide and water. During this stage the exothermic reaction from the intense microbiological activity can cause the temperature of the waste mass to rise to 80-90°C.

The duration of this aerobic stage depends on the availability of oxygen, which is influenced by management practices on site. As oxygen becomes depleted the aerobic micro-organisms are superseded by groups of micro-organisms which can tolerate low levels of oxygen (facultative anaerobes) and then, as the anaerobic conditions develop, the anaerobic micro-organisms gradually become established.

Stage II – Hydrolysis and Fermentation

In this stage the carbohydrates, lipids and proteins are hydrolysed to simple sugars and then fermented by bacteria to soluble intermediates (such as volatile acids), acetate, carbon dioxide, hydrogen and inorganic salts (such as sulphate and ammonium). During this stage, the nitrogen is displaced by carbon dioxide and hydrogen to form leachate with a high ammoniacal nitrogen content. The temperature within the landfill drops to 30-50°C.

Stage III – Acetogenesis

During this stage bacteria convert the soluble acids formed by the activities of the fermentative bacteria of the previous stage to acetate, carbon dioxide and hydrogen. Other bacteria convert carbohydrates, hydrogen and carbon dioxide to acetic acid. In a balanced system the gases predominately generated are carbon dioxide, hydrogen and methane.

Stage IV – Methanogenesis

In this stage the methane-generating bacteria (methanogens) metabolise acetate and formate produced during the other degradation stages to form methane and carbon dioxide. Some other methanogens may be able to generate methane by

direct conversion of hydrogen and carbon dioxide. Methanogens are most active in the pH range of 6.8-7.4.

A balanced relationship usually occurs between the hydrogen-producing fermentative bacteria of the acetogenic stage and the hydrogen-utilising methanogens. If the activity is not balanced then the breakdown intermediates of the acetogenic stage accumulate in a process known as acid-souring.

Stage V- Oxidation

In this stage as the degradable components are exhausted, progressive re-establishment of aerobic conditions can occur. As the prevailing conditions permit the landfill is recolonised by facultative aerobic and aerobic micro-organisms. This may release substances such as metals which were stable during preceding anaerobic conditions.

Within the whole landfill site, all the stages of degradation may be occurring at different rates at any one time. This is the result of different times of waste emplacement, differing biodegradabilities and spatial variability in the physical and chemical environment of the waste materials.

Stage I is usually short and no substantial leachate generation will take place. Leachates generated during stage II are characterised by high concentrations of volatile fatty acids, acidic pH, high BOD to COD ratio and high levels of ammoniacal nitrogen and organic nitrogen. Andreottola and Cannas (1992) suggest that pH values typically lie in the range 5-6, BOD₅ values are commonly greater than 10,000 mg/l, and BOD to COD ratios are commonly greater than 0.7.

During Phase III, sulphate concentrations decrease. The conversion of fatty acids causes an increase in pH values and alkalinity with a consequent decrease in the solubility of calcium, iron, manganese and heavy metals (Andreottola & Cannas, 1992). A study of the composition of 35 samples of acetogenic leachates (Table 2.5) was carried out by the Department of the Environment (1995).

During Phase IV, the composition of the leachate is characterised by almost neutral pH values, low concentrations of volatile acids and total dissolved solids, relatively low BOD values and low ratios of BOD/COD. A study of the composition of 29 samples of methanogenic leachates (Table 2.6) was carried out by the Department of the Environment (1995).

Comparing the leachate produced at Silent Valley with these leachate analysed by the Department of the Environment, the Silent Valley leachate is a weak leachate. Silent Valley leachate geochemistry will be discussed in Chapter 6.

Determinand	Samples	Minimum	Maximum	Median	Mean	SD
pH value	34	5.12	7.8	6.0	6.73	-
COD	35	2740	152000	23600	36817	32718
BOD ₅	29	2000	68000	14600	18632	15643
Ammoniacal-N	34	194	3610	582	922	802
chloride	34	659	4670	1490	1805	910
BOD ₂₀	13	2000	125000	14900	25108	32870
TOC	24	1010	29000	7800	12217	10028
Fatty acids (as C)	26	963	22414	5144	8197	6786
Alkalinity (as CaCO ₃)	24	2720	15870	5155	7251	4390
Conductivity (μS/cm)	28	5800	52000	13195	16921	11602
Nitrate-N	30	<0.2	18.0	0.7	1.80	3.41
Nitrite-N	25	0.01	1.4	0.1	0.20	0.30
Sulphate (as SO ₄)	24	<5	1560	608	676	549
Phosphate (as P)	21	0.6	22.6	3.3	5.0	5.47
Sodium	26	474	2400	1270	1371	631
Magnesium	28	25	820	400	384	196
Potassium	28	350	3100	900	1143	760
Calcium	31	270	6240	1600	2241	1656
Chromium	26	0.03	0.3	0.12	0.13	0.08
Manganese	26	1.4	164.0	22.95	32.94	37.29
Iron	32	48.3	2300	475	653.8	566.2
Nickel	24	<0.03	1.87	0.23	0.42	0.48
Copper	24	0.020	1.100	0.075	0.130	0.216
Zinc	34	0.09	140.0	6.85	17.37	29.56
Cadmium	24	<0.01	0.10	0.01	0.02	0.03
Lead	24	<0.04	0.65	0.30	0.28	0.16
Arsenic	19	<0.001	0.148	0.010	0.024	0.039
Mercury	15	<0.0001	0.0015	0.0003	0.0004	0.0004
Heavy metals	24	0.34	2.57	0.95	1.03	0.56

Results in mg/l except for pH value and conductivity

Heavy metals represents the sum of concentrations of chromium, nickel, copper, cadmium, lead, arsenic and mercury.

Table 2.5 Summary of composition of acetogenic leachates sampled from large landfills with a high waste input rate, relatively dry (35 samples in all). From WMP26B (DoE, 1995).

Determinand	Samples	Minimum	Maximum	Median	Mean	SD
pH value	29	6.8	8.2	7.35	7.52	-
COD	29	622	8000	1770	2307	1527
BOD ₅	29	97	1770	253	374	378
Ammoniacal-N	29	283	2040	902	889	396
chloride	29	570	4710	1950	2074	9870
BOD ₂₀	24	110	1900	391	544	459
TOC	29	184	2270	555	733	470
Fatty acids (as C)	29	<5	146	5	18	29
Alkalinity (as CaCO ₃)	29	3000	9130	5000	5376	1664
Conductivity (μS/cm)	25	5990	19300	10000	11502	3890
Nitrate-N	27	0.2	2.1	0.7	0.86	0.53
Nitrite-N	27	<0.01	1.3	0.09	0.17	0.26
Sulphate (as SO ₄)	16	<5	322	35	67	83
Phosphate (as P)	28	0.3	18.4	2.7	4.3	4.3
Sodium	29	474	3650	1400	1480	691
Magnesium	29	40	1580	166	250	308
Potassium	29	100	1580	791	854	387
Calcium	29	23	501	117	151	106
Chromium	28	<0.03	0.56	0.07	0.09	0.11
Manganese	29	0.04	3.59	0.30	0.46	0.66
Iron	29	1.6	160	15.3	27.4	32.8
Nickel	29	<0.03	0.60	0.14	0.17	0.13
Copper	27	<0.02	0.62	0.07	0.13	0.15
Zinc	29	0.03	6.7	0.78	1.14	1.30
Cadmium	27	<0.01	0.08	<0.01	0.015	0.02
Lead	27	<0.04	1.9	0.13	0.20	0.35
Arsenic	27	<0.001	0.485	0.009	0.034	0.093
Mercury	23	<0.0001	0.0008	<0.0001	0.0002	0.0002
Heavy metals	27	0.15	2.78	0.51	0.61	0.49

Results in mg/l except for pH value and conductivity

Heavy metals represents the sum of concentrations of chromium, nickel, copper, cadmium, lead, arsenic and mercury.

Table 2.6 Summary of composition of methanogenic leachates sampled from large landfills with a high waste input rate, relatively dry (29 samples in all). From WMP26B (DoE, 1995).

2.4.2.3 Environmental Effects of Leachate

The main environmental aspects of landfill leachate are the impacts on surface water quality and groundwater quality if leachate is discharging into them. North West Waste Disposal Officers (1991) state that the polluting potential of leachate can be of the order of 10 to 100 times that of crude sewage.

2.4.2.3.1 Surface Waters

The input of high strength organic leachate and inorganic solutions of metals in a reduced state of oxidation into a watercourse will deplete the oxygen to the detriment of local flora and fauna. The inorganic fraction of the leachate may be toxic to life forms. Non-biodegradable organic compounds will persist for some time. When such compounds are assimilated into food chains they may adversely affect aquatic species (DoE, 1986).

Suspended matter and precipitation from leachate may inhibit photosynthesis. Settlement of the suspended matter may give rise to putrefaction and blanket the bed with solids reducing the abundance of flora and fauna. The visual quality of the watercourse may be affected by the formation of unsightly gelatinous microbial growths and by staining of the stream bed and plant life.

Concentrations of above a few mg/l of ammoniacal nitrogen can be directly toxic to fish (DoE, 1995).

2.4.2.3.2 Groundwater

The extent and chemical nature of leachate pollution is complex and dependent on the nature and structure of the soils and rocks, their hydraulic characteristics and the position

of the site with respect to abstractions or natural discharges. Once the groundwater has become polluted it may be unsuitable as a source of water for many years.

The effects of high strength organic leachate on groundwater will persist for a long time due to the limited amount of dissolved oxygen available and the low rates of dispersion (DoE, 1986). Some constituents in leachate will not attenuate by physical processes in the groundwater environment.

The leaking of a strongly reduced leachate, high in organic matter, into a shallow, presumably aerobic aquifer creates a sequence of redox zones downstream of the landfill. These redox zones will strongly influence the attenuation of the pollutants in the plume.

2.4.2.4 Leachate Management

Leachate management is concerned with how to 'manage' the leachate that is produced. The leachate management system is there to be an effective leachate control. It is essential as wastes can produce highly toxic effluents during their decomposition.

A good leachate management system is the prime requirement for the accelerated stabilisation of a landfill site. Investigation and risk assessment are an important factor in the production of an acceptable leachate management plan and will form an essential part of a licence application.

Important considerations which influence leachate management are:

- site lay-out

The shape of the site base and hence the drainage gradients will have a bearing on the leachate management.

- surface water control

Surface water management is required to ensure that rainwater run-off does not drain into the waste from surrounding areas and that contaminated surface water run-off from the operational area does not enter water courses.

- leachate collection

A landfill will need an efficient leachate collection and removal system to enable leachate to be removed from the site for disposal.

- leachate monitoring

The composition and volume of leachate generated will vary over time. Leachate treatment will be required to meet these long and short term variations.

- estimates of leachate production

The volumes of leachate generated will vary over time. Leachate treatment will have to cope with these changing quantities.

- daily cover

Daily cover is used primarily in preventing windblown litter and odours, deterrence to scavengers, birds and vermin and improving the site's visual appearance. It is also advocated as a means of shedding surface water during the filling sequence, thereby assisting in leachate management (DoE, 1995).

- final capping of site

A cap manages leachate production by controlling the ingress of rain and surface water into the underlying waste.

- leachate removal and treatment

The leachate removal and treatment facilities should be adequate for the varying volumes and composition of leachate generated through all stages of landfill development and restoration.

The effectiveness of the leachate management system can be monitored. Monitoring can be used to confirm that the landfill is behaving in the ways predicted when the site was first planned and licensed and to provide information needed for management decisions. The Environment Agency dictates the required level of monitoring for a site within the license agreement. The Environment Agency has the right to obtain access to the site and take its own samples.

2.4.3 LANDFILL GAS

Landfill gas is a by-product of the digestion by micro-organisms of putrescible matter present in waste deposited in landfill sites. The gas is predominantly methane (64%) with carbon dioxide (34%) and trace concentrations of a range of other gases and vapours.

2.4.3.1 Landfill Gas Generation

The important factors controlling the rates and amounts of gas likely to be generated are:

- physical dimension of the site;
anaerobic processes normally dominate in wastes at depths greater than 5 metres.
- waste type;
the composition of waste affects the rate, quality of gas generated per unit mass. Different organic materials in deposited wastes will produce slight differences in methane/carbon dioxide ratios. Mixed waste streams may also react within the site to produce other gases such as hydrogen sulphide.
- waste density;
the degree of saturation of the waste and its density depends both on void space and the absorptive capacity of the waste. The greater the waste density in a landfill the higher the theoretical yield of a landfill gas per unit volume of void space.
- waste input rates;
progressive restoration coupled with high input rates will encourage more rapid development of the anaerobic process.
- site operations;
reduction of the particle size of the waste, by pulverisation and compaction using thin layering techniques, will hasten the onset of anaerobic decomposition for the more readily degradable materials. Rapid infilling of small areas of a site will shorten the aerobic degradation phase and tend to keep waste temperatures down. Daily or intermediate cover and the use of low permeability materials in cell wall construction may encourage perched water tables to develop and have effects on moisture movement, transmission of gases and buffering of leachates.

- moisture content;
a moist landfill environment is normally associated with high rates of gas generation. Liquid movement within the waste tends to provide a more even waste moisture content. It also distributes nutrients and bacteria within the mass, which can further enhance rates of waste degradation and gas evolution.
- pH within the landfill;
the optimal range for methanogenesis is between pH 6.5 to 8.5 and outside this range it is inhibited.
- temperature;
the optimum temperature range for maximising methane production is between 35 and 45°C, which is common in deep landfill sites. A significant reduction in gas evolution occurs below 10 to 15°C.
- oxygen ingress.
the ingress of oxygen into anaerobically decomposing wastes can occur by extensive pumping rates in landfill gas extraction schemes, or through trenches dug into mature wastes for site operations. Oxygen will inhibit the methane formation.

During the aerobic phase of degradation, oxygen levels become depleted and carbon dioxide levels rise (Fig. 2.9). As the hydrolysis and fermentation stage of degradation occurs, levels of carbon dioxide and hydrogen increase and nitrogen levels fall. The concentration of methane present in the gas gradually rises as the acetogenic and methanogenic stages develop. When steady-state methanogenic conditions occur, the resulting gas composition is about 64% methane and 34% carbon dioxide.

As the degradable organic fraction within the waste becomes exhausted, methane and carbon dioxide generation decline. Hydrogen sulphide can be generated by sulphate-reducing bacteria which act on sulphate within the waste.

El-Fadel *et al* (1996a; 1996b; 1997) have developed a numerical model for simulating the spatial and temporal distribution of production and transport of landfill gas and heat. The model is based on microbiology, chemistry and physics.

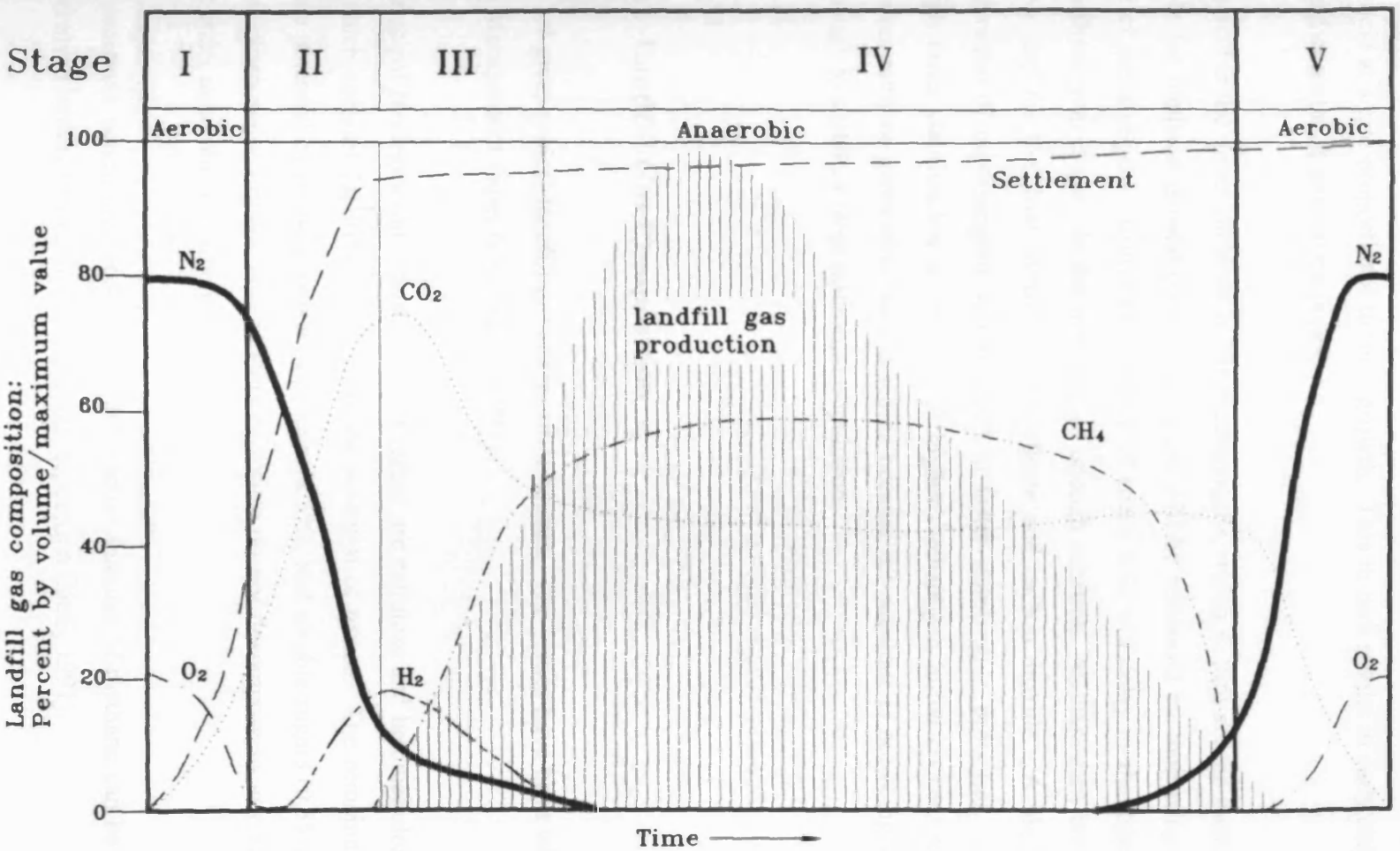


Figure 2.9 Graph showing changes in composition of landfill gas. From WMP26B (DoE, 1995).

El-Fadel *et al* (1997) found that when the acidogens grow at a fast rate, they produce acetic acid at a rate proportional to their growth. This in turn results in early stabilisation with higher methane generation peaks.

Acetic acid is the direct substrate to the methanogens, which in turn are the most essential variable for methane generation. Stabilisation will be enhanced by increasing the food source of methanogens. Conversely, a lack of acetic acid will delay methanogen growth and methane generation. In the presence of enough substrate, methanogens are the rate-limiting step for the final formation of methane and carbon dioxide. A higher initial concentration of methanogens would result in faster stabilisation processes. However, although faster stabilisation is observed at higher methanogen initial concentrations, the maximum methane generation rate decreases because the substrate is not being generated fast enough to sustain a large microbial population.

2.4.3.2 Landfill Gas Composition

Table 2.7 gives typical landfill gas composition values. The values have been taken from Waste Management Paper No 27 (DoE, 1991).

The principal biodegradable constituents of refuse are cellulose and hemicellulose (Table 2.8), which account for 91% of the methane potential of refuse. The remainder of the methane potential of refuse consists of protein (8.3%), and soluble sugars (0.5%). Lignin and the other major organic components of refuse do not decompose to any significant extent under anaerobic conditions.

Once anaerobic conditions predominate, substantial amounts of methane can be expected to be evolved within 3 to 12 months of waste deposition (DoE, 1991).

Component	Typical Value (% Volume)	Observed Maximum (% Volume)
Methane	63.8	88.0
Carbon Dioxide	33.6	89.3
Oxygen	0.16	20.9
Nitrogen	2.4	87.0
Hydrogen	0.05	21.1
Carbon Monoxide	0.001	0.09
Ethane	0.005	0.0139
Ethene	0.018	-
Acetaldehyde	0.005	-
Propane	0.002	0.0171
Butanes	0.003	0.023
Helium	0.00005	-
Higher Alkanes	<0.05	0.07
Unsaturated Hydrocarbons	0.009	0.048
Halogenated Compounds	0.00002	0.032
Hydrogen Sulphide	0.00002	35.0
Organosulphur Compounds	0.00001	0.028
Alcohols	0.00001	0.127
Other	0.00005	0.023

Table 2.7 Typical landfill gas composition values. From WMP 27 (DoE, 1994)

Chemical Constituent	% dry weight	Methane Potential
Cellulose	51.2	73.4
Hemicellulose	11.9	17.1
Protein	4.2	8.3
Lignin	15.2	0
Starch	0.5	0.7
Pectin	<3.0	-
Soluble Sugars	0.35	0.5

Table 2.8 Composition and methane potential of municipal refuse by chemical constituent. From Barlaz & Ham (1993).

2.4.3.3 Landfill Gas Production

2.4.3.3.1 Quantity

Often the total amount of gas production is calculated from measured or estimated refuse analysis. Using the carbon content of refuse, the total gas production rate is calculated using the following equation:

$$G_e = 1.868 C \quad (2)$$

where G_e is the total gas production (m^3 (STP)/t MSW), C is the carbon content (kg/t), 1.868 is a conversion factor from solid carbon to gaseous carbon, and STP is standard temperature pressure. For this equation, the assumption is that the carbon is totally biologically converted into biogas (CH_4 and CO_2) (Ehrig, 1996).

2.4.3.3.2 Production Rate

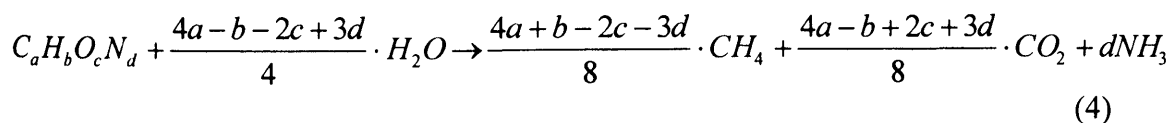
The gas production rate can be estimated using the following equation (Ehrig, 1996):

$$G_t = A (1 - e^{-tk_1}) e^{-tk_2} \quad (3)$$

where G_t is the gas production rate at time t (m^3 (STP)/t MSW \times year), A is the maximum gas production rate, and k_1 and k_2 are coefficients.

2.4.3.3.3 Landfill Gas Yields

The maximum theoretical landfill gas yield can be calculated using the equation (Cossu *et al.*, 1996):



where $C_aH_bO_cN_d$ is the empirical chemical formulation for biodegradable organics in solid waste. The equation allows the estimation of the maximum theoretical yield of landfill gas, starting from the general formula characterising solid wastes ($C_aH_bO_cN_d$). The estimation can also be carried out directly according either to the specific formula of organic compound to be decomposed or to the empirical formulae introduced to represent biodegradable fractions of MSW. Once the elementary composition of the waste is known, this equation permits evaluation of both the quantity and quality of the gas generation. The proportion of methane being generated in the gas can be calculated.

The equation above states that 1 mol of organic carbon is bioconverted to 1 mol of landfill gas. Therefore, given that 1 mol of gas at 0°C and 1 atm occupies 22.4 litres:

$$1 \text{ mol C in organic matter} = 22.4 \text{ litres gas (CH}_4 + \text{CO}_2)$$

On a weight basis:

$$1 \text{ g C in organic matter} = 1.867 \text{ litres gas (CH}_4 + \text{CO}_2)$$

Table 2.9 summarises some typical data on the elementary composition of the biodegradable fraction of MSW, expressed as percentage of dry weight.

Component	Wet weight (%)	Dry weight (%)	Elementary composition (%)					
			C	H	O	N	S	Ash
Food wastes	11.4	4.6	4.7	4.7	4.4	13.0	10.0	4.0
Paper	42.8	55.0	50.8	53.0	61.3	18.5	60.0	55.2
Cardboard	7.5	9.8	9.2	9.4	11.1	3.7	10.0	8.0
Plastics	8.8	11.9	15.1	13.8	6.8	-	-	19.8
Textiles	2.5	3.1	3.6	3.3	2.4	14.8	-	1.4
Rubber	0.6	0.9	1.4	1.4	-	1.9	-	1.4
Leather	0.6	0.7	0.9	0.8	0.2	7.4	-	1.1
Yard wastes	23.3	11.2	11.4	10.8	10.8	40.7	20.0	8.3
Wood	2.5	2.8	2.9	2.8	3.0	-	-	0.6
Total	100.0	100.0	100.0	100.0	100.0	100.0	100.0	100.0

Table 2.9 Typical data on the elementary composition of the biodegradable fraction of MSW, expressed as percentage of dry weight. From Cossu *et al.* (1996).

Table 2.10 shows values of landfill gas yields and generation rates that have been reported in the literature.

Source	LFG yields (m ³ /ton of MSW)	LFG production rates (m ³ /ton year)
Rhyne (1974)	437	
EMCON (1976)		1.22 (methane)
Tabasaran (1976)	60-180	
Rasch (1976)	300-500	
Augenstein <i>et al.</i> (1976)	128	
Bowermann <i>et al.</i> (1977)	40-50	
Rovers <i>et al.</i> (1977)		12-22
DeWalle & Chian (1978)	5.4 l/kg TS	0.181 l/kg TS d ⁻¹
Rettenberger (1978)	200	
Stegmann (1978)	250	
Ham (1978)	440	16
	120-310	
Pacey (1981)	55-225	
EMCON (1981)		9.6
Beker (1981)	250	
Hoeks & Oosthoek (1981)	200	10 m ³ /yr m ³
Bogardus (1983)		2-8
Hoeks (1983)	20	
Stegmann (1983)	120-150	
Campbell (1985)	100-400	
Stegmann (1986)	186-235 (USA)	12.8 (Palos Verdes)
	120-150 (Germany)	18.6 (Fresh Kills)
Wise <i>et al.</i> (1987)	100-400	3.9-130
AFRC (1988)	400	
Rae (1988)	400	
Willumsen (1988)		2-5
Richards (1989)	135-400	

Table 2.10 Landfill gas yields and generation rates that have been reported in the literature. From Cossu *et al.* (1996)

2.4.3.3.4 Landfill Gas Generation Time

Information concerning the generation time is provided by the half time ($t_{1/2}$), the time over which the gas generation equals half the estimated yield. By definition the $t_{1/2}$ is such that the area under the production curve is the same on both sides. In the literature (Cossu *et al.*, 1996) $t_{1/2}$ values range from 2-5 years for wet to 10-25 years for dry climates in the USA.

The half time can be calculated in first-order kinetic models by:

$$t_{1/2,i} = \ln \frac{2}{k_i} \quad (5)$$

where k_i is the decay rate constant of the i th component of organic waste.

Laboratory-scale experiment results have been transferred to full-scale landfills to give half-lives of biological degradation of 4-7.5 years (Ehrig, 1996).

2.4.3.3.5 Estimating Landfill Gas Quantity

The US Environmental Protection Agency present three methods to estimate gas flow from a landfill site (EPA, 1996). Landfill characteristics, and therefore gas generation, can vary substantially among landfills so the following methods of gas generation should be used as rough estimates only. The EPA recommend that it should be assumed that the actual gas flows may be 50% higher or lower.

2.4.3.3.5.1 Simple Approximation

A rough approximation of landfill gas production can be estimated using the amount of waste in place as the only variable. Industry experts have developed a rule of thumb, based on their experience. They found that landfill gas generation rates range from 0.05 to over 0.20 cubic feet (cf) of gas per pound (lb) of refuse per year [0.00064 to

0.00257 m³/kg], with the average landfill generating 0.10 cf of landfill gas per lb [0.00128 m³/kg] per year (EPA, 1996). This rule of thumb results in the following equation:

$$\text{Annual Landfill Gas Generation (cf)} = 0.10 \text{ cf/lb} \times 2000 \text{ lb/ton} \times \text{Waste in place (tons)} \quad (6)$$

A figure of 0.1 ft³ CH₄/wet lb-yr is often used to estimate the methane production rate from a landfill. Assuming refuse buried at 20% moisture, this converts to 7.8 litres CH₄/dry kg-yr (Barlaz & Ham, 1993).

2.4.3.3.5.2 *First Order Decay Model*

A First Order Decay Model can be used to account for the changing gas generation rates over the life of the landfill. The model requires that the following variables are known or can be estimated:

- the average annual waste acceptance rate;
- the number of years the landfill has been open;
- the number of years the landfill has been closed, if applicable;
- the potential of the waste to generate methane;
- the rate of methane generation from the waste.

The basic first order decay model is:

$$\text{LFG} = 2 L_0 R (e^{-kc} - e^{-kt}) \quad (7)$$

Where:

- LFG = Total amount of landfill gas generated in current year (cf)
- L₀ = Total methane generation potential of the waste (cf/lb)
- R = Average annual waste acceptance rate during active life (lb)
- k = Rate of methane generation (1/year)
- t = Time since landfill opened (years)
- c = Time since landfill closure (years)

Values for L_0 and k are thought to vary widely. They are dependent in part on local climatic conditions and waste composition. Ranges for L_0 and k have been developed by an industry expert and are presented in table 2.11.

Variable	Range	Suggested Values		
		Wet Climate	Medium Moisture Climate	Dry Climate
L_0 (cf/lb)	0-5	2.25-2.88	2.25-2.88	2.25-2.88
k (1/yr)	0.003-0.4	0.1-0.35	0.05-0.15	0.02-0.10

Table 2.11 Suggested values for first order decay model variables. From EPA (1996).

Due to the uncertainty in estimating L_0 and k , gas flow estimates derived from the first order decay model should be given as a range of plus or minus 50%.

2.4.3.3.5.3 Pump Test

The most accurate method for estimating gas quantity is to conduct a pump test. A pump test involves sinking test wells and installing pressure monitoring probes, then measuring the gas collected from the wells under a variety of controlled extraction rates. A benefit of this method is that the collected gas can be tested for quality as well as quantity.

2.4.3.3.6 Landfill Gas Properties

2.4.3.3.6.1 Major Constituents

Methane is both colourless and odourless, but is flammable between about 5 and 15% by volume in air at normal atmospheric pressures. This range reduces with increasing carbon dioxide and reducing oxygen content. A methane:air mixture is potentially most explosive when there is just enough oxygen to completely combust the gas (about 9.5% methane in

air). The minimum concentration of oxygen required for flame propagation in a methane:air mixture at STP is 12% by volume.

Carbon dioxide is also colourless and odourless, is non-flammable but stimulates the respiratory and central nervous systems at high concentrations.

2.4.3.3.6.2 *Minor Constituents*

Landfill gas contains many minor constituents at low concentrations. There are considerable variations in the concentration and presence of trace compounds, which are related to waste constituents, age and extent of waste degradation.

Over 100 trace compounds in landfill gas have been recognised and some groups of compounds may be related to known phases of decomposition. Many compounds present in trace amounts may be flammable, toxic or carcinogenic, or have an obnoxious odour. Such compounds include hydrogen, hydrogen sulphide, and organic compounds including volatile and halogenated varieties.

Organosulphur compounds and esters are found in gases derived from recently deposited wastes, from which odours are more obvious.

Hydrogen sulphide can be evolved in quantity from the co-deposit of sulphate containing materials, such as wastes containing gypsum from plasterboard or some colliery spoils, with biodegradable wastes.

2.4.3.3.6.3 *Density*

The density of landfill gas depends on the proportion of compounds present. The different gases have different densities; hydrogen (0.08 kg/m^3), carbon dioxide (1.98 kg/m^3) and methane (0.72 kg/m^3). Thus a mixture of 10% hydrogen and 90% carbon dioxide, which is typically evolved in the early stage of anaerobic degradation, will be denser than air. A

mixture of 60% methane and 40% carbon dioxide will be slightly lighter than air. The evolution of warm landfill gas gives it buoyancy in colder air. As a result of different densities and buoyancies, landfill gas may collect in the bottoms of trenches or excavations, or may rise up and accumulate beneath structures and foundations.

2.4.3.4 Environmental Effects of Landfill Gas

Emissions of landfill gas lead to pollution of the environment, and have the potential to produce malodours, cause damage to vegetation, destruction of property or harm to human health. Landfill gas emissions lead to reduced air quality.

2.4.3.4.1 Atmospheric Pollution

The dominant landfill gases, methane and carbon dioxide, are the two main greenhouse gases produced as a result of human activity. Methane is thought to be 20-30 times more effective than carbon dioxide in blocking the long wave energy radiated from the Earth's surface. Using 1990 estimates, landfill accounts for over 39% of all UK methane emissions, with an estimated total of over one million tonne escaping from landfill sites each year (Warwickshire Environmental Protection Council, 1995).

2.4.3.4.2 Soil Pollution

Stressed vegetation is commonly associated with the presence of landfill gas within soils, but the extent will be dependent on a species' tolerance of methane and carbon dioxide, and oxygen depletion. These conditions may arise from the displacement of air by a high flux of landfill gas through the soil. Where emissions are lower methane-oxidising bacteria within the soil can oxidise residual methane to carbon dioxide and where recharge

with air is slow, i.e. in cohesive soils, oxygen depletion can result in stressed vegetation. The level of oxidation will be dependent on soil types and thickness, moisture content, temperature and retention time of the methane within the soil.

2.4.3.4.3 Damage to Health

Carbon dioxide stimulates the respiratory and central nervous systems at high concentrations. It is a highly soluble gas and this leads to a rapid appearance of physiological effects when exposed to high concentrations. Carbon dioxide is naturally present in air at about 0.03%. At 0.5% in air, breathing becomes slightly deeper and at a level of 3% in air the breathing rate is doubled. There is a steady increase in breathing rate between 3 and 10% in air, leading to headaches and exhaustion. Complete recovery will usually occur on removal from the oppressive environment. Above 10% in air breathing becomes very distressful and severe headaches are experienced with convulsions due to acute depression of the brain stem. An individual may collapse if subjected to concentrations above 10% in air and death usually results above 25% (Warwickshire Environmental Protection Council, 1995).

Oxygen depletion usually accompanies elevated levels of landfill gas, due either to dilution or oxidation of methane to carbon dioxide. Exposure to an oxygen deficient atmosphere may result in asphyxiation. A normally healthy person will first experience symptoms of anoxia at about 16% oxygen, with serious distress and fatigue resulting when the oxygen level drops to about 14% by volume. Unconsciousness may result in oxygen concentrations below 10% and death at less than 6% (Warwickshire Environmental Protection Council, 1995). The HSE Guidance Note EH40 suggests that no one should enter or remain in an unventilated area where oxygen has fallen below 18%.

2.4.3.4.4 Flammability

When methane or hydrogen is mixed with air, within certain concentration limits known as the flammable or explosive range, the resultant mixtures may ignite to produce fires and explosions. The concentration limits are commonly known as the "Lower Explosive Limit" (LEL) and the "Upper Explosive Limit" (UEL). The LEL is reached when there is sufficient flammable gas in air to sustain combustion. With an increasing concentration of flammable gas the amount of available oxygen will reduce to a point at which combustion cannot be sustained, the Upper Explosive Limit.

The flammable ranges of methane and hydrogen are 5-15% and 4-74% by volume respectively (DoE, 1991). The presence of carbon dioxide affects these ranges, but there is little change at the lower limit. When oxygen concentration falls to below 13% by volume, under normal conditions methane cannot ignite.

There is generally little risk of an explosion from landfill gas venting to atmosphere, though there may be a possibility of a flash fire if accumulation occurs in poorly ventilated areas.

2.4.3.4.5 Toxicity

Some of the minor constituents of landfill gas have toxic effects if present in high enough concentrations. Trace gases do not usually represent a health hazard following normal atmospheric dilution. At present there is little information available regarding the accumulation effect of low concentrations of potentially harmful gases.

2.4.3.4.6 Corrosive Properties

Some of the components of landfill gas, or the derivatives thereof, have a corrosive potential.

Carbon dioxide is soluble in water and will give rise to an ionised solution of carbonic acid in aqueous condensates associated with the gas. Such condensates can corrode a range of metals (DoE, 1991).

The combustion of landfill gas will give rise to a high temperature environment in which some trace components, such as halogenated or sulphuretted compounds, may give rise to highly acidic and aggressive derivatives. At such elevated temperatures, carbon dioxide, hydrogen, hydrocarbons and water vapour can be involved in decarbonisation (removal of carbon) or carburization (coking) reactions with alloys strengthened by the addition of interstitial carbon (DoE, 1991).

2.5 HYDROLOGY / HYDROGEOLOGY OF LANDFILLS

2.5.1 WATER BALANCE

A water balance or water budget analysis can be used to estimate the potential leachate production. Knowledge of the possible range of leachate production is important for sizing the leachate collection system and in making decisions about how to manage treatment of the leachate.

Water balance analysis accounts for the effects of many hydrologic processes on water movement at a site. Potential pathways of water movement are shown in figure 2.10.

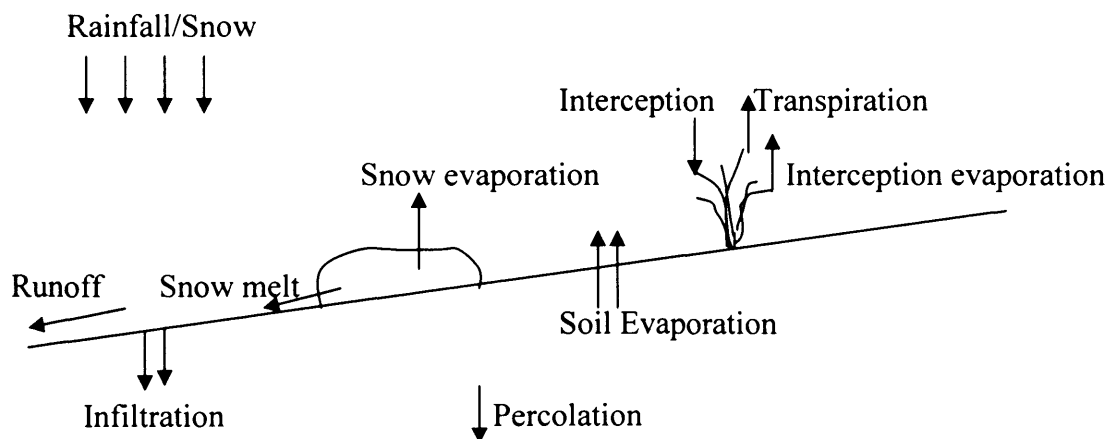


Figure 2.10 Potential pathways of water movement on a landfill site.

The leachate potential of landfilled municipal solid waste is commonly evaluated by water balance methods. Water balance calculations handle volume inputs, outputs and absorptive capacity by empirically derived bulk coefficients. A standard water balance equation may be written as (McDougall *et al*, 1996):

$$P = R - SR - E - \Delta M \quad (8)$$

where:

P = percolation

R = rainfall

SR = surface runoff

E = evapotranspiration

ΔM = change in moisture retained within the waste fill.

2.5.1.1 Precipitation

Precipitation represents the largest single contribution to the production of leachate. Once precipitation strikes a site, it may:

- be intercepted by vegetation and subsequently be evaporated
- be stored temporarily on the surface in the form of snow or ice
- run off the surface
- infiltrate into the cover

2.5.1.2 Infiltration

Water that is not intercepted or does not run-off may infiltrate into the soil. Water infiltrating the soil may:

- be transpired to the atmosphere via plants
- evaporate from the surface soil into the atmosphere
- be stored in the soil
- percolate downward through the soil and past the evaporative zone.

As with all cases of infiltration, the most critical situation occurs during periods of light rainfall over long a long elapse of time. Short bursts of heavy rainfall during a storm result in a quick saturation of the cover material with the remainder being shed as run-off (Canziani & Cossu, 1989).

2.5.1.3 Run-Off

The most important factors that influence the run-off of rainwater are:

- topography;
- morphology of the soil;
- type of soil cover;
- vegetation;
- permeability of the soil;
- drainage system installed.

It is possible to make estimates of run-off. Two methods commonly used are the rational method and the infiltration curve method. The Infiltration Curve method is recommended for calculating daily fluctuations in run-off whereas the rational method is more use for calculations of run-off over longer periods of time.

2.5.1.3.1 Rational Method

The rational method is based on the general formula:

$$R = c \times P \quad (9)$$

where:

R = run-off

P = rainfall

c = an empirical coefficient which varies in function with the nature of soil, the slope of the site, the presence and type of vegetation.

Values of c adopted for the evaluation of the hydrological balance around a landfill site have been proposed (Table 2.12) by Salvato *et al.* 1971 (in Canzizni & Cossu, 1989).

Soil Cover	Soil Texture			
	Slope (%)	Sandy loam	Loamy clay	Clay
Grassed soil	0-5	0.10	0.30	0.40
	5-10	0.16	0.36	0.55
	10-30	0.22	0.42	0.60
Bare soil	0-5	0.30	0.50	0.60
	5-10	0.40	0.60	0.70
	10-30	0.52	0.72	0.82

Table 2.12 Values of c for the evaluation of the hydrological balance around a landfill site. From Canzizni & Cossu (1989).

2.5.1.3.2 Infiltration Curve Method

The United States Department of Agriculture and Soil Conservation Service (USDA-SCS) formulated the infiltration curve method in 1947. It calculates the run-off taking into account various factors such as the permeability of the topsoil, type of vegetation growing, the slope of the site and the moisture content of the soil at the moment for which the estimation is to be made.

2.5.1.4 Evaporation

If the number of water molecules passing to the vapour state exceeds the number of molecules joining the liquid, the result is evaporation. Evaporation will continue until the air becomes saturated with moisture.

The absolute humidity of a given air mass is the number of grams of water per cubic meter of air. At any given temperature, air can hold a maximum amount of moisture, called the

saturation humidity, which is directly proportional to the temperature of the air (Table 2.13). The relative humidity of an air mass is the percent ratio of the absolute humidity to the saturation humidity for the temperature of the air mass. As the relative humidity approaches 100%, evaporation ceases.

Temperature (°C)	Saturation Humidity (g/m ³)
-25	0.705
-20	1.074
-15	1.605
-10	2.358
-5	3.407
0	4.874
5	6.797
10	9.399
15	12.83
20	17.30
25	23.05
30	30.38

Table 2.13 Saturation humidity of air (g/m³). From Fetter (2001).

When an air mass is cooled and the saturation humidity value drops, condensation occurs as the air mass can no longer hold all of its humidity. If the absolute humidity remains constant, the relative humidity will rise. When it reaches 100%, any further cooling will result in condensation. The dew point for an air mass is the temperature at which condensation will begin.

There are two characteristics of an uncovered landfill that affect the evaporation in opposite directions: the high infiltration capacity and the heat production in the top layer (Bendz & Bengtsson, 1996). The high infiltration capacity diminishes the evaporation because of rapid transportation of precipitation into the landfill. Campbell (1983) estimates that the evaporation from an operational landfill surface in the UK could annually be as low as 40% of the precipitation due to the high infiltration capacity. The

heat production in the top layer contributes to the energy available for evaporation. For most active landfills the high infiltration seems to be the dominant process of the two.

Evaporation from a landfill with a soil cover that is not thin and has well-established vegetation is comparable to the regional evaporation.

Bendz and Bengtsson (1996) conducted experiments in an active landfill site in Sweden. They investigated the contribution of the heat of biodegradation by measuring the temperature gradient in the top layer of the landfill. The evaporation was calculated by combining the energy budget with an expression for sensible heat flux, and taking the atmospheric stability into account by introducing the similarity theory of Monin and Obukhov. It was found that the biological heat enhanced the net energy flux and the actual evaporation by 20% and 10%, respectively.

2.5.1.5 Evapotranspiration

Evapotranspiration refers to the transfer of water from the soil directly to the atmosphere (evaporation), and to the removal of water by plants and transfer of that water to the atmosphere by those same plants (transpiration).

The growth of vegetation causes water loss to the atmosphere by evapotranspiration, which is greater than that which could be lost by evaporation from the soil alone without any vegetation.

For European climates the formula developed by Thornthwaite, corrected by coefficients to take into account latitude, seems closest to reality (Canziani & Cossu, 1989).

$$PE_i = 16 \left(\frac{10T_i}{I_i} \right)^a C_i \quad (10)$$

where:

PE_i = potential evapotranspiration in the i -th month (mm/month)

T_i = monthly average temperature (°C)

$$a = 6.75 \times (10^{-7} \times I_t^3) + 7.71 \times (10^{-5} \times I_t^2) + 1.79 \times (10^{-2} \times I_t) + 0.49239 \quad (11)$$

I_t = annual thermal indice

$$I_t = \sum_{i=1}^{12} i \left(\frac{T_i}{I_t} \right)^{1.514} \quad (12)$$

C_i = correction coefficient relative to the month which takes account of the variation in length of day at various latitudes

2.5.2 WATER BALANCE ANALYSIS ON A LANDFILL CAP

2.5.2.1 Computer Analysis

The computer programme HELP (Hdraulic Evaluation of Landfill Performance) employs the same principals as the method of the hand analysis described in Section 2.5.2.2. The programme uses daily (rather than monthly) time step and employs more sophisticated algorithms for many of the computations. The model accepts weather, soil, and design data, and uses solution techniques that account for the effects of surface storage, snowmelt, runoff, infiltration, evapotranspiration, vegetative growth, storage of soil moisture, lateral drainage of water in drainage layers, leachate recirculation, vertical percolation of soil water, and leakage through hydraulic barriers (Koerner & Daniel, 1997).

2.5.2.2 Hand Analysis

One of the first decisions that must be made when carrying out water balance analysis is what time-scale to use – hourly, daily or monthly. When performing the analysis by hand over long periods of time it is more convenient to look at monthly averages.

Koerner & Daniel (1997) and the US Environmental Protection Agency (2003) give details of a spreadsheet (Table 2.14) that can be set up for analysing the annual water balance on a landfill cap using monthly averages.

This method is used in Chapter 5 using data for Silent Valley to work out the water balance on the capped Southern Slope.

Row	Parameter	Month												Total
		J	F	M	A	M	J	J	A	S	O	N	D	
A	Av. Monthly Temp (°C)													
B	Monthly Heat Index (H_m)													
C	Unadjusted Daily Potential Evapotranspiration (UPET) (mm)													
D	Possible Monthly Duration of Sunlight (N)													
E	Potential Evapotranspiration (PET) (mm)													
F	Precipitation (P) (mm)													
G	Runoff Coefficient (C)													
H	Runoff (R) (m)													
I	Infiltration (IN) (mm)													
J	IN – PET (mm)													
K	Accumulated Water Loss (WL) (mm)													
L	Water Stored (WS) (mm)													
M	Change in Water Storage (CWS) (mm)													
N	Actual Evapotranspiration (AET) (in)													
O	Percolation (PERC) (mm)													
P	Check (CK) (mm)													
Q	Percolation Rate (FLUX) (m/s)													

Table 2.14 Spreadsheet used for water balance analysis. From Koerner & Daniel (1997).

2.5.2.2.1 Row A: Average Monthly Temperature

The average monthly temperature ($^{\circ}\text{C}$) is recorded in Row A (Table 2.14).

2.5.2.2.2 Row B: Monthly Heat Index (H_m)

The monthly heat index (H_m) is a dimensionless, empirical parameter used to estimate evapotranspiration. The monthly heat index is calculated as follows:

$$H_m = (0.2 T)^{1.514} \quad (\text{for } T > 0^{\circ}\text{C}) \quad (13)$$

$$H_m = 0 \quad (\text{for } T \leq 0^{\circ}\text{C}) \quad (14)$$

where T is the average monthly temperature from row A.

The monthly values can be summed to determine the annual heat index (H_a), which is entered into the 'total' column.

2.5.2.2.3 Row C: Unadjusted Daily Potential Evapotranspiration (UPET)

The unadjusted daily potential evapotranspiration (UPET) refers to the maximum amount of evapotranspiration that would occur if the soil were saturated with water. The amount of actual evapotranspiration will depend on the water content of the soil and will usually be less than the unadjusted daily potential evapotranspiration. Unadjusted daily potential evapotranspiration can be calculated as follows:

$$\text{UPET} = 0 \quad (\text{for } T \leq 0^{\circ}\text{C}) \quad (15)$$

$$\text{UPET} = 0.53(10T/H_a)^a \quad (\text{for } 0^{\circ}\text{C} < T < 27^{\circ}\text{C}) \quad (16)$$

$$\text{UPET} = -0.015T^2 + 1.093T - 14.208 \quad (\text{for } T \geq 27^{\circ}\text{C}) \quad (17)$$

where T is the temperature in $^{\circ}\text{C}$, H_a is the annual heat flux, and a is a dimensionless empirical factor that is computed as follows:

$$a = (6.75 \times 10^{-7})H_a^3 - (7.71 \times 10^{-5})H_a^2 + 0.01792H_a + 0.49239 \quad (18)$$

2.5.2.2.4 Row D: Monthly Duration of Sunlight (N)

The mean possible monthly duration of sunlight (N) is corrected for possible amount of sunlight and expressed in units of 12 hour periods. The value of N depends on the latitude and month of the year. It can be determined by looking at tables (Appendix A) developed for the northern and southern hemispheres by Thornthwaite and Mather (Koerner & Daniel, 1997).

2.5.2.2.5 Row E: Potential Evapotranspiration (PET)

The potential evapotranspiration is calculated by multiplying the values for the unadjusted daily potential evapotranspiration (Row C) and the monthly duration of sunlight (Row D).

2.5.2.2.6 Row F: Precipitation (P)

The mean monthly precipitation (P) for the site is entered in Row F. Precipitation varies from year to year, so it is important to consider the purpose of the water balance analysis (e.g. Maximum expected percolation through cap, long-term average) when deciding on monthly values.

2.5.2.2.7 Row G: Runoff Coefficient (C)

The runoff coefficient (C) is dimensionless and is defined as the ratio of runoff to precipitation. It can vary widely and is difficult to predict accurately. If no site-specific information is available, then it is recommended to use guidance developed by Fenn *et al*, which is summarised in table 2.15 (Koerner & Daniel, 1997).

Description of Soil	Slope	Runoff coefficient
Sandy Soil	Flat ($\leq 2\%$)	0.05-0.10
Sandy Soil	Average (2-7%)	0.10-0.15
Sandy Soil	Steep ($\geq 7\%$)	0.15-0.20
Clayey Soil	Flat ($\leq 2\%$)	0.13-0.17
Clayey Soil	Average (2-7%)	0.18-0.22
Clayey Soil	Steep ($\geq 7\%$)	0.25-0.35

Table 2.15 Suggested runoff coefficients. From Koerner & Daniel (1997).

2.5.2.2.8 Row H: Runoff (R)

Runoff (R) is calculated from precipitation (Row F) and the runoff coefficient (C) (Row G):

$$R = PC \quad (19)$$

2.5.2.2.9 Row I: Infiltration (IN)

The monthly infiltration (IN) is defined as the amount of water entering the surface of the cover and is assumed to equal precipitation (Row F) minus runoff (Row H):

$$IN = P - R \quad (20)$$

2.5.2.2.10 Row J: Infiltration minus Potential Evapotranspiration ($IN - PET$)

The difference between infiltration (Row I) and potential evapotranspiration (Row E) ($IN - PET$) is entered into Row J. A positive value indicates potential accumulation (storage) of water in the cover soil and a negative value indicates that the soil is drying.

2.5.2.2.11 Row K: Accumulated Water Loss (WL)

The accumulated water loss (WL) is the sum of the negative monthly values of IN-PET (Row J) since the beginning of the year.

2.5.2.2.12 Row L: Water Stored in Root Zone (WS)

The water stored in the root zone (WS) is defined as the amount of water stored in the portion of the soil cover that can be tapped by plant roots for evapotranspiration. The amount of water stored in the root zone is calculated from the volumetric water content (θ) of the soil and the depth of the root zone (H_{root}) as follows:

$$WS = \theta H_{root} \quad (21)$$

The volumetric water content (θ) is defined as the volume of water (V_w) divided by the total volume of the soil (V).

2.5.2.2.13 Row M: Change in Water Storage (CWS)

The change in water storage (CWS) in a month is the water stored (WS) (Row L) in that month minus the water stored in the previous month. If CWS is negative then the soil in the root zone is losing water and if it is positive it is gaining water.

2.5.2.2.14 Row N: Actual Evapotranspiration (AET)

The actual evapotranspiration (AET) depends on whether infiltration exceeds potential evapotranspiration. If there is less infiltration than potential evapotranspiration, the soil in the root zone is losing water through evapotranspiration.

$$AET = PET \quad (\text{if } (IN - PET) \geq 0) \quad (22)$$

$$AET = PET + [(IN - PET) - CWS] \quad (\text{if } (IN - PET) < 0) \quad (23)$$

2.5.2.2.15 Row O: Percolation (PERC)

Percolation (*PERC*) is the amount of water draining from the root zone and is calculated as follows:

$$PERC = 0 \quad (\text{if } (IN - PET) \leq 0) \quad (24)$$

$$PERC = (IN - PET) - CWS \quad (\text{if } (IN - PET) > 0) \quad (25)$$

The monthly percolation should be summed to obtain the annual amount of percolation.

2.5.2.2.16 Row P: Check for Calculations (CK)

The idea of water balance calculations is to account for all of the precipitation that falls on the cover. For each month it is possible to check the previous calculations as follows:

$$CK = PERC + AET + CWS + R \quad (26)$$

Each monthly value and the yearly total should equal precipitation *P*, i.e. Row P should equal Row F for each column.

2.5.2.2.17 Row Q: Percolation Rate (FLUX)

The rate of percolation (*FLUX*) is the flux of water passing through the cover soil. It should be calculated for months where *PERC* > 0 as follows:

$$FLUX = (PERC \cdot 0.001) / t \quad (27)$$

where *t* is the number of seconds in the month.

2.6 RESEARCH BY THE WASTE MANAGEMENT INFORMATION BUREAU (WMIB)

With funding from the Department of the Environment, the Waste Management Information Bureau (WMIB, 1995) produced a report for them reviewing the composition of leachates from domestic wastes in landfill sites.

2.6.1 VALLEY LANDFILLS WITH GROUNDWATER INGRESS

Natural valleys were often identified as suitable areas for the deposition of household and other wastes. The most common problem encountered at such sites relates to the uncontrolled entry of groundwater into wastes from either springs along the valley walls or from streams in the base of the valley.

Streams were often culverted beneath the site. Culverts must be watertight, designed to accommodate the anticipated external loadings, and constructed with concrete suitably corrosion-resistant to the aggressive conditions present in the base of landfills. The granular materials used around the culvert could provide a pathway for leachate to travel along the side of the culvert, either to enter it at a point of weakness, or discharge with it at its outlet.

Waste Management Paper 26 (DoE, 1986) warns about the risks of valley landfills, recommending detailed investigation of site hydrology to identify all springs, streams and watercourses. It did not regard landfilling over culverts as good practice, unless a well designed and properly engineered culvert can be provided.

The Waste Management Information Bureau examined detailed leachate monitoring records from eight landfill sites. They found a consistency in leachate composition from the sites examined (Table 2.16).

Landfill Site	Operational		Present Leachate Composition						
	Opened	Closed	pH	COD	BOD ₅	NH ₄ -N	Cl ⁻	Na	Fe
Dean House Farm	1980	1984	7.3	84	4.5	64	1280	658	3.4
Conygar Coppice	1966	1978	6.7	94	~1.0	43	345	225	38.8
Sherbourne	1976	~1994	7.1	174	~14	97	360	210	35.4
Farthinghoe	1972	1983	7.0	133	<0.5	54	200	171	13.5
Cannon Bridge	1968	1993	7.0	195	71	77	161	88	22.8
Faygate	1969	1993	7.5	257	14.7	166	403	262	21.8
Stangford	1982	1990	6.8	330	~50	161	311	351	27.0
Fowlchurch	~1965	1994	7.1	373	25	328	824	631	11.2

Results in mg/l, except for pH value.

Table 2.16 Summary of leachate quality in 1995 at valley landfills with groundwater ingress. From Waste Management Information Bureau (1995).

Leachate quality at each site is characterised by neutral pH, very low BOD₅ values (often less than 10 mg/l), but relatively high and persistent residual concentrations of ammoniacal-N and chloride. While these very low levels of biodegradable organic compounds indicate that methanogenic conditions have become established, as supported by generally low sulphide concentrations, the relatively high rates of water ingress appear to have prevented pH values of 8 or above from being established, as might otherwise be the case. A consequence of continuing pH values close to 7.0 is that relatively high residual concentrations of soluble iron (typically 20 to 40 mg/l) remain in the leachate.

Results for leachate at Silent Valley show similar results to those in table 2.16. Leachate geochemistry for Silent Valley will be discussed in detail in Chapter 6.

CHAPTER 3

DESK STUDY

Silent Valley landfill site (SO 185 075) has been in operation as a landfill site since 1981. Before accepting municipal waste it received large quantities of waste from the iron and steel works at Ebbw Vale. The site is licensed to accept household waste.

This chapter gives a description of the site, the geology, hydrology, hydrogeology, site history and the present site operating conditions.

3.1 SITE DESCRIPTION

3.1.1 SITE LOCATION

Silent Valley Landfill Site is located in the Cwm Merddog, an eastern tributary valley that joins the Ebbw Fawr at the village of Cwm (Fig. 3.1). The site is 1.2 km east of the village of Waunlwyd and lies to the southeast of Ebbw Vale. It is located at National Grid Reference SO 185 075.

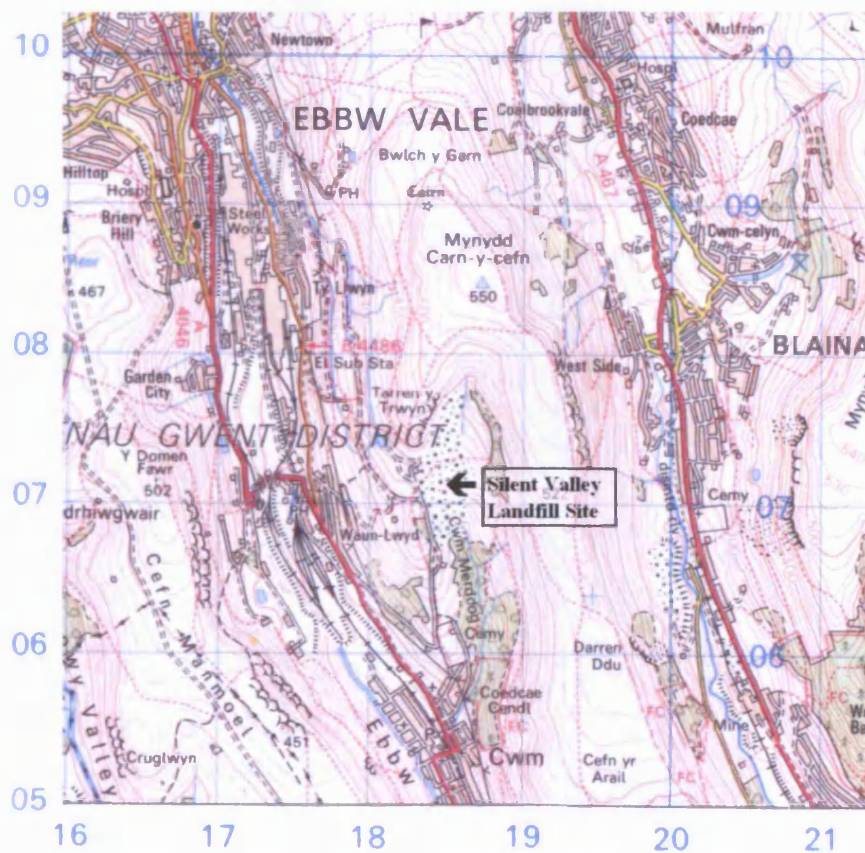


Figure 3.1 Map showing the location of Silent Valley landfill site. From OS Landranger Series 161.

3.1.2 SITE ACCESS

The site is reached via an access road, between Cwm and Waunlwyd, off the A4046. The turnoff is signed. The access road also leads to Cwm Cemetery. The A4046 joins the A467 and links Ebbw Vale with Newport.

3.1.3 SITE OF SPECIAL SCIENTIFIC INTEREST (SSSI)

A leaflet about Cwm Merddog is available from the Gwent Wildlife Trust. Many of the details given below are taken from the leaflet.

The site has been declared by the Blaenau Gwent County Borough Council as a Local Nature Reserve. Much of the site was notified in 1984 as a Site of Special Scientific Interest. It was purchased by the Gwent Wildlife Trust with financial help from Blaenau Gwent Borough Council, WWF and the Nature Conservancy Council.

Silent Valley Local Nature Reserve covers approximately 50 hectares. It is made up of a number of plant communities including grassland, wetlands, heaths and woodlands. Species such as narrow buckler fern, greater tussock sedge and heath spotted orchid can be found. The Reserve attracts a lot of birds, including finches, Bramblings, Green Woodpecker, Pied Flycatcher, Redstart and buzzard.

The two main blocks of beech woodland are found at Cwm Merddog, which straddles the Nant Merddog stream, and Coed Tyn y Gelli, which is the highest known site of beech in the UK. There, at an altitude of up to 1500 feet (460 m) the trees are stunted and gnarled and many grow little taller than 2 m.

Gwent Wildlife Trust in partnership with the Countryside Council for Wales, Blaenau Gwent County Borough Council, Silent Valley Waste Services Ltd is developing an education and community resource. The project is funded through the Silent Valley Environmental Trust (landfill tax) and the European Regional Development Fund. It aims to enhance the Silent Valley Local Nature Reserve as an important wildlife site to be enjoyed by the local community and as an educational resource for schools.

3.2 GEOLOGY

The site is located within the Carboniferous Upper Coal Measures, Westphalian C and D series (Golder Associates, 1993a; 1993b). The Hughes Beds form the top of the sequence and belong to the Upper Pennant Measures. Below the Hughes Beds are the Brithdir and Rhondda Beds of the Lower Pennant Measures. The solid geology is overlain by a mixture of boulder clay, head deposits and made ground. Figure 3.2 shows the regional geology of Silent Valley and the surrounding area.

The landfill site lies at elevations below the outcrop of the Brithdir Seam and consequently rests on the Rhondda Beds (Fig. 3.3).

3.2.1 SOLID GEOLOGY

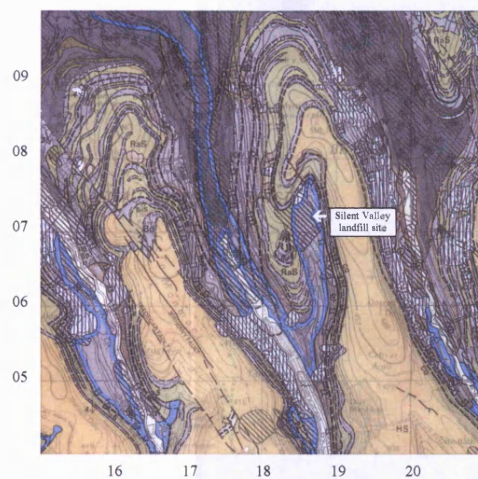
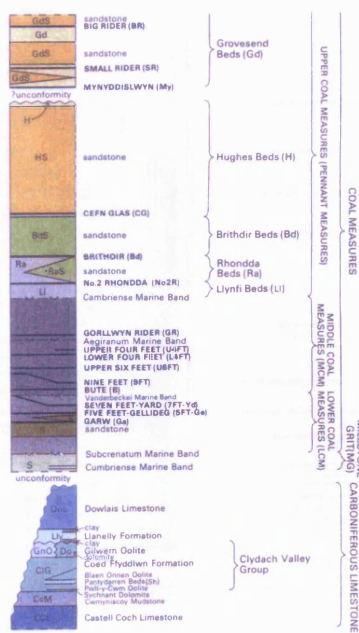
3.2.1.1 Llynfi Beds

The Llynfi Beds consist of mudstones and sandstones occurring in approximately equal proportions. The sandstones are typically quartzitic sandstones, commonly pebbly and conglomeratic. Red beds appear towards the top of the formation in the Ebbw Fach Valley (Barclay, 1989).

The No. 3 Rhondda, locally called Old Man's Coal, is the most persistent coal in the Llynfi Beds.

3.2.1.2 Rhondda Beds

The Rhondda Beds in the area are about 100m thick with the No. 2 Rhondda coal defining the base of the formation. The lower part of the formation comprises mainly pebbly coarse-grained orthoquartzitic sandstones and polymitic conglomerates. In the upper part



EXPLANATION OF GEOLOGICAL SYMBOLS

- + Horizontal strata
- ∕ Gently inclined strata
- ∕ Inclined strata, dip in degrees
- ∕ General dip of strata, dip in degrees
- Geological boundary, Drift
- Geological boundary, Solid
- Coal crop
- Fault at surface, crossmark indicates downthrow side
- Marine Band (MB)
- In general, broken lines denote uncertainty. Drift boundaries on this sheet are shown as continuous lines regardless of their certainty or uncertainty.
- Borehole
- ⊕ Pit or mine shaft, open at time of survey
- ⊖ Pit or mine shaft, abandoned
- ∕ Adit or mine mouth, showing direction of entry
- ⊖ Adit or mine mouth, abandoned, showing direction of entry
- ***** Cross measures drift
- ▨ Landslip
- ▨ Area of founded strata
- ▨ Worked out opencast coal area
- ▨ Made ground
- Fossil locality

Figure 3.2 Geological map of area surrounding Silent Valley landfill site. From British Geological Survey. Solid and Drift Geology. England and Wales Sheet 232, Abergavenny.

of the succession the quartzite strata are interbedded with mudstones, coal and associated seatearths. The mudstones are predominantly red and know as Deri Beds (Golder Associates, 1993a; 1993b).

3.2.1.3 Brithdir Beds

The boundary between the Rhondda and the overlying Brithdir Beds is formed by the Brithdir coal seam. In the past, two mines worked this seam to the north of the site and two mines to the east (Golder Associates, 1993a; 1993b).

Pennant sandstones, about 16m thick overlie the Brithdir on the west side of the Ebbw Fawr Valley and on the east side of the valley near Cwm, but mudstones overlie the coal in the Cwm Merddog (Barclay, 1989).

The Brithdir Rider, a thin inferior coal seam overlies the mudstones and is itself overlain by about 25 m of strong massive conglomeritic to fine grained orthoquartzitic sandstones.

The base of the Cefn Glas coal seam, known locally as the Tillery Rider, defines the top of the Brithdir Beds (Barclay, 1989).

3.2.1.4 Hughes Beds

The Hughes Beds extend from the base of the Cefn Glas coal seam to the base of the Mynyddislwyn seam. Pennant sandstones dominate the formation, with only thin and impersistent mudstones. On the west side of the Ebbw Fawr Valley the Cefn Glas is 0.12 m thick in a disused quarry at Victoria [1694 0630]. On the east side of the Ebbw Fawr Valley the coal is thick enough to have been worked from crop levels in Cwm Merddog (Barclay, 1989).

	Head Deposits Range	Silty CLAY Range	Guidelines NRA
Natural Moisture Content %	15-17 (3)	13-26 (15)	-
Liquid Limit %	23-47 (4)	30-57 (15)	<90
Plastic Limit %	8-26 (4)	11-34 (15)	<65
Clay Content %	5-12 (6)	18-47 (4)	>10
Specific Gravity Mg/m ³	2.65-2.68 (2)	2.71-2.80 (6)	-
Optimum Moisture Content %	8.5-10 (2)	9-18 (6)	-
Maximum Dry Density Mg/m ³	2.00-2.11 (2)	1.76-2.06 (6)	-
Permeability m/s	2.35-7.18×10 ⁻⁹ (3)	2.85×10 ⁻⁹ – 8.9×10 ⁻¹⁰ (10)	<1×10 ⁻⁸
Undrained Shear Strength kN/m ²	-	75-10 (4)	-

Figures in brackets represent number of samples tested.

Table 3.1 Summary of laboratory results (BGBC and Golder Associates) and NRA guidelines for landfill lining material. From Golder Associates (1993c).

3.3 HYDROLOGY

3.3.1 SURFACE WATER

3.3.1.1 Surface Water Catchment

Golder Associates and Ove Arup & Partners have made calculations of the landfill site catchment area. Golder Associates (1993b) calculated a surface water catchment area of 106 hectares.

Ove Arup & Partners (1995) calculated that at the downhill toe of the landfill, the theoretical catchment of the Nant Merddog is about 110 hectares, of which the landfill site occupies 20 hectares. The effective catchment of the Nant Merddog upstream of inlet A (Fig. 3.32) is about 30 hectares. The remaining 60 hectares of catchment is from the interfluvial ridges to the east and west of the site where little run-off occurs.

In another report Ove Arup & Partners (1997) give the surface water catchment area (upper part of Cwm Merddog) as an area of approximately 120 ha.

The main surface water running through the site is the Nant Merddog stream. It is a subsidiary of the Ebbw Fawr River, which it joins to the south of the site near Cwm. The Nant Merddog is culverted to the east of the site.

3.3.1.2 General Quality Assessment of the Ebbw Fawr

The General Quality Assessment scheme (GQA) is the Environment Agency's method for classifying water quality in rivers and canals. The scheme provides a way of comparing quality from one river to another and for looking at changes through time. Water quality is assessed for:

- Chemistry

- Biology
- Nutrients
- Aesthetics.

The following information comes from the Environment Agency website (accessed in February 2004, http://www.environment-agency.gov.uk/yourenv/eff/water/213902/river_qual/gqa2000/?version=1&lang=_e).

3.3.1.2.1 Chemistry

The grade (Table 3.2) is defined by standards for biochemical oxygen demand (BOD), ammonia and dissolved oxygen. These determinands are indicators of pollution that apply to all rivers, first because of the widespread risk of pollution from sewage or farms, and second because of the toxicity of ammonia and the requirement for dissolved oxygen for aquatic life.

In 2002 the Ebbw Fawr had a river classification for chemistry as fairly good and good upstream of the landfill site and good downstream (Fig. 3.4).

Chemical Grade		Dissolved oxygen (% saturation) 10-percentile	Biochemical Oxygen Demand (mg/l) 90-percentile	Ammonia (mg/l) 90-percentile	Likely uses and characteristics*
A	Very Good	80	2.5	0.25	All abstractions Very good salmonid fisheries Cyprinid fisheries Natural ecosystems
B	Good	70	4	0.6	All abstractions Salmonid fisheries Cyprinid fisheries Ecosystems at or close to natural
C	Fairly Good	60	6	1.3	Potable supply after advanced treatment Other abstractions Good cyprinid fisheries Natural ecosystems, or those corresponding to good cyprinid fisheries
D	Fair	50	8	2.5	Potable supply after advanced treatment Other abstractions Fair cyprinid fisheries Impacted ecosystems
E	Poor	20	15	9.0	Low grade abstraction for industry Fish absent or sporadically present, vulnerable to pollution** Impoverished ecosystems**
F	Bad	<20	-	-	Very polluted rivers which may cause nuisance Severely restricted ecosystems

* Provided other standards are met

** Where the grade is caused by discharges of organic pollution

Table 3.2 Table showing the General Quality Assessment scheme grades for chemistry.

3.3.1.2.2 Biology

The biological scheme (Table 3.3) is based on the macro-invertebrate communities of rivers and canals. The variety of macro-invertebrates differs from site to site and from river to river even when there is no pollution or physical disturbance. This is because they

are affected by the size, slope, altitude and geographical location of the watercourse, the nature of the stream bed, the river flow and the geology of the catchment. Because of these natural differences, it is best to describe biological quality as the difference between the macro-invertebrate community actually found in the river and that which would be expected under natural conditions.

Grade	Quality	
A	Very Good	The biology is similar to (or better than) that expected for an average, unpolluted river of this size, type and location. There is a high diversity of families, usually with several species in each. It is rare to find a dominance of any one family.
B	Good	The biology shows minor differences from Grade 'a' and falls a little short of that expected for an unpolluted river of this size, type and location. There may be a small reduction in the number of families that are sensitive to pollution, and a moderate increase in the number of individuals in the families that tolerate pollution (like worms and midges). This may indicate the first signs of organic pollution.
C	Fairly Good	The biology is worse than that expected for an unpolluted river of this size, type and location. Many of the sensitive families are absent or the number of individuals is reduced, and in many cases there is a marked rise in the numbers of individuals in the families that tolerate pollution.
D	Fair	The biology shows considerable differences from that expected for an unpolluted river of this size, type and location. Sensitive families are scarce and contain only small numbers of individuals. There may be a range of those families that tolerate pollution and some of these may have high numbers of individuals.
E	Poor	The biology is restricted to animals that tolerate pollution with some families dominant in terms of the numbers of individuals. Sensitive families will be rare or absent.
F	Bad	The biology is limited to a small number of very tolerant families, often only worms, midge larvae, leeches and the water hog-louse. These may be present in very high numbers but even these may be missing if the pollution is toxic. In the very worst case there may be no life present in the river.

Table 3.3 Table showing the General Quality Assessment scheme grades for biology.

The Environment Agency use a computer-based system to predict the macro-invertebrates that would be found if the river was unpolluted and undamaged. The system is called RIVPACS (River Invertebrate Prediction and Classification System). The classification of waters is not precise and there is an average risk of 22% that rivers may be classed wrongly. It is unusual, however, for this error to extend beyond the neighbouring grade.

In 2002 the Ebbw Fawr had a river classification for biology as fairly good and fair upstream of the landfill site and good and fairly good downstream (Fig. 3.5).

3.3.1.2.3 Nutrients

Samples are analysed for their concentrations of two nutrients: nitrate and phosphate. The data are collected over three years to determine average nutrient concentrations. So the classification for the year 2002 includes the results for 2000 and 2001. Data from three years (36 samples per site) is used to reduce any variation due to unusual weather conditions.

A grade from 1 to 6 is allocated for both phosphate (Table 3.4) and nitrate (Table 3.5). These are not combined into a single nutrients grade. There are no set ‘good’ or ‘bad’ concentrations for nutrients in rivers in the way that we describe chemical and biological quality. Rivers in different parts of the country have naturally different concentrations of nutrients. ‘Very low’ nutrient concentrations, for example, are not necessarily good or bad; the classifications merely states that concentrations in this river are very low relative to other rivers.

Classification for Phosphate	Grade limit (mgP/l) Average	Description
1	<0.02	Very low
2	>0.02 to 0.06	Low
3	>0.06 to 0.1	Moderate
4	>0.1 to 0.2	High
5	>0.2 to 1.0	Very high
6	>1.0	Excessively high

Table 3.4 Table showing the General Quality Assessment scheme grades for phosphate.

Classification for Nitrate	Grade limit (mg NO ₃ /l) Average	Description
1	<5	Very low
2	>5 to 10	Low
3	>10 to 20	Moderately low
4	>20 to 30	Moderate
5	>30 to 40	High
6	>40	Very high

Table 3.5 Table showing the General Quality Assessment scheme grades for nitrate.

In 2002 the Ebbw Fawr had a river classification for phosphate as low upstream of the landfill site and very low downstream (Fig. 3.6). Nitrate was classed as very low upstream of the landfill site and very low downstream (Fig. 3.7).

3.3.1.2.4 Aesthetics

The aesthetic quality of rivers and canals is based on:

- litter (gross litter, general litter, sewage litter and dog faeces)
- oil, surface scum, foam, sewage fungus, ochre
- colour and odour.

The standard sampling unit consists of an area extending 50 m along the riverbank and up to 5 m from the water's edge plus the river and its bed. Each parameter is assigned a class in the following way:

- Litter is classified on the total number of items counted for each parameter.
- Oil, scum, foam, sewage fungus and ochre are classified on the percentage cover of the water.
- Colour is classified according to its hue and intensity.
- Odour is classified according to the type of odour and its intensity.

The overall grade for a site is derived from the 'score' allocated to each parameter.

The classification of a site for aesthetic quality is one of four grades:

- Grade 1 - good
- Grade 2 - fair
- Grade 3 - poor
- Grade 4 - bad

In 2000 the aesthetic quality of some rivers and canals was assessed. The Ebbw Fawr was not assessed (Fig. 3.8). At a couple of locations north of the Ebbw Fawr, the assessment had been good. A location in Newport had been assessed as poor.

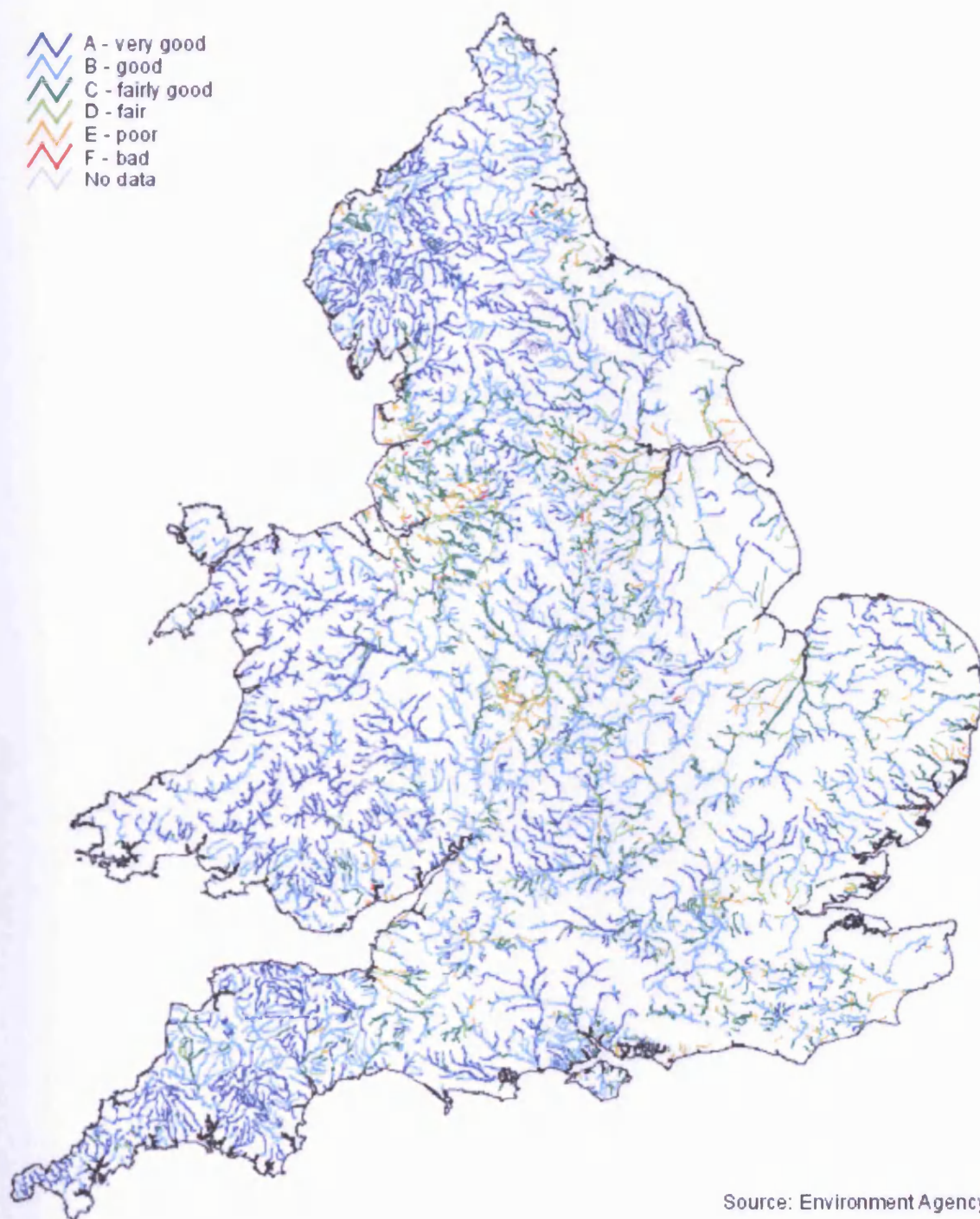


Figure 3.4 Classification under the General Quality Assessment scheme (GQA) for river chemistry in 2002.

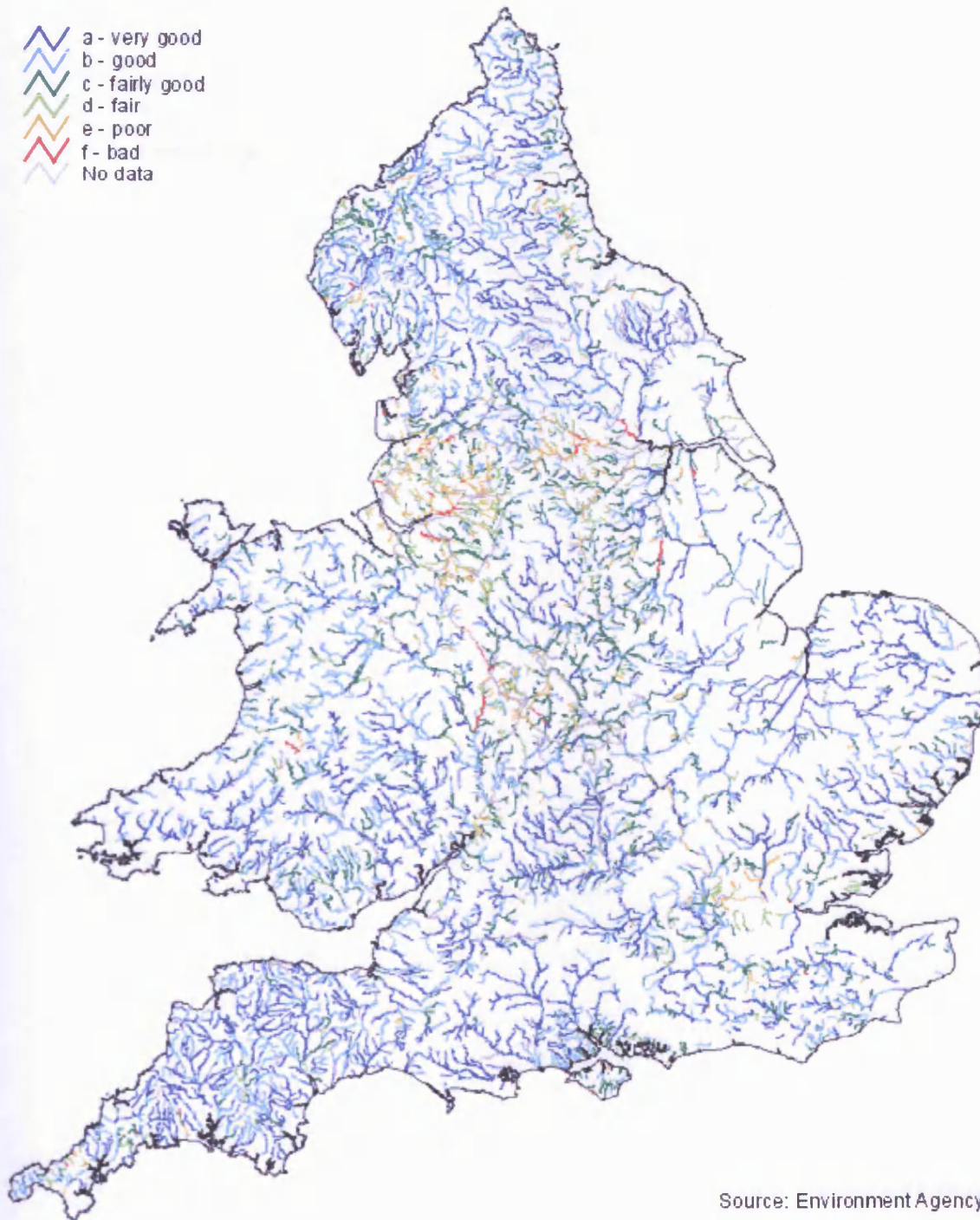


Figure 3.5 Classification under the General Quality Assessment scheme (GQA) for river biology in 2002.

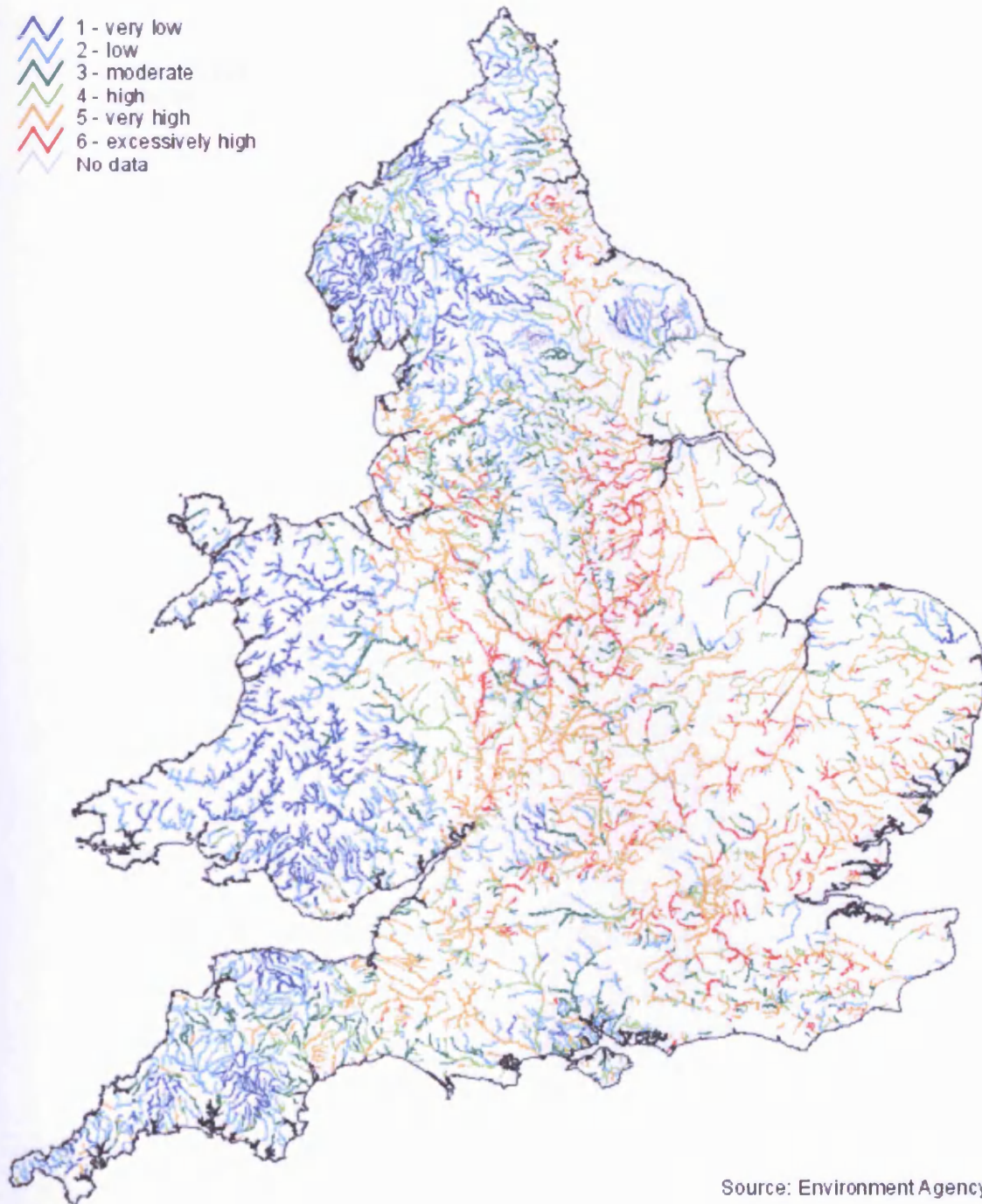


Figure 3.6 Classification under the General Quality Assessment scheme (GQA) for river phosphate in 2002.

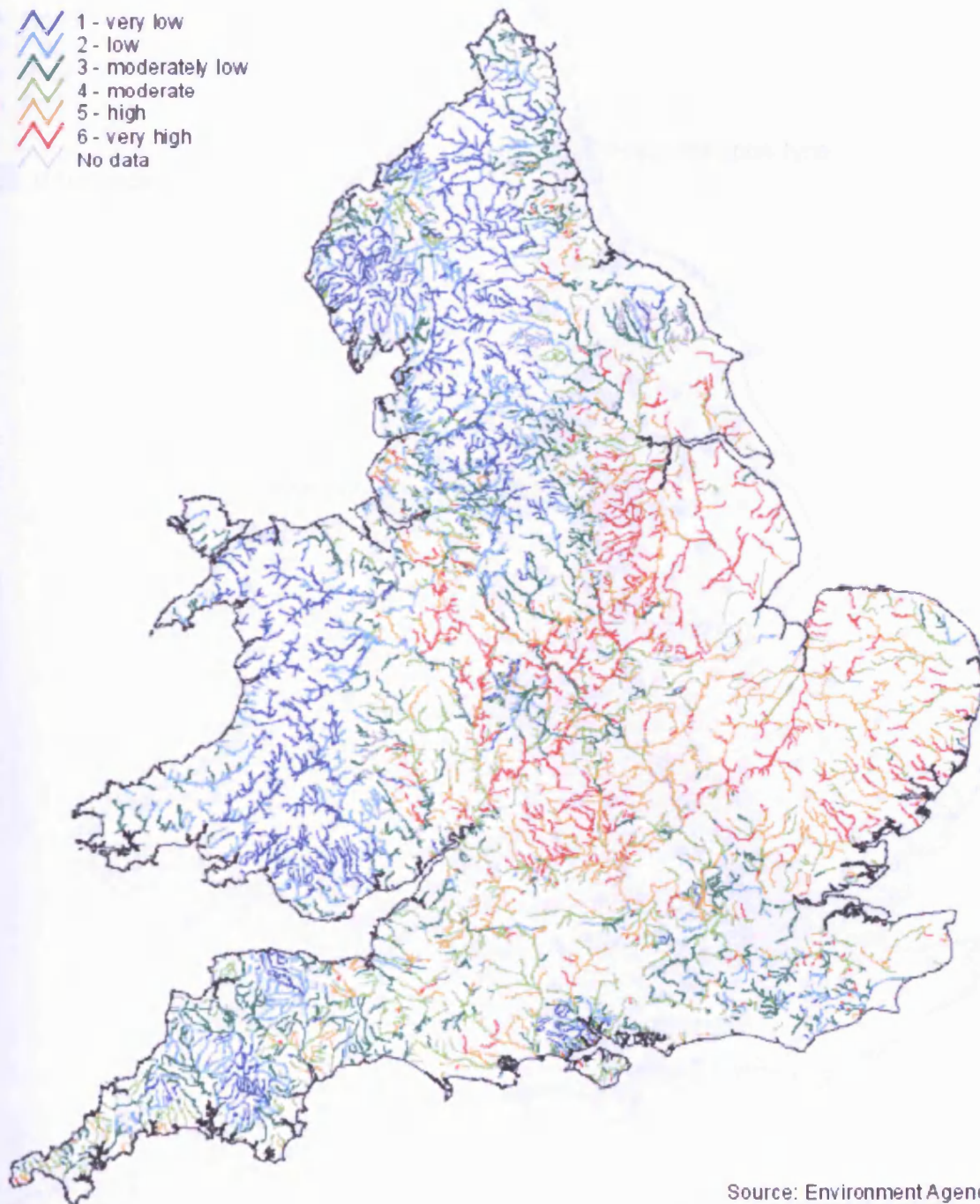


Figure 3.7 Classification under the General Quality Assessment scheme (GQA) for river nitrate in 2002.

3.3.2 MAINFALL

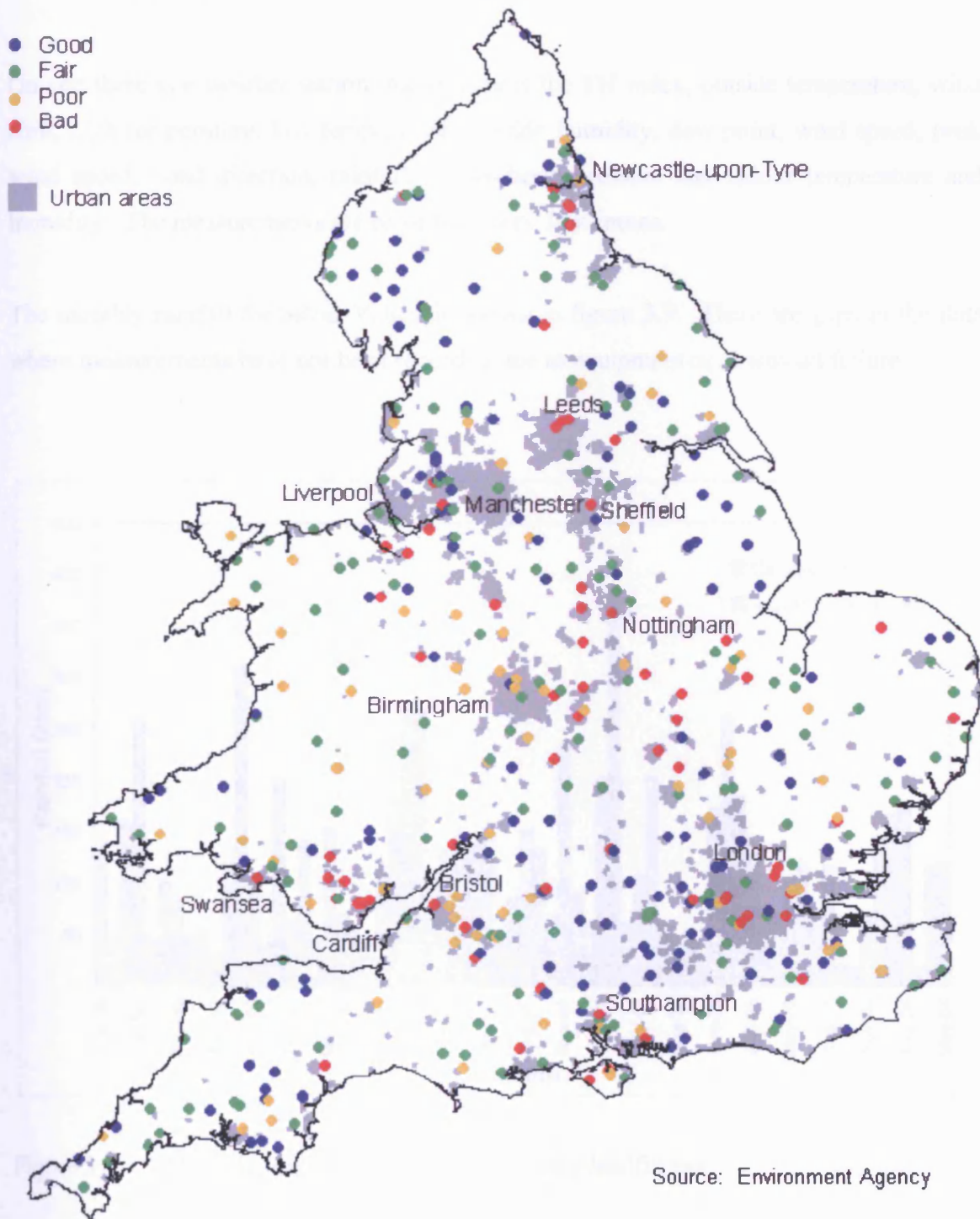


Figure 3.8 Classification under the General Quality Assessment scheme (GQA) for river aesthetics in 2000.

3.3.2 RAINFALL

On site there is a weather station that measures the TH index, outside temperature, wind chill, high temperature, low temperature, outside humidity, dew point, wind speed, peak wind speed, wind direction, rainfall, atmospheric pressure and indoor temperature and humidity. The measurements are recorded every 30 minutes.

The monthly rainfall for Silent Valley is shown in figure 3.9. There are gaps in the data where measurements have not been recorded due to equipment or download failure.

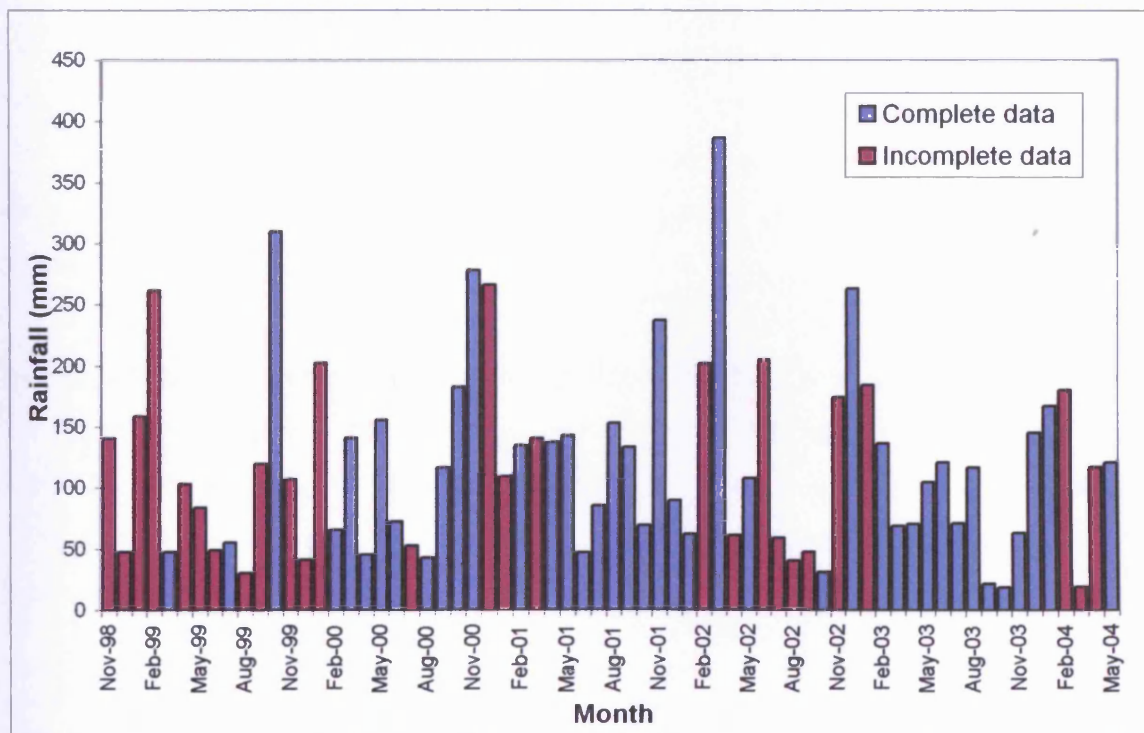


Figure 3.9 Monthly rainfall data for Silent Valley landfill site.

Golder Associates (1993b) obtained the long term annual rainfall from the Meteorological Office for MORECS square 146 as 1257.8 mm.

Effective rainfall for the Silent Valley area is estimated to be of the order of 60% of rainfall (Ove Arup & Partners, 1999).

The rainfall at the site will be dealt with in more detail in Section 5.2.

3.4 HYDROGEOLOGY

3.4.1 REGIONAL HYDROGEOLOGY

Studies carried out on the sediments underlying the site show that the arenaceous deposits and mudstones of the Rhondda Beds are characterised by an intergranular permeability several orders of magnitude greater than that of the less permeable mudstones. The folding, faulting and fracturing of the sequence subsequent to deposition has led to a secondary permeability within the sandstones which is likely to increase the transmissivity of these horizons.

The sandstone beds predominantly control the movement of groundwater in the Upper Coal Measures and that movement is more likely to occur horizontally along bedding planes than vertically across sandstone/mudstone interfaces. This sequence of high and low permeability layers forms a multi-layer aquifer system with individual water pressures in each sandstone aquifer horizon.

Springs commonly emerge along the boundaries of the high permeable sandstones with low permeable mudstones or coal/seatearths. Water is also issuing from disused mine adits. The adit at the north-western end of the site has an engineered drainage system. From the two mines on the eastern valley side water is issuing from their entrances and free draining downslope.

No site specific data are available from published material regarding the hydraulic properties of the aquifer horizons. However, transmissivity values of the coal measure sandstone horizons are reported to range between 0.1-20 m²/d with porosity values of around 0.02 expected (Barclay, 1989).

3.4.2 SITE HYDROGEOLOGY

According to the NRA Document on Policy and Practice for the Protection of Ground Water, Silent Valley landfill is lying in a catchment source protection zone (Golder Associates, 1993b).

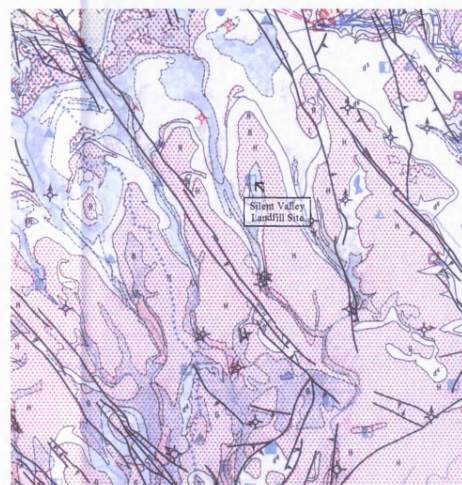
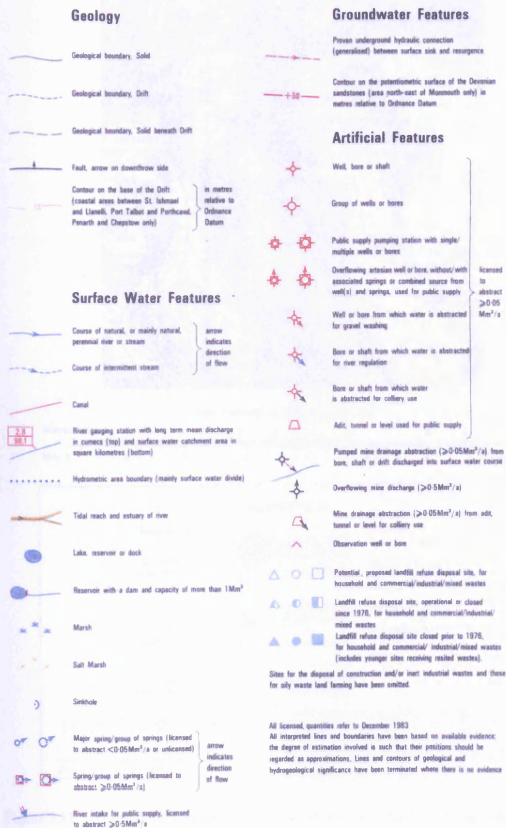
The hydrogeological map (Fig. 3.10) produced by the British Geological Survey has the landfill site marked. The map shows sites of overflowing mine drainage ($\geq 0.5\text{Mm}^3/\text{a}$) to the south of the site and a licensed abstraction point ($\geq 0.05\text{Mm}^3/\text{a}$) to the northwest.

The groundwater vulnerability map (Fig. 3.11) produced by the Environment Agency identifies the vulnerability of groundwater to contamination. An assessment of the physical and chemical properties of the soil is overlain onto geological information to produce 7 groundwater vulnerability classes. Silent Valley Landfill site is treated as a Minor Aquifer (variably permeable) with soils of high leaching potential (H).

The minor aquifer is classified as seldom producing large quantities of water for abstraction but they are important both for local supplies and in supplying base flow to rivers.

Soils of high leaching potential (H) are soils with little ability to attenuate diffuse source pollutants and in which non-adsorbed diffuse source pollutants and liquid discharges have the potential to move rapidly to underlying strata or to shallow groundwater. The soils at Silent Valley have been classified in the sub-class H3; coarse textured or moderately shallow soils which readily transmit non-adsorbed pollutants and liquid discharges but which have some ability to attenuate adsorbed pollutants because of their clay or organic matter contents.

EXPLANATION OF LINES AND SYMBOLS USED ON THE CENTRAL MAP



Scale 1:125,000

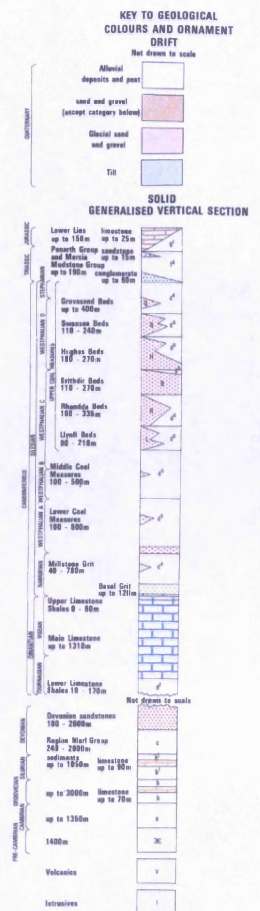


Figure 3.10 Hydrogeological map of Silent Valley and surrounding area. From BGS 1:125,000 Hydrogeological Map of South Wales.

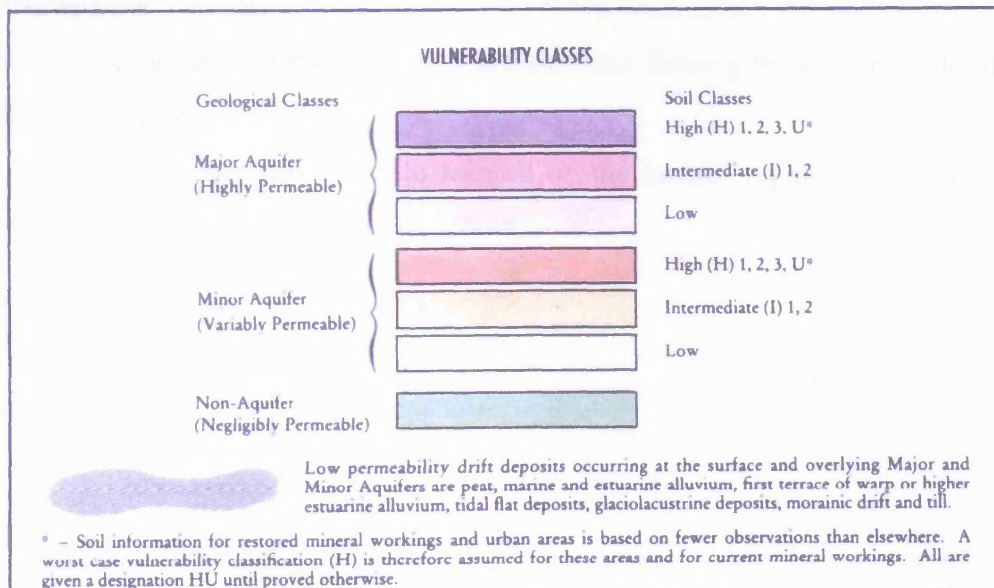
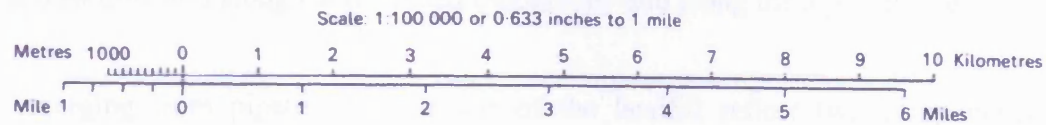
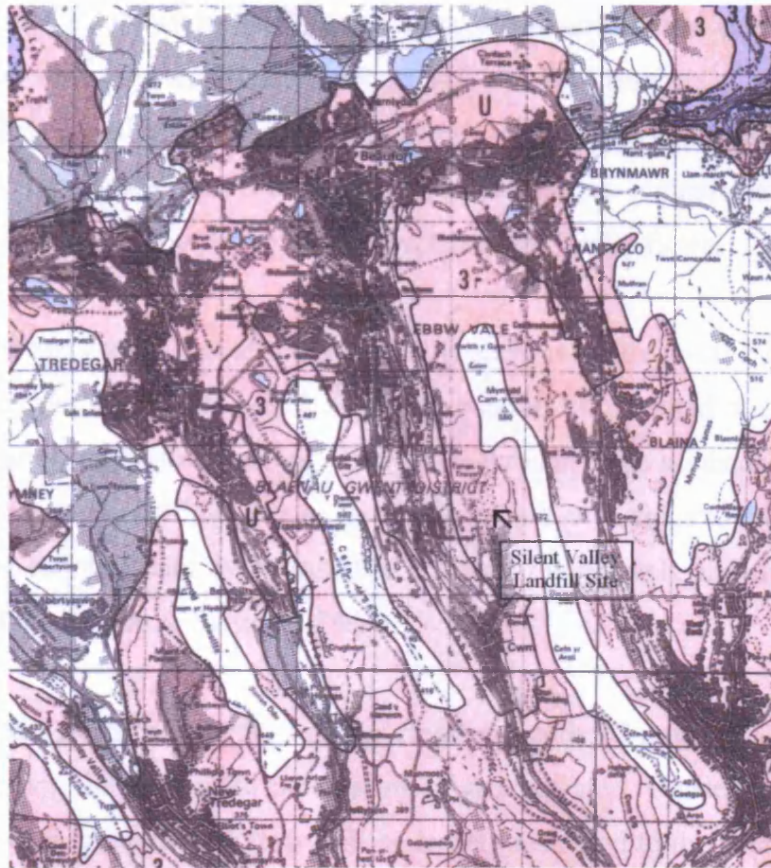


Figure 3.11 Groundwater vulnerability map of area surrounding Silent Valley landfill site. Adapted from Environment Agency map, sheet 36.

There is likely to be a contrast in conductivity between the landfill and underlying boulder clay. Combined with the steep valley topography and the presence of underdrains and pipelines the effect would be the rapid drainage of leachate, with little opportunity for the build-up of leachate heads. Infiltration and percolation of groundwater through the landfill is therefore characterised by short transit times and peaky flows.

To the north-east and north-west of the landfill site there is little run-off. These areas are underlain by massive sandstones which in places contain fissures and open joints which are largely the result of previous mining. Rainwater through these sandstones would enter extensive workings in the Brithdir Seam. In the Tarren y Trwyn ridge to the north-west of the landfill, pipe-rubble drains were installed to drain these levels and discharge away from the landfill (Ove Arup & Partners, 1995).

Below the Brithdir Seam, the strata contain frequent bands of mudstone, which act as aquicludes inhibiting the downward percolation of groundwater. Consequently, downhill of the Brithdir Seam, groundwater flow will be largely restricted to the near surface strata and will flow downhill along the rockhead topography and along the dip of the beds.

Flows emerging from pipelines at the toe of the landfill reflect two components of groundwater flow:

- seasonally changing baseflows due to groundwater flowing through the natural strata before entering the landfill;
- short duration, peaky flows due to rainfall on the landfill rapidly percolating to the downhill toe (Ove Arup & Partners, 1996b).

3.4.3 ANALYSIS OF GROUNDWATER FLOWS

In 1993 Golder Associates (1993b) carried out a site investigation to assess the feasibility of a proposed extension of the site. As part of the investigation 4 groundwater monitoring boreholes were drilled to assess the hydrological regime beneath the site (Fig. 3.12).

The drilling showed that there is a sequence of mudstones and sandstones of various thicknesses underlying the site. Correlation between the boreholes was not possible due to differences in their elevation and the wide spacing between them. The boreholes therefore measured water pressures in different horizons and so the data could not be used to construct contour maps showing groundwater flow across the site.

A numerical model of the site could not be produced due to the layering of the coal measure strata and the scarcity of data available. The standard Modflow package is not suitable. There are other packages for modelling that are commercially available. It was therefore decided to estimate the occurring groundwater flow underneath the site for a single 50 m thick layer with a hydraulic conductivity representing the mudstone/sandstone sequence encountered in the boreholes. A single idealised equivalent layer is created.

The thickness of the mudstones and sandstones in each well are taken from the borehole logs and the hydraulic conductivities were assumed to be 10^{-5} m/s for a sandstone and 10^{-7} m/s for a mudstone (no measurements of hydraulic conductivity for the horizons were available). For each well the hydraulic conductivity of the equivalent layer to the depth of that well is calculated according to the formula:

$$K_x = \sum_{i=1}^n \frac{K_i d_i}{d} \quad (28)$$

where K_i = individual hydraulic conductivity [m/s]

d_i = thickness of individual layer [m]

d = total thickness of n layer [m]

The hydraulic conductivity of the equivalent layer for the boreholes was as follows:

GA/5 $K_x = 3.9 \times 10^{-6}$ m/s

GA/6 $K_x = 4.4 \times 10^{-6}$ m/s

$$\text{GA/7} \quad K_X = 6.3 \times 10^{-6} \text{ m/s}$$

$$\text{GA/8} \quad K_X = 1.8 \times 10^{-6} \text{ m/s}$$

Giving an average for the equivalent layer of:

$$K_X (\text{av.}) = 3.7 \times 10^{-6} \text{ m/s}$$

Assuming a repetitive sequence of the coal measure strata, the calculated average value can be used to determine the flow through the top 50 m below the site. This provides a simple model that assumes that the flow is parallel to the strata.

The hydraulic gradient (*i*) of the site can be calculated between GA/4 and GA/8.

$$i = \frac{\Delta h}{\Delta l} \quad (29)$$

where Δh = difference in head = 100 m

Δl = distance between GA/4 and GA/8 = 800 m

$$i = \frac{100}{800} = 0.125$$

Assuming that the flow occurs across the width of the valley of 500 m, the flow can be calculated using Darcy's Equation,

$$Q = Aki \quad (30)$$

where A = cross-sectional area of flow [m^2]

K = hydraulic conductivity [m/s]

i = hydraulic gradient [-]

$$= 50 \text{ m} \times 500 \text{ m} \times 3.7 \times 10^{-6} \text{ m/s} \times 0.125$$

$$= 1.2 \times 10^{-2} \text{ m}^3/\text{s}$$

$$\approx 1.0 \times 10^{-2} \text{ m}^3/\text{s}$$

This value must balance with the recharge to the aquifer which can be estimated. Golder Associated took the likely area contributing to the recharge of the sequence as 705000 m^2 (Fig. 3.12).



Figure 3.12 Estimated recharge area for calculation of flow through the equivalent layer. From Golder Associates (1993b).

Golder Associates obtained the long term annual rainfall from the Meteorological Office for MORECS square 146 as 1257.8 mm. Using the potential evaporation, the long term average effective rainfall is calculated as 734.3 mm. It was assumed that 30% of the effective rainfall can infiltrate through the coal measure strata, giving an estimate for the potential annual recharge as 220 mm/yr. Over the total area this gives a volume of:

$$\begin{aligned} 705000 \text{ m}^2 \times 0.22 \text{ m/y} &= 155100 \text{ m}^3/\text{y} \\ &= 0.5 \times 10^{-2} \text{ m}^3/\text{s} \end{aligned}$$

Golder Associates compared the volume of groundwater flow with the annual flow estimates of 527000 m³/y through the lagoon. Adding the groundwater flow to the flow through the lagoon gave a total water throughput of:

$$\begin{aligned} &527000 \text{ m}^3/\text{y} \quad (\text{Lagoon}) \\ + &315000 \text{ m}^3/\text{y} \quad (\text{Groundwater Flow}) \\ &\quad (\text{Golder Associates used } 1.0 \times 10^{-2} \text{ m}^3/\text{s} \text{ rather than } 1.2 \times 10^{-2} \text{ m}^3/\text{s}) \\ = &842000 \text{ m}^3/\text{y} \quad (\text{Total flow through site}) \end{aligned}$$

If $1.2 \times 10^{-2} \text{ m}^3/\text{s}$ is used rather than $1.0 \times 10^{-2} \text{ m}^3/\text{s}$ for the groundwater flow, the extra $0.2 \times 10^{-2} \text{ m}^3/\text{s}$ or 63072 m³/y increases the total flow through the site to 905000 m³/y.

The total flow through the site should balance with the available water for infiltration and surface run-off, i.e. the effective rainfall over the whole of the surface water catchment area (Fig. 3.13) of 1060000 m², giving a volume of:

$$1060000 \text{ m}^2 \times 0.734 \text{ m/y} = 780000 \text{ m}^3/\text{y}$$

It is considered that this value is in reasonable agreement with the total flow through the site given the uncertainty of the data used.

Under the existing operating conditions, the likely quantities through the lagoon can be calculated. As before it is still assumed that 70% of the effective rainfall falling on the coal measure strata becomes run-off and that all the effective rainfall falling onto Phases I and II will infiltrate to become leachate.

Phase I:	$201775 \text{ m}^2 \times 0.734 \text{ m/y}$	$= 148103 \text{ m}^3/\text{y}$
Phase II:	$135440 \text{ m}^2 \times 0.734 \text{ m/y}$	$= 99413 \text{ m}^3/\text{y}$
Rest of surface water catchment area:	$722785 \text{ m}^2 \times 0.514 \text{ m/y}$	$= 371511 \text{ m}^3/\text{y}$



Figure 3.13 Estimated surface water catchment area. From Golder Associates (1993b).

3.5 SITE HISTORY

Golder Associates and Ove Arup & Partners have undertaken extensive research to establish the development of Silent Valley. They used Ordnance Survey maps and Country Series maps in addition to information from local people. The information below is a combination of their research and mine.

1880 Cwm Merddog was under agricultural use (Fig. 3.14). Trees and hedges occurred along many field boundaries with occasional coppices on the valley sides. Woodland extended along the Nant Merddog stream in the bottom of the valley and to the east of Ty'n-t-gelli. Within the site three tributary streams flowed into the Nant Merddog, the southern most originating from a spring on the east side of the valley.

There were two farms within the site boundary – Ty'n-y-gelli on the eastern valley side and Pen-y-crûg in the west.

A small quarry exists above the woodland to the east of Blaen-y-cwm and a coal level near the stream exists to the north-northeast of Blaen-y-cwm (just off the north of the map).

1886 This map shows nothing different from the previous edition.

1901 The field boundaries, homesteads and old coal level and quarry to the north remain the same (Fig. 3.15).

A tramway has been constructed along the side of the valley to the trees about 100 m south-southeast of Ty'n-y-gelli. At this location the 'North Level' has been opened up.

The small quarry above the woodland to the east of Blaen-y-cwm is described as Old Quarry. Along the tramway three Old Coal Levels

are noted (only one visible in figure). To the south of the Old Coal Level it appears that there is some rubble. To the south of the landfill boundary one coal level is related to a small spoil tip.

1904 & 1908 Old photographs show a spoil tip encroaching across Nant Merddog from the west.

1920 The North Level is now described as disused (Fig. 3.16). Many of the hedges and trees along field boundaries are no longer present.

The old quarry to the east of Blaen-y-cwm is located but not mentioned. The old coal level to the north remains the same.

1933 - 1934 Old photographs indicate that the spoil tips in the western area were a distinct conical shape (Maclane cones) with a similar height to Tarren-y-Twyn headland.

1948 This map indicates the Old Coal levels along the eastern valley side, the Old Tramway, the spoil tip to the east appears slightly larger than the 1901 edition. Ty'n-y-gelli is no longer present.

A spoil tip to the north of Pen-y-crug has appeared on the western valley side and south of Tarren-y-Trwyn.

The aerial photo (Fig. 3.17) shows the Maclane cones produced from the iron and steel works.

1951 The aerial photo (Fig. 3.18) shows the Maclane cones produced from the iron and steel works.

1956 The Agricultural land Classification of England and Wales confirms that Silent Valley was generally used for land primarily in non-agricultural use.

1969 The spoil tip on the western area has developed to cover an area approximately 146,000 m² (14.6 ha) (Fig. 3.19). An additional feature to the north of the spoil tip, suggests another tip or that a landslide deposit may be present immediately to the southeast of Tarren y Trwyn.

On the eastern side of the valley there is a tip that was visible as some rubble on the 1901 map to the south of the Old Coal Level.

1960s – early 1980 Llanwern Slag Ltd was involved in the removal of blast furnace slag to use as aggregate. Heckett Ltd recovered the metals from the slag and sold them back to British Steel.

1970s British Steel Corporation culverted the Nant Merddog beneath part of the steelworks waste tips in a 750 mm internal diameter concrete pipeline, the BSC pipeline.

1979 Geological Map (Fig. 3.3) showing adits and shafts that are in use and have been abandoned. A thick slag heap is shown across the site.

1981 In 1981 the site was sold by British Steel to Blaenau Gwent Borough Council and was licensed to accept domestic refuse. It was run as Silent Valley Landfill by Blaenau Gwent Borough Council. At this time major civil engineering works were carried out to culvert the Nant Merddog along with additional drainage along the eastern slopes in order to control the surface water run off.

1983 A new pipeline was constructed to convey the Nant Merddog to the east of the original stream course.

1986 – 1988 Carn Tillery workings in the Brithdir Seam upper leaf were carried out beneath the hillside scarp to the north of the site.

- 1990 The spoil tip on the western flanks is now described as disused with a dismantled tramway leading up to it from the main valley of Ebbw Vale. A Nature Reserve exists to the south on the eastern valley slopes.
- 1992 An adit to the north of the existing landfill site was closed.
- 1993 Blaenau Gwent Borough Council installed a plastic drain along the valley between the slag on the western side of the valley and the landfill on the east to collect drainage from the upper parts of the valley and divert it beneath the proposed landfill.
- 1994 Silent Valley Waste Services Limited, a LAWDC undertook the responsibility of waste disposal in the valley in August 1994.
- 2000 Aerial photograph (Fig. 3.20) showing the landfill site.
- 2001 The Southern Flank was capped, with 850 mm of overburden and then hydroseeded, to reduce infiltration into the landfill. Drainage ditches around the site were lined with concrete to reduce their erosion.

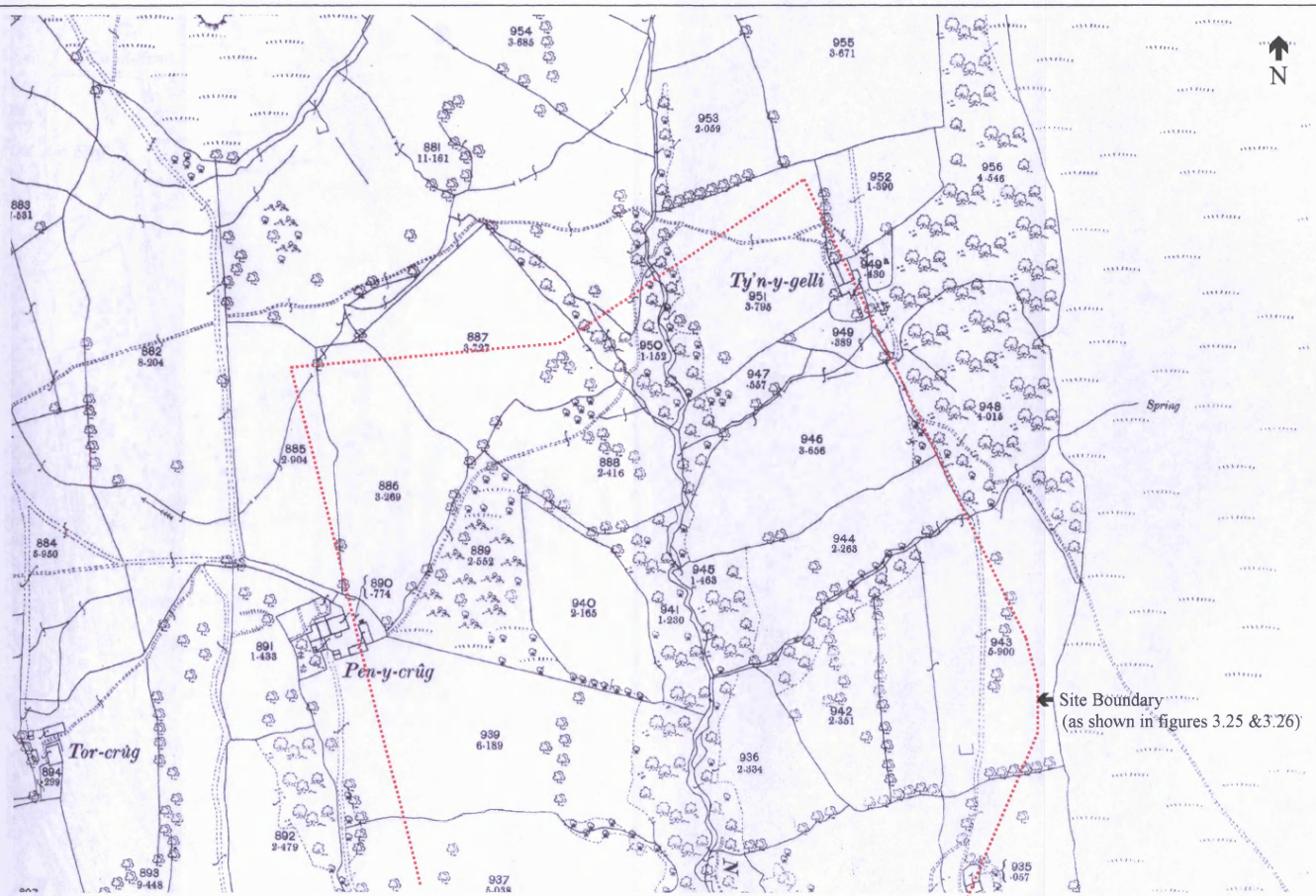


Figure 3.14 Map taken from the 1880 1:2500 Monmouthshire map. Reproduced to scale.

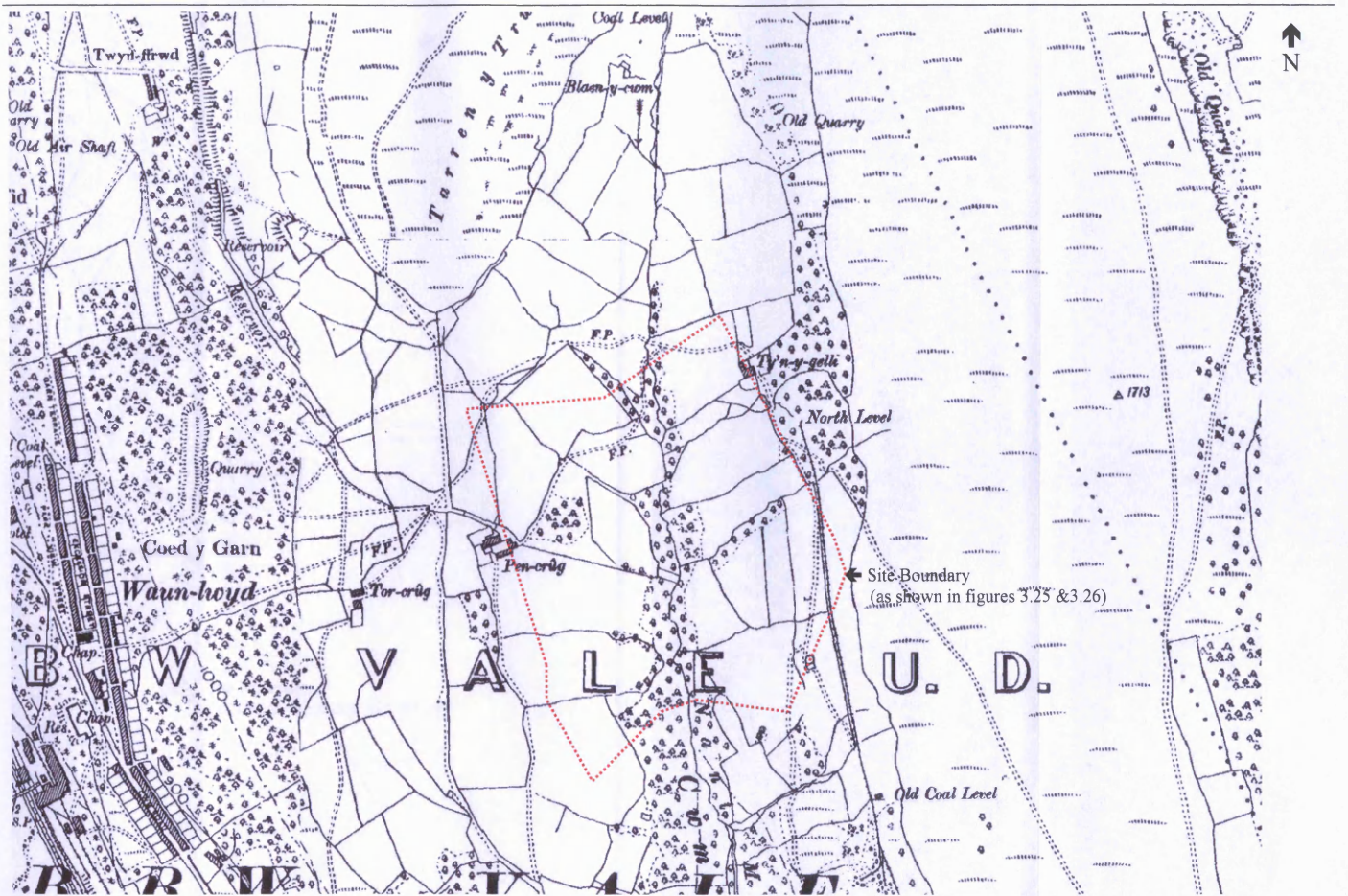


Figure 3.15 Map taken from the 1901 1:10,560 Monmouthshire map. Reproduced to scale.

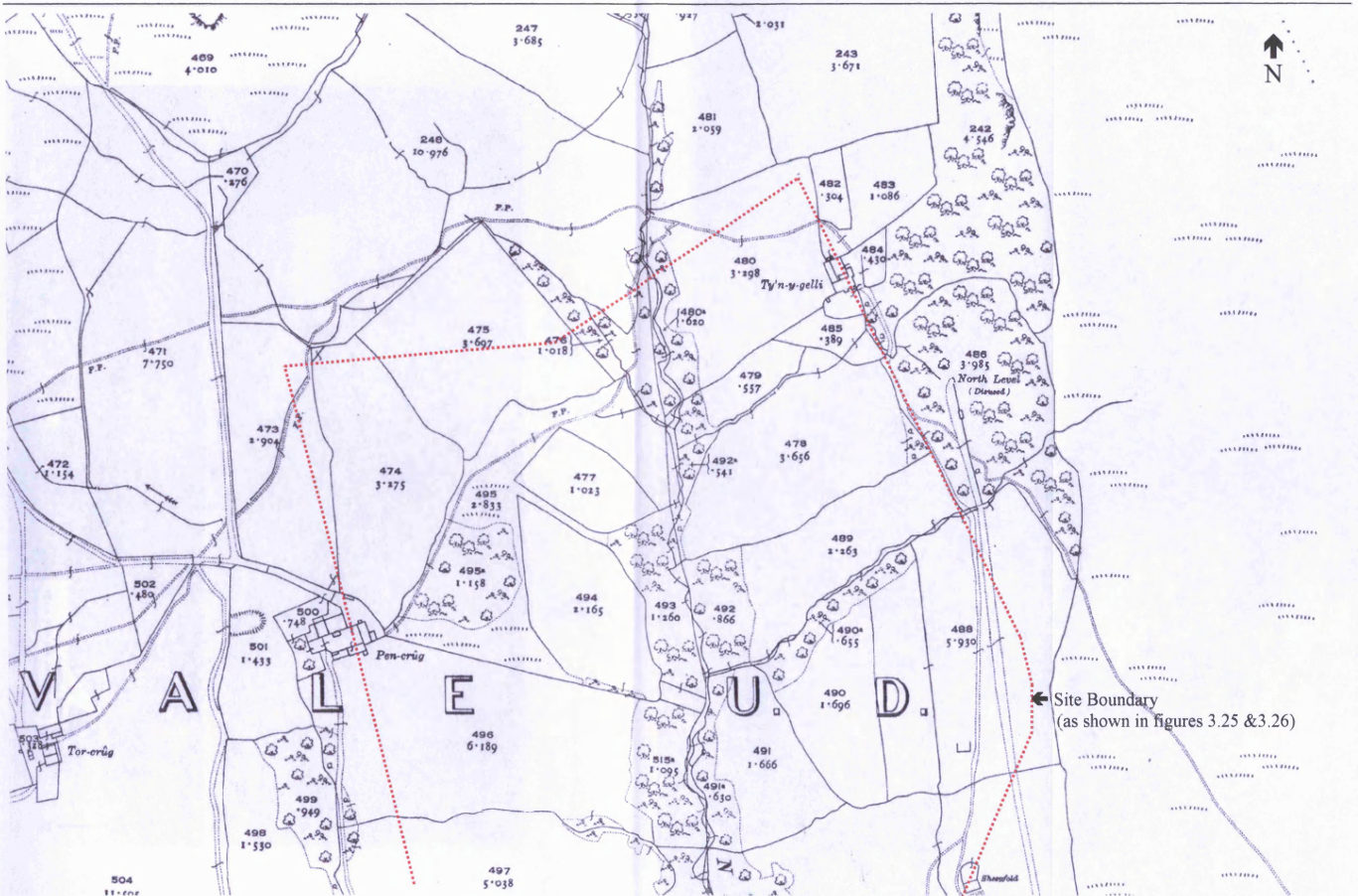


Figure 3.16 Map taken from the 1920 1:2500 Monmouthshire map. Reproduced to scale.

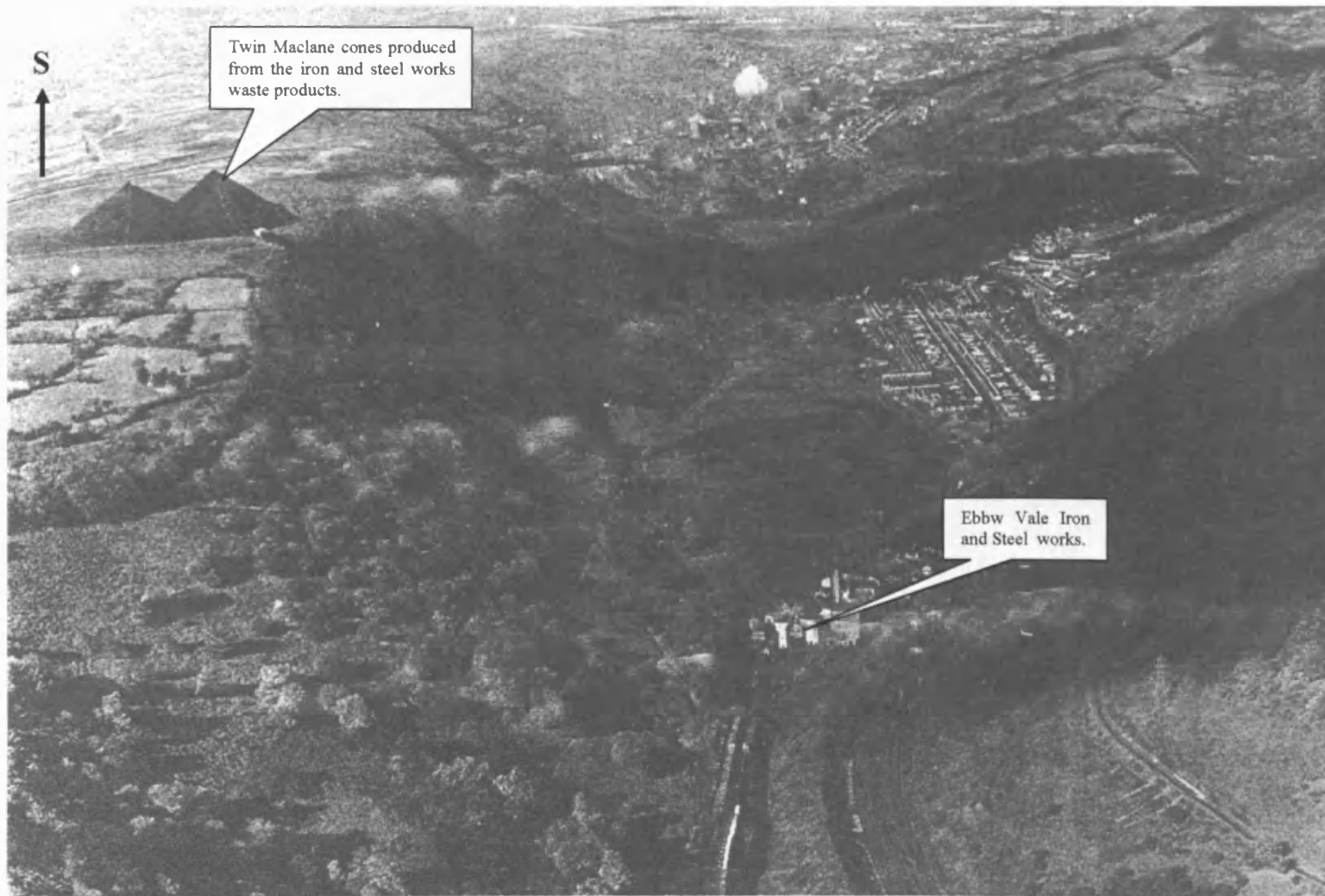


Figure 3.17 Oblique aerial photograph showing the twin Maclane cones at Cwm Merddog taken on 26th October 1948 (supplied courtesy of the Welsh Office, 2002).

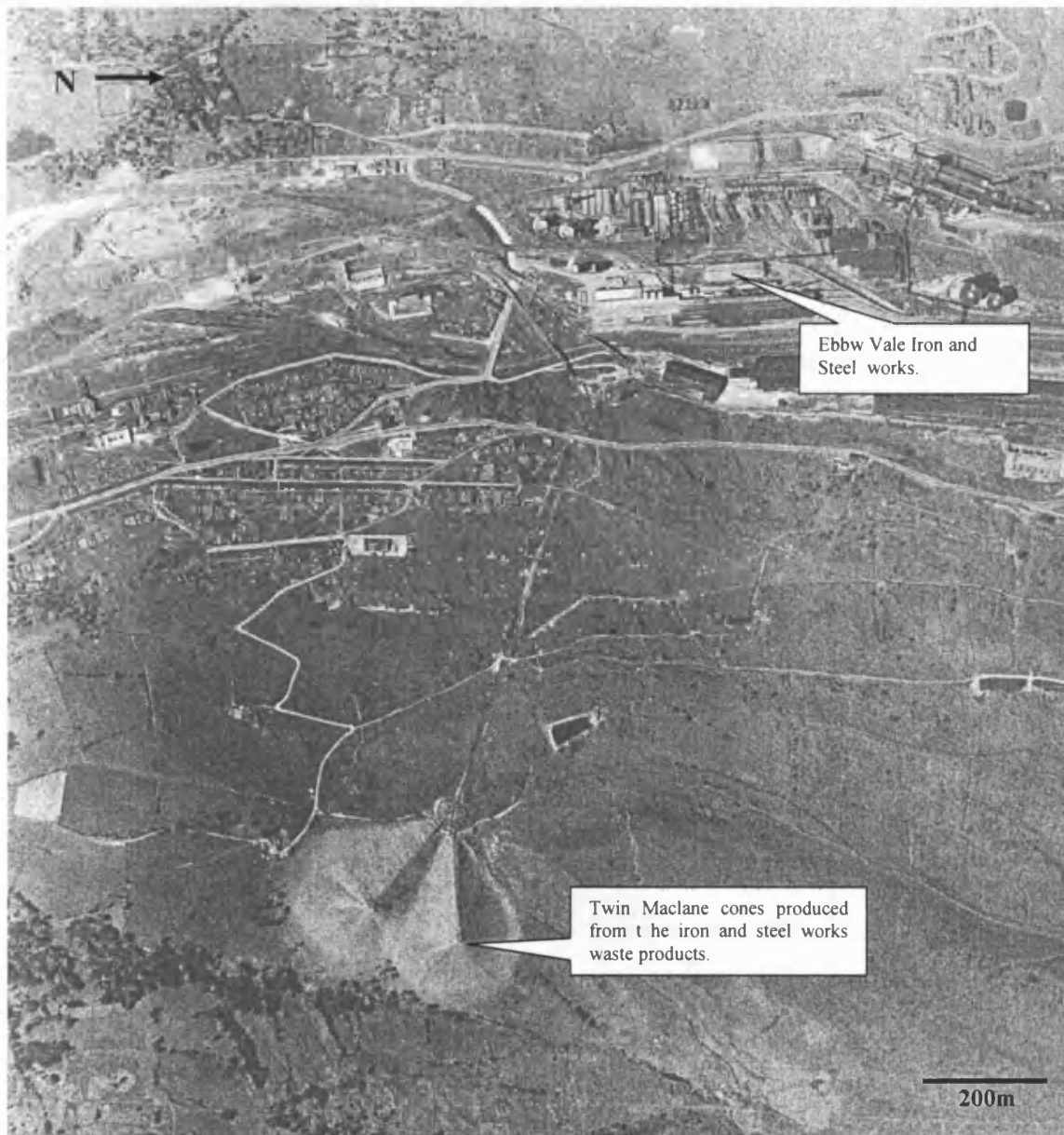


Figure 3.18 Aerial photograph showing the twin Maclane cones at Cwm Merddog taken on 12th May 1951 (supplied courtesy of the Welsh Office, 2002).



<p>Abbreviations</p> <p>Boundary Post or Stone BP, BS</p> <p>Church Ch</p> <p>Fire Engine Station FE Sta</p> <p>Five Bridge FB</p> <p>Footpath Fp</p> <p>Grade Post GP</p> <p>Mile Post MP</p> <p>Mile Stone MS</p> <p>Police Station Pol Sta</p> <p>Post Office PO</p> <p>Public Convenience PC</p> <p>Public House PH</p> <p>Signal Box SB</p> <p>Springs Sp</p> <p>Telephone Call Box TCB</p> <p>Telephone Call Post TCP</p> <p>Well W</p>	<p>Boundaries</p> <p>Geographical County - - - - -</p> <p>Administrative County, County Borough or County of City - - - - -</p> <p>Municipal Borough, Urban or Rural District, Borough or District Council - - - - -</p> <p>Civil Parish - - - - -</p> <p>Borough, Borough or County Constabulary - - - - -</p>	<p>Heights</p> <p>Values are given in feet above Mean Sea Level at Newlyn. Contours are at 100 feet interval.</p> <p>Surface heights determined by ground survey or survey.</p>	<p>Rock Features</p> <p>Lime Rock, Bracken, Dolomite, Stone</p>
--	--	--	--

<p>Road - - - - -</p> <p>Track - - - - -</p> <p>Path - - - - -</p> <p>Ministry of Transport Road Numbering</p> <p>M1 (M AEM)</p> <p>Trunk Road A17</p> <p>Main Road B16</p> <p>Secondary Road B16</p>	<p>Railways</p> <p>Cutting - - - - -</p> <p>Embankment - - - - -</p> <p>Standard Gauge - - - - -</p> <p>Narrow Gauge - - - - -</p>	<p>Lake, Loch or Pond - - - - -</p> <p>Gravel Pit - - - - -</p> <p>Sand Pit - - - - -</p> <p>Overgrown Pit or Clay Pit - - - - -</p> <p>Refuse or Slag Heap - - - - -</p> <p>Brickworks - - - - -</p> <p>Quarry, Chalk or Clay Pit - - - - -</p> <p>Antiquity (site of) - - - - -</p> <p>Triangulation Station - - - - -</p> <p>Dunes - - - - -</p>
---	---	---

Figure 3.19 1969 map of area around Silent Valley landfill site. Sheet SO 10 NE.

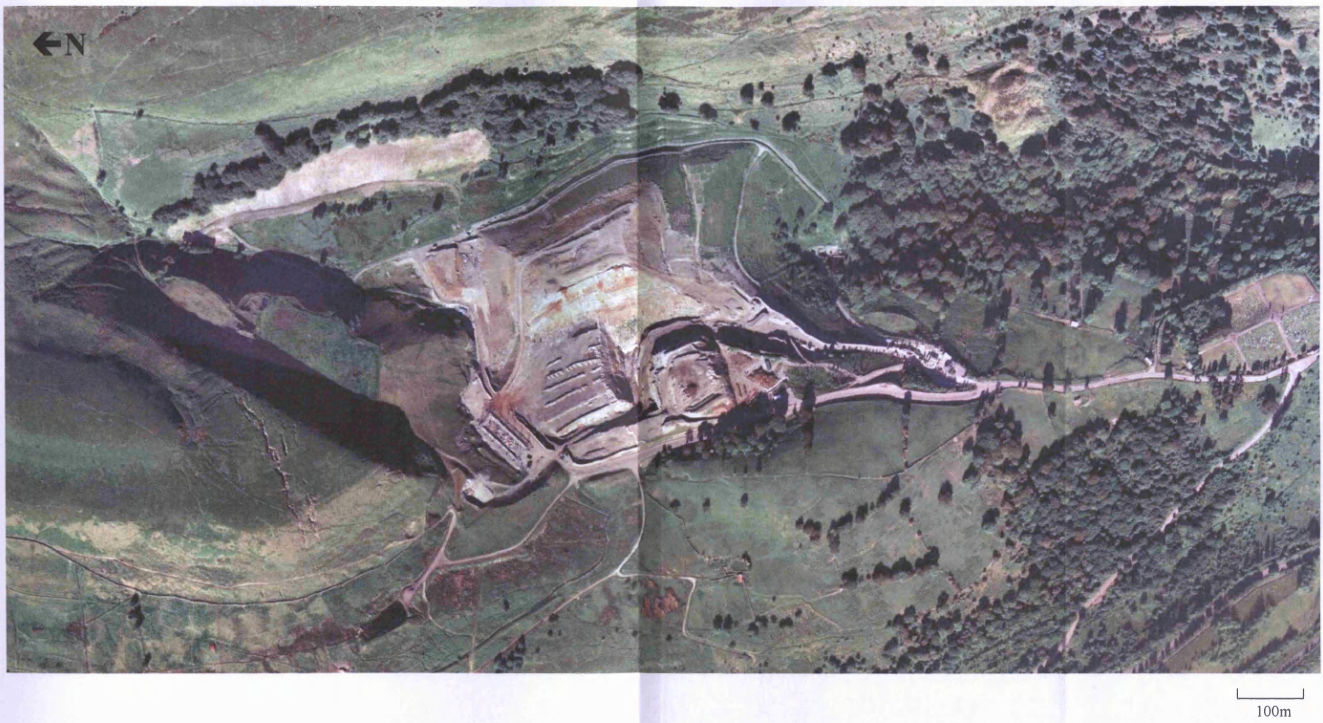


Figure 3.20 Georeferenced photograph of Silent Valley taken in 2000. From Getmapping.com

3.6 PRESENT SITE CONDITIONS

3.6.1 SITE LAYOUT

The operational site can be divided into two areas. Phase I (20.1 ha) is active at present and Phase II (13.5 ha) is the proposed area for future development (Fig. 3.21). Phase I is located to the south of the site. The southern face was filled, in an uncontrolled manner, during the early 1980s while Blaenau Gwent Borough Council ran the site. Phase IA is the present day active phase, which is working northward from this face.

The site has offices located to the south of the site where all visitors must report. A road leads from the site offices around the western periphery of the site. There is a weighbridge along this road that monitors all fill entering the site. At the top of this road, where vehicles exit the active area of the site, there is a wheel wash. To the north of the site there is a waste paper containment cell.

Next to the site offices there is a civil amenity site open to the public. There are large skips and some facilities for recycling.

At the south end of the site there is the settlement tank that receives the collected leachate and contaminated water. From here the wastewater goes to the foul sewer.

The site is surrounded by 2 main blocks of semi-natural beech woodland; found at Cwm Merddog (south) and Coed Tyn y Gelli (east). The area has been declared as a Local Nature Reserve with much of it designated as a SSSI.

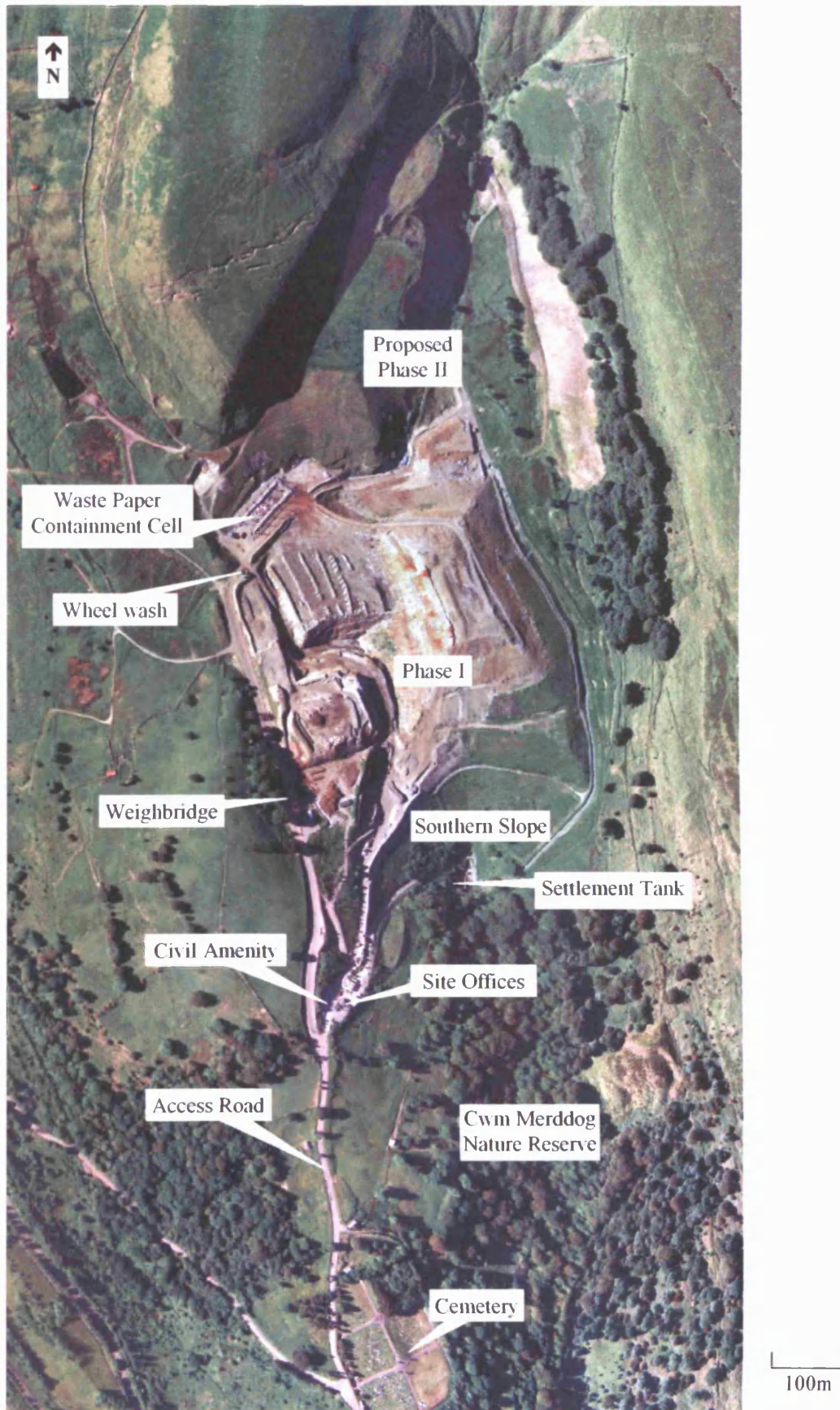


Figure 3.21 Photograph (taken 2000) showing the layout of Silent Valley landfill site.

3.6.2 GROUND CONDITIONS

3.6.2.1 Superficial Deposits

3.6.2.1.1 Made Ground

Broadly speaking, the eastern part of the site is occupied by landfill and the western part by the pre-existing slag bank.

3.6.2.1.1.1 Landfill

The landfill consists of layers of industrial, commercial and domestic refuse. In 1994 the household waste comprised about 33% of the total and about 26% of the total in 1995 (Ove Arup & Partners, 1996b).

The landfill is constructed by heavily compacting the waste in normally 2 m thick layers and covering it with a normally 0.15 m thick cover layer, generally of slag material. Slag fill is also used in the construction of cells and haul roads.

Waste Management Paper 26B (DoE, 1995) suggests that landfill density in the range 0.65 to 0.85 tonnes/m³ should be used for planning purposes. Using weighings of incoming material and site surveys, the average unit weight of the as placed materials in 1989 was 1.15 tonnes/m³. A field measurement in 1992, on six month old waste, gave a unit weight of 1.37 tonnes/m³. A survey in 1995 found that the incoming waste occupied space at a rate of 1.1 tonnes/m³. The proportion of cover layer and contaminant bund was assessed to be in the range of 20% to 30% by volume. Using an average density of 1.5 tonnes/m³ for the slag construction material, the overall average density of the as placed material would be in the range 1.2 to 1.4 tonnes/m³ (Ove Arup & Partners, 1996b). Subsequent increases in moisture content, depth of burial, degradation and settlement would all increase density after placement.

3.6.2.1.1.2 Steelworks Waste

Slag fill occupies a large part of the western part of the site and is up to 21 m thick in borehole GA/93/6B (Golder Associates, 1993d). The slag is thickest to the southern end of the site, thinning to the north. Golder Associates (1993d) suggest that the slag between GA/93/1D and GA/93/11 and between GA/93/1D and GA/93/6B may be up to 36 m thick (Fig. 3.24; Fig. 4.1).

The slag is variable ranging from fine ash like material to cobble and boulder sized fragments. The slag appears to be layered, as observed in the faces of the slag tip where it has been excavated for use as daily cover (Fig. 3.22). Within the slag, layers of soft clay and also large timbers and metal fragments can be found. Damp layers associated with the soft clays suggest that they are generating local perched water tables.

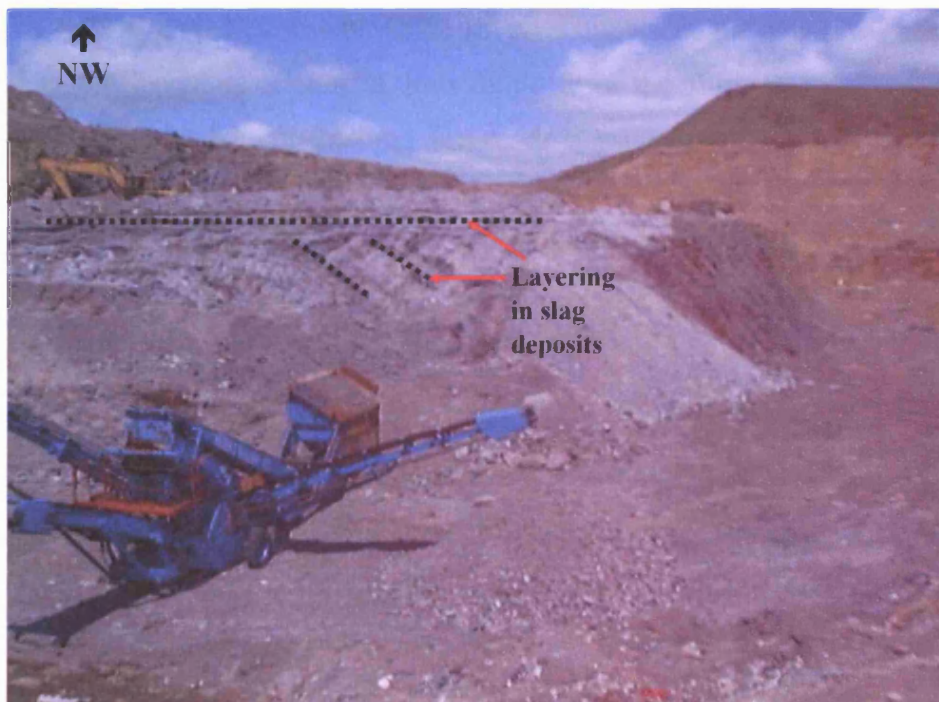


Figure 3.22 Photograph showing layering within the slag deposits taken June 2001.

Golder Associates (1993d) collected 4 samples of slag for laboratory testing. Two of the samples were predominately medium to coarse gravel while the other two were fine-medium gravel with a significant proportion of coarse sand sized material. Compaction

test results gave maximum dry density of 1.76 – 2.32 Mg/m³ [1.76 – 2.32 tonnes/m³]. The maximum dry density are likely to be influenced by the particle density of the material which may vary considerably depending on the proportion of metals within the slag.

Waste palm oil from the British Steel Corporation tinplate works was disposed of in trenches dug into the slag banks across the northwest plateau. The British Steel plant used a lubrication during cold rolling processes, which was primarily beef tallow fat, containing small amounts of pressure additives and preservatives, which during the rolling process become adulterated with mineral oils and iron. The final waste oil was disposed as an aqueous emulsion containing approximately 70% water. It was estimated that 8000 tonnes of this effluent was disposed at Silent Valley annually (Celtic Technologies, 1995).

Celtic Technologies (1995) analysed the slag at Silent Valley. It was found that clean slag on site consists of approximately 18% iron. Samples from other areas of the site ranged between 0.79% and 33.3% with 89% of all samples below the level for clean slag, indicating the leaching of iron as iron oxide from the fill. In many areas there was evidence of this seen by a distinct red iron oxide staining on the surface.

3.6.2.1.2 Landslip Deposits

Landslip deposits were encountered in several boreholes that were sunk by Exploration Associates Ltd and supervised and logged by Ove Arup & Partners to the north of the site in Phase 2. The deposit was characterised by a yellow plastic clay flush return during open-hole drilling. Rotary coring was carried out to determine the nature of the deposits and to identify the base of the landslip deposits.

The landslip deposits were generally heterogeneous, consisting mainly of gravelly clay with frequent boulders and cobbles. Changes in bedding angle revealed where boreholes had penetrated boulder deposits and blocks of displaced strata.

In boreholes EA3A and EA4 (Fig. 3.24; Fig. 4.1), slickensided slip surfaces within thin layers of soft, grey very plastic clay were recovered from the base of the landslip deposits. Direct shear testing of the slip surface found in BH3A, gave a residual effective shear strength of $c_r'=0$, $\phi_r'=16^\circ$. Ring shear testing performed on 2 disturbed samples from BH4 gave a residual strength of $c_r'=0$, $\phi_r'=17.5^\circ$ for both samples (Ove Arup & Partners, 1996a).

3.6.2.2 Geological Structure

The dip of the strata at the site is approximately 4 degrees towards the south-west, although there is some local variation.

There are a number of faults on the plateau to the east of the site (Fig. 3.3), which trend northwest-southeast and are often expressed at the surface as deep fissures. It is possible that some of these faults are derived from collapse subsequent to coal extraction, rather than geological processes.

Discontinuities are well developed in the Brithdir and Hughes sandstones and to a lesser degree in the argillaceous beds of the Rhondda and Brithdir beds. They tend to be subvertical and parallel to the major fault structures, with a secondary set at right angles. Within the arenaceous beds the discontinuities are extremely persistent and are generally open, thus having a significant effect on permeability and rock slope stability (Golder Associates, 1993a; 1993b).

The landslip survey of the South Wales Coalfield (Institute of Geological Science, 1980) indicates that the slip on the west side of Cwm Merddog below Tarren y Trwyn (SO 185 075) is a shallow translational slip in the Rhondda shale and superficial materials with a slope angle of 16.7° . At present it is dormant and has an area of 2 hectares and extends on the valley side between 390 and 420 m AOD.

The other landslide affecting the Silent Valley site is that on the Eastern bank of Cwm Merddog (SO 189 066) opposite the spoil tip. It is described as a translational debris flow in superficial material and occurs within the Rhondda and Brithdir shales with a slope angle of 15.7°. The lower part of the slip is covered by spoil. At present it is dormant, has an area of 2 hectares and is at a height between 405 and 360 m (Golder Associates, 1993a; 1993b).

The Darren Ddu landslip was caused by the reactivation of fault planes and the formation of subsidence fissures by undermining (Barclay, 1989).

There is a significant arcuate tension crack at the edge of the hillside to the north of the site following mining of the Brithdir Seam upper leaf at Carn Tillery workings (Fig 3.23). Ove Arup & Partners (1996a) determined that the tension crack appeared between 1985 and 1991 by looking at aerial photographs. The position of the tension crack corresponds with a typical angle of draw of 70° from the edge of the mine workings (Ove Arup & Partners, 1996a).

3.6.2.3 Stability

3.6.2.3.1 Phase 1A

Golder Associates (1994) performed a probabilistic risk assessment to assess the consequences of collapse of the plastic pipe on stability. The plastic pipe was installed in 1993 to collect all rainfall runoff from the area to the north-west of the landfill. The assessment examined the effect of an increase in the leachate level due to the pipe breaking or inefficient drainage.

Their input parameters included waste parameters, clay parameters, site geometry, BSC and Armco pipe performance and initial leachate head in the landfill. Many of the figures used by Golder Associates were based on empirical data. Their results indicated the probability of instability as follows:

- Both plastic pipe and stream diversion working and draining their respective catchment areas
16% (1 in 6.3 chance) in 50 years or 21% (1 in 4.7 chance) in 1000 years
- Plastic pipe damaged and all of its catchment water running into the landfill
16% (1 in 6.3 chance) in 50 years or 21% (1 in 4.7 chance) in 1000 years
- Plastic pipe damaged and stream diversion blocked, i.e. the whole catchment area water running into the landfill
18% (1 in 5.7 chance) in 50 years or 24% (1 in 4.2 chance) in 1000 years

Their analysis indicated that the material parameters of the clay have a significant effect on the stability.

Ove Arup & Partners (1995) consider that the stability analysis conducted by Golder Associates is based on unreasonable assumptions and that their results are not considered to be meaningful. Additional stability analysis, performed by Ove Arup & Partners, in terms of effective stress show that the landform rising to 414 mAOD has comfortably adequate factors of safety under the most severe foreseeable conditions.

Ove Arup & Partners (1996b) reviewed the stability of Phase 1A of the landfill site. Their stability analyses confirmed that the proposed mound to 414 mAOD will be adequately stable under the existing hydrogeological regime.

The risk of instability lies with a build up of water table levels considerably higher than have been found to date. As parts of the site are completed and capped and the surface drainage improved, the amount of water entering the landfill will be significantly reduced. Deterioration of the pipelines beneath the landfill could reduce the outflow capacity and cause an increase in the height of the water table. Ove Arup & Partners determined that this is likely to be a gradual process that could be monitored for.

3.6.2.3.2 Phase 2

Analysis of the existing profile of Phase 2 (Fig. 3.23) indicates that the presence of the steelworks waste tip increases the stability of the landslip by about 100%, compared with the pre-tipping profile (Ove Arup & Partners, 1996a). The increase in stability is because the tip increases the toe weight, increases the normal stresses acting on the basal slip surface and reduces the average pore pressure ratio. Ove Arup & Partners (1996a) computed minimum factors of safety in excess of 2.2, even when using the ‘worst’ piezometric conditions.

Reprofiling of the steelworks waste tip would remove toe weight and reduce the normal stresses acting on the basal slip surface. Under the proposed reprofiling, the computed minimum factor of safety for overall stability is 1.41 using the ‘worst’ piezometric conditions, which is considered as adequate for an extreme event. The factor of safety increases to 1.71 with the maximum recorded piezometric surface (Ove Arup & Partners, 1996a).

3.6.2.4 Economic Geology

3.6.2.4.1 Coal

In the main Ebbw Valley deep mining of the Middle and Lower Coal Measures have been carried out from Waunlywd Colliery (1876 to 1963) and the Marine Colliery at Cwm (1889). The Ebbw Vale Steel, Iron and Coal Company sank the Marine Colliery. Beneath Silent Valley the Old Coal was worked between 1983 to 1986.

A series of levels and trails have been driven into the eastern flanks of the main Ebbw Valley and into the Nant Merddog Valley. These were driven into the Rhondda, Rider, Brithdir Coal seams and Cefn Glas coal seam. In 1992 two adits to the north of the existing waste disposal site were closed (Golder Associates, 1993a; 1993b).

Silent Valley Licenced Opencast Mine operated to the north-east of the site in 1994/95 (Ove Arup & Partners, 1995).

3.6.2.4.2 Iron Ore

Ironstones occur as thin tabular beds or nodular concretions in the Lower and Middle Coal Measures. In the main Ebbw Valley the operation of Ironworks commenced in 1790. This eventually developed into steel works under the British Steel Corporation in 1949. The steel works is responsible for the spoil tip on the western flanks of the Nant Merddog valley, which was transported via a tramway on the valley side.

3.6.2.4.3 Mineral Extraction

During the 1960's blast furnace slag was viewed as a resource and several companies were involved in the excavation of the spoil tip, and subsequent processing and utilisation of the

materials. Heckett Ltd recovered the metals from the slag and sold them back to British Steel.

Llanwern Slag Ltd was involved for 15 to 20 years in the removal of blast furnace slag from Silent Valley. They are reputed to have removed millions of tonnes of material. The material was screened depending on use and demand and was typically used for road building, foundation works, filter beds on sewage farms and drainage medium. Llanwern Slag went into liquidation in 1987 (Golder Associates, 1993a; 1993b).

3.6.3 TOPOGRAPHY & MORPHOLOGY

The morphology of Cwm Merddog is of glacial origin. Cwm Merddog once housed a small tributary glacier (Barclay, 1989).

Silent Valley Landfill is situated at a level between 310 and 440 m AOD. The north-south trending Merddog Valley consists of a cliffed headwall of Cefn-y-Areal with gentle slopes to the south, with an approximate 1:8 gradient. The Cwm Merddog joins the Ebbw Fawr Valley to the south.

The Nant Merddog stream originally flowed down the valley, however this has been diverted to flow along the eastern boundary of the landfill site.

Ove Arup & Partners (1995; 1996b) produced cross-sections (Fig. 3.24) to illustrate the ground conditions at the site. Original ground levels were estimated using aerial photos from 1955. The sections also show the surface as it was in 1994 and the proposed profile upon completion.

The National Remote Sensing Centre (NRSC) undertook photogrammetric work to produce ground contours for the site based on 1955 aerial photographs (Fig. 3.25). The NRSC stated an accuracy of ± 1.5 m for the contours (Ove Arup & Partners, 1995; 1996b). The contours clearly show the Maclane cones (Fig. 3.17; Fig. 3.18) of the spoil from the iron and steel works at Ebbw Vale.

Ordnance Survey undertook photogrammetric work to produce approximate 'base of refuse' contours using aerial photographs from 1983 (Fig. 3.26). The Ordnance Survey stated an accuracy of ± 0.6 m for the contours. The spoil of the Maclane cones have been reprofiled. Much of the material used for daily cover and to construct the cells was quarried locally from the banks of steelworks wastes, so the 1983 'base of refuse' contours will have been modified where these excavations took place (Ove Arup & Partners, 1995; 1996b).

A georeferenced image is a digital image, such as an air photograph, where each pixel has a known geographical reference. This allows the image to be placed correctly on top of a map or a 3D landscape surface. Figure 3.27a and 3.27b shows Silent Valley landfill site and the surrounding area as a 3D surface¹. The image used is an air photograph taken in 2000 and obtained from Getmapping.com.

¹ Images produced by Dr Peter Brabham, School of Earth, Ocean & Planetary Sciences, Cardiff University.

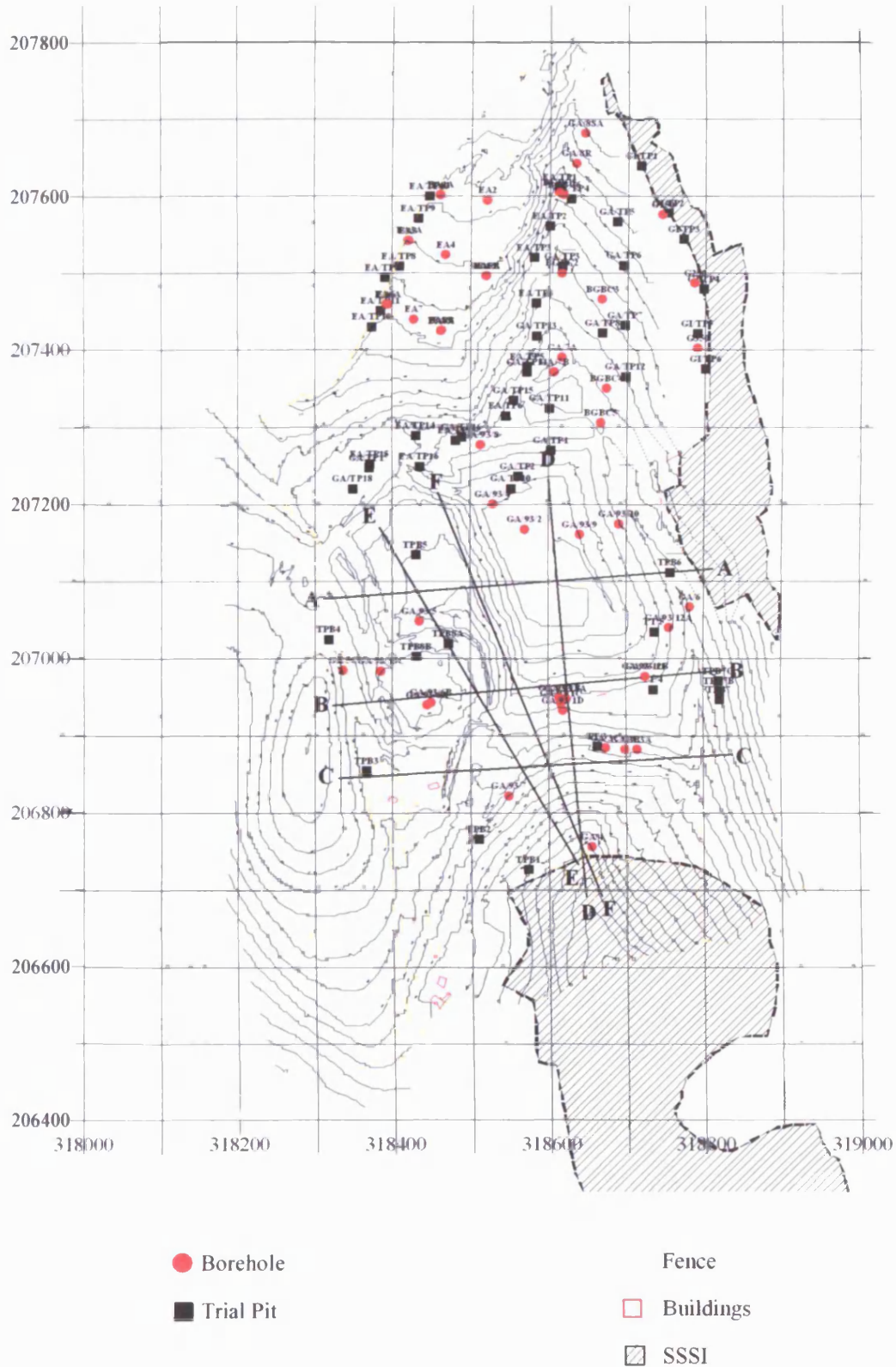
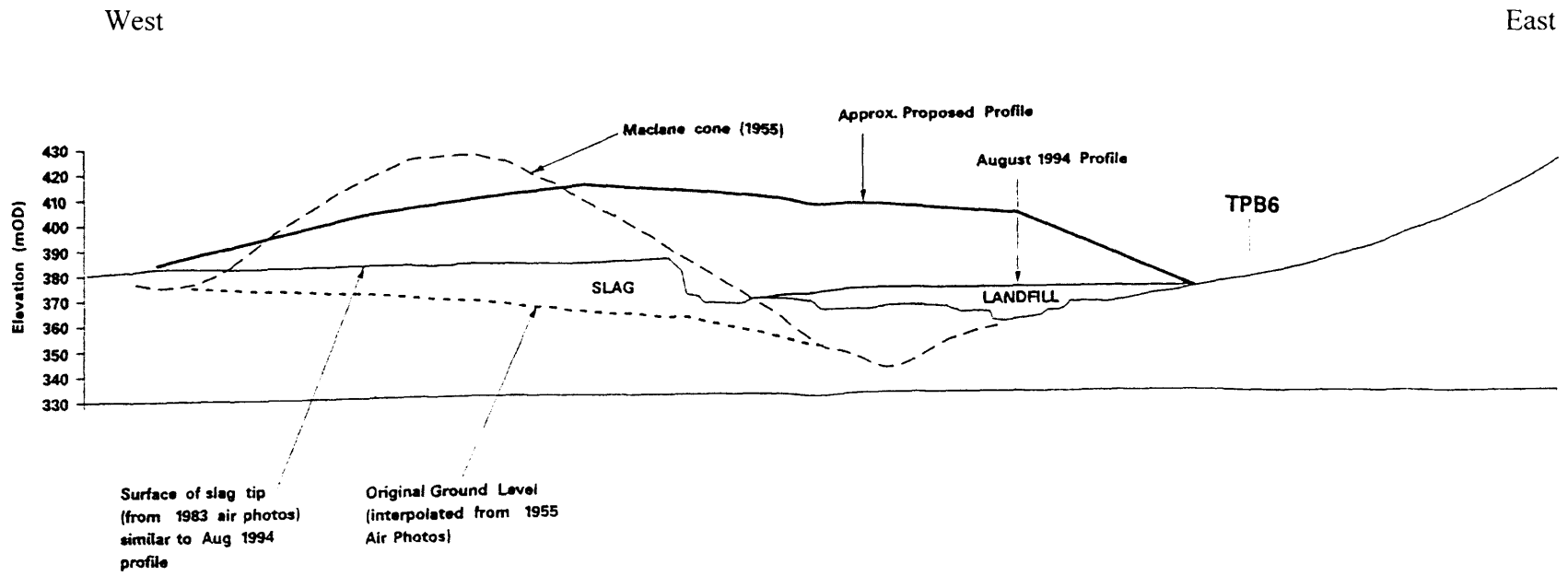
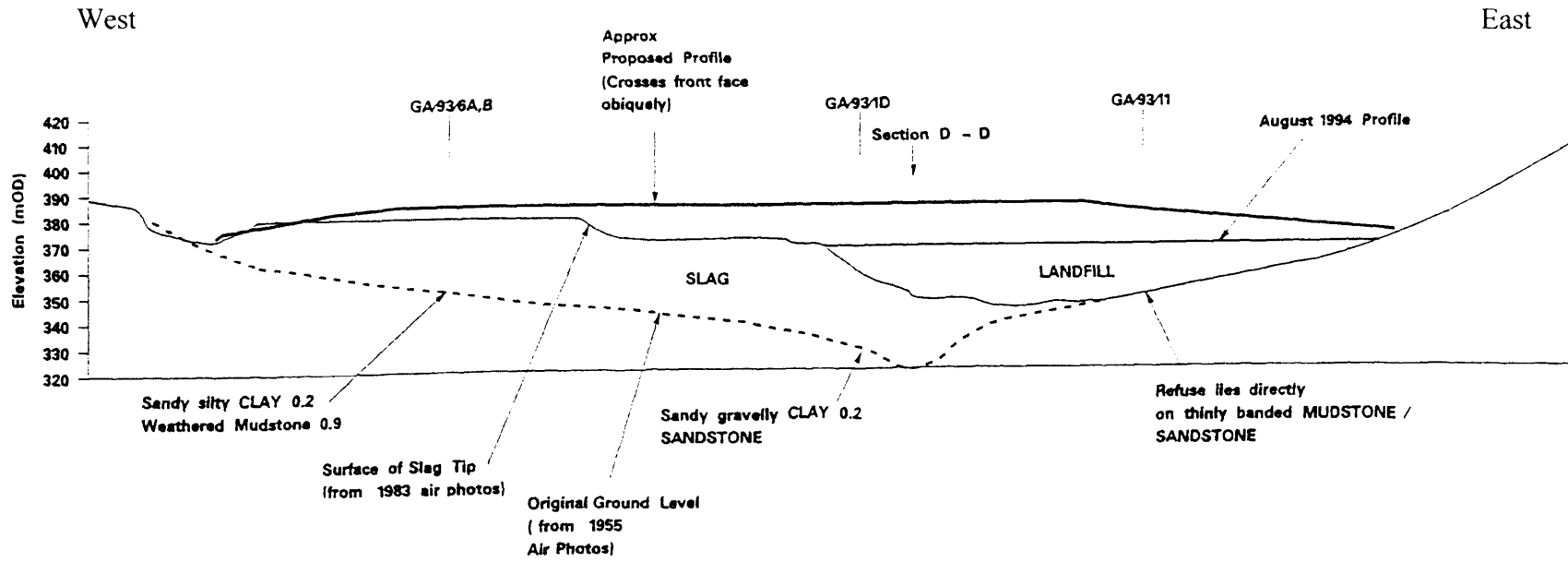


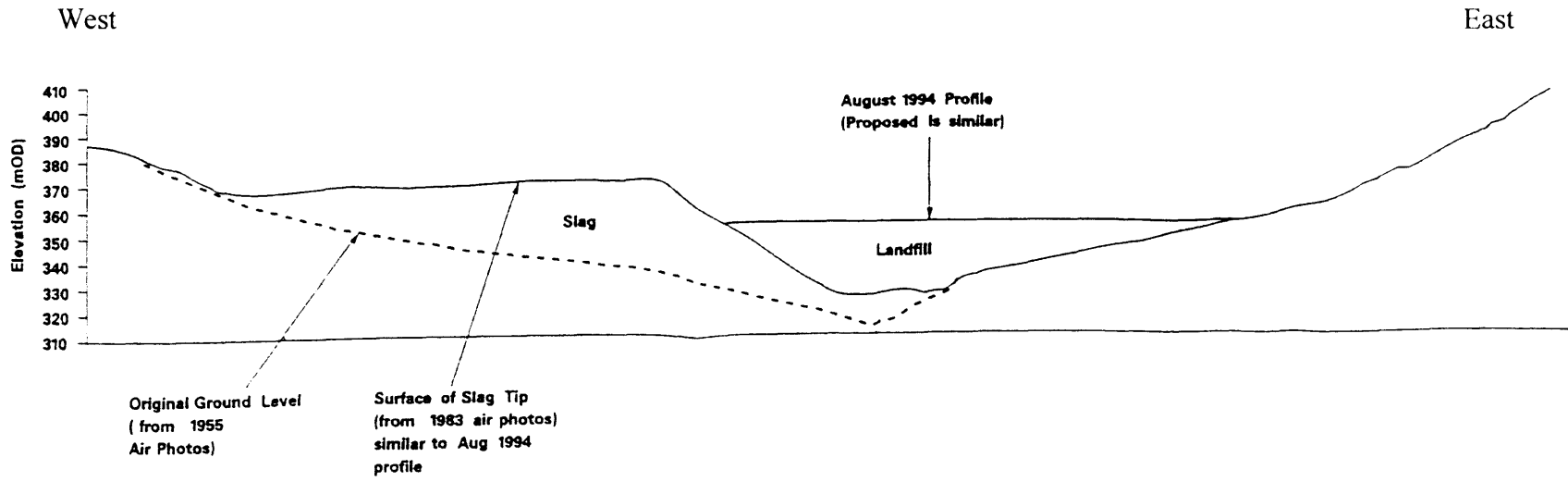
Figure 3.24 Map showing the location of the following cross-sections. Adapted from Ove Arup & Partners (1995; 1996b).



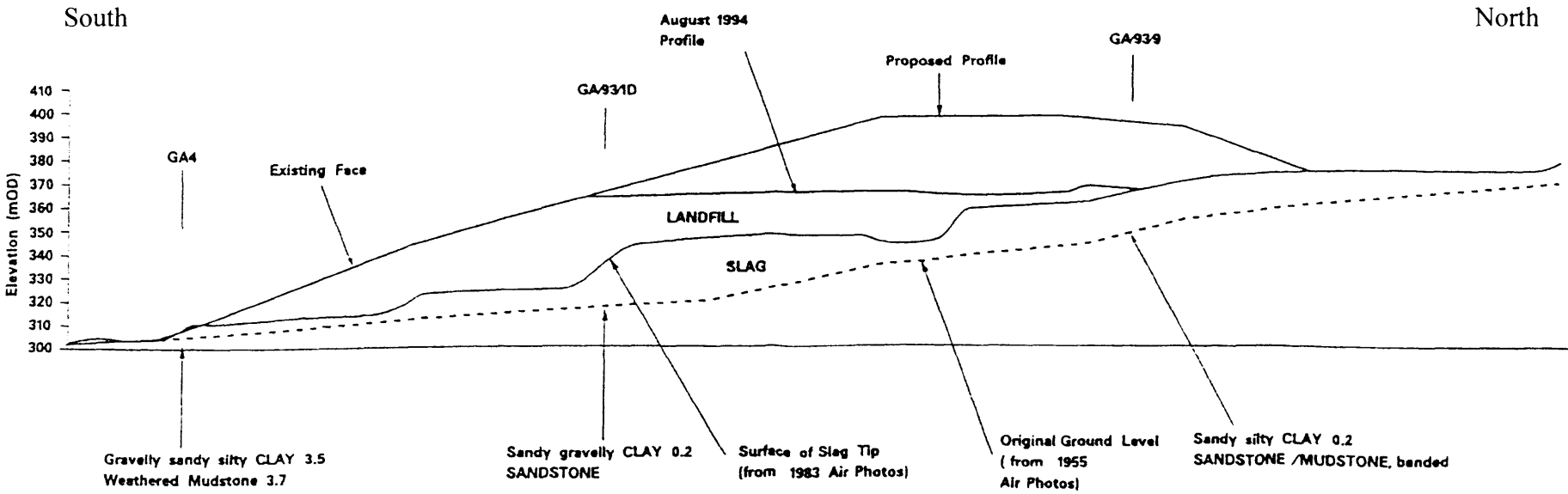
Cross section A-A



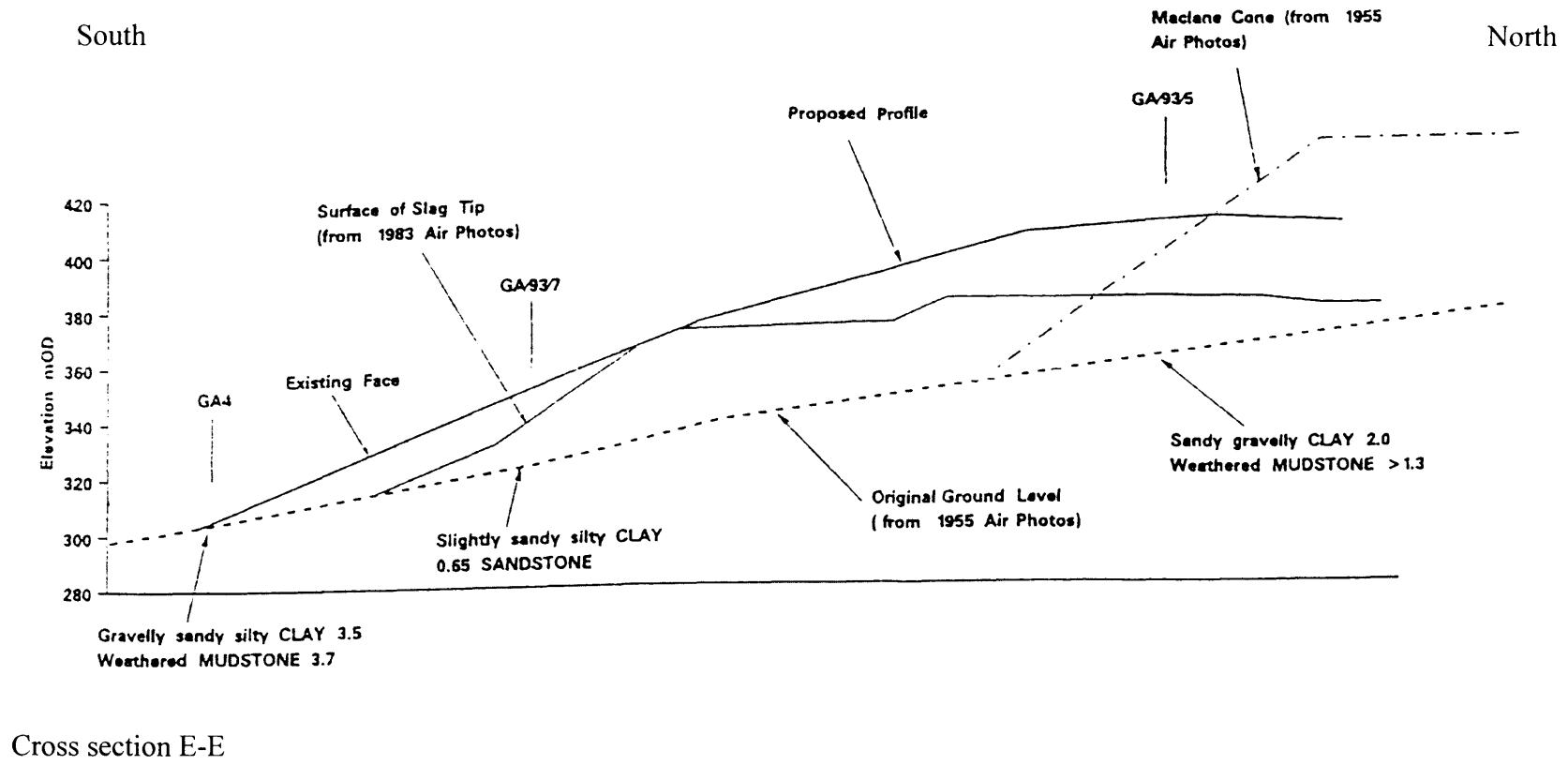
Cross section B-B

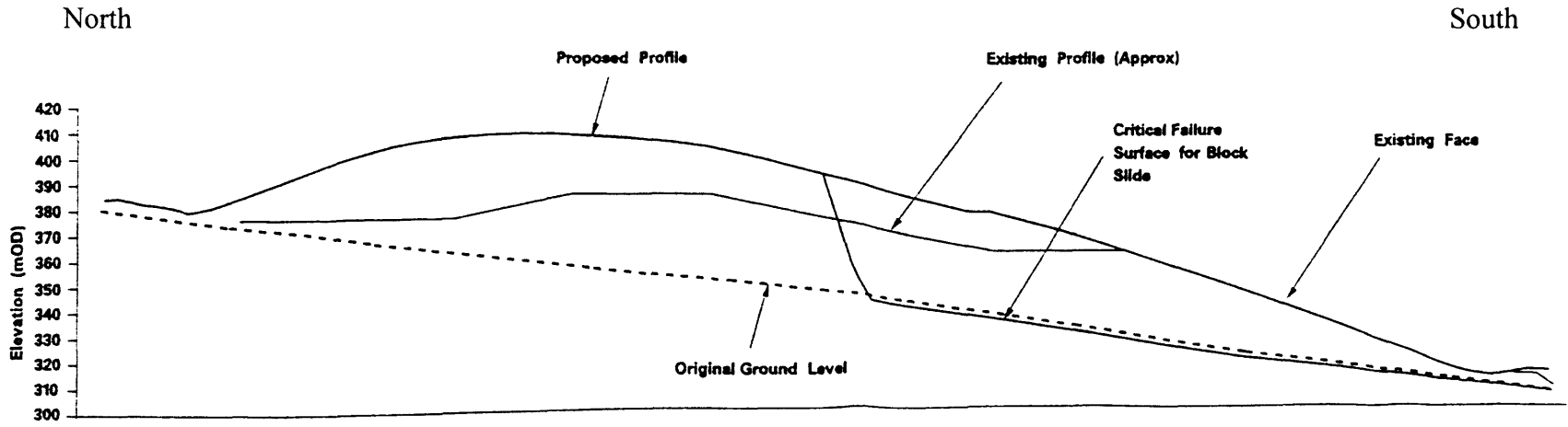


Cross section C-C



Cross section D-D





Cross section F-F

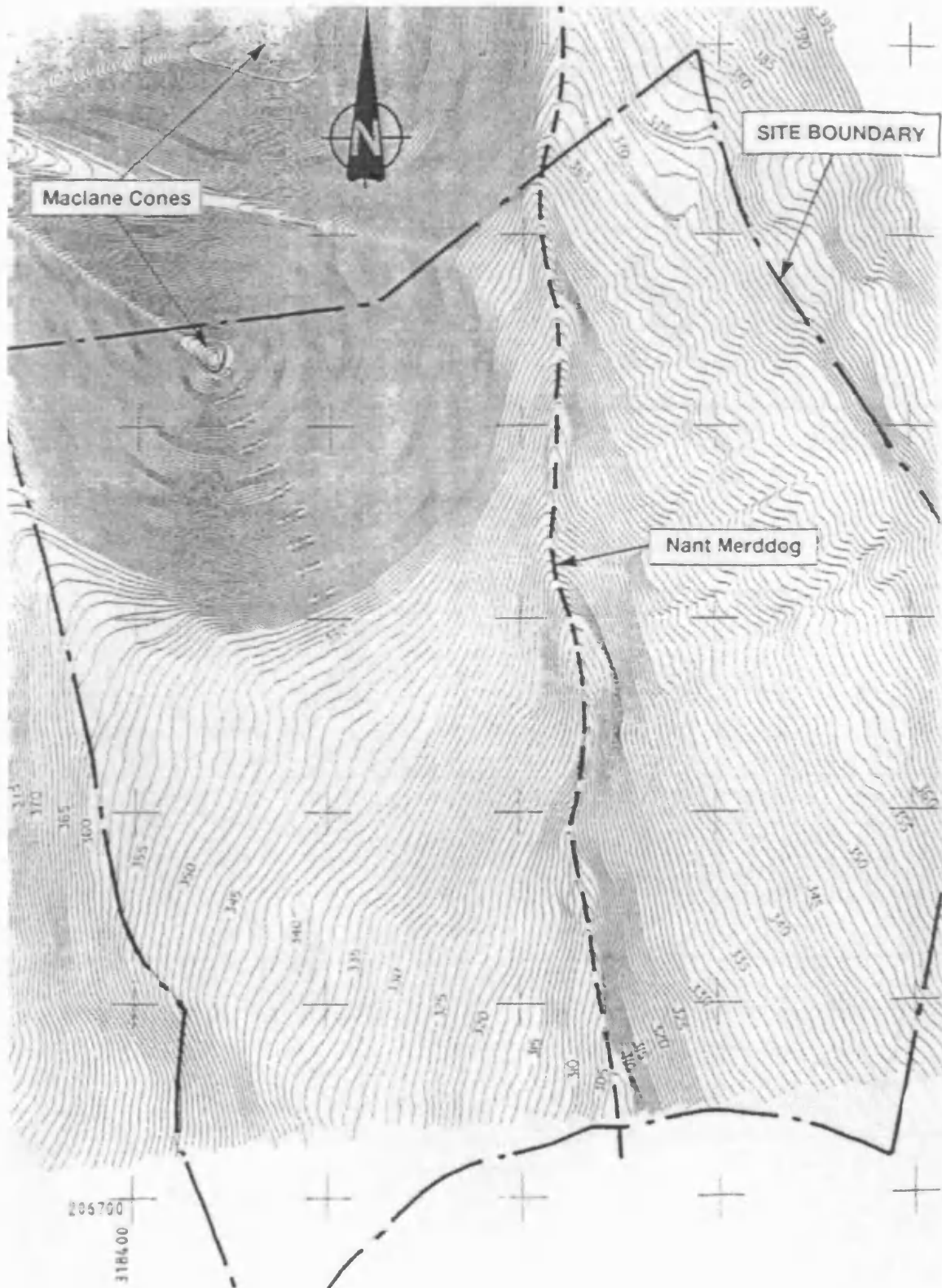


Figure 3.25 Contours of the site based on photogrammetric work of 1955 aerial photographs. From Ove Arup & Partners (1995; 1996b).

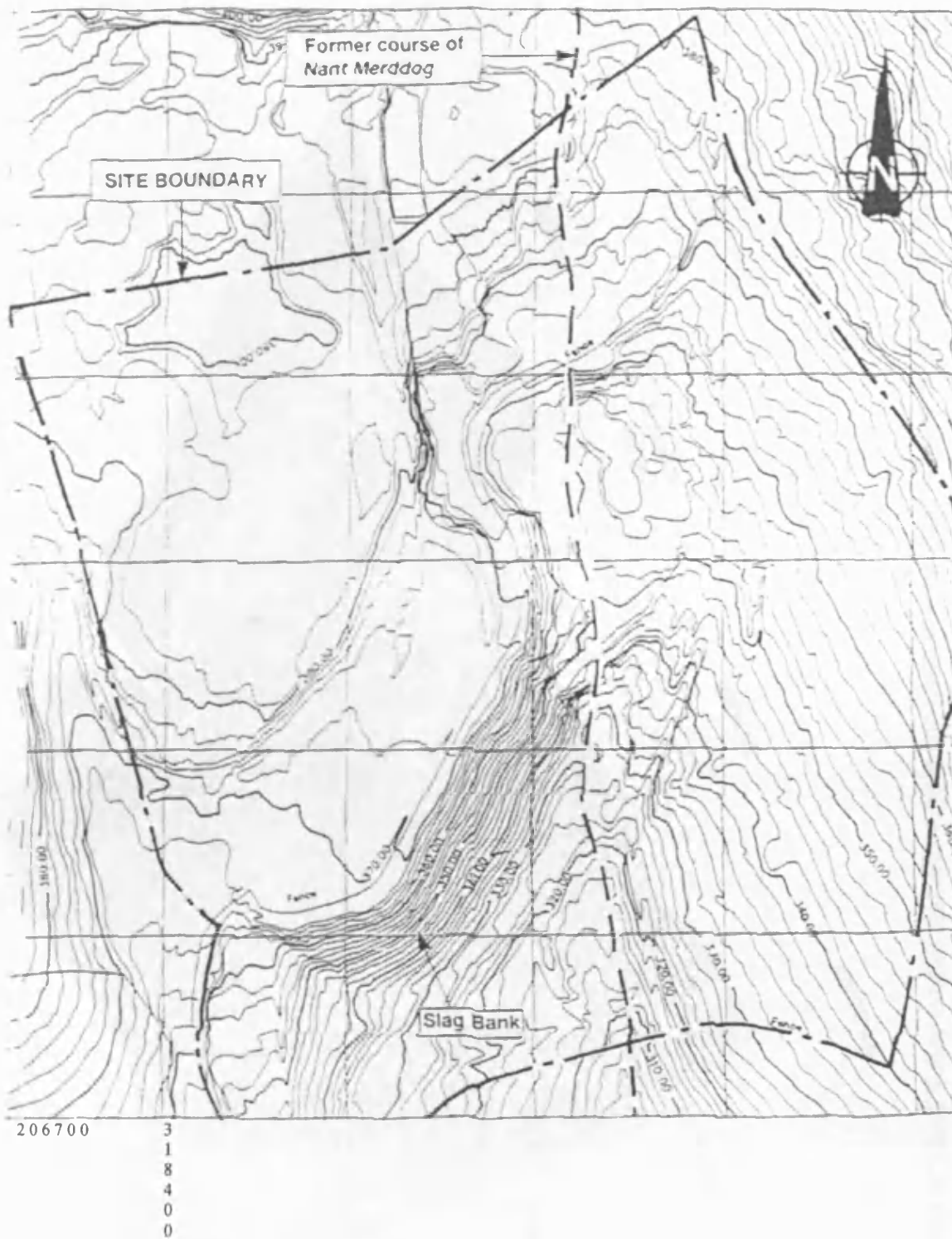


Figure 3.26 Contours of the site based on photogrammetric work of 1983 aerial photographs. From Ove Arup & Partners (1995; 1996b).

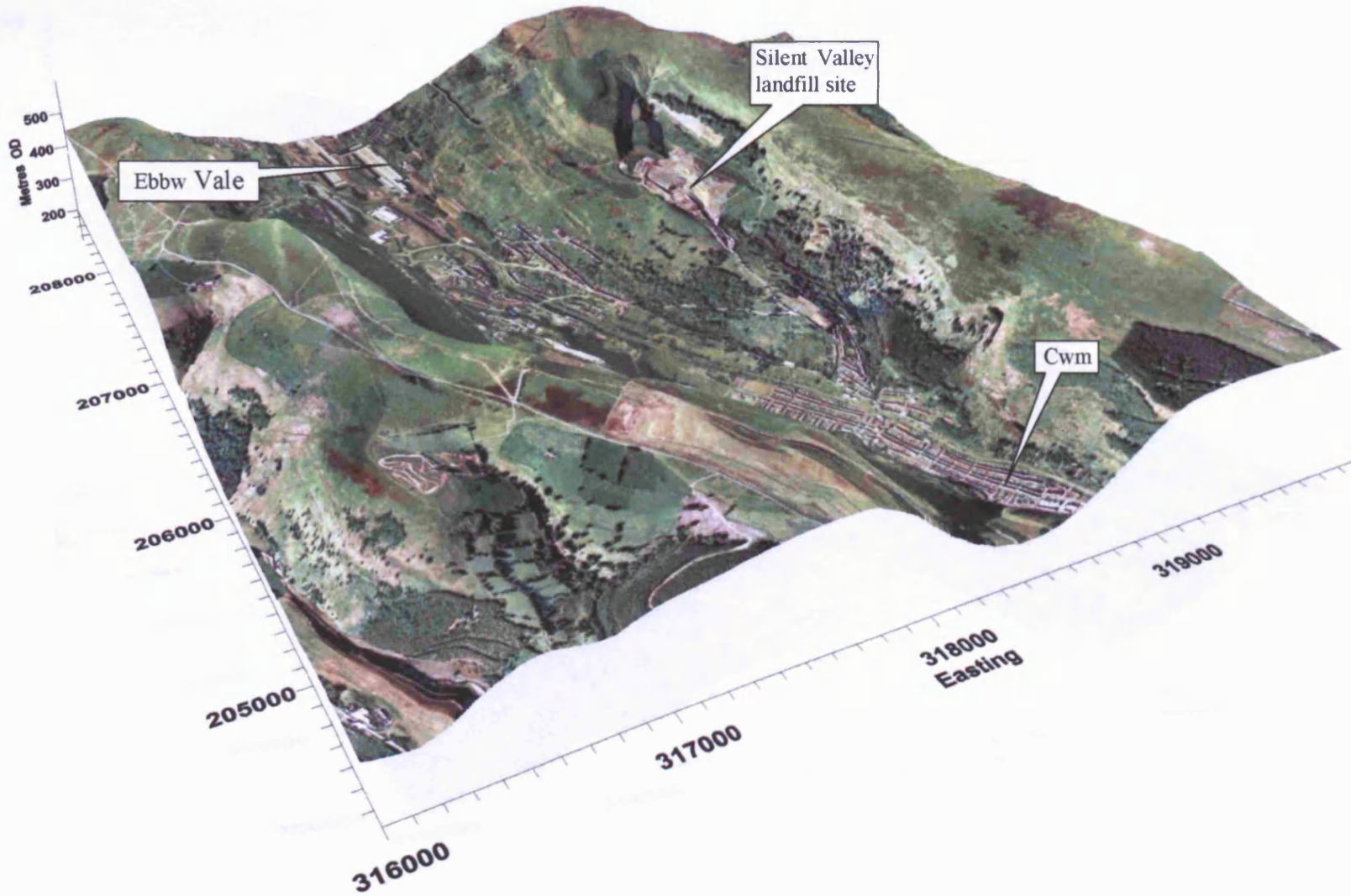


Figure 3.27a 3D surface of Silent Valley landfill site, Ebbw Vale and Cwm using a georeferenced air photograph taken in 2000. Image produced by Dr Peter Brabham, School of Earth, Ocean & Planetary Sciences, Cardiff University.

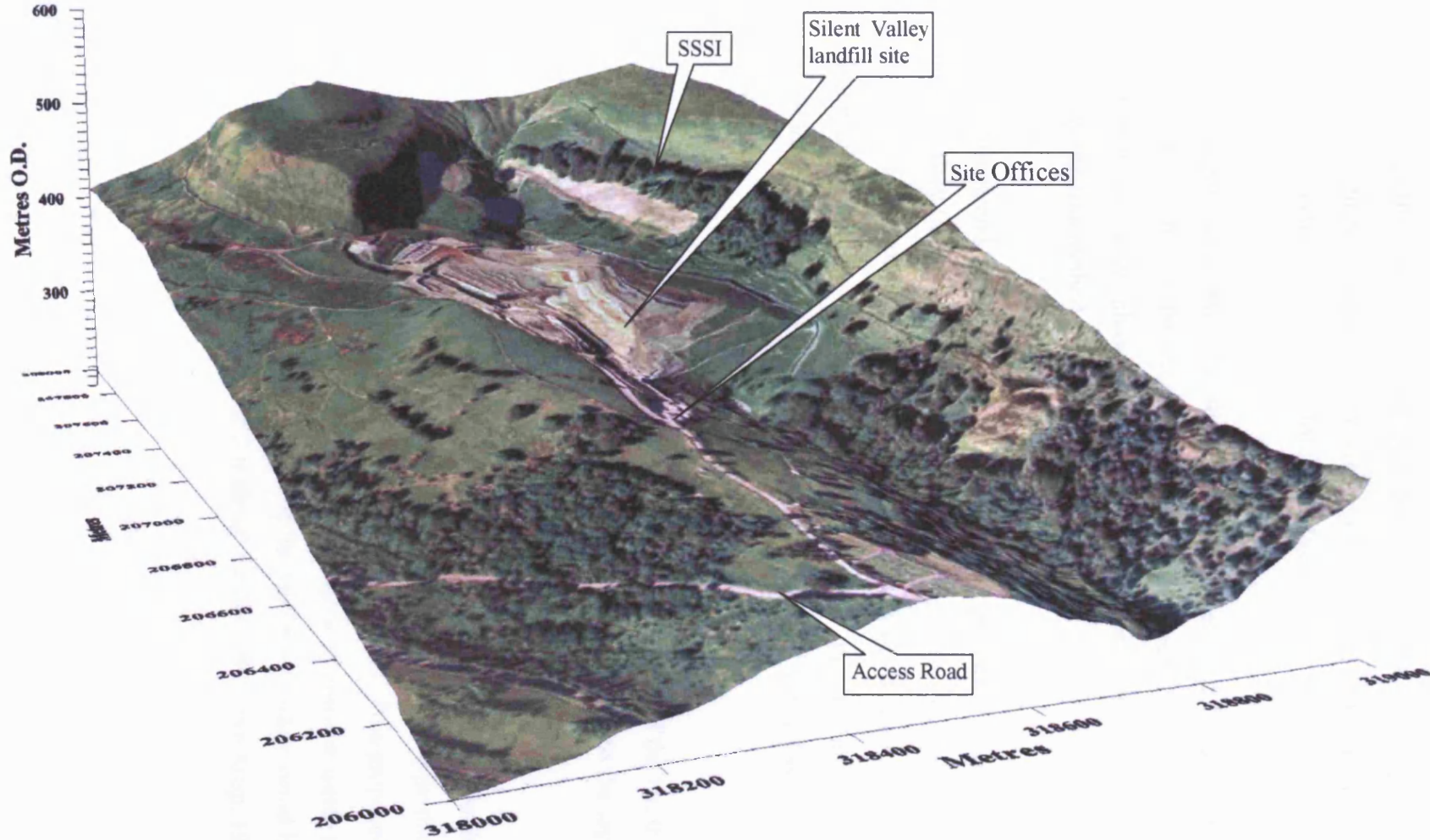


Figure 3.27b 3D surface of Silent Valley landfill site using a georeferenced air photograph taken in 2000. Image produced by Dr Peter Brabham, School of Earth, Ocean & Planetary Sciences, Cardiff University.

3.6.4 SITE OPERATION

Silent Valley landfill site is operated by Silent Valley Waste Services (SVWS). The operational site can be divided into two areas. Phase I (20.1 ha) is active at present and Phase II (13.5 ha) is the proposed area for future development.

Phase I is located to the south of the site. The southern face was filled, in an uncontrolled manner, during the early 1980s while Blaenau Gwent Borough Council ran the site. Phase IA is the present day active phase, which is working northward from this face. It is being infilled using the area method (Fig. 3.28).

The site is unlined and works on a dilute and attenuate principal. The clay rich deposits covering the valley floor act as a relatively impermeable layer. The thickness of the clay varies across the site from 0.2 m to in excess of 3.5 m (Golder Associates, 1993c). The clay permeability met the NRA guideline of $<1 \times 10^{-8}$ m/s for an acceptable lining material (Golder Associates, 1993b), although natural variability has not been investigated.

The leachate is collected through the drainage network at the base of the landfill and flows into a sump. The leachate and contaminated water is then pumped into the lagoon. Water is discharged from the lagoon to foul sewer.

Phase II of the landfill site will be developed as a containment site with a leachate collection system. The area will receive the same volume and waste type that is entering the site at present. Infilling of waste will be on a cellular basis. It is proposed to develop Phase 2 of the landfill site by reprofiling the spoil heap of steelworks waste in the north-west part of the site. Assuming that the faces of the steelworks waste could be reprofiled to 1 on 3, the potential capacity of Phase 2 is about 3 million m³ (Ove Arup, 1996a).

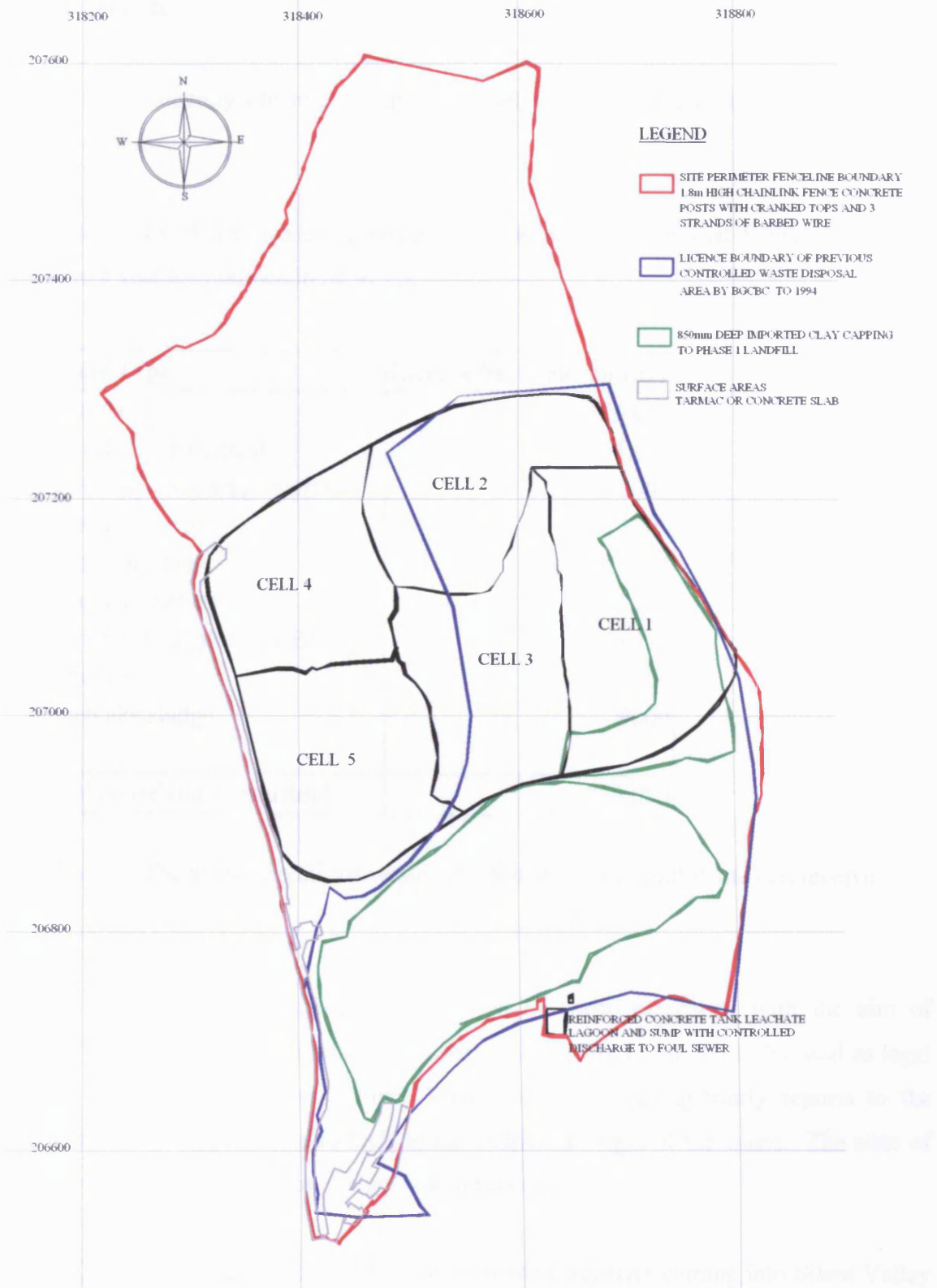


Figure 3.28 Location of the approximate base area of Phase 1A landfill cells 1 to 5. Adapted from Silent Valley Waste Services drawing number ESID6-1.

3.6.4.1 Waste

There is a civil amenity site available at Silent Valley that is available free of charge to the local community.

Under the terms of the licence agreement, the permitted wastes that Silent Valley can receive in a year are outlined in table 3.6.

Waste Type	Licence Maxima (tonnes)
Household	120,000
Industrial/commercial	156,000
Screenings ex sewage works	1000
Road sweepings	1000
Colostomy bags	200
Animal carcasses	300
Contaminated tallow ex BSC	10,000
Asbestos	2500
Filtercake sludge	9000
Total household + Industrial	250,000

Table 3.6 The annual permitted wastes that Silent Valley landfill site can receive.

In 1999 the Environment Agency issued a list of waste categories with the aim of grouping together wastes of similar properties. The guidelines are not to be used as legal guidance on waste definitions. Silent Valley Landfill sends quarterly reports to the Environment Agency, which also include the district of origin of the waste. The state of the waste, either solid, liquid or sludge, is also recorded.

Figure 3.29 shows the proportions of different waste categories coming into Silent Valley landfill between July 1999 and June 2000 (collected by SVWS). At this time the waste that entering the site was 2% liquid (29A Organic Chemical Wastes - Special Waste), 3% sludge (22E Sewage & 29A Organic Chemical Wastes - Special Waste) and the remaining 95% was solid.

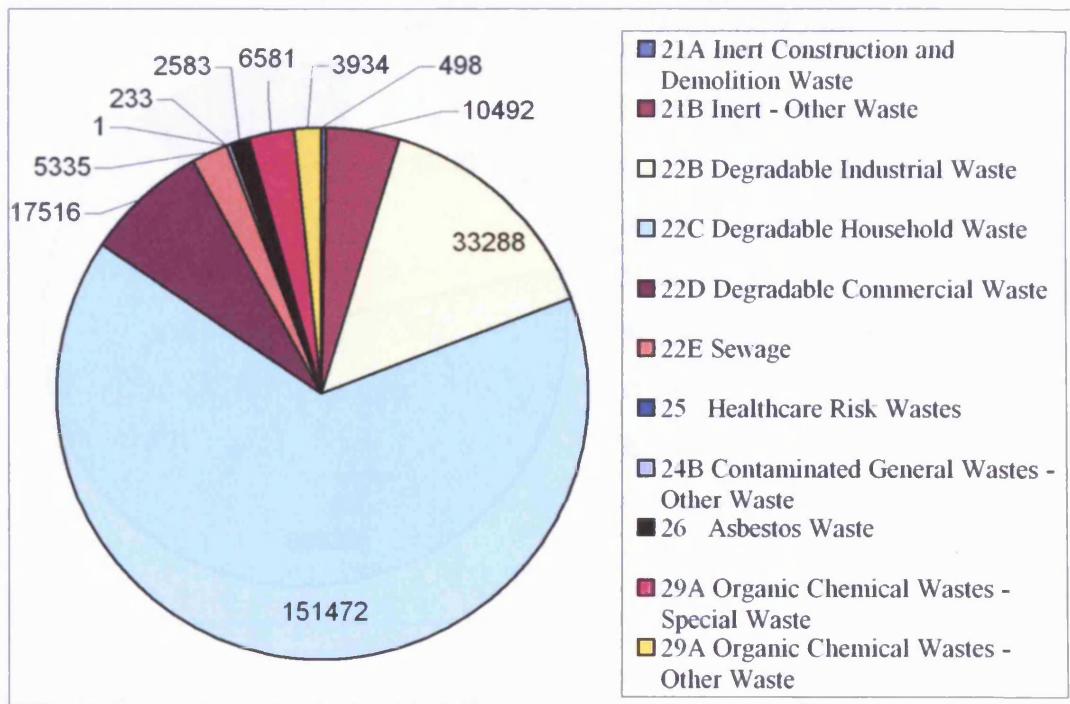


Figure 3.29 The proportions of different waste categories that entered Silent Valley landfill site between July 1999 and June 2000. The values indicate the waste volume to the nearest tonne. Data collected by SVWS.

Four years later the waste stream had altered (Fig. 3.30) due to the Landfill Directive and the waste was now all solid with no special waste.

Waste (23B Metals and Discarded (Scrap) Composite Equipment - Other Waste) is now taken off site for recycling. Between January and March 2004 4.9 tonnes were taken off site for recycling.

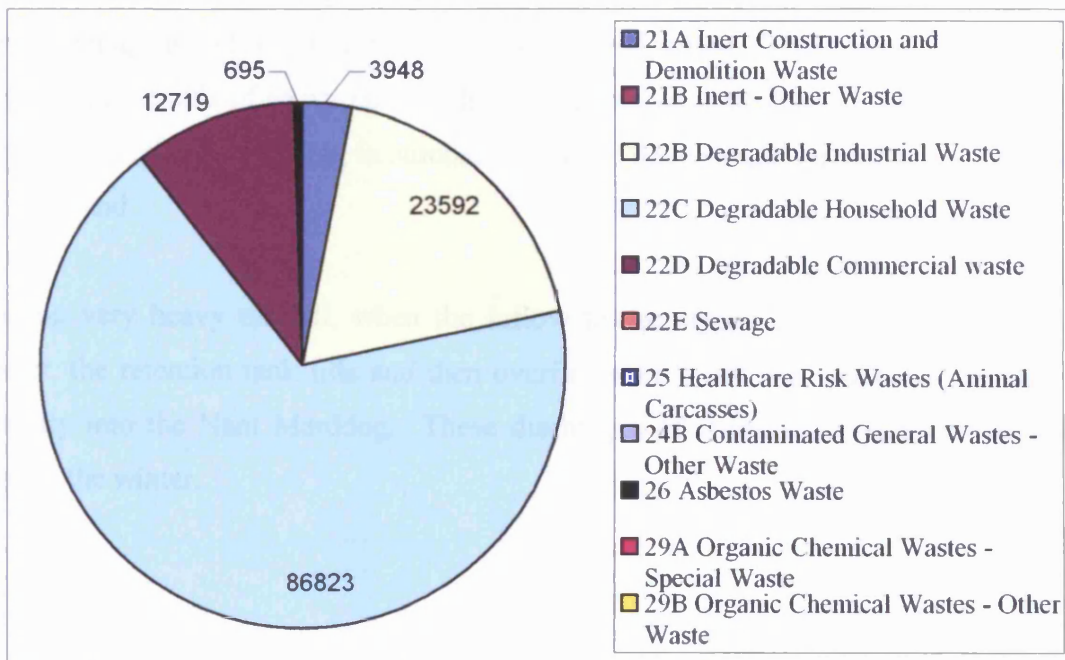


Figure 3.30 The proportions of different waste categories that entered Silent Valley landfill site between April 2003 and March 2004. The values indicate the waste volume to the nearest tonne. Data collected by SVWS.

3.6.4.2 Leachate Management

At present there are a number of monitoring and sampling points situated on and off the landfill site (Fig. 3.31). At the north of the site there are twelve groundwater piezometers. Seven groundwater wells and a groundwater stream sampling point are situated around the perimeter of the site. Five of the six surface water sampling points are located outside the inner site fence with the sixth on site. Four leachate wells are located across the southern face.

Leachate is currently disposed of to a 150 mm diameter sewer from the lagoon at the toe of the landfill. This sewer connects into the Welsh Water foul sewer system in Cwm. The

hydraulic capacity of the 150 mm sewer is about 20 l/s (1,700 m³/day). However, flows in excess of 10 l/s are discharged directly to the Nant Merddog stream, the discharge into the sewer being limited to 10 l/s to avoid risk of overloading. There have been complaints that during periods of heavy rainfall the 150 mm sewer is unable to cope with the flow of leachate entering it, resulting in surcharge of some downstream manholes and pollution of private land.

During very heavy rainfall, when the inflow to the lagoon exceeds the outflow to the sewer, the retention tank fills and then overflows via a 450 mm diameter overflow pipe directly into the Nant Merddog. These discharges of untreated leachate are significant during the winter.

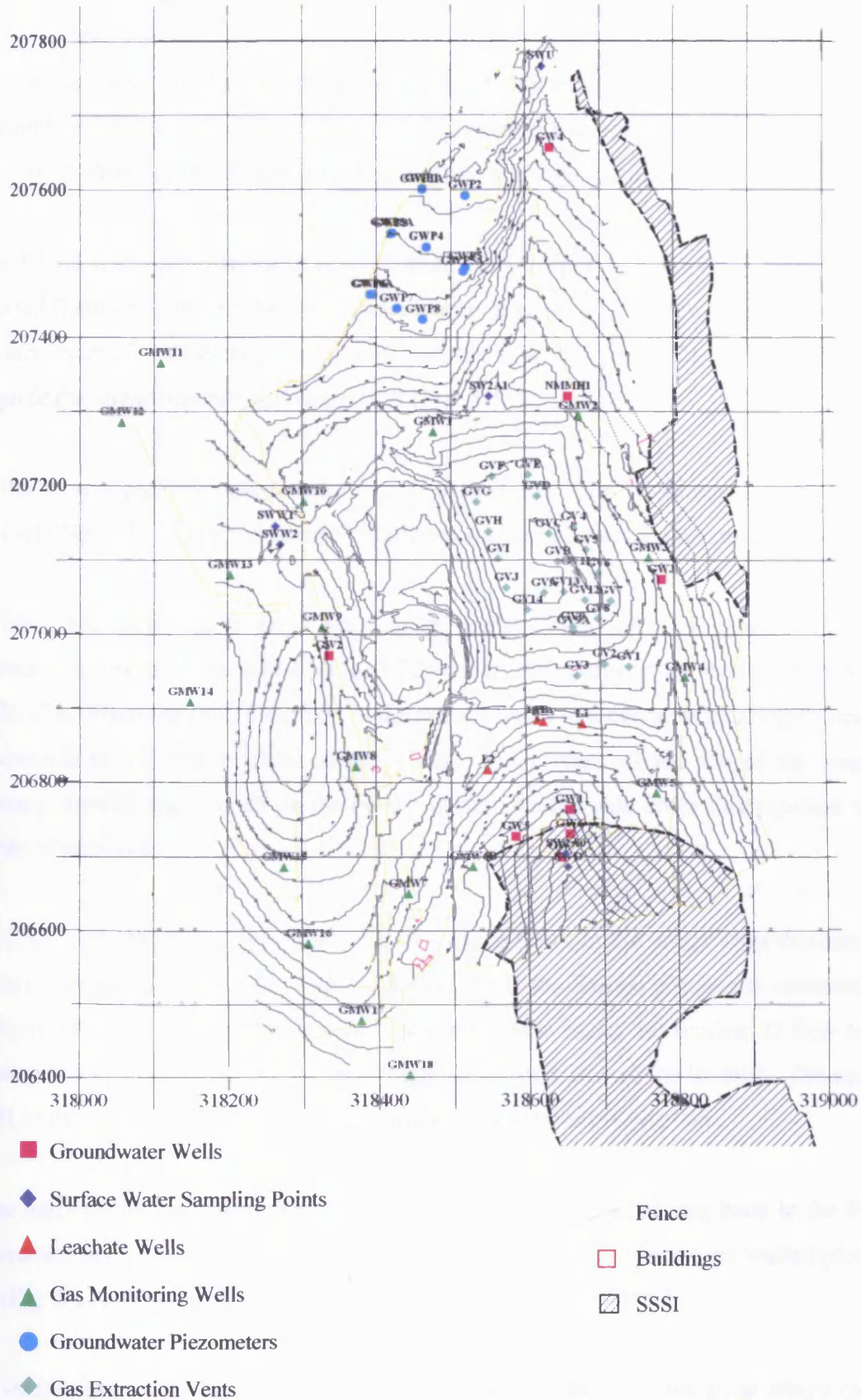


Figure 3.31 Map showing the location of monitoring points at Silent Valley landfill.

3.6.4.2.1 Drainage

Ove Arup & Partners (1995, 1996b) have detailed the drainage installations at the site and a summary of this is given below. Figure 3.32 has been adapted from a map produced by Ove Arup & Partners (1995, 1996b) and shows the drainage installations on site.

In the 1970s, under the ownership of the British Steel Corporation, the Nant Merddog was culverted beneath part of the steelworks waste tips in a 750 mm internal diameter (900 mm external diameter) concrete pipeline, the BSC pipeline. The pipeline was laid alongside the stream course, following G-H (Fig. 3.32).

In 1983 a new pipeline was constructed to convey the Nant Merddog to follow route D-E-F-H (Fig. 3.32) along the Armco pipeline to the east of the original stream course.

The Nant Merddog was diverted again in the early 1990s and now enters a 500 mm diameter concrete pipeline A-B-C (Fig. 3.32) which skirts around the eastern side of the landfill site. From the outfall at point C the stream flows in a concrete lined open channel and cascade to join the original stream course downstream of the toe of the landfill. Tributary streams and French drains on the eastern valley side enter this pipeline via a number of manholes.

At E (Fig. 3.32), the Armco pipeline collects surface flows in the valley floor downstream of A and groundwater flows via French drains. At B the Armco pipeline is connected to the Nant Merddog diversion pipeline enabling clean flows in section D-E-B to be discharged at C and then enter the Nant Merddog downstream of the landfill. The section B-F-H of the Armco pipeline collects groundwater and possibly leachate.

To the north of the landfill, groundwater issues from the toe of the slag bank in the Phase 2A area and is conveyed away in a 400 mm diameter polypropylene twin walled pipeline N-H (Fig. 3.32). The pipeline was installed towards the end of 1993.

Two other pipelines J-K and L-M (Fig. 3.32) convey water from two areas where strong issues emerge from the base of the slag bank in the Phase 2A area. These issues occur

close to where springs are shown on Old Ordnance Survey Plans. The pipelines convey the water to open channels leading away from the landfill site.

The BSC pipeline at present collects contaminated water flowing through the landfill site and discharges it into the leachate lagoon.

A CCTV survey was carried out in May 1996 on the downstream end of the BSC and sections of the Armco pipeline. It showed that the BSC pipeline is in reasonably sound condition. Some circumferential cracks are present that probably developed as a result of ground loading. There was no evidence from the survey of any chemically induced deterioration.

The sections of the Armco pipeline surveyed by CCTV appeared to be in good condition with no evidence of distortion. A dye tracer test from the land drain entry showed that the flow to the outlet took in excess of 45 minutes for a distance of about 500 m (less than 0.2 m/s) suggesting that partial obstructions may exist within the section of the pipeline that was not CCTV surveyed (Ove Arup & Partners, 1995; 1996b).

To the north of the current tipping area, SVWS have carried out works in an attempt to reduce the volume of clean water entering the tip. Ditches have been cut along the approximate boundary between the slag and underlying clay to intercept the issues from the base of the slag tip (Figure 3.33). Intercepted flows have been directed to a pump-house, where the water is pumped through a rising main to the diverted Nant Merddog. The pumping system is self-actuating thus minimising the infiltration from this source. Along part of the ditch, little or no flow is being intercepted from the slag tip but water is issuing at a lower level. This flow then disappears and it is assumed that it is entering the tip (Gwent Consultancy, 2000).

The Southern Flank was capped during 2001 to reduce infiltration into the landfill. It was covered with 850 mm of overburden and then hydroseeded (Fig. 3.33).

Drainage ditches around the site have been lined with concrete to reduce their erosion.

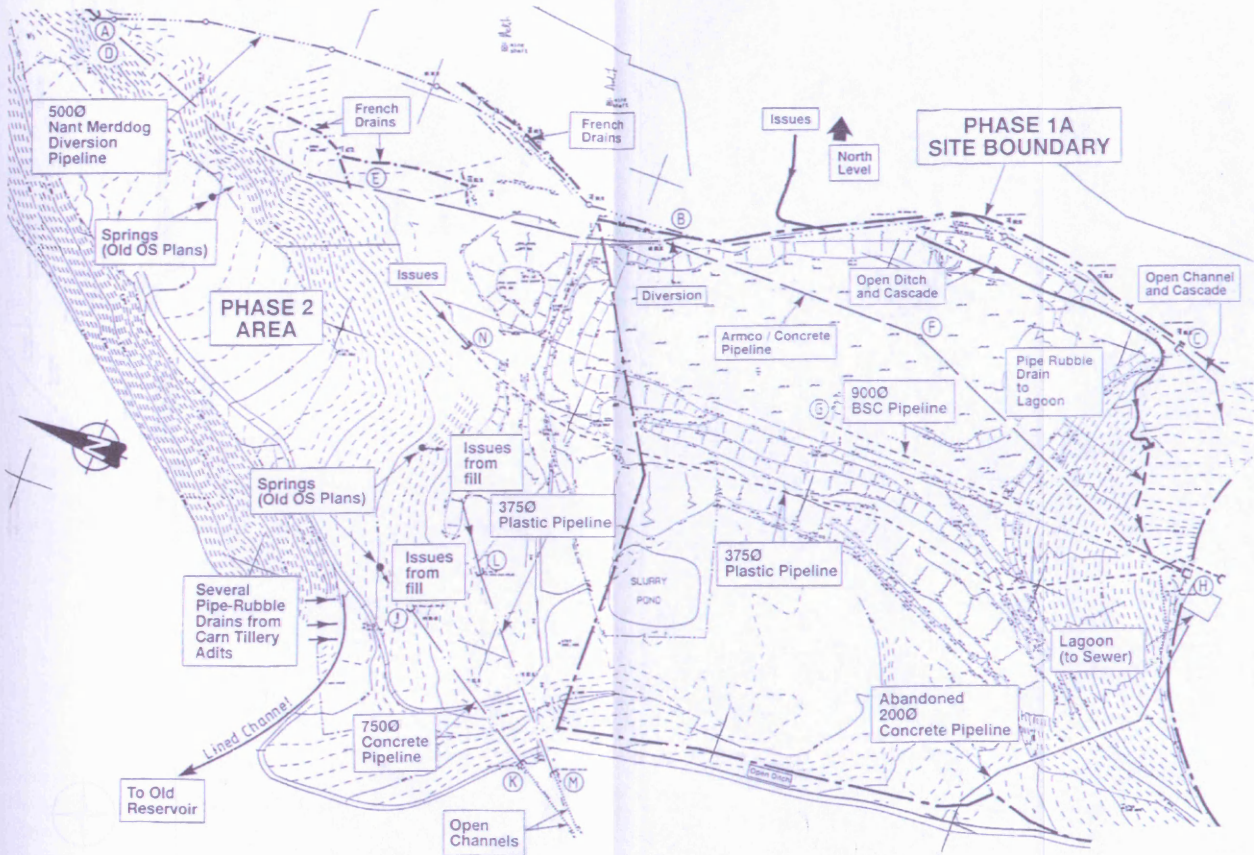


Figure 3.32 Drainage map of Silent Valley. After Ove Arup & Partners (1995, 1996b).

3.6.4.3 Gas Management

There are eighteen gas monitoring wells situated across the site and the surrounding area (Fig. 3.31). Twenty four gas extraction vents are located in the central part of the site.

Gas monitoring is carried out at gas monitoring wells GMW2, GMW3, GMW4, GMW5, GMW6B, GMW7, GMW8, GMW9 and GMW10. The wells are all monitored at 4 m and 14 m and at 25.5 m in all except GMW7 and GMW8. They are monitored for methane (%), carbon dioxide (%), oxygen (%), hydrogen sulphide (ppm), and hydrogen cyanide (ppm) and gas temperature (°C). The atmospheric pressure (mb) and differential pressure (mb) are also recorded. In 2003, the wells were monitored 18 times but twice water was sucked up, so no readings were taken.

Gas chromatography analysis is carried out annually. The gas composition percentages for oxygen, nitrogen, hydrogen, carbon dioxide, carbon monoxide, methane, ethane, propane, butane and water vapour are calculated. In 2003, the samples were taken on 10th September. All the wells except one showed the major constituent as nitrogen (59-90%), with varying amounts of oxygen (0.2-21%) and carbon dioxide (0-10%). In GMW10 at 19.50 m the gas composition was 62.3% methane, 30.3% carbon dioxide, 6.5% nitrogen and 0.3% oxygen.

Gas extraction will take place from the gas extraction vents located in the central part of the site. The gas extracted will be used to generate electricity.

3.6.4.4 Monitoring

Flow measurements are recorded for the Settlement Tank and the BSC Pipe. Flow monitoring is discussed in more detail in Section 5.1.1. Conductivity readings are also recorded for the Settlement Tank and the BSC Pipe (discussed in Section 6.3). Surface water, groundwater, leachate and gas samples are collected from monitoring points around the site and analysed. All the data are recorded. Leachate sampling will be discussed in Chapter 6.

CHAPTER 4

INTERNAL STRUCTURE

This chapter gives details of site investigations that have been performed across Silent Valley landfill. The results of the investigations have been summarised in tables. Resistivity surveys have been performed at Silent Valley landfill site to help improve the understanding of the internal structure of the landfill. The chapter concludes by using the information presented in Chapters 3 and 4 to produce a Conceptual Site Model of the landfill site.

4.1 BOREHOLE AND TRIAL PIT DATA

A series of site investigations have been carried out across Silent Valley (BGBC, Golder Associates (1993a; 1993d), Sir Alexander Gibb & Partners, Exploration Associates (1996)). Figure 4.1 shows the borehole and trial pit locations.

Many of the boreholes drilled had installations installed so that they could be used as monitoring wells for leachate, groundwater or gas.

4.1.1 BLAENAU GWENT BOROUGH COUNCIL

In 1992 Blaenau Gwent Borough Council drilled six 150 mm boreholes (BGBC1 to BGBC6) by shell and auger to depths between 5.8 and 7.7 m below ground level on the eastern flank of the valley, to the north-east of the landfill. A summary of the borehole logs is given in table 4.1.

	Surface elevation (mAOD)	Subsoil	Fill		Clay	Rockhead	
		from – to (m)	from – to (m)	Type of fill	from – to (m)	Depth to (m)	Type
BGBC1	409.067	0.00 - 0.15	0.15 – 1.30	slag	1.30 – 5.00	5.00	mudstone
BGBC2	392.150	0.00 – 0.40	-	-	0.40 – 5.70	5.70	mudstone
BGBC3	399.205	0.00 – 0.15	-	-	0.15 - >7.00	>7.00	-
BGBC4	386.658	-	-	-	0.00 – 7.40	7.40	mudstone
BGBC5	381.627	-	0.00 – 1.20	slag	1.20 – 4.10	4.10	mudstone
BGBC6	408.869	-	-	-	0.00 - >6.80	>6.80	-

Table 4.1 Summary of borehole logs data for Blaenau Gwent Borough Council site investigation.

The logs indicate a variable thickness of clay (2.9 m to 7.4 m, or >6.8 m where rockhead not encountered) overlying mudstone. BGBC1 and BGBC5 encountered about 1.2 m of made ground at the surface consisting of blast furnace slag.

Water levels for four boreholes were recorded three times during early June 1992. BGBC4 and BGBC5 were dry, BGBC3 had water levels around 398.45 m (0.75 mbgl) and BGBC6 had water levels around 406.02 m (2.85 mbgl).

4.1.2 GOLDER ASSOCIATES

Golder Associates (1993a; 1993d) carried out site investigations from November 1992 to January 1993 and in September and October 1993.

4.1.2.1 1992 Site Investigation

The 1992 site investigation was carried out from 23 November 1992 to 8 January 1993. The site investigation aimed to establish the type of superficial deposits, the level of rock head, groundwater levels, measure in situ hydraulic properties and obtain groundwater and blast furnace slag samples for analysis.

The site investigation consisted of eighteen trial pits (GA/TP1 to GA/TP18), two shell and auger boreholes (GA/7 and GA/8) and six rotary openhole boreholes (GA/3 to GA/8).

4.1.2.1.1 Trial Pits

A summary of the trial pit logs is given in table 4.2. In the trial pits, four units were identified:

1. A top layer of fill material is often encountered consisting of blast furnace slag, bricks, clinker and, in the area of Phase I, domestic waste. The fill is absent in the north eastern area of Phase II.
2. The fill is typically underlain by Head Deposits ranging in thickness between 1.4m and 5.5m, consisting predominantly of brown to grey sandy silty clays with sub-

	Fill		Head Deposits		Silty Clay		Rockhead	
	from – to (m)	thickness (m)	from – to (m)	thickness (m)	from – to (m)	thickness (m)	depth to	type
TP1	0 – 5.1	5.1	5.1	-				
TP2	0 – 0.6	0.6	0.6 – 3.3	2.7	3.3 – 4.1	0.8		
TP3	0 – 0.7	0.7	0.7 – 2.5	1.8	2.5 – 3.4	0.9	3.4	weathered mudstone sandstone
TP4/4a			0 – 3.2	3.2	3.2 – 4.5	1.3	4.5	weathered mudstone
TP5			0.2 – 4.1	3.9				
TP6			0.2 – 1.8	1.6			1.8	sandstone
TP7			0 – 5.0	5	5.0 – >5.35	>0.35	> 5.35	
TP8			0.2 – 4.4	4.2	4.4 – 4.6	0.2	4.6	weathered mudstone
TP9	0 – 3.5	3.5						
TP10	0 – 1.7	1.7	2.6 – 4.0	1.4	1.7 – 2.6	0.9		
TP11	0 – 1.8	1.8	1.8 – 3.4	1.6	3.4 – 4.5	1.1	4.5	weathered mudstone
TP12			0 – 5.5	5.5			5.5	weathered siltstone
TP13					0 – 1.4	1.4	1.4	weathered silt-/sandstone
TP14			0 – 2.7	2.7	2.7 – 3.0	0.3		
TP15	0 – 0.8	0.8	0.8 – 4.0	3.2			4	sandstone
TP16	0 – 0.6	0.6			0.6 – 1.6	1	1.6	weathered sandstone
TP17	0 – 1.8	1.8			1.8 – 4.7	2.9	4.7	weathered mudstone
TP18	0 – 1.1	1.1			1.1 – 4.8	3.7	4.8	weathered mudstone

Table 4.2 A summary of the trial pit logs from the 1992 Golder Associates site investigation. From Golder Associates (1993a).

angular to angular fine to coarse mudstone and sandstone gravel. The thickest layer of Head Deposits occurs in the north eastern part of Phase II.

3. The Head Deposits are generally underlain by a sequence of firm to stiff, reddish orange mottled brown silty clays. The silty clay material comprises glacial boulder clay and in situ completely weathered mudstone. The thickness of this layer ranges between 0.2 m and 3.7 m, with the thickest layer found along the southern end of Phase II.
4. The rockhead underlying the silty clay consisted mainly of variably weathered mudstone, siltstone or occasionally sandstone. The depth to the rockhead is variable across the site, ranging from 1.4 m near the valley bottom to greater than 5.35 m on the eastern side slope (Golder Associates, 1993a).

4.1.2.1.2 Boreholes

A shell and auger rig was used to sample the superficial deposits (GA/7 and GA/8) and a rotary percussive drilling rig was used to investigate the solid geology and groundwater regime (GA/3 to GA/8). The boreholes were 150 mm in diameter and to depths between 2.0 and 51.6 m below ground level. A summary of the borehole logs is given in table 4.3.

	BH depth (m)	Surface elevation (mAOD)	Fill		Clay	Rockhead	
			from – to (m)	Type of fill	from – to (m)	Depth to (m)	Type
GA/3A	4.50	385 est	0.00 – 4.50	waste	-	-	-
GA/3B	19.00	385 est	0.00 – 19.00	waste	-	-	-
GA/3C	24.00	385 est	0.00 – 22.20	waste	22.20 - >24.00	-	-
GA/4	17.90	312.7	-	-	0.00 -		
GA/5C	32.00	356.9	0.00 – 0.60	rubble	0.60 – 2.50	2.50	sandstone
GA/6	51.60	373.0	0.00 – 1.10	slag	1.50 – 5.10	5.10	sandstone
GA/7A	2.40	385 est	0.00 – 2.00	slag	-	-	-
GA/7B	2.00	385 est	-	-	0.00 - >2.00	-	-
GA/7R	14.70	385 est	0.00 – 1.20	slag	1.20 – 2.80	2.80	sandstone
GA/8R	17.40	418.8	-	-	0.00 – 5.30	5.30	mudstone
GA/8SA	4.80	420est	-	-	0.20 - >4.00	-	-

Table 4.3 Summary of borehole logs data for 1992 Golder Associates site investigation.

Below the superficial deposits interbedded mudstones and sandstones were found in variable thicknesses. The mudstones are grey to brown or red to brown coloured, weak to strong weathered often silty mudstones. The sandstones are characterised by a red-brown, occasionally grey colour. They range from fine to coarse grain size and are predominantly quartzitic (Golder Associates, 1993a).

In boreholes GA/4, GA/6 and GA/7R coal bands (0.1 m to 0.4 m) are found at various levels. Due to the regional dip (4°) of the strata, the coal bands cannot be related to each other.

Groundwater monitoring installations were installed in GA/3C, GA/4, GA/5C, GA/6 and GA/8R.

4.1.2.2 1993 Site Investigation

Golder Associates (1993d) carried out this site investigation between 15 September and 25 October 1993. The site investigation set out to determine the thickness and variability of in situ clay underlying the existing landfill and valley, characteristics of the clay, permeability of the clay and parameters of the existing waste.

The site investigation consisted of eighteen rotary openhole boreholes (GA/93/1 to GA/93/13), fourteen trial pits (B1 to B8) and hand augers and three trial trenches (TT3 to TT5). Laboratory testing was performed on the samples obtained.

4.1.2.2.1 Trial Pits and Hand Auger

The trial pits (B1 to B8) were 0.4 to 5.1 m deep. A summary of the trial pit and hand auger data are given in table 4.4. Clay, identified as weathered mudstone was found across the site in most of the trial pits. A number of the trial pits and hand auger holes

failed to penetrate fill deposits and therefore no information on natural soils and rocks is available at these locations.

4.1.2.2.2 Trial Trenches

The trial trenches were excavated with the aim to establish the strength parameters for the waste. Once excavated, the trenches were accurately measured and left exposed over a number of days. The trenches were then remeasured and the surrounding area examined for signs of failure or movement, which could then be used to establish a failure surface for the trench. The failure surface could then be back analysed, using a computer programme to deduce the strength parameters necessary to produce such a failure surface (Golder Associates, 1993d).

After 5 days, the degree of movement in all the trenches was negligible and no evidence of ground movement was found in the area around each trench. The result meant that it was not possible for Golder Associates to perform the proposed back analysis.

Trial Pit No.	Surface elevation of TP (mAOD)	Fill		Clay			Rockhead		Depth of base of TP (mbgl)	Elevation of base of TP (mAOD)	Remarks
		Depth of fill (m)	Type of fill	Depth to top of clay (mbgl)	Elevation of top of clay (mAOD)	Type of clay	Depth to rockhead (mbgl)	Elevation of rockhead (mAOD)			
B1	320	0.2	slag	0.2	319.80	wmst	1.05	318.95	1.25	315.90	Hand Auger
B2	334	none	-	0.2	333.80	wmst	-	-	0.80	329.90	Hand Auger
B2 (ii)	334	none	-	0	334	wmst	-	-	0.95	328.90	Hand Auger
B2 (iii)	334	none	-	0	334	wmst	-	-	0.90	330	Hand Auger
B3	367.19	1.7	waste	1.7	365.49	wmst	3.60	363.59	4.10	362.39	
B4	376.17	1.7	waste	1.9	374.27	wmst	3.45	372.72	4.10	375.72	
B4 (i)	377.76	2.3	slag	2.3	375.46	wmst	4.74	373.01	5.10	377.36	
B5	384	3.4	slag	3.4	380.60	wmst	-	-	4	383.30	
B6	372.70	1	slag	1.3	371.40	Head	-	-	4.80	371.40	
B7	370	none	-	0	370	wmst	-	-	0.45	368.50	Hand Auger
B7B	370	none	-	0	370	wmst	-	-	0.40	370	Hand Auger
B7C	370	none	-	0	370	wmst	-	-	0.70	370	Hand Auger
B8A	382.24	-	slag	none	-	-	-	-	1.30	382.24	
B8B	381.78	-	slag	none	-	-	-	-	1.50	381.78	

wmst = weathered mudstone

Table 4.4 Summary of trial pit and hand auger data for 1993 Golder Associates site investigation. From Golder Associates (1993d).

4.1.2.2.3 Boreholes

The boreholes were to depths between 2.5 and 39.0 m below ground level. A summary of the borehole logs is given in table 4.5.

Clay was found across most of the site. No clay was found in boreholes GA/93/11 and GA/93/13. Where clay was encountered the thickness varied from 0.2 m to in excess of 3.5 m.

Leachate monitoring wells were completed in boreholes GA/93/1D, GA/93/2 and GA/93/7. Borehole GA/93/8 was installed as a groundwater monitoring borehole within shallow sandstone, the sandstone being isolated by bentonite seals at the top and bottom of the screened section. Boreholes GA/93/9 and GA/93/10 were backfilled and a 50 mm perforated riser pipe was inserted in the top 2-3 m as a means of monitoring gas in the landfill.

BH No.	Surface elevation (mAOD)	Fill			Clay				Rockhead			Depth to water (mbgl)	BH depth (m)	
		Elevation of base of fill (mAOD)	Thickness of fill (m)	Type of fill	Depth to top of clay (mbgl)	Elevation of top of clay (mAOD)	Thickness of clay (m)	Type of clay	Depth to rockhead (mbgl)	Elevation of rockhead (mAOD)	Type			
GA/93/1A	363	unknown	unknown	waste	-	-	-	-	-	-	-	-	-	21.85
GA/93/1B	362	unknown	unknown	waste	-	-	-	-	-	-	-	-	-	3.45
GA/93/1C	362	unknown	unknown	waste	-	-	-	-	-	-	-	-	-	11.10
GA/93/1D	361.42	341.22	20.20	waste	-	-	-	-	-	-	-	-	-	-
GA/93/1D	-	324.12	17.10	slag	37.30	324.12	0.20	wmst	37.50	323.92	sst	-	-	39
GA/93/2	369.91	356.41	13.50	waste	13.50	356.41	0.40	wmst	13.90	356.01	mst	-	-	15
GA/93/4	363.87	362.97	0.90	slag	0.90	362.97	0.60	wmst	1.50	362.37	sst	-	-	2.50
GA/93/5	382.71	360.21	22.50	slag	22.50	360.21	2	Till	24.50	358.21	mst	-	-	25.80
GA/93/6A	381	unknown	unknown	slag	-	-	-	-	-	-	-	-	-	11.45
GA/93/6B	381.33	350.53	30.80	slag	30.80	350.53	0.20	wmst	31	350.33	sst	30.18	-	32.20
GA/93/7	348.94	328.79	20.15	waste	20.15	328.79	0.25	wmst	20.80	328.14	sst	-	-	22.30
GA/93/8	375.01	374.41	0.60	slag	0.60	374.41	0.50	wmst	1.10	373.91	sst	0.60	-	15.95
GA/93/9	377.01	359.26	17.75	waste	17.75	359.26	0.20	wmst	17.95	359.06	sst	-	-	20.10
GA/93/10	376.58	367.63	8.95	waste	8.95	367.63	0.25	wmst	9.20	367.38	sst	-	-	11.50
GA/93/11	369.48	347.58	21.90	waste	-	-	-	-	21.90	347.58	sst	-	-	23.50
GA/93/12	368	unknown	unknown	waste	-	-	-	-	-	-	-	-	-	6.20
GA/93/12	371.17	358.67	12.50	waste	12.50	358.67	1.10	wmst	13.60	357.57	mst	-	-	14.30
GA/93/13	381.32	unknown	unknown	slag	-	-	-	-	-	-	-	-	-	6.50
GA/93/13	381.32	unknown	unknown	slag	-	-	-	-	-	-	-	-	-	3
GA/93/13	381.32	360.22	21.10	slag	-	-	-	-	21.10	360.22	mst	-	-	22.50

Table 4.5 Summary of borehole logs data for 1993 Golder Associates site investigation. From Golder Associates (1993d).

4.1.3 SIR ALEXANDER GIBB & PARTNERS

For Walters Mining Ltd., Sir Alexander Gibb & Partners drilled three boreholes and excavated six trial pits to the north east of the Phase 1A landfill site along the eastern boundary of the land reclamation site in January and February 1994.

4.1.3.1 Trial Pits

The trial pits (GI/TP1 to GI/TP6) were 3.0 to 3.4 m deep (Table 4.6). They indicated 200/300 mm topsoil overlying approximately 2 m of silty clay above weathered siltstone. Trial pit one (GI/TP1) revealed a layer of silty fine to medium sand between 0.8 m and 2.0 m depth. Groundwater was only encountered in one trial pit (GI/TP3).

	TP depth (m)	Surface elevation (mAOD)	Topsoil	Clay	Rockhead		Groundwater encountered?
			from – to (m)	from – to (m)	Depth to (m)	Type	
GI/TP1	3.40	432.5	0.00 – 0.20	0.20 – 3.00	3.00	siltstone	no
GI/TP2	3.20	429.8	0.00 – 0.30	0.30 – 2.00	2.00	siltstone	no
GI/TP3	3.40	430.0	0.00 – 0.30	0.30 – 2.10	2.10	siltstone	yes
GI/TP4	3.20	427.5	0.00 – 0.30	0.30 – 2.50	2.50	siltstone	no
GI/TP5	3.20	420.0	0.00 – 0.20	0.20 – 1.25	1.25	siltstone	no
GI/TP6	3.00	418.0	0.00 – 0.20	0.20 – 2.00	2.00	siltstone	no

Table 4.6 Summary of trial pit logs for Sir Alexander Gibb & Partners site investigation.

4.1.3.2 Boreholes

The three boreholes (G150, G250, and G350) were drilled by rotary openhole and coring methods to between 13.30 m and 15.50 m deep (Table 4.7). The logs indicated a variable (1.3 to 5.0 m) thickness of boulder clay overlying a 400 mm thick coal seam. Borehole G150 also showed a 1.6 m layer of weathered mudstone above the coal. This coal was laid upon a sequence of mudstone, siltstone, sandstone and thin coal seams.

	Surface elevation (mAOD)	BH depth (m)	Clay	Rockhead		Water struck during drilling?
			from – to (m)	Depth to (m)	Type	
G150	427.5	14.70	0.00 – 2.00	2.00	mudstone	dry
G250	425.0	15.50	0.00 – 5.00	5.00	coal	5.00m
G350	417.0	13.30	0.00 – 1.30	1.30	coal	dry

Table 4.7 Summary of borehole logs for Sir Alexander Gibb & Partners site investigation.

4.1.4 EXPLORATION ASSOCIATES

Fifteen boreholes were drilled and eighteen trial pits excavated between 23 November and 5 December 1995 to the northwest of the site. The site investigation was logged and directed by Ove Arup & Partners. The investigation was required to determine the nature, depth and engineering properties of the materials at the site.

4.1.4.1 Trial Pits

Trail pits EA/TP1 to EA/TP18 were excavated. A summary of the trail pits logs is given in table 4.8.

4.1.4.2 Boreholes

The boreholes (EA1 to EA8B) were drilled using open hole and coring methods. Soil samples were taken for analysis. A summary of the borehole logs is given in table 4.9.

	TP depth (m)	Made Ground		Superficial deposits		Rockhead	
		from – to (m)	Type	from – to (m)	Type	Depth to (m)	Type
EA/TP1	5.00	0.00 – 2.50	sand	0.00 – 2.50	Till	-	-
EA/TP2	2.20	-	-	0.00 – 1.60	Till	1.60	sandstone
EA/TP3	4.20	0.00 – 0.20	slag	0.20 – 4.00	Till	4.00	sandstone
EA/TP4	3.80	-	-	0.00 – 3.40	Till	3.40	sandstone
EA/TP5	2.50	-	-	0.00 – 2.00	LD	2.00	sandstone
EA/TP6	1.80	0.00 – 0.30	slag	0.30 – 1.10	Till	1.10	sandstone
EA/TP7	1.20	0.00 – 0.25	clay	0.25 – 1.20	Till	1.20	sandstone
EA/TP8	4.00	0.00 – 3.60	slag	3.60 - >4.00	LD	-	-
EA/TP9	3.60	0.00 – 2.50	slag	2.50 - >3.60	LD	-	-
EA/TP10	0.45	-	-	0.00 – 0.45	scree	-	-
EA/TP11	4.00	1.20 – 4.00	slag	0.00 - 1.20	scree	-	-
EA/TP12	5.00	-	-	0.00 – >5.00	LD	-	-
EA/TP13	4.00	-	-	0.00 – 3.50	LD	3.50	sandstone
EA/TP14	4.70	-	-	0.00 - >4.70	Till	-	-
EA/TP15	5.20	-	-	0.00 – 5.00	clay	5.00	sandstone
EA/TP16	2.40	0.00 – 0.10	clay	0.10 – 2.40	Till	2.40	sandstone

LD = Landslide Deposits

Table 4.8 Summary of trial pit logs for Exploration Associates site investigation.

	Surface elevation (mAOD)	BH depth (m)	Fill		Superficial deposits		Rockhead	
			from – to (m)	Type	from – to (m)	Type	Depth to (m)	Type
EA1	430.86	34.30	0.00 – 3.50	slag	3.50 – 18.00	LD	18.00	mudstone
EA1A	430.97	17.00	0.00 – 3.50	slag	3.50 - >17.00	LD	-	-
EA2	431.28	30.00	0.00 – 13.10	slag	13.10 – 22.30	LD	23.00	mudstone
EA3	425.10	29.50	0.00 – 2.40	slag	2.40 – 8.10	LD	8.10	sandstone
EA3A	425.03	16.00	0.00 – 3.00	slag	Part of log missing			
EA4	425.97	35.00	0.00 – 11.50		11.50 – 19.45	LD	19.45	mudstone
EA5	423.58	35.10	0.00 – 23.50		23.50 – 26.30	BC	28.30	mudstone
EA5A	423.00	8.00	0.00 - >8.00		-	-	-	-
EA5B	423.00	24.00	0.00 – 23.30		23.30 - >24.00	BC	-	-
EA6	416.65	25.70	0.00 – 4.00	slag	4.00 – 17.00	LD	17.00	mudstone
EA6A	416.76	17.00	0.00 – 5.00	slag	5.00 - >17.00	LD	-	-
EA7	417.58	34.75	0.00 – 14.50		14.50 – 25.70	LD	25.70	siltstone
EA8	417.25	7.50	0.00 - >7.50		-	-	-	-
EA8A	417.00	1.50	0.00 - >1.50		-	-	-	-
EA8B	417.00	31.35	0.00 – 18.00		18.00 – 27.35	BC/clay	27.35	mudstone

LD = Landslide Deposits BC = Boulder Clay

Table 4.9 Summary of borehole logs for Exploration Associates site investigation.

4.2 RESISTIVITY SURVEYING

In order to obtain a two-dimensional model of the Southern Slope of the site, geophysical investigations were employed, specifically resistivity survey. The aim was to identify areas of lower resistivity, which are likely to correspond with areas of leachate saturation.

4.2.1 ELECTRICAL RESISTIVITY

The property of the electrical resistance (R) of a material is usually expressed in terms of its resistivity (ρ). The resistivity of a material is defined as the resistance in ohms between the opposite faces of a unit cube of material. The SI unit of resistivity is the ohm-metre (Ωm).

Electrical conduction in most rocks is essentially electrolytic. This is because most mineral grains (except metallic ores and clay minerals) are insulators. Groundwater filling the pore space of a rock is a natural electrolyte.

Resistivity is an extremely variable parameter. There is no general correlation of the lithology with resistivity, although a broad classification is possible (Table 4.10). As a rule, the more porous a rock and the larger its groundwater content, the higher the conductivity and the lower the resistivity. If clay minerals are present in a water-bearing rock, ion exchange processes may release a relatively large number of ions. The ions released add to the normal ion concentration in the pore water, with the net result being an increased conductivity. Dissolved contaminants within the leachate contribute to the ion content of the water, which results in an increased conductivity and therefore a reduced resistivity.

Material	Resistivity (Ωm)
Granite	$3 \times 10^2 - \times 10^6$
Consolidated Shales	$20 - 2 \times 10^3$
Sandstones	$1 - 7.4 \times 10^8$
Limestones	$5 \times 10^1 - 10^7$
Clays	$1 - 10^2$
Top Soil	250 – 1700
Unsaturated Landfill	30 – 100
Saturated Landfill	15 – 30
Landfill Runoff	<10 - 50

Table 4.10 Resistivities of common geologic materials. Adapted from Reynolds (1997).

4.2.2 RESISTIVITY SURVEY

In a resistivity survey electrical currents are introduced into the ground and the resulting potential differences are measured at the surface. Deviations from the pattern of potential differences expressed from homogeneous ground provide information on the form and electrical properties of subsurface inhomogeneities.

In homogeneous ground the depth of current penetration increases as the separation of the current electrodes is increased.

Vertical Electrical Sounding (VES) is used mainly in the study of horizontal or near-horizontal interfaces. The current and potential electrodes are maintained at the same relative spacing and the whole spread is progressively expanded about a fixed central point. Consequently, readings are taken as the current reaches progressively deeper depths.

Constant Separation Traversing (CST) is used to determine lateral variations of resistivity. The current and potential electrodes are maintained at a fixed separation and progressively moved along a profile.

The value of resistivity that is measured is an average of a volume of ground proportional to the electrode spacing. This value is called the apparent resistivity (ρ_a). Apparent resistivity can be measured using any configuration of electrodes as long as the distance between them is known. There are common electrode configurations such as the Wenner, Schlumberger and Double Dipole configurations.

4.2.2.1 Electrode Configurations

The two types of electrode configurations that have been used on Silent Valley are the Wenner and Schlumberger arrays. The two arrays have different suitability (Table 4.11).

Criteria	Wenner	Schlumberger
Vertical Resolution	✓✓✓	✓✓
Depth Penetration	✓	✓✓
Suitability to VES	✓✓	✓✓✓
Suitability to CST	✓✓✓	✗
Sensitivity of Orientation	Yes	Yes
Sensitivity to Lateral Inhomogeneities	High	Moderate
Labour Intensive	Yes (No*)	Moderate (No*)
Availability of Interpretational Aids	✓✓✓	✓✓✓

✓ = poor; ✓✓ = moderate; ✓✓✓ = good; ✗ = unsuitable

* When using a multicore cable and automated electrode array

Table 4.11 Comparison of Wenner and Schlumberger electrode arrays. Adapted from Reynolds (1997).

4.2.2.1.1 Wenner Array

In the Wenner array (Fig. 4.2) four electrodes are equally spaced along a straight line. The distance between adjacent electrodes is called the array spacing, a (Sharma, 1997). For this configuration the equation of (apparent) resistivity (ρ_a), for the midpoint between the potential electrodes, P₁P₂ is:

$$\rho_a = 2\pi.a.\frac{\Delta V}{I} \quad (32)$$

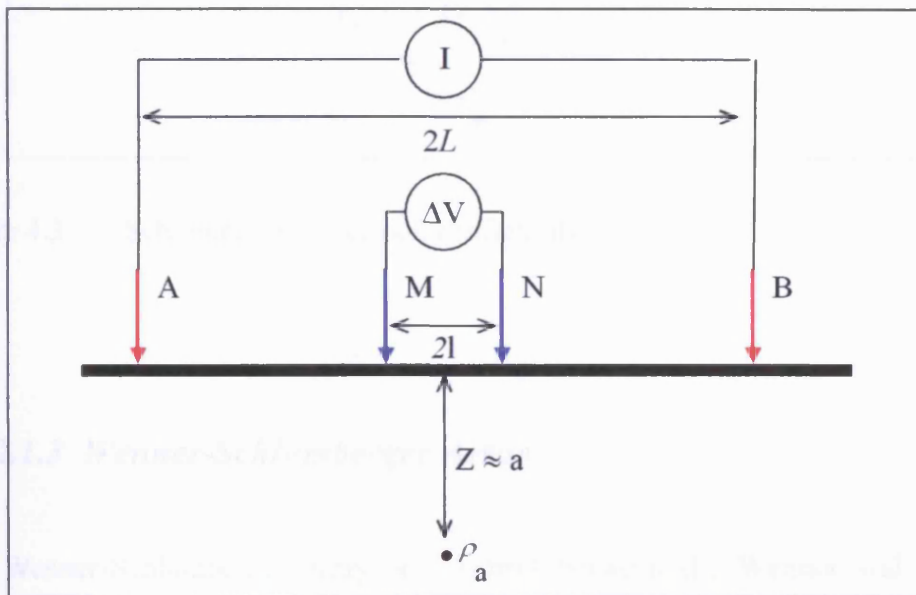


Figure 4.2 Wenner electrode configuration.

4.2.2.1.2 Schlumberger Array

In the Schlumberger (symmetrical) array (Fig. 4.3) measurements of apparent resistivity are made by keeping the potential electrodes (M,N) about the midpoint of the array while the current electrodes (A,B) are symmetrically moved outwards in steps (Sharma, 1997). In the Schlumberger array the formula for (apparent) resistivity is:

$$\rho_a = \frac{\pi L^2}{I} \frac{\Delta V}{2l} \quad (33)$$

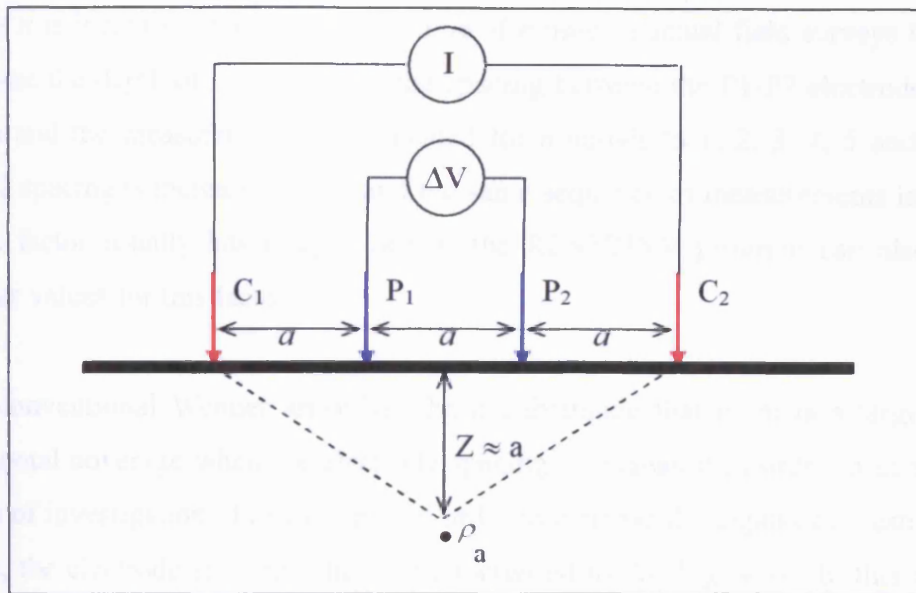


Figure 4.3 Schlumberger electrode configuration.

4.2.2.1.3 Wenner-Schlumberger Array

The Wenner-Schlumberger array is a hybrid between the Wenner and Schlumberger arrays. The apparent resistivity value for the Wenner-Schlumberger array is given by:

$$\rho = \pi n(n+1) a R \quad (34)$$

where,

R = measured resistance

a = spacing between the P1 and P2 electrodes

n = the ratio of the distances between the C1-P1 and the P1-P2 electrodes (Loke, 1999a).

This array effectively becomes the Schlumberger array when the n factor is greater than 2. The normal Wenner array is actually a special case of the Wenner-Schlumberger array where the n factor is equal to 1. Thus the array is a combination of the Wenner and Schlumberger arrays adapted for use with a line of electrodes with a constant spacing.

Since the potential between the P1 and P2 electrodes decreases when the electrode spacing factor n is increased, the maximum value of n used in actual field surveys is about 8. To increase the depth of investigation, the spacing between the P1-P2 electrodes is increased to $2a$ and the measurements are repeated for n equals to 1, 2, 3, 4, 5 and 6. Next, the P1-P2 spacing is increased to $3a$, and the same sequence of measurements is made. While the n factor usually has integer values, the RES2DINV program can also accept non-integer values for this factor.

The conventional Wenner array has the disadvantage that there is a large reduction in horizontal coverage when the electrode spacing is increased in order to achieve a deeper depth of investigation. For example, in order to increase the depth of investigation by two times, the electrode spacing a has to be increased to $2a$ (Fig. 4.4). In this case, the total length of the array is increased from $3a$ to $6a$.

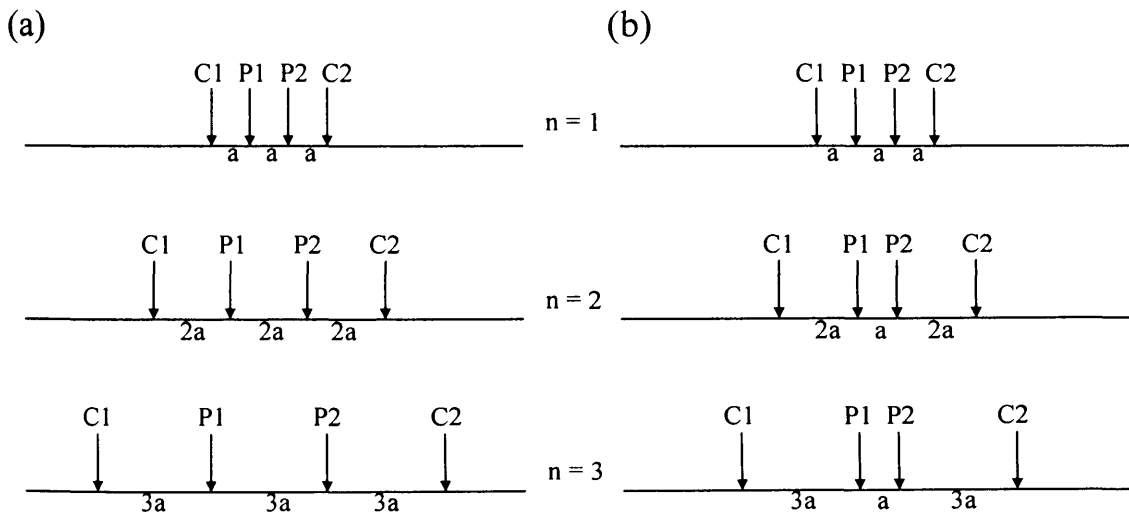


Figure 4.4 The steps used by the (a) Wenner and the (b) Wenner-Schlumberger arrays to increase the depth of investigation.

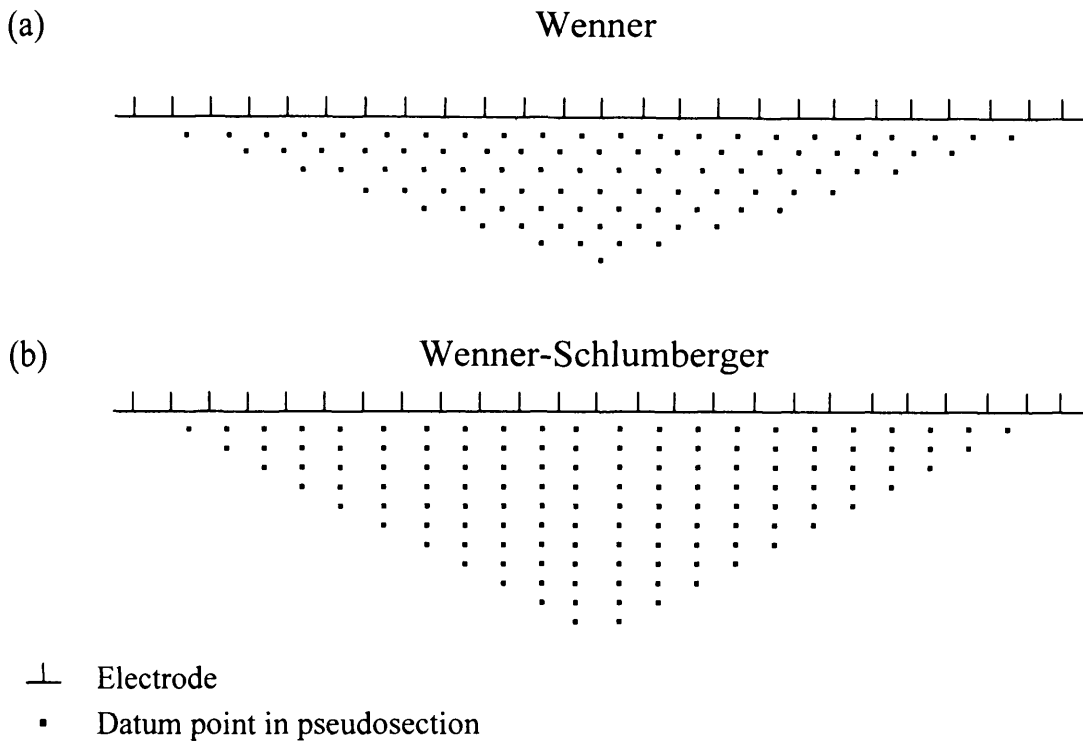


Figure 4.5 Schematic showing the arrangement of data points in the pseudosections for the (a) Wenner and the (b) Wenner-Schlumberger arrays.

The Wenner-Schlumberger array has a better horizontal coverage compared with the Wenner array. For the Wenner array each deeper data level has 3 data points less than the previous data level, while for the Wenner-Schlumberger array there is a loss of 2 data points with each deeper data level (Fig. 4.5). Besides better horizontal coverage, the maximum depth of penetration of the Wenner-Schlumberger array is about 15% larger than the Wenner array.

4.2.2.2 Resistivity Surveying Equipment

Resistivity surveys can be carried out with simple equipment consisting of a high-tension battery pack as the source current, four metal stakes, an ammeter, a voltmeter, and insulated cable. The electrodes (metal stakes) are commonly made of aluminium, copper or steel.

To improve the ease of data acquisition, electrodes are connected by a multicore cable to a switching box. The data acquisition is software controlled from a laptop computer.

Resistivity surveying instruments are designed to be capable of reading the very low levels of resistance of the ground. Apparent resistivity values are computed from the resistance measurements using the formula relevant to the electrode configuration used.

Most modern resistivity meters use low-frequency alternating current. The periodic reversal of the current prevents accumulation of ions around the electrodes and thus overcomes electrolytic polarisation. The use of an alternating current also overcomes the effects of telluric currents, which are natural electric currents in the ground that flow parallel to the Earth's surface and cause regional potential gradients. The frequency of the alternating current used depends upon the required depth of penetration.

4.2.2.3 Data Processing

Data processing is based on an iterative routine involving determination of a 2D simulated model of the subsurface that is then compared to the observed data and revised. Convergence between the theoretical and observed data is achieved by non-linear least squares optimisation. The procedure is smoothness constrained to improve stability in the iterative process, the degree of smoothness being determined by a user-specified damping factor. The extent to which the observed and calculated theoretical models agree is an indication of the validity of the true resistivity model (indicated by the root-mean-squared (RMS) error).

4.2.2.4 Limitations of Resistivity Surveying

Resistivity surveying suffers from a number of limitations (Kearey & Brooks, 1991):

- Interpretation is limited to simple structural configurations. Any deviations from these simple situations may be impossible to interpret.
- The depth of penetration is limited by the maximum electrical power that can be introduced into the ground and by the practical difficulties of laying out long lengths of cable.
- Topography and the effects of near surface resistivity variations can be mask the effects of deeper variations.

4.2.2.5 Interpretation of Resistivity Data

The data of resistivity surveys can be presented in two forms, profiles and maps. In a profiling survey with a constant electrode spacing, the data may be presented as graphs showing the resistivity variation along the traverse, or as a contour map showing the lines of equal resistivity.

The interpretation of resistivity tomography data is based on the known physical properties of the sub-surface materials.

Near-surface layers tend to be modelled more accurately than those at depth, primarily because field data from shorter electrode separations tend to be more reliable than data from very large separation, owing to higher signal-to-noise ratios.

The calculated resistivity value is not the *true* resistivity of the subsurface, but an *apparent* value, which is the resistivity of a homogeneous ground that will give the same resistance value for the same electrode arrangement. The relationship between the *apparent* resistivity and the *true* resistivity is complex. To determine the true subsurface resistivity, an inversion of the measured apparent resistivity values using a computer program must be carried out.

The RES2DINV program is used to interpret the resistivity data collected at Silent Valley. It uses iterative inversion methods.

4.2.2.5.1 Inversion method

All inversion methods essentially try to find a model for the subsurface whose response agrees with the measured data.

The RES2DINV program uses an iterative method whereby starting from an initial model, the program tries to find an improved model whose calculated apparent resistivity values are closer to the measured values.

The difference between the calculated and measured apparent resistivity is frequently given as a RMS (root-mean-squared) value. This is the quantity that the inversion method seeks to reduce, after each iteration, in an attempt to find a better model.

Besides trying to minimise the difference between the measured and calculated apparent resistivity values, the inversion method also attempts to reduce other quantities that will produce certain desired characteristics in the resulting model. The additional constraints also help to stabilise the inversion process.

4.2.2.5.2 RES2DINV Program

The RES2DINV program used to interpret the Silent Valley data is a computer program that will automatically determine a two dimensional (2D) resistivity model for the subsurface for the data obtained from electrical imaging surveys.

The program is designed to operate, as far as possible, in an automatic and robust manner with minimal input from the user. It has a set of default parameters which guides the inversion process. In most cases the default parameters give reasonable results.

The computer program RES2DINV.EXE will automatically subdivide the subsurface into a number of blocks, and it then uses a least-squares inversion scheme to determine the appropriate resistivity value for each block. The model parameters are the resistivity values of the model blocks, while the data are the measured apparent resistivity values.

The problem of non-uniqueness is well known in the inversion of resistivity sounding and other geophysical data. For the same measured data set, there is wide range of models giving rise to the same calculated apparent resistivity values. To narrow down the range of possible models, normally some assumptions are made concerning the nature of the subsurface that can be incorporated into inversion subroutine. In almost all surveys, something is known about the geology of the subsurface. In some cases it is known whether the subsurface bodies of interest have gradational boundaries, such as pollution plumes or bedrock with a thick transitional weathered layer. In such cases, the conventional smoothness-constrained inversion gives a model, which more closely corresponds with reality. This is the default method used by the RES2DINV program. In others, the subsurface might consist of discrete geological bodies that are internally almost homogeneous with sharp boundaries between different bodies. For such cases, a robust model inversion constrain is more suitable.

The quality of the field data are important. Good quality data usually show a smooth variation of apparent resistivity values in the pseudosection. To get a good model, the data must be of equally good quality. Bad data points could be due to the failure of the relays at one of the electrodes, poor electrode ground contact due to dry soil, or shorting across the cables due to very wet ground conditions. These bad data points usually have apparent resistivity values that are obviously too large or too small compared to the neighbouring data points.

If the data are of poor quality there are several things that could be done. With the RES2DINV program, you can plot the data in profile form that helps to highlight the bad

datum points, and remove them from the data set manually (Fig. 4.6). The damping factors can also be increased to exclude bad data. A larger damping factor would tend to produce smoother models with less structure, and thus poorer resolution, but it would be less sensitive to noisy data.

The second setting is the robust data constrain option. The inversion subroutine normally tries to reduce the *square* of the difference between the measured and calculated apparent resistivity values. Data points with a larger difference between the measured and calculated apparent resistivity values are given a greater weight. This normally gives acceptable results if the noise is random in nature. However, in some cases, a few bad data points with unusually low or high apparent resistivity values (outliers) could distort the results. To reduce the effect of such bad datum points, the robust data constrain causes the program to reduce the *absolute* difference between measured and calculated apparent resistivity values. The bad datum points are given the same weight as the other data points, and thus their effect on the inversion results is considerably reduced.

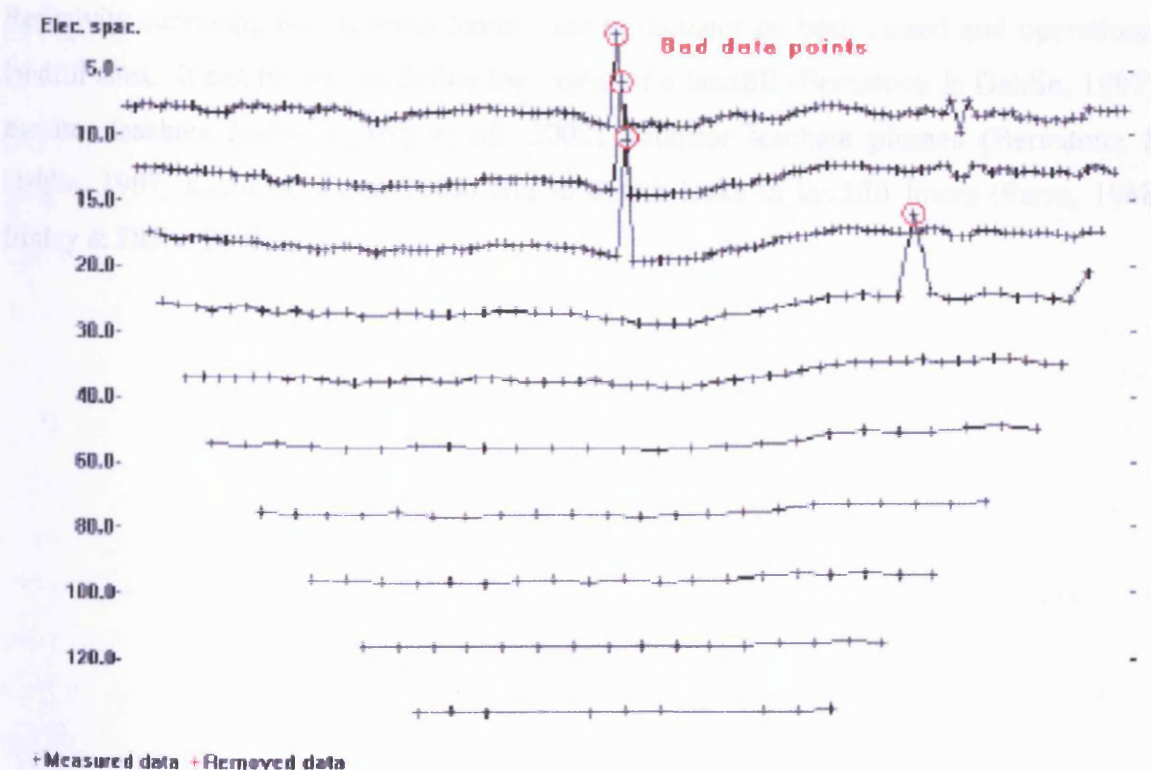


Figure 4.6 An example of a field data set with a few bad data points. From Loke (1999a).

4.2.2.6 The use of Resistivity on Landfill Sites

There is an increasing amount of interest in the use of high-resolution resistivity surveys in the investigation of landfills, particularly with respect to potential leachate migration. Both resistivity sounding and sub-surface imaging have been used very successfully (Reynolds, 1997).

Bernstone *et al.* (2000) performed 2D DC resistivity surveys across two old landfills with the objective to test the capability of resistivity as a characterisation method. They surveyed two landfills in southern Sweden. After the resistivity surveys were completed, the landfills were excavated and characterised. They found that the most important potential information which can be recovered from the surveys is an indication of the hydraulics of the waste piles; leachate pathways, fringing leachate pockets and the level of saturated waste. They were not able to correlate the waste type against the resistivity models.

Resistivity surveying is frequently being used in industry on both closed and operational landfill sites. It can be used to define the extent of a landfill (Bernstone & Dahlin, 1997), monitor leachate levels (Ogilvy *et al.*, 2002), monitor leachate plumes (Bernstone & Dahlin, 1997; Karlik & Kaya, 2001) and to detect leaks in landfill liners (Parra, 1988; Binley & Daily, 2003).

4.2.3 RESISTIVITY SURVEYS UNDERTAKEN AT SILENT VALLEY

Three Cardiff University MSc students have undertaken resistivity surveys across the southern slope (Phase 1) of Silent Valley landfill site, assisted and/or supervised by the author.

A permanent set of electrodes was installed on the southern slope at Silent Valley in December 2001. Surveys were repeated across the same area of landfill once a month for a year.

4.2.3.1 Summer 2000 Survey

Four resistivity survey lines (Fig. 4.7) were carried out by Mara Lopes in June/July (Lopes, 2000). The resistivity lines ran east to west, were parallel with each other and roughly followed the contours.

The survey was performed with the University's resistivity equipment using the Wenner array. The electrodes were connected by a multicore cable to a switching unit and a laptop. The computer runs the Campus Imager programme, which performs a number of readings of constant separation along the array. It then performs more traverses along the array with increasing electrode spacing. To extend the survey area covered, a roll-along method was used. After completing the sequence of measurements the cable was moved on by 12 electrodes, so that readings overlapped with readings of the previous survey.

Using the RES2DINV inversion program, a depth-corrected model of the calculated true resistivity was produced and compared with the field readings of apparent resistivity. A finite model of the resistivity distribution in the ground was generated and adjusted to fit the data iteratively, and the smaller the error between sections the more accurate the model. The final apparent resistivity model could then be used for the final interpretation.

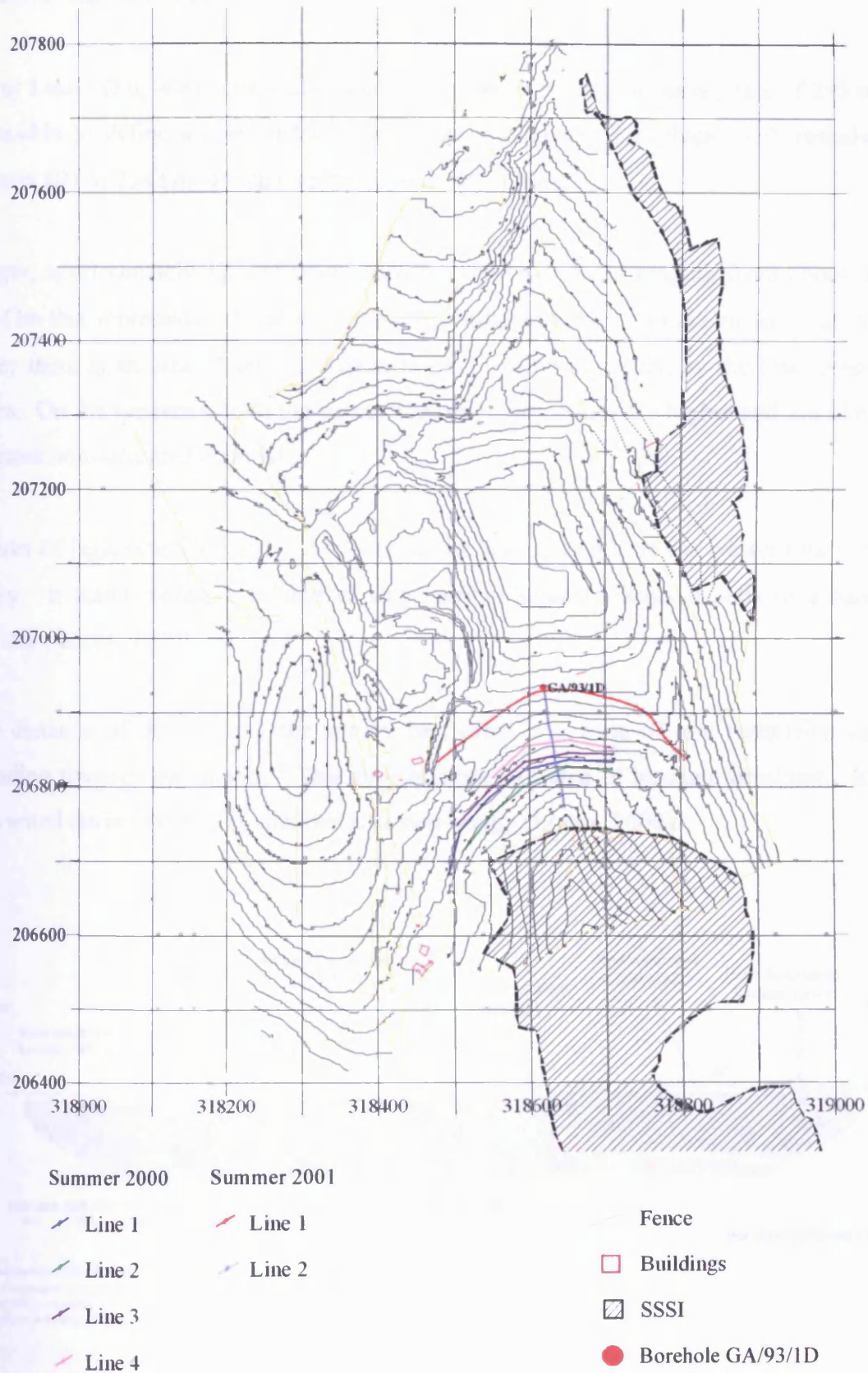


Figure 4.7 Map showing the locations of the Summer 2000 and 2001 resistivity surveys.

4.2.3.1.1 Survey Line 1

Survey Line 1 (Fig. 4.8) consisted of four traverses, giving a total survey line of 295 m. It is possible to define a near surface layer, approximately 2.5 m thick, with resistivities between 101 to 254 Ωm which could represent dry rubble.

A layer, approximately 17.5 m thick, shows resistivity values ranging from about 10 to 63.5 Ωm that represents a layer of compacted refuse material. On the eastern side of the survey there is an area of saturated material that can be identified by the low resistivity values. On the western side of the survey the resistivity values are higher and are likely to represent non-saturated material.

An area of high resistivity (101-254 Ωm) can be seen at depth on the western part of the survey. It could represent a bund of slag used to separate disposal cells or a haulage roadway (Lopes, 2000).

At a distance of 90 m along the survey line there is a zone of low resistivity values extending towards the surface. This may indicate an area of leachate breakout. It had been noted during the survey that this area was boggy (Lopes, 2000).

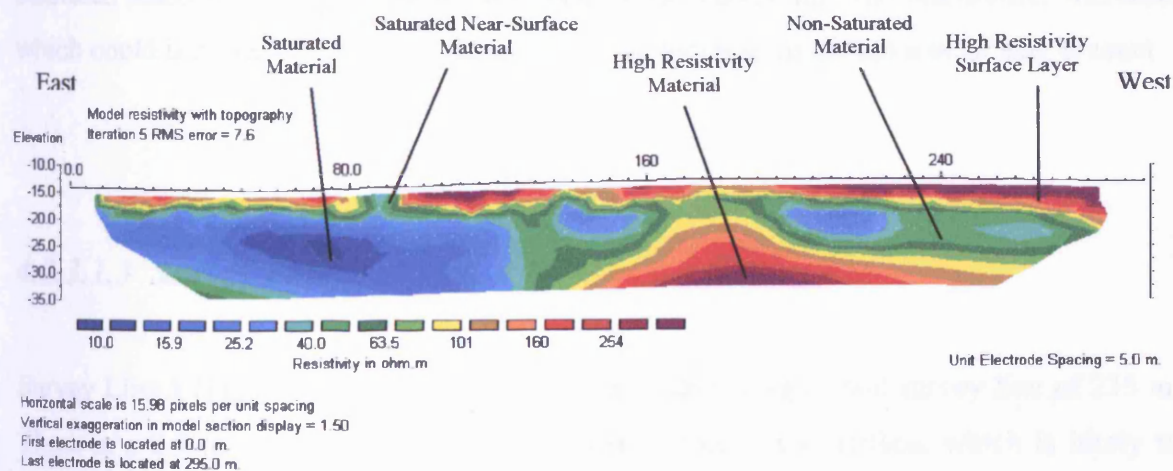


Figure 4.8 Line 1 of the summer 2000 resistivity survey. Adapted from Lopes (2000).

4.2.3.1.2 Survey Line 2

Survey Line 2 (Fig. 4.9) consisted of three traverses giving a total survey line of 235 m. It is possible to define an approximately 2.5 m thick near surface layer with resistivities between about 63.5 and 254 Ωm . It is likely that this represents slag and rubble.

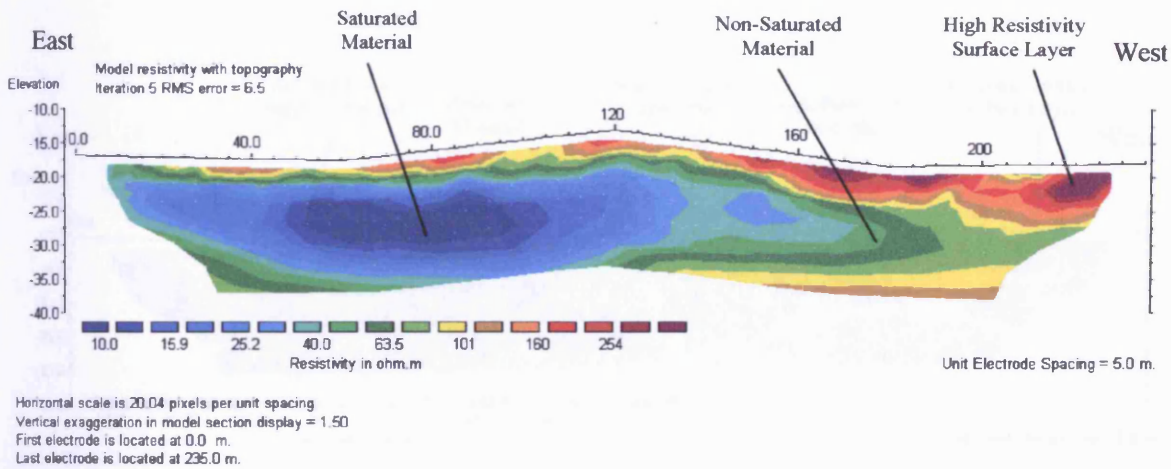


Figure 4.9 Line 2 of the summer 2000 resistivity survey. Adapted from Lopes (2000).

There is a large area represented by low resistivity values (10 to 22.5 Ωm) that represents saturated material. Towards the western end of the survey line the resistivities increase, which could indicate a decrease in saturation or an increase in the amount of slag present.

4.2.3.1.3 Survey Line 3

Survey Line 3 (Fig. 4.10) consisted of three traverses giving a total survey line of 235 m. There is a 2.5 to 5 m thick layer of high resistivities at the surface, which is likely to represent dry rubble and slag.

A large area of saturated material can be identified by the low resistivities.

An area of high resistivity can be seen at depth on the western part of the survey. It could represent a bund of slag used to separate disposal cells or a haulage roadway. It is likely that it is a continuation of the feature seen in Line 1 (Lopes, 2000).

At a distance of 60 m along the survey line there is a zone of low resistivity values extending towards the surface. This suggests saturation of near surface material. This may be the continuation of the feature seen in Line 1 (Lopes, 2000).

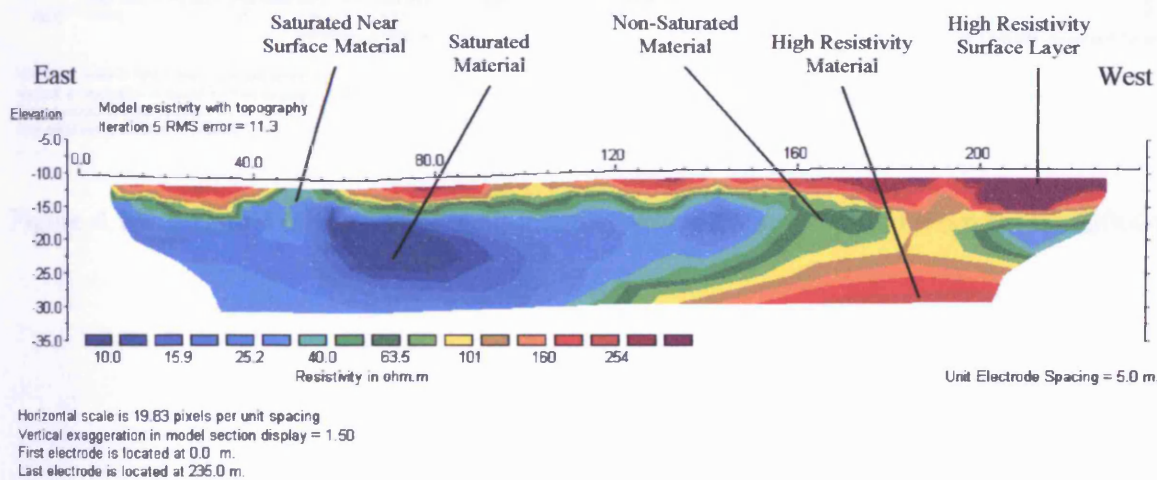


Figure 4.10 Line 3 of the summer 2000 resistivity survey. Adapted from Lopes (2000).

4.2.3.1.4 Survey Line 4

Survey Line 4 (Fig. 4.11) consisted of two traverses giving a total survey line of 175 m. A surface layer approximately 2.5 m thick can be identified by high resistivities.

The survey line shows a large area of low resistivities that represent saturated material. Some of the area has lower resistivities, which could represent different water contents within the material.

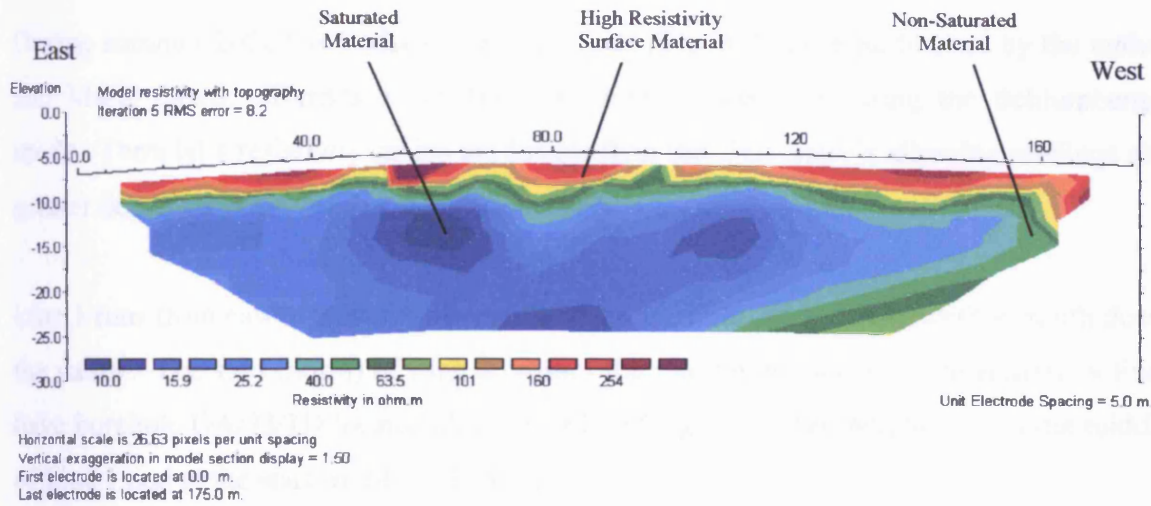


Figure 4.11 Line 4 of the summer 2000 resistivity survey. Adapted from Lopes (2000).

4.2.3.2 Summer 2001 Survey

During summer 2001 two resistivity survey lines (Fig. 4.7) were performed by the author and Marta Otero. Terradat's resistivity equipment was used using the Schlumberger mode. Terradat's resistivity cables are longer than the University's allowing readings at a greater depth.

Line 1 runs from east to west following the contour. Line 2 runs from north to south down the valley. The start (north) of Line 2 crosses the middle of Line 1. Both resistivity lines have borehole GA/93/1D located along their line (Fig. 4.7). The borehole is in the middle of Line 1 and at the start (north) of Line 2.

Borehole GA/93/1D was drilled by Golder Associates in 1993. The borehole is situated at location 318619, 206932. At the time of drilling, the surface elevation was 361.42 m. The current surface level at that location is about 370 m. The borehole was drilled to a depth of 39 m using a rotary percussive drill. Natural ground (clay) was hit at a depth of 37.30 m (324.12 mAOD) and rockhead (sandstone) was at a depth of 37.50m (323.92 mAOD).

4.2.3.2.1 Survey Line 1

Survey Line 1 (Fig. 4.12) was 400 m long and ran from east to west, roughly following the contour.

Low resistivity values can be seen across the survey line down to depths generally less than 15 m. These values represent areas of leachate saturated material. In the centre of the survey line low resistivity values continue down to the base of the profile. It is likely that the low resistivity readings at depth are an effect of the 'principal of equivalence' and are shown at a greater depth than they exist. In a three-layered model, if the middle layer has a lower resistivity to the layers on either side, the current flow will concentrate into the middle layer and will be almost parallel to the layer. The resistance of an elementary

block of length Δl and cross-section $h\Delta m$ to such a current flow is $R = \rho\Delta l/(h\Delta m)$, which will be unaltered if we increase ρ but at the same time increase h in the same proportion. Thus all such middle layers for which the ratio h/ρ is the same are electrically equivalent. On the other hand, if the resistivity of the middle layer is much larger than the other layers either side, the electric current will tend to avoid it and take the shortest route to the lower layer. The lines of current flow will be almost perpendicular to the layer. The resistance of an elementary block to this flow will be $R = \rho h/\Delta A$ where ΔA is the cross-section. In this case all layers for which the product is the same are electrically equivalent so that, again h and ρ cannot be determined separately. Essentially the flow path of the electrical current is not accurately modelled in the inversion, resulting in a low resistivity mid layer appearing to extend downwards below its true location. Therefore, it is likely that much higher resistivities should occur at the base of the section in figure 4.12.

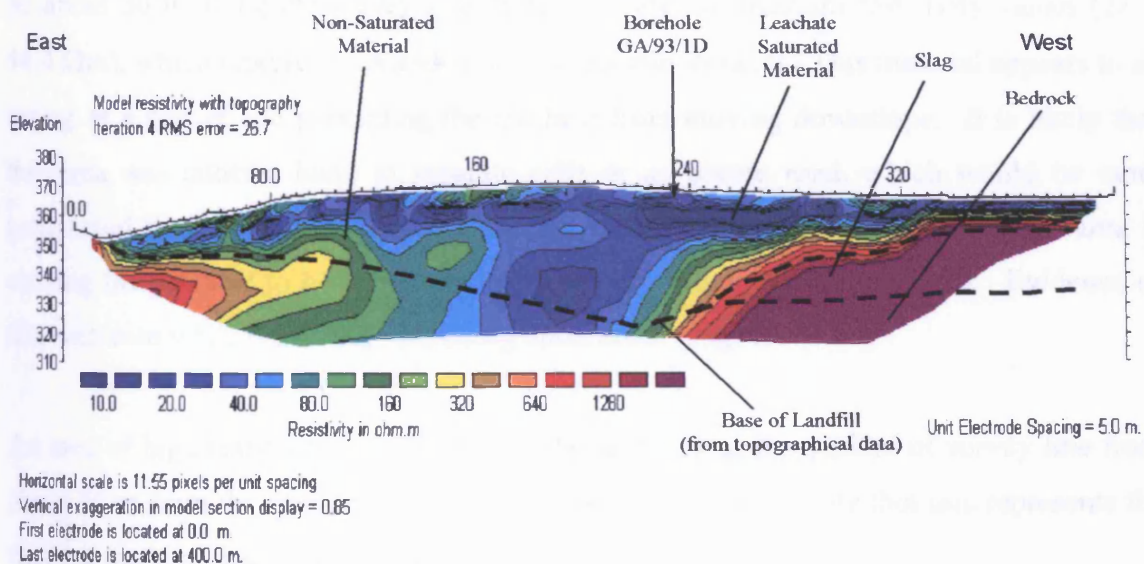


Figure 4.12 Line 1 of the summer 2001 resistivity survey.

An area of very high resistivity ($>1280 \Omega m$) can be seen on the western part of the survey. It is likely that this represents the slag and natural bedrock.

The location of borehole GA/93/1D has been indicated on the resistivity profile. At this location natural ground was encountered at an elevation of 324.12 mAOD. This can be marked on the resistivity survey line and used to help interpret the data. The cross sections of the site (Fig. 3.24) produced by Ove Arup & Partners (1995; 1996b) can also be used to aid in the interpretation of the survey.

4.2.3.2.2 *Survey Line 2*

Survey Line 2 (Fig. 4.13) was 175 m long and ran from north to south. Large areas of low resistivity values can be seen across the survey and represent areas of leachate saturated material.

At about 30 m along the survey line there is an area of medium resistivity values (28 – 44.4 Ωm), which represents an area of lower moisture content. This material appears to be acting as a barrier and preventing the leachate from moving downslope. It is likely that this area was either a bund to separate cells or an access road, which would be more compacted than surrounding fill. The change in hydraulic conductivity of this area is causing the leachate to be forced up to the surface where it is seeping out. Evidence of this was seen while the survey was being undertaken (Fig. 4.14).

An area of high resistivity (>112 Ωm) can be seen across the surface of survey line from about 50 m from the start of the survey line to the end. It is likely that this represents the capping material that is being placed on site.

The survey line crossed leachate monitoring well L1A, its location has been marked on the profile. The location of borehole GA/93/1D has been indicated on the resistivity profile. At this location natural ground was encountered at an elevation of 324.12 m. This can be marked on the resistivity survey line and used to help interpret the data. The cross sections of the site (Fig. 3.24) produced by Ove Arup (1995; 1996) can also be used to aid in the interpretation of the survey.

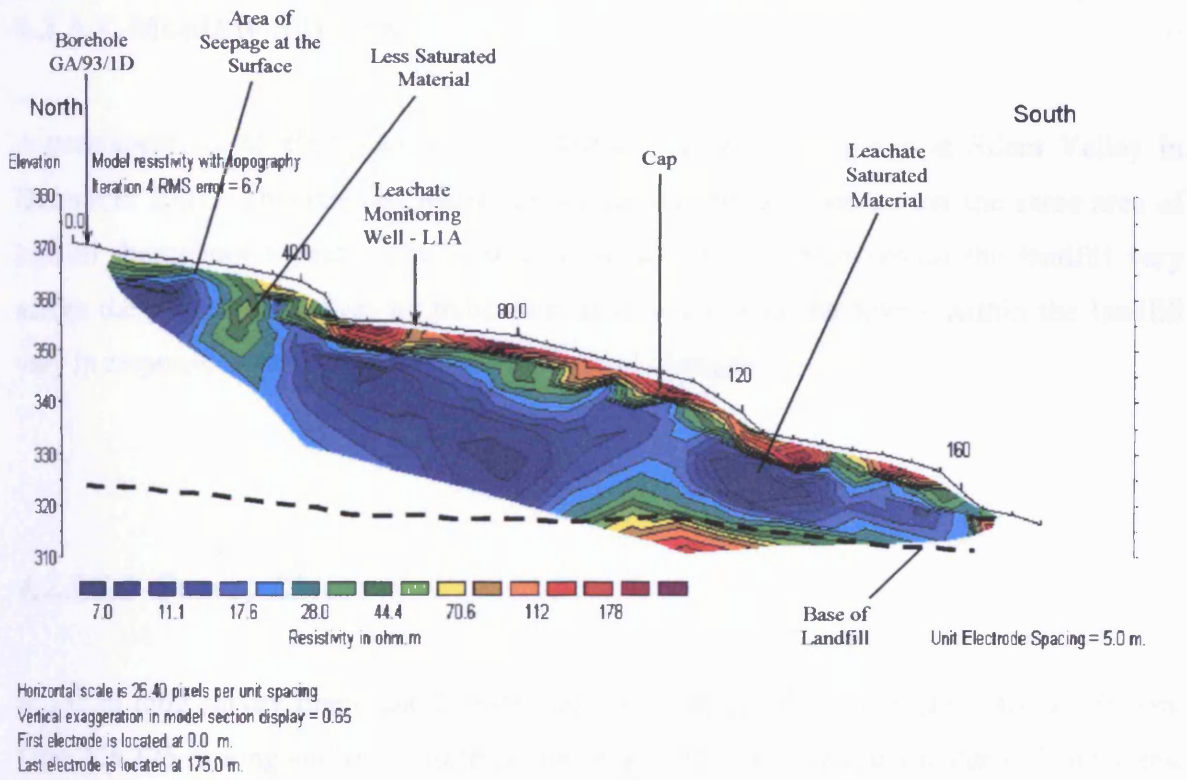


Figure 4.13 Line 2 of the summer 2001 resistivity survey.

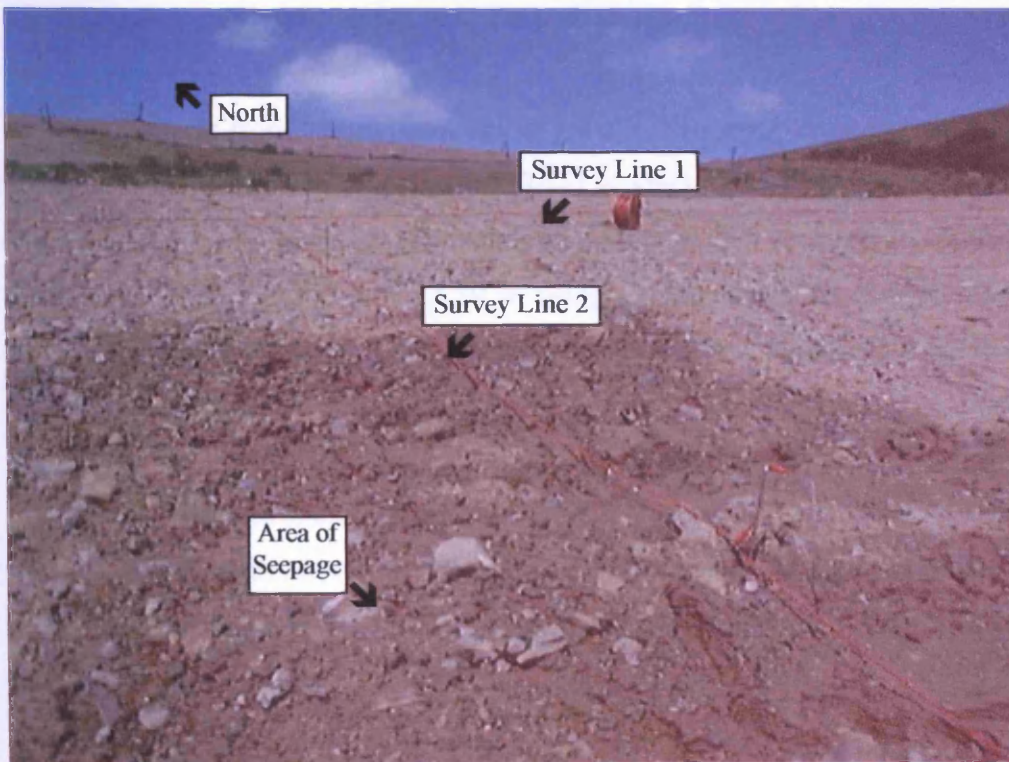


Figure 4.14 Photo (taken June 2001) showing the area where seepage is evident at the surface.

4.2.3.3 Monthly Surveys

A permanent set of electrodes was installed on the southern slope at Silent Valley in December 2001. This enabled resistivity surveys to be repeated across the same area of landfill throughout a year. The results show how resistivities within the landfill vary across the year, which gives an indication of how the leachate levels within the landfill vary in response to seasonal hydrometeorological changes.

4.2.3.3.1 Survey Lines

A 355 m long survey line (Line 1) runs East-West across the valley (Fig. 4.15). Survey Line 2 is 175 m long and runs North-South (Fig. 4.15). It is perpendicular to Line 1 and crosses Line 1 170 metres from its eastern end. Resistivity Line 1 is comprised of 72 electrodes and Line 2 is made up of 36 electrodes. Bamboo canes were inserted into the ground next to the electrodes to mark their location, which became invaluable as vegetation grew across the slope.

At about 8 metres from the northern end of Line 2 the survey crosses over the point where Golder Associates drilled borehole GA/93/1D in 1993. At the time of drilling, the surface elevation was 361.42 m. The current surface level at that location is about 370 m. The borehole was drilled to a depth of 39 m using a rotary percussive drill. Natural ground (clay) was hit at a depth of 37.30 m (324.12 mAOD) and rockhead (sandstone) was at a depth of 37.50 m (323.92 mAOD).

Line 2 passes through monitoring well L1A/L1B (about 62 metres from the north end of the line), which is monitored every month by Silent Valley Waste Services. About 100 metres from the north end of Line 2 there is a well (W1) that is not regularly monitored and is silted up.

The Wenner-Schlumberger array is used for the permanent set of resistivity lines installed at Silent Valley. The electrodes are at a spacing of 5 metres.

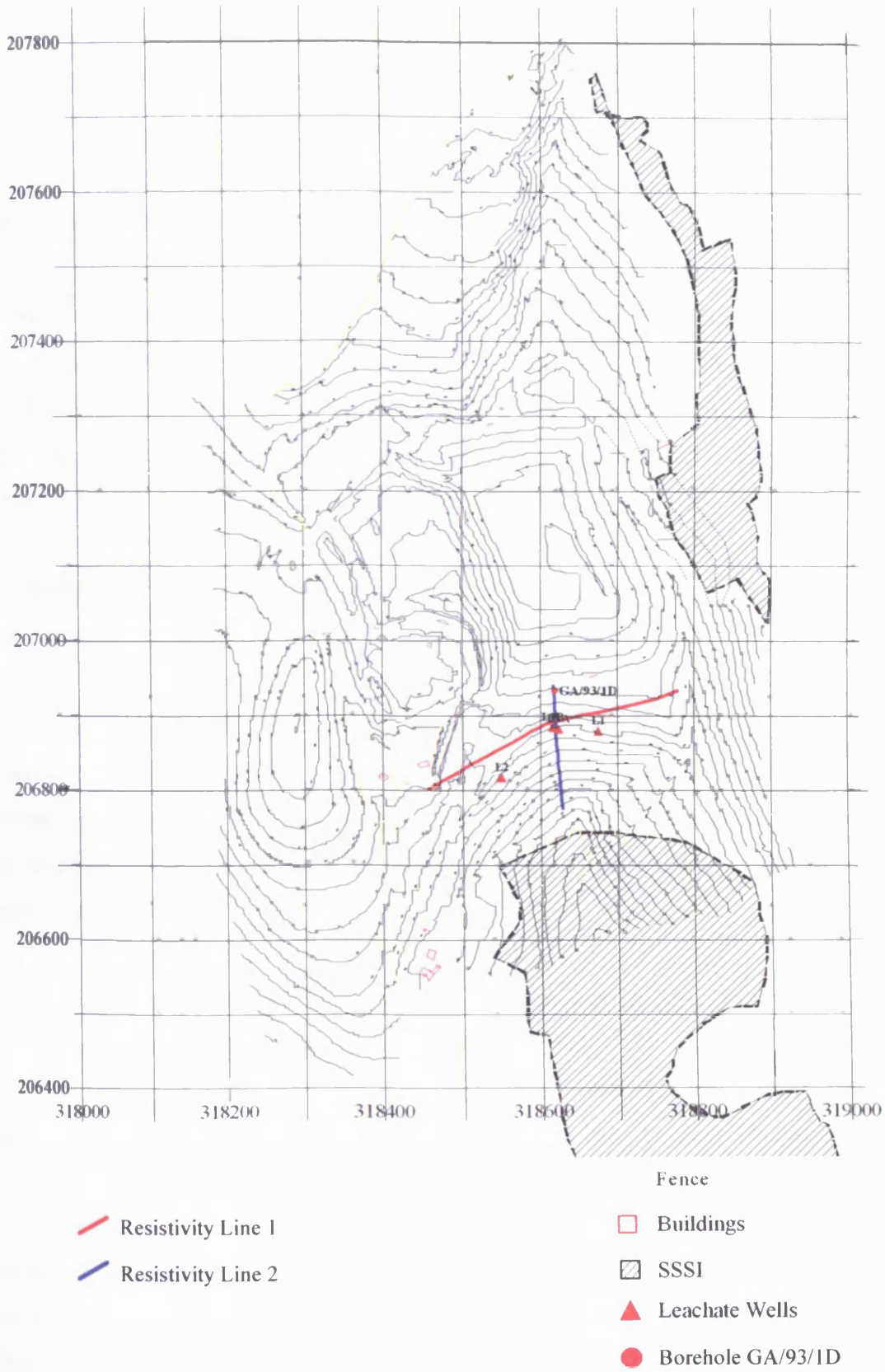


Figure 4.15 Map showing location of survey lines 1 and 2.

4.2.3.3.2 Data Analysis

The RES2DINV program was used to analyse and display the data.

4.2.3.3.3 Results

The results (Figures 4.16 and 4.17. For larger images see Appendix B) obtained for resistivity surveys performed for Line 1 and Line 2 are of a high quality. The structure of the landfill remains the same for surveys performed in different months indicating that the survey line and the equipment used has a very good repeatability. The only changes between months occur in the areas of saturation (areas of low resistivity – blue).

Due to problems with the resistivity equipment it was only possible to perform a survey for Line 1 in September 2002.

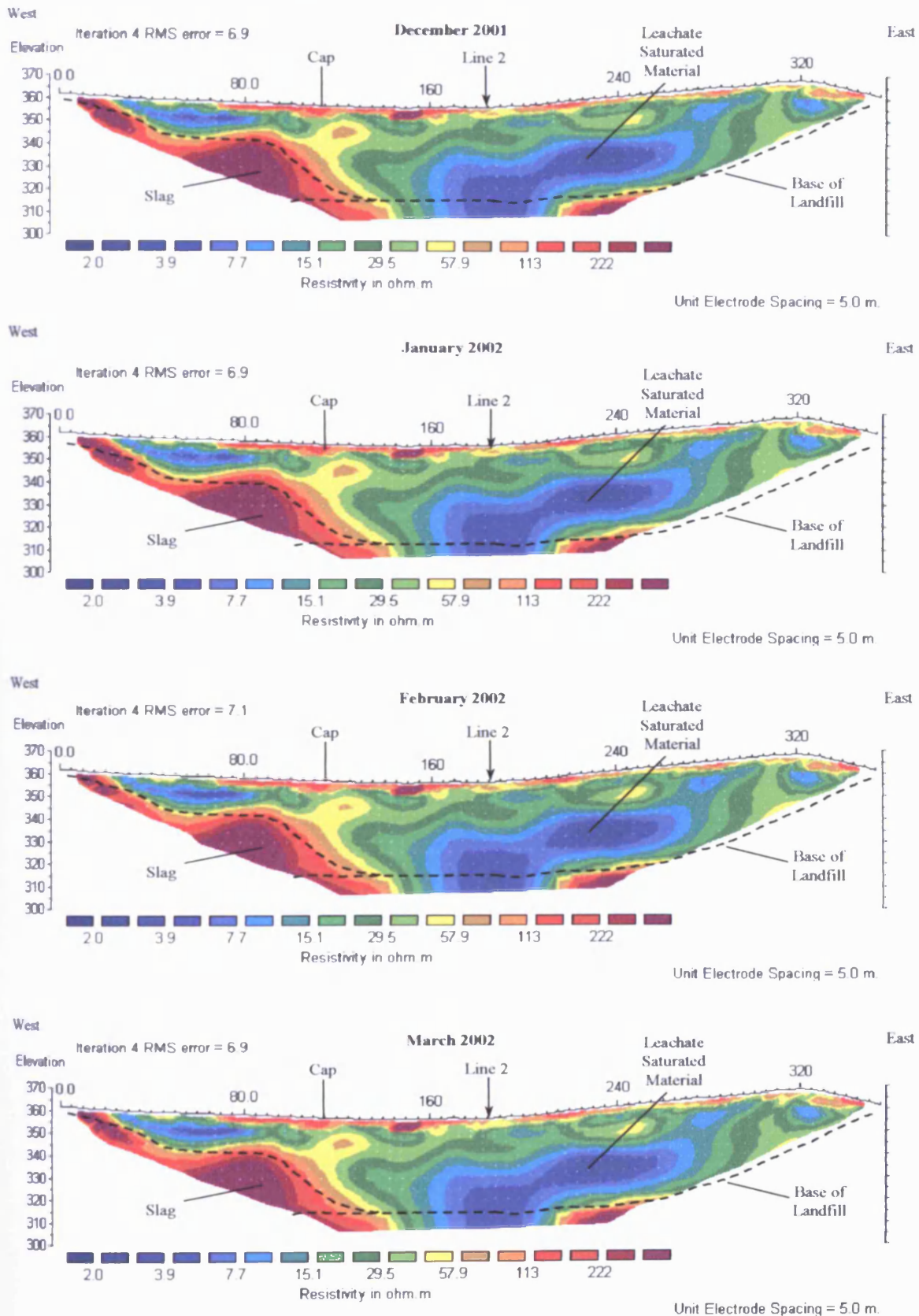
The sections show an area of high resistivity at the surface (orange/red), which is the cap. Dry waste (orange) and areas of saturated waste (green) can be seen across the sections. At increasing depth the lower resistivity values (green) are more widespread, indicating more saturated waste. Very low resistivity (blue) values indicate areas of leachate saturated waste.

Survey Line 1 shows an area of high resistivity (red/purple) at depth to the west there is likely represent the presence of slag within the fill material.

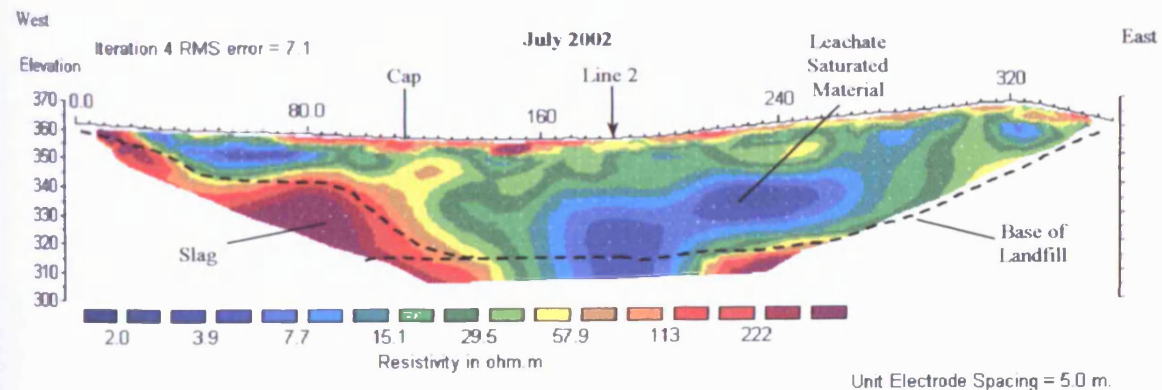
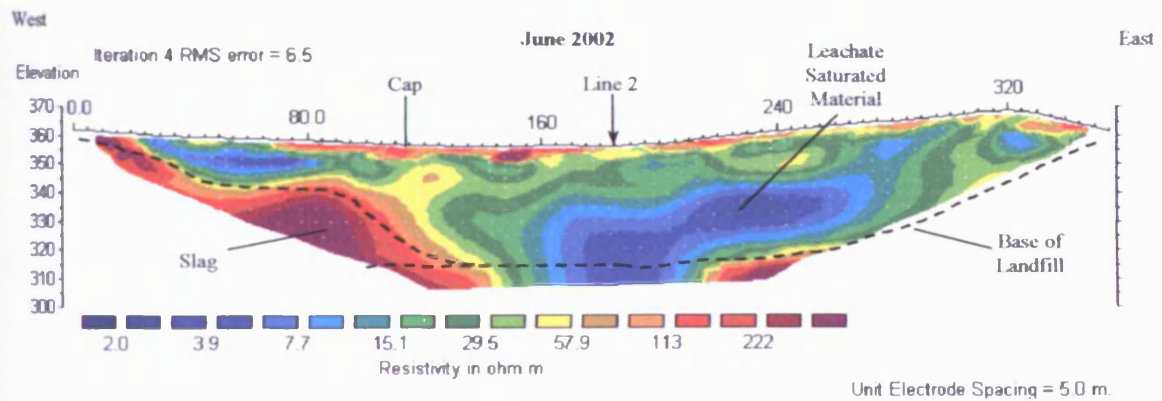
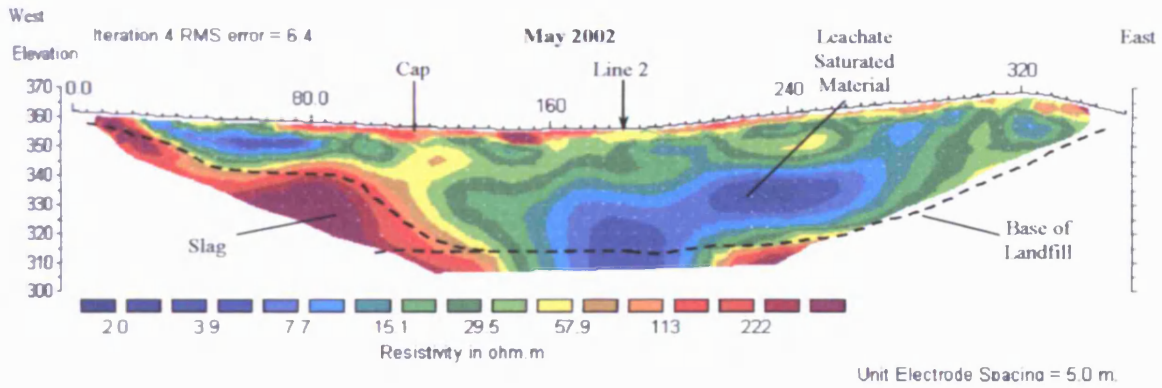
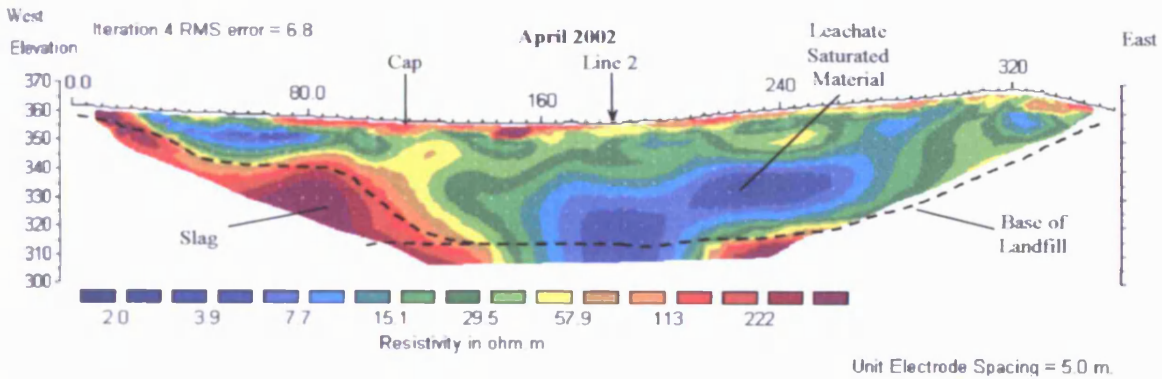
At depth to the south of survey Line 2 there are high resistivity values. This represents the original valley bottom.

Water levels at the monitoring wells L1 and L1A have been collected, on the day that the resistivity surveys were performed, using a dip meter. Unfortunately the dip meter belonging to the University broke after a few months and was not replaced until after the final monthly survey was done. The monitoring wells were partially silted up, so readings were only available when the water level was above the silt.

Figure 4.16 Resistivity profiles for survey Line 1 between December 2001 and November 2002.



Chapter 4 – Internal Structure.



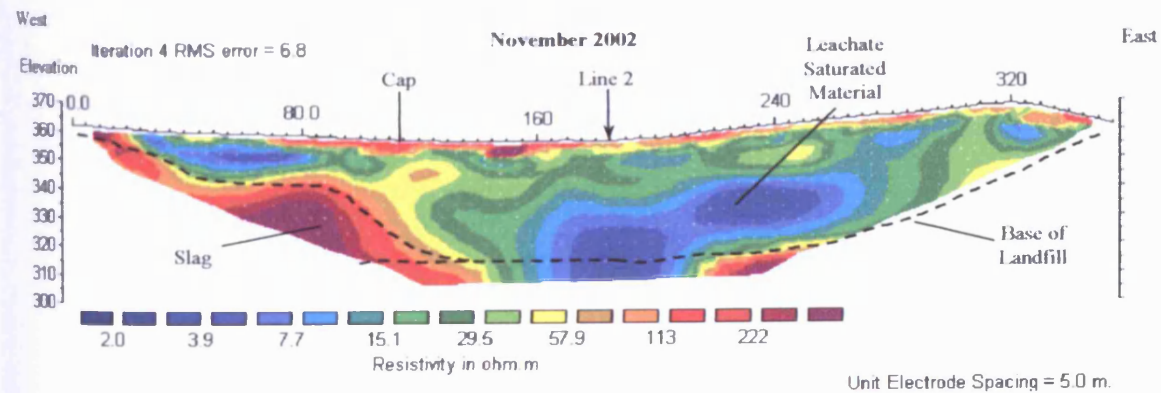
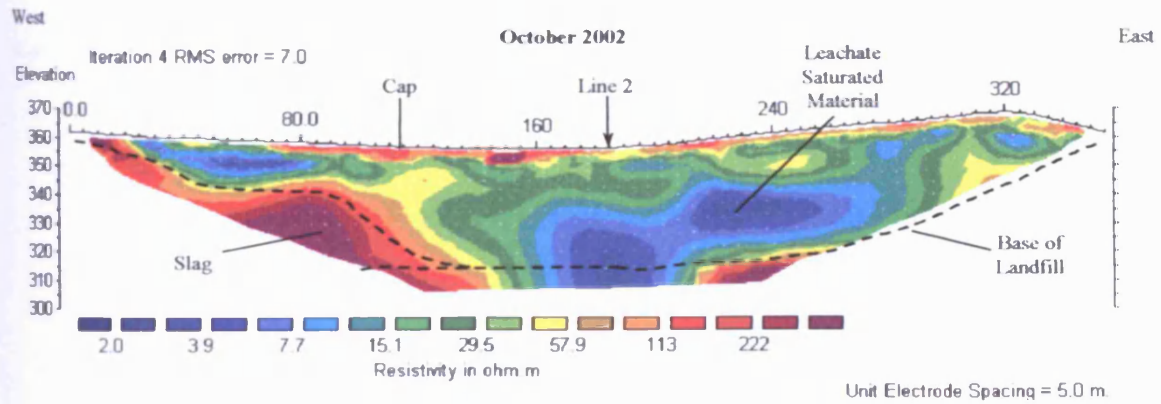
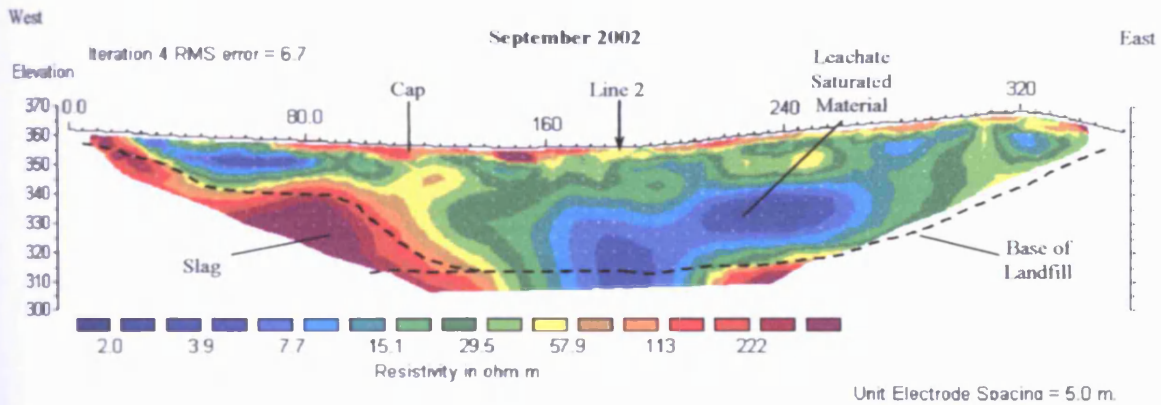
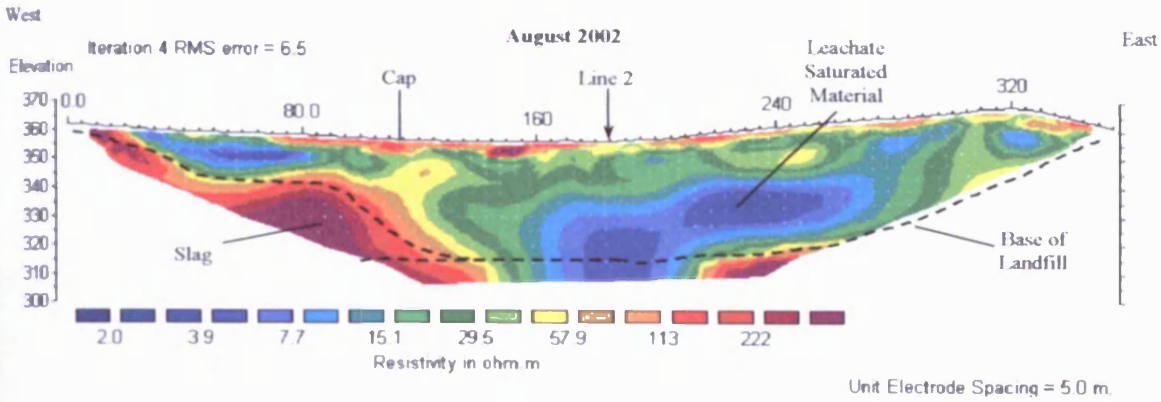
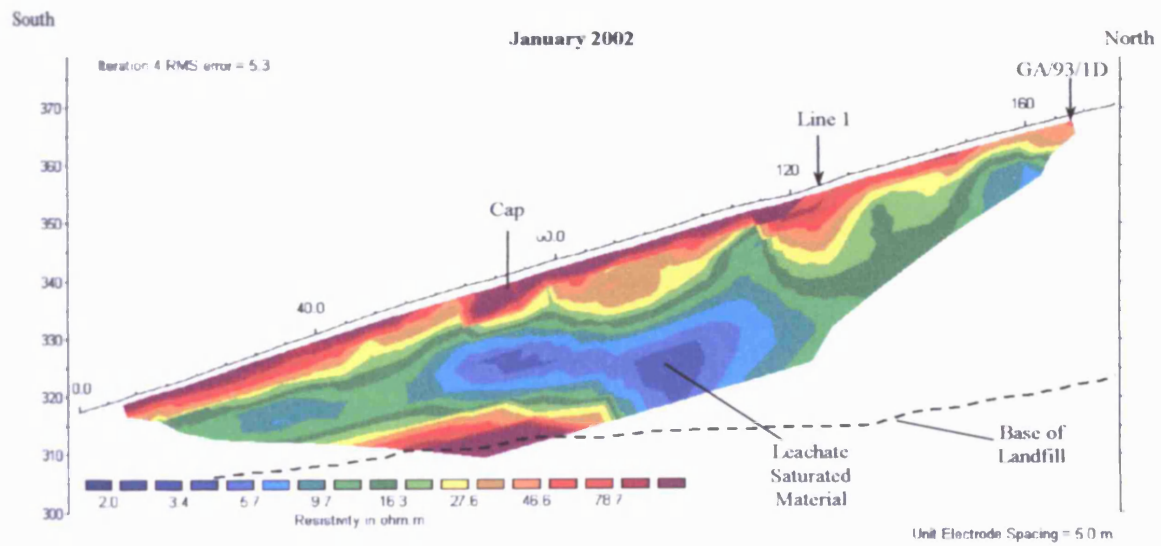
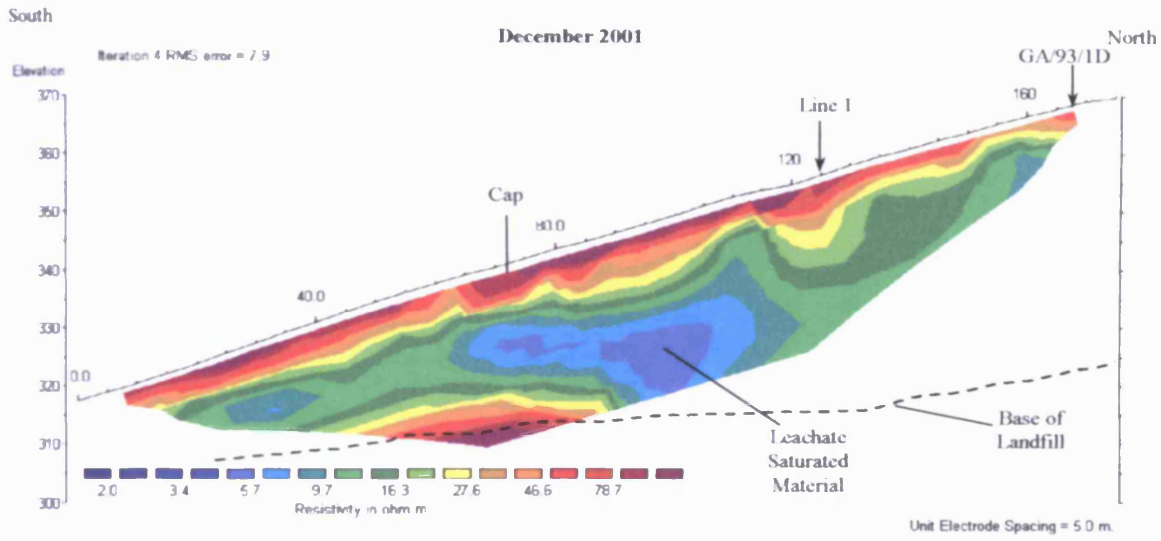
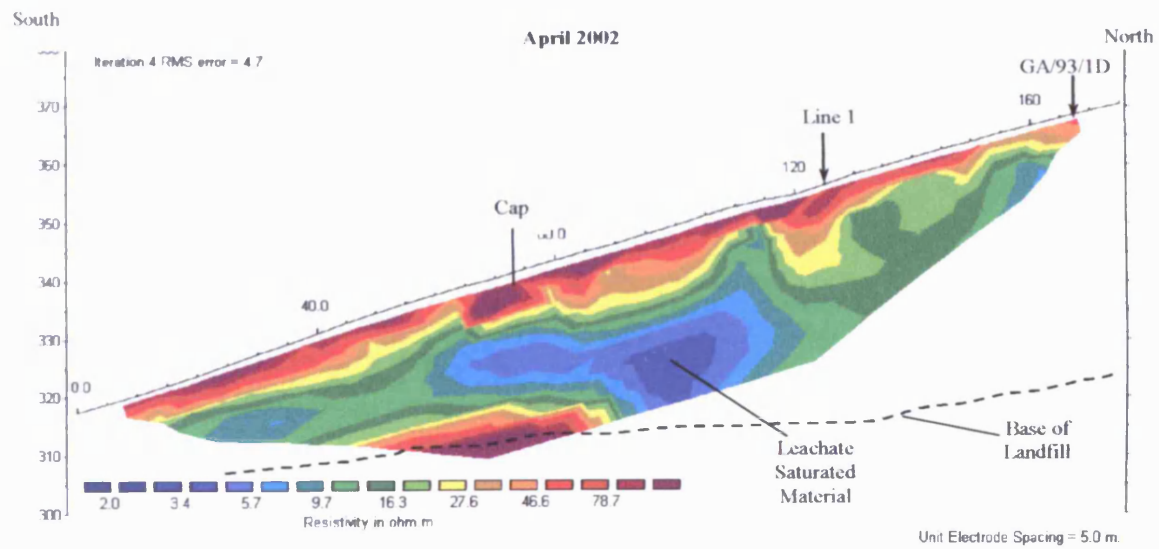
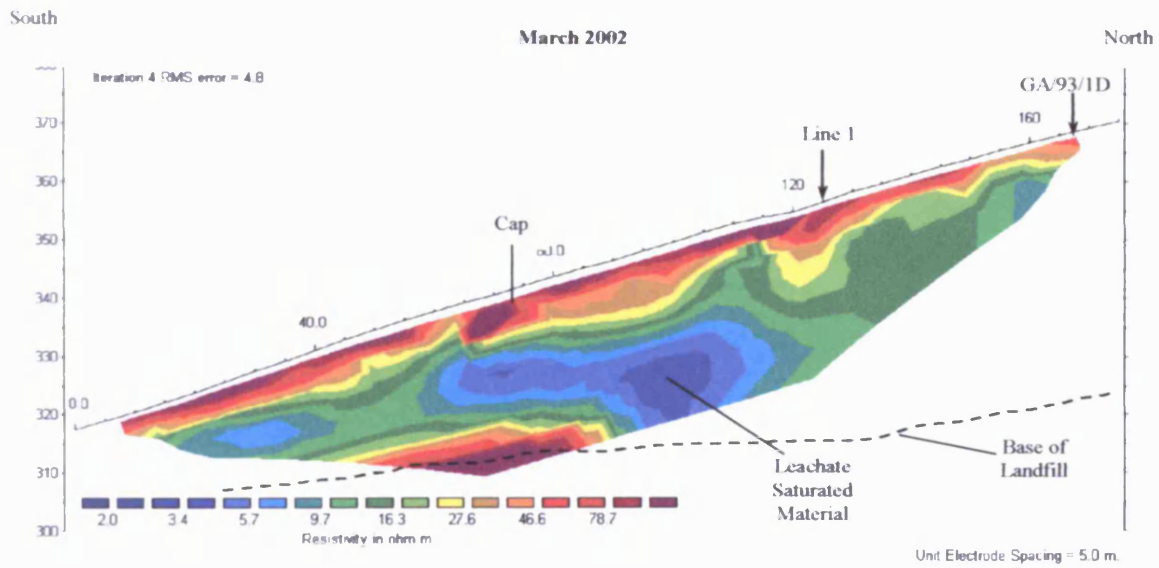
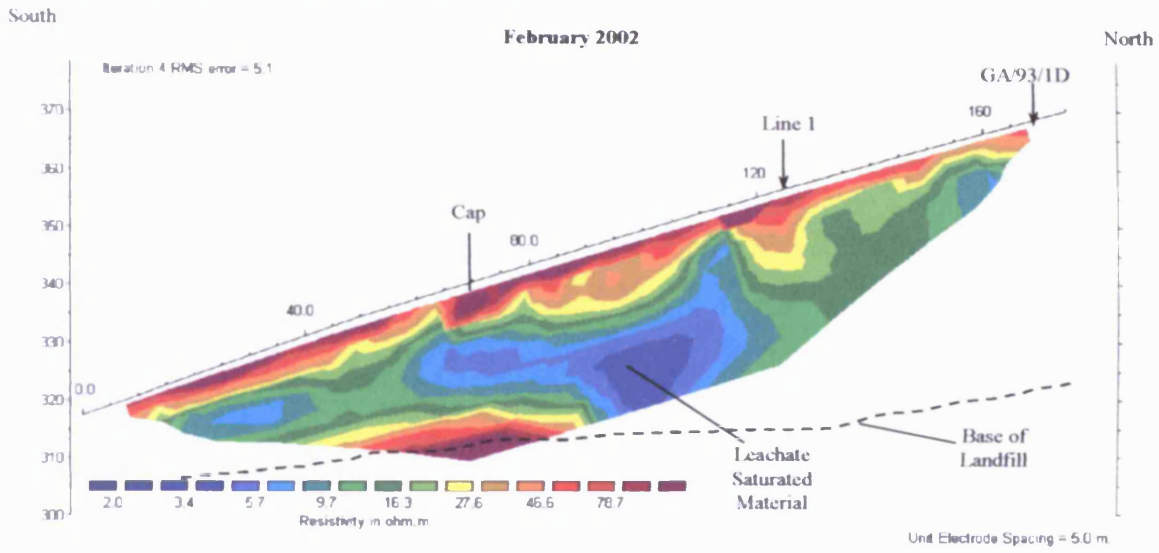
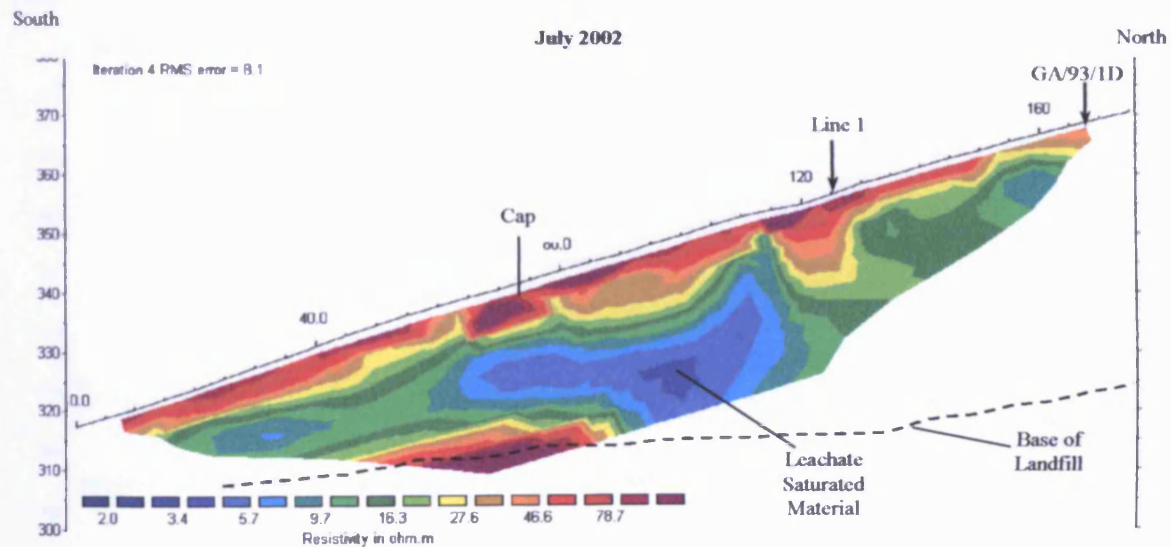
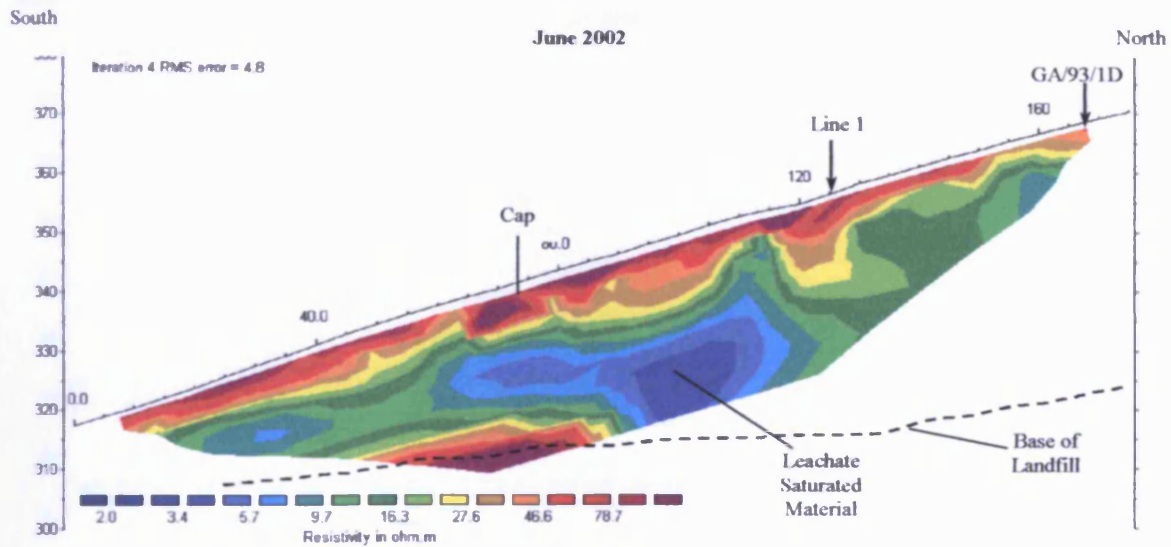
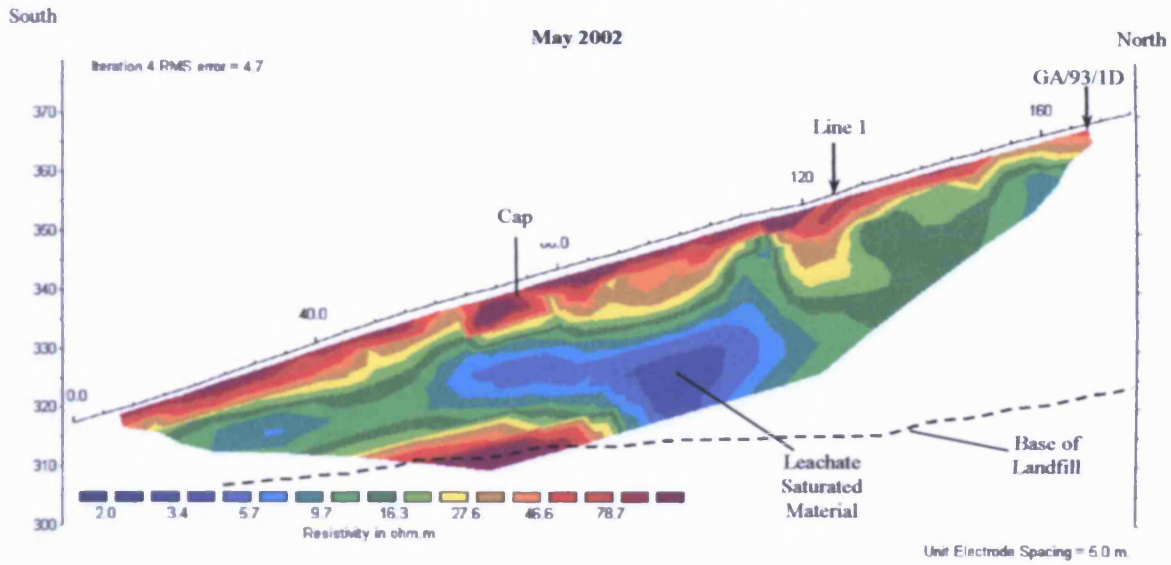
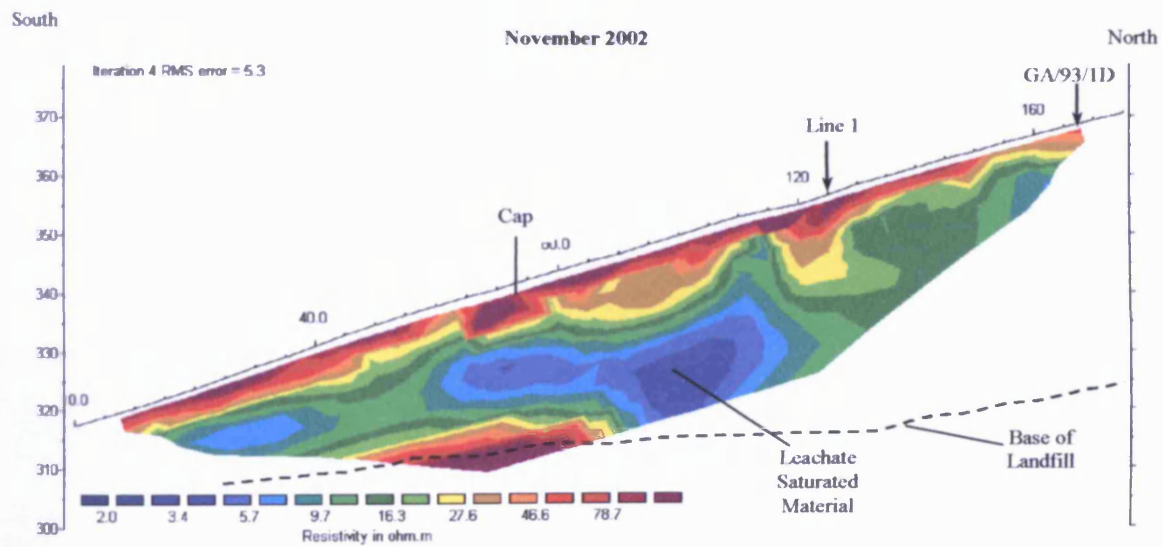
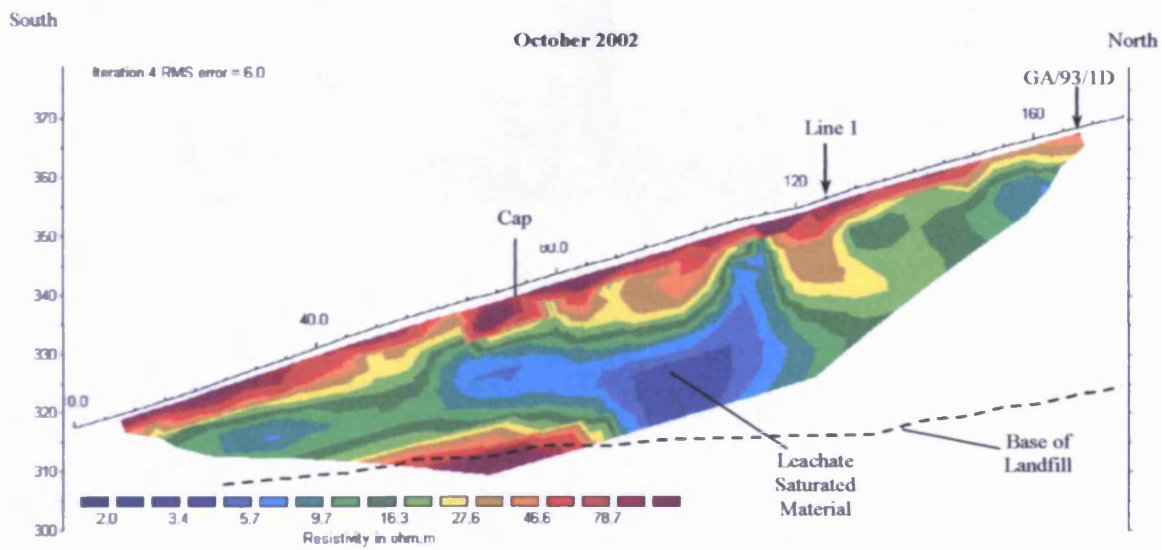
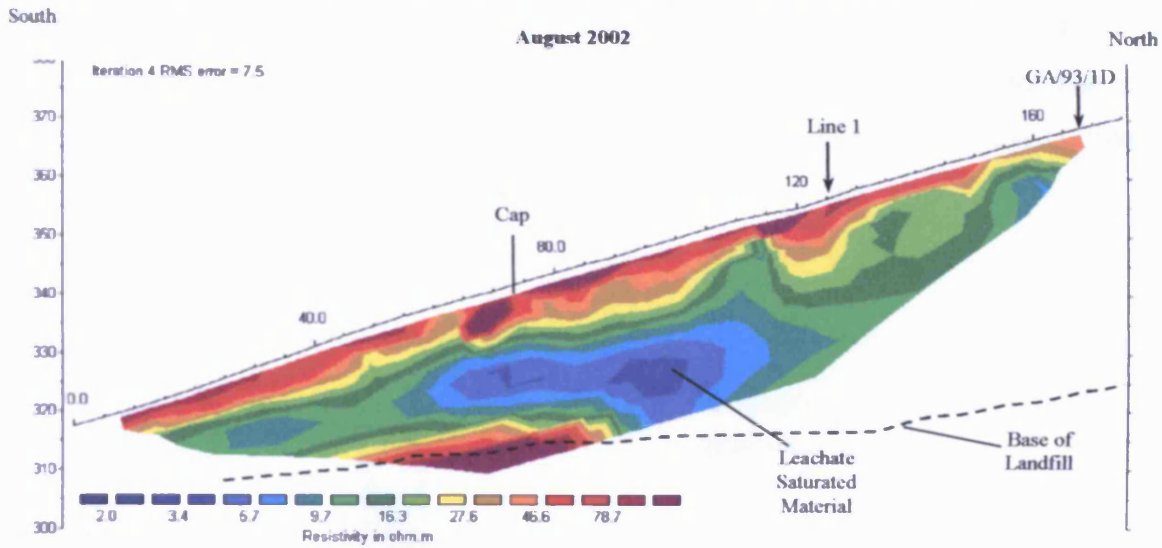


Figure 4.17 Resistivity profiles for survey Line 2 between December 2001 and November 2002.









The sections can be compared with the rainfall recorded at Silent Valley (Fig 4.18). For the survey period, the highest rainfall was in February 2002. The section for that month shows slightly lower resistivity values (darker blue) in the centre of Line 1 than the previous month indicating increased saturation.

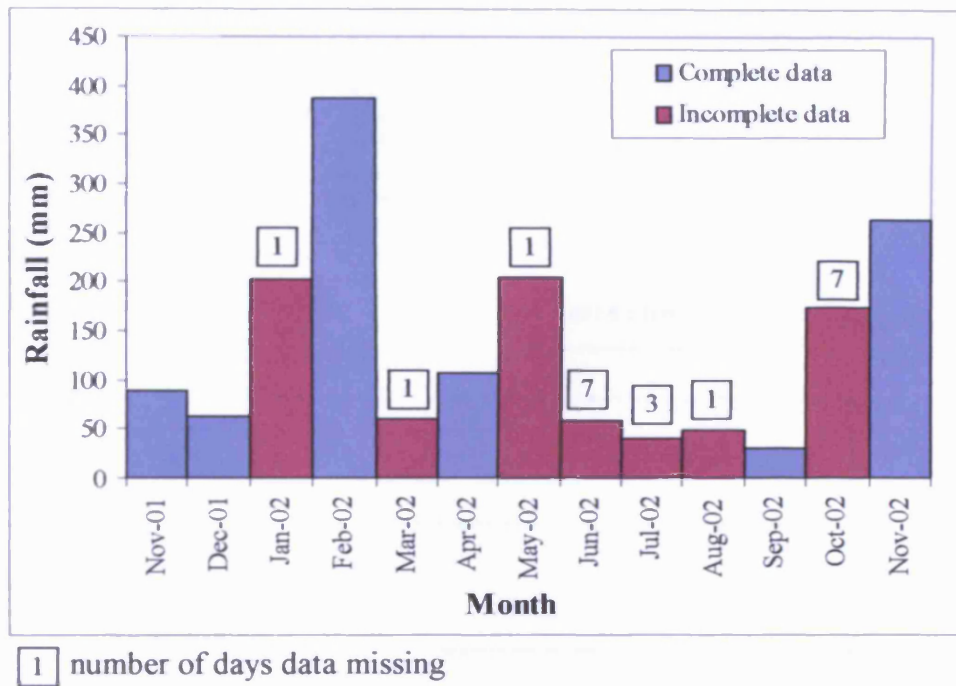


Figure 4.18 Rainfall recorded at Silent Valley by Silent Valley Waste Services.

4.2.3.4 3D Survey

The electrodes for 3D surveys are normally arranged in a rectangular grid with a constant spacing between the electrodes (Fig. 4.19). However, the RES3DINV resistivity and IP inversion program can also handle grids with a non-uniform spacing between the rows or columns of electrodes.

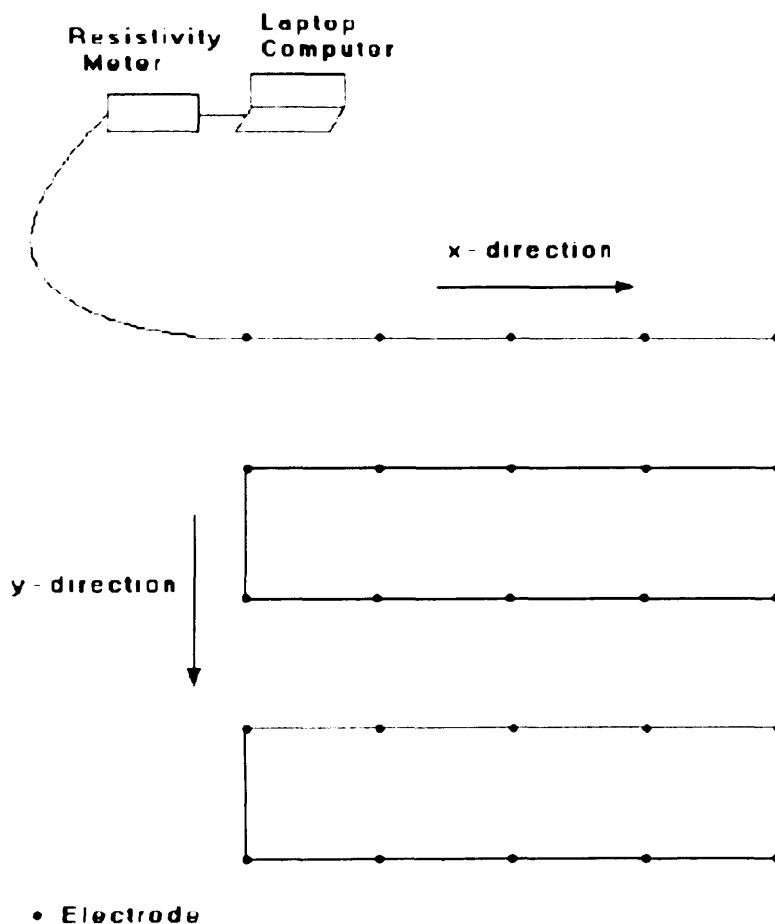
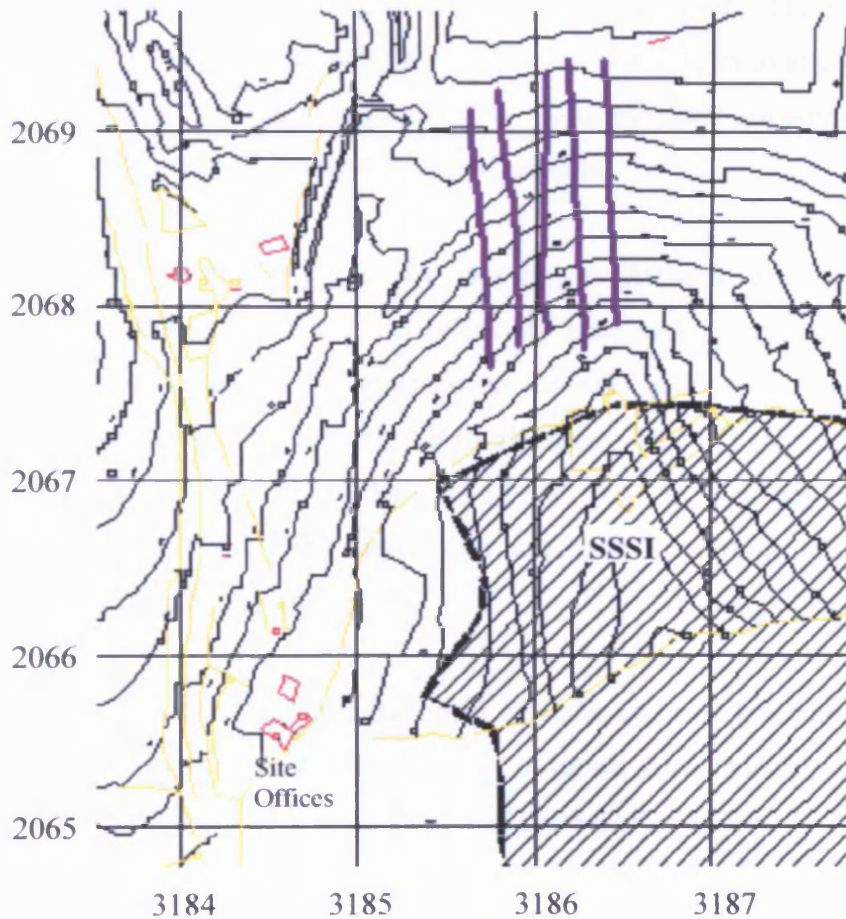


Figure 4.19 The arrangement of the electrodes for a 3D survey. From Loke (1999a).

In some cases, measurements are made only in one direction. The 3D data set consists of a number of parallel 2D lines. The data from each 2D survey line is initially inverted independently to give 2D cross-sections then combined into a 3D data set and is inverted with RES3DINV to give a 3D picture. The quality of the 3D model is expected to be poorer than that produced with a complete 3D survey.

In June 2002 five parallel resistivity surveys were performed (Fig. 4.20) by the author and Guy Cassidy, an MSc student. The survey lines are at a spacing of approximately 20 m. Each survey line has an electrode spacing of 3 m and is 159 m in length. One of the survey lines covers the same area as the monthly survey line.



Key

-  Resistivity Survey Lines
-  Contours
-  Fence
-  Buildings

Figure 4.20 Map showing the location of the resistivity survey lines.

Analysis of the resistivity data for each array, using the inversion modelling computer package *RES2DINV*, gives a 2 dimensional 'slice' through the underlying landfill (Fig. 4.21).

The resistivity profiles (Fig. 4.21) show capping material at the surface represented by high resistivities (purple). The eastern survey lines have lower resistivities than those in the west, indicating that the survey lines to the west are drier. The survey line furthest west shows high resistivities indicating materials of low void ratio and permeability. It is likely that there is a high slag content present. At depth there are areas of low resistivity (blue) that indicate areas of leachate saturated material.

The 3D inversion package *RES3DINV* was not available to process the data, so the sequence of two-dimensional vertical resistivity data points were integrated using the *Surfer* contouring computer programme to provide a three-dimensional model of resistivity in the fill material beneath the survey area. This 3D model was then sliced at different depths (0.75 m, 2.25 m, 3.80 m, 5.56 m, 7.46 m, 9.56 m, 11.87 m, 14.40 m, 17.19 m and 20.26 m) below the surface and parallel to it, to show spatial distribution of resistivity at each depth (Fig. 4.22).

Zones of low resistivity (high conductivity) indicate areas of leachate saturation, while areas of high resistivity indicate low leachate contents, corresponding principally to soil bunds and cover materials where void ratio and permeability is low.

In the field it was possible to detect an area (the north-west of the area covered in this survey) where surface water was present. From the results of the resistivity surveying it is unlikely that the leachate is breaking out at this point, instead surface water is issuing further up the slope and running along the surface. This is indicated by the high resistivity values shown at 0.75 m below the surface beneath these surface seepage areas. If the surface of the landfill were saturated with leachate then lower resistivity values would be expected within the underlying soil capping.

The very high resistivity values (purple) found close to the surface (0.75 m below ground level) represent the cap of the landfill. High resistivity values are present at 2.25 m below

the surface representing material with a low moisture content. This suggests that the cap is limiting infiltration into the landfill.

Resistivity values decrease with depth indicating waste material, areas of saturation and the presence of leachate.

The resistivity plot for 3.80 m below the surface indicates the presence of dry waste (orange) and areas of saturated waste (green). At increasing depth the lower resistivity values (green) are more widespread, indicating more saturated waste.

Low resistivity (blue) values from 11.87 m deep indicate areas of leachate saturated waste. At 20.26 m below the surface the area of low resistivity (blue) is decreasing indicating a decrease in the leachate saturation.

It is likely that the high resistivity values at depth to the west of the survey area represent the presence of slag within the fill material in which low void ratios result in low leachate contents.

Pages 232 to 236

Figure 4.22 Resistivity modelled on surfaces at increasing depth, based on integration of five 2D resistivity tomography models.

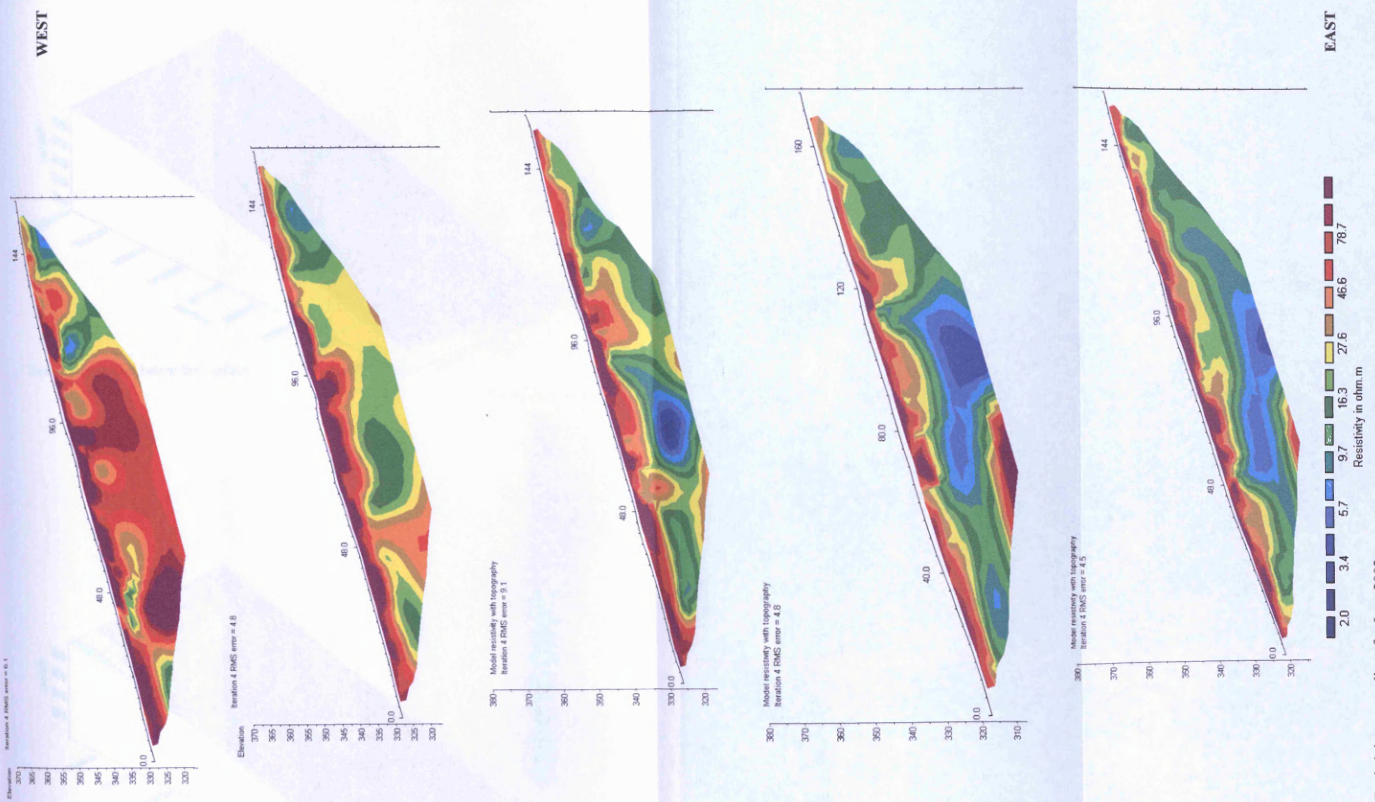
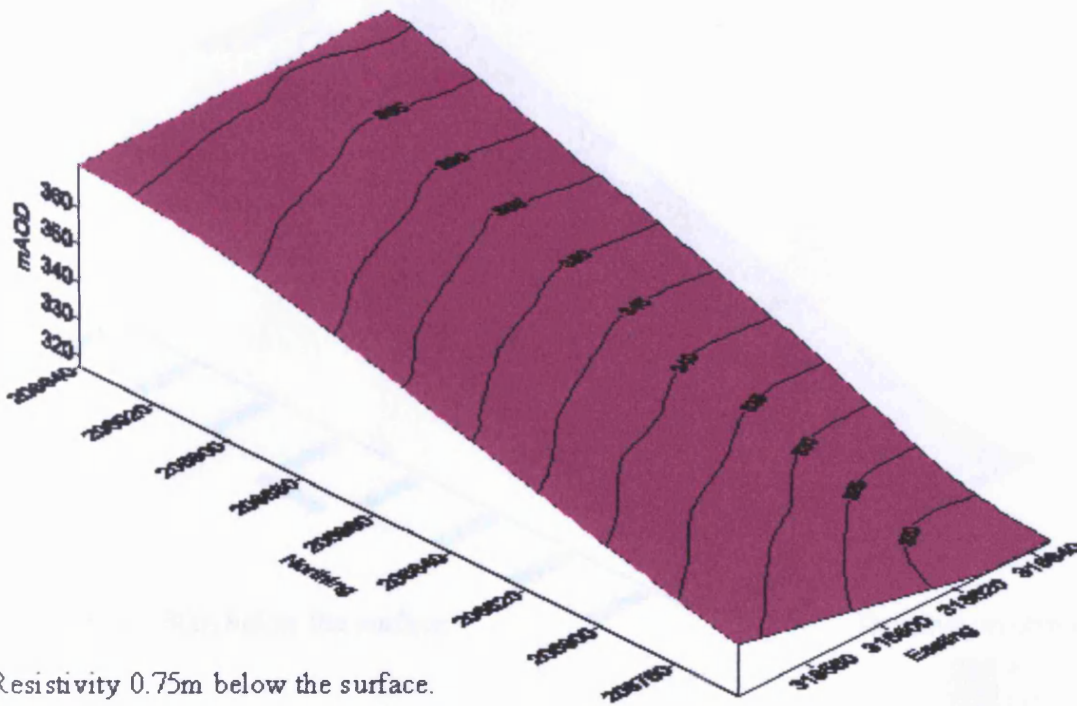
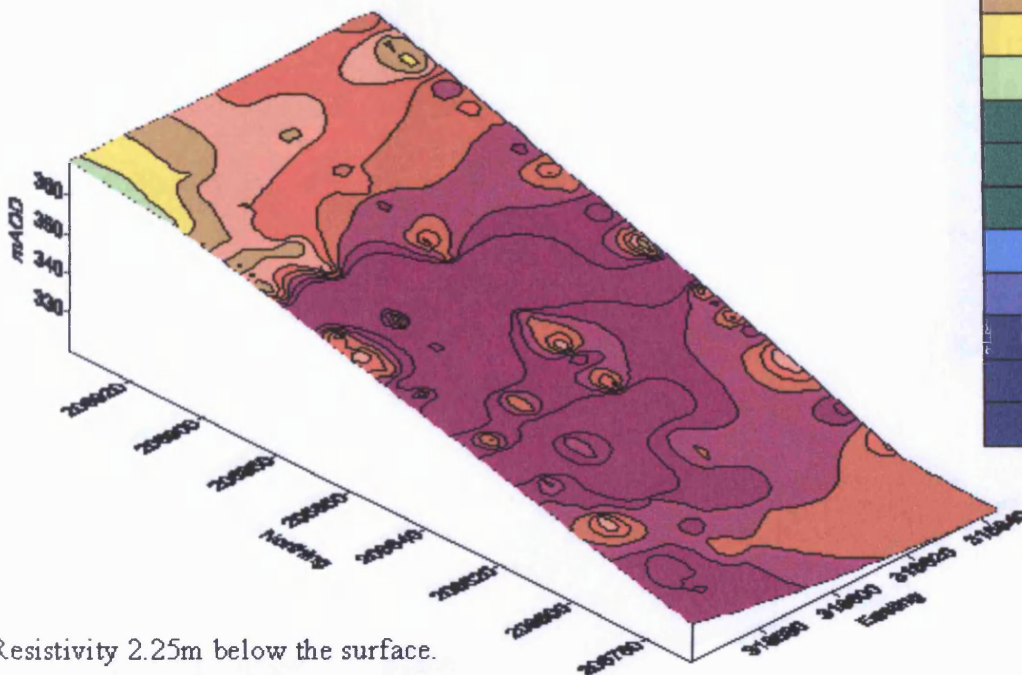
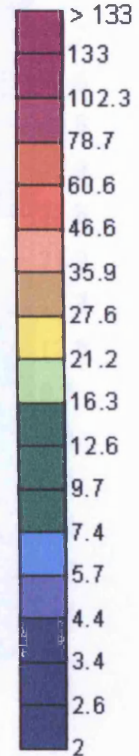


Figure 4.21 Resistivity survey lines for June 2002.

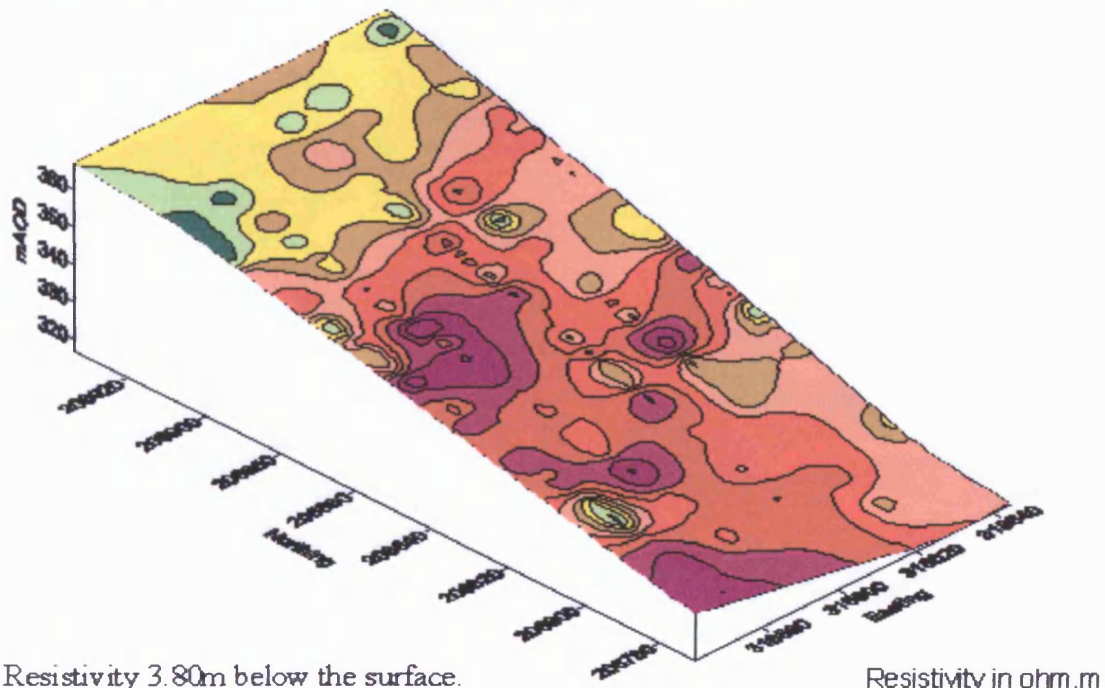


Resistivity 0.75m below the surface.

Resistivity in ohm.m

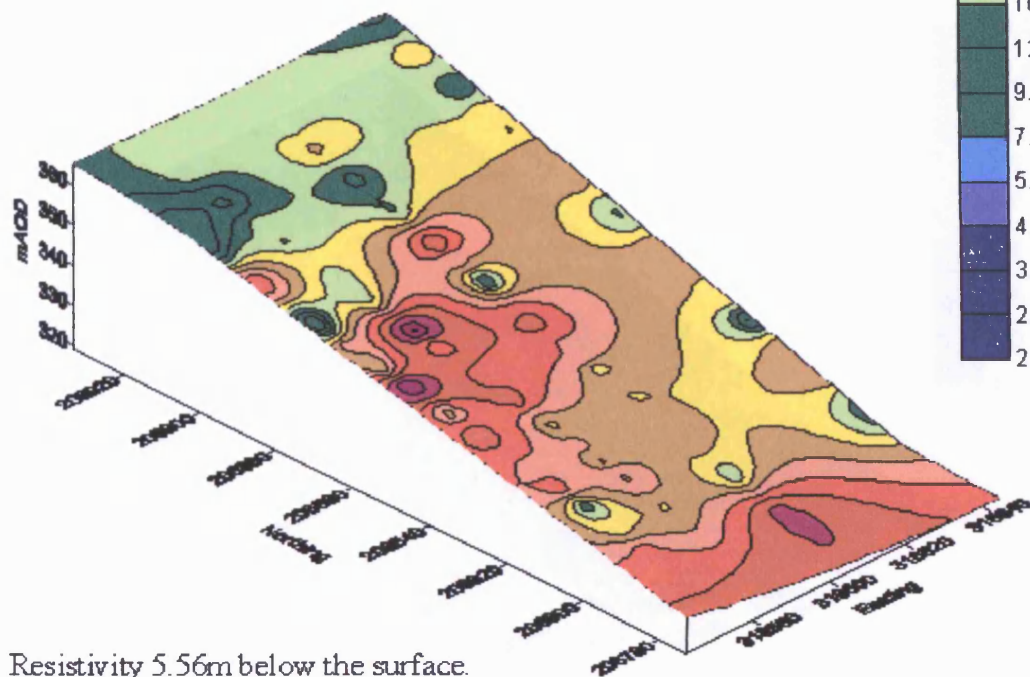
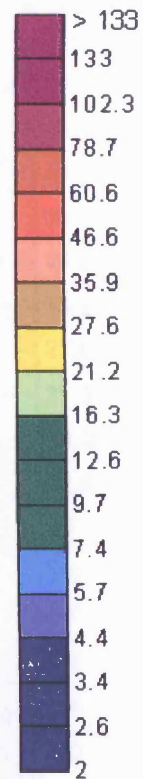


Resistivity 2.25m below the surface.

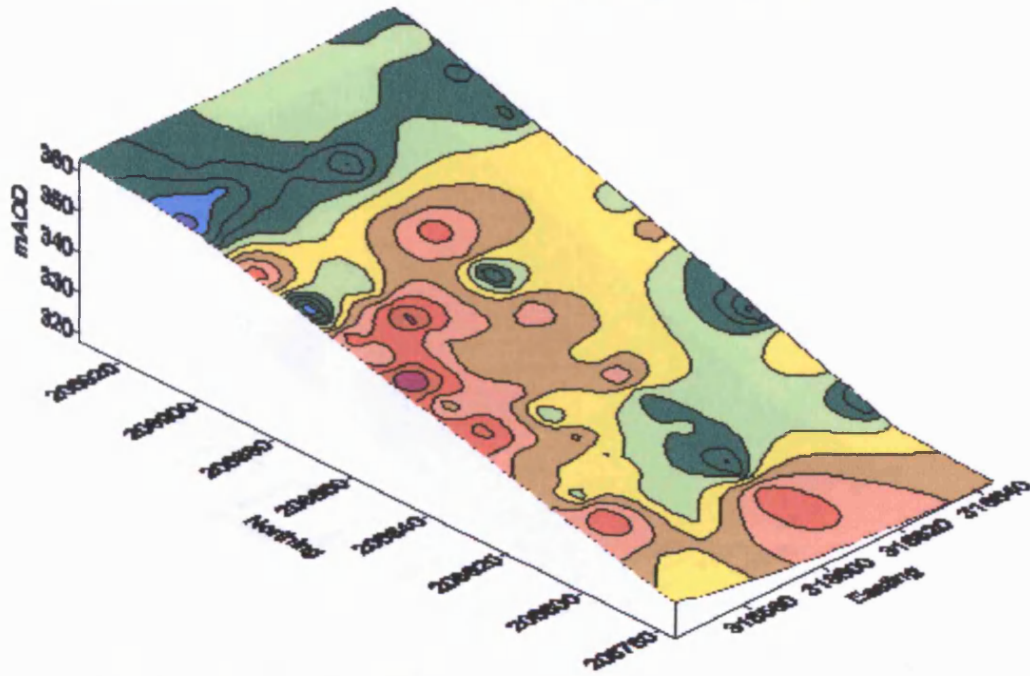


Resistivity 3.80m below the surface.

Resistivity in ohm.m

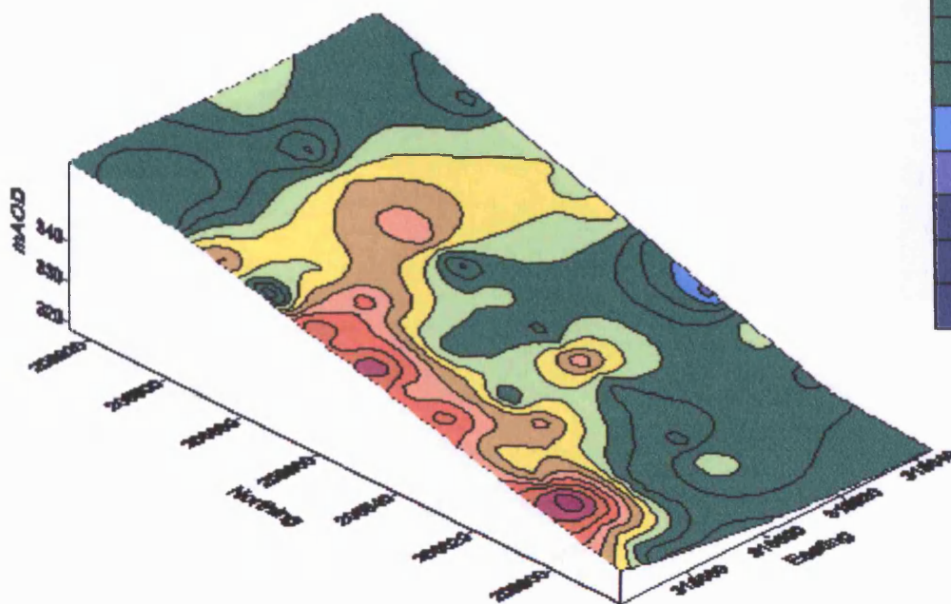
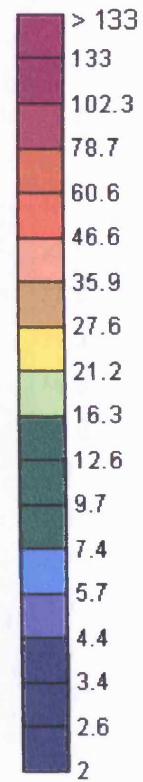


Resistivity 5.56m below the surface.

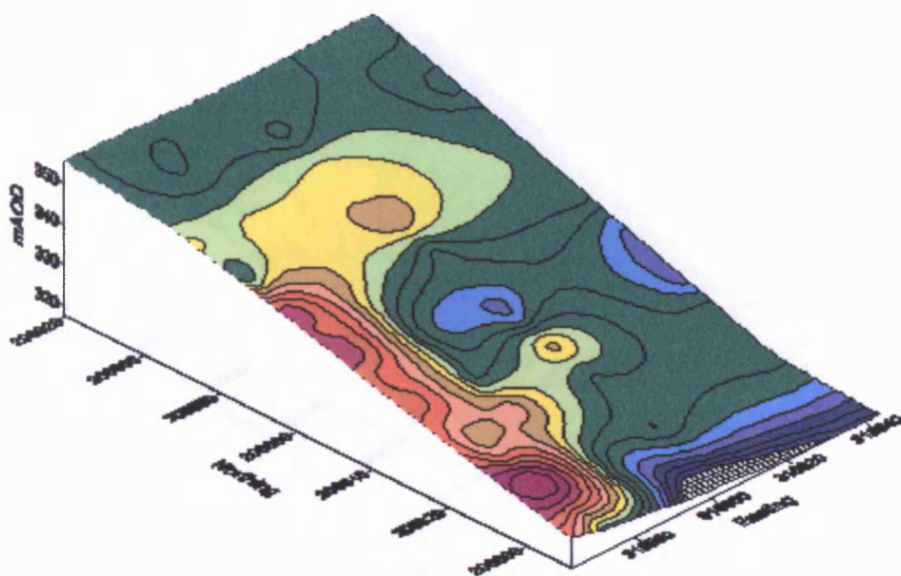


Resistivity 7.46m below the surface.

Resistivity in ohm.m

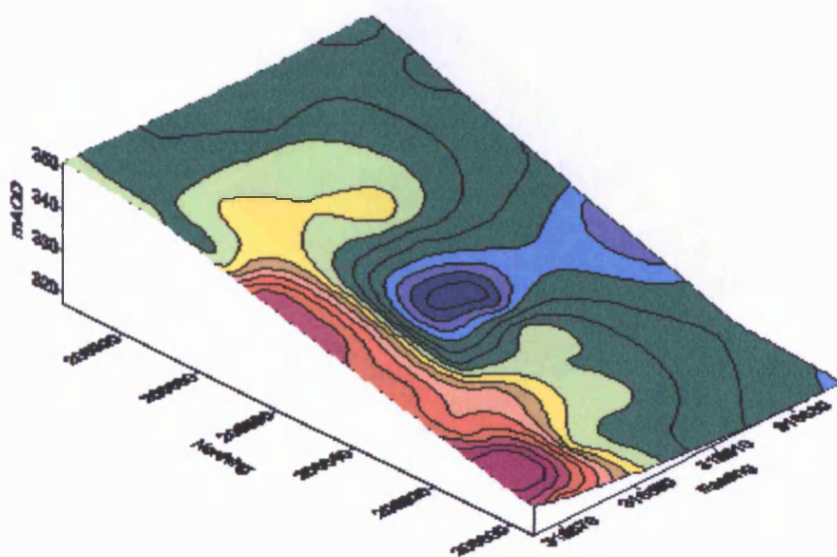
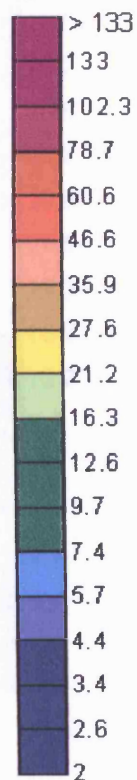


Resistivity 9.56m below the surface.

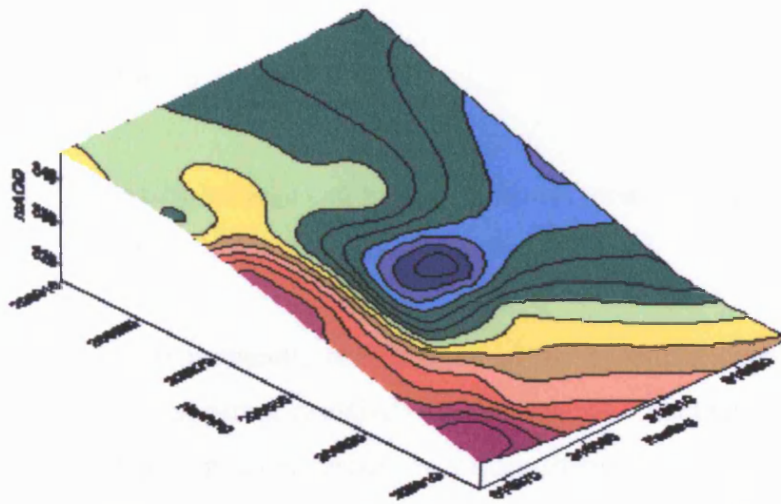


Resistivity 11.87m below the surface.

Resistivity in ohm.m

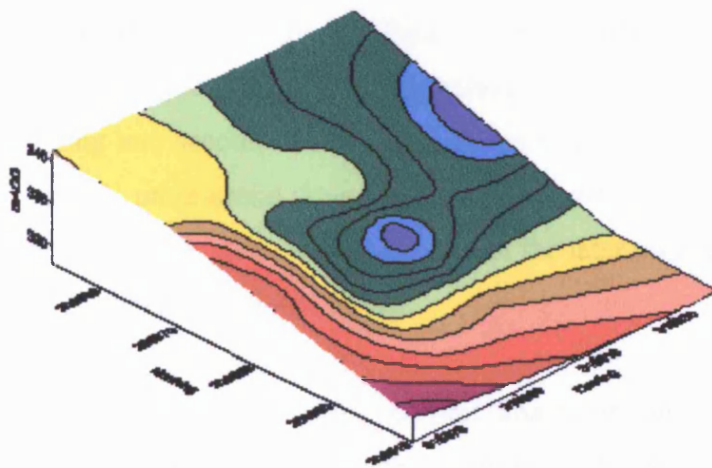
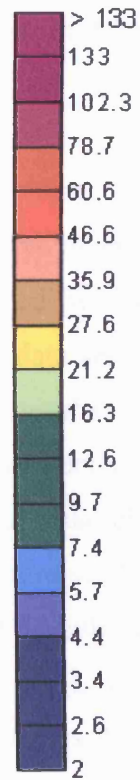


Resistivity 14.40m below the surface.



Resistivity 17.19m below the surface.

Resistivity in ohm.m



Resistivity 20.26m below the surface.

4.2.3.5 Time-Lapse Resistivity

4.2.3.5.1 Theory

Resistivity imaging surveys can be carried out in time as well as space, which enables the changes of the subsurface to be monitored through time.

For time-lapse experiments, the changes in the subsurface resistivity are estimated by using changes in apparent resistivity measurements. Accurate results can therefore only be obtained if the apparent resistivity values themselves are sufficiently accurate. It is preferable to use the Wenner-Schlumberger array as the dipole-dipole and pole-dipole arrays due to the relatively low signal to noise ratios for experiments with large spacings (Geotomo Software, 2002).

Normally, the data from the surveys conducted at different times are inverted independently, frequently with a smoothness-constrained least-squares inversion method. The changes in the subsurface resistivity values are then determined by comparing the model resistivity values obtained from the inversions of an initial data set and the later data sets. In many cases, such an approach has given satisfactory results. However, in theory, since the inversion of each data set is carried out independently, there is no guarantee that the differences in the resistivity values are only due to actual changes in the subsurface resistivity with time. Each inversion attempts to minimise the difference between the observed and calculated apparent resistivity values for an individual data set without taking into account the model obtained from the initial data set (Loke, 1999b). In the RES2DINV programme there is a joint inversion technique that uses the model from the initial data set to constrain the inversion of the later time data sets to minimise possible distortions (Geotomo Software, 2002).

By default, the model obtained for the first data set is used as the reference model for all the later time data sets, i.e. the same reference model is used for all the other data sets. Where there is a large change in resistivity of the models from the first to the last data set, an option is provided where the model for the preceding data set is used as the reference model. In this case the model for the first data set is used as the reference model for the

second data set, while the model for the second data set is used as the reference model for the third data set (Geotomo Software, 2002).

In the software the time-constrain weight gives the relative importance given to keeping the later models as similar as possible to the reference model. If a large weight is used (eg. 10), the models for the later data sets will be kept very similar to the reference model, which effectively minimises changes across the time models. This reduces the possibility of noise in the data sets causing spurious changes between models but at the expense of increasing the data misfit, i.e. the RMS differences between the calculated and measured data. A value of 1 gives equal importance to minimising the time changes in the model and minimising the RMS data error. The programme uses a default value of 3 for the time-constrain weight (Geotomo Software, 2002).

The software can display the change in the model resistivity obtained from the inversion of the later time data set compared with the reference model from the inversion of the first data set. The changes in resistivity will indicate changes in saturation.

4.2.3.5.2 Results

RES2DINV was used to investigate the change in resistivity of Line 1 over the year. Simultaneous inversions were carried out using the first data set (December 2001) as the reference model and a time constraint weight of 3. The results from the initial data set form the base model in the joint inversion with the later data sets.

Figure 4.23 shows the time-lapse data (in this case time series 10, i.e. October 2002 compared with December 2001) for the initial data set, a subsequent data set and the percentage change in resistivity between them.

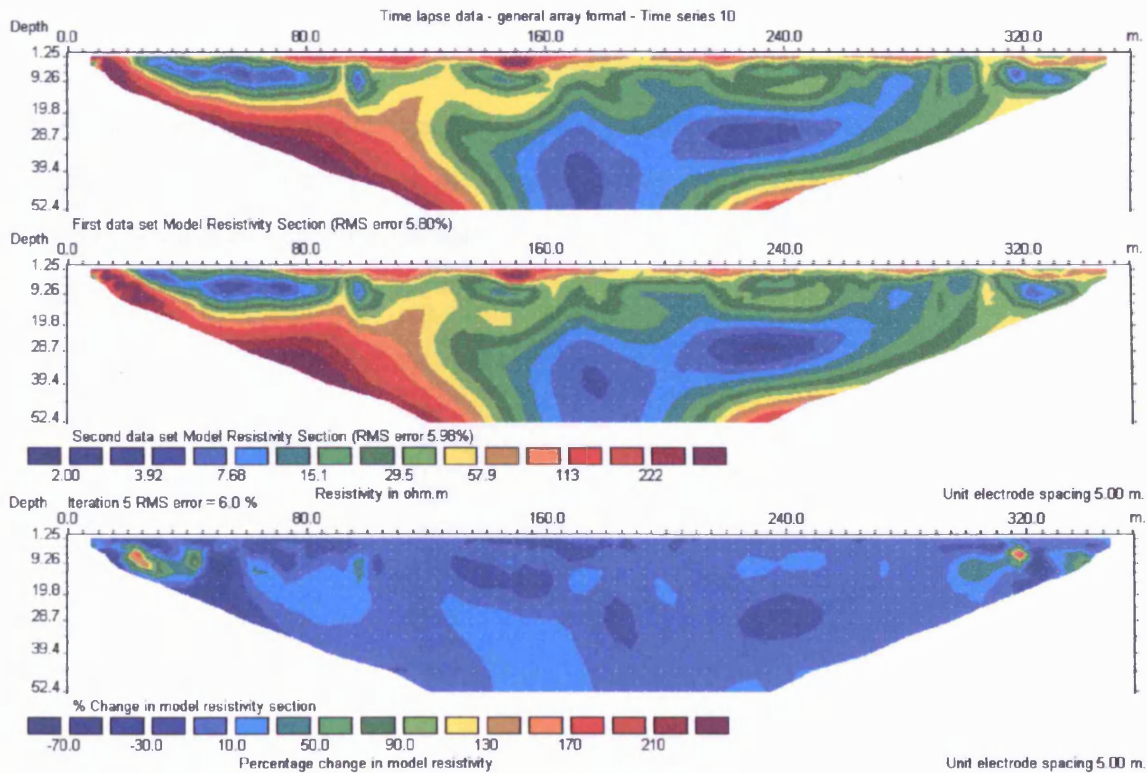


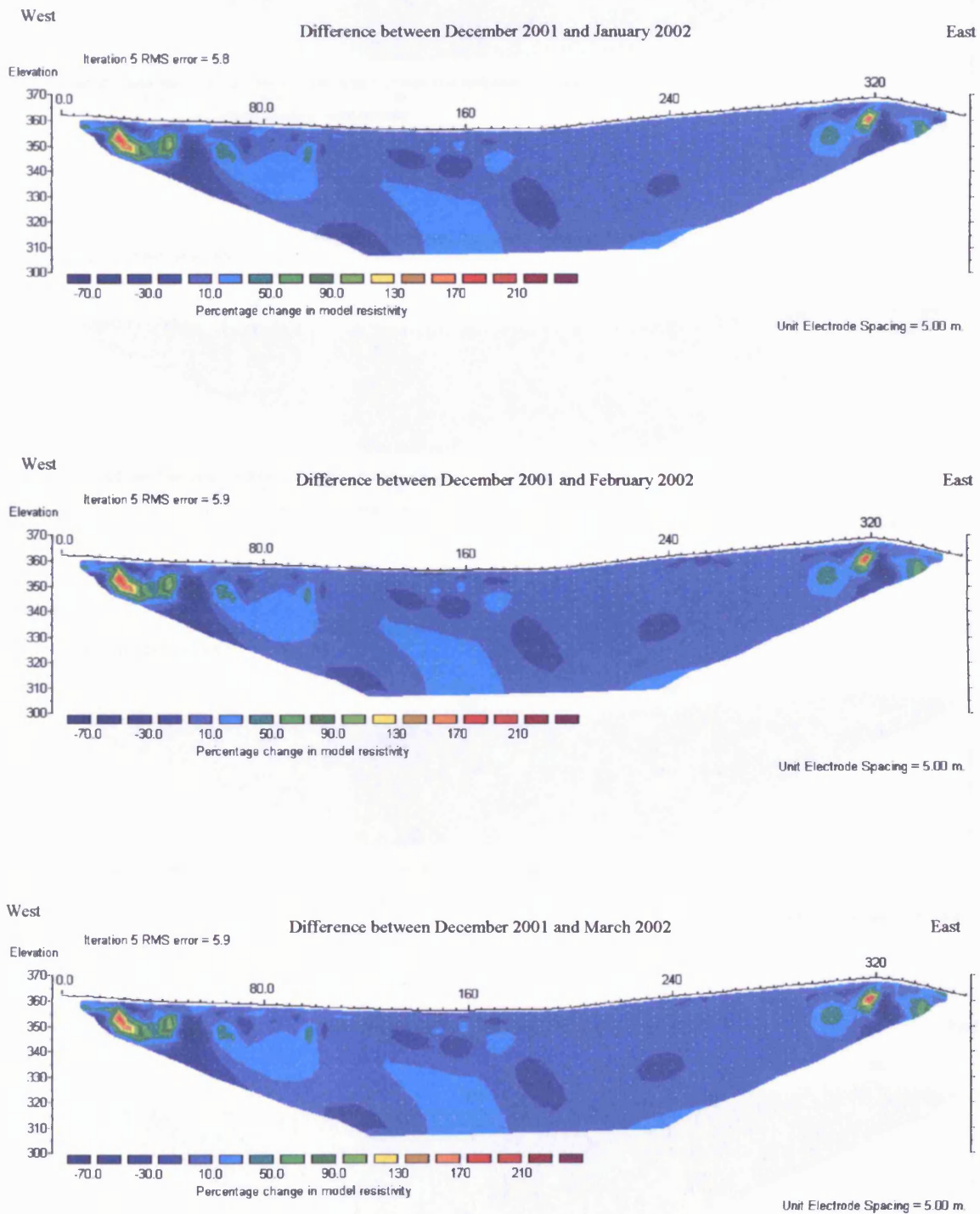
Figure 4.23 Time-lapse data for time series 10 for the initial data set (December 2001), a subsequent data set (October 2002) and the percentage change in resistivity between them.

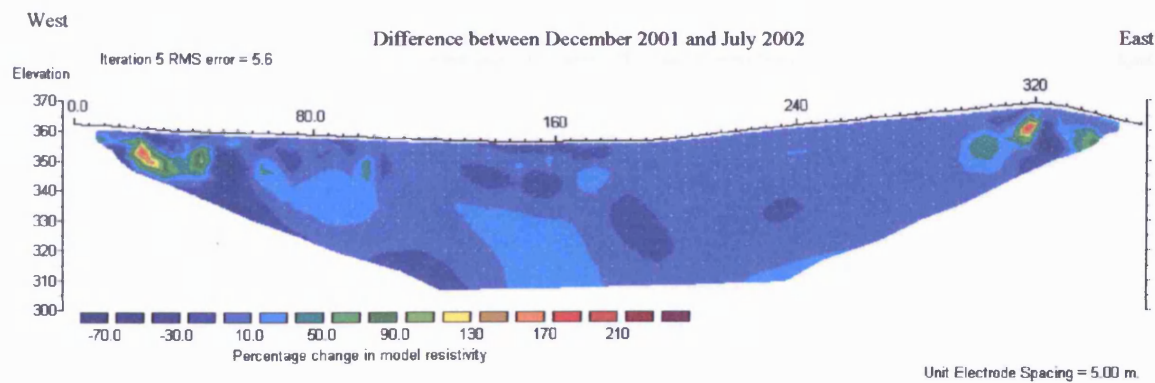
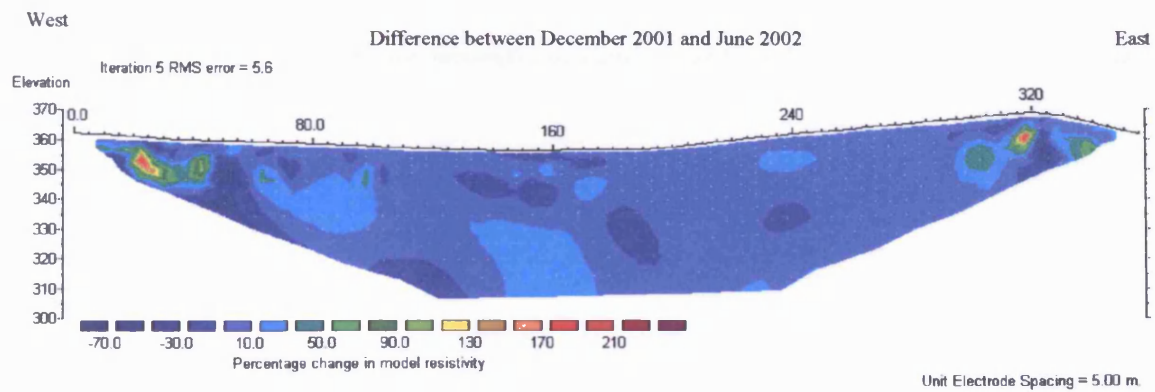
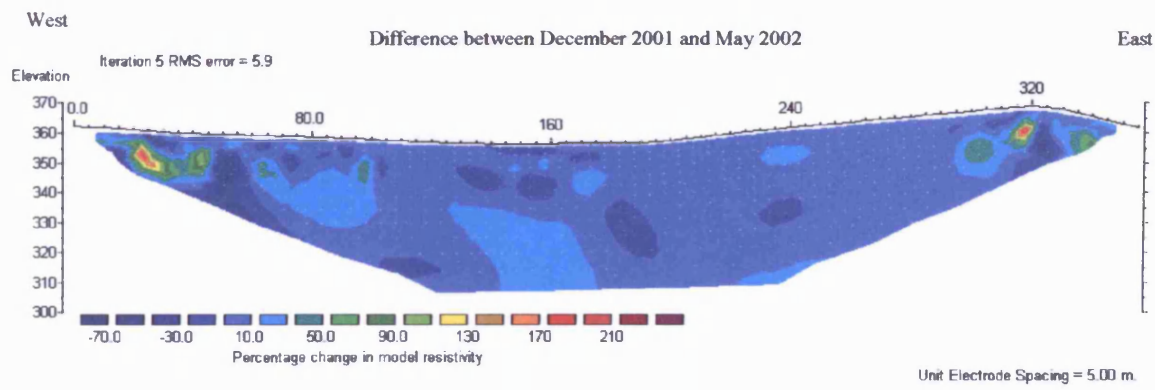
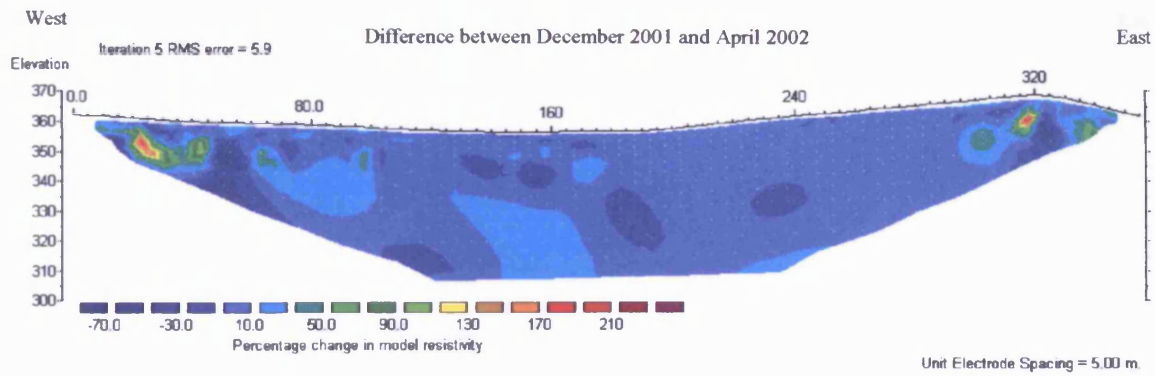
The plots (Fig. 4.24) show the percentage change in resistivity for Line 1 between the survey done in December 2001 and the other surveys carried out between January and November 2002.

There is not a lot of change across the section throughout the year. Increases in resistivity indicate that the area is dryer than when the first survey was done in December 2001. Decreases in resistivity indicate that the area is now more saturated or more saturated with stronger leachate than the area was when the first survey was done in December 2001. The central part of the section varies by +30 to -30%, indicating some variation in moisture content. Since the main part of the section has resistivity measurements less than 60 Ωm , a change of 30% is not a very significant resistivity variation indicating little change throughout the year.

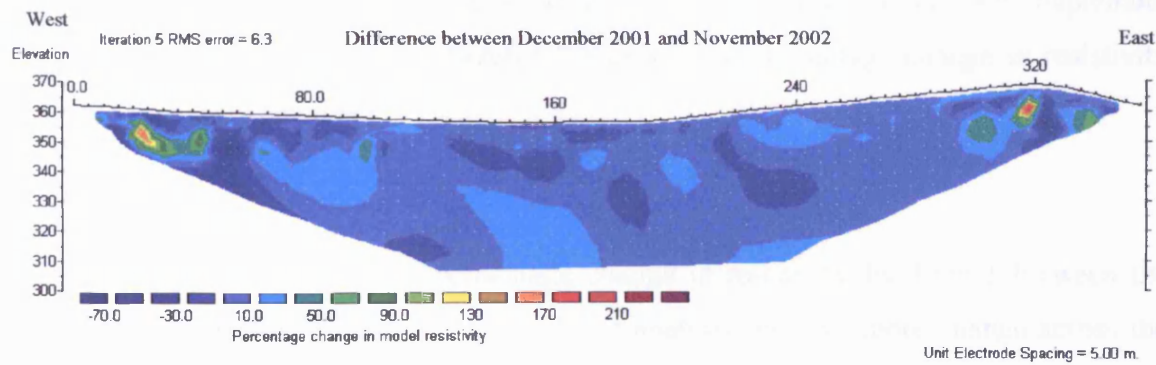
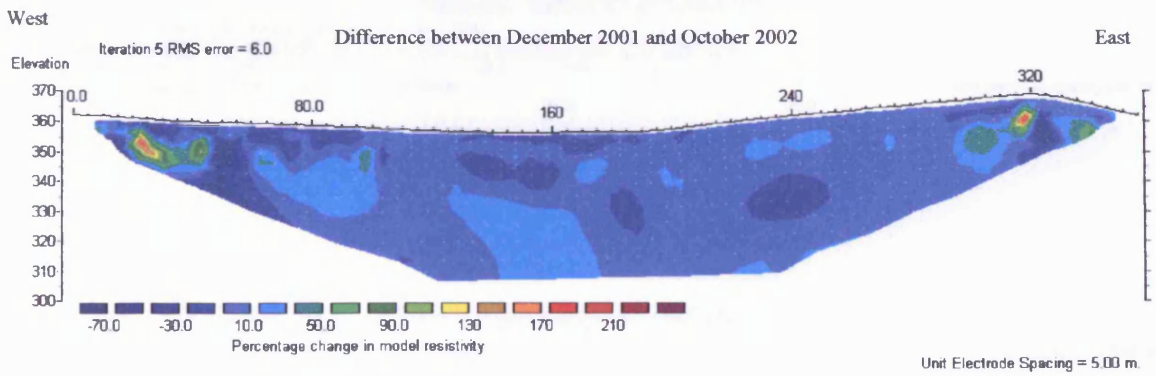
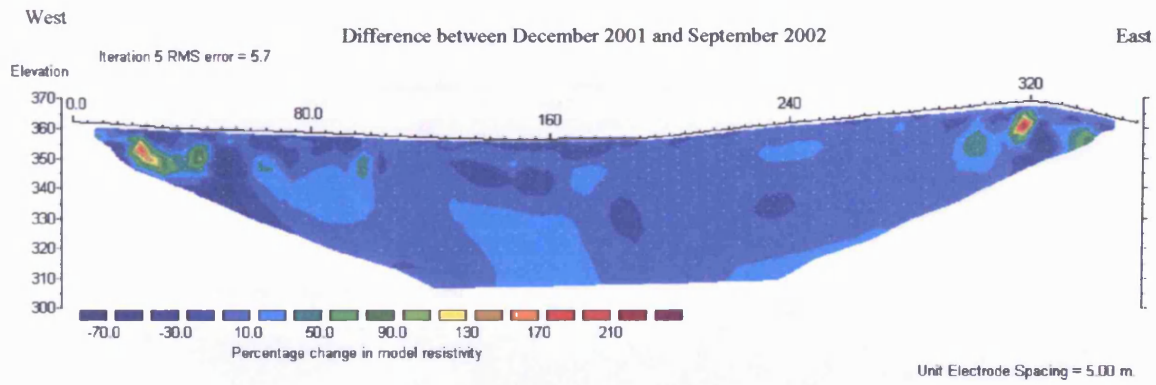
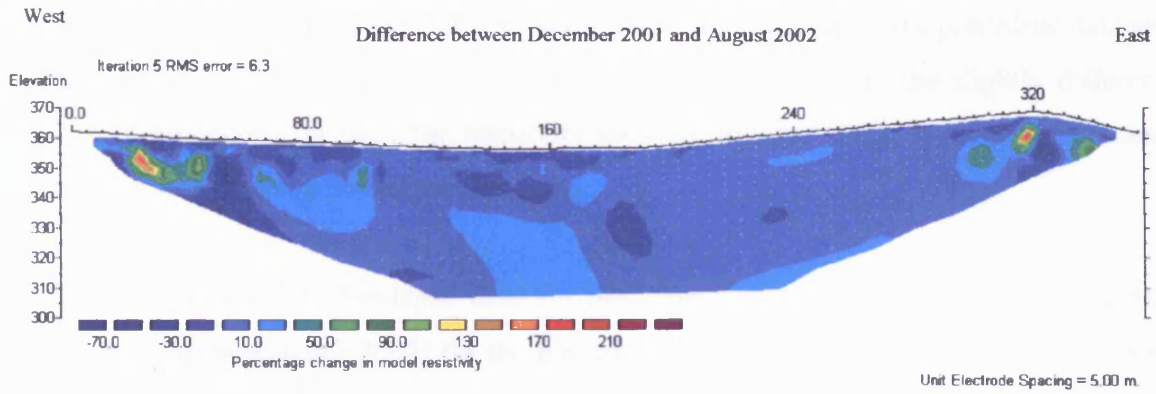
In the west and east of the section there are patches that vary by over +100%. It is likely that these areas represent slag that is dry. It is possible that electrodes in this area are not making such a good contact with the ground as they did when the initial survey was done when the electrodes were first set out.

Figure 4.24 Profiles of Line 1 showing the percentage change in resistivity between December 2001 and surveys done between January and November 2002.





Chapter 4 – Internal Structure.



RES2DINV was also used to perform simultaneous inversions using the preceding data set as the reference model and a time constraint weight of 3. Due to the slightly different method of processing the data, the resistivity sections obtained differ from those obtained using the first data set as the reference model.

Figure 4.25 shows the time-lapse data (in this case time series 10, i.e. October 2002 compared with September 2002) for the preceding data set, a data set and the percentage change in resistivity between them.

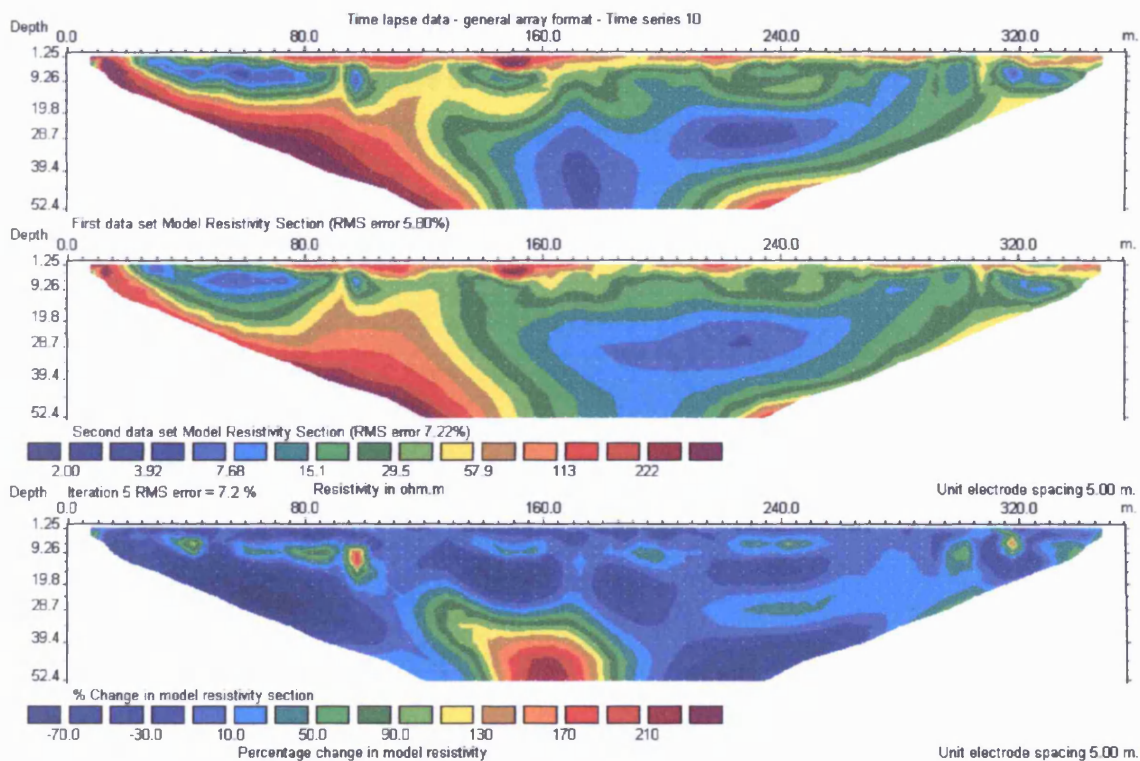


Figure 4.25 Time-lapse data for time series 10 for the preceding data set (September 2002), a data set (October 2002) and the percentage change in resistivity between them.

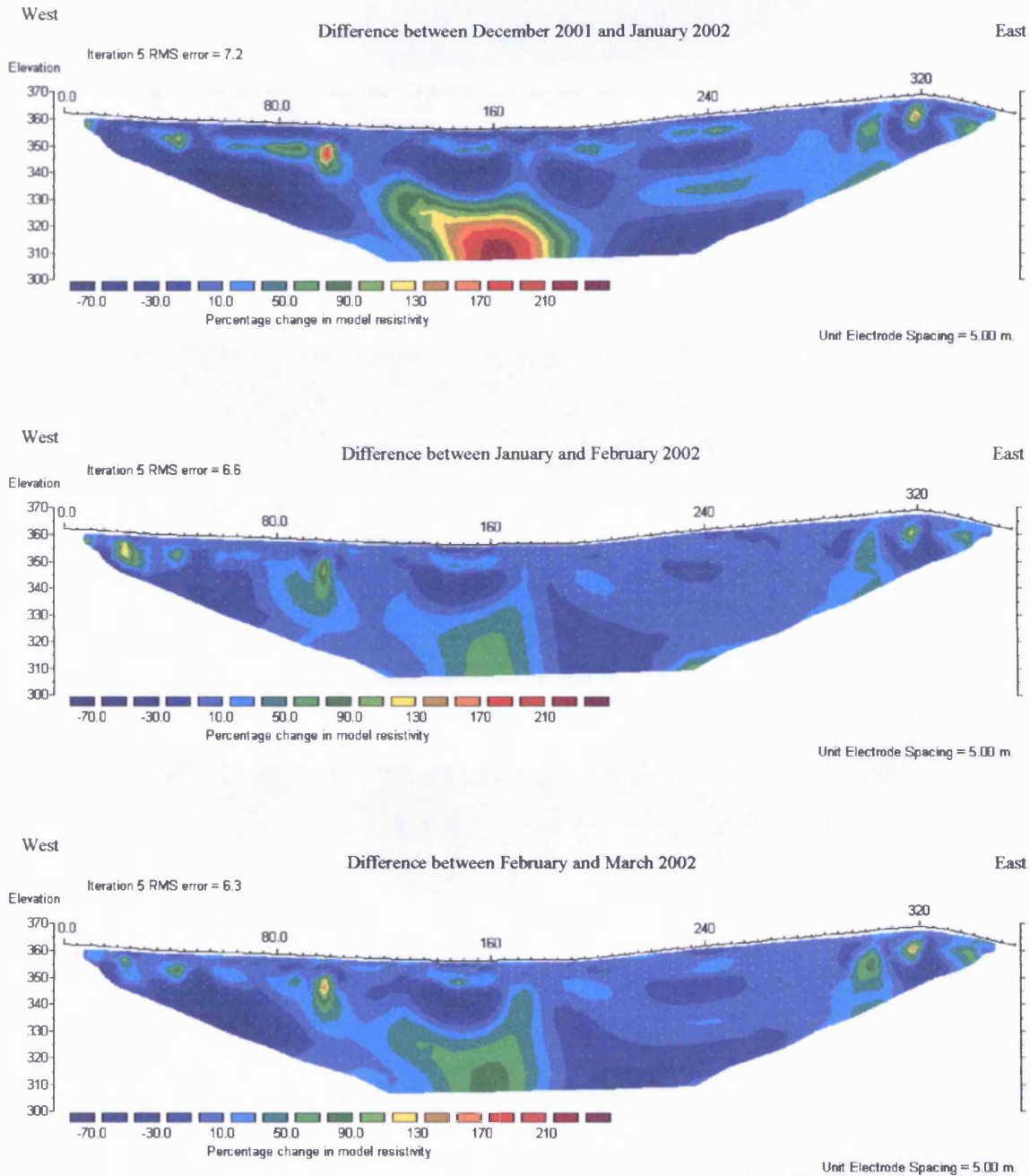
The plots (Fig. 4.26) show the percentage change in resistivity for Line 1 between the surveys. This method of doing the time-lapse analysis displays more change across the section throughout the year. Increases in resistivity indicate that the area is dryer than the

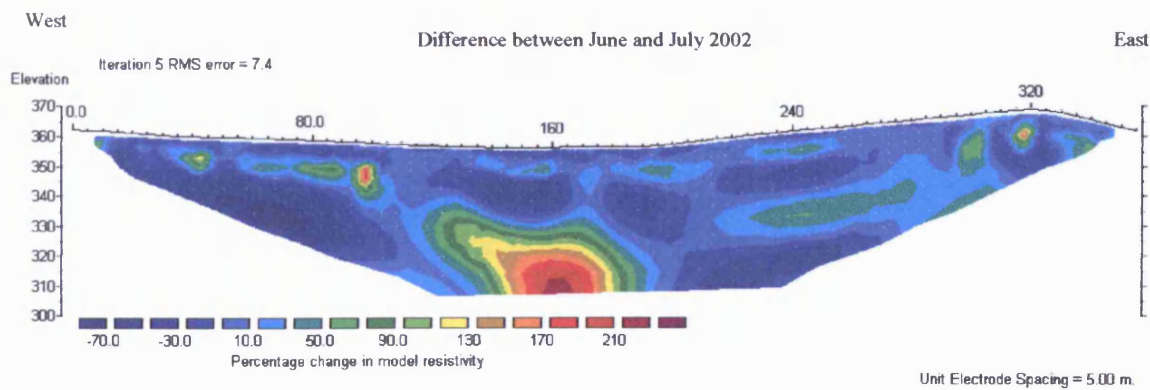
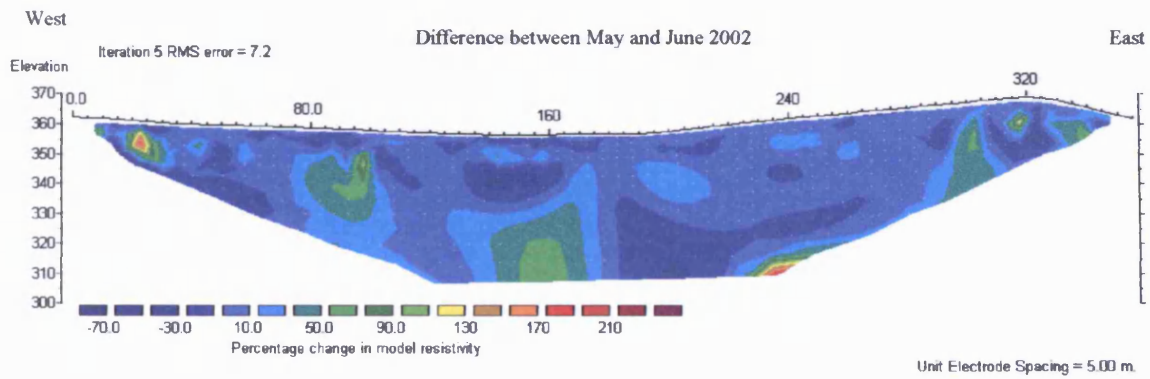
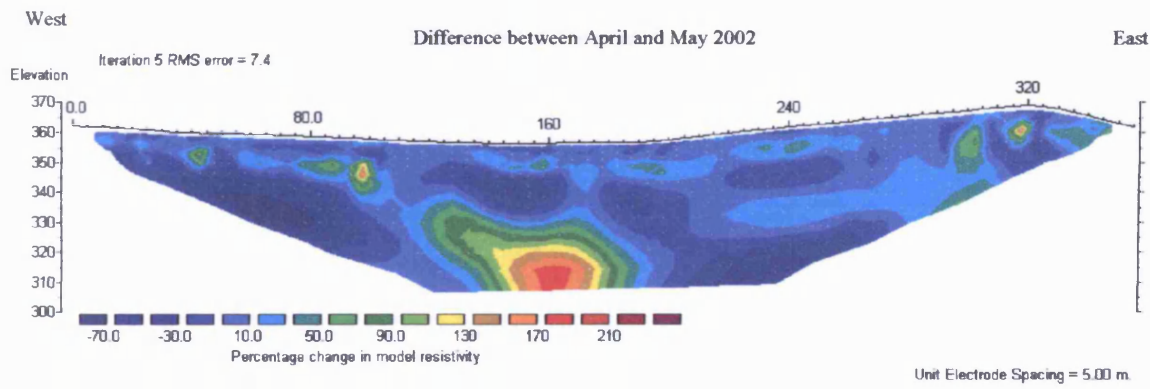
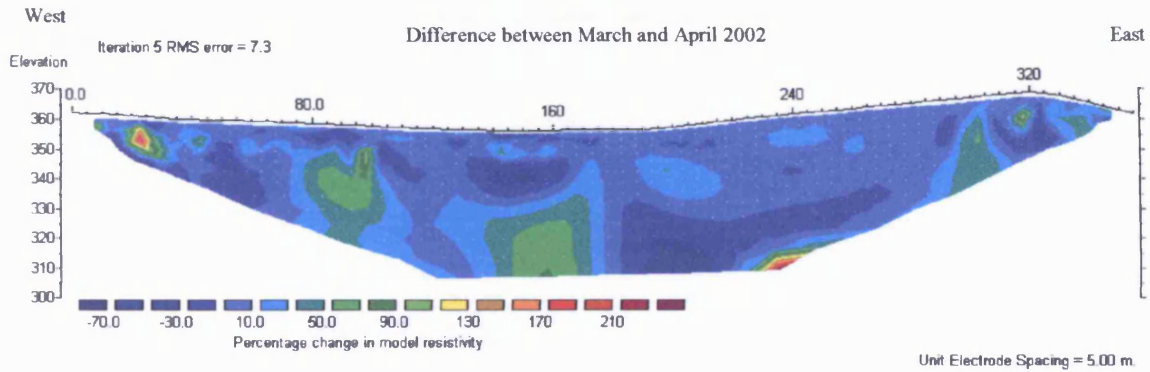
previous month. Decreases in resistivity indicate that the area is more saturated than the previous month. It is possible that changes in resistivity are also due to changes in the leachate geochemistry; a diluted leachate might contain less ions and therefore be less conductive.

The central part of the section varies the most by up to 210%. Since the central part of the section has resistivity measurements less than $29.5 \Omega\text{m}$, the change is not very significant.

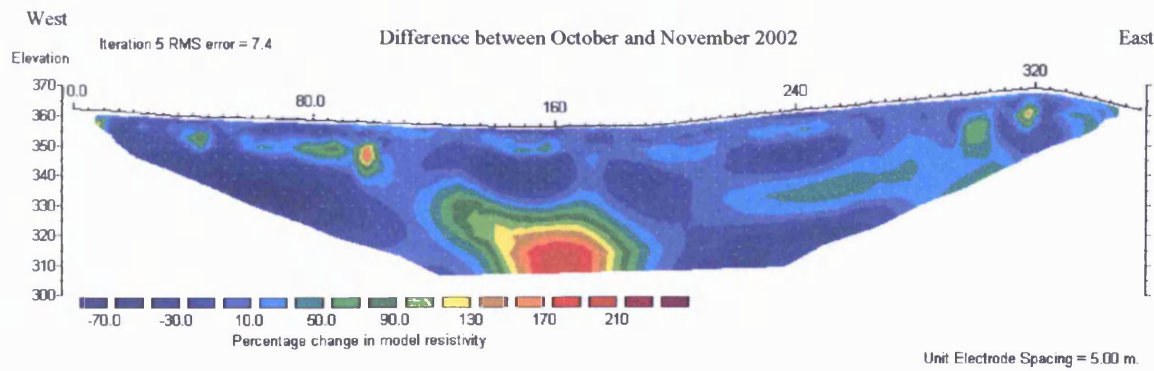
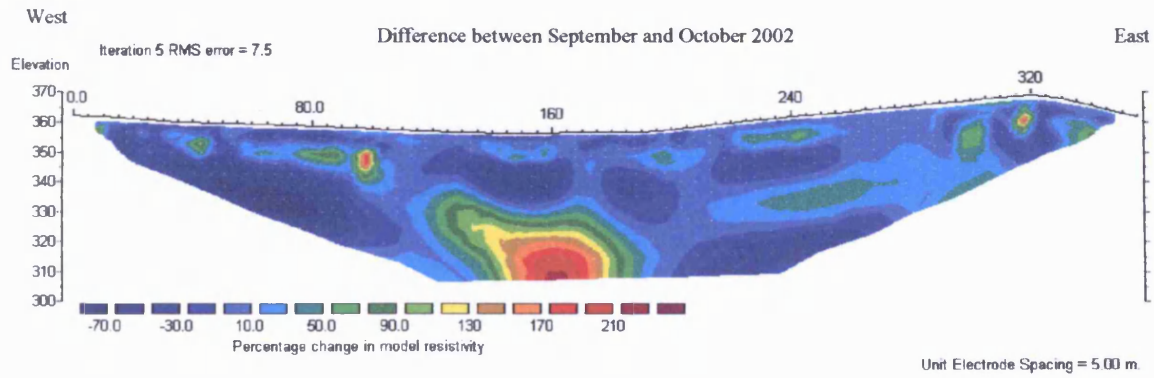
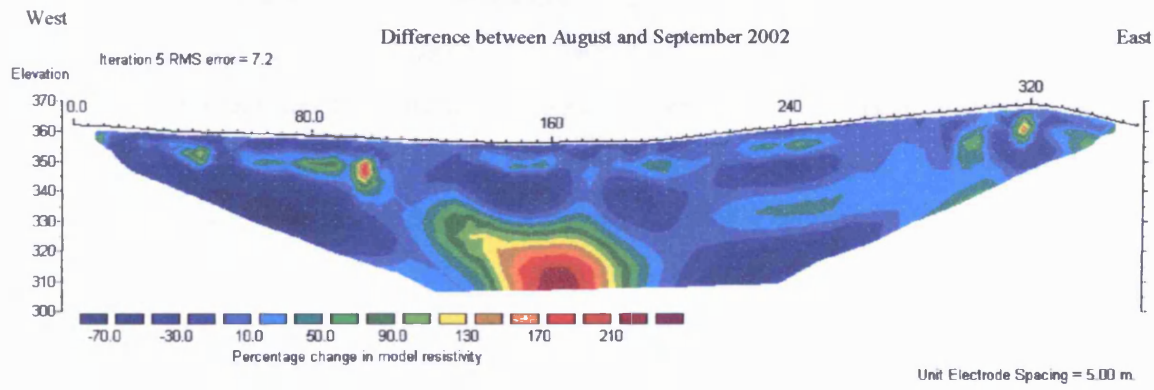
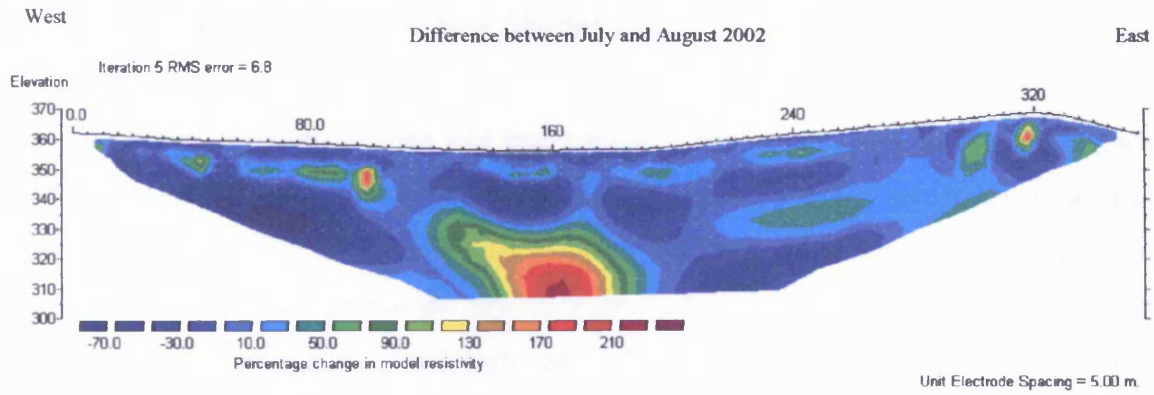
Comparing changes in the resistivity sections and rainfall data, it appears that the central sections exhibit a decrease or increase in resistivity the month after the rainfall amount increased or decreased (Figure 4.18). This may be interpreted as reflecting an increase or decrease respectively in the degree of saturation of the fill, rather than a change in leachate concentrations, however, it is likely that some dilution of leachate occurs as a result of rainfall ingress.

Figure 4.26 Profiles of Line 1 showing the percentage change in resistivity between months.





Chapter 4 – Internal Structure.



4.2.3.6 General Interpretative Model based on Geophysics.

With reference to borehole data and interpreting zones of high resistivity as areas with lower leachate content and vice-versa, a simple geological model of the frontal zone of the landfill can be developed (Figures 4.16, 4.17 and 4.22). It appears that leachate-saturated fill occurs in the central part of the landfill, extending downslope above the location of the LP1 leachate drainage pipe. The tomography model is almost certainly a simplification of the actual hydrogeological conditions, however, since with surface-downward resistivity survey it is impossible to identify sequences of perched water tables since the uppermost low resistivity zone casts a “shadow” downwards in the model. Recent research (George, 2004) has demonstrated that lateral borehole to borehole resistivity tomography is much more effective in identifying such stacked zones of saturation caused by leachate perched above zones of lower permeability within the landfill waste mass.

4.3 CONCEPTUAL SITE MODEL (CSM)

Silent Valley landfill site has been in operation as a landfill site since 1981. Before accepting municipal waste it received large quantities of waste from the iron and steel works at Ebbw Vale. Phase I is active at present and covers 20.1 ha.

The site is situated at a level between 310 and 440 m AOD. It lies in the north-south trending Merddog Valley of glacial origin that joins the Ebbw Fawr Valley to the south.

The two beech woods of Cwm Merddog, which straddles the Nant Merddog stream, and Coed Tyn y Gelli, which is the highest known site of beech in the UK, are Sites of Special Scientific Interest (SSSI). In 1998 these separate woodland blocks were joined together to form The Silent Valley Local Nature Reserve (approximately 50 hectares).

The landfill site rests on the Rhondda Beds below the outcrop of the Brithdir Seam. Quartzite strata are interbedded with mudstones, coal and associated seatearths. The strata at the site dip approximately 4 degrees towards the south-west. The solid geology is overlain by a mixture of Boulder clay, Head Deposits and made ground. The thickness of clay varies considerably across the site ranging from nothing to in excess of 3.5 m. The lower slopes of the valley are overlain by boulder clay, with the higher slopes covered with periglacial Head Deposits.

There are a number of faults on the plateau to the east of the site, which trend northwest-southeast and are often expressed at the surface as deep fissures. Discontinuities tend to be subvertical and parallel to the major fault structures, with a secondary set at right angles.

A series of levels have been driven into the eastern flanks of the main Ebbw Valley and into the Nant Merddog Valley. These were driven into the Rhondda, Rider, Brithdir Coal seams and Cefn Glas coal seam.

The long term annual rainfall from the Meteorological Office for MORECS square 146 is 1257.8 mm.

The main surface water running through the site is the Nant Merddog stream. It is a subsidiary of the Ebbw Fawr River, which it joins to the south of the site near Cwm. The Nant Merddog is culverted to the east of the site.

Estimates for the catchment at the downhill toe of the landfill, the theoretical catchment of the Nant Merddog vary between 106 ha and 120 ha.

The arenaceous deposits and mudstones of the Rhondda Beds are characterised by an intergranular permeability several orders of magnitude greater than that of the less permeable mudstones.

The landfill consists of layers of industrial, commercial and domestic refuse. The waste streams have altered over the operation of the site. Due to the implementation of the Landfill Directive waste accepted at the site now is all solid waste with no special waste.

Slag fill occupies a large part of the western part of the site. The slag is variable ranging from fine ash like material to cobble and boulder sized fragments. Waste palm oil from the British Steel Corporation tinplate works was disposed of in trenches dug into the slag banks across the northwest plateau.

Leachate is currently disposed of to a 150 mm diameter sewer from the lagoon at the toe of the landfill. During periods of heavy rainfall the 150 mm sewer is sometimes unable to cope with the flow of leachate entering it, resulting in surcharge of some downstream manholes and pollution of private land. When the inflow to the lagoon exceeds the outflow to the sewer, the retention tank fills and then overflows via a 450 mm diameter overflow pipe directly into the Nant Merddog.

Figures 4.27 and 4.28 show east-west and north-south cross-sections across the site. The February 2000 profile is used for the landfill surface. The contour maps produced from aerial photos for 1955 (Fig. 3.25) and 1983 (Fig. 3.26) are used for the original ground surface (except in the area containing the Maclane cones) and the surface of the slag tip respectively. Where there are borehole logs along the cross-sections these have been plotted to scale in the correct location to aid in the creation of the cross-sections.

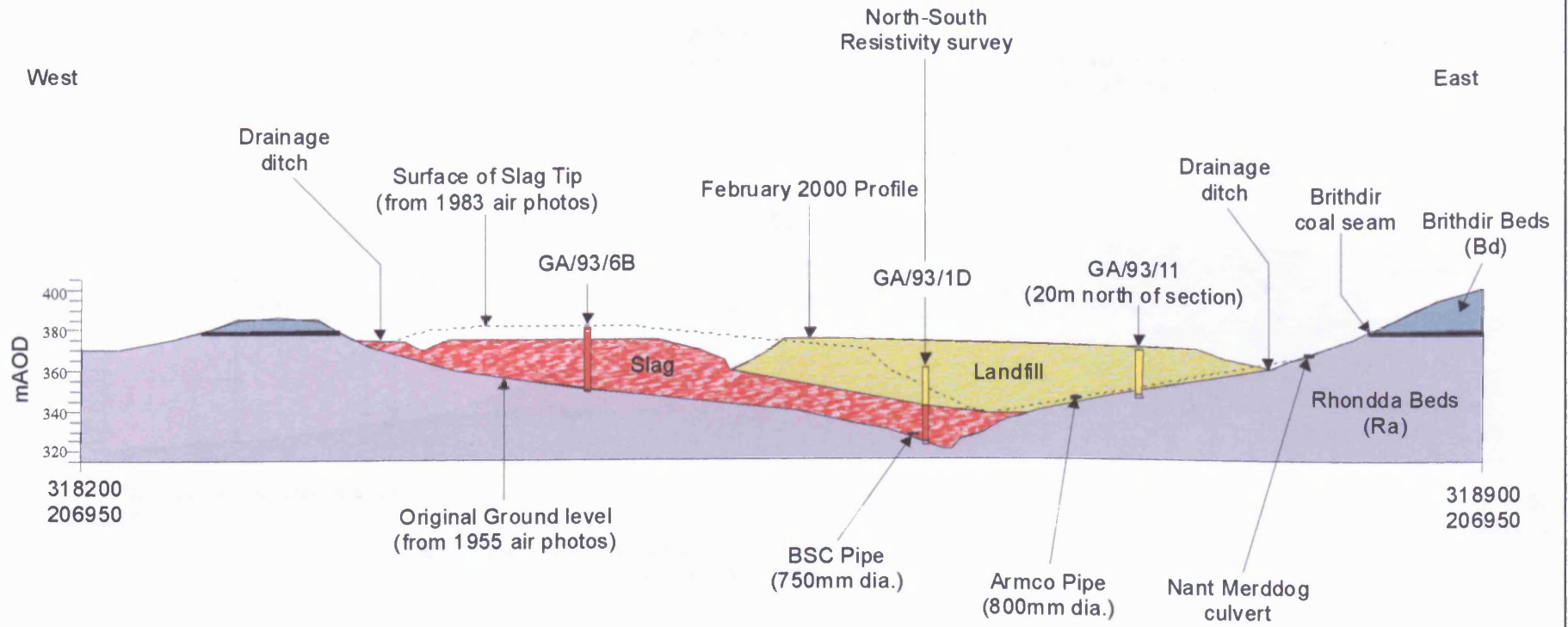


Figure 4.27 Cross-section across northling 206950.

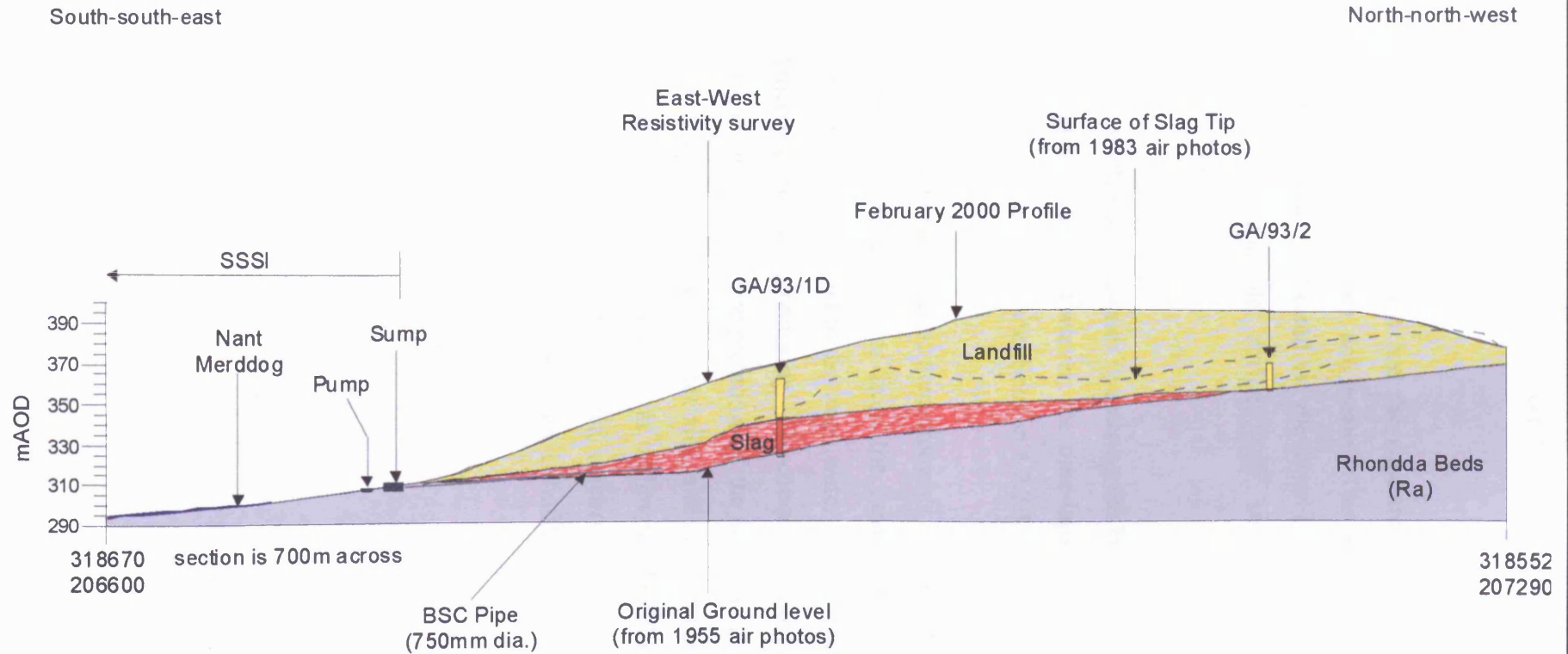


Figure 4.28 Cross-section running south-south-east north-north-west between 318670 206600 and 318552 207290.

The cross-sections have been used to create a conceptual site model of the landfill (Fig. 4.29 and 4.30).

The landfill, leachate, landfill gas and the slag are sources of contaminants including organic and inorganic compounds, and metals. The possible groundwater, surface water, air and soil pathways are indicated on the cross-sections. The possible receptors of contaminants are the groundwater, surface water, soil, the SSSI, the Nant Merddog, and the residents of Cwm.

It is not known whether groundwater is entering the landfill and slag or whether leachate is entering the groundwater. However, the time-lapse resistivity analysis suggests that groundwater may be entering the site (Section 4.2.3.5.2).

In the context of the present thesis, measurements of rainfall inputs to the landfill are compared with measured discharges from the landfill in an attempt to quantify the hydrogeological system. Interaction between water and fill materials are then examined through detailed geochemical monitoring. The conceptual model presented in this chapter provides the background for interpretation of the leachate geochemistry. Clearly the presence of large amounts of steel furnace slag, and its use as an engineering material for the construction of bunds and cover soils within the landfill, adds an important and potentially distinctive element to the chemical reactions and resulting chemical loadings of the leachate discharged from the Silent Valley Landfill.

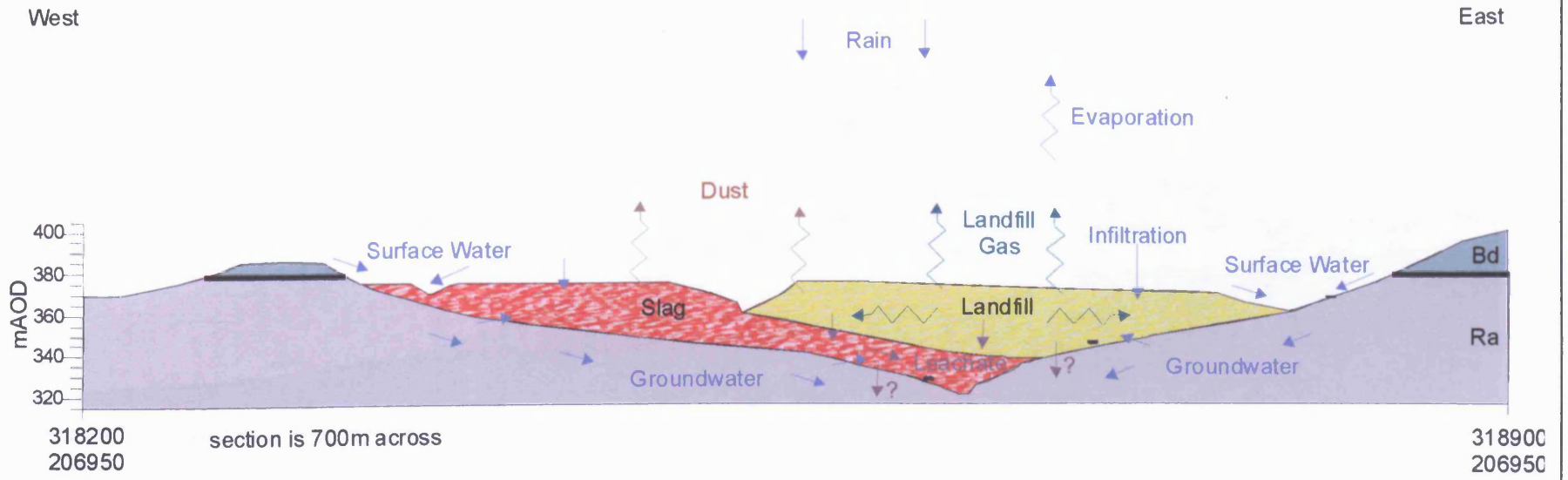


Figure 4.29 Conceptual Site Model across northling 206950.

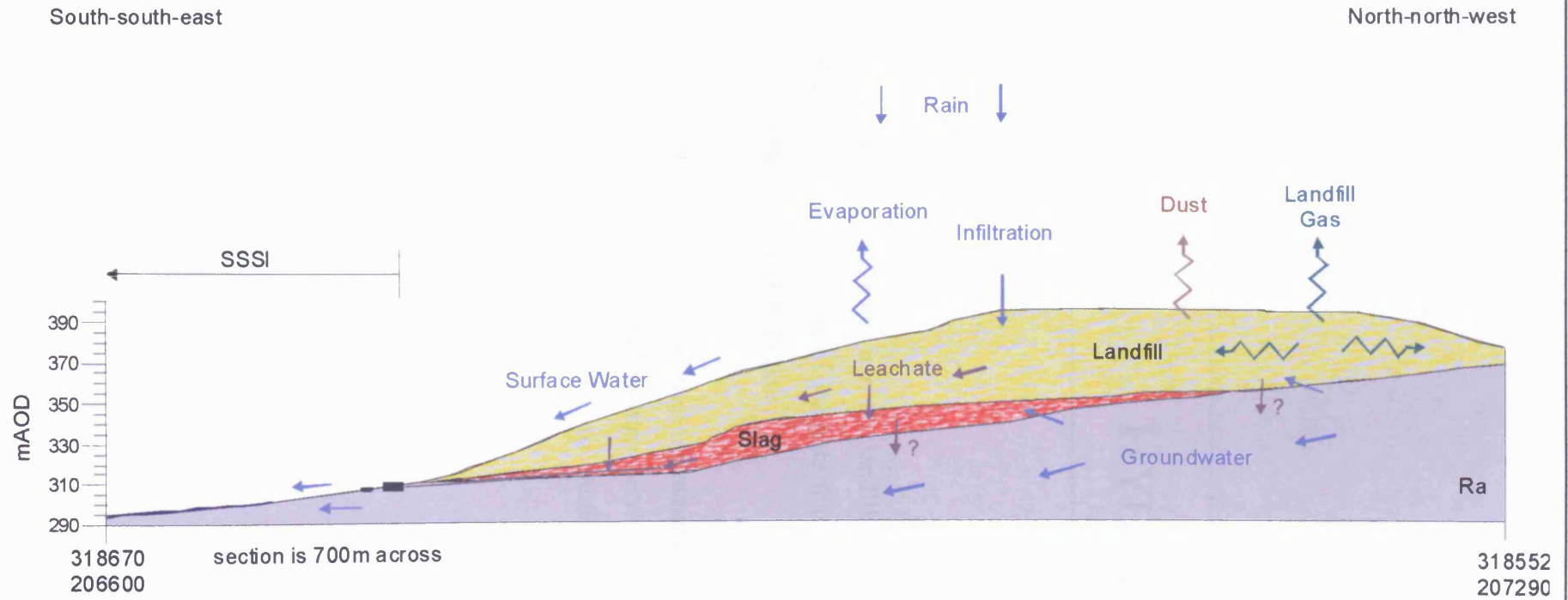


Figure 4.30 Conceptual Site Model running south-south-east north-north-west between 318670 206600 and 318552 207290.

CHAPTER 5

HYDRO-METROLOGY

Rainfall causes infiltration of water into the landfilled waste and also the generation of leachate. Prediction of the volume of leachate that can be generated from a landfill is generally based on water budget principals.

In this chapter the flow and meteorological instrumentation installed at the Silent Valley landfill site are described and relationships between the rainfall and flow data are analysed. Regression analysis is used to model the discharge of leachate from meteorological data.

5.1 INSTRUMENTATION

5.1.1 WEATHER STATION

Silent Valley Waste Services (SVWS) have a weather station (*Weather Monitor II* by Davis Instruments) located at the weighbridge (Grid Ref: SO 184 068, approximately 370 mAOD). It records measurements of temperature (inside and outside the building), humidity (inside and out), rainfall, barometric pressure, TH index (temperature-humidity index), dew point, wind speed, wind direction and wind chill.

The *Weather Monitor II* station is connected to *WeatherLink*, which provides data logging and a serial interface to a computer.

The system can be set to record the data at different intervals (archive period). Silent Valley has set the archive period to 30 minutes. Data have been recorded since October 1998. There are some gaps in the data where there were problems with the equipment or download.

5.1.1.1 Outside Temperature

The outside air temperature is measured in degrees Centigrade (°C). The temperature sensor is a precision platinum wire thermistor, which produces a resistance change proportional to temperature.

- Range -45 °C to 60 °C
- Accuracy ±0.5 °C
- Resolution 0.1 °C

The minimum, maximum and average temperatures are recorded for the previous 30 minutes. Between October 1998 and June 2004, the following temperatures were recorded:

- Mean 9.1 °C
- Minimum -8.2 °C on 20 December 1999
- Maximum 33.7 °C on 8 August 2003

Figure 5.1 shows the seasonal variation in average daily temperature recorded at Silent Valley between October 1998 and June 2004. Variations are also recorded throughout the day.

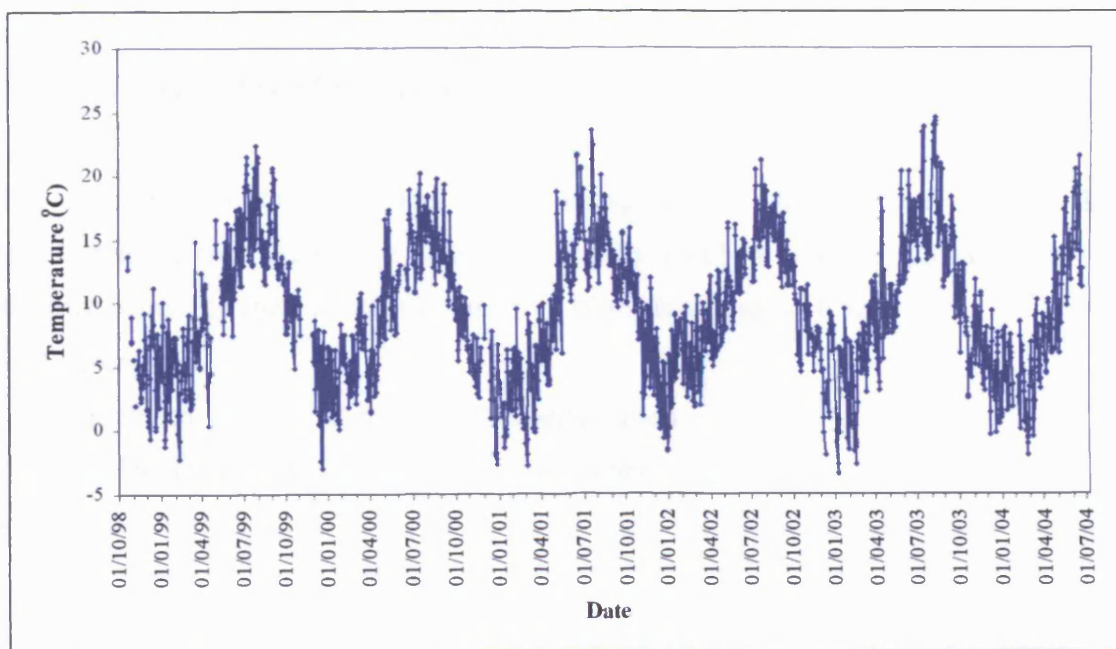


Figure 5.1 Graph showing the average daily temperature recorded at Silent Valley between October 1998 and June 2004.

5.1.1.2 Rainfall

Silent Valley Waste Services have a raingauge installed at the weighbridge (approximately 370 mAOD). Rain enters the collector cone, passes through a debris-filtering screen, and collects in one chamber of the tipping bucket. The bucket tips when it has collected 0.2 mm, which causes a switch closure and brings the second tipping bucket chamber into

position. The rainwater drains out through the screened drains in the base of the collector. Measurements are recorded every 30 minutes.

The rainfall data will be discussed in detail in Section 5.3.

5.1.1.3 Wind

5.1.1.3.1 *Wind Speed/Direction*

The anemometer installed includes both wind speed and wind direction sensors. It is installed above the weighbridge building at approximately 4 m above ground level. The standard height for anemometer placement is 10 m above ground level.

- Sensor Type
 - Wind Speed Wind cups and magnetic switch
 - Wind Direction Wind vane and potentiometer
- Range
 - Wind Speed 0 to 280 km/hr
 - Wind Direction 16 compass points
- Accuracy
 - Wind Speed $\pm 5\%$
 - Wind Direction $\pm 7^\circ$
- Resolution
 - Wind Speed 1 km/hr
 - Wind Direction 22.5° between compass points

The average and maximum wind speeds are recorded for the previous 30 minutes. The prominent wind direction is also recorded. Between October 1998 and June 2004, the following wind speeds were recorded:

- Mean 8.57 km/h
- Minimum 0 km/h

- Maximum 122.3 km/h West on 26 February 2002

The windrose for the site (Fig. 5.2) reflects the local topography of the site, which is situated within a hanging valley that is orientated north-south.

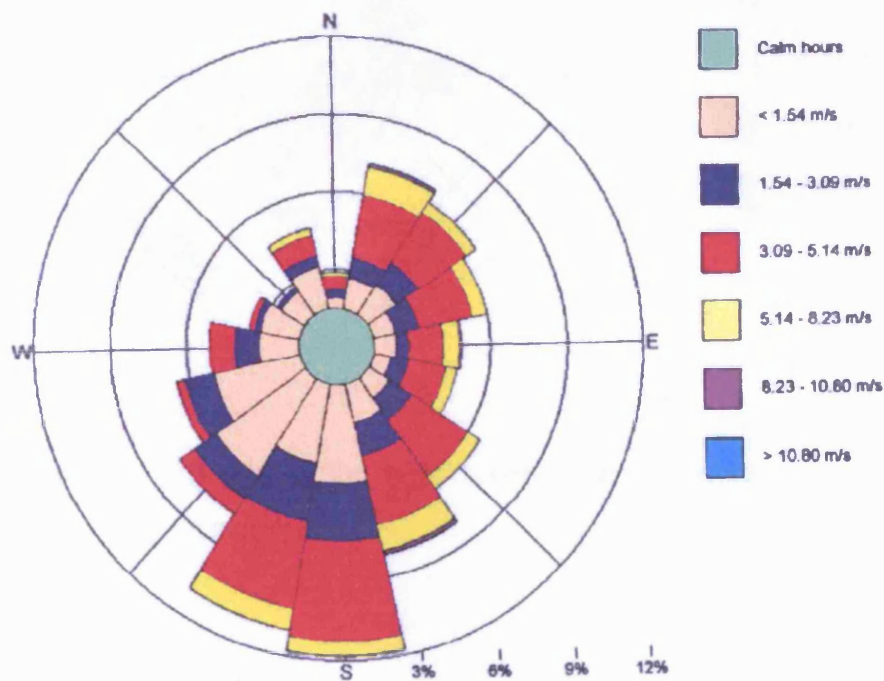


Figure 5.2 Windrose for wind recorded at Silent Valley in 2003. From Golder Associates, 2004.

There is a Met Office wind speed gauge at Sennybridge, 45 km northwest of Silent Valley (Grid Reference 289400 241700). The wind velocities recorded at Silent Valley appear to be significantly lower than those recorded at Sennybridge (Fig. 5.3).

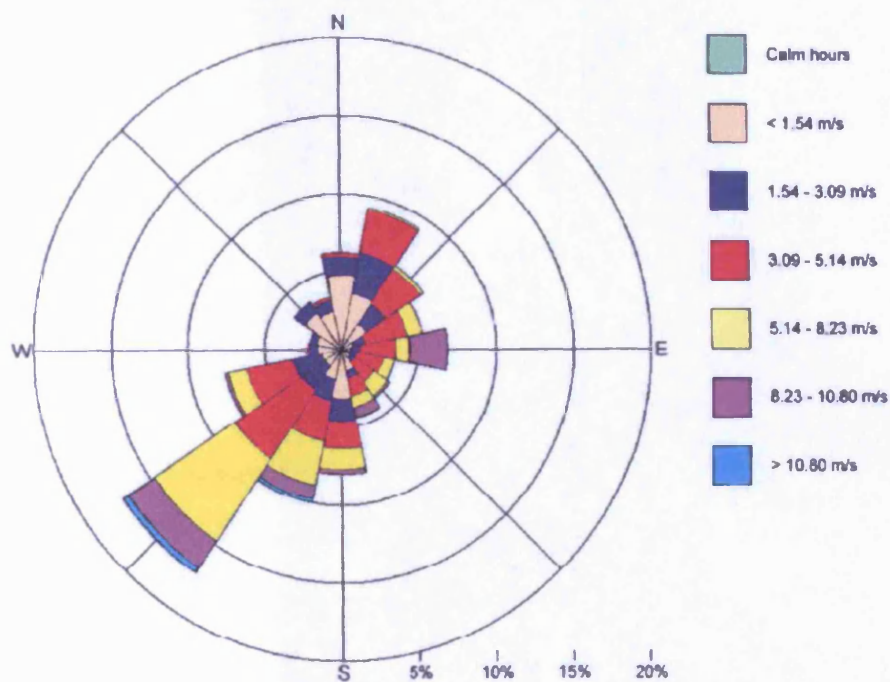


Figure 5.3 Windrose for wind recorded at Sennybridge in 2003. From Golder Associates, 2004.

5.1.1.3.2 Wind Chill

Wind chill is a measure of the effect of wind on our perception of temperature. Through convection, wind cools by transferring heat more quickly into the surrounding air. As a result, when the wind is blowing, temperature is perceived to be cooler than it actually is. The *Weather Monitor II* automatically calculates wind chill using the wind speed and the outside temperature readings. Wind chill is expressed as a temperature reading.

- Resolution 1 °C
- Range -92 °C to 37 °C
- Accuracy ± 2 °C

The following wind chills were recorded between October 1998 and June 2004:

- Mean 6.8 °C
- Minimum -20.4 °C on 30 January 2003
- Maximum 32.4 °C on 8 August 2003

5.1.1.4 Humidity

The humidity sensor is a thin film capacitor element. A dielectric polymer layer absorbs water molecules from the air through a thin metal electrode, which causes a change in capacitance proportional to relative humidity.

- Range 0-100% relative humidity
- Accuracy $\pm 3\%$ (1 to 90% RH), $\pm 4\%$ (90 to 100% RH)
- Resolution 1%

The relative humidity recorded at Silent Valley was either not recorded or recorded a value of 100%. The humidity measurements are used in calculating the TH Index and dew point making these reading unreliable.

5.1.1.5 TH Index

A temperature-humidity index has been developed by the U.S. National Weather Service that gives a single numerical value reflecting the outdoor atmospheric conditions of temperature and humidity as a measure of comfort (or discomfort) during warm weather. It uses temperature and relative humidity to determine how hot the air actually "feels". When humidity is low, the apparent temperature will be lower than the air temperature, since perspiration evaporates rapidly to cool the body. However, when humidity is high (i.e. the air is saturated with water vapour) the apparent temperature "feels" higher than the actual air temperature, because perspiration evaporates more slowly.

The *Weather Monitor II* station uses the temperature and humidity that it records to calculate the TH index and it records the average every 30 minutes. The following TH indexes were recorded between October 1998 and June 2004:

- Mean 9.7
- Minimum -7.9 on 20 December 1999
- Maximum 65.6 on 28 July 2001, 15 July 2003 and 8 August 2003

Since the humidity readings are unreliable, the TH Index values are also unreliable, so the TH Index should not be used in any calculations.

5.1.1.6 Dew Point

All air contains water vapour of varying quantities. Dew Point Temperature is the temperature to which air would have to cool (at constant pressure and constant water vapour content) to reach saturation. At saturation point, the air holds the maximum amount of moisture possible at that temperature and pressure. Dew point temperature is useful because it gives information about how much moisture is present in the air - the higher the dewpoint temperature, the more moisture there is in the air. When the dew point temperature and the air temperature are the same, the air is saturated ie at 100% relative humidity. Dew point temperature can never be higher than the air temperature. So if the air cools, some of the moisture must be removed from the atmosphere by condensation. Tiny droplets of water form in the air, as clouds, fog, frost or even as rain.

- Range -73 °C to 60 °C
- Accuracy ±2 °C
- Resolution 1 °C

The dew point is recorded every 30 minutes. The following dew points were recorded between October 1998 and June 2004:

- Mean 9.5 °C
- Minimum -7.9 °C on 20 December 1999
- Maximum 32.4 °C on 8 August 2003

Since the humidity readings are unreliable, the dew points reading are also unreliable. Where humidity readings have been recorded they are 100%, so when the dew point is calculated the value is the same as the outside temperature. Dew point should not be used in any calculations.

5.1.1.7 Pressure

The *Weather Monitor II* uses a solid state transducer to measure atmospheric pressure. Since atmospheric pressure varies with altitude, the console adjusts this measurement to give the equivalent sea level pressure, referred to as "barometric pressure". *The Weather Monitor II* has been set up to display barometric pressure in millibars (mb).

- Resolution 0.1 mb
- Range 880.0 to 1080.0 mb
- Accuracy ± 1.7 mb (at room temperature)

Between October 1998 and June 2004, the following pressures were recorded:

- Mean 974 mb
- Minimum 923 mb on 11 October 2000
- Maximum 1006.2 mb on 16 March 2003

In the British Isles the average sea-level pressure is about 1013 mb and it is rare for pressure to rise above 1050 mb or fall below 950 mb. The pressure recorded at Silent Valley is lower than values that would be expected. It is likely that the relative change in pressure is accurate but the absolute values are too low, and that the barometer has not been correctly adjusted to the altitude of the site.

5.1.2 FLOW MONITORING

The WJ460, manufactured by Warren Jones, (Fig. 5.4) is used at Silent Valley to monitor the discharge from the site. It is installed by the sump at the base of the landfill (Fig. 5.5). The flow is determined by measuring the upstream water level with a through air ultra-sonic sensor (Table 5.2). This level, along with the dimensions of the weir or flume, is used by the WJ460 (Table 5.1) to carry out full hydrometric calculations. The WJ460 contains a selection of standard types of weirs and flume, which the instrument uses to automatically calculate flow using the formulae specified in BS3680 part 4A and 4C. Alternatively the user can enter a flow curve for any non-standard structure.

On the LCD display the depth of water, flow rate and total flow can be viewed but only the flow rate is recorded. Data are stored in the build-in datalogger, which can be downloaded to a PC using the FLARE software package. At Silent Valley flow measurements are recorded every 15 minutes and are stored on the data logger.

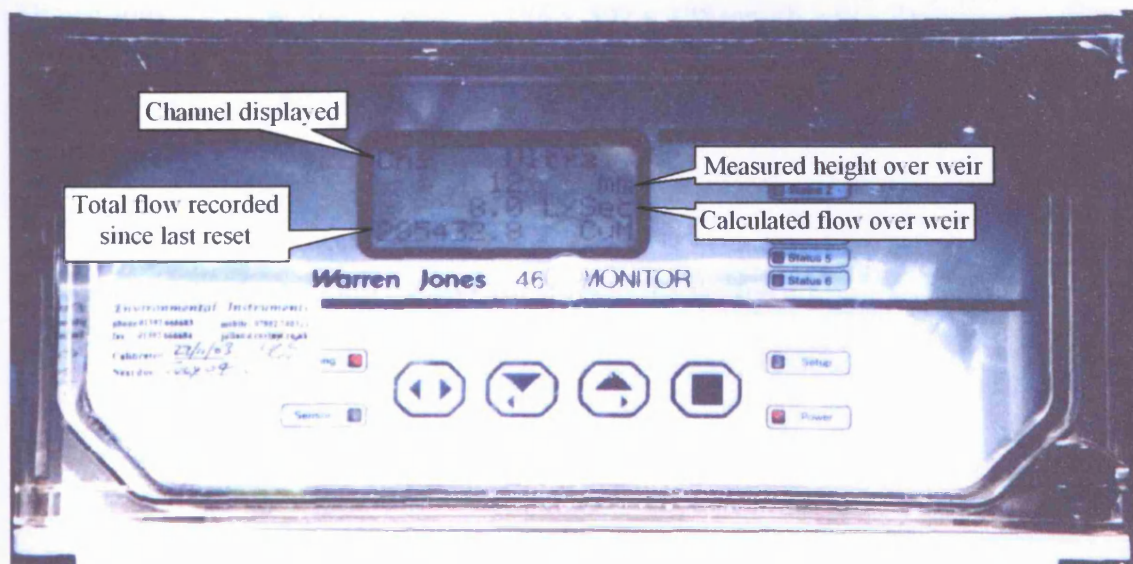


Figure 5.4 Photograph showing the WJ460 box

Enclosure	Wall mounted case: Polyester with transparent cover, IP67 rating with cover open Panel mounted case: Aluminium alloy, painted and anodised, IP54 rating
Display	LCD graphical display
Controls	4 keys
Input	4 channels. SART ultra-sonic sensor and/or analogue 4-20mA depending on model
Outputs	Fixed: 2 × 4-20 mA isolated outputs into 1 Kohm (max) 6 × alarm relays 5 A load at 240 V RS232 with RTS-CTS handshaking to 9600 baud Portable: 4 × alarm relays 1 A load at 24 VDC RS232 with RTS-CTS handshaking to 9600 baud
Data Recording	32K rollover memory (128K option) configurable
Power	Fixed: 98-123 V or 196-264 V, 50/60 Hz, 1ph 12-30 VDC (15 watts max) Portable: Internal rechargeable battery, separate charger
Dimensions	Wall mounted: 186 × 302 × 175 mm (h × w × d) Portable: 210 × 352 × 200 mm Panel Mounted: 144 × 288 × 232 mm
Weight (approx.)	Fixed: 4 kg Portable: 11 kg

Table 5.1 Table showing the specification of the WJ460.

Type	Pulse-echo sonic air-ranging with integral fast response compensation for changes in temperature
Construction	IP68 ABS body with anodised aluminium temperature sensor, fitted with M20 mounting stud
Range	0.25 to 2.0 m
Resolution	0.2 mm
Accuracy	0.5 mm or 0.05% of range (whichever is greater)
Repeatability	0.2 mm at 250 mm range, 0.5 mm at 2 m range
Temp compensation	Fully compensated over -20 to $+60^{\circ}\text{C}$
Cable	Supplied with 10 m cable (max 200 m)
Dimensions	103 mm diameter \times 190 mm long
Weight	0.8 kg

Table 5.2 Table showing the specification of the ultra-sonic device.

The different weir and meter configurations used at Silent Valley enable different maximum flow rates to be accommodated (Table 5.3). The BSC Pipe (LP1) has a maximum range of 150 litres per second, the LP2A V-notch weir a maximum of 7 litres per second, and the Settlement Tank a maximum of 500 litres per second.

PARAMETER	SETTLEMENT TANK	FLUME	BSC PIPE	NANT MERDDOG	LP2A
Weir type	Rectangular weir	Rectangular flume	Rectangular weir	Crump weir	V-notch weir
Alpha (deg)					
Weir's notch width, b (mm)	3000	150	700		
Length of flume throat, L (mm)		400			
Channel width, B (mm)	9999	250	900	1500	
Crest height, P (mm)	100		320		
Hump (mm)				200	
K_s (mm)		0.06		0.06	
Maximum expected flow rate, Q_{max} (l/s)	500	30	150	901	7
Maximum expected head on the weir, h_{max} (mm)	207	237	233	400	

Table 5.3 Weir configurations at Silent Valley landfill site.

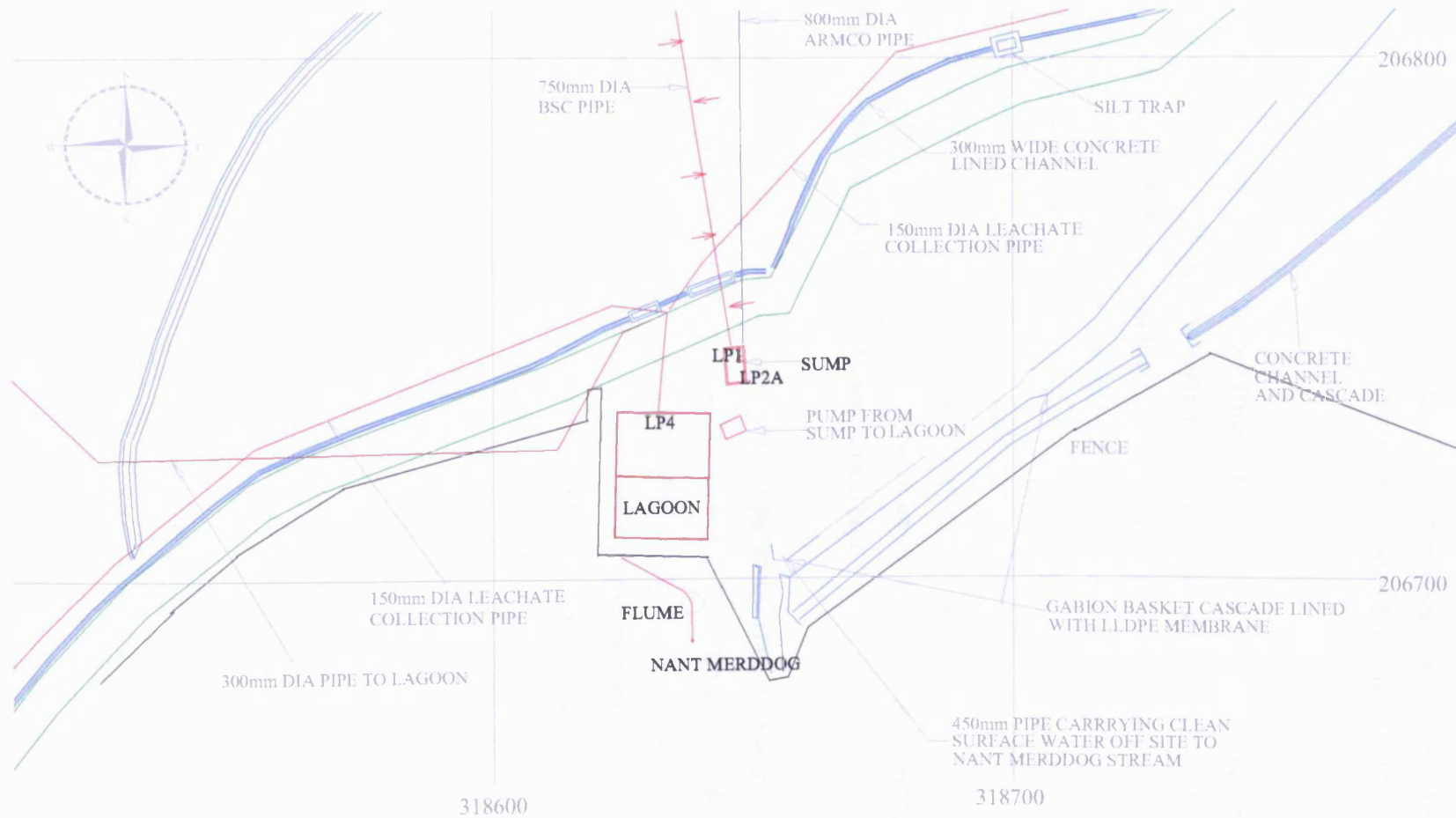


Figure 5.5 Schematic showing the location of the leachate sampling points, the sump and lagoon (Settlement Tank). Adapted from Silent Valley Waste Services drawing number ESID6-1.

5.1.2.1 Settlement Tank

All of the leachate collected at Silent Valley passes through the Settlement Tank (lagoon) (Fig. 5.5). A pipe enters the northern edge of the Settlement Tank carrying leachate that has been collected from the toe of the landfill. Samples collected at this point are labelled LP4.

Leachate is pumped into the Settlement Tank from the sump. Samples collected at this point are labelled LP3A. The sump has a number of different flows entering it. Leachate from the base of the old southern slope of the landfill enters the sump via the BSC Pipe (sample LP1). The Armco pipe transports leachate to the sump from inside the southern slope. Some of the runoff collected from the landfill in drainage ditches around the site enters the sump via pipes. There are also some pipes entering the sump that were installed when the sump was being constructed to relieve the pressure from the surrounding groundwater. Sample point LP2A is made up of these discharges along with discharges from the drainage ditch pipes and the Armco pipe.

The settlement tank is divided into two compartments (Fig. 5.6) with the first acting as a settling tank to remove suspended solids. Leachate flows from this tank over a rectangular weir (Fig. 5.7) to the second larger compartment, which has an estimated capacity of about 500 m³. This second compartment provides a degree of retention. Water is discharged from this tank to the sewer via a drain in the tank floor. The leachate passes through a pipe then through a flume before it enters the sewer.



Figure 5.6 Photograph of the settlement tank at Silent Valley Landfill site. Photograph taken looking south.

With the low flows present over the rectangular weir in the settlement tank, the accuracy is limited. To comply with BS3680 would require a depth over the weir of at least 50 mm or a flow rate greater than 60 l/s. The weir can accommodate flows up to 500 l/s and a depth over the weir up to 207 mm. At present the flow rate is generally significantly below the required 60 l/s. To increase the efficiency of the flow meter, the width of the weir should be shortened. At present it is 3000 mm wide. With a shorter weir the depth of water going over the weir would increase. Any inaccuracies in measuring the depth of water over the weir would become a smaller proportion of the depth and so there would be a smaller margin of error. BGBG are currently investigating shortening the weir.

Flow from the Settlement Tank will be discussed in Section 5.4.1.

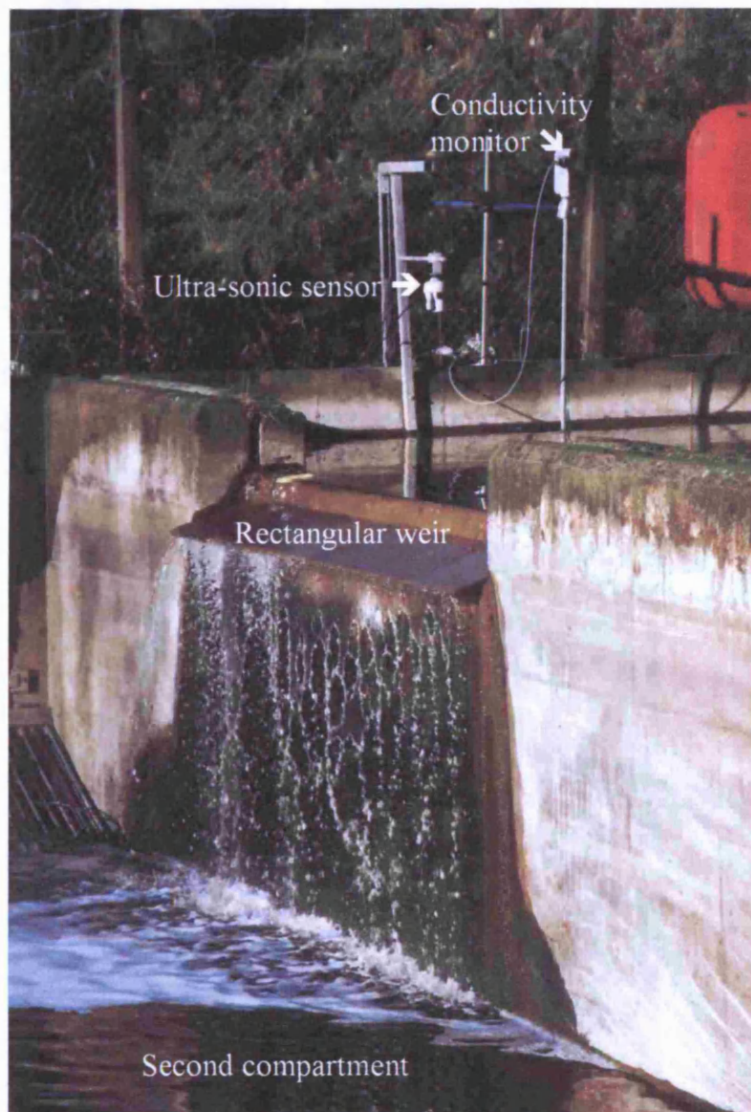


Figure 5.7 Photograph of the settlement tank rectangular weir at Silent Valley Landfill site.

5.1.2.2 BSC Pipe (LP1)

A flow meter measures the flow from the BSC Pipe (LP1) (Fig. 5.5) as it goes over a rectangular weir (Fig. 5.8) 700 mm in width. The BSC Pipe goes along the base of the landfill under the southern slope. The weir installed can measure flows up to 150 l/s.

In July 2001 the weir on the flow meter measuring discharges from the BSC pipe was raised. This has helped to cut down on the amount of foam formed at this point and so increase the accuracy of the meter. The flow meter was calibrated for the amendments.

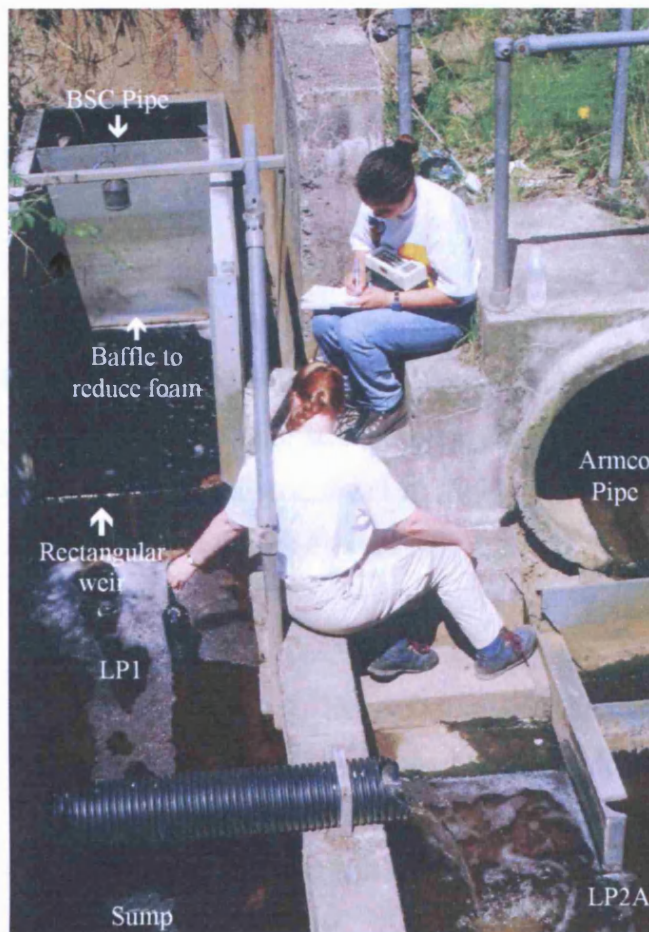


Figure 5.8 Photograph showing the BSC Pipe (LP1).

Flow from the BSC Pipe will be discussed in Section 5.4.2.

5.1.2.3 Flume

In July 2001 a flume was installed to measure the flow that enters the sewer from the settlement tank (Fig. 5.5). The flow passes through a rectangular flume (flume throat 150 mm) and an ultrasonic flow meter measures the head in the flume upstream of the throat - in the so-called "approach channel".

The flume suffers from foam building up and interfering with the ultra-sonic sensor. The foam develops due to the turbulence as the leachate comes down a pipe at an angle from the Settlement Tank and hits the level approach channel.

5.1.2.4 Nant Merddog

A crump weir is installed on the Nant Merddog at the site boundary to monitor flows through the stream (Fig. 5.5). The weir can measure flows up to 903 l/s. In February 2001 a new cable was connected between the Nant Merddog flow monitoring station and the monitoring box as the old cable had become damaged. The flow meter was then calibrated. Measurements were discontinued in November 2002. The weir had problems with silting and regularly needed to be cleared out. Limited data are available for the Nant Merddog.

The mean flow recorded for October, November and December 2001 was 26 l/s (daily average discharge of 2270 m³). The flow in the Nant Merddog, as expected, responds to rainfall (Fig. 5.9). There is a strong correlation ($r = 0.68$) between rainfall and discharge for data collected in October, November and December 2001 (Fig. 5.10).

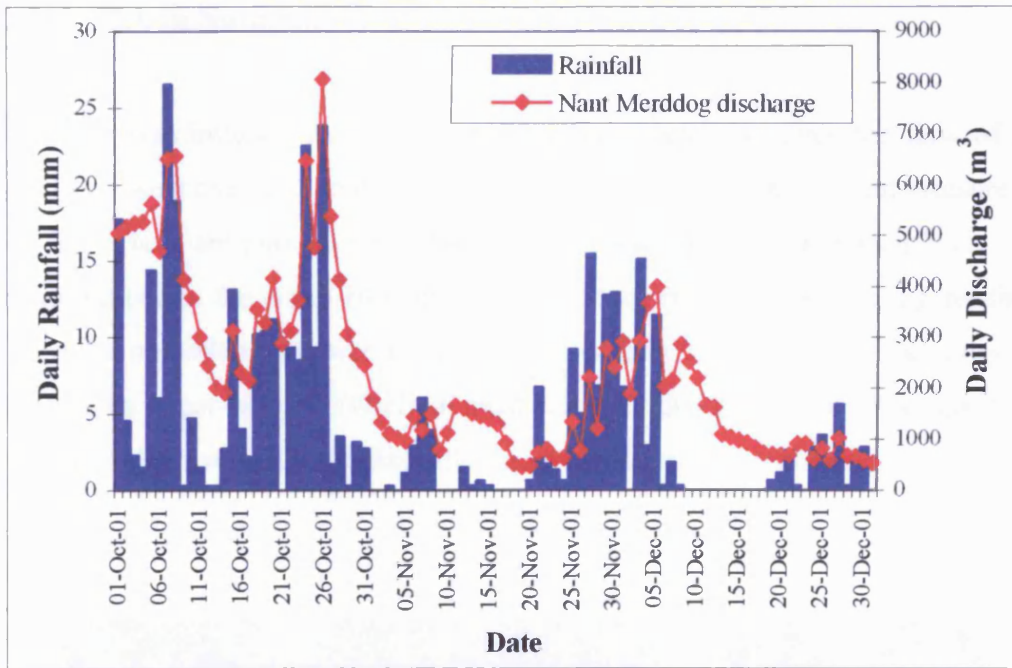


Figure 5.9 Graph showing total daily rainfall and discharge over the crump weir in the Nant Merddog between 1 October and 31 December 2001.

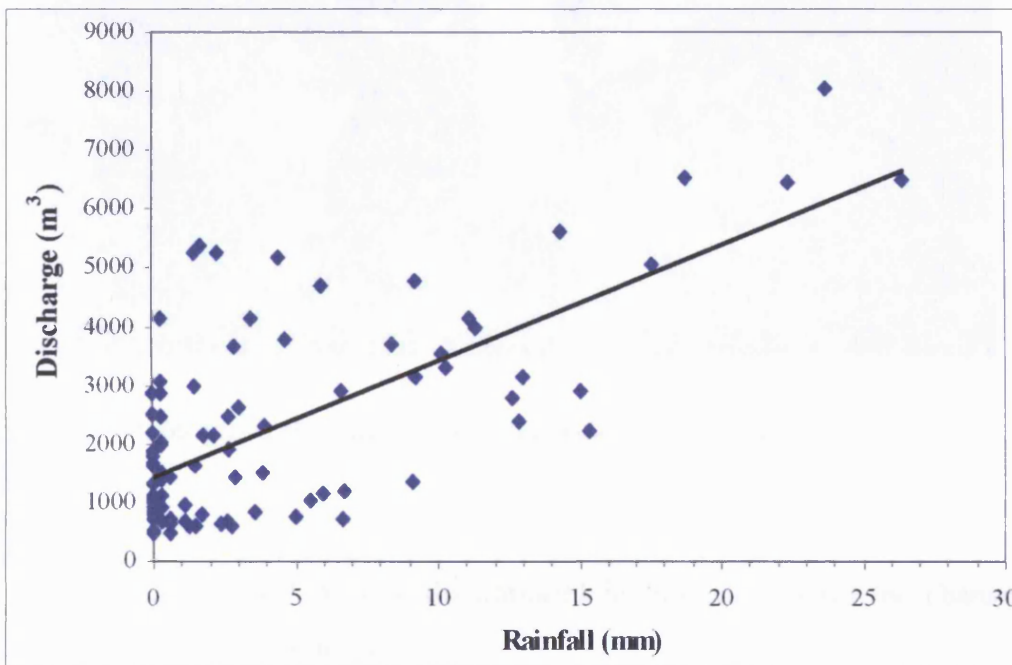


Figure 5.10 Graph showing the relationship between daily rainfall and discharge over the crump weir in the Nant Merddog between 1 October and 31 December 2001.

5.1.2.5 LP2A in Sump

A flow meter was installed in the sump. This flow meter measures the flow of LP2A (Fig. 5.5) as it went over a V-notch weir (Fig. 5.11). The V-notch weir can measure flows up to 7 l/s. There are periods when the weir recorded flows greater than 7 l/s. When refuelling the pump, the sump fills up and flows back over the weir giving readings of 7 l/s. It is not possible to say whether flows greater than 7 l/s are due to the sump filling while the pump is not working (likely in most cases) or due to genuine flows greater than 7 l/s. Flow readings were 1.5 l/s (daily discharge of 126 m³) on average.

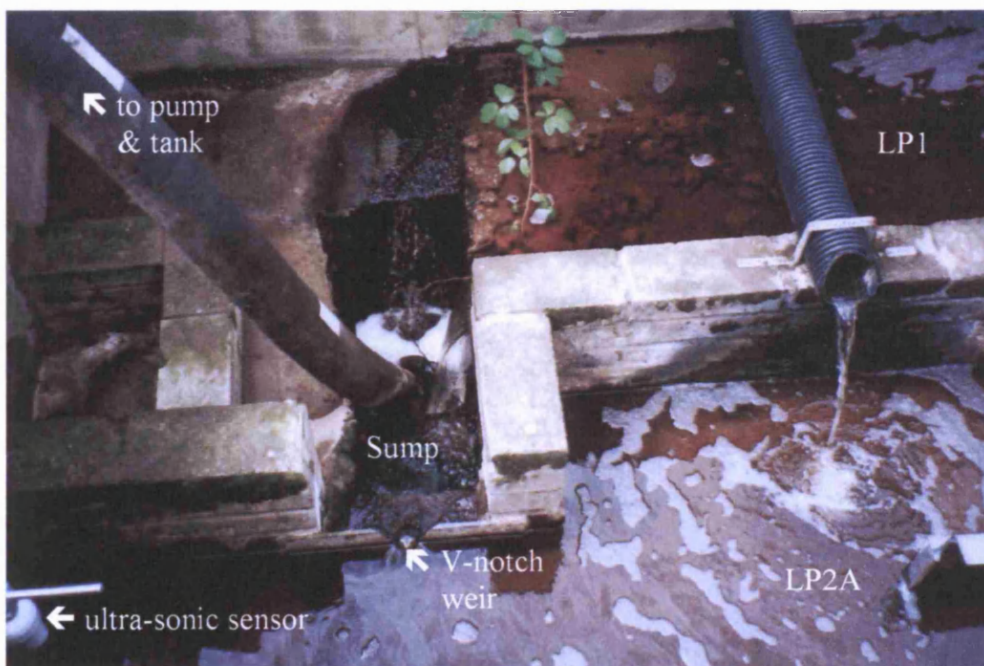


Figure 5.11 Photograph showing the V-notch weir measuring LP2A.

Flow measurements of LP2A were discontinued in July 2001 when the channel was needed for the flume measurements.

Many of the issues entering LP2A are groundwater from around the sump and are uncontaminated. The discharge from the Armco pipe (Fig. 5.8) has been separated from the rest of LP2A since it originates from the landfill. It has been proposed to discharge the

uncontaminated groundwater entering the sump directly to the Nant Merddog. The Environment Agency requested samples for dry and wet periods to determine if the water poses a threat to the river. Blaenau Gwent are waiting for the Environment Agency to make a decision.

Data are available for LP2 from March 2000, when LP2, LP3, LP5, LP6 and LP7 were combined to form sampling point LP2A, to July 2001. Data from LP2A are not used in this analysis due to the uncertainty concerning its validity and the short period for which data were collected.

5.1.3 REAL TIME DATA RETRIEVAL

In July 2001, a radio transmitter was installed to the south of the landfill next to the flow monitoring data loggers (Fig. 5.5). It is connected to the raingauge and the monitoring boxes of the flow monitoring equipment. The data are transmitted to a receiver, which is connected to a computer at the site office.

Using a modem connected to the site office computer, it is possible to download the data remotely. Regular downloading and viewing of the data enables faults to be detected and fixed quickly.

Data from the remote download can be compared with data downloaded directly from the data logger. The data should be the same within margins of error. Examples of typical data are given in Table 5.4. It is possible to see that the values downloaded from the remote download do not match those downloaded directly from the datalogger. Figure 5.12 shows a typical graph of the flow in the Settlement Tank with values from the datalogger and remote download. The flow data downloaded directly from the datalogger varies over the 5 days. The flow data downloaded via the remote download facility varies, although it appears to vary randomly about a midpoint.

The remote download facility stopped working in September 2003. The transmitter was no longer transmitting data to the site office. In view of uncertainty in the transmitted data, it was decided to abandon the remote download facility and utilise data only directly downloaded from the datalogger. In the analysis presented here only data from the datalogger is used.

Date & Time	Flow directly from datalogger (l/s)	Flow from remote download (l/s)
03/08/03 04:00	9.8	11.941
03/08/03 04:15	9.8	11.477
03/08/03 04:30	9.8	12.283
03/08/03 04:45	9.8	10.512
03/08/03 05:00	9.8	11.343
03/08/03 05:15	9.8	10.793
03/08/03 05:30	9.8	10.634
03/08/03 05:45	9.8	10.39
03/08/03 06:00	9.8	13.333
03/08/03 06:15	9.8	11.831
03/08/03 06:30	9.8	10.17
03/08/03 06:45	9.8	12.417
03/08/03 07:00	9.8	12.234
03/08/03 07:15	9.8	12.637
03/08/03 07:30	5.9	10.976
03/08/03 07:45	5.9	10.891
03/08/03 08:00	7.8	11.684
03/08/03 08:15	7.8	12.429
03/08/03 08:30	3.9	11.794
03/08/03 08:45	2	11.196
03/08/03 09:00	2	10.989
03/08/03 09:15	2	13.565
03/08/03 09:30	2	11.379
03/08/03 09:45	7.8	9.597
03/08/03 10:00	7.8	10.793
03/08/03 10:15	7.8	10.903
03/08/03 10:30	7.8	10.28
03/08/03 10:45	7.8	11.733
03/08/03 11:00	7.8	12.82
03/08/03 11:15	7.8	10.61
03/08/03 11:30	7.8	12.527
03/08/03 11:45	7.8	11.684
03/08/03 12:00	7.8	11.172
03/08/03 12:15	7.8	10.305
03/08/03 12:30	7.8	9.926
03/08/03 12:45	7.8	12.673
03/08/03 13:00	7.8	9.914
03/08/03 13:15	7.8	11.379
03/08/03 13:30	7.8	10.122
03/08/03 13:45	7.8	10.989
03/08/03 14:00	7.8	10.476

Table 5.4 Table showing typical flow data for the Settlement Tank downloaded directly from the datalogger and from the remote download.

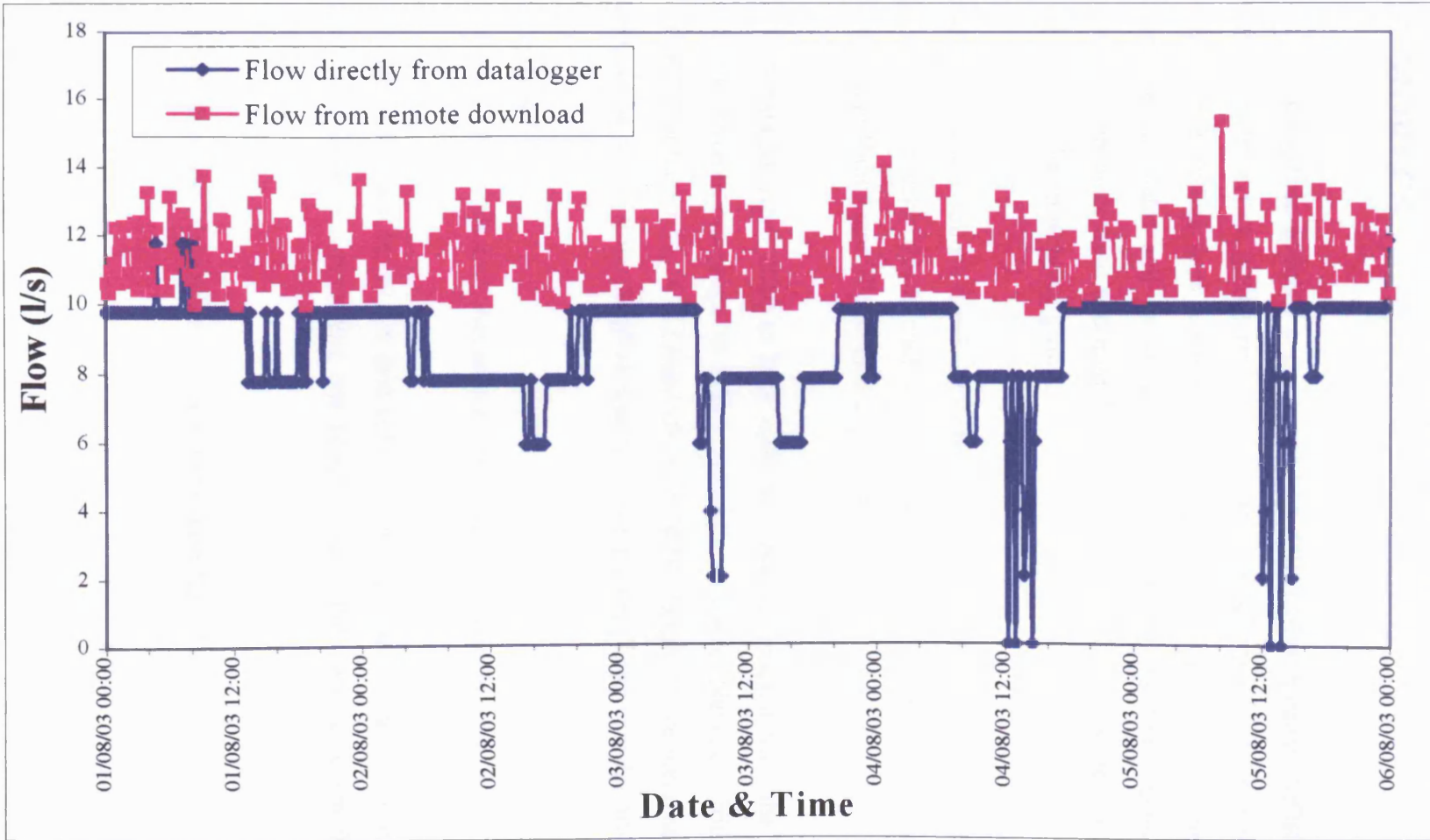


Figure 5.12 Graph showing typical flow data for the Settlement Tank downloaded directly from the datalogger and from the remote download.

5.2 RAINFALL DATA

5.2.1 MORECS

Meteorological Office Rainfall and Evaporation Calculation System (MORECS) is the only nationwide service giving real time assessments of rainfall, evaporation and soil moisture. The system uses a sophisticated equation based on the Penman-Monteith method that calculates soil moisture and evaporation values from measurements of temperature, sunshine, wind and humidity. The equation also allows for local variations in soil type and the crops being grown.

MORECS calculates soil state and evaporation for both a 40 km by 40 km grid nationwide (Fig. 5.13) on a weekly operational basis, and at individual recording sites for hindsight studies. Silent Valley landfill site falls in grid 146.

MORECS data for April 2000 to May 2004 have been purchased from the Met Office. The closest suitable raingauge to Silent Valley is at Cwm (National Grid Reference: SO 183057 (Latitude = 51:74 N Longitude = 03:18 W), height above mean sea-level: 213 metres), so the MET Office supplied data from this gauge. Their calculations were based on:

- Crop type – Upland
- Soil type - Real soils data, Actual Average available water capacity.

The nationwide 40 km by 40 km grid covers large areas of varying conditions, so it was fortunate that there is a recording site based about 2 km away at Cwm for hindsight measurements.

Data bought from the Met Office are given in Section 5.3.1.2.

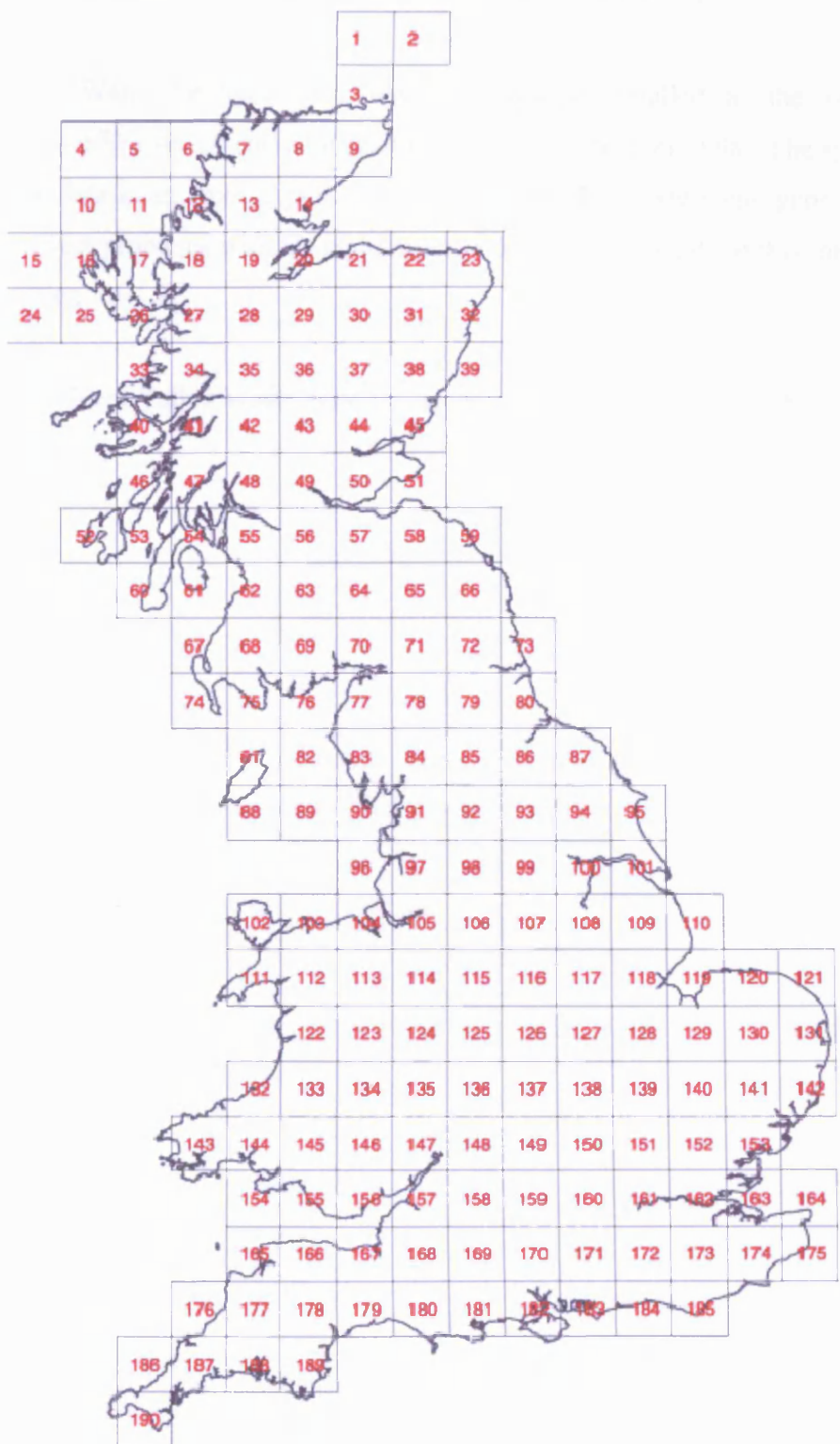


Figure 5.13 A map showing the location of the 40 km squares and their associated reference number.

5.2.2 SILENT VALLEY WASTE SERVICES (SVWS)

Silent Valley Waste Services have had a raingauge installed at the weighbridge (approximately 370 mAOD) collecting rainfall data since October 1998. The system is set to record the data at an archive period to 30 minutes. There are some gaps in the data where there were problems with the equipment or download. Details of this raingauge are given in Section 5.1.1.2.

Data from the Silent Valley Waste Services raingauge are given in Section 5.3.1.1.

5.2.3 RAINGAUGE – REMOTE LINK

A raingauge (Fig. 5.14) was installed at the end of July 2001 at the base of the landfill by the sump and flow monitoring data loggers (approximately 310 mAOD). It is a tipping bucket raingauge. Rain collects in a small bucket until the weight of the rainwater tips the bucket, discharging the collected water. At each tip of the bucket a magnet passes a reed switch, closes the contact and causes a pulse to be emitted. The raingauge on site measures 0.2 mm for every tip (pulse). The raingauge is connected to the radio transmitter and the data are logged at the office.

Rainfall measurements have not been obtained from this raingauge since September 2003 when the remote download facility stopped working.

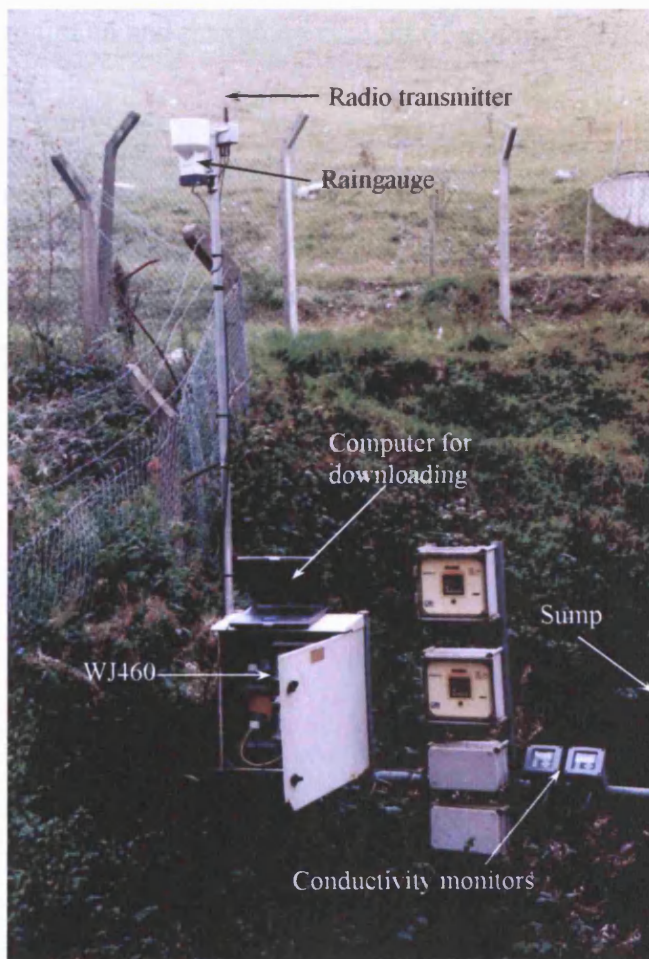


Figure 5.14 Raingauge installed at the base of the landfill by the sump and flow monitoring data loggers (approximately 310 mAOD).

5.3 ANALYSIS OF RAINFALL DATA

5.3.1 RAINFALL RECORD

5.3.1.1 Silent Valley Waste Services Data

Rainfall data collected by Silent Valley Waste Services between October 1998 and June 2004 is given in figure 5.15. There are gaps in the data where data have not been recorded because of equipment problems, power failures or data have been lost if it has not been downloaded regularly enough.

The rainfall data have been analysed. Rolling totals were calculated for different time periods. The minimum and maximum amount of rainfall recorded for each time period is given in table 5.5.

The longest recorded period without rainfall was recorded as 488 hours between 8am on the 11 September and 4pm on the 1 October 2002. The second longest recorded period without rainfall was recorded as 342 hours and 30 minutes between 9:30am on the 13 July to 4pm on the 27 July 2000.

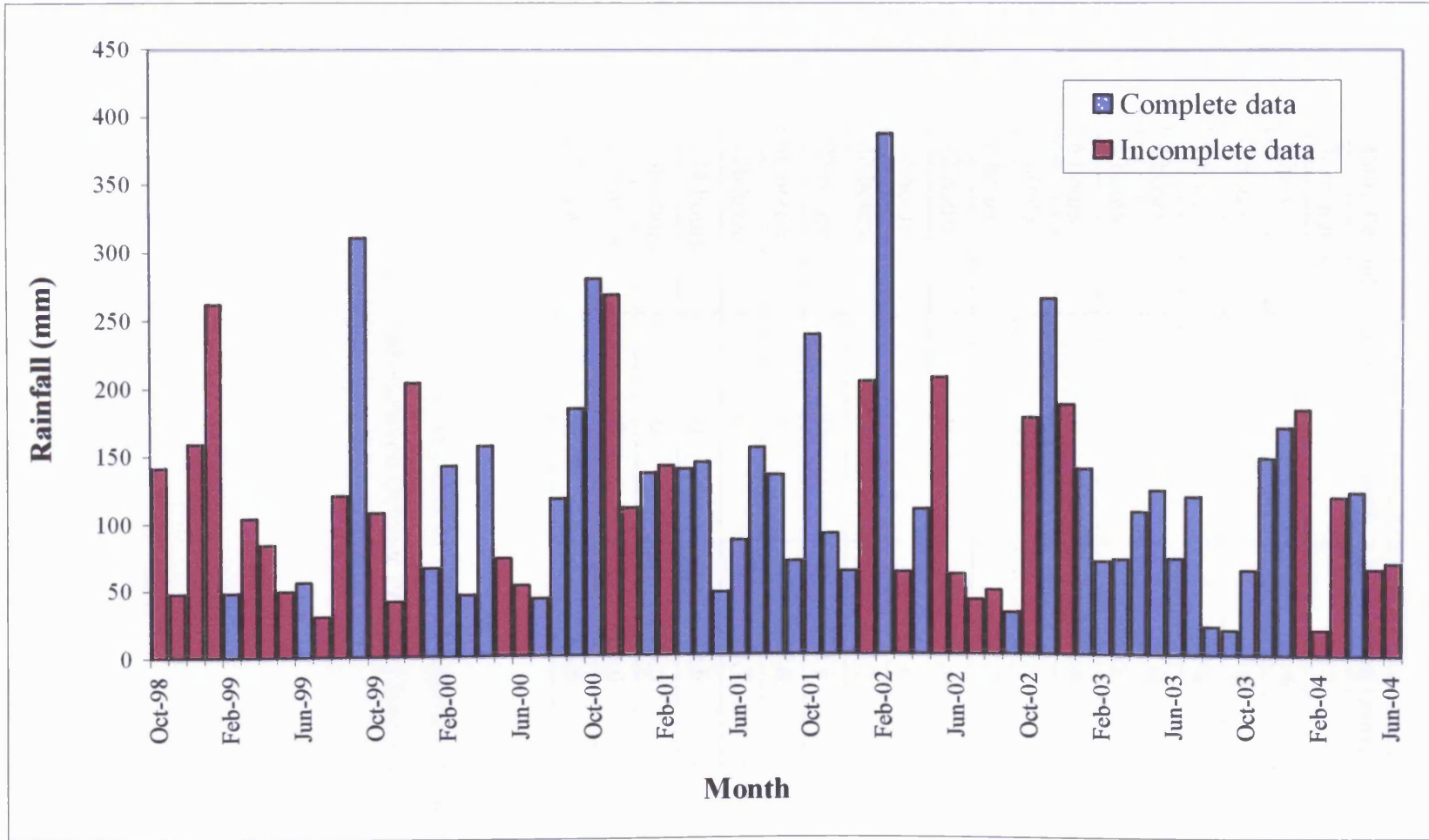


Figure 5.15 Graph showing the monthly rainfall totals recorded at Silent Valley by Silent Valley Waste Services.

Time Period	Minimum (mm)	Maximum (mm)
30 minutes	0	14.2
1 hour	0	23.6
2 hours	0	33.6
3 hours	0	42.8
4 hours	0	47.6
5 hours	0	49.6
6 hours	0	51.6
7 hours	0	57.6
8 hours	0	62.8
12 hours	0	85.4
24 hours	0	105.0
48 hours	0	124.2
72 hours	0	132.6
96 hours	0	171.6
120 hours	0	179.7
144 hours	0	180.6
168 hours	0	186.5
192 hours	0	194.0
336 hours	0	285.6

Figure 5.5 Minimum and maximum amounts of rainfall recorded at Silent Valley for different time periods between October 1998 and June 2004.

5.3.1.2 Met Office Data

Monthly rainfall data for Cwm and daily Potential Evaporation (PE), Actual Evaporation (AE) and Effective Rainfall values were bought from the Met Office for April 2000 to May 2004.

5.3.1.2.1 Potential Evaporation (PE)

Potential Evaporation (PE) is defined as the amount of water that could be evaporated were it available. It is a function of surface and air temperatures, insulation, and wind, all of which affect water-vapour concentrations immediately above the evaporating surface.

Figure 5.16 shows the Potential Evaporation for Cwm calculated by the Met Office. The PE losses exhibit a strong annual cycle, peaking normally around July. The annual PE losses occurring during the October-March period were 19.5%, 20% and 24.4% for 2001, 2002 and 2003 respectively. The remaining 75-80% PE loss occurs in the 6 month period between April and September.

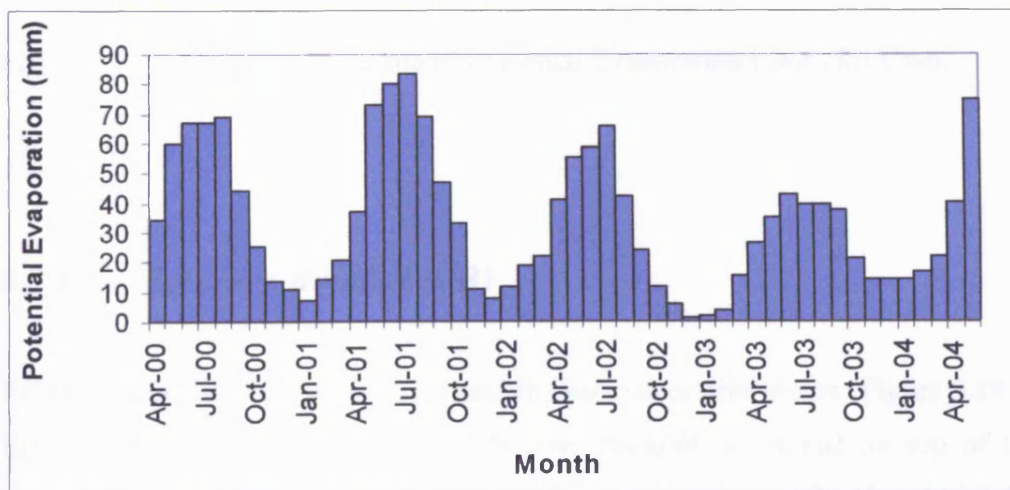


Figure 5.16 Graph showing monthly Potential Evaporation values for Cwm.

5.3.1.2.2 Actual Evaporation (AE)

Figure 5.17 shows the Actual Evaporation for Cwm calculated by the Met Office. The AE losses exhibit the same strong annual cycle as for Potential Evaporation. The annual AE losses occurring during the October-March period were 20.2%, 20.2% and 24.6% for 2001, 2002 and 2003 respectively. The remaining 75-80% AE loss occurs in the 6 month period between April and September.

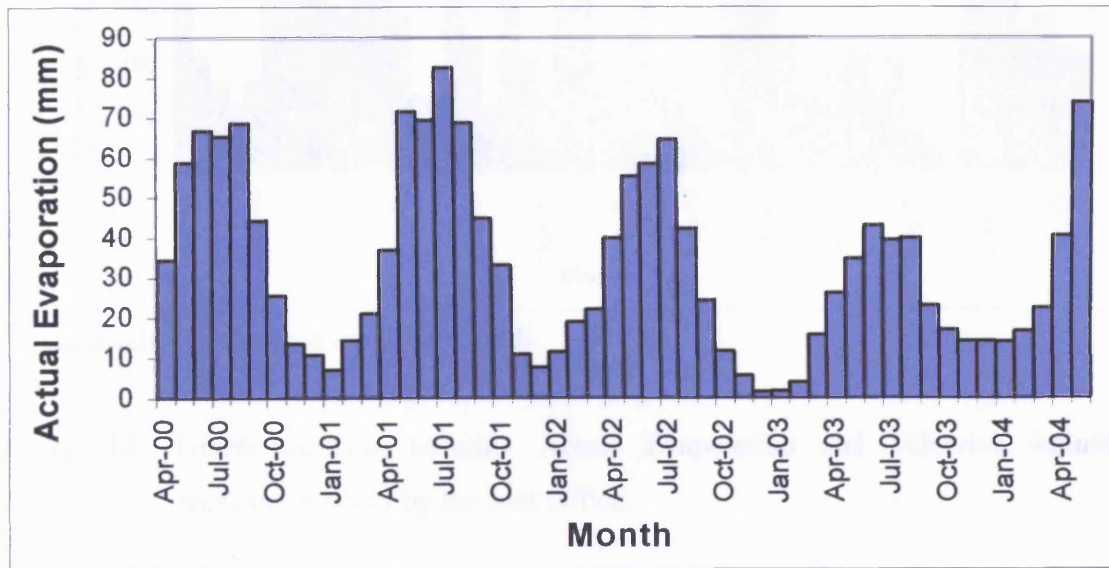
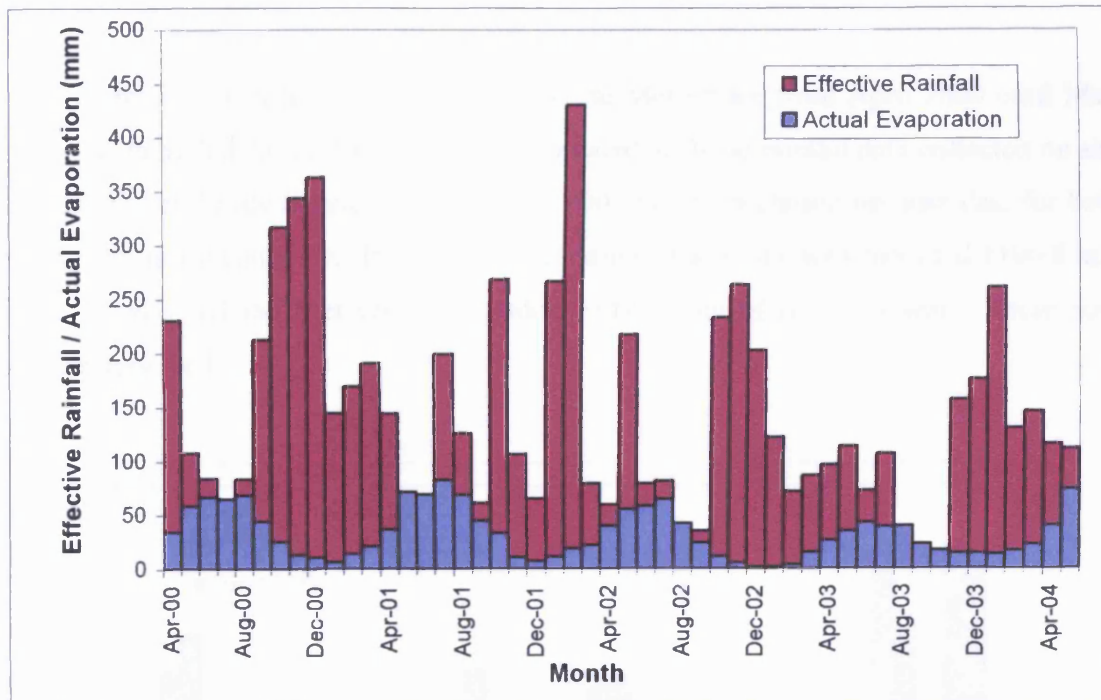


Figure 5.17 Graph showing monthly Actual Evaporation values for Cwm.

5.3.1.2.3 Effective Rainfall (ER)

Effective Rainfall is the remaining rainfall after evaporative losses. Figure 5.18 shows the Effective Rainfall for Cwm. The Effective Rainfall is stacked on top of the Actual Evaporation to give the total recorded rainfall. For some months (July 2000, May, June 2001, August 2002, August, September, October 2003) all the rainfall is lost as Actual Evaporation giving no Effective Rainfall.



Total height of column is equal to rainfall.

Figure 5.18 Graph showing monthly Actual Evaporation and Effective Rainfall recorded at Cwm by the Met Office.

Over the long-term, the Effective Rainfall represents 77% of the rainfall recorded at Cwm by the Met Office.

5.3.2 COMPARISON OF MET OFFICE AND SILENT VALLEY DATA

Rainfall data for Cwm has been bought from the Met Office from April 2000 until May 2004. The rainfall data for 2003 has been compared with the rainfall data collected on site by Silent Valley Waste Services (Fig. 5.19). 2003 has been chosen because data for both sets of records are complete. In 2003, Silent Valley Waste Services recorded 1106.8 mm of rain on site and the Met Office recorded 1114.1 mm of rain at Cwm. These data compare very well.

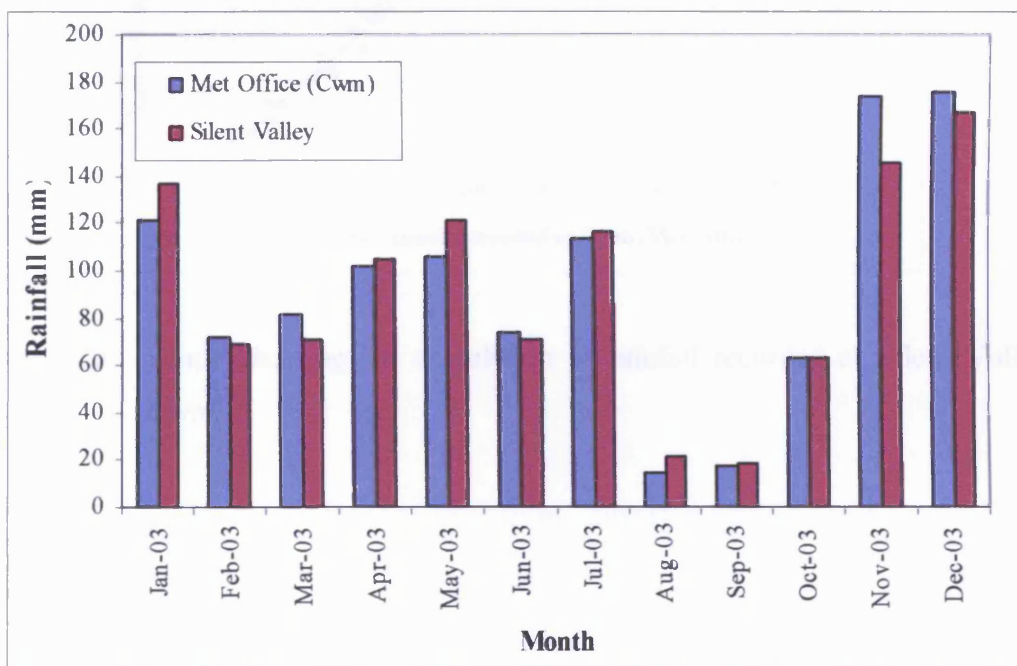


Figure 5.19 Rainfall data collected on site by Silent Valley Waste Services and at Cwm by the Met Office between January and December 2003.

By comparing rainfall data for Silent Valley and Cwm (months with complete data sets only) it is possible to see a very strong positive correlation ($r = 0.98$) (Fig. 5.20). In the long term, the rainfall recorded at Silent Valley represents about 93% of the rainfall recorded at Cwm.

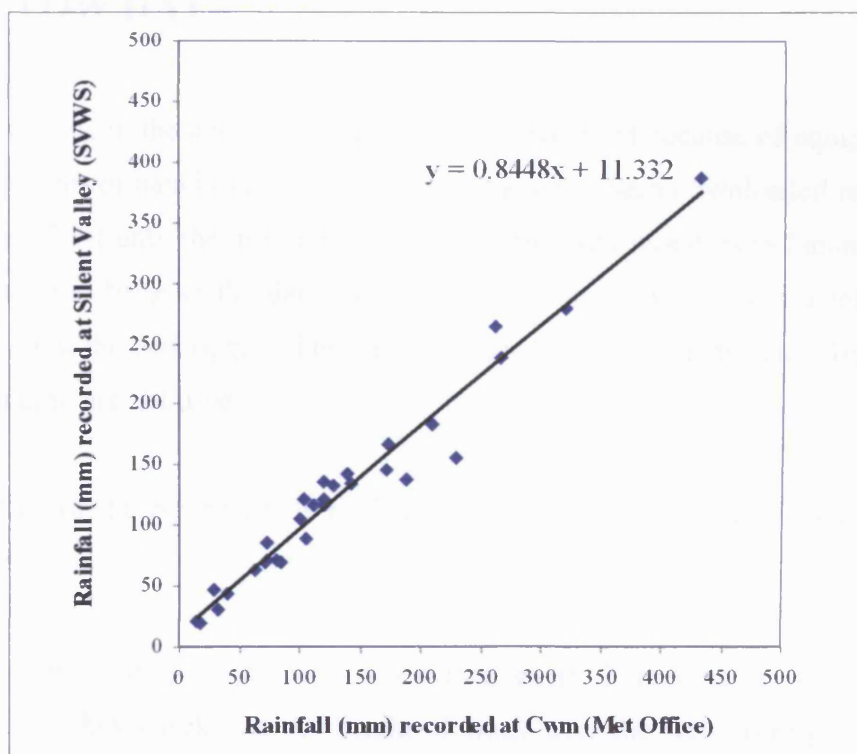


Figure 5.20 Graph showing the correlation of rainfall recorded at Silent Valley and Cwm.

5.4 FLOW DATA

There are gaps in the data where data were not recorded because of equipment problems, power failures or data have been lost if they have not been downloaded regularly enough. From July 2001 until the installation of the conductivity monitors in January 2003, gaps in the data occur because the data were generally only downloaded via telemetry and not directly from the datalogger. The data downloaded via telemetry have been shown to be unreliable, so are not used.

Calibration of the equipment is performed when the equipment is installed or a part is replaced.

The flow monitoring equipment is serviced every 3 months by the instrumentation contractor. They check that the height of water over the weir corresponds to the value measured by the equipment. Any debris collecting on the weir is cleared.

Engineering works were undertaken in 2001 with the aim to reduce the amount of water entering the site. Channels and drainage ditches were constructed around the site and a capping layer was placed on the Southern Slope (details given in Section 3.6.4.2.1).

5.4.1 BSC PIPE

Flow over the rectangular weir in the BSC Pipe has been recorded since February 1994.

The discharge for the BSC Pipe has been plotted (Fig. 5.21) as a time series. Some of the data points are suspect; much higher than expected. The flow from the BSC Pipe is pumped up to the Settlement Tank with the other flows (LP2A) entering the sump. The leachate then goes over the Settlement Tank weir. Assuming that no fluid is lost between going over the BSC weir and the Settlement Tank weir, the flow over the BSC Pipe weir should not exceed the flow over the Settlement Tank. The very high flows recorded are likely to be wrong. It is possible that foam has built up under the ultra-sonic sensor to give an artificially high reading.

Discharge for the BSC Pipe can be plotted as a time series with the suspect data points removed (Fig. 5.22). Over the years the flow appears to have decreased very slightly. Due to the gaps in the data it is not possible to say whether there is an overall decrease in discharge or whether this is simply an apparent decrease due to gaps in the data set. It is also possible that the decrease is due to recording errors or drift in the instrumentation. However, since equipment is periodically serviced by the instrumentation contractor, it is unlikely that serious consistent drift in recording has actually occurred.

Between 28 November 2003 and 7 July 2004 discharge over the weir in the Settlement Tank was recorded as 331482 m³ while a discharge of 96448 m³ was recorded over the rectangular weir in the BSC Pipe. For this period, the flow from the BSC Pipe represents 29% of the flow through the Settlement Tank.

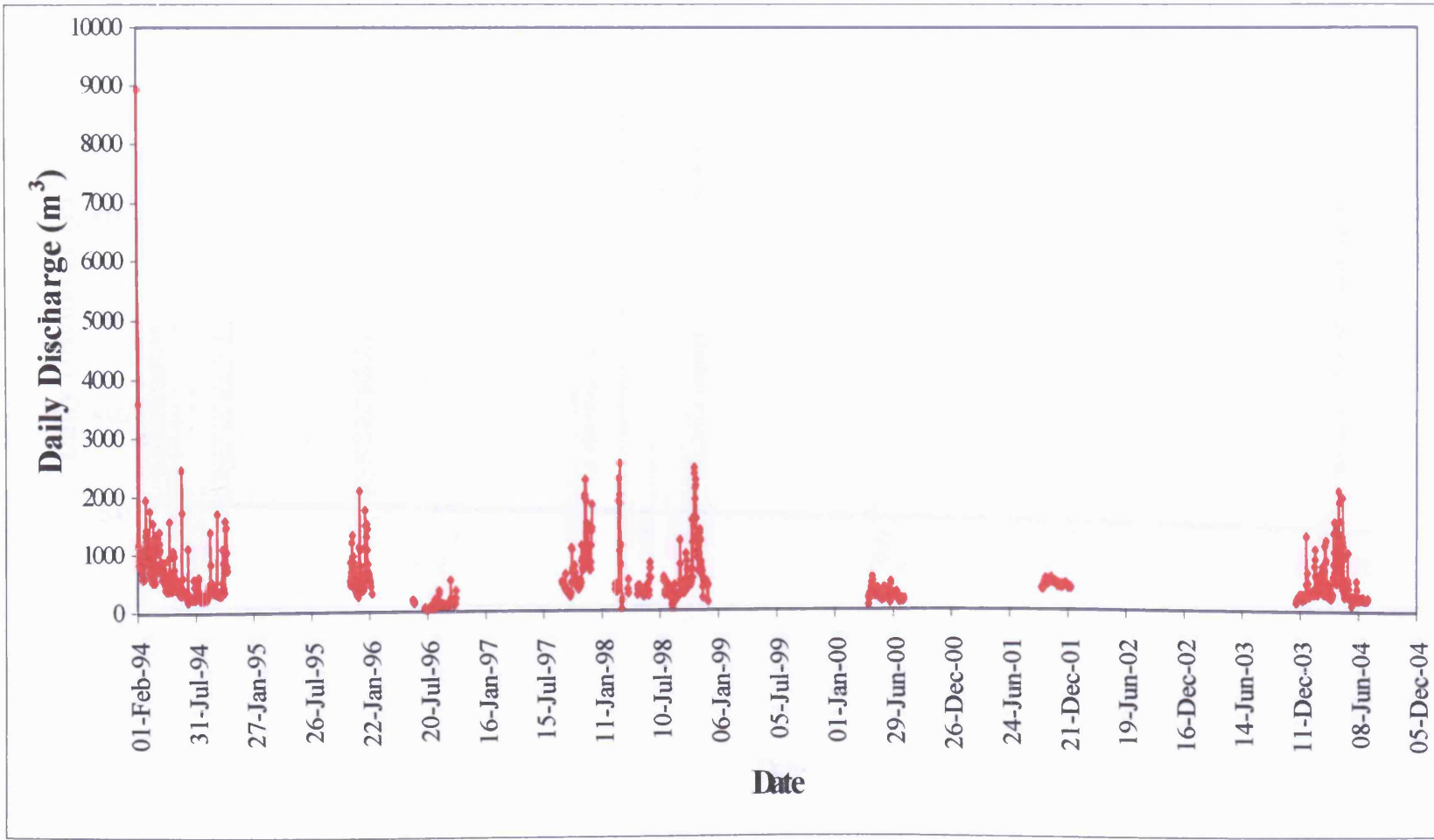


Figure 5.21 Graph showing total daily discharge over the weir in the BSC Pipe between February 1994 and July 2004.

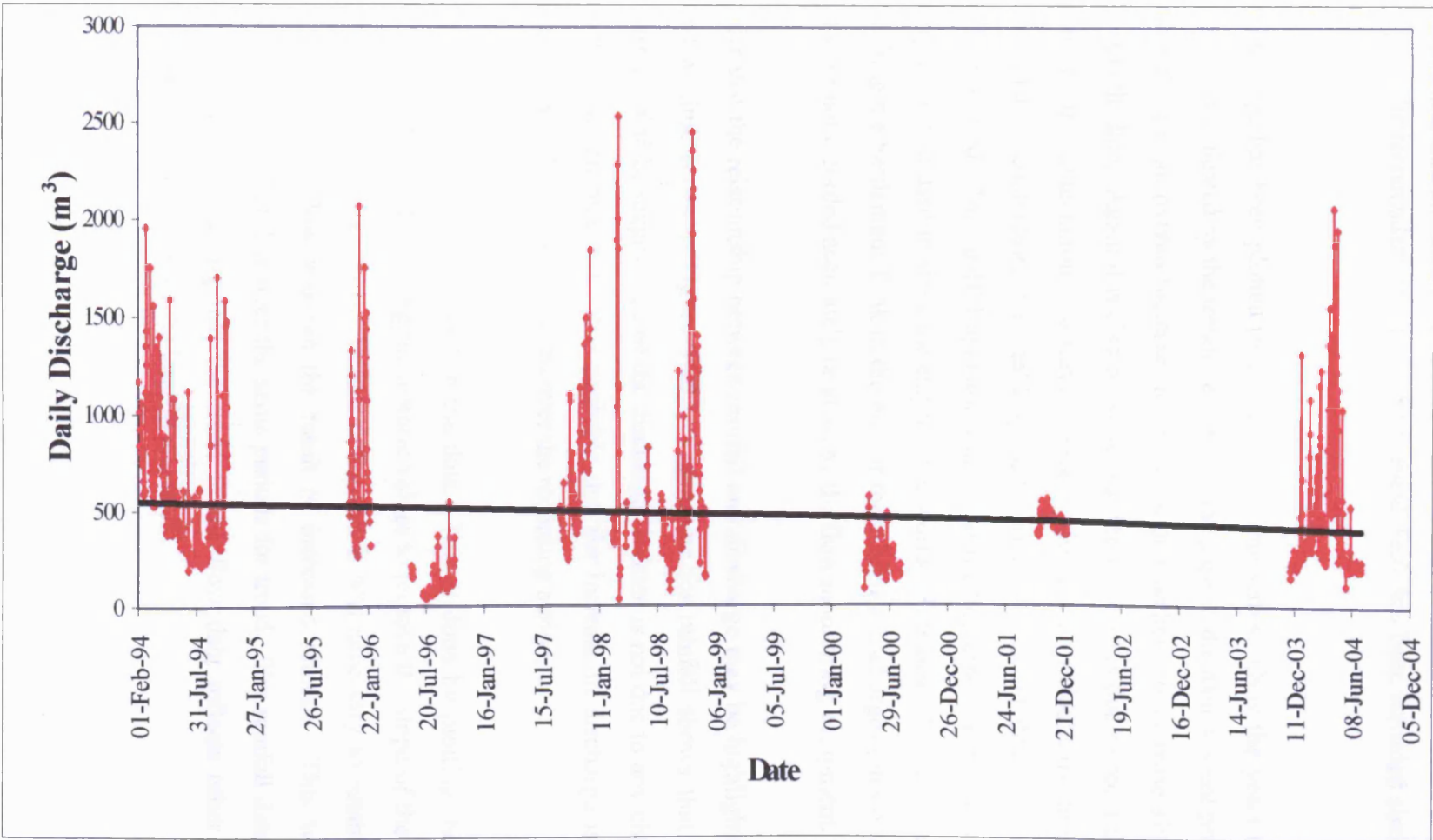


Figure 5.22 Graph showing total daily discharge (suspect data removed) over the weir in the BSC Pipe between February 1994 and July 2004.

5.4.2 SETTLEMENT TANK

Flow over the rectangular weir in the Settlement Tank has been recorded since December 1993.

The discharge has been plotted (Fig. 5.23) as a time series. Over the years the flow has increased, as indicated by the trendline. Due to the gaps in the data it is not possible to say whether there is an overall increase in discharge or whether this increase simply reflects the available data. Again it is also possible that the increase is due to recording errors or drift in the instrumentation. However, since equipment is periodically serviced by the instrumentation contractor, it is unlikely that serious consistent drift in recording has actually occurred. The landfill operator thinks that the Settlement Tank does not get full as frequently as it used to since the engineering works. This could be due to a lower flow rate exiting the Settlement Tank in the past or these higher discharges (anecdotal evidence only) were not recorded accurately or at all by the flow monitoring equipment.

In order that the relationship between rainfall and discharge may be highlighted, both are plotted as time series in Figure 5.24. A trendline for rainfall shows that there is no increase in rainfall, suggesting that the discharge increase is not due to any changes in the amount of rainfall received. It is probable that the increase in discharge is due to the increase in landfill size that occurred over the recording period.

It is possible to remove the trend in the data. This is done by plotting the flow data, adding a trendline and adjusting the historic values to remove the slope of the trendline to make it horizontal (Fig. 5.25). Before doing this it was necessary to establish that the trend of increased flow was not the result of increased rainfall. This was done by examining the rainfall data over the same periods for trend. The rainfall data showed no significant trend suggesting that the trend in the flow data reflects other factors, for instance changes in the size of the landfill site itself.

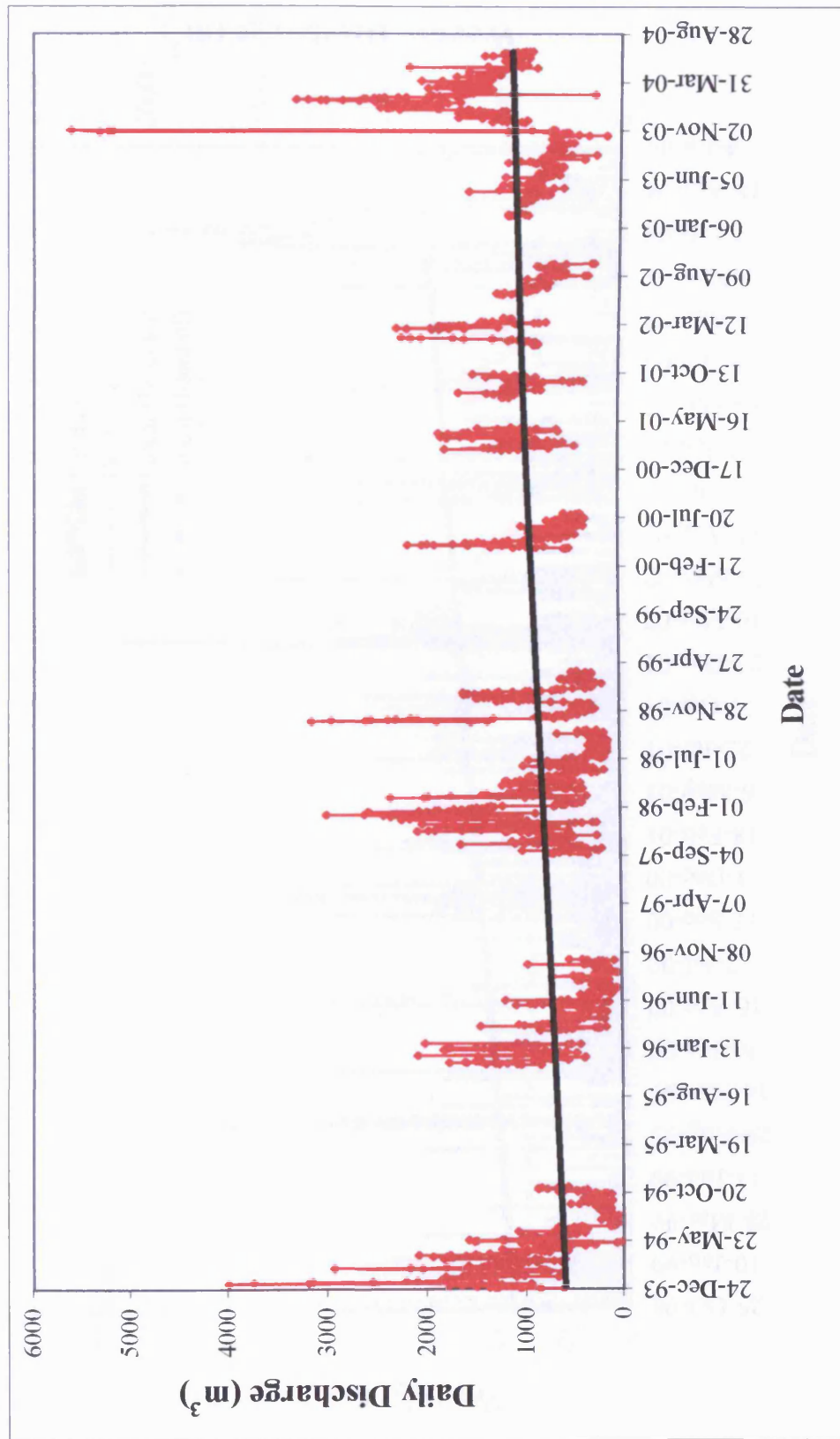


Figure 5.23 Graph showing total daily discharge over the weir in the Settlement Tank between December 1993 and July 2004.

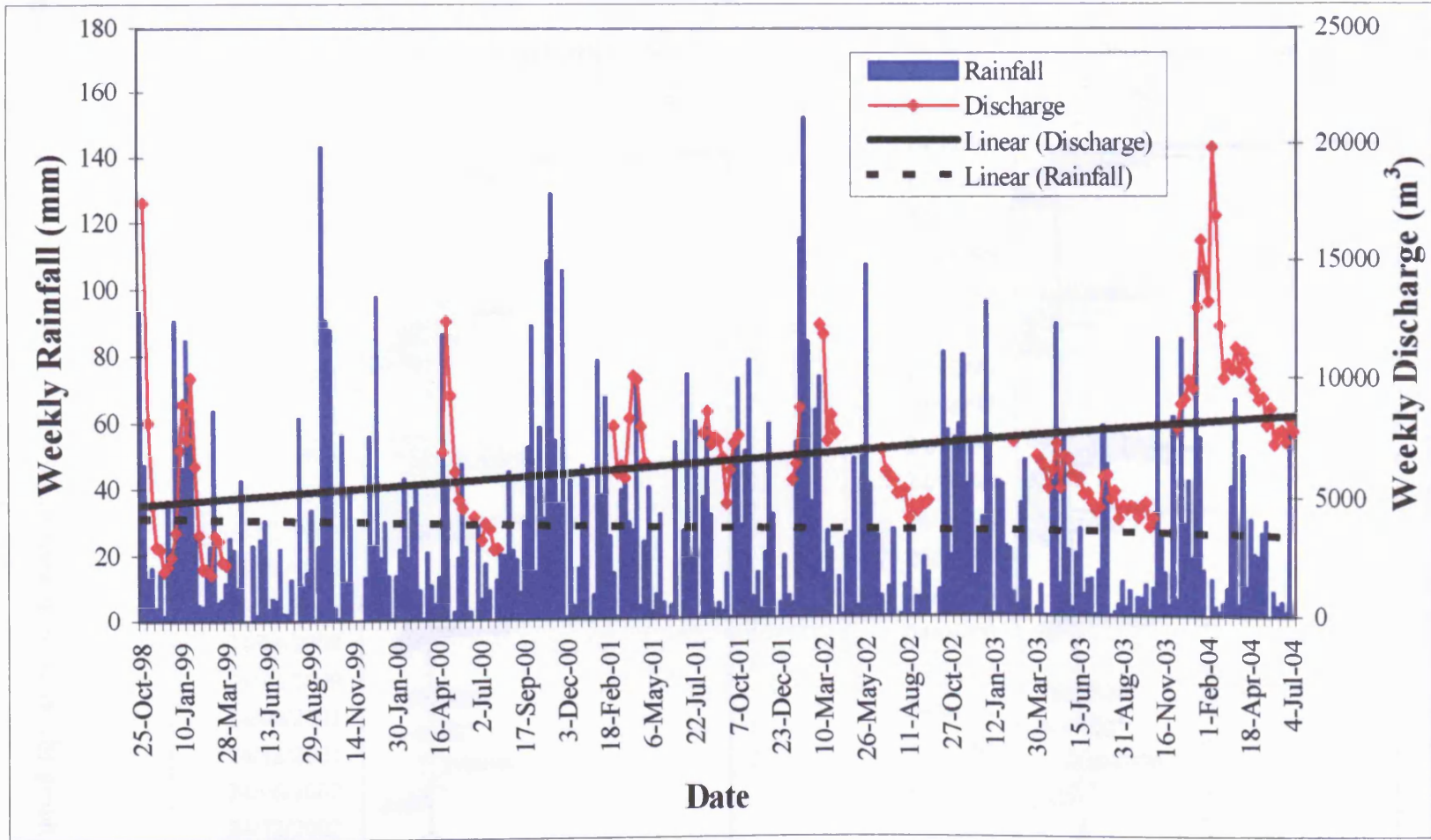


Figure 5.24 Graph showing total weekly Settlement Tank discharge and rainfall between October 1998 and June 2004.

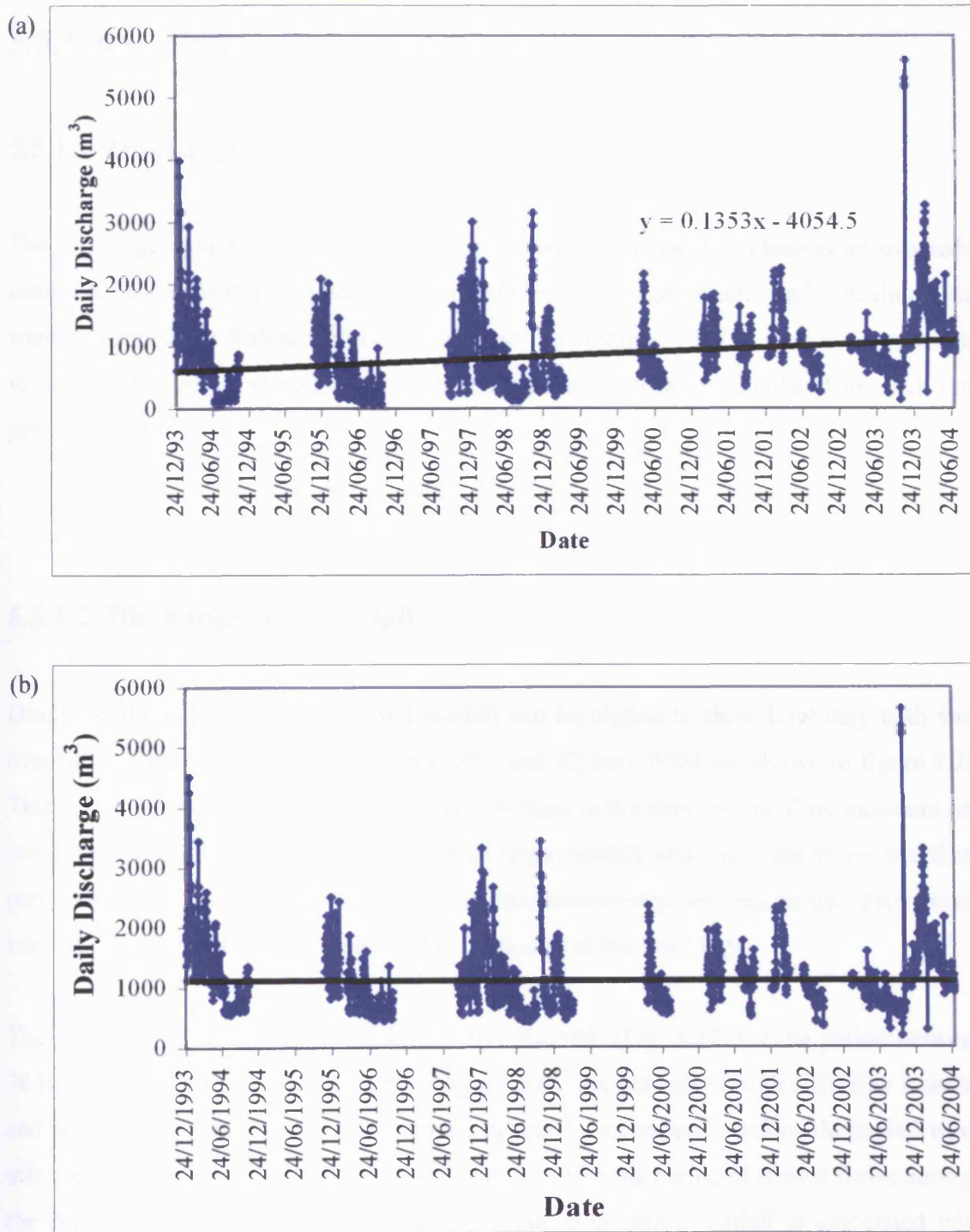


Figure 5.25 (a) Graph showing the discharge data with trend, (b) graph showing the discharge data with the trend removed.

5.5 ANALYSIS OF FLOW DATA

5.5.1 BSC PIPE

5.5.1.1 Discharge

The discharge data for the BSC Pipe is presented below and its relationship to rainfall analysed. The flow rate (l/s) has been converted to discharge volume (m³). Rolling totals were calculated for different time periods and the minimum value recorded, maximum value recorded, mean, standard deviation and median value were calculated for each time period (Table 5.6).

5.5.1.2 Discharge and Rainfall

Discharge through the BSC Pipe and rainfall can be plotted to show how they both vary over time. Data between 28 November 2003 and 22 June 2004 are shown in figure 5.26. This period was selected because there are few gaps in the data and the flow monitors had just been calibrated. There are periods of high rainfall and high discharge but these periods do not overlap. There appears to be little relationship between rainfall occurrence, intensity and duration with changes in the discharge of the BSC Pipe.

The discharge has been plotted with Effective Rainfall (Fig. 5.27) for the period between 28 November 2003 and 31 May 2004. Again there are periods of high Effective Rainfall and high discharge but these periods do not appear to correspond. In fact, the period when effective rainfall was highest (winter) corresponds with the period of lowest flows through the BSC Pipe, while in early summer the reduced effective rainfall is associated with increased daily discharge.

Figure 5.28, a cumulative graph for discharge through the BSC Pipe, rainfall and effective rainfall shows lower total and effective rainfall in the summer periods, when the

cumulative curves are less steep, and, as expected, much higher rainfall (total and effective) in winter. Increases and decreases in discharge from the BSC pipe appear to lag behind this rainfall pattern. This may reflect lags between rainfall and recharge of the landfill leachate system and possibly longer lag-times between rainfall and recharge of local groundwater system, if (as is possible) a proportion of the discharge through the BSC pipe is a result of groundwater seepage into the landfill base.

	15 mins	30 mins	1hr	2hrs	4hrs	6hrs	8hrs	12hrs	18hrs
Data points	44778	44771	44757	44729	44673	44617	44561	44449	44281
Min recorded	0	0	0	0	0	0	0	1.6	50.2
Max recorded	76.2	150.8	293.8	548.9	874.5	1107.3	1461.9	2027.8	2266.6
Mean	4.6	9.2	18.4	36.7	73.4	110.1	146.8	220.1	329.9
Standard Deviation	4.9	9.7	19	37.2	72	104.9	136.2	194.6	275.7
Median	3.2	6.4	13.2	27.4	55.8	84.2	113.7	172.6	260.5

	24hrs	36hrs	48hrs	60hrs	72hrs	96hrs	120hrs	168hrs
Data points	44113	43777	43441	43105	42769	42097	41425	40081
Min recorded	108.8	144	228.7	265.2	357.9	490.2	621	889.4
Max recorded	2588.8	3795.4	4766.3	5700.2	6669	8821.6	11037.2	14744.6
Mean	439.7	658.9	877.4	1094.9	1311.5	1741.9	2169.4	3013
Standard Deviation	357.1	522.9	680.3	837	985.8	1268.3	1534.5	2008.7
Median	347.8	531	710	887.8	1077.8	1452.2	1854	2665.7

Table 5.6 Discharge (m^3) recorded through the BSC Pipe between October 1998 and July 2004 for different time scales.

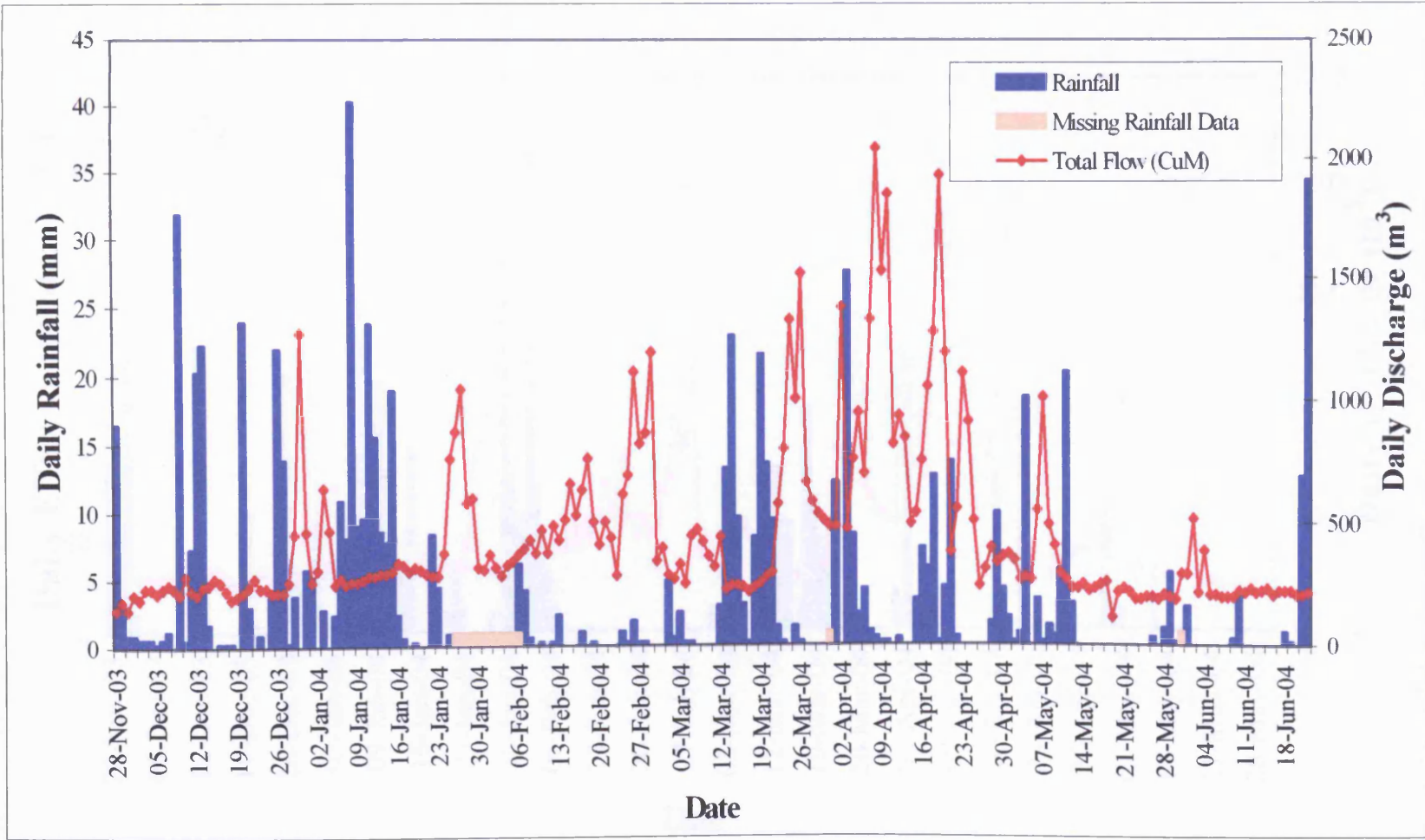


Figure 5.26 Graph showing discharge through the BSC Pipe and rainfall between 28 November 2003 and 22 June 2004.

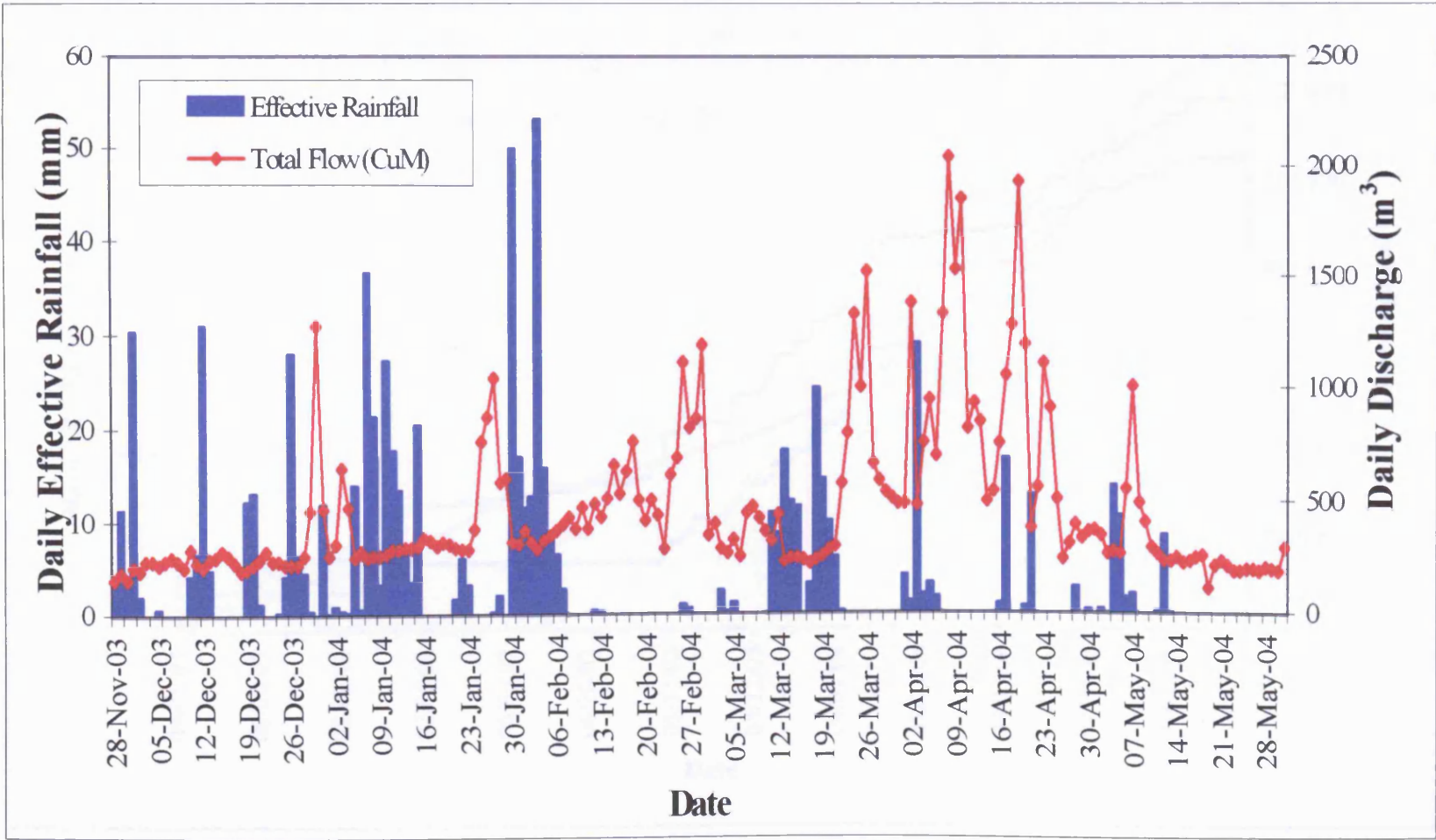


Figure 5.27 Graph showing discharge through the BSC Pipe and Effective Rainfall between 28 November 2003 and 31 May 2004.

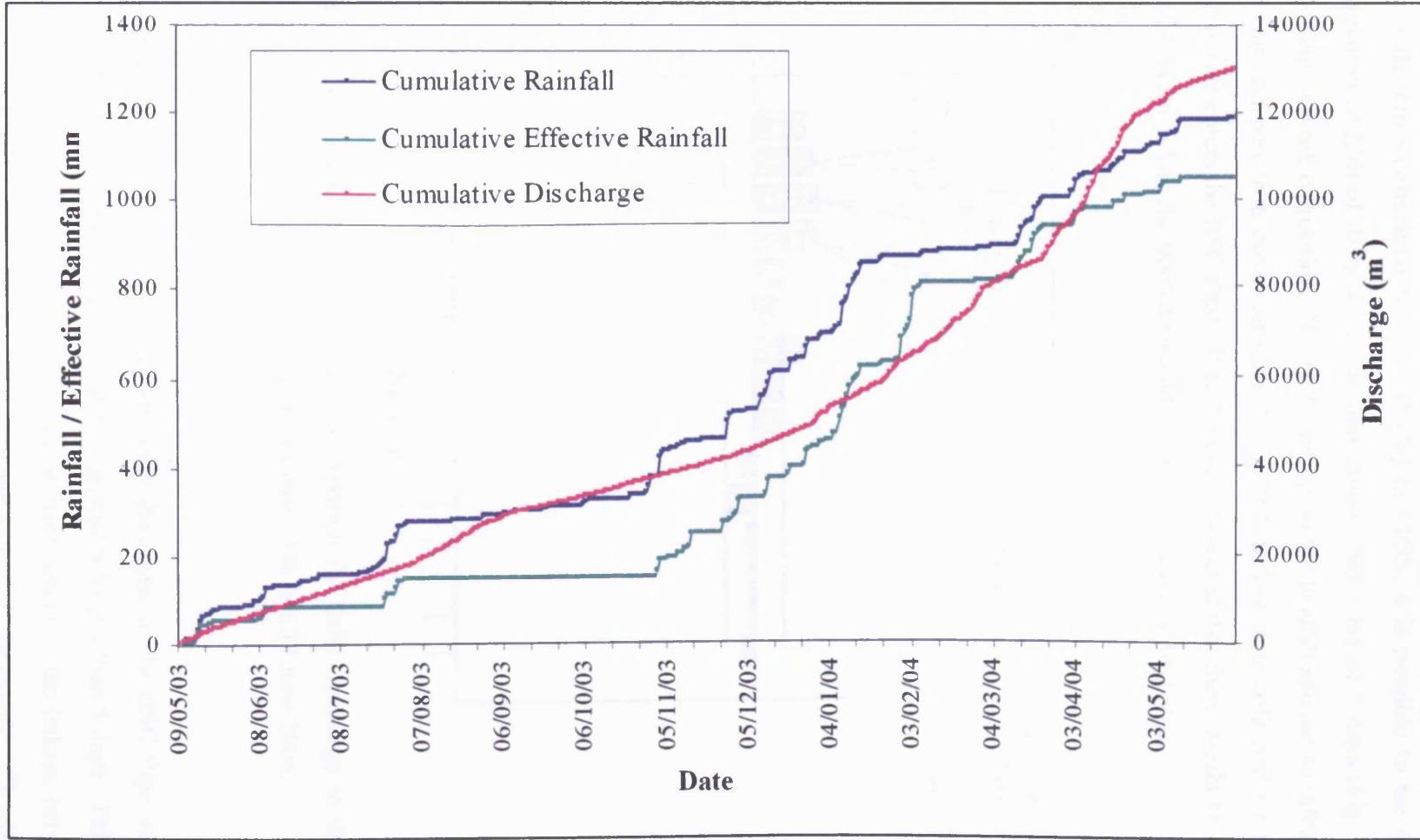


Figure 5.28 Cumulative graph showing discharge through the BSC Pipe, rainfall and Effective Rainfall between 9 May 2003 and 31 May 2004.

5.5.1.3 Lag Time

Using the cross-correlation function (CCF) in SPSS, it is possible to see that the best correlation (0.220) of daily discharge and rainfall has a lag of 5 days (Fig. 5.29). This represents a weak correlation. Rainfall landing on the landfill site has to infiltrate through the cap and percolate down through the landfill before it is collected by the drainage system that enters the BSC Pipe. It is therefore expected that there would be delay after a rainfall event before the leachate would show an increase in discharge.

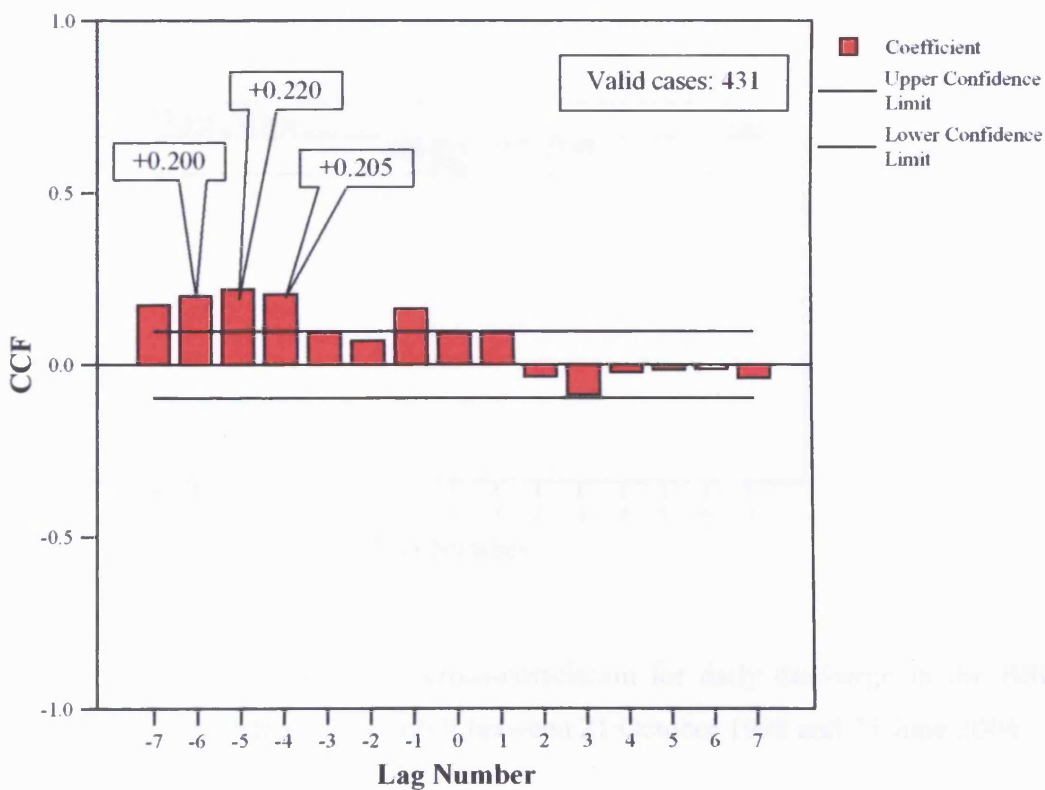


Figure 5.29 Chart showing the cross-correlation for daily discharge in the BSC Pipe with Rainfall between 21 October 1998 and 23 June 2004.

No significant correlation is found for daily discharge in the BSC Pipe with Effective Rainfall (Fig. 5.30), though the lag time suggested is longer than 5 days. This analysis of rainfall and effective rainfall indicates the indirect nature of the linkage between rainfall events and discharge through the basal drainage system of the landfill. Clearly recharge of

leachate, leachate storage, possibly flows from higher perched water tables to the main leachate water table in the base of the landfill all attenuate the rainfall signal, so that it does not correlate strongly with fluctuations in leachate drainage through the BSC Pipe.

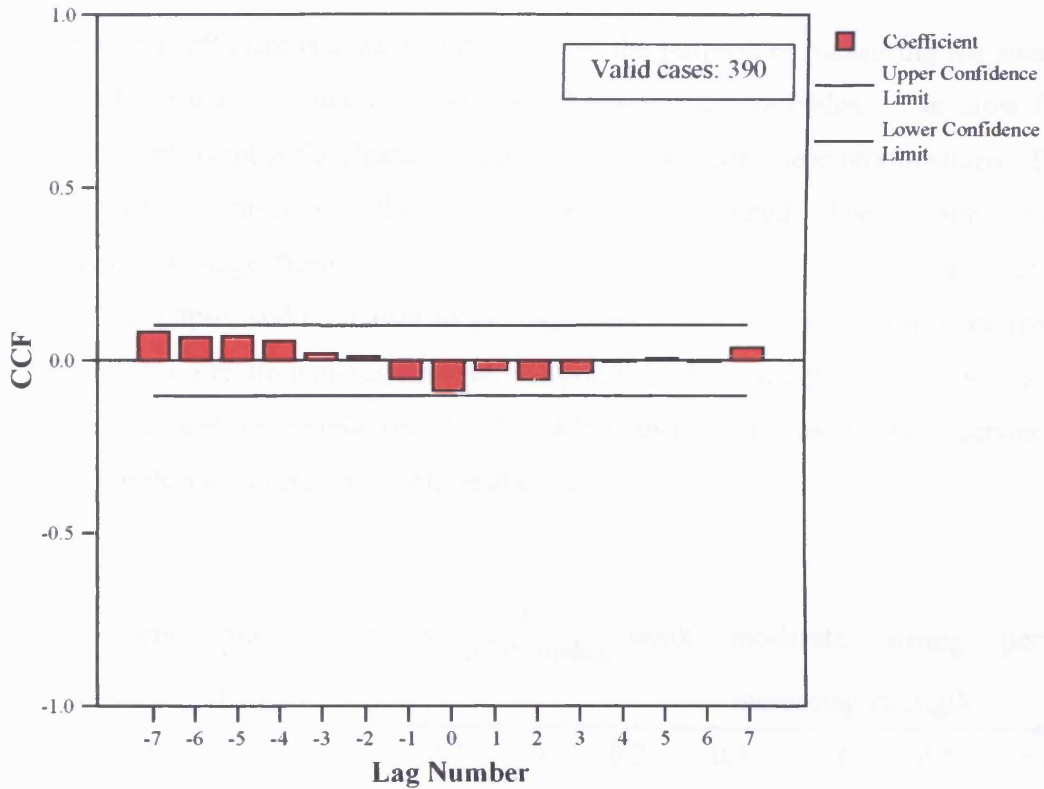


Figure 5.30 Chart showing the cross-correlation for daily discharge in the BSC Pipe with Effective Rainfall between 21 October 1998 and 23 June 2004.

5.5.1.4 Regression Analysis

There are a set of techniques, known as regression methods, which utilise the presence of an association between two variables to predict the values of one (the dependent variable) from those of another (the independent variable).

A correlation coefficient is a statistic devised for the purpose of measuring the strength of a supposed linear or polynomial association between two variables. The most familiar correlation coefficient is the Pearson correlation (r) used for linear relationships. Pearson correlation coefficients assume the data are normally distributed. The Pearson correlation has values that range from -1 to $+1$ (Fig. 5.31). The larger the absolute value, the narrower the ellipse, and the closer to the regression line the points in the scatterplot will fall. A perfect correlation arises when all the points in the scatterplot lie on the regression line giving a Pearson correlation of ± 1 . When there is no association between two variables the Pearson correlation will be about zero.

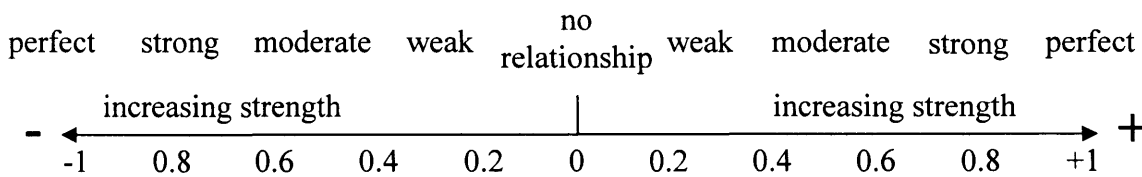


Figure 5.31 Scale of correlation.

Strong correlations are not necessarily significant (probably true; not due to chance). To assess the significance of a correlation, reference is made to the t -test table (Appendix C), which assesses the significance against the number of data pairs (N). The significance level (or p -value) is the probability of obtaining results by chance as high as the one observed. If the significance level is very small (<0.05 i.e., a 95% chance of being true) then the correlation is significant and the two variables are linearly related. If the significance level is large (for example, >0.50) then the correlation is not significant and the two variables are not linearly related. Even if the correlation between two variables is not significant, the variables may be correlated but with a non-linear relationship.

The discharge from the BSC Pipe between October 1998 and June 2004 has been plotted as a histogram (Fig. 5.32) with a normal curve with the same mean and variance as the discharge data. From this it is possible to see that the data do not fit a normal distribution very well. However, since the population size, N , is large and therefore the sample mean, \bar{x} , is approximately normally distributed, correlation analysis can still be performed on these data.

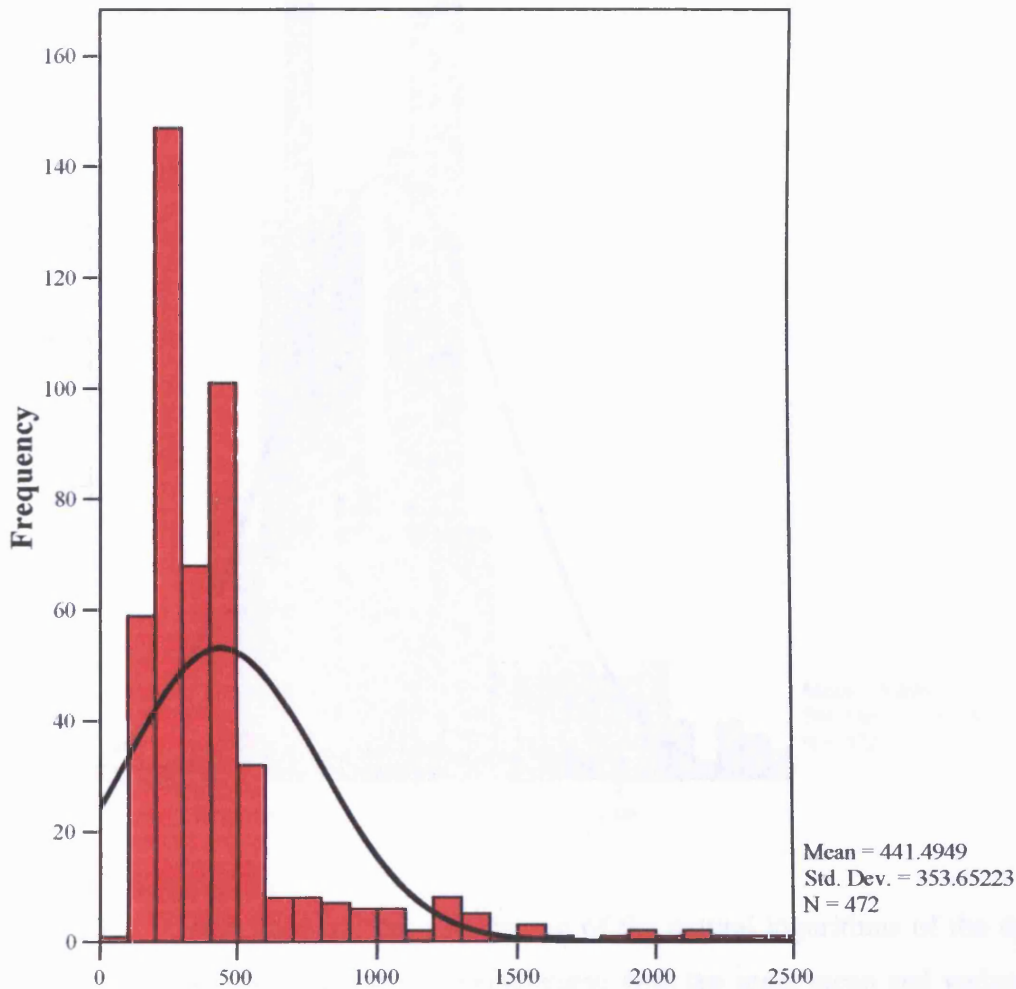


Figure 5.32 Graph showing the distribution of daily BSC Pipe discharge and a normal curve with the same mean and variance as the data.

Natural (base e) logarithms of values instead of the values themselves can be used for data which is characterised by an extended right hand tail distribution and can be used for both small and large values. Figure 5.33 shows that the distribution of the natural logarithms of the daily BSC Pipe discharge fit a normal distribution better than the raw discharge values.

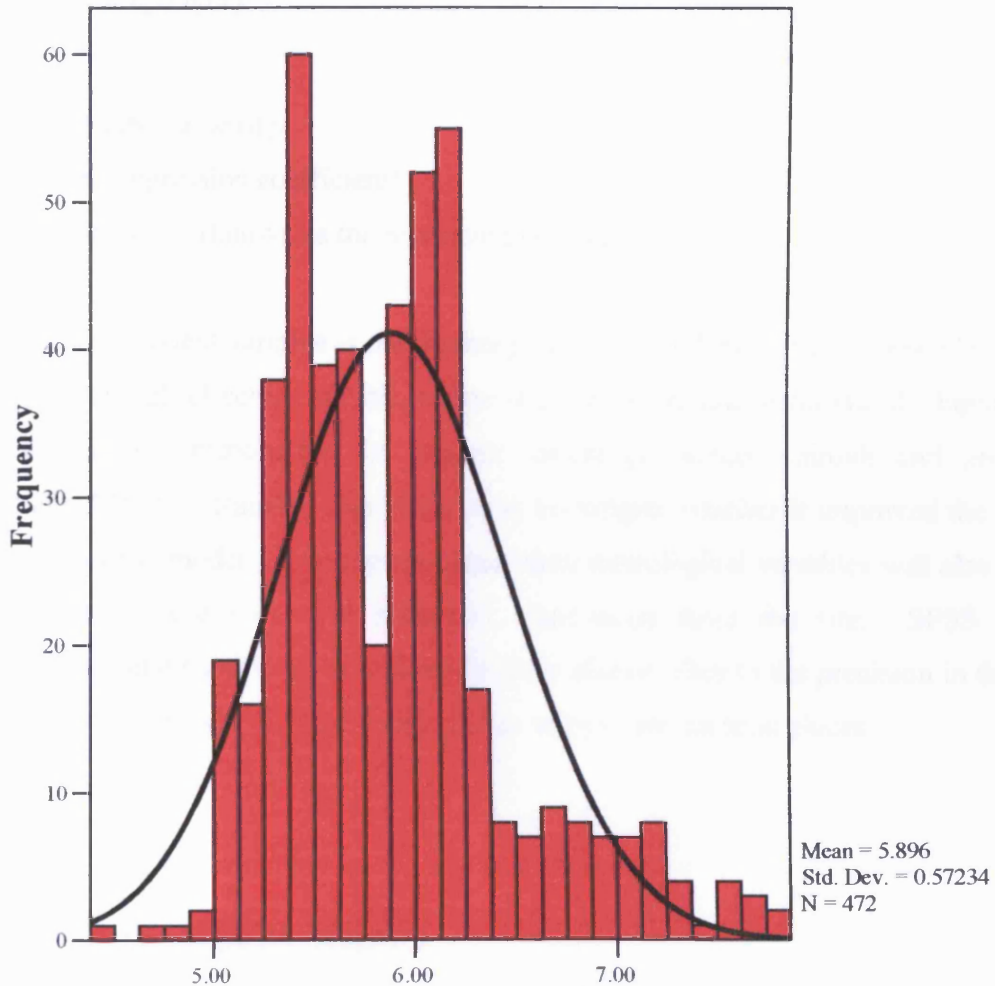


Figure 5.33 Graph showing the distribution of the natural logarithms of the daily BSC Pipe discharge and a normal curve with the same mean and variance as the data.

5.5.1.4.1 Simple, Two-Variable Regression

In simple, two-variable regression, the values of one variable (the dependent variable, y) are estimated from those of another (the independent variable, x) by a linear regression equation:

$$y' = b_0 + b_1(x) \quad (35)$$

where

y' = estimated value of y

b_1 = slope (regression coefficient)

b_0 = the intercept (known as the regression constant).

Here the dependent variable is the discharge through the BSC Pipe. Independent variables include rainfall, effective rainfall, temperature, pressure and wind speed. Inputs into the landfill system responsible for leachate discharge include rainfall and groundwater seepage. Effective Rainfall was included to investigate whether it improved the predictive strength of the model. It is expected that other metrological variables will also affect the discharge because they will influence evaporation from the site. SPSS calculates coefficients and significances to three decimal places. Due to the precision in the original data, coefficients will only be quoted to the nearest two decimal places.

5.5.1.4.1.1 Discharge and Rainfall

If the BSC Pipe daily discharge is plotted against the daily rainfall (Fig. 5.34), a Pearson coefficient of 0.09 is obtained with a significance of 0.05, which represents a significant very weak correlation. The general trend is that as the rainfall increases the discharge increases, which would be expected.

The best lag time was shown to be around 5 days (Section 5.5.1.3). A better correlation is obtained when comparing the rainfall and flow moved back by 5 days (i.e. compared with rainfall recorded 5 days before the discharge measurement) (Fig. 5.35). A Pearson coefficient of 0.22 with significance 0.00 is obtained, which represents a significance

weak correlation. The general trend is that as the rainfall increases the discharge increases, which would be expected.

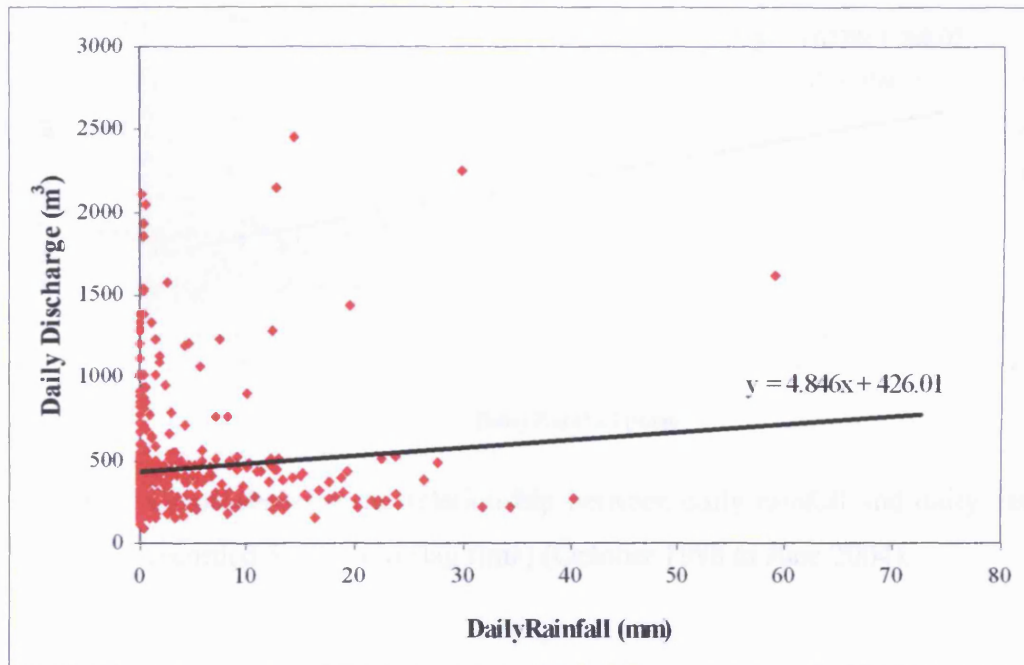


Figure 5.34 Graph showing the relationship between daily rainfall and daily discharge (October 1998 to June 2004).

The natural logarithms of the discharge is plotted against the rainfall (Fig. 5.36). The natural logarithms of the discharge has been moved back by 5 days (i.e. compared with rainfall recorded 5 days before the discharge measurement). A Pearson coefficient of 0.16 is obtained, which represents a very weak correlation. This is a weaker correlation than comparing the unadjusted daily discharge. The general trend is that as the rainfall increases the discharge increases, which would be expected.

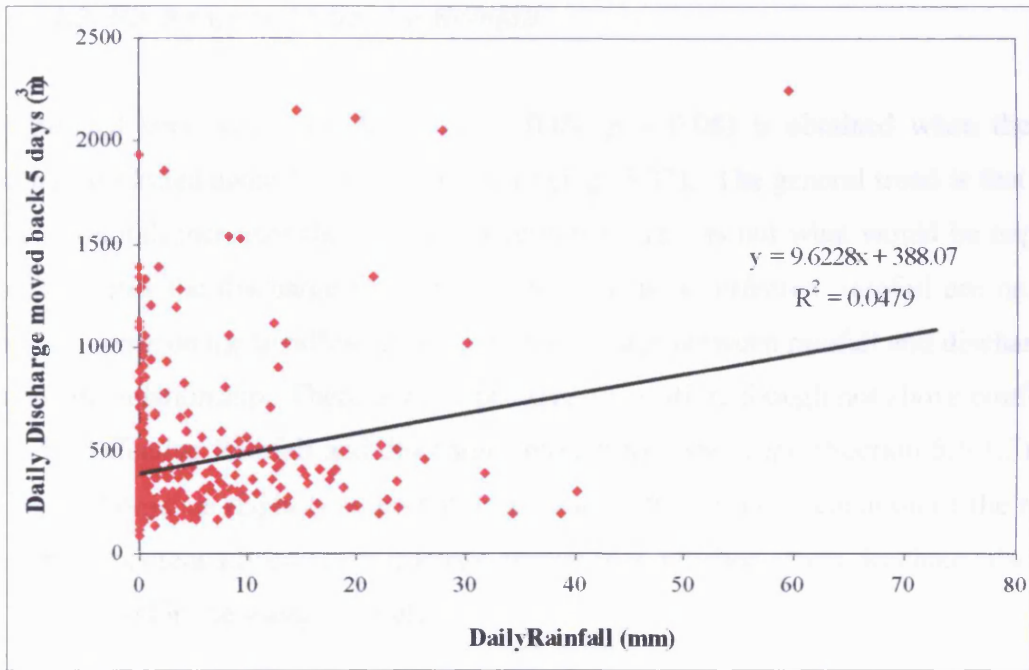


Figure 5.35 Graph showing the relationship between daily rainfall and daily discharge recorded 5 days ago (lag time) (October 1998 to June 2004).

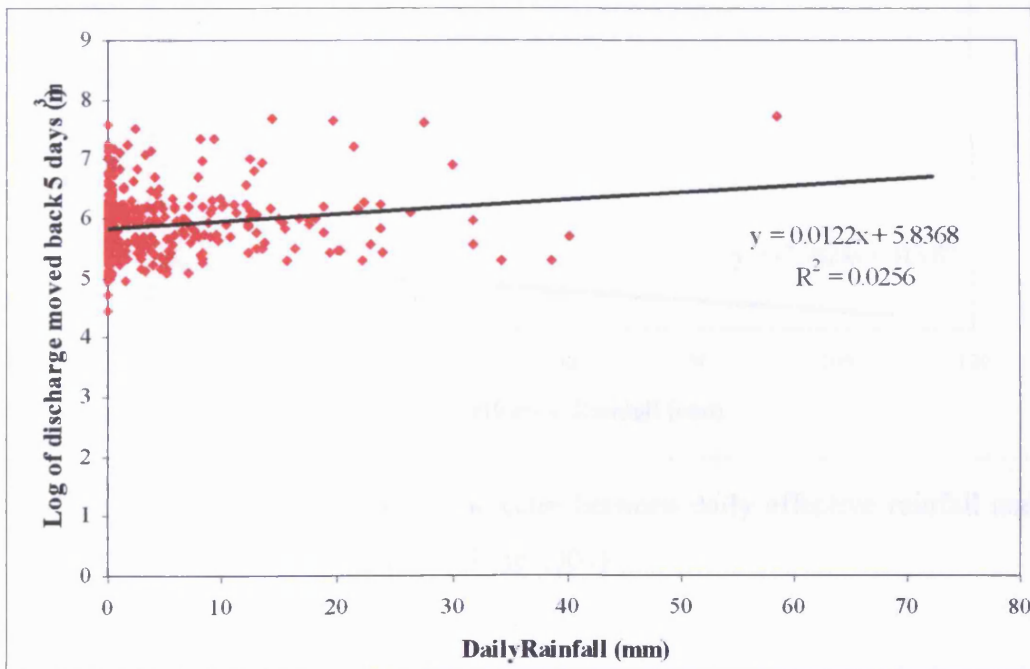


Figure 5.36 Graph showing the relationship between daily rainfall and the natural logarithms of daily discharge recorded 5 days ago (lag time) (October 1998 to June 2004).

5.5.1.4.1.2 Discharge and Effective Rainfall

A significant very weak correlation ($r = -0.09$, $p = 0.08$) is obtained when the daily discharge is plotted against Effective Rainfall (Fig. 5.37). The general trend is that as the effective rainfall increases the discharge decreases. This is not what would be expected. It is likely that the discharge readings when there is no effective rainfall are having a strong influence on the trendline, and the effects of lags between rainfall and discharge are masking the relationship. There is weak positive correlation, though not above confidence limits for Effective Rainfall and discharge through the BSC Pipe (Section 5.5.1.3) when lagged by 7 days, as might be expected as a result of the strong attenuation of the rainfall signal by the potentially complex leachate system (e.g. perched levels, leachate adsorption and storage within the waste mass etc.).

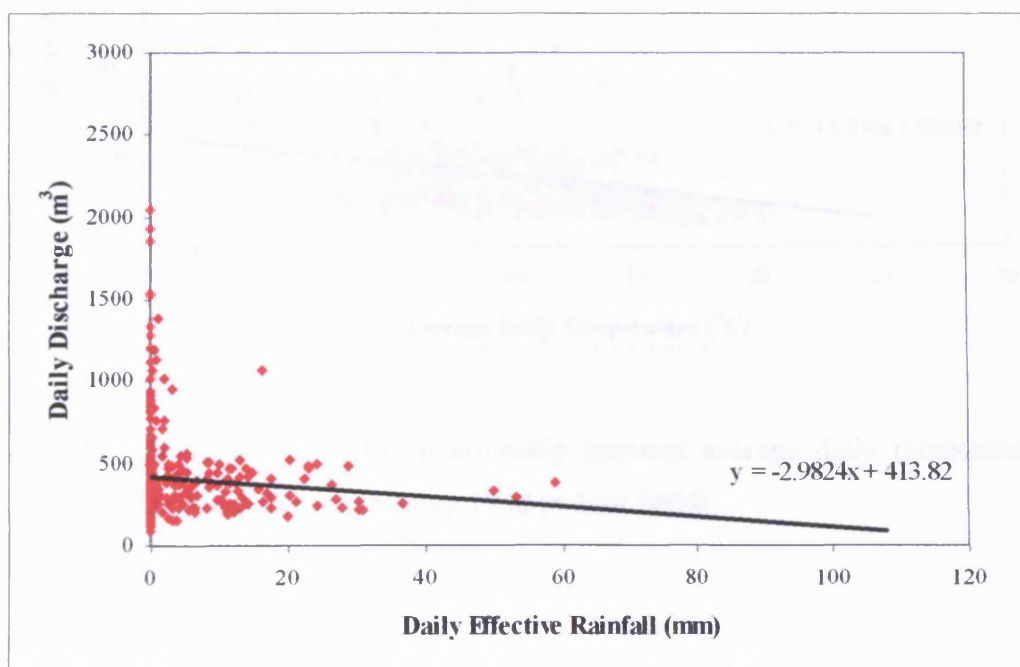


Figure 5.37 Graph showing the relationship between daily effective rainfall and daily discharge (April 2000 to June 2004).

5.5.1.4.1.3 Discharge and Temperature

A significant ($p = 0.00$) weak correlation of -0.26 is obtained when the daily discharge is plotted against the average daily temperature (Fig. 5.38). The general trend is that as the average temperature increases the discharge decreases. This is what would be expected since higher temperatures would promote increased evaporation.

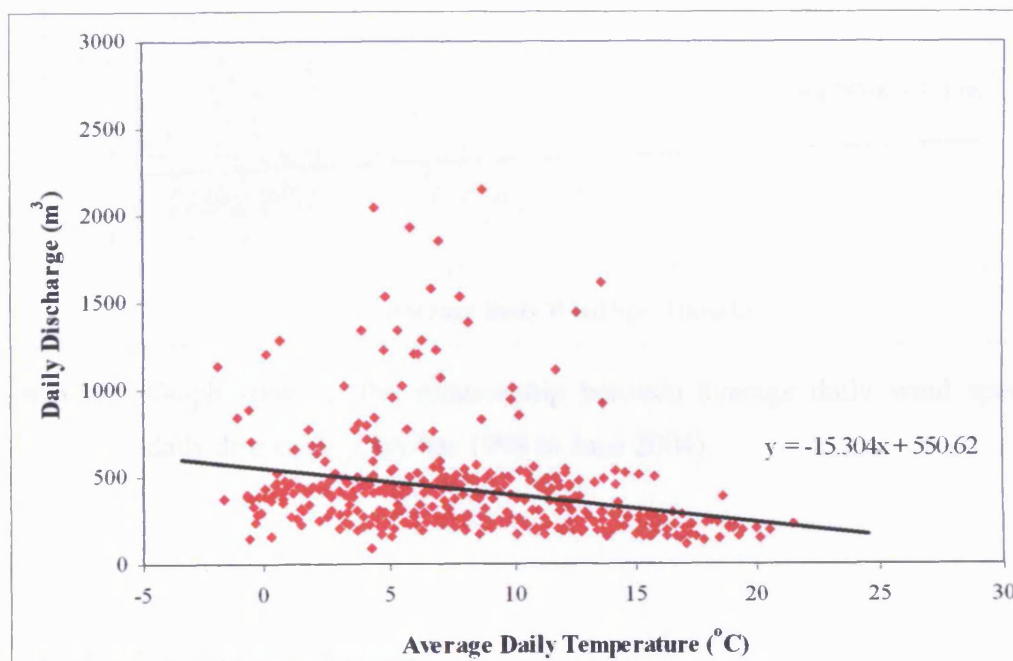


Figure 5.38 Graph showing the relationship between average daily temperature and daily discharge (October 1998 to June 2004).

5.5.1.4.1.4 Discharge and Average wind speed

A significant ($p = 0.03$) very weak correlation of 0.11 is obtained when the daily discharge is plotted against the average daily wind speed (Fig. 5.39). The general trend is that as the average daily wind speed increases the discharge increases. It is likely that this relationship is linked to the weather since periods of higher wind speeds are often associated with periods of rainfall.

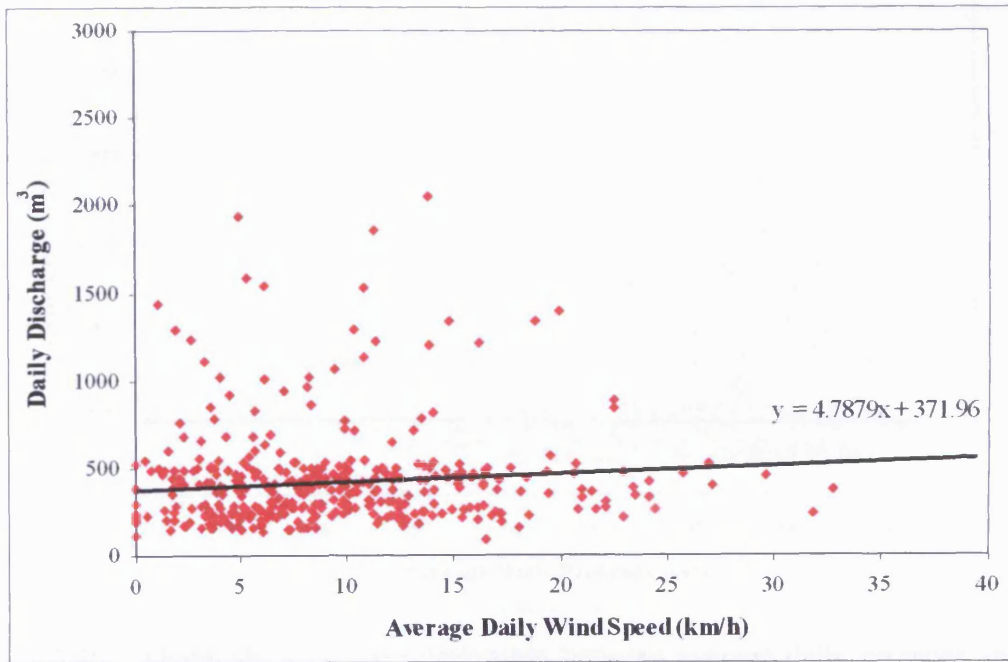


Figure 5.39 Graph showing the relationship between average daily wind speed and daily discharge (October 1998 to June 2004).

5.5.1.4.1.5 Discharge and Pressure

No correlation ($r = -0.01$, $p = 0.83$) is obtained when the daily discharge is plotted against the average daily pressure (Fig. 5.40). Horizontal lines do not represent a relationship between two variables.

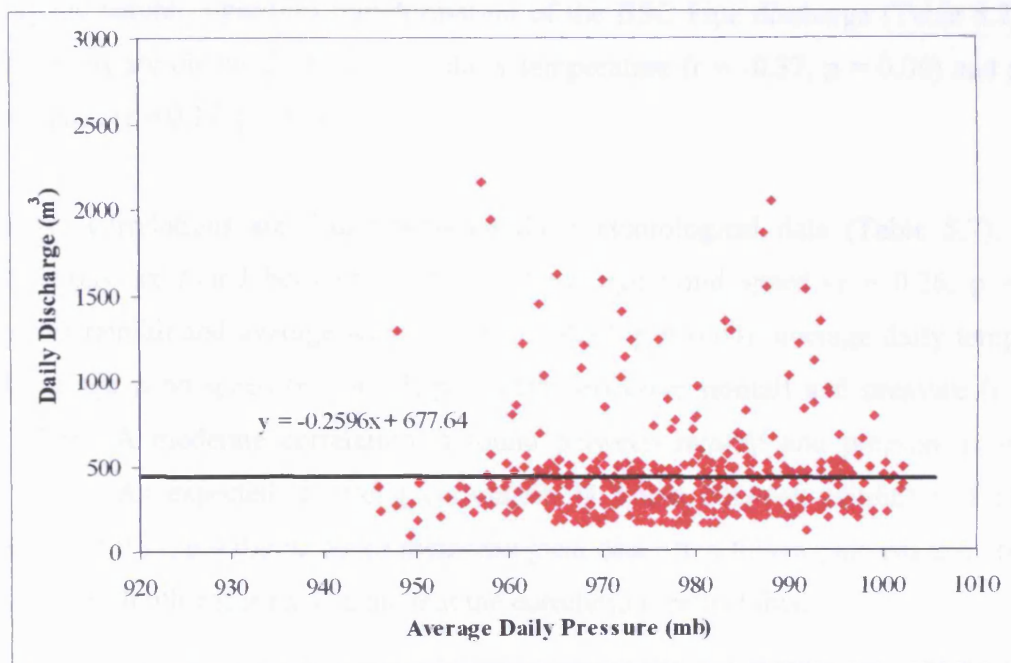


Figure 5.40 Graph showing the relationship between average daily pressure and daily discharge (October 1998 to June 2004).

5.5.1.4.1.6 Summary

Table 5.7 provides a summary of bivariate analysis. As well as the correlations described above it provides correlation coefficients and significance for the natural logarithms of the discharge and the meteorological data compared against each other.

The strongest correlation with the discharge through the BSC Pipe is with average daily temperature ($r = -0.26$, $p = 0.00$). On a scale of correlation (Fig. 5.31) this is only considered as a weak correlation.

A lag time of 5 days was suggested by comparing the rainfall and discharge at different lag intervals (Section 5.5.1.3). A very weak correlation ($r = 0.09$) is obtained between discharge and rainfall when there is no lag. However, this increases to $r = 0.22$ when a lag of 5 days is considered.

Using the natural logarithm transformation of the BSC Pipe discharge (Table 5.7) better correlations are obtained for average daily temperature ($r = -0.37$, $p = 0.00$) and average wind speed ($r = 0.17$, $p = 0.00$).

Stronger correlations are found between the meteorological data (Table 5.7). Weak correlations are found between rainfall and average wind speed ($r = 0.26$, $p = 0.00$); effective rainfall and average wind speed ($r = 0.30$, $p = 0.00$); average daily temperature and average wind speed ($r = -0.35$, $p = 0.00$); effective rainfall and pressure ($r = 0.35$, $p = 0.00$). A moderate correlation is found between rainfall and pressure ($r = -0.46$, $p = 0.00$). As expected, a strong correlation is found between rainfall and effective rainfall ($r = 0.71$, $p = 0.00$). Since meteorological data often follow patterns and are partly linked to each other it is reasonable that the correlations reflect this.

The bivariate analysis does not give a good predictive tool for discharge through the BSC Pipe. This is due to the complexity of the system within the landfill. It is also possible that preferential water movement paths only operate under certain conditions e.g. rainfall inputs, water table levels.

		Daily BSC Pipe discharge	Natural Logarithm of Daily BSC Pipe discharge	Average daily temperature	Daily rainfall	Average daily pressure	Daily Effective Rainfall	Average wind speed	BSC discharge moved back by 5 days (lag time)
Daily BSC Pipe discharge	Pearson Correlation	1	.92**	-.26**	0.09	-0.01	-0.09	.11*	.60**
	Significance	.	0.00	0.00	0.05	0.83	0.08	0.03	0.00
	N	472	472	415	431	415	390	410	450
Natural Logarithm of Daily BSC Pipe discharge	Pearson Correlation	.92**	1	-.37**	0.06	0.03	-0.05	.17**	.59**
	Significance	0.00	.	0.00	0.29	0.60	0.34	0.00	0.00
	N	472	472	415	431	415	390	410	450
Average daily temperature	Pearson Correlation	-.26**	-.37**	1	-.07**	.11**	-.14**	-.35**	-.19**
	Significance	0.00	0.00	.	0.00	0.00	0.00	0.00	0.00
	N	415	415	1931	1931	1930	1447	1815	414
Daily rainfall	Pearson Correlation	0.09	0.06	-.07**	1	-.46**	.71**	.26**	.22**
	Significance	0.05	0.29	0.00	.	0.00	0.00	0.00	0.00
	N	431	431	1931	1973	1930	1473	1815	429
Average daily pressure	Pearson Correlation	-0.01	0.03	.11**	-.46**	1	-.35**	-.15**	0
	Significance	0.83	0.60	0.00	0.00	.	0.00	0.00	0.97
	N	415	415	1930	1930	1930	1446	1814	414
Daily Effective Rainfall	Pearson Correlation	-0.09	-0.05	-.14**	.71**	-.35**	1	.30**	0.07
	Significance	0.08	0.34	0.00	0.00	0.00	.	0.00	0.15
	N	390	390	1447	1473	1446	1522	1447	395
Average wind speed	Pearson Correlation	.11*	.17**	-.35**	.26**	-.15**	.30**	1	.11*
	Significance	0.03	0.00	0.00	0.00	0.00	0.00	.	0.03
	N	410	410	1815	1815	1814	1447	1815	409
BSC discharge moved back by 5 days (lag time)	Pearson Correlation	.60**	.59**	-.19**	.22**	0	0.07	.11*	1
	Significance	0.00	0.00	0.00	0.00	0.97	0.15	0.03	-
	N	450	450	414	429	414	395	409	467

** Correlation is significant at the 0.01 level

* Correlation is significant at the 0.05 level

Table 5.7 Table of correlations for the BSC Pipe discharge and meteorological data.

5.5.1.4.2 Multiple Regression

In multiple regression, the values of one variable (the dependent variable, y) are estimated from those of two or more other variables (the independent variables, x_1, x_2, \dots, x_p). This is achieved by the construction of a linear multiple regression equation:

$$y' = b_0 + b_1(x_1) + b_2(x_2) + \dots + b_p(x_p) \quad (36)$$

where

b_1, b_2, \dots, b_p = partial regression coefficients

b_0 = regression constant (intercept)

The package SPSS can be used to perform multiple regression analysis. The multiple regression is set up so that the discharge through the BSC Pipe is the dependent variable and rainfall, average daily temperature, average daily wind speed and pressure are the independent variables. Since the best correlation between the discharge and the rainfall is with a lag of 5 days, rainfall readings moved on by 5 days will be used in the calculations.

Effective Rainfall has not been included due to its strong correlation with daily rainfall, which represents a similar variable. Collinearity, where the correlations among the independent variables are high, is undesirable. Rainfall gave the better correlation of the two when considering correlation with the discharge (Section 5.5.1.3). Adding Effective Rainfall into the analysis does not have a significant effect on the R value obtained. Again due to the precision in the original data, coefficients will only be quoted to the nearest two decimal places although SPSS quotes to three decimal places.

5.5.1.4.2.1 Simultaneous Multiple Regression

SPSS is used to perform simultaneous multiple regression. In simultaneous multiple regression all the available independent variables are entered in the equation directly.

SPSS produces a table of correlations (Table 5.8) for the data. There are 397 days (N) where there are complete data for all the variables between October 1998 and June 2004.

Due to this difference in sample, different correlation coefficients are obtained here than in the simple regression analysis (Section 5.5.1.4.1). The table also shows that the dependent variable BSC Pipe discharge correlates significantly with average daily temperature.

	BSC Pipe discharge	
Pearson Correlation	BSC Pipe discharge	1
	Average daily temperature	-.31
	Average wind speed	.14
	Daily rainfall (5 day lag)	.11
	Pressure	.08
Significance	BSC Pipe discharge	.
	Average daily temperature	.00
	Average wind speed	.00
	Daily rainfall (5 day lag)	.01
	Pressure	.07
N	397	

Table 5.8 Table of correlations for simultaneous multiple regression for discharge through the BSC Pipe.

For this model, the multiple correlation coefficient (R) is 0.33 (Table 5.9). The adjusted R square value, the estimate of the proportion of variance accounted for by the regression, is 0.10, i.e. 10%. For the coefficient for individual variables (Table 5.8), the best correlation coefficient was -0.31 for average daily temperature, so adding more independent variables has improved the predictive power of the regression equation.

Model	R	R Square	Adjusted R Square	Std. Error of the Estimate
1	.33	.11	.10	250.72

Table 5.9 Table giving the value of R for simultaneous multiple regression for discharge through the BSC Pipe.

Using the outputs (column B) in Table 5.10, it is possible to construct the multiple regression equation of BSC Pipe discharge (*BSC*) from average daily temperature (*temp*), average wind speed (*wind*), daily rainfall with 5 day lay (*rain*) and pressure (*mb*) as:

$$BSC' = -1230.71 + -14.42(temp) + 1.97(wind) + 4.42(rain) + 1.76(mb) \quad (37)$$

where *BSC'* is the predicted BSC Pipe discharge.

Model	Unstandardised Coefficients		Standardized Coefficients	t	Significance
	B	Std. Error	Beta		
1 (Constant)	-1230.71	1067.50		-1.15	.25
Average daily temperature	-14.42	2.67	-.28	-5.40	.00
Average wind speed	1.97	2.21	.05	.89	.37
Daily rainfall (5 day lag)	4.42	1.95	.11	2.27	.02
Pressure	1.76	1.08	.08	1.62	.11

Table 5.10 The regression equation and associated statistics for simultaneous multiple regression for discharge through the BSC Pipe.

The beta coefficients (column headed Beta in Table 5.10) give the number of standard deviations change on the dependent variable that will be produced by a change of one standard deviation on the independent variable concerned. For these data, the average daily temperature makes the greatest contribution. This results in the predicted cyclicity in leachate discharge, with highest flows in winter and lowest flows in summer (Fig. 5.41). The actual data shows significant short-term fluctuations that cannot be modelled using this simple multiple regression based approach (Fig. 5.42).

A Root Mean Squared Error (RMSE) of 255 is obtained for the 381 days with recorded and predicted discharge for the BSC Pipe between 1 April 2000 and 22 June 2004. Considering the mean recorded discharge for the same period is 388 m³ per day, this is a large error.

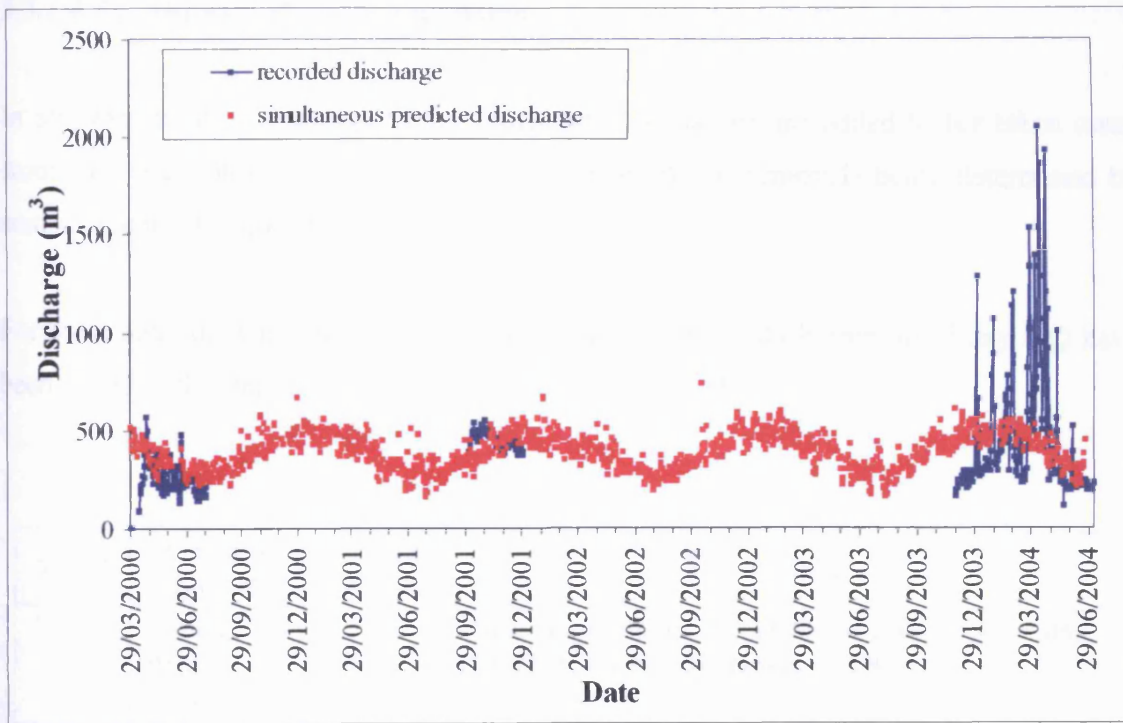


Figure 5.41 Graph showing the recorded and predicted discharge through the BSC Pipe using simultaneous regression.

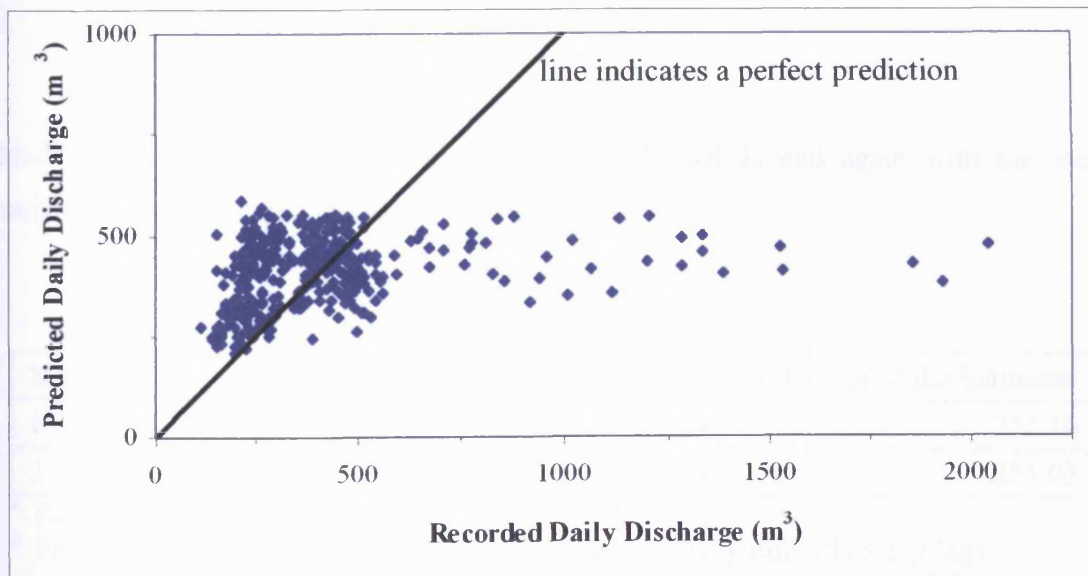


Figure 5.42 Graph showing the recorded against the predicted discharge through the BSC Pipe using simultaneous regression.

5.5.1.4.2.2 Stepwise Multiple Regression

In stepwise multiple regression, the independent variables are added to (or taken away from) the equation one at a time, the order of entry (or removal) being determined by statistical considerations (Kinnear & Gray, 2000).

For these data, the variables average daily temperature and daily rainfall (5 day lag) have been added to the stepwise multiple regression (Table 5.11).

Model	Variables Entered	Variables Removed	Method
1	Average daily temperature	.	Stepwise (Criteria: Probability-of-F-to-enter \leq .050, Probability-of-F-to-remove \geq .100).
2	Daily rainfall (5 day lag)	.	Stepwise (Criteria: Probability-of-F-to-enter \leq .050, Probability-of-F-to-remove \geq .100).

Table 5.11 List of variables entered into the stepwise multiple regression for discharge through the BSC Pipe.

Models are run with the first variable entered (Model 1) and again with the second variable added to the first (Model 2) (Table 5.12).

Model	R	R Square	Adjusted R Square	Std. Error of the Estimate
1	.31 ^a	.09	.09	252.16
2	.32 ^b	.10	.10	251.03

^a Predictors: (Constant), average daily temperature

^b Predictors: (Constant), average daily temperature, Daily rainfall (5 day lag)

Table 5.12 Value of R and associated statistics for each model in the stepwise multiple regression for discharge through the BSC Pipe.

The value of R for Model 2 (0.32) (Table 5.12) is smaller than the value (0.33) given for the simultaneous regression of BSC Pipe discharge upon average daily temperature, average wind speed, daily rainfall and pressure but only slightly so. This shows the lack of predictive value of the excluded variables (average wind speed and pressure).

Using the outputs (column B) in Table 5.13, it is possible to construct the multiple regression equation of BSC Pipe discharge (BSC) from average daily temperature ($temp$), and daily rainfall ($rain$) as:

$$BSC' = 517.47 + -15.55(temp) + 4.14(rain) \quad (38)$$

where BSC' is the predicted BSC Pipe discharge. Since the increment in R with the inclusion of the remaining variables (average wind speed and pressure) does not reach the necessary criterion for the stepwise program, these variables are excluded from the final equation.

Model	Unstandardised Coefficients		Standardized Coefficients	t	Significance
	B	Std. Error	Beta		
1 (Constant)	534.77	24.23		22.07	.00
Average daily temperature	-15.77	2.48	-.31	-6.36	.00
2 (Constant)	517.47	25.44		20.34	.00
Average daily temperature	-15.55	2.47	-.30	-6.30	.00
Daily rainfall (5 day lag)	4.14	1.94	.10	2.14	.03

Table 5.13 The regression coefficients for the single variable (Model 1) and the two variables (Model 2) remaining in the stepwise regression analysis.

Table 5.14 details the variables excluded from the stepwise regression analysis. Beta In is the standardised regression coefficient that would result if the variable were entered into the equation at the next step. The t -test is a test of significance of the regression coefficient. Partial correlation is the correlation that remains between two variables after removing the correlation that is due to their mutual association with the other variables. Collinearity is the undesirable situation where the correlations among the independent variables are high. Collinearity can be detected by the Tolerance statistic, which is the

proportion of a variable's variance not accounted for by the other independent variables in the equation. A variable with very low tolerance contributes little information to a model (Kinnear & Gray, 2000).

Model	Beta In	t	Significance	Partial Correlation	Collinearity Statistics
					Tolerance
1 Average wind speed	.03 ^a	.63	.53	.03	.87
Daily rainfall (5 day lag)	.10 ^a	2.14	.03	.11	1.00
Pressure	.06 ^a	1.23	.22	.06	1.00
2 Average wind speed	.03 ^b	.57	.57	.03	.87
Pressure	.07 ^b	1.47	.14	.07	.99

^a Predictors in the Model: (Constant), average daily temperature

^b Predictors in the Model: (Constant), average daily temperature, Daily rainfall (5 day lag)

Table 5.14 The variables excluded from the stepwise regression analysis.

Again, the low adjusted *R* square value suggests that the multiple regression model predicts a relatively low percentage of variation within the data set. The influence of temperature is again clearly demonstrated, with the predicted cyclicity in discharge mirroring that predicted by the simultaneous multiple regression analysis (Fig. 5.43). The large excursions in the real data marking short-term fluctuations in discharge cannot be modelled here (Fig. 5.44). The dataset available for leachate discharge from the BSC pipe contains too many gaps to conclusively validate the annual cycles in leachate discharge predicted by the multiple-regression based models. However what data are available (especially that for 2003-4) does suggest higher winter discharges, and that the model prediction is not equivalent to a low flow (base flow) component of the system, but rather an approximate average between the short duration higher values and the recorded low "base flow" values.

A Root Mean Squared Error (RMSE) of 256 is obtained for the 381 days with recorded and predicted discharge for the BSC Pipe between 1 April 2000 and 22 June 2004. Considering the mean recorded discharge for the same period is 388 m³ per day, this is a large error.

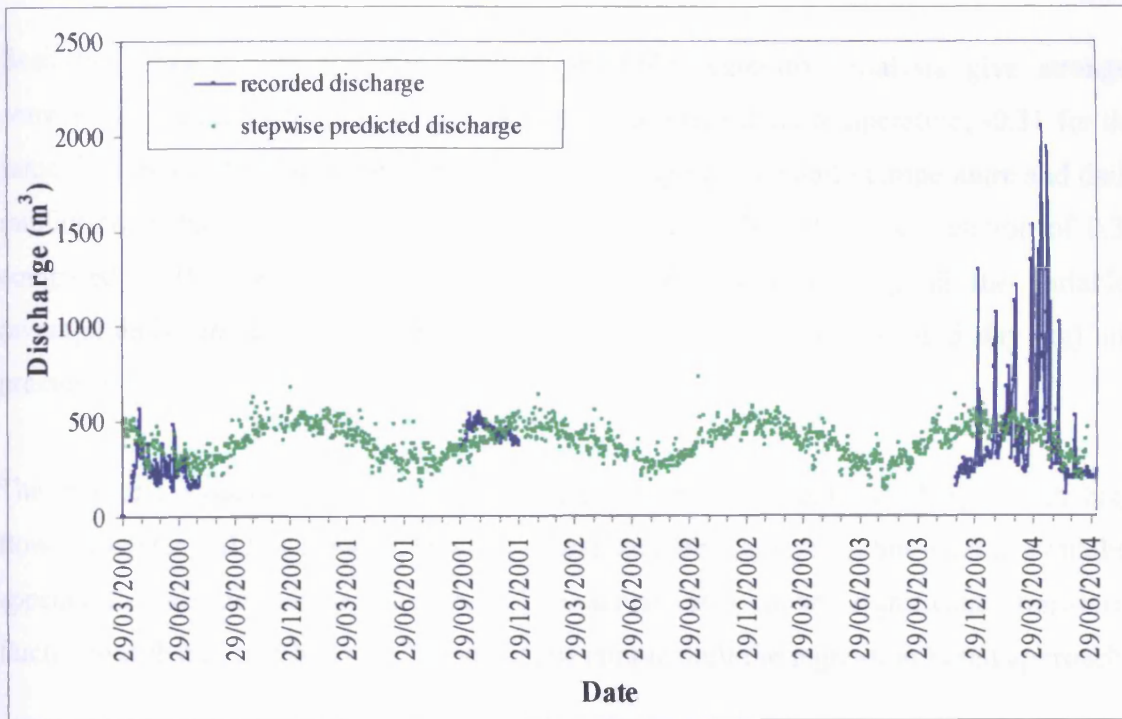


Figure 5.43 Graph showing the recorded and predicted discharge through the BSC Pipe using stepwise regression.

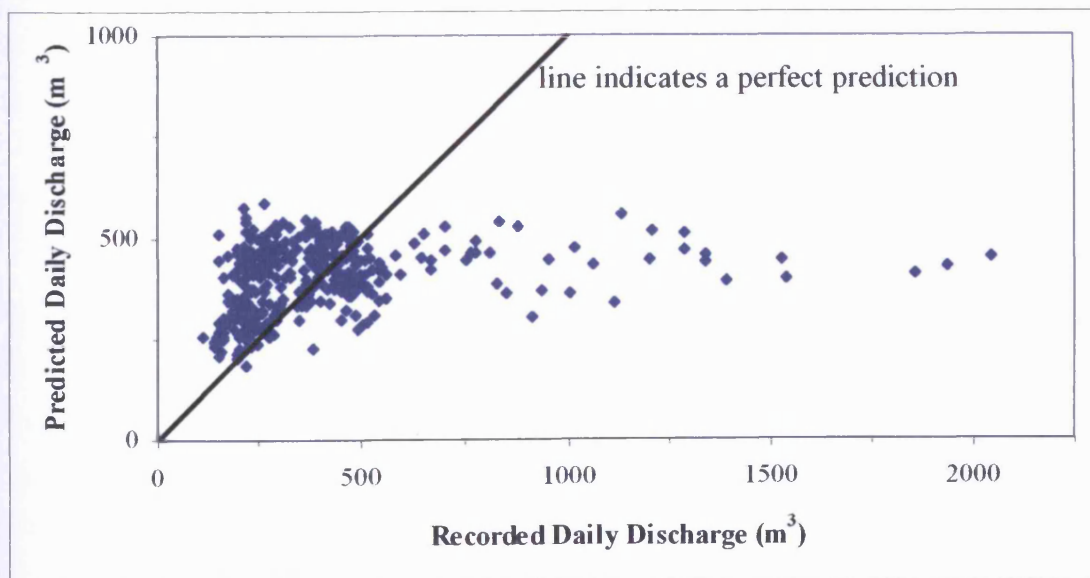


Figure 5.44 Graph showing the recorded against the predicted discharge through the Settlement Tank using stepwise regression.

5.5.1.4.2.3 Summary

Both the simultaneous and the stepwise multiple regression analysis give stronger correlations than the strongest single correlation (average daily temperature, -0.31 for the same data as the multiple regression analysis). Using average daily temperature and daily rainfall (with the 5 day lag) the stepwise regression analysis has a correlation of 0.32 compared to 0.33 with the simultaneous regression analysis using all the variables (average daily temperature, average wind speed, daily rainfall (with the 5 day lag) and pressure).

The resulting models both show seasonal fluctuation in leachate discharge, with high flows in winter and low flows in summer. Real data are inadequate, but what is available appears to validate this conclusion. The actual data shows significant short-term fluctuations that cannot be modelled using this simple multiple regression based approach.

5.5.2 SETTLEMENT TANK

5.5.2.1 Discharge

In analysing the discharge data, the flow rate (l/s) has been converted to discharge (m^3). Rolling totals were calculated for different time periods and the minimum value recorded, maximum value recorded, mean, standard deviation and median value were calculated for each time period (Table 5.15).

5.5.2.2 Discharge and Rainfall

Time Series for discharge through the Settlement Tank and rainfall are plotted for the period 28 November 2003 to 22 June 2004 (Fig. 5.45). This period was selected because there are few gaps in the data and the flow monitors had just been calibrated. Clearly the discharge is closely related to rainfall with an apparent lag time of one or two days. Input into the Settlement Tank includes runoff collected from the landfill and the data suggest that surface runoff predominates over leachate drainage in the total Settlement Tank discharge.

A similar relationship is shown when discharge is plotted with Effective Rainfall (Fig. 5.46) for the period between 28 November 2003 and 31 May 2004.

Figure 5.47, a cumulative graph for discharge through the Settlement Tank, rainfall and Effective Rainfall shows lower total and effective rainfall in the summer periods, when the cumulative curves are less steep, and, as expected, much higher rainfall (total and effective) in winter. The discharge rate from the Settlement Tank mirrors the rainfall and Effective Rainfall rates with the steepest section of the discharge curve occurring over the same period (winter) as the steepest sections of the rainfall and Effective Rainfall curves.

	15 mins	30 mins	1hr	2hrs	4hrs	6hrs	8hrs	12hrs	18hrs
Data points	97042	97031	97009	96965	96877	96789	96701	96525	96261
Min recorded	0	0	0	0	0	0	0	0	0
Max recorded	90	180	360	720	1440	1899.2	2001.1	2895.7	4250.9
Mean	10.2	20.3	40.6	81.2	162.4	243.7	324.9	487.3	731
Standard Deviation	6.4	12.7	25.3	50.3	99.6	148.2	196.2	290.5	429.5
Median	8.8	17.6	35.3	70.6	141.2	213.5	285.8	432.4	652.8

	24hrs	36hrs	48hrs	60hrs	72hrs	96hrs	120hrs	168hrs
Data points	95997	95516	95036	94556	94076	93116	92156	90236
Min recorded	50.9	157.1	238.2	310.6	402.4	571.8	771.2	1295.3
Max recorded	5604.3	8129.4	10783.3	13424.9	16001.1	21316.3	22730.4	24080
Mean	974.9	1463	1951.3	2439.9	2928.7	3906	4886.8	6806.2
Standard Deviation	567.2	839.6	1105.9	1367.9	1624.8	2126.2	2599.9	3513.7
Median	871.8	1316	1760.2	2214.2	2666.3	3564.4	4447.9	6311.2

Table 5.15 Discharge (m³) recorded in the Settlement Tank between October 1998 and July 2004 for different time scales

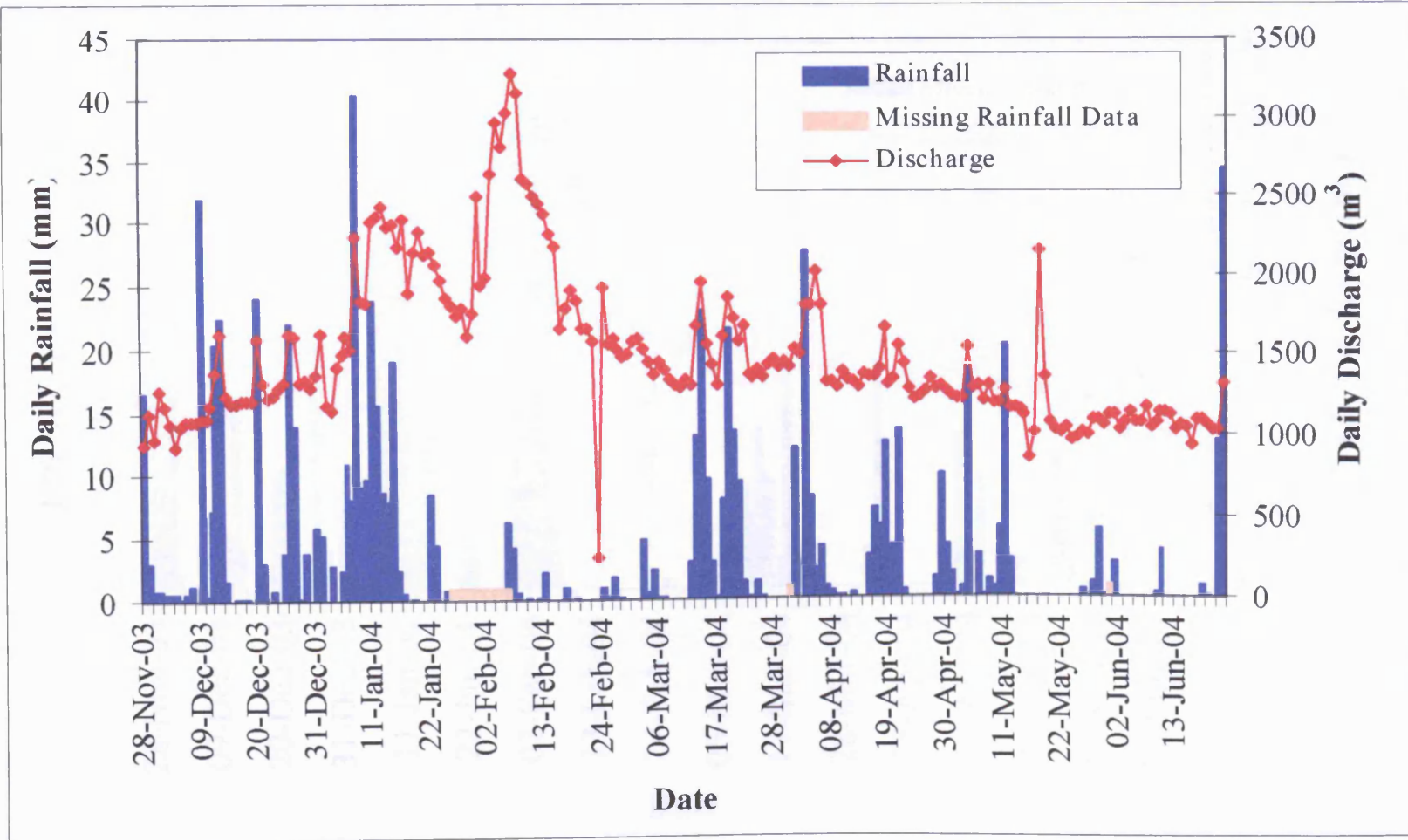


Figure 5.45 Graph showing discharge through the Settlement Tank and rainfall between 28 November 2003 and 22 June 2004.

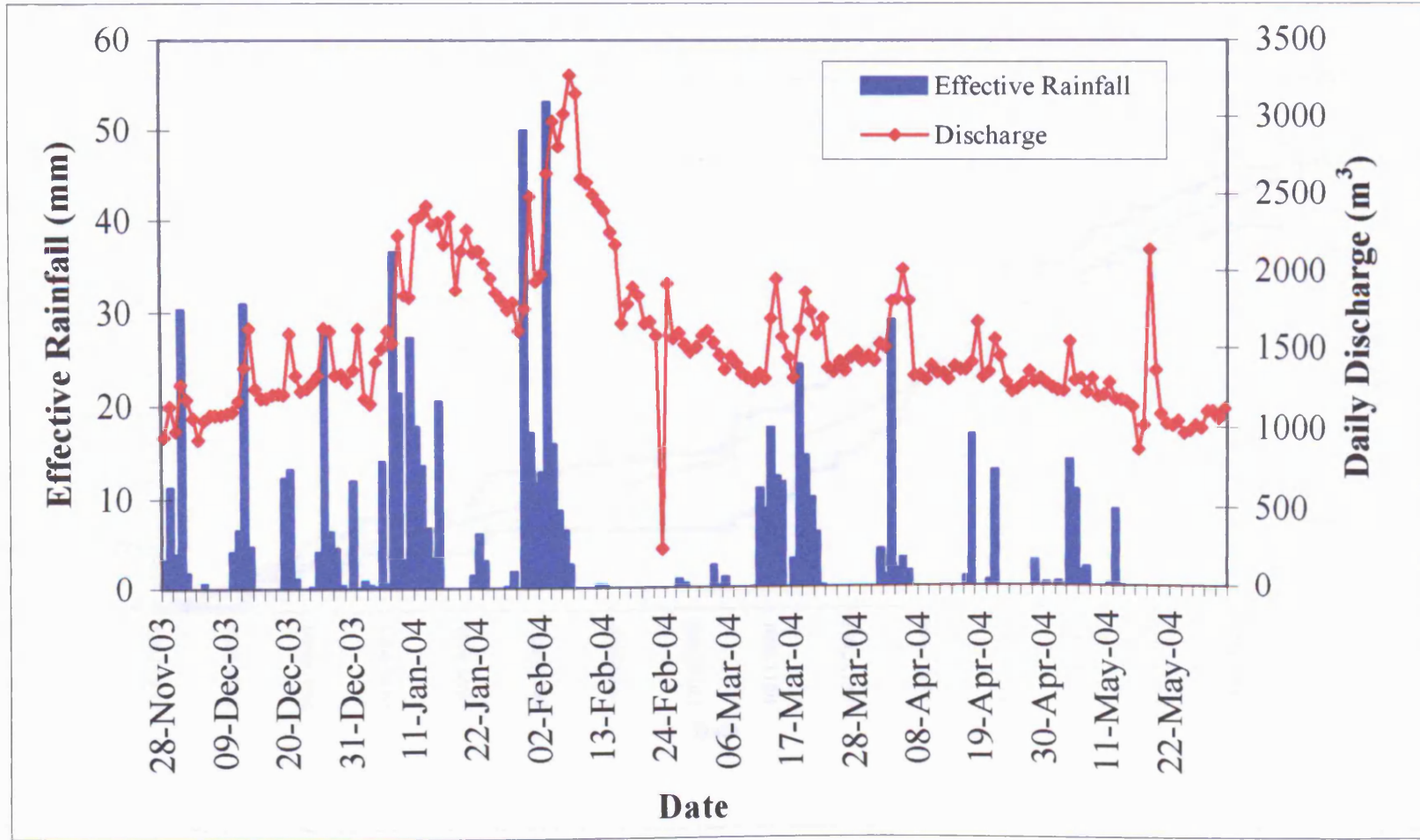


Figure 5.46 Graph showing discharge through the Settlement Tank and effective rainfall between 28 November 2003 and 31 May 2004.

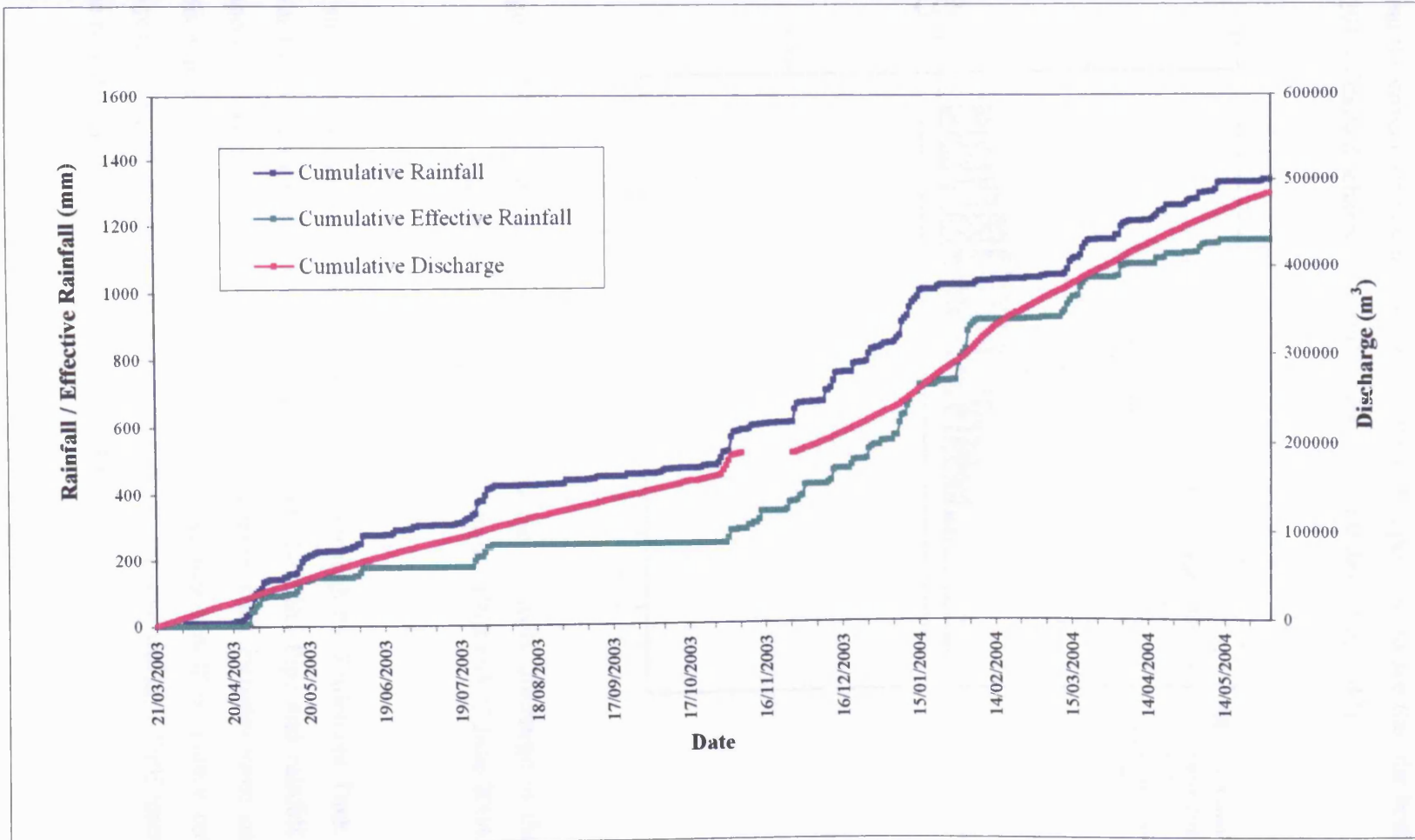


Figure 5.47 Cumulative graph showing discharge through the Settlement Tank, rainfall and Effective Rainfall between 9 May 2003 and 31 May 2004.

5.5.2.3 Lag Time

Using the cross-correlation function in SPSS, it is possible to see that the best correlation (0.291) of daily discharge and rainfall has a lag of 0 days (Fig. 5.47).

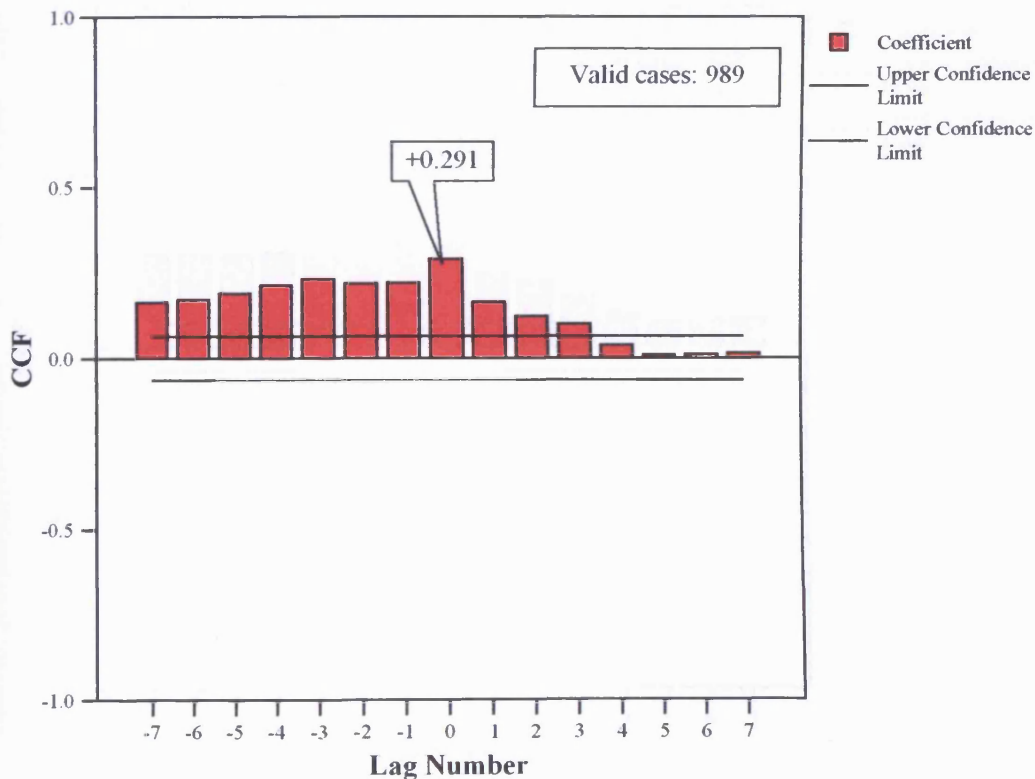


Figure 5.48 Chart showing the cross-correlation for daily discharge in the Settlement Tank with Rainfall between 21 October 1998 and 23 June 2004.

A stronger correlation is seen for the discharge through the Settlement Tank with rainfall than the correlation between discharge through the BSC Pipe and rainfall. This is as expected since the discharge through the Settlement Tank includes some surface runoff, which is a direct response to rainfall. Clearly, this runoff is mainly collected from impermeable, often smooth surfaces (engineered drainage works, HDPE liner etc.) so that the runoff is rapid, with no discernible lag time.

A slightly stronger correlation is obtained for daily discharge through the Settlement Tank and daily Effective Rainfall (Fig. 5.49). A slightly stronger correlation (0.307) is found for a lag of 1 day rather than a lag of 0 days (0.294), which was the strongest correlation for lag for the rainfall.

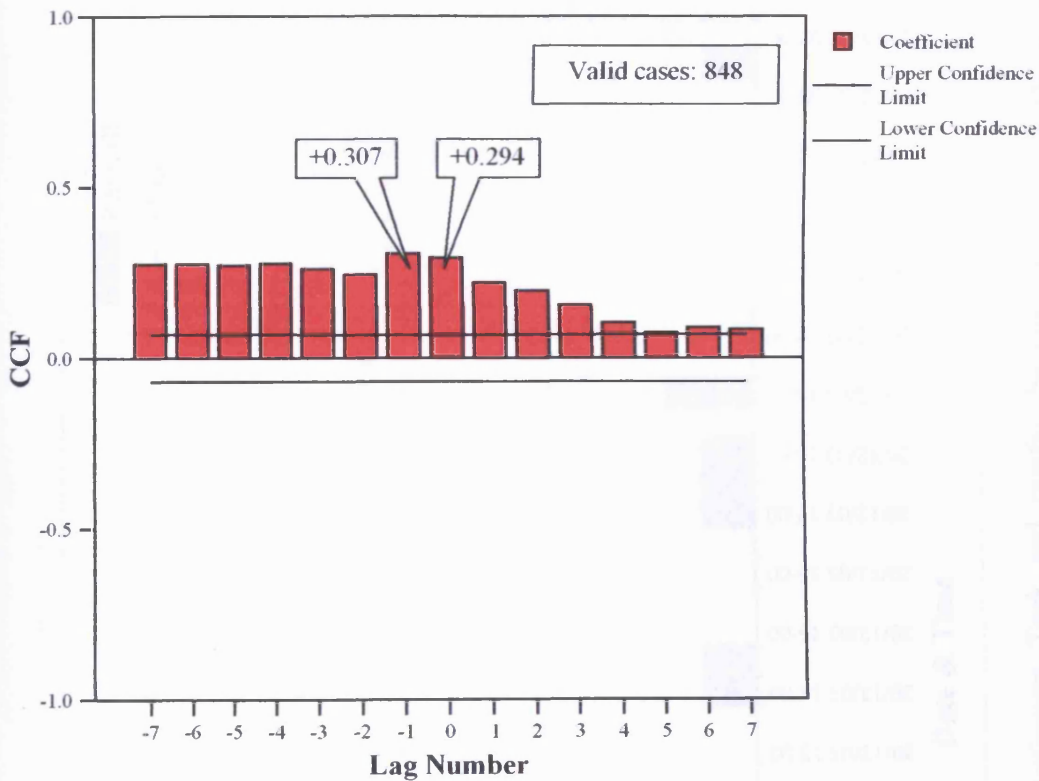


Figure 5.49 Chart showing the cross-correlation for daily discharge in the Settlement Tank with Effective Rainfall between 21 October 1998 and 23 June 2004.

Using the data for every 30 minutes the cross-correlation function in SPSS gives the best correlation (0.189) of half hourly discharge and rainfall with a lag of 3 intervals - one and a half hours (Fig. 5.50). This implies that the discharge shows a rapid response to rainfall events. This rapid response to rainfall is demonstrated by figure 5.51. It is likely that the rapid response is derived largely from surface runoff across the landfill that is collected by drainage ditches and enters the Settlement Tank.

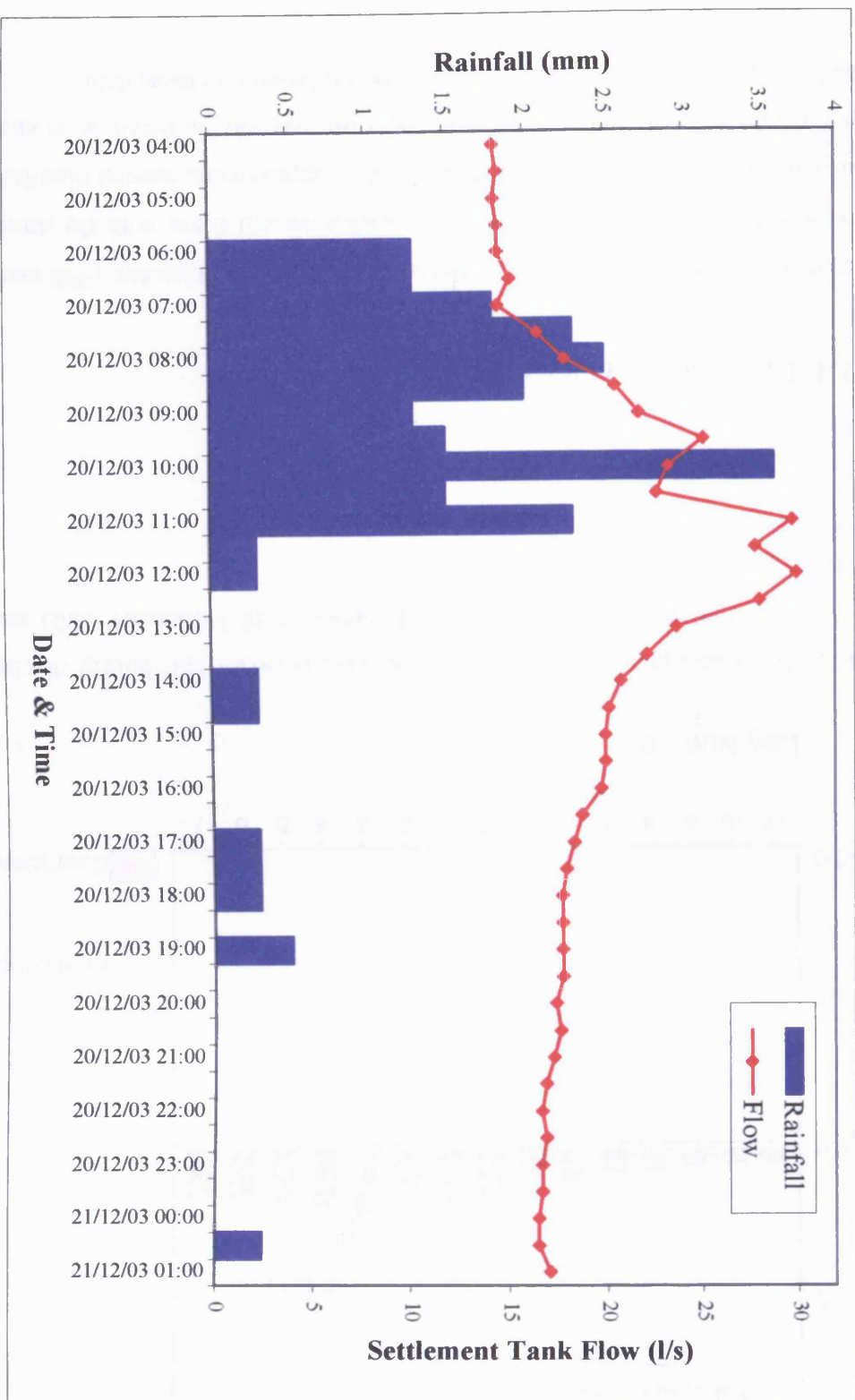


Figure 5.51 Graph showing discharge through the Settlement Tank and rainfall between 4am on 20 December 2003 and 1am on 21 December 2003.

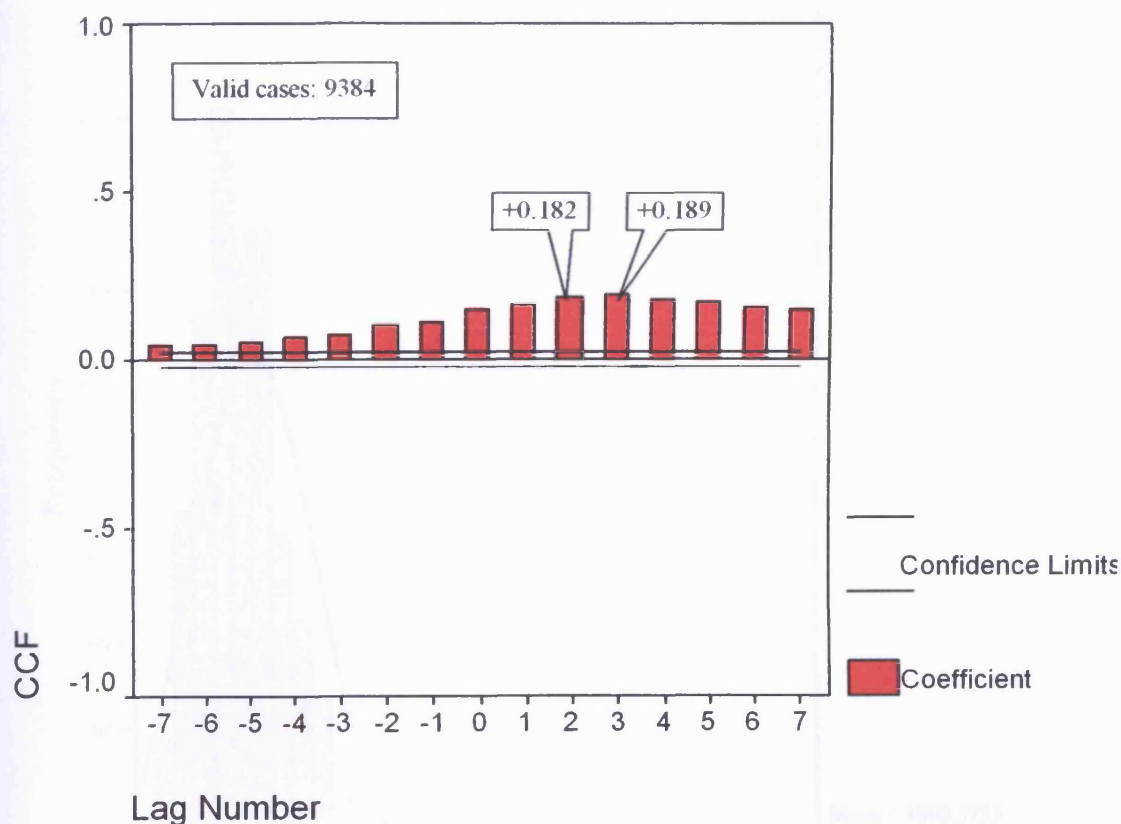


Figure 5.50 Chart showing the cross-correlation between half hourly discharge in the Settlement Tank and Rainfall between 28 November 2003 and 24 June 2004.

5.5.2.4 Regression Analysis

The discharge over the weir in the Settlement Tank between October 1998 and June 2004 has been plotted as a histogram (Fig. 5.52) with a normal curve with the same mean and variance as the discharge data. The data show an approximate normal distribution. Since the population size, N , is also large and therefore the sample mean, \bar{x} , is approximately normally distributed correlation analysis can be performed on these data.

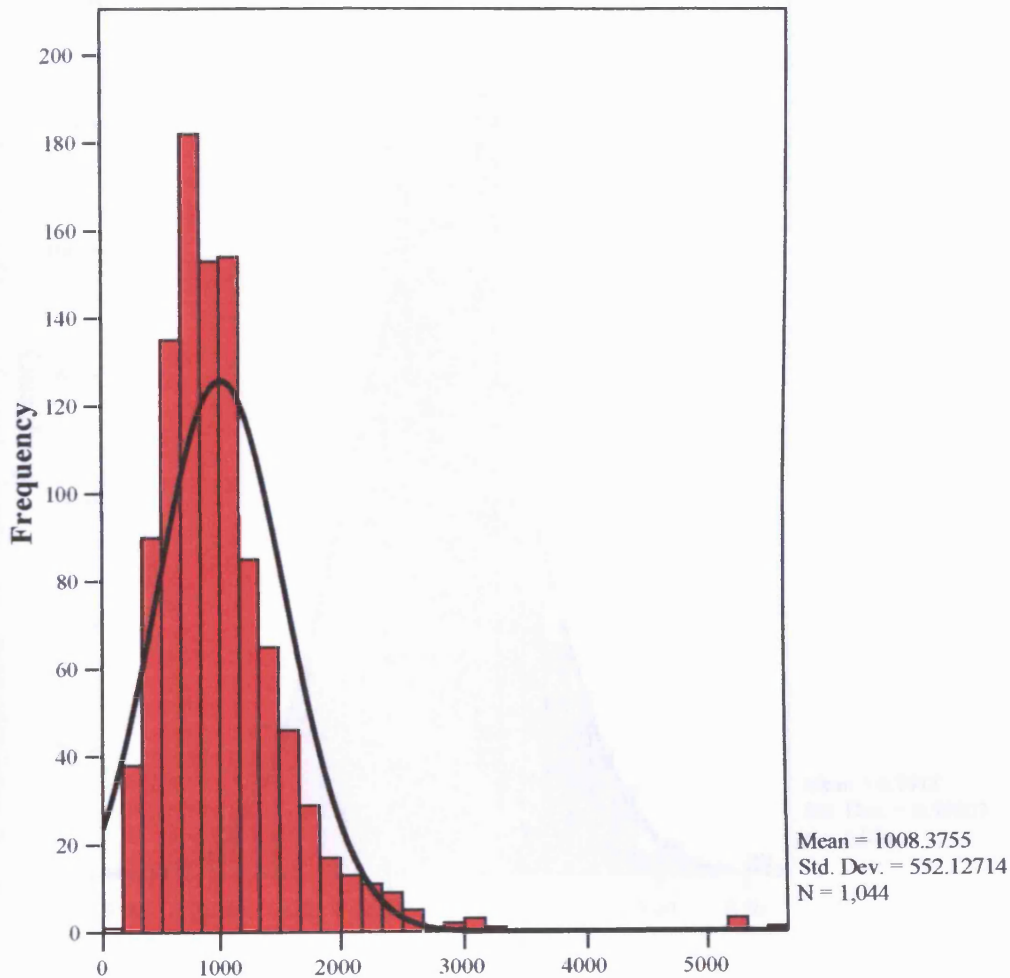


Figure 5.52 Graph showing the distribution of daily Settlement Tank discharge and a normal curve with the same mean and variance as the data.

Figure 5.53 shows that the distribution of the natural logarithms of the daily Settlement Tank discharge fit a normal distribution better than the raw discharge values. Correlation and regression analysis may therefore provide stronger relationships between the rainfall and the transformed discharge data.

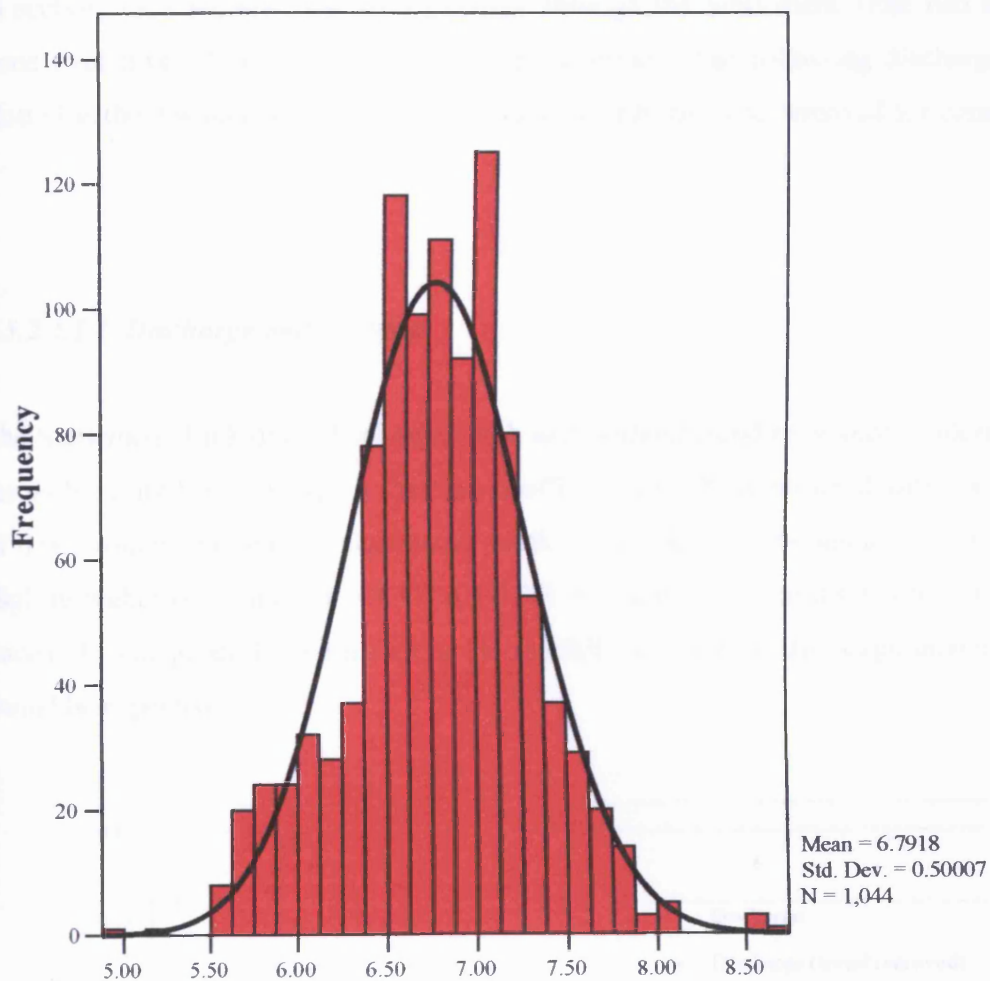


Figure 5.53 Graph showing the distribution of the natural logarithms of the daily Settlement Tank discharge and a normal curve with the same mean and variance as the data.

5.5.2.4.1 Simple, Two-Variable Regression

Again due to the precision in the original data, coefficients will only be quoted to the nearest two decimal places although SPSS quotes to three decimal places.

In section 5.4.2 we saw that the discharge through the Settlement Tank had an upward trend over time. It is possible to remove the trend. The following discharge data are plotted as the raw unadjusted discharge data and with the trend removed for comparison.

5.5.2.4.1.1 Discharge and Rainfall

The Settlement Tank daily discharge (with and without trend removed) is plotted against the daily rainfall (Fig. 5.54). A Pearson coefficient of 0.29 is obtained with a significance of 0.00, which represents a significant weak correlation for the unaltered discharge. A slightly higher correlation ($r = 0.31$, $p = 0.00$) is obtained for the discharge with the trend removed. The general trend is that as the rainfall increases the discharge increases, which would be expected.

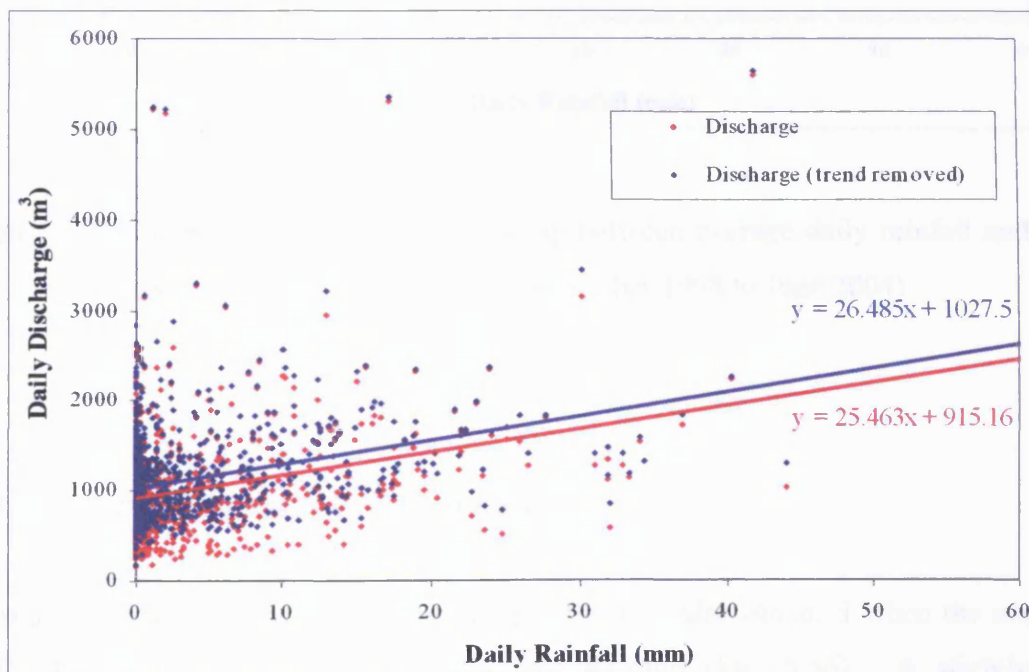


Figure 5.54 Graph showing the relationship between average daily rainfall and daily discharge (October 1998 to June 2004).

The natural logarithms of the discharge is plotted against the daily rainfall (Fig. 5.55). A Pearson coefficient of 0.27 is obtained, which represents a weak correlation slightly lower than that of the unadjusted daily discharge. The general trend is that as the rainfall increases the discharge increases, which would be expected.

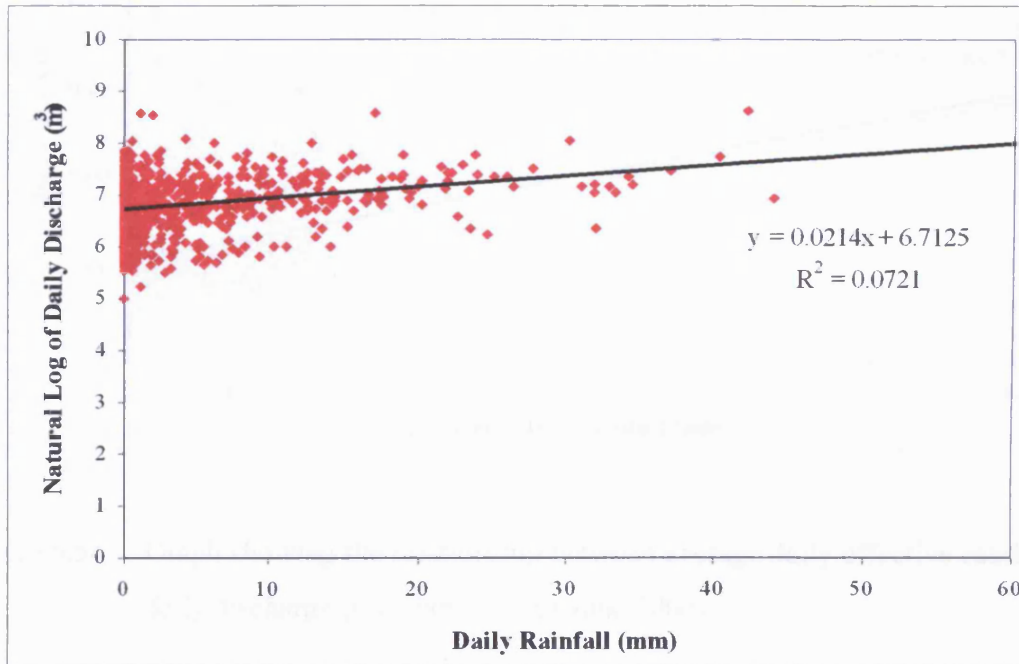


Figure 5.55 Graph showing the relationship between average daily rainfall and natural logarithms of daily discharge (October 1998 to June 2004).

5.5.2.4.1.2 Discharge and Effective Rainfall

A significant weak correlation ($r = 0.29$, $p = 0.00$) is also obtained when the unadjusted daily discharge is plotted against Effective Rainfall (Fig. 5.56). A slightly higher correlation ($r = 0.30$, $p = 0.00$) is obtained for the discharge with the trend removed. The general trend is that as the effective rainfall increases the discharge decreases, which is as expected.

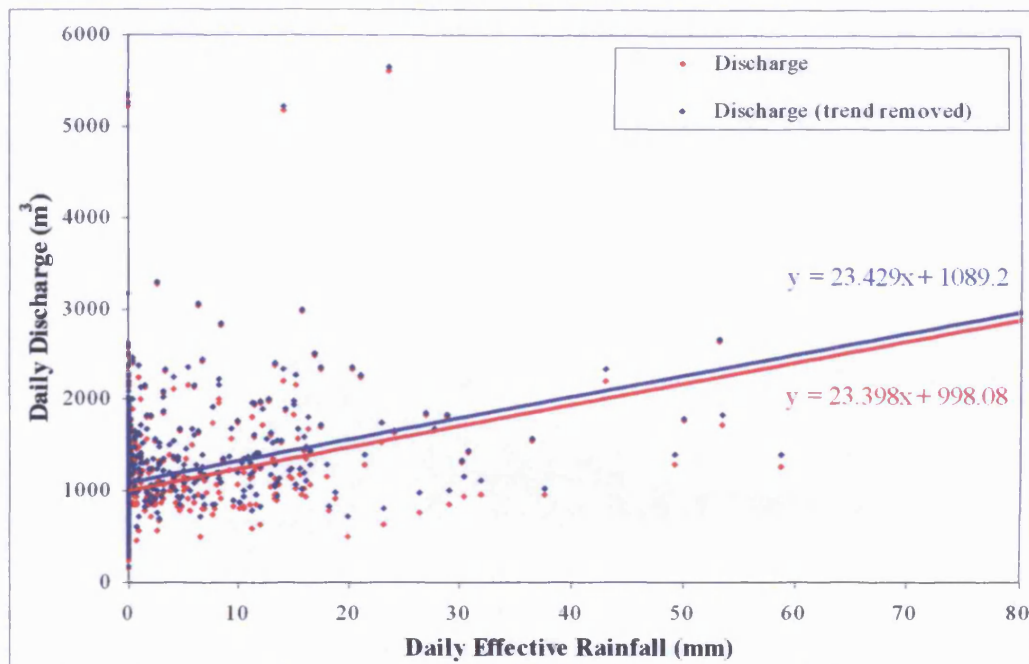


Figure 5.56 Graph showing the relationship between average daily effective rainfall and daily discharge (October 1998 to June 2004).

5.5.2.4.1.3 Discharge and Temperature

A significant weak correlation ($r = -0.25$, $p = 0.00$) is obtained when the unaltered daily discharge is plotted against the average daily temperature (Fig. 5.57). A slightly higher correlation ($r = -0.30$, $p = 0.00$) is obtained for the discharge with the trend removed. The general trend is that as the average temperature increases the discharge decreases. This is expected since higher temperatures are associated with dry sunny days in the summer when rainfall is low and evaporation is high.

Taking the summer period only, when the temperature is high and rainfall is generally low, a strong relationship can be seen between average temperature ($^{\circ}\text{C}$) and flow rate (l/s) recorded every 30 minutes. Figure 5.58, from May 2000 shows a typical period when the flow variation shows a strong diurnal relationship with the average temperature.

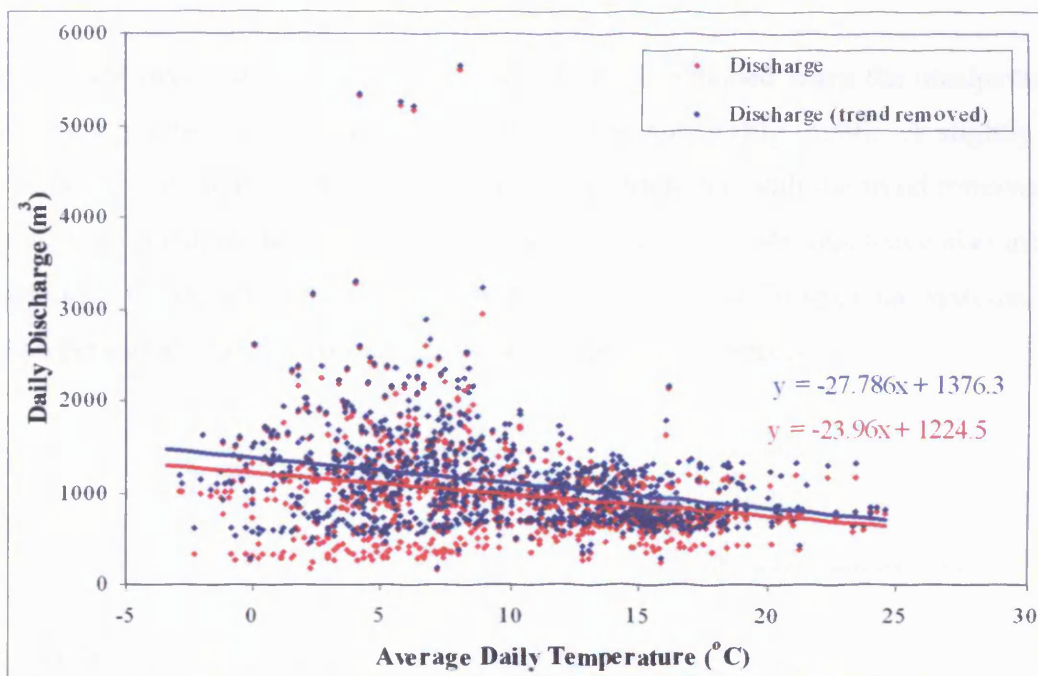


Figure 5.57 Graph showing the relationship between average daily temperature and daily discharge (October 1998 to June 2004).

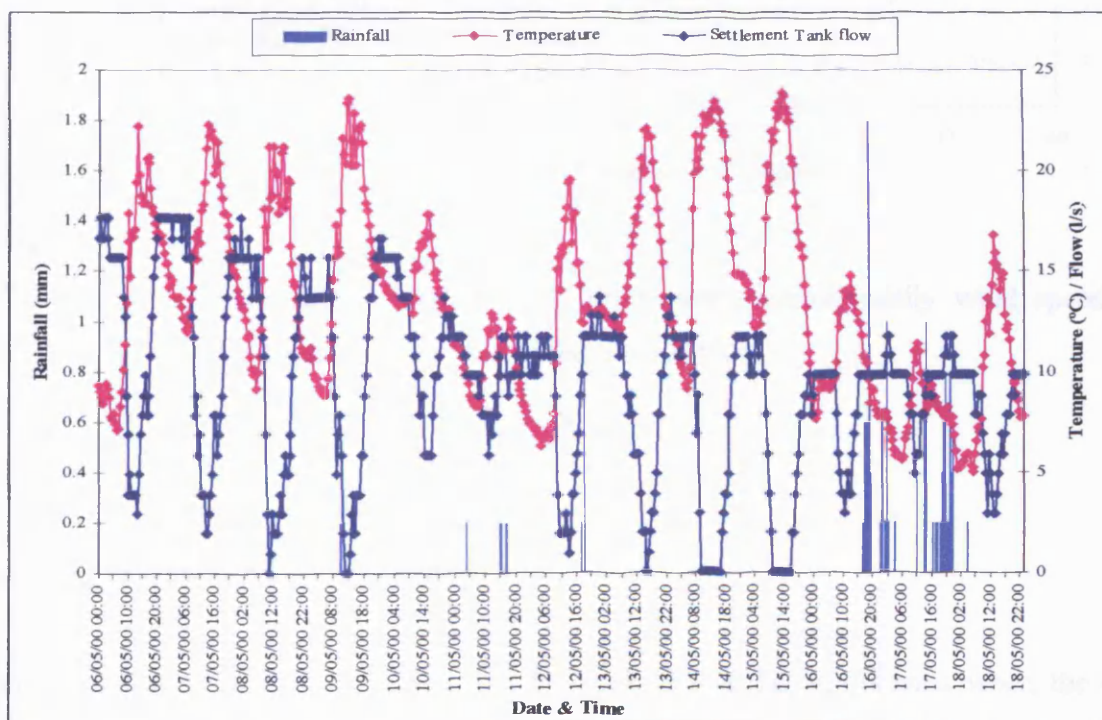


Figure 5.58 Graph showing the relationship between temperature and flow through the Settlement Tank.

5.5.2.4.1.4 Discharge and Average wind speed

A significant weak correlation ($r = 0.15$, $p = 0.00$) is obtained when the unadjusted daily discharge is plotted against the average daily wind speed (Fig. 5.59). A slightly higher correlation ($r = 0.16$, $p = 0.00$) is obtained for the discharge with the trend removed. The general trend is that as the average daily wind speed increases the discharge also increases. This reflects the fact that rainfall in south Wales is dominated by cyclonic systems, so that rainfall periods are likely to be associated with higher wind speeds.

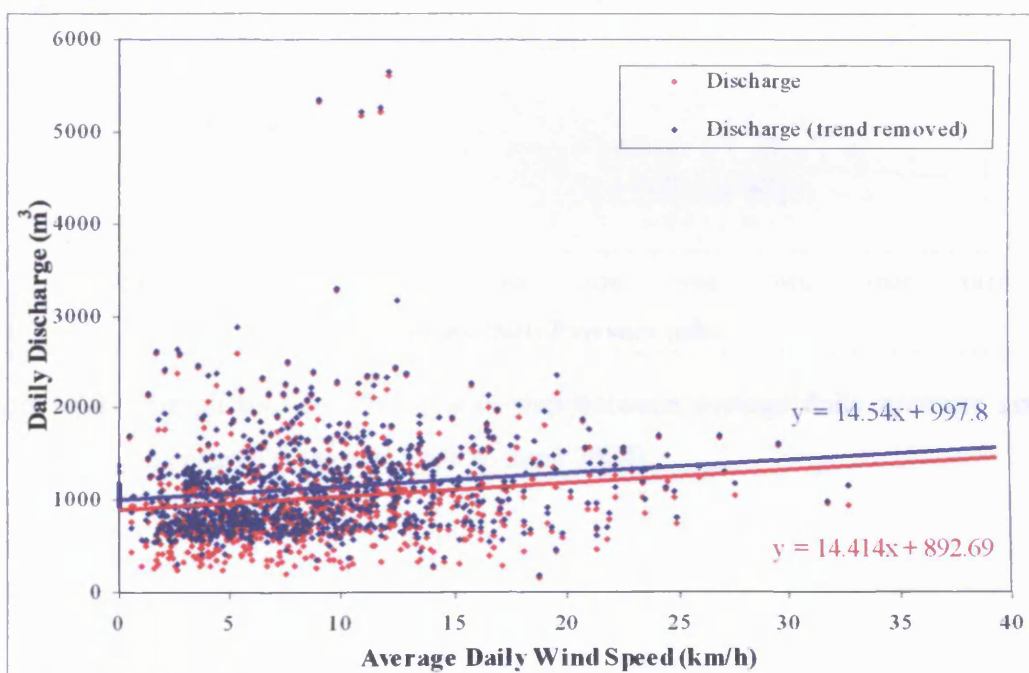


Figure 5.59 Graph showing the relationship between average daily wind speed and daily discharge (October 1998 to June 2004).

5.5.2.4.1.5 Discharge and Pressure

A significant very weak correlation ($r = -0.09$, $p = 0.01$) is obtained when the daily discharge is plotted against the average daily pressure (Fig. 5.60), with discharge tending to be higher with lower pressure, as might be expected, since precipitation is generally

associated with frontal depressions. A higher correlation ($r = -0.18$, $p = 0.00$) is obtained for the discharge with the trend removed.

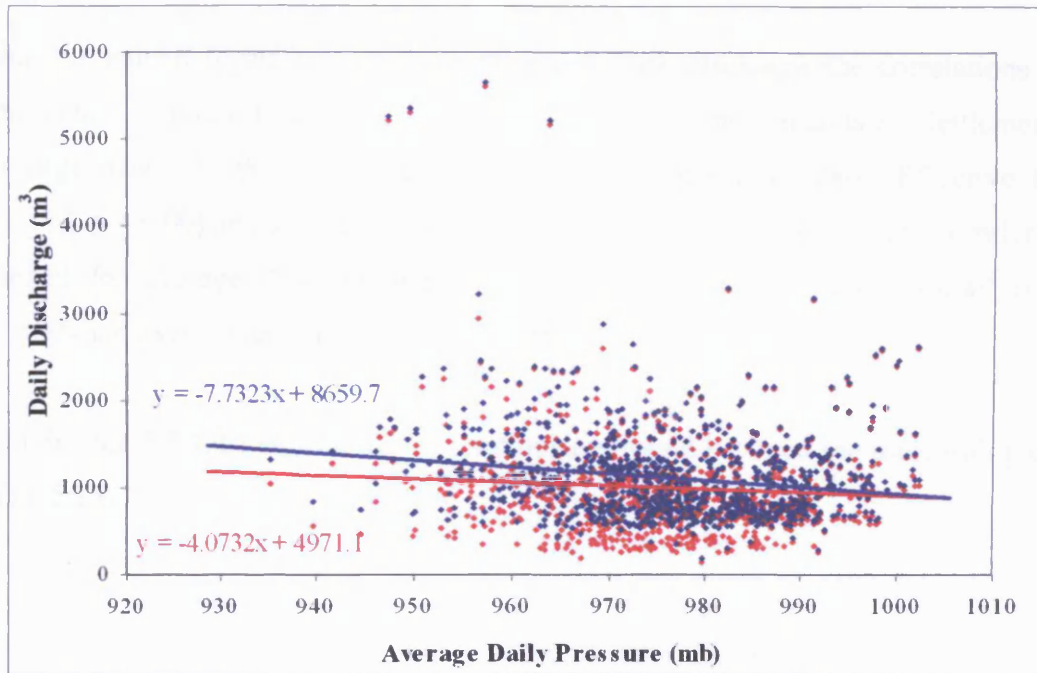


Figure 5.60 Graph showing the relationship between average daily pressure and daily discharge (October 1998 to June 2004).

5.5.2.4.1.6 Summary

Table 5.16 provides a summary of bivariate analysis. As well as the correlations described above it provides correlation coefficients and significance for the natural logarithms of the discharge and the meteorological data compared against each other.

The strongest correlation with the unadjusted discharge through the Settlement Tank is with daily rainfall ($r = 0.29$, $p = 0.00$) and daily effective rainfall ($r = 0.29$, $p = 0.00$). On a scale of correlation (Fig. 5.31) these are only considered as a weak correlations. The Settlement Tank receives discharge from the BSC Pipe, in addition to a range of other sources (LP2A, LP4), so it is not really surprising that the correlation is not stronger.

Slightly better correlations are obtained with all the meteorological data when using the discharge values with the long-term trend removed. This suggests that the trend observed is real.

Using the natural logarithms of the Settlement Tank discharge the correlations are not significantly different (Table 5.16) from those for the raw unadjusted Settlement Tank discharge data. Slightly better correlations are obtained for daily Effective Rainfall ($r = 0.30$, $p = 0.00$) and average wind speed ($r = 0.16$, $p = 0.00$) but worse correlations are obtained for average daily temperature ($r = -0.17$, $p = 0.00$), daily rainfall ($r = 0.27$, $p = 0.00$) and average daily pressure ($r = -0.04$, $p = 0.21$).

As in Section 5.5.1.4.1.6, stronger correlations are found between the meteorological data (Table 5.16).

		Daily Settlement Tank discharge	Natural Logarithm of Daily Settlement Tank discharge	Daily Settlement Tank discharge (trend removed)	Average daily temperature	Daily rainfall	Average daily pressure	Daily Effective Rainfall	Average wind speed
Daily Settlement Tank discharge	Pearson Correlation	1	.91**	.99**	-.25**	.29**	-.09**	.29**	.15**
	Significance	.	0.00	0.00	0.00	0.00	0.01	0.00	0.00
	N	1044	1044	1044	967	987	966	848	916
Natural Logarithm of Daily Settlement Tank discharge	Pearson Correlation	.91**	1	.88**	-.17**	.27**	-0.04	.30**	.16**
	Significance	0.00	.	0.00	0.00	0.00	0.21	0.00	0.00
	N	1044	1044	1044	967	987	966	848	916
Daily Settlement Tank discharge (trend removed)	Pearson Correlation	.99**	.88**	1	-.30**	.31**	-.18**	.30**	.16**
	Significance	0.00	0.00	.	0.00	0.00	0.00	0.00	0.00
	N	1044	1044	1044	967	987	966	848	916
Average daily temperature	Pearson Correlation	-.25**	-.17**	-.30**	1	-.07**	.11**	-.14**	-.35**
	Significance	0.00	0.00	0.00	.	0.00	0.00	0.00	0.00
	N	967	967	967	1931	1931	1930	1447	1815
Daily rainfall	Pearson Correlation	.29**	.27**	.31**	-.07**	1	-.46**	.71**	.26**
	Significance	0.00	0.00	0.00	0.00	.	0.00	0.00	0.00
	N	987	987	987	1931	1973	1930	1473	1815
Average daily pressure	Pearson Correlation	-.09**	-.04	-.18**	.11**	-.46**	1	-.35**	-.15**
	Significance	0.01	0.21	0.00	0.00	0.00	.	0.00	0.00
	N	966	966	966	1930	1930	1930	1446	1814
Daily Effective Rainfall	Pearson Correlation	.29**	.30**	.30**	-.14**	.71**	-.35**	1	.30**
	Significance	0.00	0.00	0.00	0.00	0.00	0.00	.	0.00
	N	848	848	848	1447	1473	1446	1522	1447
Average wind speed	Pearson Correlation	.15**	.16**	.16**	-.35**	.26**	-.15**	.30**	1
	Significance	0.00	0.00	0.00	0.00	0.00	0.00	0.00	.
	N	916	916	916	1815	1815	1814	1447	1815

** Correlation is significant at the 0.01 level

* Correlation is significant at the 0.05 level

Table 5.16 Table of correlations for the Settlement Tank discharge and meteorological data.

5.5.2.4.2 Multiple Regression

The multiple regression is set up so that the discharge through the Settlement Tank is the dependent variable and Effective Rainfall, average daily temperature, average daily wind speed and pressure are the independent variables.

Effective Rainfall and rainfall have a strong correlation with each other and represent similar variables. Collinearity, where the correlations among the independent variables are high, is undesirable. If daily rainfall and Effective Rainfall are used in the simultaneous regression analysis independently then better R values were obtained when using Effective Rainfall rather than daily rainfall. A slightly better correlation was obtained for Effective Rainfall when looking at the lag in Section 5.5.2.3. Slightly better R values are obtained if both Effective Rainfall and rainfall are used but since they represent similar inputs it was decided to exclude daily rainfall from the simultaneous regression analysis.

In stepwise multiple regression, the independent variables are added to (or taken away from) the equation one at a time, the order of entry (or removal) being determined by statistical considerations. For this reason, both daily rainfall and Effective Rainfall have been presented to allow the analysis to determine which is the most significant.

Regression analysis will be performed for both the unadjusted discharge and the discharge with the long-term trend removed.

Again due to the precision in the original data, coefficients will only be quoted to the nearest two decimal places although SPSS quotes to three decimal places.

5.5.2.4.2.1 Simultaneous Multiple Regression - Unadjusted Discharge

SPSS is used to perform simultaneous multiple regression. The package produces a table of correlations (Table 5.17) for the data. There are 801 days (*N*) where there are complete data for all the variables. Due to this difference in sample population, different correlation coefficients are obtained here than in the simple regression analysis (Section 5.5.2.4.1). The table also shows that the dependent variable Settlement Tank discharge correlates significantly with all the independent variables.

		Settlement Tank discharge
Pearson Correlation	Settlement Tank discharge	1
	Average daily temperature	-.43
	Average wind speed	.16
	Pressure	-.13
	Effective Rainfall	.25
Significance	Settlement Tank discharge	.
	Average daily temperature	.00
	Average wind speed	.00
	Pressure	.00
	Effective Rainfall	.00
N		801

Table 5.17 Table of correlations for simultaneous multiple regression for discharge (unadjusted) through the Settlement Tank.

For this model, the multiple correlation coefficient (*R*) is 0.47 (Table 5.18). The adjusted *R* square value, the estimate of the proportion of variance accounted for by the regression, is 0.21, i.e. 21%. For the coefficient for individual variables (Table 5.17), the best correlation coefficient was -0.43 for average daily temperature, so adding more independent variables has improved the predictive power of the regression equation.

If daily rainfall had been used instead of Effective Rainfall, a multiple correlation coefficient of 0.40 is obtained. If daily rainfall and Effective Rainfall had both been used, an R value of 0.51 is obtained.

Model	R	R Square	Adjusted R Square	Std. Error of the Estimate
1	.47	.22	.21	472.11

Table 5.18 Table giving the value of R for simultaneous multiple regression for discharge (unadjusted) through the Settlement Tank.

Using the outputs (column B) in Table 5.19, it is possible to construct the multiple regression equation of Settlement Tank discharge (ST) from average daily temperature ($temp$), average wind speed ($wind$), pressure (mb) and Effective Rainfall (ER) as:

$$ST' = 3129.38 + -41.08(temp) + -5.75(wind) + -1.67(mb) + 13.80(ER) \quad (39)$$

where ST' is the predicted Settlement Tank discharge.

Model	Unstandardized Coefficients		Standardized Coefficients	t	Significance
	B	Std. Error	Beta		
1 (Constant)	3129.38	1527.98		2.05	.04
Average daily temperature	-41.08	3.35	-.42	-12.25	.00
Average wind speed	-5.75	3.41	-.06	-1.69	.09
Pressure	-1.67	1.56	-.04	-1.08	.28
Effective Rainfall	13.80	2.91	.17	4.75	.00

Table 5.19 The regression equation and associated statistics for simultaneous multiple regression for discharge (unadjusted) through the Settlement Tank.

The beta coefficients (column headed Beta in Table 5.19) give the number of standard deviations change on the dependent variable that will be produced by a change of one standard deviation on the independent variable concerned. For these data, the average daily temperature makes the greatest contribution followed by Effective Rainfall.

As indicated by the low adjusted R square value, and figures 5.61 and 5.62, the simultaneous regression analysis model does not have the power to accurately predict the more extreme excursions in discharge values, although the clear seasonal fluctuation in the modelled predictions agree well with the broad average values in the measured discharge.

A Root Mean Squared Error (RMSE) of 467 is obtained for the 823 days with recorded (unadjusted) and predicted discharge for the Settlement Tank between 1 April 2000 and 22 June 2004. Considering the mean recorded discharge (unadjusted) for the same period is 1060 m^3 per day, this is a large error.

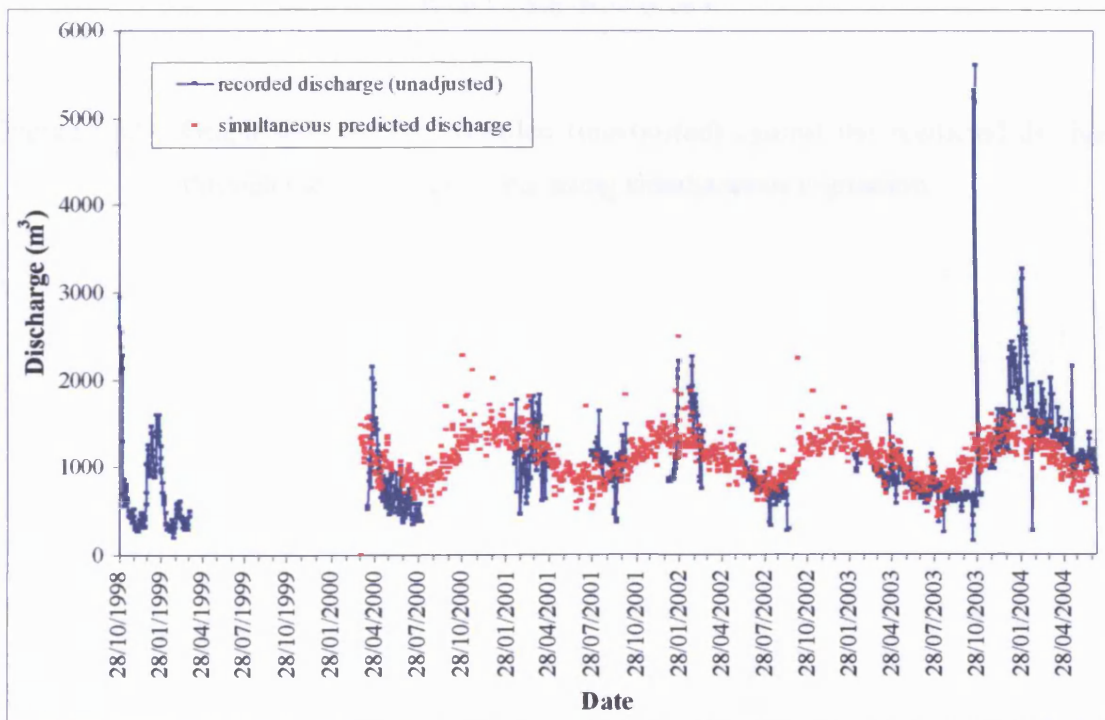


Figure 5.61 Graph showing the recorded (unadjusted) and predicted discharge through the Settlement Tank using simultaneous regression.

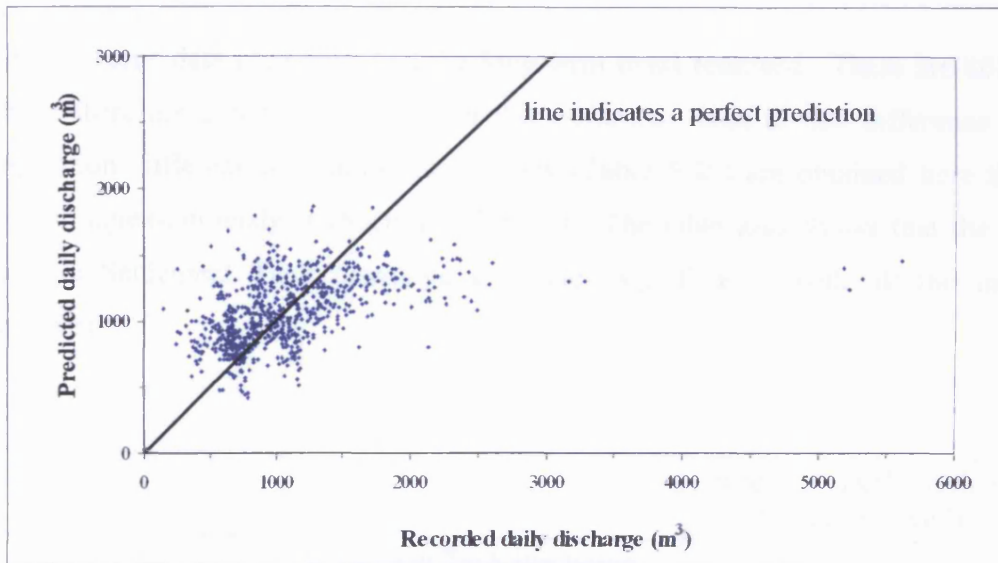


Figure 5.62 Graph showing the recorded (unadjusted) against the predicted discharge through the Settlement Tank using simultaneous regression.

5.5.2.4.2 Simultaneous Multiple Regression – Trend removed from Discharge

The discharge data used have had the long-term trend removed. There are 801 days (N) where there are complete data for all the variables. Due to this difference in sample population, different correlation coefficients (Table 5.20) are obtained here than in the simple regression analysis (Section 5.5.2.4.1). The table also shows that the dependent variable Settlement Tank discharge correlates significantly with all the independent variables.

		Settlement Tank discharge (trend removed)
Pearson Correlation	Settlement Tank discharge (trend removed)	1
	Average daily temperature	-.43
	Average wind speed	.16
	Pressure	-.20
	Effective Rainfall	.26
Significance	Settlement Tank discharge (trend removed)	.
	Average daily temperature	.00
	Average wind speed	.00
	Pressure	.00
	Effective Rainfall	.00
N		801

Table 5.20 Table of correlations for simultaneous multiple regression for discharge (trend removed) through the Settlement Tank.

For this model, the multiple correlation coefficient (R) is 0.48 (Table 5.21). The adjusted R square value is 0.23, i.e. 23%. For the coefficient for individual variables (Table 5.20), the best correlation coefficient was -0.43 for average daily temperature, so adding more independent variables has improved the predictive power of the regression equation.

If daily rainfall had been used instead of Effective Rainfall, a multiple correlation coefficient of 0.43 is obtained. If daily rainfall and Effective Rainfall had both been used, an R value of 0.51 is obtained.

Model	R	R Square	Adjusted R Square	Std. Error of the Estimate
1	.48	.23	.23	459.94

Table 5.21 Table giving the value of R for simultaneous multiple regression for discharge (trend removed) through the Settlement Tank.

Using the outputs (column B) in Table 5.22, it is possible to construct the multiple regression equation of Settlement Tank discharge (ST) from average daily temperature ($temp$), average wind speed ($wind$), pressure (mb) and Effective Rainfall (ER) as:

$$ST' = 6422.27 + -39.63(temp) + -5.87(wind) + -4.96(mb) + 12.34(ER) \quad (40)$$

where ST' is the predicted Settlement Tank discharge.

Model	Unstandardized Coefficients		Standardized Coefficients	t	Significance
	B	Std. Error	Beta		
1 (Constant)	6422.27	1488.58		4.31	.00
Average daily temperature	-39.63	3.27	-.41	-12.13	.00
Average wind speed	-5.87	3.33	-.06	-1.77	.08
Pressure	-4.96	1.52	-.11	-3.27	.00
Effective Rainfall	12.34	2.83	.15	4.36	.00

Table 5.22 The regression equation and associated statistics for simultaneous multiple regression for discharge (trend removed) through the Settlement Tank.

The beta coefficients (column headed Beta in Table 5.22) give the number of standard deviations change on the dependent variable that will be produced by a change of one standard deviation on the independent variable concerned. For these data, the average daily temperature makes the greatest contribution followed by Effective Rainfall.

As indicated by the low adjusted R square value, and figures 5.63 and 5.64, the simultaneous regression analysis model does not have the power to accurately predict the more extreme excursions in discharge values, although the clear seasonal fluctuation in the modelled predictions agree well with the broad average values in the measured discharge.

A Root Mean Squared Error (RMSE) of 454 is obtained for the 823 days with recorded (trend removed) and predicted discharge for the Settlement Tank between 1 April 2000 and 22 June 2004. Considering the mean recorded discharge (trend removed) for the same period is 1147 m^3 per day, this is a large error.

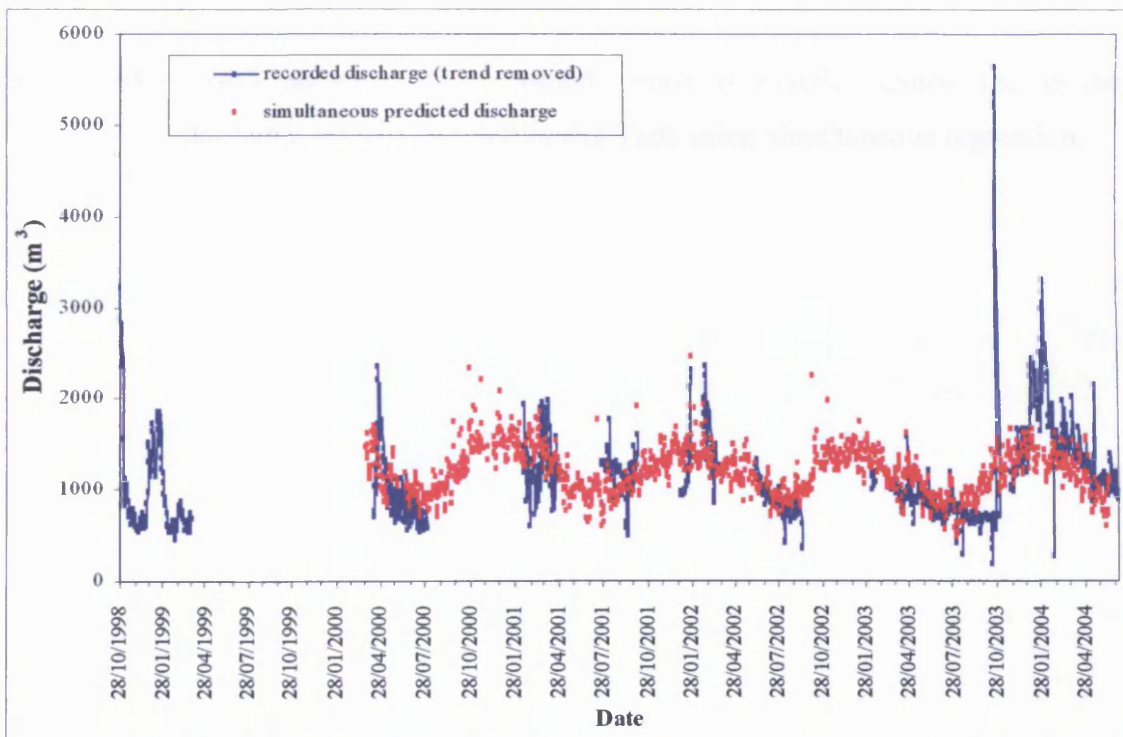


Figure 5.63 Graph showing the recorded (trend removed) and predicted discharge through the Settlement Tank using simultaneous regression.

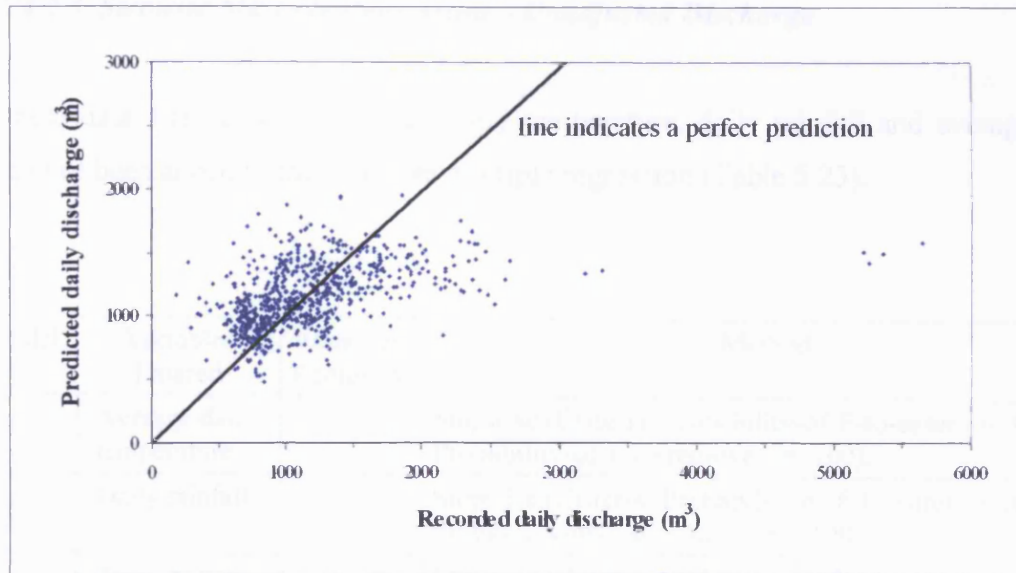


Figure 5.64 Graph showing the recorded (trend removed) against the predicted discharge through the Settlement Tank using simultaneous regression.

5.5.2.4.2.3 Stepwise Multiple Regression – Unadjusted Discharge

For these data, the variables average daily temperature, daily rainfall and average wind speed have been added to the stepwise multiple regression (Table 5.23).

Model	Variables Entered	Variables Removed	Method
1	Average daily temperature	.	Stepwise (Criteria: Probability-of-F-to-enter \leq .050, Probability-of-F-to-remove \geq .100).
2	Daily rainfall	.	Stepwise (Criteria: Probability-of-F-to-enter \leq .050, Probability-of-F-to-remove \geq .100).
3	Average wind speed	.	Stepwise (Criteria: Probability-of-F-to-enter \leq .050, Probability-of-F-to-remove \geq .100).

Table 5.23 List of variables entered into the stepwise multiple regression for discharge (unadjusted) through the Settlement Tank.

Models are run with the first variable entered (Model 1) and again with the second variable added to the first (Model 2) and again with the third variable added to the first and second (Model 3) (Table 5.24).

The value of R for Model 3 (0.51) (Table 5.24) is slightly better than that for the simultaneous regression (0.47) of Settlement Tank discharge (unadjusted) upon average daily temperature, average wind speed, pressure and Effective Rainfall.

Model	R	R Square	Adjusted R Square	Std. Error of the Estimate
1	.43 ^a	.19	.19	480.12
2	.51 ^b	.26	.25	460.41
3	.51 ^c	.26	.26	459.47

^a Predictors: (Constant), Average daily temperature

^b Predictors: (Constant), Average daily temperature, Daily rainfall

^c Predictors: (Constant), Average daily temperature, Daily rainfall, Average wind speed

Table 5.24 Value of *R* and associated statistics for each model in the stepwise multiple regression for discharge (unadjusted) through the Settlement Tank.

Using the outputs (column B) in Table 5.25, it is possible to construct the multiple regression equation of Settlement Tank discharge (*ST*) from average daily temperature (*temp*), daily rainfall (*rain*) and average wind speed (*wind*) as:

$$ST' = 1454.95 + -40.87(temp) + 23.82(rain) + -6.79(wind) \quad (41)$$

where *ST'* is the predicted Settlement Tank discharge. Since the increment in *R* with the inclusion of the remaining variables (effective rainfall and pressure) does not reach the necessary criterion for the stepwise program, these variables are excluded from the final equation.

Model	Unstandardized Coefficients		Standardized Coefficients	t	Significance
	B	Std. Error	Beta		
1 (Constant)	1492.00	36.58		40.79	.00
Average daily temperature	-42.60	3.13	-.43	-13.62	.00
2 (Constant)	1373.55	37.80		36.34	.00
Average daily temperature	-38.45	3.04	-.39	-12.65	.00
Daily rainfall	22.74	2.70	.26	8.42	.00
3 (Constant)	1454.95	54.55		26.67	.00
Average daily temperature	-40.87	3.25	-.42	-12.57	.00
Daily rainfall	23.82	2.75	.27	8.67	.00
Average wind speed	-6.79	3.29	-.07	-2.07	.04

Table 5.25 The regression coefficients for the single variable (Model 1), the two variables (Model 2) and the three variables (Model 3) remaining in the stepwise regression analysis for the unadjusted discharge.

Table 5.26 details the variables excluded from the stepwise regression analysis.

Model	Beta In	t	Sig.	Partial Correlation	Collinearity Statistics
					Tolerance
1 Average wind speed	-.01 ^a	-.40	.69	-.01	.85
Daily rainfall	.26 ^a	8.42	.00	.29	.97
Pressure	-.08 ^a	-2.63	.01	-.09	.99
Effective Rainfall	.17 ^a	5.16	.00	.18	.96
2 Average wind speed	-.07 ^b	-2.07	.04	-.07	.82
Pressure	.04 ^b	1.24	.22	.04	.78
Effective Rainfall	-.01 ^b	-.12	.90	-.00	.57
3 Pressure	.04 ^c	1.07	.29	.04	.78
Effective Rainfall	.01 ^c	.15	.88	.01	.56

^a Predictors in the Model: (Constant), Average daily temperature

^b Predictors in the Model: (Constant), Average daily temperature, Daily rainfall

^c Predictors in the Model: (Constant), Average daily temperature, Daily rainfall, Average wind speed

Table 5.26 The variables excluded from the stepwise regression analysis for the unadjusted discharge.

The resulting predicted discharge once again identifies a seasonal variation in Settlement Tank discharge that agrees well with the measured data (Fig. 5.65). The predicted discharge is virtually identical to the simultaneous multiple regression model (Fig. 5.66). Again the short term extreme discharge excursions cannot be simulated using the stepwise multiple regression model.

A Root Mean Squared Error (RMSE) of 455 is obtained for the 824 days with recorded (unadjusted) and predicted discharge for the Settlement Tank between 1 April 2000 and 22 June 2004. Considering the mean recorded discharge (unadjusted) for the same period is 1060 m³ per day, this is a large error.

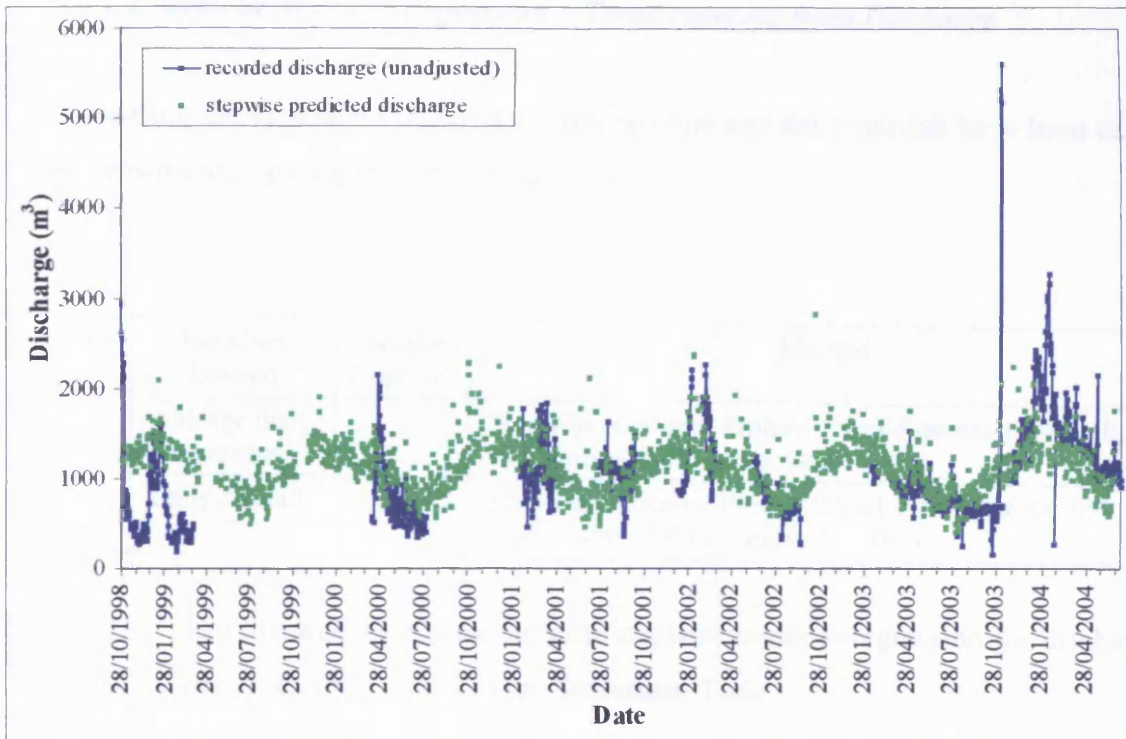


Figure 5.65 Graph showing the recorded (unadjusted) and predicted discharge through the Settlement Tank using stepwise regression.

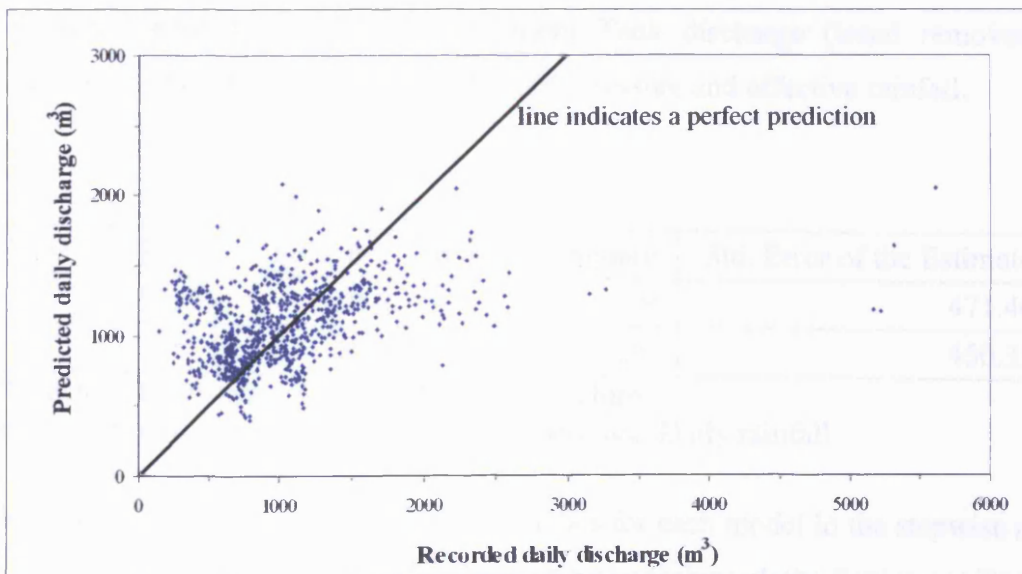


Figure 5.66 Graph showing the recorded (unadjusted) against the predicted discharge through the Settlement Tank using stepwise regression.

5.5.2.4.2.4 Stepwise Multiple Regression – Trend removed from Discharge

For these data, the variables average daily temperature and daily rainfall have been added to the stepwise multiple regression (Table 5.27).

Model	Variables Entered	Variables Removed	Method
1	Average daily temperature	.	Stepwise (Criteria: Probability-of-F-to-enter \leq .050, Probability-of-F-to-remove \geq .100).
2	Daily rainfall	.	Stepwise (Criteria: Probability-of-F-to-enter \leq .050, Probability-of-F-to-remove \geq .100).

Table 5.27 List of variables entered into the stepwise multiple regression for discharge (trend removed) through the Settlement Tank.

Models are run with the first variable entered (Model 1) and again with the second variable added to the first (Model 2) (Table 5.28).

The value of R for Model 2 (0.51) (Table 5.28) is slightly better than that for the simultaneous regression (0.48) of Settlement Tank discharge (trend removed) upon average daily temperature, average wind speed, pressure and effective rainfall.

Model	R	R Square	Adjusted R Square	Std. Error of the Estimate
1	.43 ^a	.19	.19	471.46
2	.51 ^b	.26	.26	450.33

^a Predictors: (Constant), Average daily temperature

^b Predictors: (Constant), Average daily temperature, Daily rainfall

Table 5.28 Value of R and associated statistics for each model in the stepwise multiple regression for discharge (trend removed) through the Settlement Tank.

Using the outputs (column B) in Table 5.29, it is possible to construct the multiple regression equation of Settlement Tank discharge (ST) from average daily temperature ($temp$) and daily rainfall ($rain$) as:

$$ST' = 1454.95 + -40.87(temp) + 23.82(rain) \quad (42)$$

where ST' is the predicted Settlement Tank discharge. Since the increment in R with the inclusion of the remaining variables (average wind speed, Effective Rainfall and pressure) does not reach the necessary criterion for the stepwise program, these variables are excluded from the final equation.

Model	Unstandardized Coefficients		Standardized Coefficients	t	Significance
	B	Std. Error	Beta		
1 (Constant)	1570.69	35.92		43.73	.00
Average daily temperature	-41.53	3.07	-.43	-13.52	.00
2 (Constant)	1449.33	36.97		39.20	.00
Average daily temperature	-37.28	2.97	-.39	-12.54	.00
Daily rainfall	23.30	2.64	.27	8.82	.00

Table 5.29 The regression coefficients for the single variable (Model 1) and the two variables (Model 2) remaining in the stepwise regression analysis for the discharge with the trend removed.

Table 5.30 details the variables excluded from the stepwise regression analysis.

Model	Beta In	t	Sig.	Partial Correlation	Collinearity Statistics
					Tolerance
1 Average wind speed	-.01 ^a	-.20	.85	-.01	.85
Pressure	-.15 ^a	-4.80	.00	-.17	.99
Effective Rainfall	.18 ^a	5.50	.00	.19	.96
Daily Rainfall	.27 ^a	8.82	.00	.30	.97
2 Average wind speed	-.07 ^b	-1.93	.05	-.07	.82
Pressure	.04 ^b	-1.06	.29	-.04	.78
Effective Rainfall	-.00 ^b	.02	.98	.00	.57

^a Predictors in the Model: (Constant), Average daily temperature

^b Predictors in the Model: (Constant), Average daily temperature, Daily rainfall

Table 5.30 The variables excluded from the stepwise regression analysis for the discharge with the trend removed.

As with the predicted discharge using stepwise regression on the unadjusted discharge data, totals once again identify a seasonal variation in Settlement Tank discharge that agrees well with the measured data (Fig. 5.67). The predicted discharge is virtually identical to the simultaneous multiple regression model and the stepwise regression model using the unadjusted discharge data. Again the short term extreme discharge excursions cannot be simulated using the stepwise multiple regression model (Fig. 5.68).

A Root Mean Squared Error (RMSE) of 448 is obtained for the 824 days with recorded (trend removed) and predicted discharge for the Settlement Tank between 1 April 2000 and 22 June 2004. Considering the mean recorded discharge (trend removed) for the same period is 1147 m³ per day, this is a large error.

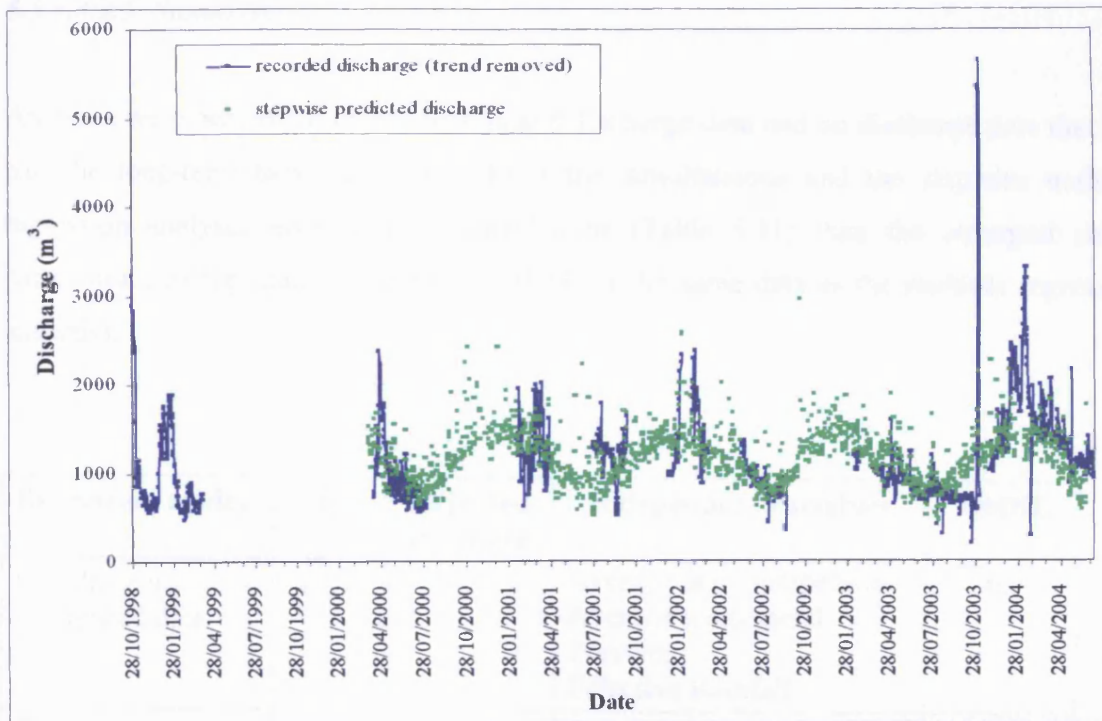


Figure 5.67 Graph showing the recorded (trend removed) and predicted discharge through the Settlement Tank using stepwise regression.

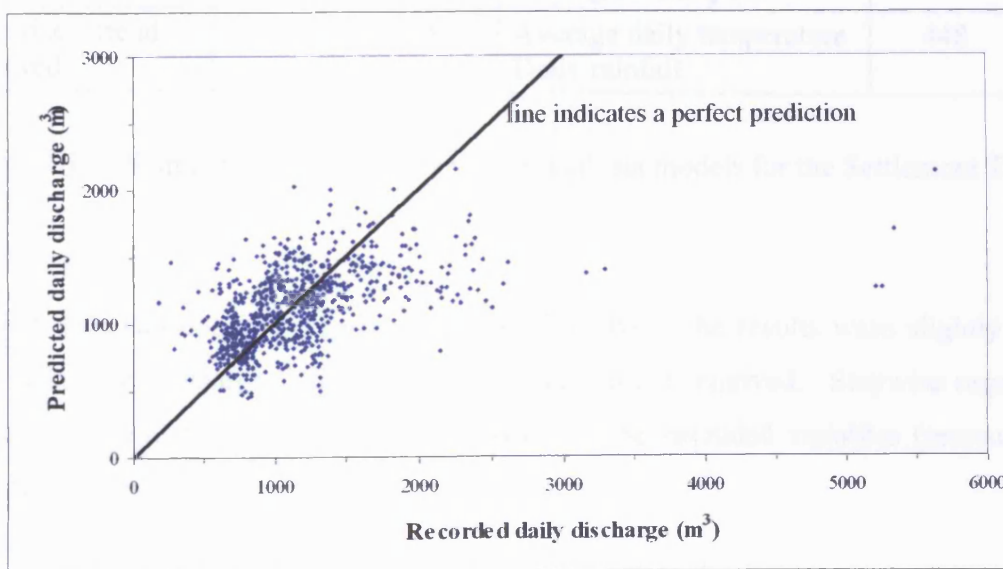


Figure 5.68 Graph showing the recorded (trend removed) against the predicted discharge through the Settlement Tank using stepwise regression.

5.5.2.4.2.5 Summary

Analyses were performed on the unadjusted discharge data and on discharge data that had had the long-term trend removed. Both the simultaneous and the stepwise multiple regression analyses give stronger correlations (Table 5.31) than the strongest single correlation (average daily temperature, -0.43 for the same data as the multiple regression analysis).

Regression model	R	Adjusted R square	Independent variables	RMSE
Simultaneous – unadjusted data	0.47	0.21	Average daily temperature Average wind speed Pressure Effective Rainfall	467
Simultaneous – trend removed	0.48	0.23	Average daily temperature Average wind speed Pressure Effective Rainfall	454
Stepwise – unadjusted data	0.51	0.26	Average daily temperature Daily rainfall Average wind speed	455
Stepwise – trend removed	0.51	0.26	Average daily temperature Daily rainfall	448

Figure 5.31 Summary of multiple regression analysis models for the Settlement Tank.

For both simultaneous and stepwise regression analysis, the results were slightly better when using the discharge data with the long-term trend removed. Stepwise regression analysis highlights the lack of predictive power of the excluded variables (pressure and average wind speed).

The best regression method for the data was using stepwise regression on the discharge data with the trend removed. This produced the highest *R* and *R* square values and the lowest RMSE (Table 5.31).

It is interesting that using Effective Rainfall produced better results when using simultaneous regression analysis but daily rainfall gave better results for the stepwise analysis.

In all the models short-term extreme discharge variations could not be predicted. However, the seasonal cyclicality in “average” measured discharge values appears to correspond closely with modelled data. Reasons for this will be discussed in Chapter 8. It is notable that observed discharge through 2003/4, however, generally exceeds the predicted totals based on the longer time series model.

5.5.2.4.3 Seasonal Data

It is likely that different variables have different predictive powers at different times of the year. Any seasonal variations will show up better for the discharge through the Settlement Tank since it accepts all the leachate and contaminated runoff produced on site.

The data have been separated into two data sets. Data collected between April and September form a summer data set and data collected between October and March forms the winter data set. These data can then be analysed independently.

5.5.2.4.3.1 Simple, Two-Variable Regression

Simple regression analysis of the Settlement Tank discharge with the meteorological data shows different correlations between using all year around data or the summer or winter data (Table 5.32). The best of the correlations are considered as weak.

Using data from throughout the year, the best correlation of Settlement Tank discharge is with Effective Rainfall ($r = 0.29$, $p = 0.00$) and Rainfall ($r = 0.29$, $p = 0.00$). Daily rainfall provides the best correlation with the Settlement Tank discharge ($r = 0.24$, $p = 0.00$) with data collected in the winter (October to March). The summer (April to September) data shows the strongest correlations with average daily temperature ($r = -0.37$, $p = 0.00$), daily rainfall ($r = 0.34$, $p = 0.00$) and effective rainfall ($r = 0.26$, $p = 0.00$).

For the data for throughout the year and the summer data, all the correlations are significant ($p < 0.05$). For the winter data only correlations with daily rainfall and effective rainfall are significant ($p < 0.05$).

		Summer Settlement Tank discharge	Winter Settlement Tank discharge	All year Settlement Tank discharge
Average daily temperature	Pearson Correlation	-.37**	-.01	-.25**
	Significance	.00	.78	.00
	N	541	426	967
Average wind speed	Pearson Correlation	.17**	.06	.15**
	Significance	.00	.25	.00
	N	541	375	916
Daily rainfall	Pearson Correlation	.34**	.24**	.29**
	Significance	.00	.00	.00
	N	549	438	987
Pressure	Pearson Correlation	-.14**	-.04	-.09**
	Significance	.00	.38	.01
	N	540	426	966
Effective Rainfall	Pearson Correlation	.26**	.21**	.29**
	Significance	.00	.00	.00
	N	547	301	848

** Correlation is significant at the 0.01 level

* Correlation is significant at the 0.05 level

Table 5.32 Table showing the correlations for the Settlement Tank discharge and meteorological data for all the year, Summer (April to September) and Winter (October to March).

5.5.2.4.3.2 Multiple Regression

Simultaneous and stepwise multiple regression analysis have been performed on the winter and summer data (Table 5.33) to see how separating the data affects the analysis. Collinearity is undesirable so daily rainfall and Effective Rainfall have not both been used in the simultaneous regression analysis. Daily rainfall gave better correlations for the seasonal data than Effective Rainfall, which is the opposite when using all the data.

Although better correlations are obtained for simple regression of the summer data rather than all the data (Table 5.32), when using multiple regression analysis the best correlations are obtained when using all the data set (Table 5.33). This could be related to the amount of data available for the analysis.

Data used in model	Model	R	R Square	Adjusted R Square	Std. Error of the Estimate
All data	Simultaneous	.40 ^{Rain}	.16	.16	490.13
	Simultaneous	.47 ^{ER}	.22	.21	472.11
	Stepwise 1	.43 ^{1a}	.19	.19	480.12
	Stepwise 2	.51 ^{1b}	.26	.25	460.41
	Stepwise 3	.51 ^{1c}	.26	.26	459.47
Summer	Simultaneous	.45	.20	.19	281.40
	Stepwise 1	.40 ^{2a}	.16	.16	290.87
	Stepwise 2	.46 ^{2b}	.22	.21	281.03
Winter	Simultaneous	.28	.08	.07	683.95
	Stepwise 1	.28 ^{3a}	.07	.07	684.29

^{Rain} Predictors: (Constant), Average daily temperature, Daily rainfall, Pressure, Average Wind Speed

^{ER} Predictors: (Constant), Average daily temperature, Effective Rainfall, Pressure, Average Wind Speed

^{1a} Predictors: (Constant), Average daily temperature

^{1b} Predictors: (Constant), Average daily temperature, Daily rainfall

^{1c} Predictors: (Constant), Average daily temperature, Daily rainfall, Average wind speed

^{2a} Predictors: (Constant), Summer average daily temperature

^{2b} Predictors: (Constant), Summer average daily temperature, Summer daily rainfall

^{3a} Predictors: (Constant), Winter daily rainfall

Table 5.33 Table showing value of R and associated statistics for each simultaneous and stepwise multiple regression for discharge through the Settlement Tank using all the data, winter data and summer data.

5.5.3 SUMMARY

Regression analysis was used as a predictive tool for modelling discharge through the BSC Pipe and the Settlement Tank. The results for the Settlement Tank give stronger correlation coefficients than the results for the BSC Pipe.

5.5.3.1 BSC Pipe

Using the cross-correlation function (CCF) in SPSS, there is a weak correlation (0.22) between daily discharge and rainfall with a lag of 5 days. No significant correlation is found for daily discharge in the BSC Pipe with Effective Rainfall, though the lag time suggested is longer at 7 days. Rainfall landing on the landfill site has to infiltrate through the cap and percolate down through the landfill before it is collected by the drainage system that enters the BSC Pipe. This analysis indicates the indirect nature of the linkage between rainfall events and discharge through the basal drainage system of the landfill. Clearly recharge of leachate, leachate storage, possibly flows from higher perched water tables to the main leachate water table in the base of the landfill all attenuate the rainfall signal, so that it does not correlate strongly with fluctuations in leachate drainage through the BSC Pipe.

The strongest correlation with the discharge through the BSC Pipe is with average daily temperature ($r = -0.26$, $p = 0.00$). Using the natural logarithm transformation of the BSC Pipe discharge better correlations are obtained for average daily temperature ($r = -0.37$, $p = 0.00$) and average wind speed ($r = 0.17$, $p = 0.00$). Stronger correlations are found between the meteorological data.

BSC Pipe discharge was considered as the dependant variable with meteorological data as the independent variables for multiple regression analysis. Both the simultaneous and the stepwise multiple regression analysis give stronger correlations than the strongest single correlation (average daily temperature, -0.31 for the same data as the multiple regression analysis). Using average daily temperature and daily rainfall (with the 5 day lag) the

stepwise regression analysis has a correlation of 0.32 compared to 0.33 with the simultaneous regression analysis using all the variables (average daily temperature, average wind speed, daily rainfall (with the 5 day lag) and pressure). This shows the lack of predictive power of pressure and average wind speed.

The resulting models both show seasonal fluctuations in leachate discharge, with high flows in winter and low flows in summer. The actual data shows significant short-term fluctuations that cannot be modelled using this simple multiple regression based approach. The multiple regression analysis has however highlighted average daily temperature as the most important variable in determining discharge for the BSC Pipe.

5.5.3.2 Settlement Tank

Using the cross-correlation function (CCF) in SPSS, there is a weak correlation (0.291) between daily discharge and rainfall with a lag of 0 days. Using rainfall data for every 30 minutes, the best correlation (0.189) of half hourly discharge and rainfall occurs with a lag of 3 intervals - one and a half hours. This implies that the discharge shows a rapid response to rainfall events. It is likely that the rapid response is derived largely from surface runoff across the landfill that is collected by drainage ditches and enters the Settlement Tank.

Slightly stronger correlations are obtained for daily discharge through the Settlement Tank and daily Effective Rainfall for a lag of 1 day (0.307) and a lag of 0 days (0.294).

The strongest correlation with the unadjusted discharge through the Settlement Tank is with daily rainfall ($r = 0.29$, $p = 0.00$) and daily effective rainfall ($r = 0.29$, $p = 0.00$). Slightly better correlations are obtained with all the meteorological data when using the discharge values with the long-term trend removed. This suggests that the trend observed is real.

Using the natural logarithms of the Settlement Tank discharge the correlations are not significantly different from those for the raw unadjusted Settlement Tank discharge data.

Settlement Tank discharge was considered as the dependant variable with meteorological data as the independent variables for multiple regression analysis. Analysis was performed on unadjusted discharge data and discharge data that had had the long-term trend removed.

Both the simultaneous and the stepwise multiple regression analyses give stronger correlations than the strongest single correlation (average daily temperature, -0.43 for the same data as the multiple regression analysis). For both simultaneous and stepwise regression analysis, the results were slightly better when using the discharge data with the long-term trend removed.

The best regression method for the data was using stepwise regression on the discharge data with the trend removed, with the highest R (0.51) and R square values (0.26) and the lowest RMSE (448).

The resulting models show seasonal fluctuations in leachate discharge, with high flows in winter and low flows in summer. The actual data shows significant short-term fluctuations that cannot be modelled using this simple multiple regression based approach. The multiple regression analysis has however highlighted average daily temperature as the most important variable in determining discharge for the Settlement Tank.

5.5.3.3 Seasonal Data

Settlement Tank discharge data in the winter (October to March) and summer (April to September) were analysed separately. Stronger correlations for simple bivariate regression and multiple regression were obtained for the summer data than for the winter, emphasising the importance of temperature on evaporative losses.

Although better correlations are obtained for simple regression of the summer data rather than all the data, when using multiple regression analysis the best correlations are obtained when using all the data set.

5.6 WATER BALANCE

5.6.1 WATER BALANCE ACROSS SITE

The active part of the landfill, Phase I is 20.1 ha. Golder Associates (1993b) estimated the surface water catchment area as 1060000 m² (106 ha). There are a number of drainage ditches around the site intercepting surface runoff preventing it from entering the landfill site.

5.6.1.1 Water Catchment area as 106 ha

The following calculation assumes that the rainfall catchment that feeds into the landfill is the 106 ha estimated by Golder Associates (1993b) as the surface water catchment. The data used is between April 01 and May 04 where there are synchronous discharge and rainfall data (819 days contain both data). The water balance across the site is calculated as follows:

Total discharge through Settlement Tank	= 872521 m ³
Total rainfall input over 106 ha catchment	= 2219004 m ³
Percentage of discharge accounted for by rainfall input	= 249%

The following calculation also assumes that the rainfall catchment is 106ha but uses Effective Rainfall values. The water balance across the site is calculated as follows:

Total discharge through Settlement Tank	= 872521 m ³
Total Effective Rainfall input over 106 ha catchment	= 3259712 m ³
Percentage of discharge accounted for by rainfall input	= 374%

Using at catchment of 106 ha there is more water entering the site as rainfall than exiting. Either the catchment is too big or water is being lost from the site to groundwater. Since surface water catchment ditches surround the active part of the landfill, it is fair to assume that the catchment size used in this analysis is too big.

5.6.1.2 Water Catchment is landfill area (20.1 ha)

The following calculation assumes that the rainfall catchment that feeds into the landfill is the active landfill area (20.1 ha). The data used were collected between April 01 and May 04 where there are discharge and rainfall data for both days (819 days contain both data).

The water balance across the site is calculated as follows:

Total discharge through Settlement Tank	= 872521 m ³
Total rainfall input over 20.1 ha catchment	= 618115 m ³
Percentage of discharge accounted for by rainfall input	= 70.8%

The following calculation also assumes that the rainfall catchment is 20.1 ha but uses Effective Rainfall values. The water balance across the site is calculated as follows:

Total discharge through Settlement Tank	= 872521 m ³
Total Effective Rainfall input over 20.1 ha catchment	= 464940 m ³
Percentage of discharge accounted for by rainfall input	= 53.3%

Using a catchment of 20.1 ha there is more water exiting the site than is entering as rainfall. Either the effective catchment is bigger or there is water entering the site as groundwater. It is likely that both these are the case.

5.6.1.3 Calculation of Catchment Area to account for all Rainfall Input

The catchment area can be calculated assuming that all the rainfall landing on site is collected and is discharged through the Settlement Tank with no groundwater additions or losses to groundwater. The data used is between April 01 and May 04 where there are discharge and rainfall data for both days (819 days). The catchment area can be calculated as follows:

Total discharge through Settlement Tank	= 872521 m ³
If rainfall input was the same as the discharge	= 872521 m ³
Rainfall depth over period when discharge was measured	= 3.08 m
Catchment required to produce rainfall input	= 283728 m ²

$$= 28.37 \text{ ha}$$

Assuming that all the Effective Rainfall landing on site is collected and is discharged through the Settlement Tank with no groundwater additions or losses to groundwater, the catchment area can be calculated as follows:

Total discharge through Settlement Tank	= 872521 m ³
If rainfall input was the same as the discharge	= 872521 m ³
Rainfall depth over period when discharge was measured	= 2.09 m
Catchment required to produce rainfall input	= 416796 m ²
	= 41.68 ha

5.6.1.4 Water Catchment area estimated as 25 ha

Looking at the drainage map of the site (Figure 3.33), it appears that the area within the drainage ditches is approximately 25 ha. This is a smaller catchment than the catchments calculated above based on rainfall/Effective Rainfall as the only input. This suggests that groundwater is entering the site.

The data used were collected between April 01 and May 04 where there are discharge and rainfall data for both days (819 days contain both data). The water balance across the estimated catchment is calculated as follows:

Total discharge through Settlement Tank	= 872521 m ³
Total rainfall input over 25 ha catchment	= 768800 m ³
Percentage of discharge accounted for by rainfall input	= 88%

The following calculation also assumes that the rainfall catchment is 25 ha but uses Effective Rainfall values. The water balance across the site is calculated as follows:

Total discharge through Settlement Tank	= 872521 m ³
Total Effective Rainfall input over 20.1 ha catchment	= 523350 m ³
Percentage of discharge accounted for by rainfall input	= 60%

Assuming a catchment size of 25 ha, the percentage of discharge accounted for by rainfall input is 88% and the percentage of discharge accounted for by Effective Rainfall input is 60%. So between 104000 m³ and 350000 m³ entered the site over the 819 days as groundwater input, i.e. approximately between 46000 m³ and 156000 m³ a year. The true value is likely to be somewhere between the two.

5.6.2 WATER BALANCE ON CAPPED SOUTHERN SLOPE

Section 2.5.2.2 details a spreadsheet (Koerner & Daniel, 1997; Environmental Protection Agency, 2003) that can be set up for analysing the annual water balance on a landfill cap using monthly averages. This method was used for Silent Valley to calculate the water balance on the capped Southern Slope (Table 5.34).

5.6.2.1 Row A: Average Monthly Temperature

The average monthly temperatures (°C) recorded at Silent Valley by Silent Valley Waste Services' weather station between October 1998 and June 2004 are given in Table 5.35 and figure 5.68. The values in Table 5.35 are used in the calculation. The error bars in figure 5.69 give the minimum and maximum average monthly temperatures recorded between October 1998 and June 2004.

Month	Average Temperature (°C)
January	4.0
February	4.0
March	5.9
April	7.7
May	11.5
June	14.2
July	15.9
August	16.2
September	13.5
October	9.4
November	6.3
December	3.8

Table 5.35 Table showing average monthly temperatures recorded at Silent Valley between October 1998 and June 2004.

ROW	PARAMETER	JAN	FEB	MAR	APR	MAY	JUN	JUL	AUG	SEP	OCT	NOV	DEC	TOTAL
A	Av Monthly Temp	4	4	5.9	7.7	11.5	14.2	15.9	16.2	13.5	9.4	6.3	3.8	
B	Monthly Heat Index	0.71	0.71	1.28	1.92	3.53	4.86	5.76	5.93	4.5	2.6	1.42	0.66	33.89
C	Unadjusted daily PE	0.63	0.63	0.94	1.24	1.88	2.34	2.63	2.69	2.22	1.53	1.01	0.6	
D	Poss Monthly Dur of Sunlight	22.2	23.4	30.6	34.5	39.9	40.8	41.1	37.5	31.8	27.6	22.8	21	373.2
E	PET	13.97	14.73	28.83	42.84	75.12	95.6	108.28	100.73	70.7	42.15	22.99	12.53	628.48
F	Precipitation	198	200	121	149	106	70	79	79	86	225	222	247	1782
G	Runoff Coefficient	0.42	0.42	0.42	0.42	0.42	0.42	0.42	0.42	0.42	0.42	0.42	0.42	
H	Runoff	83.16	84	50.82	62.58	44.52	29.4	33.18	33.18	36.12	94.5	93.24	103.74	748.44
I	Infiltration	114.84	116	70.18	86.42	61.48	40.6	45.82	45.82	49.88	130.5	128.76	143.26	
J	Infiltration-PET	100.87	101.27	41.35	43.58	-13.64	-55	-62.46	-54.91	-20.82	88.35	105.77	130.73	
K	Accumulated Water Loss	0	0	0	0	-13.636	-68.631	-131.1	-186.01	-206.83	-206.83	-206.83	-206.83	
L	Water Stored	75	75	75	75	62.2523	35.3798	31.9478	35.4192	56.4315	75	75	75	
M	Change in Water Storage	0	0	0	0	-12.748	-26.872	-3.432	3.47139	21.0123	18.5685	0	0	
N	Actual ET	13.97	14.73	28.83	42.84	74.23	67.47	49.25	42.35	28.87	42.15	22.99	12.53	440.21
O	Percolation	100.87	101.27	41.35	43.58	0	0	0	0	0	69.78	105.77	130.73	593.35
P	Check	198	200	121	149	106	70	79	79	86	225	222	247	1782
Q	Percolation Rate (Flux)	3.80E-08	4.20E-08	1.50E-08	1.70E-08	0	0	0	0	0	2.60E-08	4.10E-08	4.90E-08	

Root Depth	200	200	200	200	200	200	200	200	200	200	200	200	200
Field Capacity	0.375	0.375	0.375	0.375	0.375	0.375	0.375	0.375	0.375	0.375	0.375	0.375	0.375
WS max	75	75	75	75	75	75	75	75	75	75	75	75	75
If IN-PET negative	297.53	299.18	131.96	136.03	62.25	35.38	31.95	35.42	56.43	250.76	318.14	447.41	
If IN-PET positive	175.87	176.27	116.35	118.58	61.36	7.26	-27.08	-22.97	14.6	144.78	180.77	205.73	

Table 5.34 Spreadsheet used to analyse the annual water balance on the Southern Slope landfill cap at Silent Valley landfill site using monthly averages.

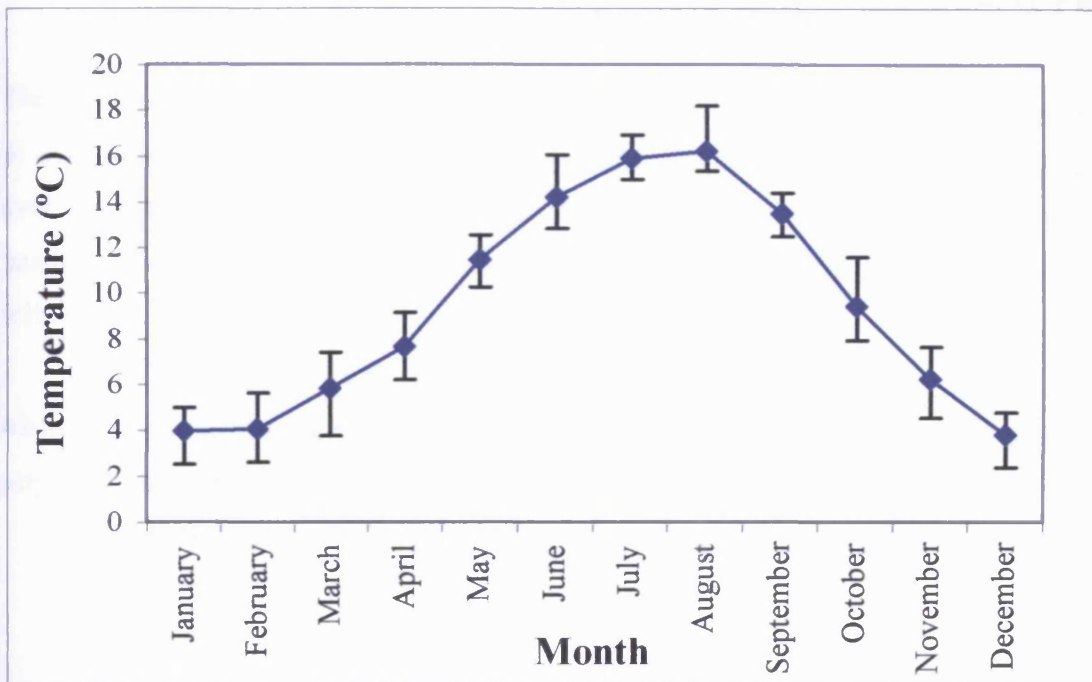


Figure 5.69 Graph showing the average, minimum and maximum monthly temperatures recorded at Silent Valley between October 1998 and June 2004.

5.6.2.2 Row B: Monthly Heat Index (H_m)

The monthly heat index (H_m) is a dimensionless, empirical parameter used to estimate evapotranspiration. Since the average monthly temperature recorded at Silent Valley is greater than 0°C , the monthly heat index is calculated using equation (13) as follows:

$$H_m = (0.2 T)^{1.514} \quad (13)$$

where T is the average monthly temperature in Row A.

The monthly values are summed to determine the annual heat index (H_a), which is entered into the 'total' column.

5.6.2.3 Row C: Unadjusted Daily Potential Evapotranspiration (UPET)

The unadjusted daily potential evapotranspiration (UPET) refers to the maximum amount of evapotranspiration that would occur if the soil were saturated with water. Since the average monthly temperature recorded at Silent Valley is between 0 °C and 27 °C, the unadjusted daily potential evapotranspiration can be calculated using equation (16) as follows:

$$UPET = 0.53(10T/H_a)^a \quad (16)$$

where T is the temperature in °C, H_a is the annual heat flux, and a is a dimensionless empirical factor that is computed as follows:

$$a = (6.75 \times 10^{-7})H_a^3 - (7.71 \times 10^{-5})H_a^2 + 0.01792H_a + 0.49239 \quad (18)$$

5.6.2.4 Row D: Monthly Duration of Sunlight (N)

The mean possible monthly duration of sunlight (N) is determined by looking at the table (Appendix C) for the northern hemisphere by Thornthwaite and Mather (Koerner & Daniel, 1997). The values are expressed as units of 12 hour periods. Silent Valley landfill is located at a latitude of 51:45 N. On the table the closest latitude is 50 degrees so this is used.

5.6.2.5 Row E: Potential Evapotranspiration (PET)

The potential evapotranspiration is calculated by multiplying the values for the unadjusted daily potential evapotranspiration (Row C) and the monthly duration of sunlight (Row D).

5.6.2.6 Row F: Precipitation (P)

The precipitation (P) for the site is entered in Row F. Since there are gaps in the rainfall data collected by Silent Valley Waste Services, the monthly rainfall bought from the Met Office will be used (Table 5.36). The monthly rainfall varies from year to year as shown by figure 5.70. The rainfall recorded by silent Valley Waste Services varies by the same amount.

Month	Average Rainfall (mm)
January	198
February	200
March	121
April	149
May	106
June	70
July	79
August	79
September	86
October	225
November	222
December	247

Table 5.36 Table showing average monthly rainfall recorded at Cwm by the Met Office between April 2000 and May 2004.

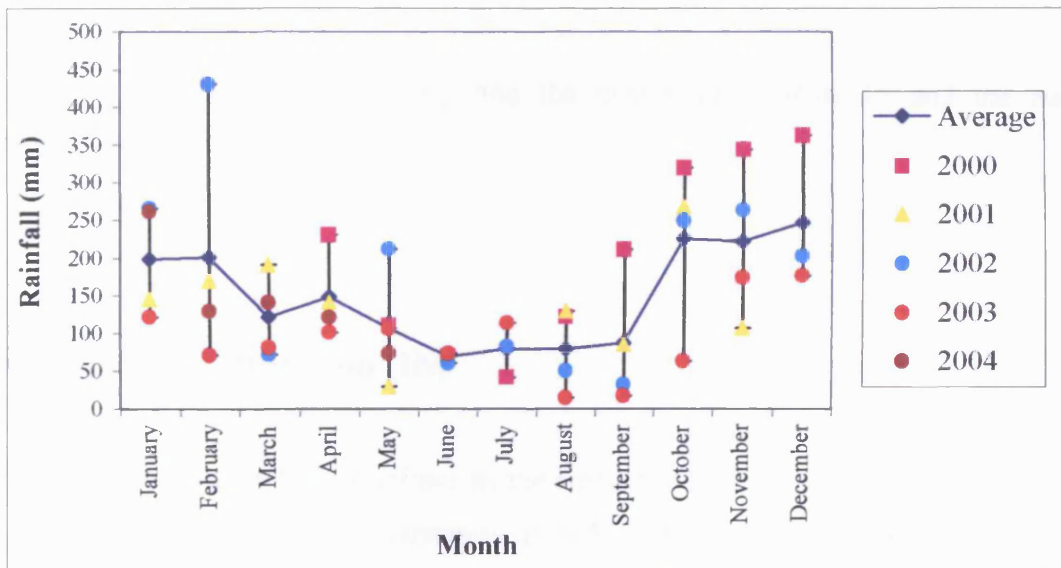


Figure 5.70 Graph showing the average, minimum and maximum monthly rainfall recorded at Cwm by the Met Office between April 2000 and May 2004.

5.6.2.7 Row G: Runoff Coefficient (C)

The runoff coefficient (C) is dimensionless and is defined as the ratio of runoff to precipitation.

No site-specific information is available for Silent Valley, so a runoff coefficient can be taken from table 2.15 or table 2.12. The southern slope at Silent Valley is about 30% and is a grassed clayey overburden. Using table 2.15, a clayey soil at a steep angle ($\geq 7\%$) gives a runoff coefficient of 0.25-0.35. Table 2.12 gives a runoff coefficient of 0.42 for a grassed loamy clay 10-30% slope. Due to the high slope angle, a runoff coefficient of 0.42 is used for this calculation.

5.6.2.8 Row H: Runoff (R)

Runoff (R) is calculated by multiplying the precipitation (Row F) and the runoff coefficient (C) (Row G).

5.6.2.9 Row I: Infiltration (IN)

The monthly infiltration (IN) is defined as the amount of water entering the surface of the cover and is assumed to equal precipitation (Row F) minus runoff (Row H):

$$IN = P - R \quad (20)$$

5.6.2.10 Row J: Infiltration minus Potential Evapotranspiration (IN-PET)

The difference between infiltration (Row I) and potential evapotranspiration (Row E) ($IN-PET$) is entered into Row J. Positive values are given for January, February, March, April, October, November and December indicating potential accumulation (storage) of water in the cover soil. Negative values are obtained for May, June, July, August and September indicating that the soil is drying.

5.6.2.11 Row K: Accumulated Water Loss (WL)

The accumulated water loss (WL) is the sum of the negative monthly values of $IN-PET$ (Row J) since the beginning of the year.

5.6.2.12 Row L: Water Stored in Root Zone (WS)

The water stored in the root zone (WS) is defined as the amount of water (in mm) stored in the portion of the soil cover that can be tapped by plant roots for evapotranspiration. The amount of water stored in the root zone is calculated from the volumetric water content (θ) of the soil and the depth of the root zone (H_{root}) using equation (21) as follows:

$$WS = \theta H_{root} \quad (21)$$

The volumetric water content (θ) is defined as the volume of water (V_w) divided by the total volume of the soil (V).

Assuming a root zone (H_{root}) of 200 mm and a volumetric water content (θ) of 0.375 (based on table 5.37), the water stored in the root zone (WS) is 75 mm.

Type of Soil	θ at Field Capacity
Fine sand	0.12
Sandy Loam	0.20
Silty Loam	0.30
Clay Loam	0.375
Clay	0.45

Table 5.37 Suggested Volumetric Water contents of various soils. From Koerner & Daniel, 1997.

5.6.2.13 Row M: Change in Water Storage (CWS)

The change in water storage (CWS) in a month is the water stored (WS) (Row L) in that month minus the water stored in the previous month. If CWS is negative (as for May, June and July) then the soil in the root zone is losing water and if it is positive it is gaining water (August, September, October). There is no change in water stored for November, December, January, February, March and April.

5.6.2.14 Row N: Actual Evapotranspiration (AET)

The actual evapotranspiration (*AET*) depends on whether infiltration exceeds potential evapotranspiration. If there is less infiltration than potential evapotranspiration, the soil in the root zone is losing water through evapotranspiration.

5.6.2.15 Row O: Percolation (PERC)

Percolation (*PERC*) is the amount of water draining from the root zone. The monthly percolation has been summed to obtain an annual percolation of 593 mm.

5.6.2.16 Row P: Check for Calculations (CK)

The previous calculations are checked. Each monthly value and the yearly total equals the precipitation *P*, i.e. Row P equals Row F for each column.

5.6.2.17 Row Q: Percolation Rate (FLUX)

The rate of percolation (*FLUX*) is the flux of water passing through the cover soil.

5.6.2.18 Summary

The percolation over a year is 593 mm, which represents 33% of the precipitation (Table 5.38). The percolation occurred over January, February, March, April, October,

November and December. This corresponds with the increase in predicted leachate discharge obtained from the multiple regression models for both the BSC Pipe and the Settlement Tank.

Parameter	Annual Amount (mm)	Percent of Precipitation
Precipitation	1782	100
Runoff	748.4	42
Actual Evapotranspiration	440.2	25
Percolation	593.3	33

Table 5.38 Table showing analysis results of the annual water balance on the southern Slope at Silent Valley landfill.

The actual evaporation calculated in this model (25%) compares well with the actual evaporation of the MORECS data for Cwm (23%) bought from the Met Office (Section 5.3.1).

If the percolation was the same over the entire landfill catchment then a percolation of 593 mm (0.593 m) over 25 ha (catchment area in section 5.6.1.4) would contribute about 148250 m³ to the discharge through the site, which is approximately a quarter of the measured discharge through the Settlement Tank. The actual percolation over the entire site is likely to contribute more than this because the southern slope has an overburden cap and a higher runoff coefficient than the rest of the site, which would lead to lower percolation on the southern slope than the rest of the site.

CHAPTER 6

LEACHATE COMPOSITION

This chapter details historical leachate analysis of LP1 exiting the BSC Pipe from 1993 to the present. In addition, Ion Chromatography (IC) analyses that have been performed as part of the present investigation on leachate exiting the BSC Pipe (LP1) and the Settlement Tank are presented.

Details are given of the two conductivity sensors that were installed in LP1 (BSC Pipe) and the Settlement Tank in January 2003. The leachate conductivity results are compared with the Ion Chromatography results.

6.1 LEACHATE ANALYSIS - PRE PROJECT

6.1.1 PAST STUDIES

A small number of short-term monitoring studies have been undertaken at Silent Valley in the past. The first was by Knox Associates (1995) who studied the leachate exiting the site between July 1993 and October 1994. They found that the leachate from the Settlement Tank and Armco pipe (a flow into LP2A; Fig. 5.8) were very similar to each other and were typical dilute methanogenic leachates. However, they found the quality of the BSC flow (LP1) to be not at all typical of landfill leachates. It was dominated by inorganic ions, particularly sulphate. The BSC flow appeared to be primarily derived from percolation through inorganic materials and not from decomposing municipal or similar wastes.

It is believed that the source of the majority of the sulphate originates from the leaching of the large area of slag deposited by the British Steel Company in the Nant Merddog Valley, and now being excavated for daily cover, which lies in the catchment area of the BSC pipe (Fig. 4.27 and 4.28). The presence of high levels of sulphate is not conducive to the process of methanogenesis, and can cause instead, the reduction of sulphate to form sulphide. It is not known to what extent this process is taking place within the landfill and whether it is affecting leachate quality (Ove Arup & Partners, 1997).

Microtox toxicity testing by the NRA of effluent from the BSC pipe has indicated that it is probably non-toxic (Ove Arup & Partners, 1997). However, the Microtox test is essentially a test of ecotoxicity and may not give information on other toxic aspects such as its carcinogenic, mutagenic, teratogenic and hormonal effects.

6.1.2 HISTORICAL DATA COLLECTED BY SILENT VALLEY

Silent Valley Waste Services collect and analyse leachate samples once a month as part of their Environment Agency monitoring programme. Blaenau Gwent Borough Council and Silent Valley Waste Services keep records of leachate that they have analysed. Data from both sources were combined for this study.

Over the years the sampling points have altered. LP1 originates from a single pipe (the BSC pipe (Fig. 5.8), and is collected as a sample before mixing with other flows. LP2A is a combination of different flows originating from different pipes. Before March 2000 the different flows were collected as separate samples, LP2, LP3, LP5, LP6 and LP7. LP3A is the combination of LP1 and LP2A and became a new sampling point in March 2000 when LP2A sampling started. LP4 originates from a pipe entering directly into the settlement tank (Fig. 5.4).

Here the results for LP1 are examined. Data for the leachate exiting the BSC Pipe goes back the furthest and can be compared with analysis performed for the current study. Results are available from July 1993 to May 2004, with a gap between February 1996 and June 1997.

The time series graphs for selected determinands are presented below, together with trendlines and R-squared values. The R-squared values can be interpreted as the proportion of the variance in y attributable to the variance in x , in this case, the degree of variation explained by time (addresses the question, is there a consistent trend?). The R-squared value displayed with a trendline is not an adjusted R-squared value. For logarithmic, power, and exponential trendlines, Microsoft Excel uses a transformed regression model.

6.1.2.1 pH

For LP1 the measured pH values vary between 6.37 and 8.81. The pH value has gradually decreased over the past 11 years, with the last couple of years showing a possible slight increase again (Fig. 6.1). The decrease in pH could indicate that the leachate exiting the BSC Pipe is being generated under different conditions now compared with 11 years ago.

The production of CO₂ by oxidation of organic matter lowers the pH of water (Deutsch, 1997). CO₂ is produced during all the stages of organic waste degradation (Fig. 2.7) so this could be a factor lowering the pH over the sample period.

6.1.2.2 Temperature

For LP1 the measured temperature varies between 11.9 °C and 35.8 °C. The temperature has gradually increased over the past 11 years (Fig. 6.2). A polynomial trendline is shown on the graph, and indicates an increase in temperature over the period. The increase in temperature could indicate that the leachate is being generated in association with greater exothermic biochemical processes, probably related to the increase in organic material within the accumulating domestic waste.

6.1.2.3 Electrical Conductivity

The conductivity of a solution is a measure of its capacity to convey an electric current. Conductivity is related to the nature and concentration of ionised substances present in the solution and to the temperature of the solution.

The historical data (SV Data) show a variation in conductivity from 0.042 to 4.24 mS (average 2.5 mS) (Fig. 6.3). If the samples (MSc Data) analysed during July 2000 for an MSc project (Paris, 2000) are included, the maximum value recorded is 5.3 mS with an

average of 2.94 mS. There is a large variation in measured conductivity that could be due to the changing constituent makeup of the leachate.

6.1.2.4 Ammoniacal Nitrogen

Ammoniacal nitrogen ($\text{NH}_4\text{-N}$) is the combined concentrations of nitrogen as ammonia and ammonium compounds. The slow leaching of wastes producing nitrogen and no significant mechanism for transformation of N-NH_3 in the landfills causes a high concentration of ammoniacal nitrogen in leachate over a long period of time. Concentrations of above a few mg/l can be directly toxic to fish.

For LP1 the measured ammoniacal nitrogen varies between 0.04 and 117 mg/l. A polynomial trendline is shown on the graph (Fig. 6.4), and indicates an increase in ammoniacal nitrogen over the monitored period. This could indicate that the conditions where the leachate is being formed is moving from oxic to anoxic conditions.

6.1.2.5 Alkalinity

Alkalinity is measured by titration and is expressed in units of milligrams per litre (mg/l) of CaCO_3 (calcium carbonate). It is a measure of the buffering capacity of water, or the capacity of bases to neutralise acids. The buffering materials are primarily the bases bicarbonate (HCO_3^-), and carbonate (CO_3^{2-}), and occasionally hydroxide (OH^-), borates, silicates, phosphates, ammonium, sulphides, and organic ligands. Above pH 8.3, alkalinity is mostly in the form of carbonate (CO_3^{2-}); below 8.3, alkalinity is present mostly as bicarbonate (HCO_3^-).

Levels of 20-200 mg/l are typical of fresh water. A total alkalinity level of 100-200 mg/l will stabilise the pH level in a stream. Levels below 10 mg/l indicate that the system is poorly buffered, and is very susceptible to changes in pH from natural and human-caused

sources. Alkalinity not only helps regulate the pH of a water body, but also the metal content. Bicarbonate and carbonate ions in water can remove toxic metals (such as lead, arsenic, and cadmium) by precipitating the metals out of solution (Murphy, 2002).

For LP1 the measured alkalinity varies between 43 and 1380 mg/l. A polynomial trendline is shown on the graph (Fig. 6.5), and indicates an increase in alkalinity over the period. Alkalinity concentrations are generally expected to increase during Phase III of leachate generation owing to conversion of fatty acids (Andreottola & Cannas, 1992).

Large amounts of CO₂ produced during the breakdown of waste often give rise to carbonate dissolution and to strongly enhanced alkalinity. It is possible that fatty acids in the leachate are also contributing to the alkalinity (Appelo & Postma, 1996).

6.1.2.6 Chemical Oxygen Demand (COD)

Chemical oxygen demand is a measure of the total amount of chemically oxidisable material present in the liquid. It is a measure of potential energy available for animals.

For LP1 the measured COD varies between 21 and 752 mg/l. A power trendline is shown on the graph (Fig. 6.6), and indicates an increase in COD over the period. More organics are appearing in the leachate over time.

6.1.2.7 Biochemical Oxygen Demand (BOD)

Biochemical oxygen demand is a measure of the amount of material present in water that can be readily oxidised by micro-organisms and thus a measure of the power of that material to take up the oxygen in water (DoE, 1995). The COD value is normally higher than the BOD value because more organics can be oxidised chemically than are biodegradable in the BOD test.

For LP1 the measured BOD varies between 1.2 and 33 mg/l. A power trendline is shown on the graph (Fig. 6.7), and indicates an increase in BOD over the period. Again this shows that more organics are appearing in the leachate over time.

6.1.2.8 BOD/COD Ratio

The BOD/COD ratio is an indication of the proportion of biologically degradable carbon to "total" (chemically oxidisable) carbon. The BOD/COD ratio will decrease in the methanogenic waste as the amount of degradable carbon decreases as a result of microbial activity (Westlake, 1995).

For LP1 the measured BOD/COD ratio varies between 0.006 and 0.18. A power trendline is shown on the graph (Fig. 6.8), and indicates a decrease in the BOD/COD ratio over the period, suggesting a progressive increase in methanogenic microbial activity.

6.1.2.9 Total Organic Carbon (TOC)

Total Organic Carbon (TOC) measures the amount of carbonaceous material present.

For LP1 the measured TOC varies between 9.6 and 126 mg/l. A polynomial trendline is shown on the graph (Fig. 6.9), and indicates an increase in TOC over the period. The carbonaceous material is being broken down by biological activity so higher concentrations are flowing out with the leachate.

6.1.2.10 Metals

Sodium, potassium, calcium, magnesium, iron, manganese, cadmium, chromium, copper, nickel, lead, zinc and mercury have been regularly analysed for in LP1. Their minimum, maximum and mean recorded values are given in table 6.1.

DETERMINAND	MINIMUM (mg/l)	MAXIMUM (mg/l)	MEAN (mg/l)
Sodium (Na)	175	734	433
Potassium (K)	161	396	278
Calcium (Ca)	41.1	327	174
Magnesium (Mg)	22.8	274	72
Iron (Fe)	0.1	14.4	0.85
Manganese (Mn)	0.105	2.78	0.85
Cadmium (Cd)	0.0002	0.002	0.0004
Chromium (Cr)	0.011	0.264	0.040
Copper (Cu)	0.0095	0.053	0.023
Nickel (Ni)	0.011	0.09	0.043
Lead (Pb)	0.0007	0.174	0.0085
Zinc (Zn)	0.021	0.328	0.051
Mercury (Hg)	<0.0001	0.021	<0.018

Table 6.1 Chemical analysis results for metals in LP1 between July 1993 to May 2004.

Heavy metals (specifically chromium, nickel, copper, zinc, cadmium, lead and mercury) are not generally present at significant concentrations in landfill leachates (Waste Management Information Bureau, 1995). This is the case for leachate LP1 from the BSC Pipe.

Chromium is immobile in a reducing environment. The trace metals Cu, Cd, Pd and Zn are not normally mobile at high concentrations because they form relatively insoluble carbonate, oxide or sulphide minerals in either oxidising or reducing environments (Deutsch, 1997).

Figures 6.10 and 6.11 show how the metal concentrations varied between July 1993 to May 2004. Calcium, magnesium, copper, zinc, nickel, cadmium, lead and chromium have near horizontal trendlines indicating no significant variation in concentration over time.

Sodium, potassium and manganese exhibit upward trendlines suggesting an increase in concentration over time. The dissolved concentrations of iron and manganese are generally less than 0.1 mg/l in the natural environment. When reducing leachate from a landfill contacts manganese and iron hydroxide minerals, the minerals will dissolve because they are more soluble in a reducing environment (Deutsch, 1997). This could explain the increase in manganese over time.

Iron exhibits a slight downward trendline suggesting a decrease in iron concentrations over time. Since the iron is likely to be originating in the slag, it is possible that the available iron is being slowly leached away. However, it is more likely that the iron is being fixed as iron sulphide. The reduction of sulphate to sulphide usually requires the presence of sulphate-reducing bacteria (Deutsch, 1997).

Mercury can be metabolised by bacteria in anaerobic environments to produce methylmercury. Methylmercury can be readily bioaccumulated and biomagnified in the aquatic food chain. Mercury present within the leachate is often present at <0.0001 mg/l.

Celtic Technology (1995) reported elevated concentrations of metals across the entire site during their site investigation. They concluded that the alkaline ground conditions restrict the metals amenability into aqueous solution. Leach tests of the slag showed little evidence of metals in leachate and so Celtic did not perceive metals to provide a threat in terms of off-site migration.

Clearly the geochemical processes within the waste mass are complex, involve chemical and biological interaction and are likely to be strongly influenced by spatial and temporal variation in redox potential.

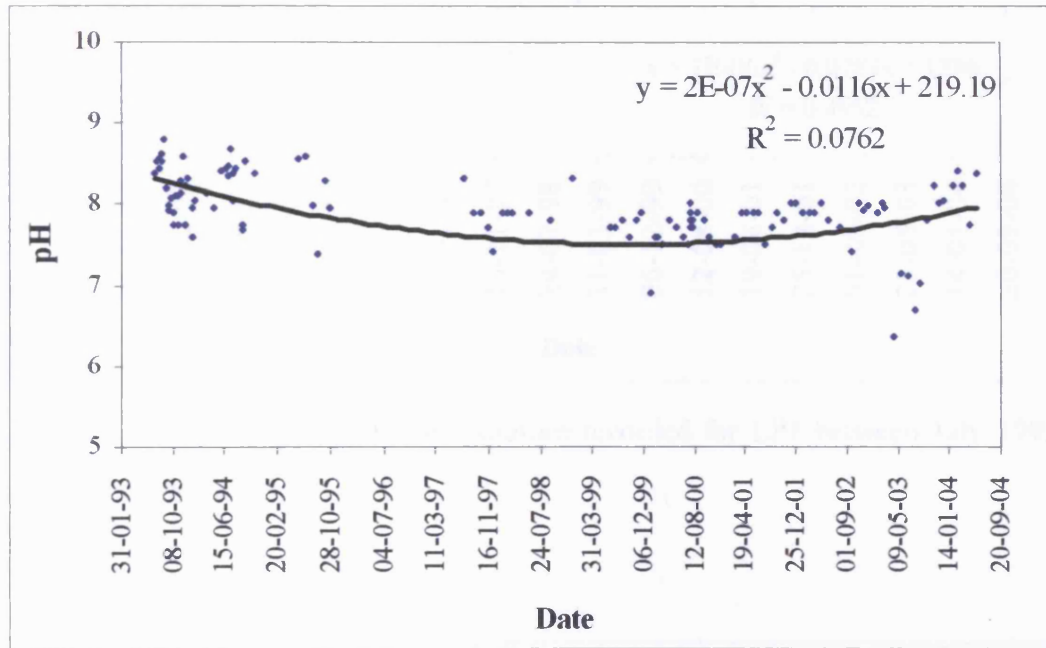


Figure 6.1 Graph showing the pH recorded for LP1 between July 1993 and May 2004.

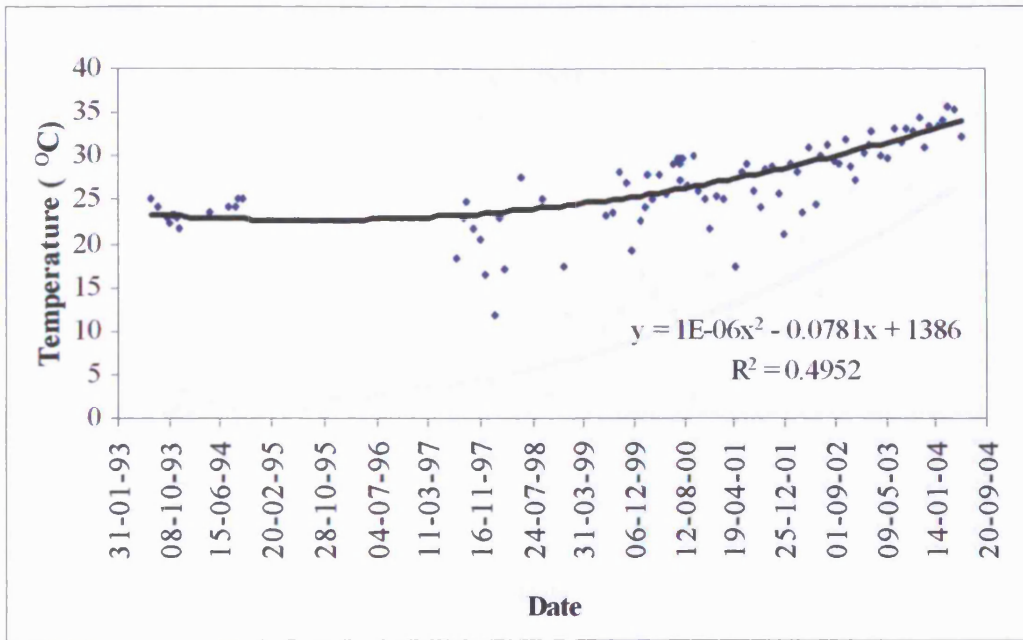


Figure 6.2 Graph showing the temperature recorded for LP1 between July 1993 and May 2004.

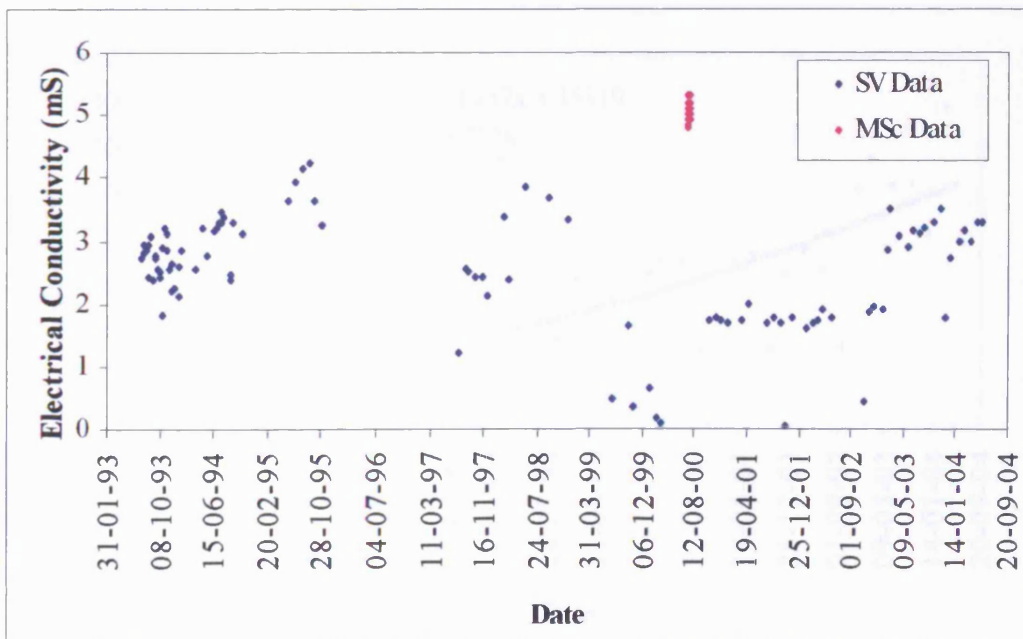


Figure 6.3 Graph showing the conductivity recorded for LP1 between July 1993 and May 2004.

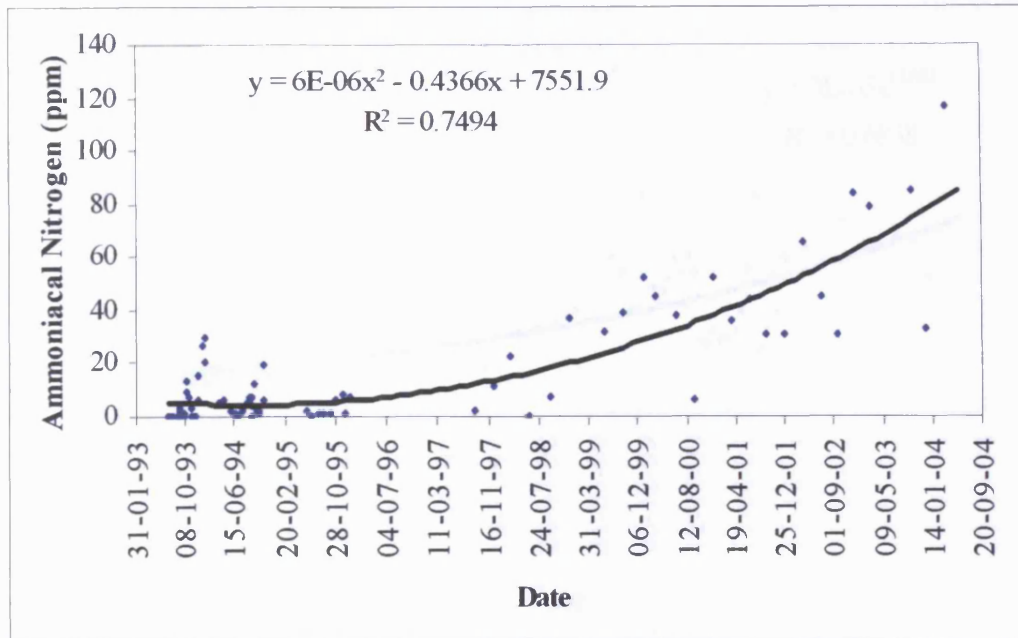


Figure 6.4 Graph showing the ammoniacal nitrogen recorded for LP1 between July 1993 and May 2004.

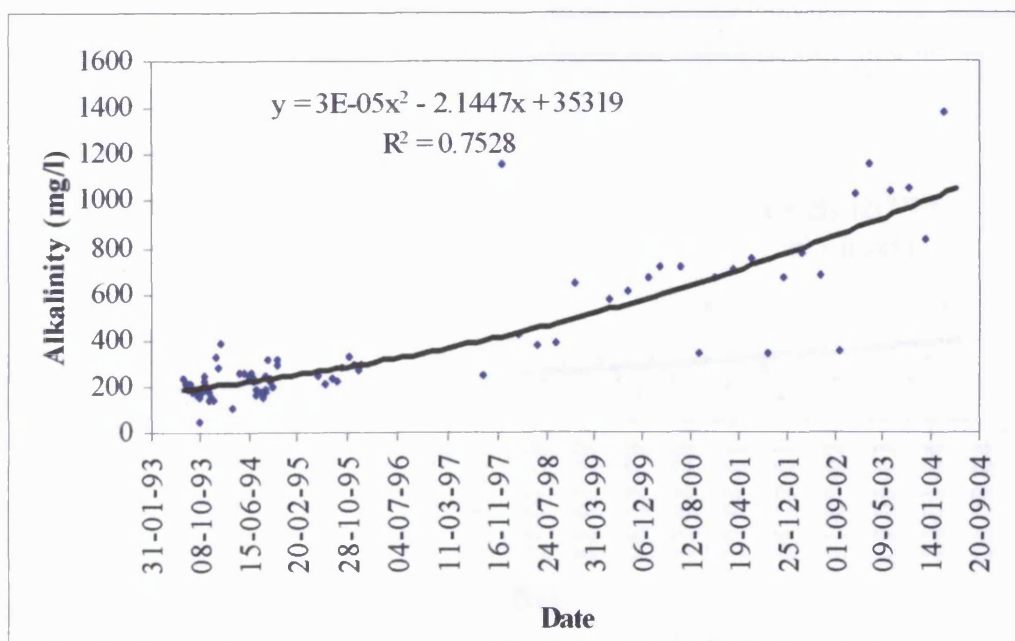


Figure 6.5 Graph showing the alkalinity recorded for LP1 between July 1993 and May 2004.

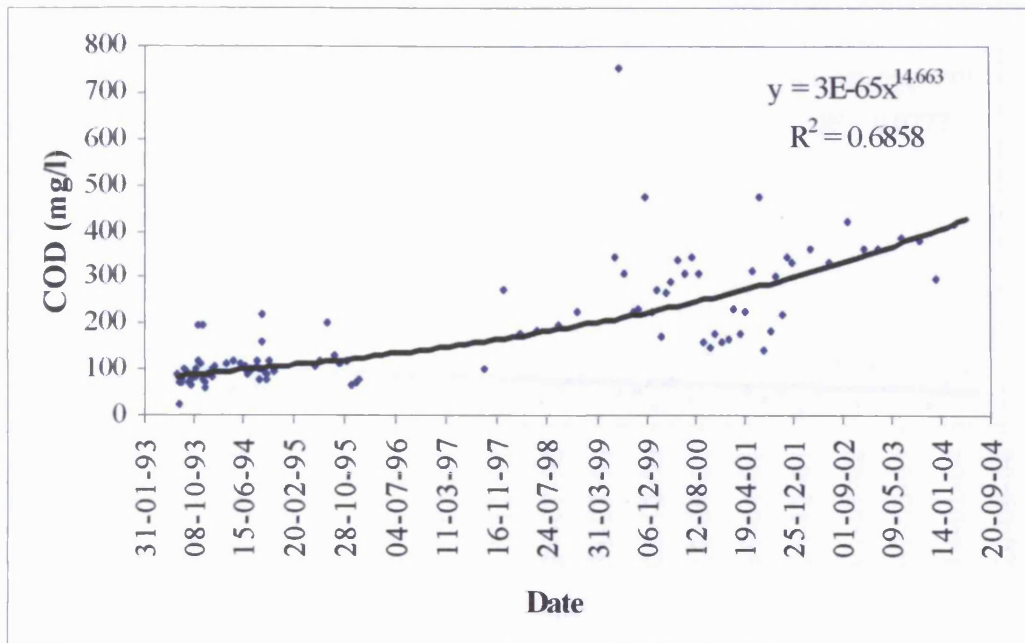


Figure 6.6 Graph showing the Chemical Oxygen Demand (COD) recorded for LP1 between July 1993 and May 2004.

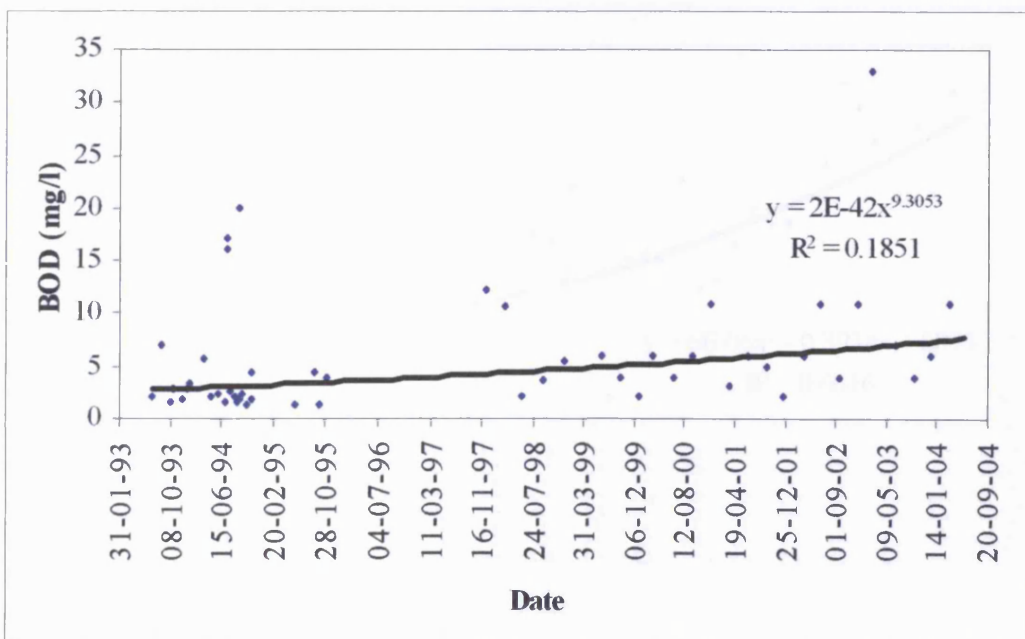


Figure 6.7 Graph showing the Biochemical Oxygen Demand (BOD) recorded for LP1 between July 1993 and May 2004.

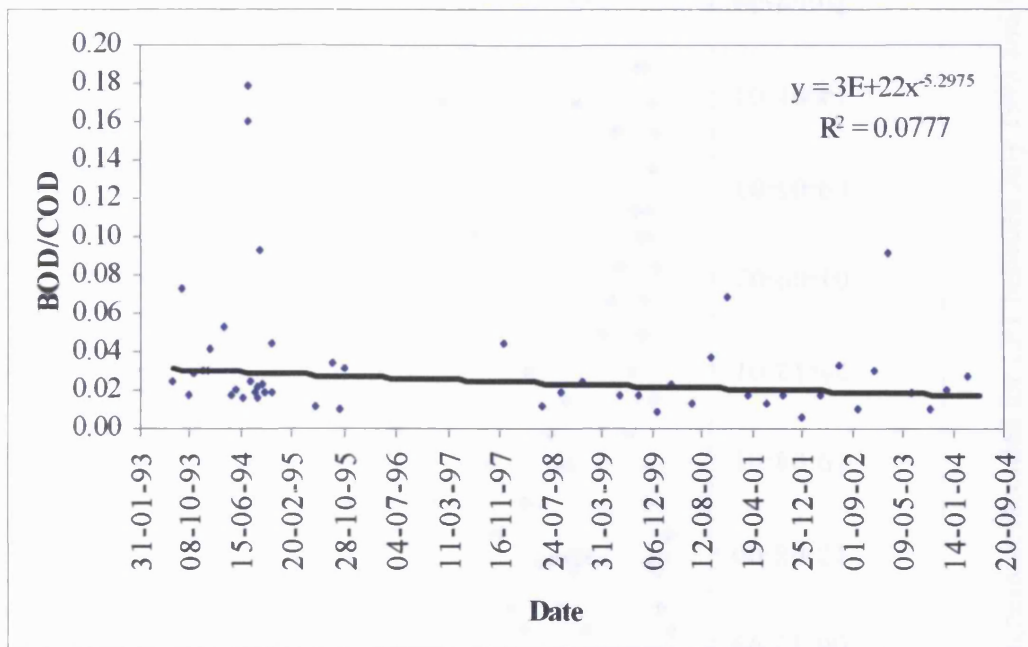


Figure 6.8 Graph showing the BOD/COD ratio recorded for LP1 between July 1993 and May 2004.

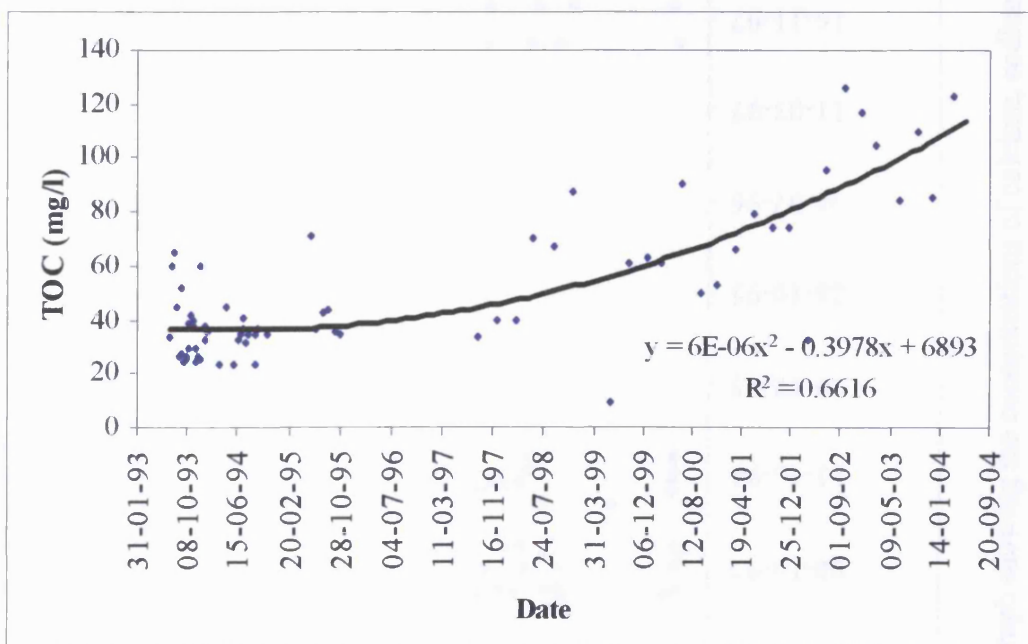


Figure 6.9 Graph showing the Total Organic Carbon (TOC) recorded for LP1 between July 1993 and May 2004.

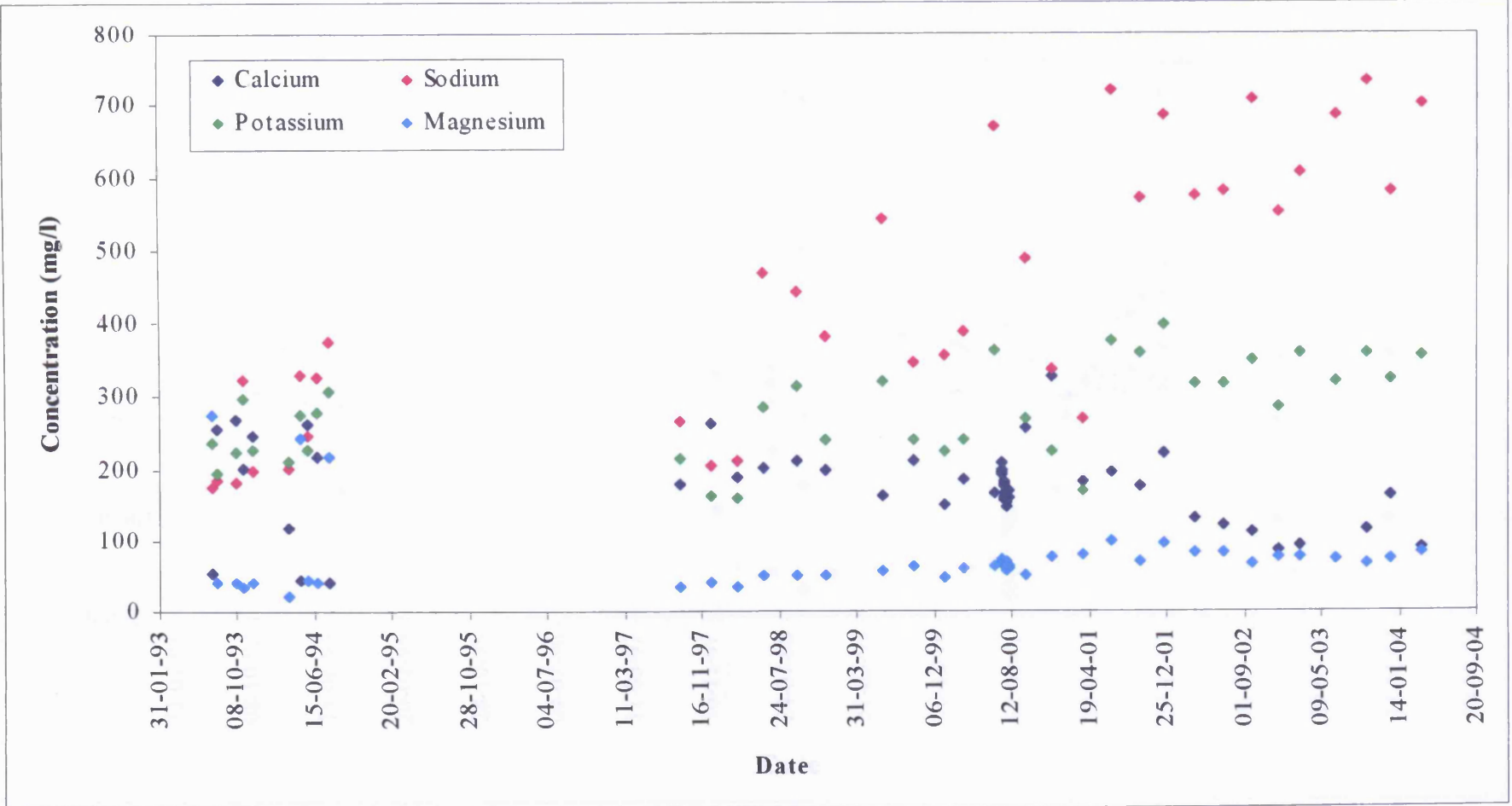


Figure 6.10 Graph showing the concentrations of calcium, sodium, potassium and magnesium recorded for LP1 between July 1993 and May 2004.

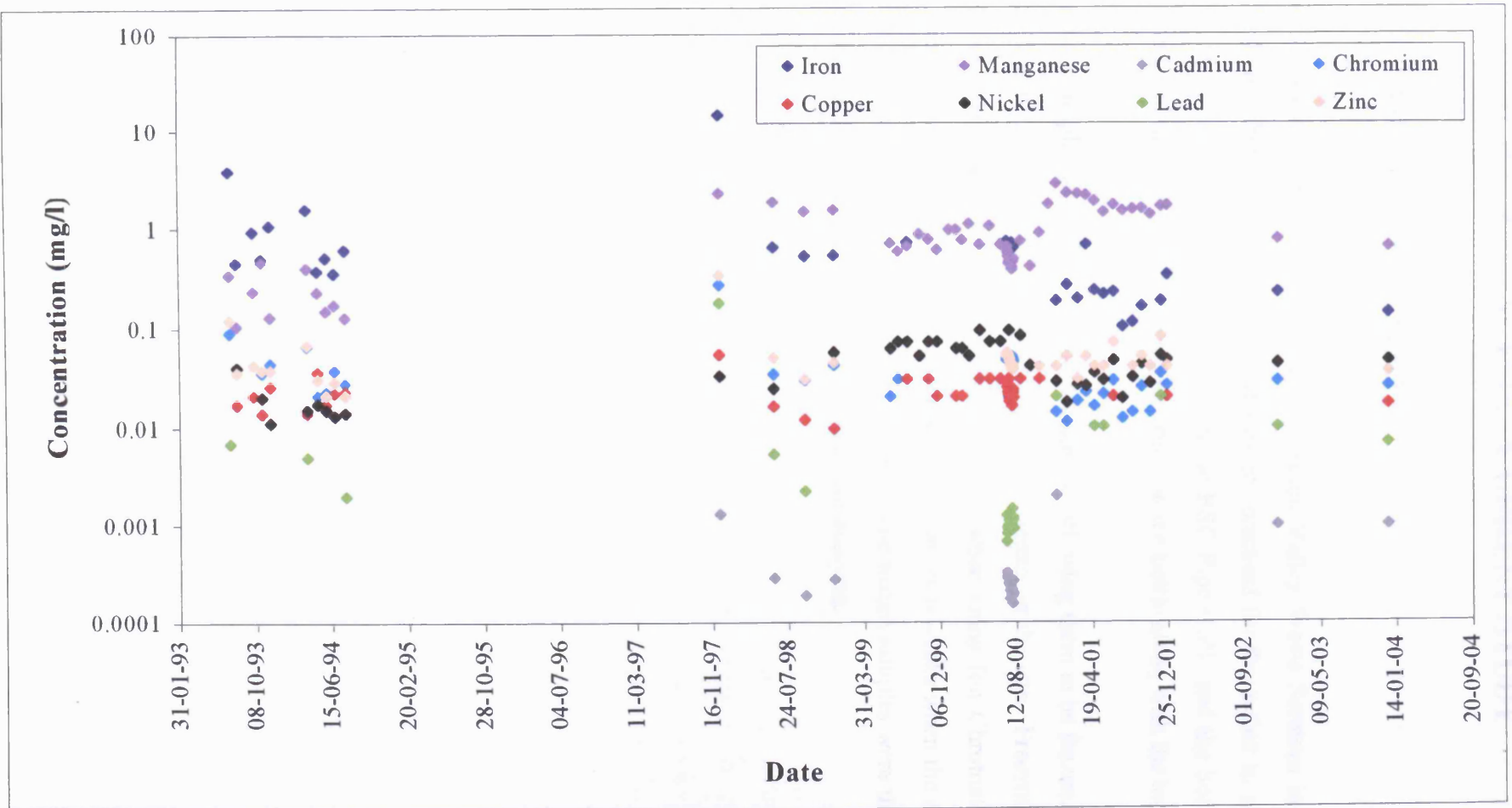


Figure 6.11 Graph showing the concentrations of iron, manganese, cadmium, chromium, copper, nickel, lead and zinc recorded for LP1 between July 1993 and May 2004.

6.2 LEACHATE ANALYSIS - CURRENT STUDY

6.2.1 SAMPLING STRATEGY

Samples were collected on weekdays by Silent Valley Waste Services in high density polyethylene bottles for the author. It was not practical for the author to go to site on a daily basis. Samples were collected from the BSC Pipe (LP1) and the Settlement Tank. The date and time of collection were recorded on the bottle along with the location.

Leachate samples were clear with no precipitate, allowing them to be frozen. The samples were frozen as soon as they were collected in a freezer at the site. Freezing the samples does not affect the results of chemical analysis when using Ion Chromatography (IC). Frozen samples were collected from the site about every 6 weeks when the author went to the site to download data from the data loggers. The frozen samples were then stored in a freezer at the University until they were ready for analysis.

6.2.2 ION CHROMATOGRAPHY (IC)

Ion Chromatography (IC) is the separation and quantification of anions and cations using Liquid Chromatography (LC). LC is an analytical technique based on the separation of the components of a mixture in solution by selective absorption. Ion chromatography is a high-performance version of ion-exchange chromatography.

In ion chromatography, a sample of the mixture to be analysed (the analyte) is applied to some stationary fixed material (the adsorbent) and then a second material (the eluent) is passed through or over the stationary phase. The compounds contained in the analyte are then partitioned between the stationary adsorbent and the moving eluent. The success of the method depends on the fact that different materials adhere to the adsorbent with different forces. So, as the eluent flows through the column, the components of the analyte will move down the column at different speeds and therefore separate from one another.

Each time analyte molecules/ions emerge from the chromatography column a detector generates a measurable signal that is usually printed out as a peak on the chromatogram. The chromatogram is a record of detector output vs. time as the analyte passes through the chromatography system. It usually consists of a series of peaks corresponding to the different times in which components of the analyte mixture emerge from the column.

6.2.2.1 Dionex DX-80

Leachate samples were analysed using a Dionex DX-80 with a column for analysing anions.

6.2.2.1.1 *Stages of Analysis*

Ion Chromatography analysis consists of four stages (Fig. 6.12):

1. Eluent Delivery

- Eluent, a liquid that helps separate the sample ions, carries the sample through the ion analyser. The DX-80 is an isocratic delivery system. This means that the eluent composition and concentration remain constant throughout the run.
- Liquid sample is injected into the eluent stream either manually or automatically.
- The pump forces the eluent and sample through a separator column

2. Separation

- As the eluent and sample are pumped through the column (a chemically-inert tube packed with a polymeric resin), the sample ions are separated. In the DX-80, the mode of separation is called ion exchange and it is based on the premise that different sample ions migrate through the IC column at different rates, depending upon the interactions with the ion exchange sites.

3. Detection

- After the eluent and the sample ions leave the column, they flow through a suppressor that selectively enhances detection of the sample ions while suppressing the conductivity of the eluent.
- A conductivity cell monitors and measures the electrical conductance of the sample ions as they emerge from the suppressor and produces a signal based on a chemical or physical property of the analyte.

4. Data Analysis

- The conductivity cell transmits the signal to a computer running chromatography software.
- The chromatography software (PeakNet® IA for the DX-80) analyses the data comparing the sample peaks in a chromatogram to those produced from a standard solution, identifying the ions based on retention time, and quantifying each analyte by integrating the peak area or peak height. The results are displayed as a chromatogram, with the concentrations of ionic analytes automatically determined and tabulated.

(Dionex Corporation, 2001)

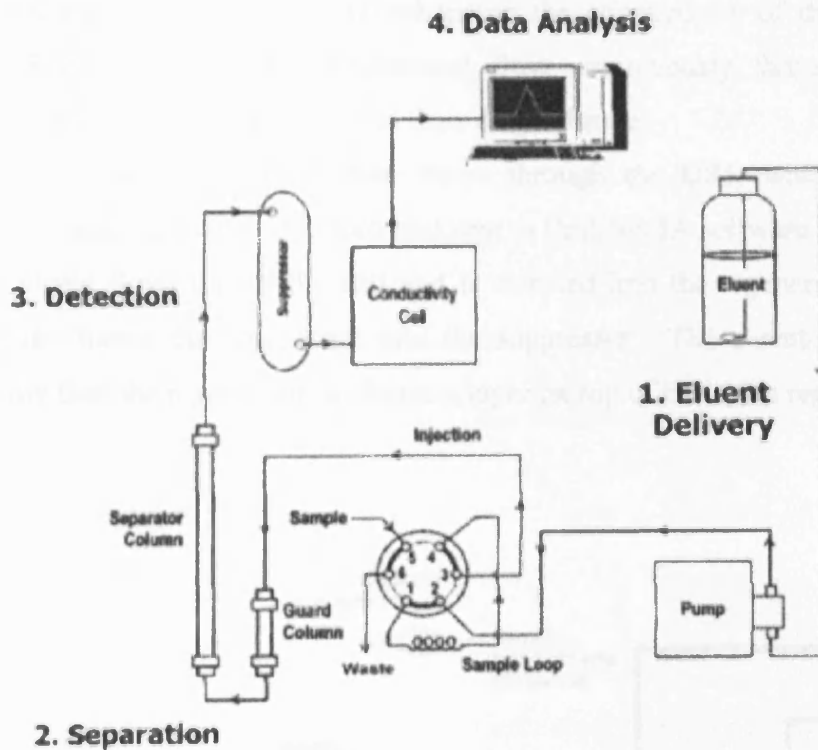


Figure 6.12 Ion analysis process. From Dionex Corporation (2001).

6.2.2.1.2 Flow path through the DX-80

Liquid flows through the DX-80 along the following path (Fig. 6.13):

- Eluent from the eluent reservoir is pressurised by gas, forced into the pump, and passes through the pressure transducer. It is then pushed through a pulse damper/restrictor assembly, which smoothes out any minor pressure variations to minimise baseline noise. The eluent then flows to the injection valve.
- The injection valve toggles to the Inject Position, when sample is loaded into the sample loop, enabling the injected sample to be combined with the eluent as it is pushed through.
- The eluent/sample mixture is pumped through the guard and separator columns, where the ions are separated by the ion exchange process. The ion exchange process allows different sample ions to migrate through the column at different rates.

- The eluent/sample mixture flows through the suppressor. There, by suppressing the conductivity of the eluent and enhancing the conductivity of the analyte detection sensitivity is enhanced. Regenerant flow continuously through the suppressor, restoring the ion exchange sites to their original state.
- The eluent/sample mixture then flows through the DS5, where the analytes are detected and a signal is produced and sent to PeakNet IA software.
- The eluent flows out of the cell and is directed into the regenerant reservoir, where pressure forces the regenerant into the suppressor. The eluent/sample has a lower density than the regenerant, so forms a layer on top of the anion regenerant.

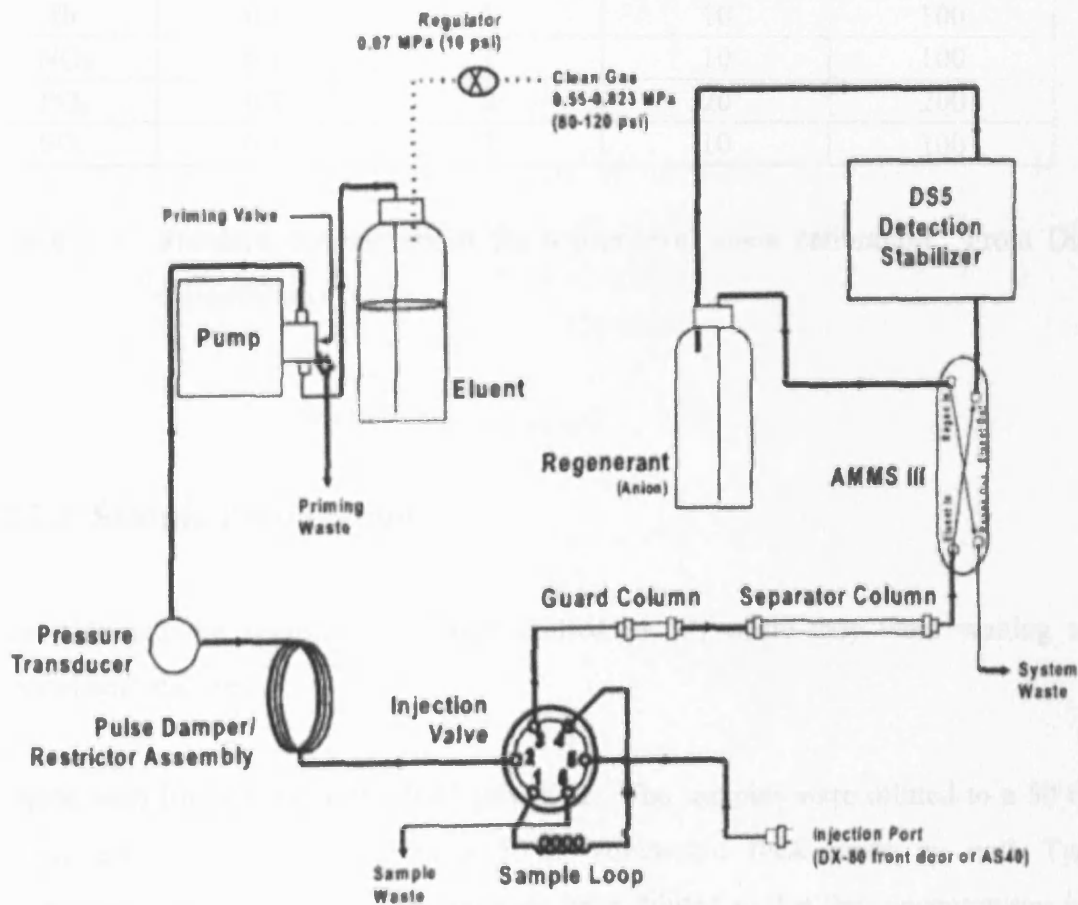


Figure 6.13 Schematic of the flow through the DX-80. From Dionex Corporation (2001).

6.2.2.1.3 Calibration

Before running a sample, the machine is calibrated using standard solutions. By comparing the data obtained from a sample to that obtained from the standard, sample ions can be identified and quantified. The DX-80 is preconfigured to perform a four-level calibration. Table 6.2 lists the standard concentrations for a four-level anion calibration.

Analyte	STD I (mg/l)	STD II (mg/l)	STD III (mg/l)	STD IV (mg/l)
F	0.02	0.2	2	20
Cl	0.1	1	10	100
NO ₂	0.1	1	10	100
Br	0.1	1	10	100
NO ₃	0.1	1	10	100
PO ₄	0.2	2	20	200
SO ₄	0.1	1	10	100

Table 6.2 Standard concentrations for a four-level anion calibration. From Dionex Corporation (2001).

6.2.2.2 Sample Preparation

Once defrosted the samples were kept chilled (4 °C) while they were waiting to be prepared and analysed.

Samples were filtered through a 0.45 µm filter. The samples were diluted to a 50 times dilution using 1 ml of sample in a 50 ml volumetric flask made up with Type I (18-megohm) deionised water. The samples were diluted so that the concentrations in the samples were in the middle of the range of the calibration for the machine.

Type I (18-megohm) deionised water was run through the IC every 10 samples. This was used to check that the IC was not drifting or that the column was not having anions

passing through slower than they should be and appearing on the next analysis. The water analysis results can also be used to calculate detection limits (Section 6.2.2.3).

Sample bottles washed and rinsed with deionised water before reuse.

6.2.2.3 Detection Limits

There are a number of different ways of calculating detection limits. The lowest calibration sample concentrations can be used since they represent the bottom of the calibration curve (Table 6.2).

The detection limits can be calculated using the analysis of blank solutions (deionised water). The mean and standard deviation of each element are calculated. 2 standard deviations give the limit at which something can be detected. 10 standard deviations give the limit at which something can be detected and its concentration given with some certainty.

	detection limit (2SD)	detection limit (10SD)
Fluoride	5.4	26.9
Chloride	5.7	28.4
Nitrite	3.0	15.2
Bromide	1.9	9.5
Nitrate	2.4	12.0
Phosphate	-	-
Sulphate	4.3	21.4

Figure 6.3 Detection limits of the anions analysed using IC.

6.2.2.4 Precision

The precision, statistical errors which reflect random fluctuations in the analytical procedures, can be calculated by repeated analysis of the same sample. Calibration standard 3 (CAL STD III) was run 10 times. The mean and standard deviation of the analyses are calculated. The samples are then quoted to 2 standard deviations of the mean for each anion (Table 6.4).

	result \pm
Fluoride	0.052
Chloride	0.230
Nitrite	0.178
Bromide	2.648
Nitrate	1.723
Phosphate	0.580
Sulfate	0.921

Table 6.4 Precision for anions analysed using IC.

6.2.2.5 Errors

Errors in results may occur in a number of ways, including errors in sampling, errors in analysis, and changes in the samples between collection and analysis.

Errors in sampling could arise if atypical samples are collected. It is not anticipated that this represents a major source of error in this case, since small samples of liquid were taken from a free flowing source that could be expected to be reasonable uniform at the time of collection.

Errors in analysis may occur as a result of errors in preparation or errors produced by the analytical equipment. In order to minimise preparation errors, dilution was undertaken

with high accuracy pipettes which used disposable elements to reduce the possibility of cross contamination.

6.2.2.6 Frozen/Chilled Samples

Although freezing samples does not affect the geochemical analysis of the samples using IC, several samples were run to confirm this. On two occasions duplicate samples were collected at each monitoring point – LP1 (L) and the Settlement Tank (S). One bottle was stored over night in a fridge until it was analysed the following day and the other sample bottle was frozen. The frozen sample was then thawed and analysed at a later date (about 6 weeks later).

Table 6.5 shows the results of the analysis. There are slight differences between the results. These can be accounted for due to errors in sample preparation and the fact that the chilled and frozen samples were collected in different bottles. This confirms that for IC analysis, freezing the samples does not affect the results.

Sample Name	Fluoride (mg/l)	Chloride (mg/l)	Nitrite (mg/l)	Bromide (mg/l)	Nitrate (mg/l)	Phosphate (mg/l)	Sulphate (mg/l)
L12-1-04 15:30 Fridge	3.2	525	3.8	11.2	109.7	-15.1	782
L12-1-04 15:30 Frozen	3.5	468	n.a.	9.4	104.9	n.a.	708
L12-1-04 15:30 Frozen Rpt	3.6	480	3.5	9.2	102.8	-14.6	735
L23-2-04 11:30 Fridge	3.5	564	n.a.	9.6	75.4	n.a.	539
L23-2-04 11:30 Fridge Rpt	6	573	n.a.	11	70.1	-14.9	533
L23-2-04 11:30 Frozen	4.8	485	n.a.	15.8	70.7	n.a.	477
L23-2-04 11:30 Frozen Rpt	3.5	504	n.a.	9.7	75.4	n.a.	481
S12-1-04 15:30 Fridge	1.3	290	n.a.	5.2	52	n.a.	452
S12-1-04 15:30 Frozen	0.9	251	n.a.	3.2	36.4	n.a.	408
S12-1-04 15:30 Frozen Rpt	1.4	272	n.a.	7.2	79.3	n.a.	438
S23-2-04 11:30 Fridge	3.4	448	n.a.	7.2	48.3	-13.8	431
S23-2-04 11:30 Fridge Rpt	1.9	475	n.a.	7.6	56.6	n.a.	457
S23-2-04 11:30 Frozen	2.3	429	n.a.	6.3	53.4	-15.6	400
S23-2-04 11:30 Frozen Rpt	3.9	442	n.a.	7.6	48.4	n.a.	460

Table 6.5 Results of analysis of samples that were analysed after being refrigerated over night and after being frozen and thawed.

6.2.3 RESULTS

The samples were analysed for fluoride, chloride, nitrite, bromide, nitrate, phosphate and sulphate. Nitrite and phosphate concentrations were around the detection limit, so readings were not obtained for them.

6.2.3.1 BSC Pipe (LP1)

6.2.3.1.1 Fluoride

Fluoride values recorded for LP1 vary between 1.0 and 19.9 mg/l (mean 3.6 mg/l) (Table 6.6). Figure 6.14 shows that other than a few outliers the concentration does not vary greatly.

6.2.3.1.2 Chloride

Chloride values recorded for LP1 vary between 265.9 and 868.0 mg/l (mean 633.2 mg/l) (Table 6.6). Figure 6.15 shows that chloride varies throughout the recording period in such a way that suggests an external influence on the concentration. The most likely such influence is discharge and this will be explored in Section 6.4.

Figure 6.16 shows the chloride values measured during this study with the historical data. The analyses using IC for this study fit in well with the general long-term trend exhibited by the historical data recorded by SVWS.

6.2.3.1.3 Bromide

Bromide values recorded for LP1 vary between 1.5 and 53.8 mg/l (mean 10.4 mg/l) (Table 6.6). Figure 6.17 shows that bromide varies throughout the recording period, again possibly in response to discharge and this will be explored in Section 6.4. There are also a number of outlying data points.

6.2.3.1.4 Nitrate

Nitrate values recorded for LP1 vary between 6.9 and 465.5 mg/l (mean 160.9 mg/l) (Table 6.6). Figure 6.18 shows that nitrate varies throughout the recording period, and again the possible external influence is discharge, which will be explored in Section 6.4.

Figure 6.19 shows the nitrate values measured during this study with the historical data. The analyses using IC for this study are higher than those in the historical data recorded by SVWS.

6.2.3.1.5 Sulphate

Sulphate values recorded for LP1 vary between 342.6 and 948.2mg/l (mean 677.3 mg/l) (Table 6.6). Figure 6.20 shows that this significant variation in sulphate concentrations may also reflect changes in leachate discharge volumes, as discussed in Section 6.4.

Figure 6.21 shows the sulphate values measured during this study with the historical data. The analyses using IC for this study agree well with the general long-term trend exhibited by the historical data recorded by SVWS.

	Fluoride	Chloride	Bromide	Nitrate	Sulphate
Minimum	1.0	265.9	1.5	6.9	342.6
Maximum	19.9	868.0	53.8	465.5	948.2
Mean	3.6	633.2	10.4	160.9	677.3
Standard Deviation	1.5	116.4	4.8	88.4	122.4

Table 6.6 Minimum, maximum, mean and standard deviation of determinands in LP1 analysed using IC.

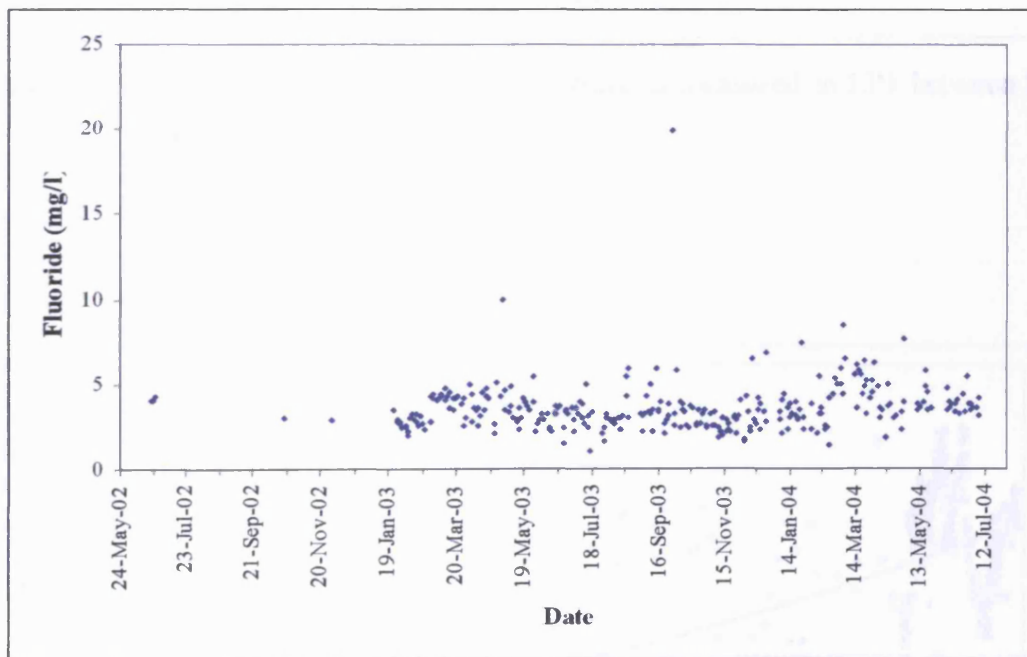


Figure 6.14 Graph showing fluoride concentrations measured in LP1 between 22 June 2002 and 7 July 2004.

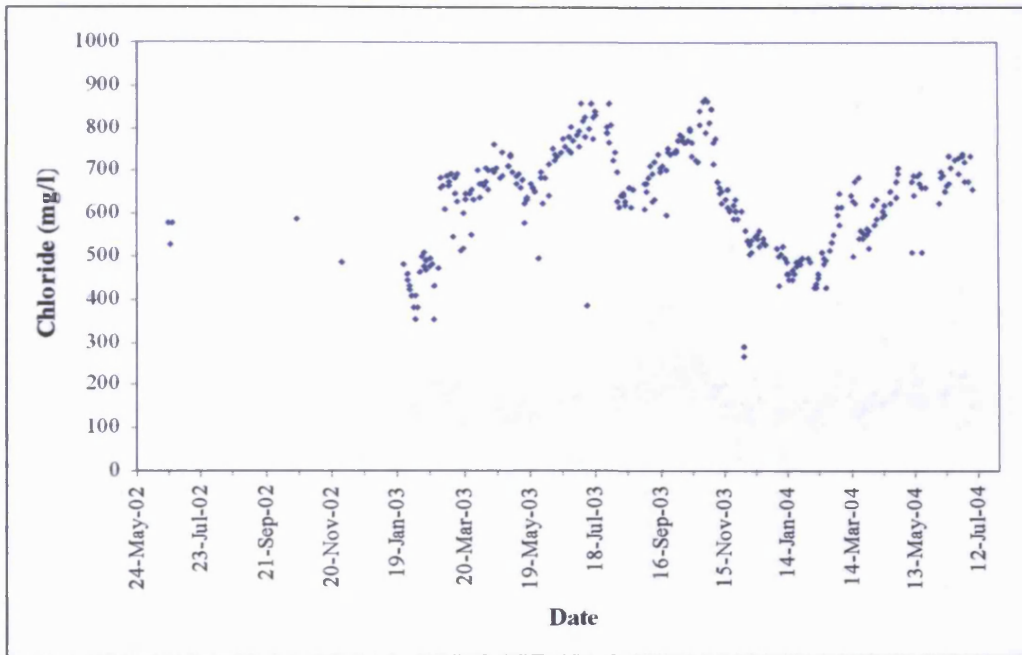


Figure 6.15 Graph showing chloride concentrations measured in LP1 between 22 June 2002 and 7 July 2004.

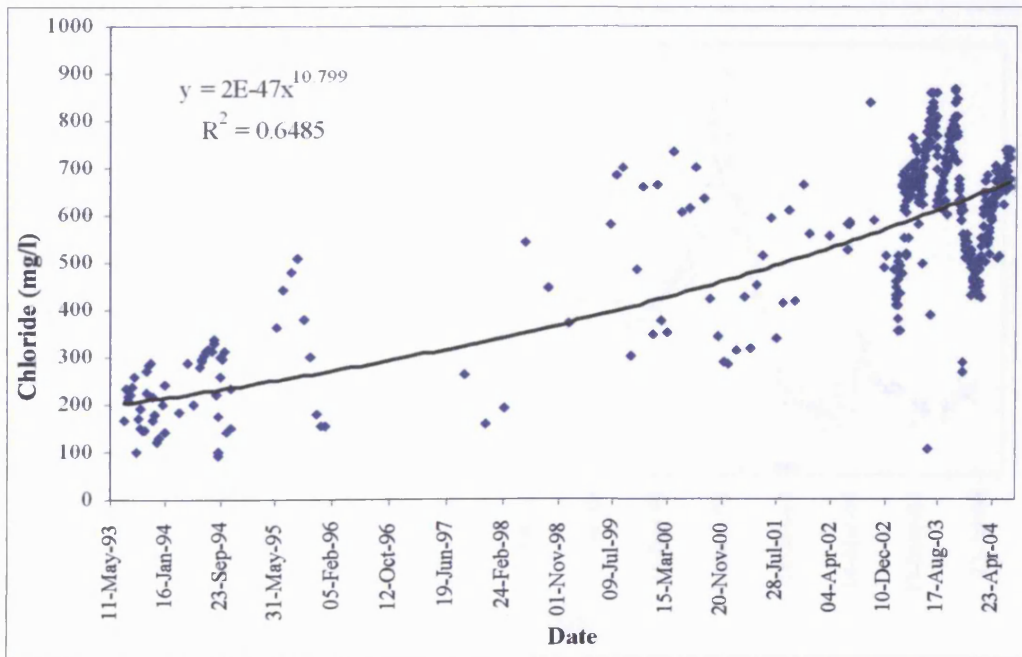


Figure 6.16 Graph showing chloride concentrations measured in LP1 between July 1993 and July 2004.

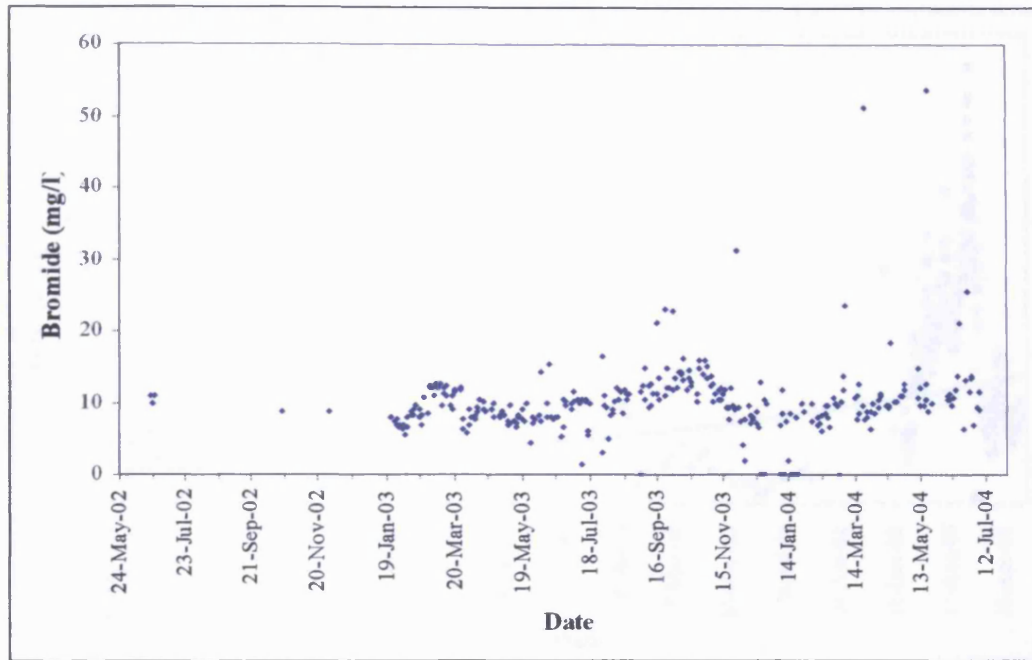


Figure 6.17 Graph showing bromide concentrations measured in LP1 between 22 June 2002 and 7 July 2004.

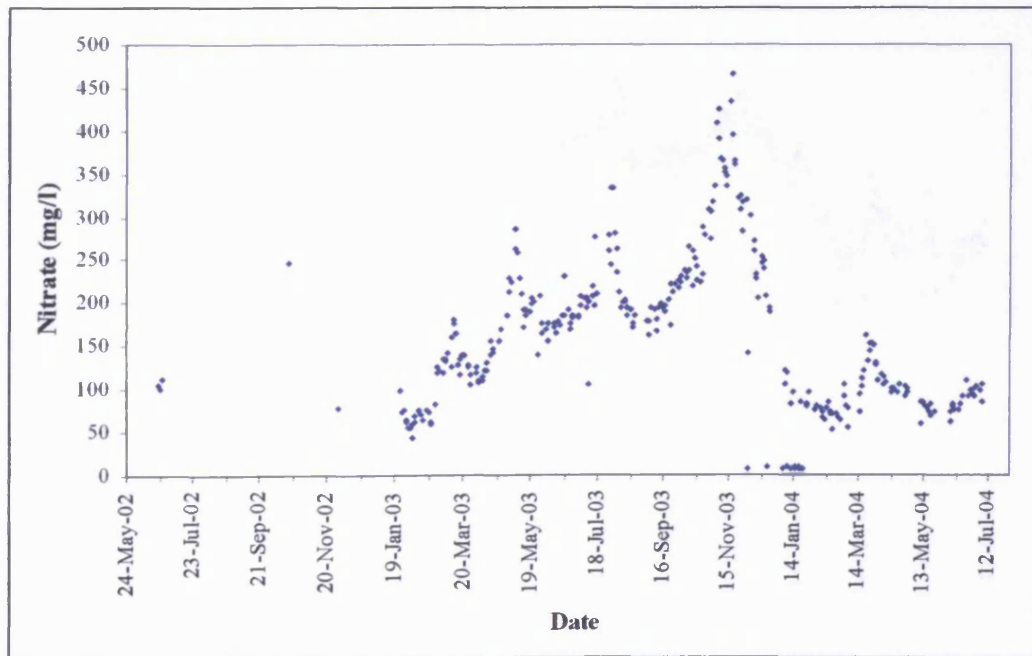


Figure 6.18 Graph showing nitrate concentrations measured in LP1 between 22 June 2002 and 7 July 2004.

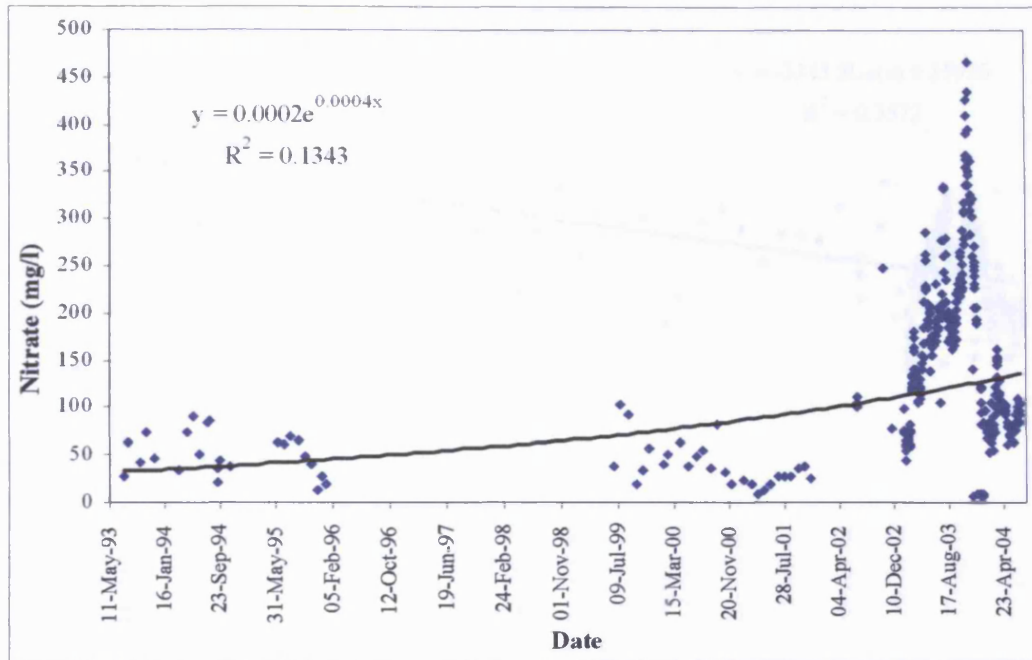


Figure 6.19 Graph showing nitrate concentrations measured in LP1 between July 1993 and July 2004.

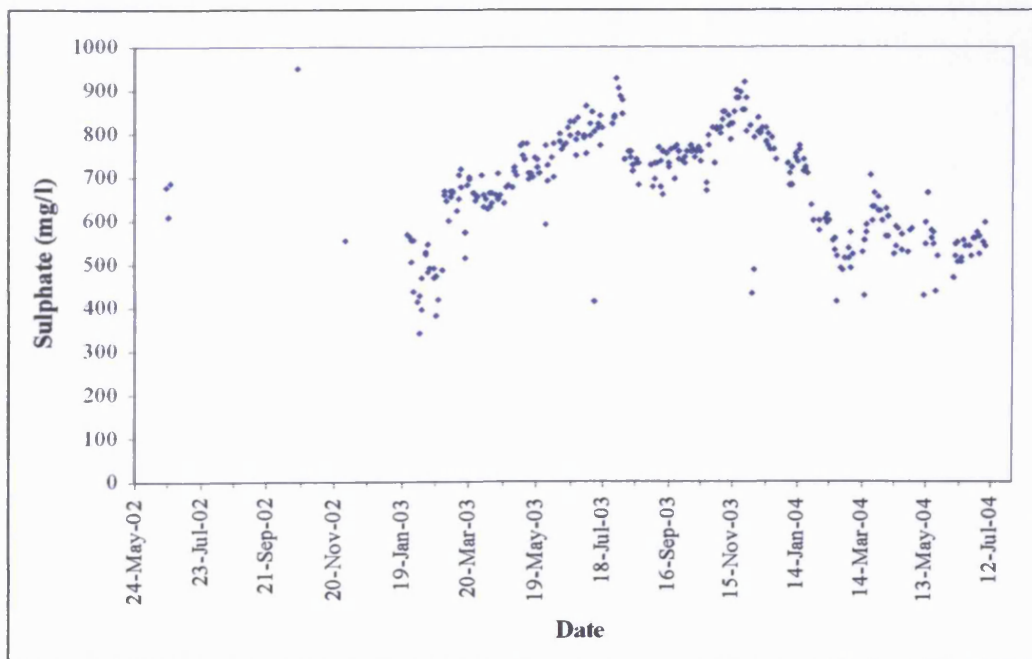


Figure 6.20 Graph showing sulphate concentrations measured in LP1 between 22 June 2002 and 7 July 2004.

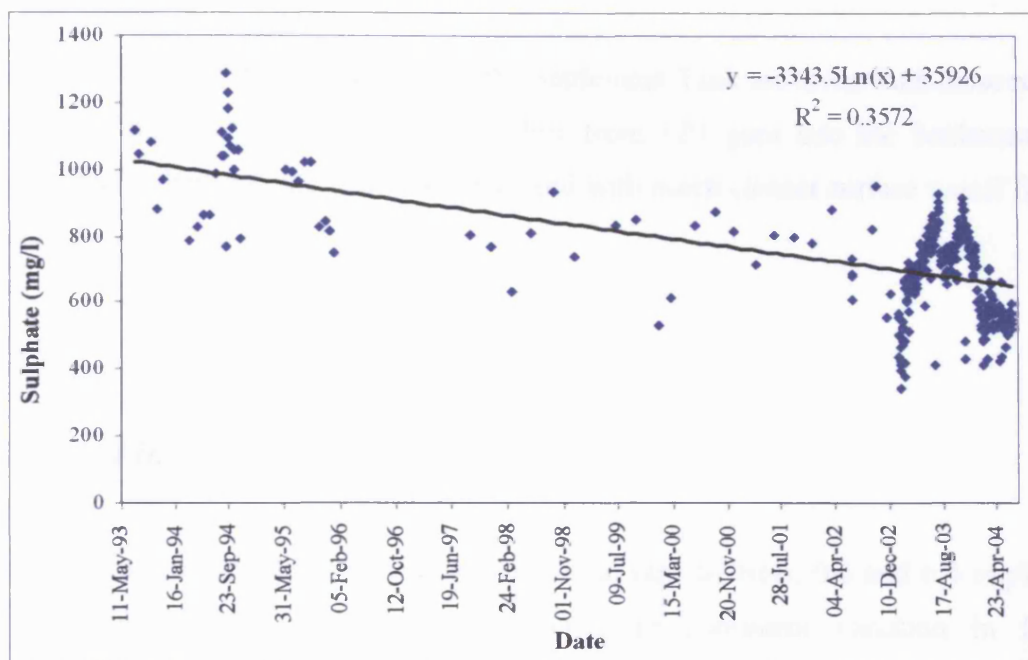


Figure 6.21 Graph showing sulphate concentrations measured in LP1 between July 1993 and July 2004.

6.2.3.2 Settlement Tank

Values of ion concentration recorded in the Settlement Tank are lower than those recorded for LP1. This is as expected since the flow from LP1 goes into the Settlement Tank together with other leachate flows and is mixed with much cleaner surface runoff from the landfill.

6.2.3.2.1 Fluoride

Fluoride values recorded for the Settlement Tank vary between 0.6 and 6.4 mg/l (mean 2.6 mg/l) (Table 6.7). Figure 6.22 shows little consistent variation in fluoride concentration, although the wide scatter of values makes detection of trends difficult.

6.2.3.2.2 Chloride

Chloride values recorded for the Settlement Tank vary between 124.6 and 692.5 mg/l (mean 486.1 mg/l) (Table 6.7). Figure 6.23 shows that chloride varies throughout the recording period in a similar manner to that recorded for LP1, and the effect of discharge variation will be discussed in Section 6.4.

6.2.3.2.3 Bromide

Bromide values recorded for the Settlement Tank vary between 0.5 and 23.2 mg/l (Fig. 6.24) (mean 7.7 mg/l, Table 6.7). Again, the influence of discharge is discussed in Section 6.4.

6.2.3.2.4 Nitrate

Nitrate values recorded for the Settlement Tank vary between 3.0 and 305.3 mg/l (mean 118.8 mg/l) (Table 6.7) and this variation in concentration (Fig 6.25) is discussed in relation to discharge in Section 6.4.

6.2.3.2.5 Sulphate

Sulphate values recorded for the Settlement Tank vary between 140.4 and 750.7 mg/l (mean 513.7 mg/l) (Table 6.7). Figure 6.26 shows that sulphate concentrations are likely to vary with discharge (see Section 6.4.)

	Fluoride	Chloride	Bromide	Nitrate	Sulphate
Minimum	0.6	124.6	0.5	3.0	140.4
Maximum	6.4	692.5	23.2	305.3	750.7
Mean	2.6	486.1	7.7	118.8	513.7
Standard Deviation	0.9	105.5	3.1	57.4	100.3

Table 6.7 Minimum, maximum, mean and standard deviation of determinands in the Settlement Tank discharge analysed using IC.

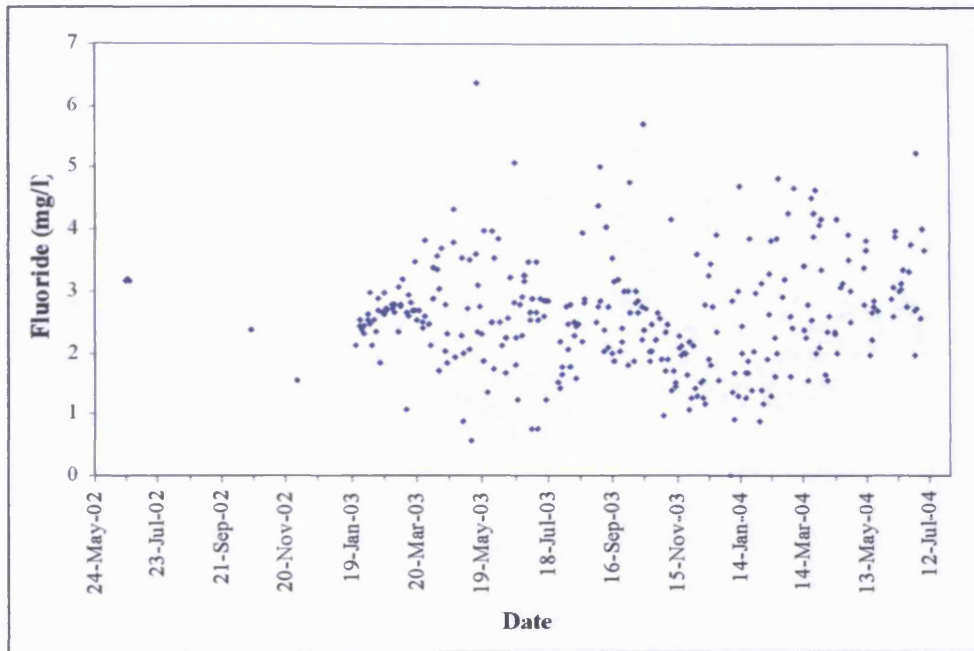


Figure 6.22 Graph showing fluoride concentrations measured in the Settlement Tank between 22 June 2002 and 7 July 2004.

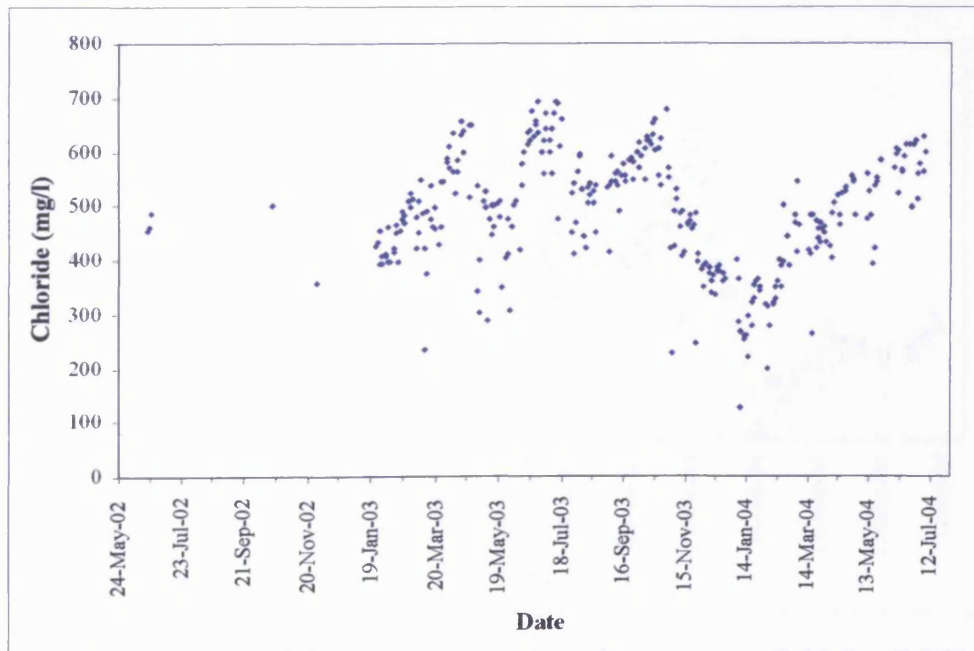


Figure 6.23 Graph showing chloride concentrations measured in the Settlement Tank between 22 June 2002 and 7 July 2004.

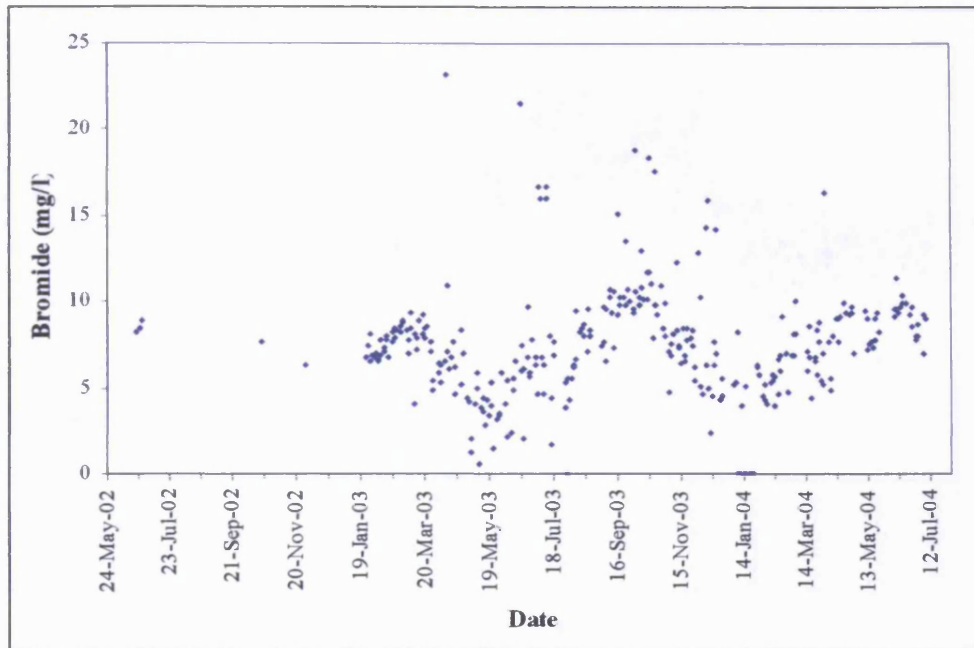


Figure 6.24 Graph showing bromide concentrations measured in the Settlement Tank between 22 June 2002 and 7 July 2004.

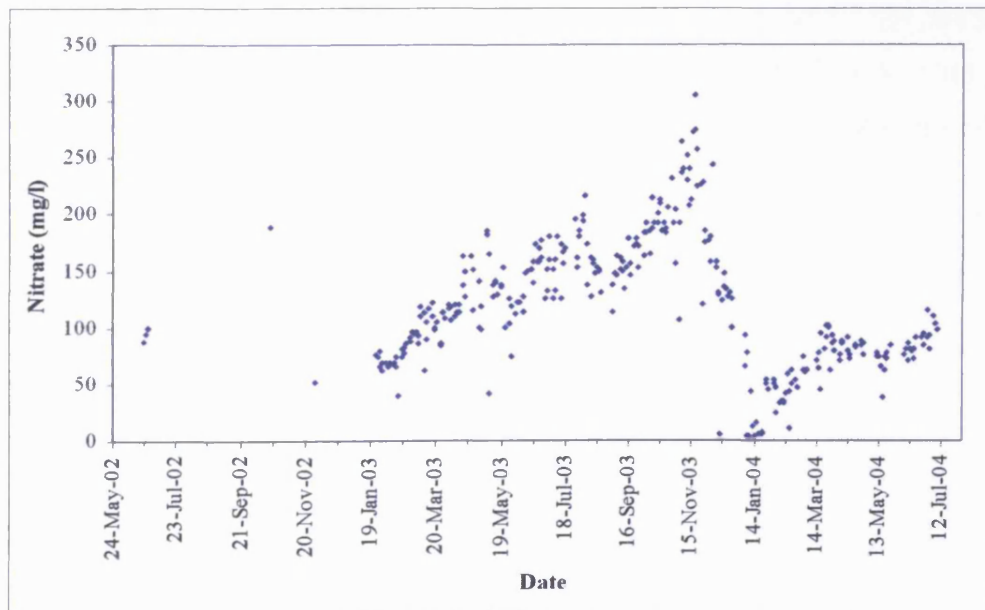


Figure 6.25 Graph showing nitrate concentrations measured in the Settlement Tank between 22 June 2002 and 7 July 2004.

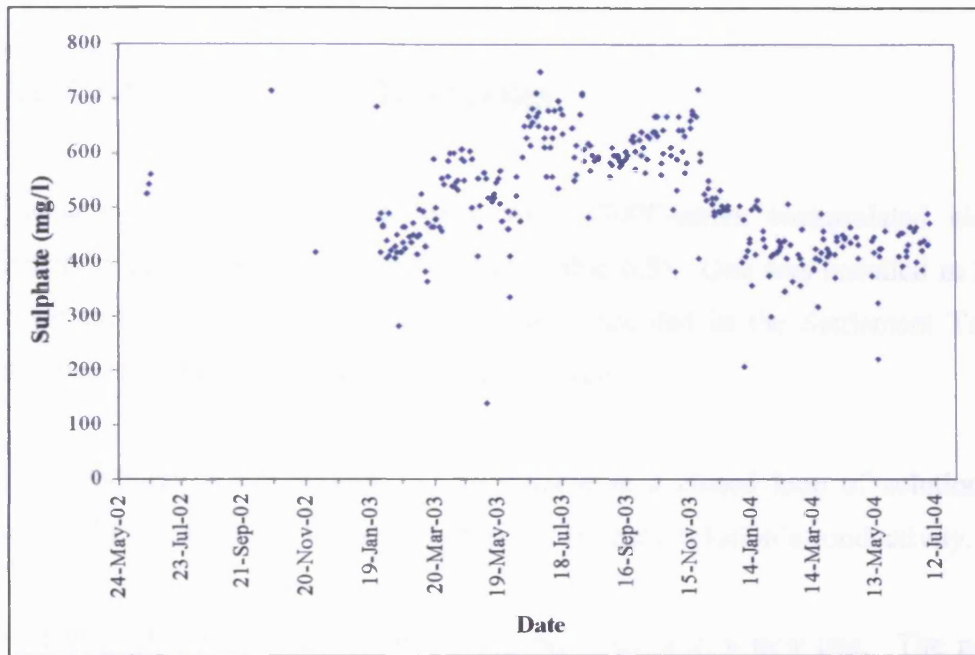


Figure 6.26 Graph showing sulphate concentrations measured in the Settlement Tank between 22 June 2002 and 7 July 2004.

6.3 CONDUCTIVITY MONITORING

6.3.1 CONDUCTIVITY MONITORS

In January 2003 two E53 analysers with 3700E-series encapsulated electrodeless conductivity sensors were installed on site (Table 6.8). One was installed in LP1 as the leachate exits the BSC Pipe. The other was installed in the Settlement Tank by the ultrasonic sensor monitoring the flow over the weir.

The electrodeless sensor induces a low current in a closed loop of solution and then measures the magnitude of this current to determine the solution's conductivity.

One of the old WJ460 flow monitors was replaced with a new one. The new WJ460 monitor has 2 channels dedicated to flow readings and 2 channels that can be used for other measurements – in this case conductivity. The sensors continuously monitor the conductivity and readings are recorded every 15 minutes, which is the same frequency as the flow readings.

Although the analyser and conductivity sensor measures conductivity readings to 2 decimal places, the datalogger records measurements to the closest value it can allocate a reading to. The values that readings can be assigned to are at a spacing of 0.1 and 0.2 mS/cm.

6.3.2 RESULTS

6.3.2.1 BSC Pipe (LP1)

Conductivity for LP1 varied between 1.9 and 8.5 mS/cm (mean 6.0 mS/cm, Standard Deviation ± 1.1 mS/cm) between January 2003 and June 2004 (Fig. 6.27). The data appears to show rapid increases in conductivity within the time series, separated by less rapid declines.

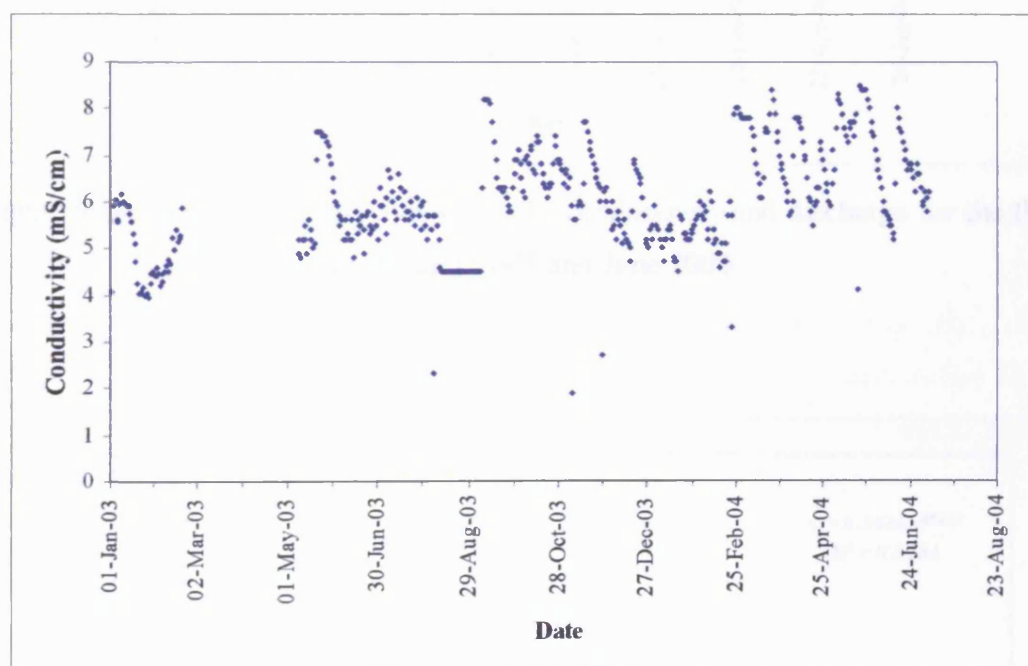


Figure 6.27 Graph showing how average daily conductivity varies for LP1 between January 2003 and June 2004.

Figure 6.28 shows how the conductivity varies with the BSC Pipe (LP1) discharge. A weak correlation ($R^2 = 0.0284$) is obtained for these data (Fig. 6.29). An exponential trendline shows a decrease in conductivity with an increase in discharge, which could represent dilution, but the degree of scatter particularly for lower flows suggests that this is not a dominant control on conductivity.

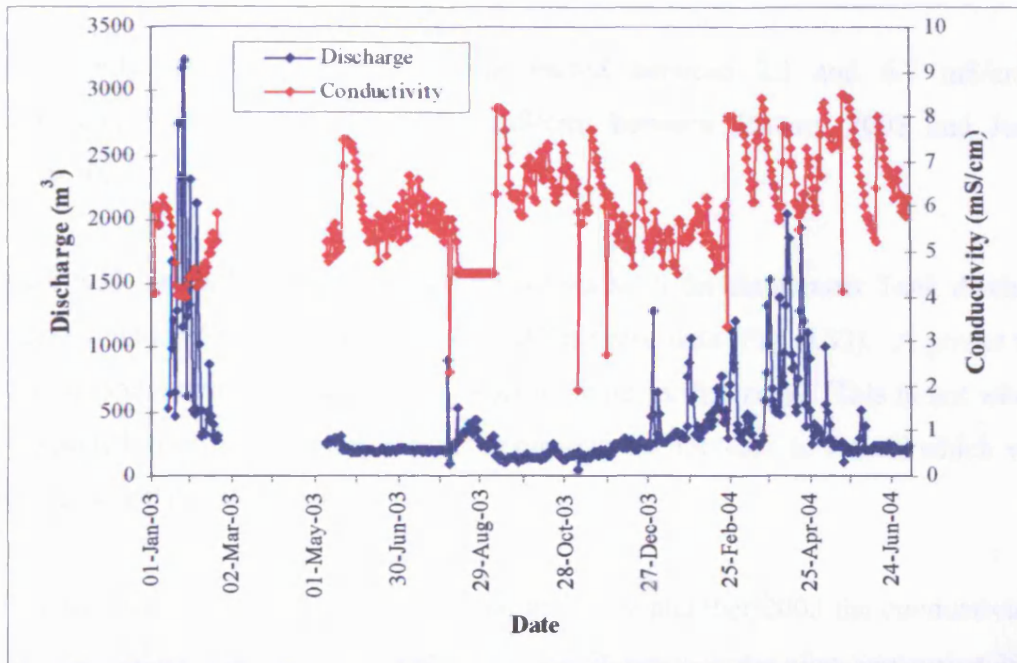


Figure 6.28 Graph showing average daily conductivity and discharge for the BSC Pipe (LP1) between January 2003 and June 2004.

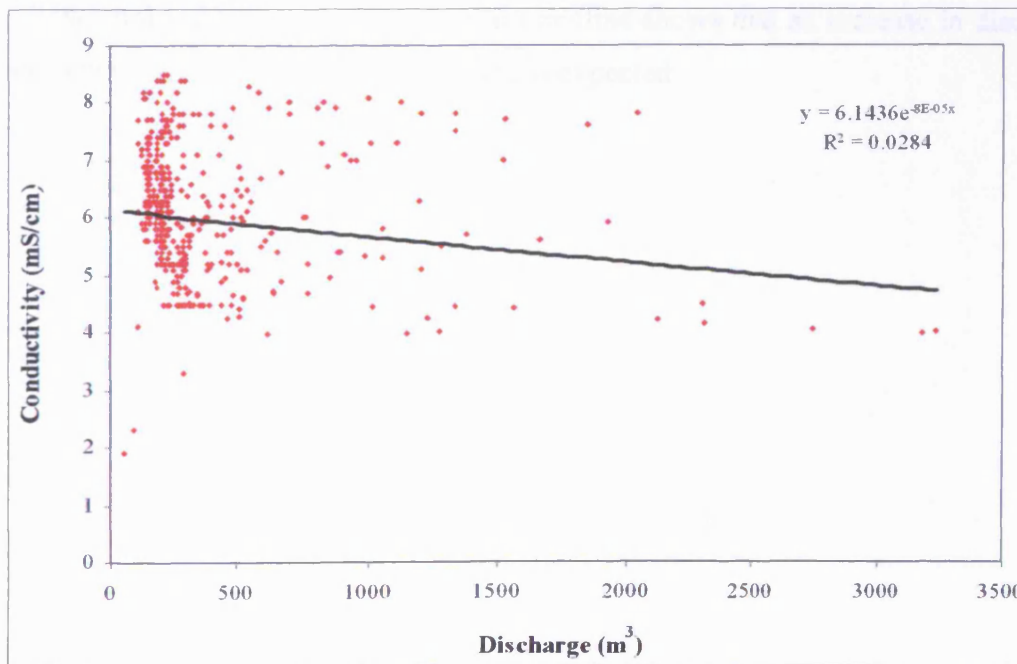


Figure 6.29 Graph showing discharge for the BSC Pipe (LP1) against average daily conductivity between January 2003 and June 2004.

6.3.2.2 Settlement Tank

Conductivity for the Settlement Tank varied between 2.3 and 6.7 mS/cm (mean 4.3 mS/cm, Standard Deviation ± 1.4 mS/cm) between January 2003 and June 2004 (Fig. 6.30).

Figure 6.31 shows how the conductivity varies with the Settlement Tank discharge. A weak correlation ($R^2 = 0.0118$) is obtained for these data (Fig. 6.32). A power trendline shows an increase in conductivity with an increase in discharge. This is not what would be expected since increased discharge represents an increase in runoff which would be expected to dilute the discharge.

In detail, however, figure 6.31 shows that before September 2003 the conductivity varied very little and did not show any response to discharge whereas after September 2003 there appears to be a relationship between discharge and conductivity. It is possible that the conductivity readings for January to September 2003 are unreliable. Figure 6.33 shows a strong ($R^2 = 0.4614$) relationship between conductivity and discharge when data from 8 September 2003 are used (excluding 4 very high discharge readings between 30 October and 2 November 2003). The exponential trendline shows that an increase in discharge is associated with a decrease in conductivity, as expected.

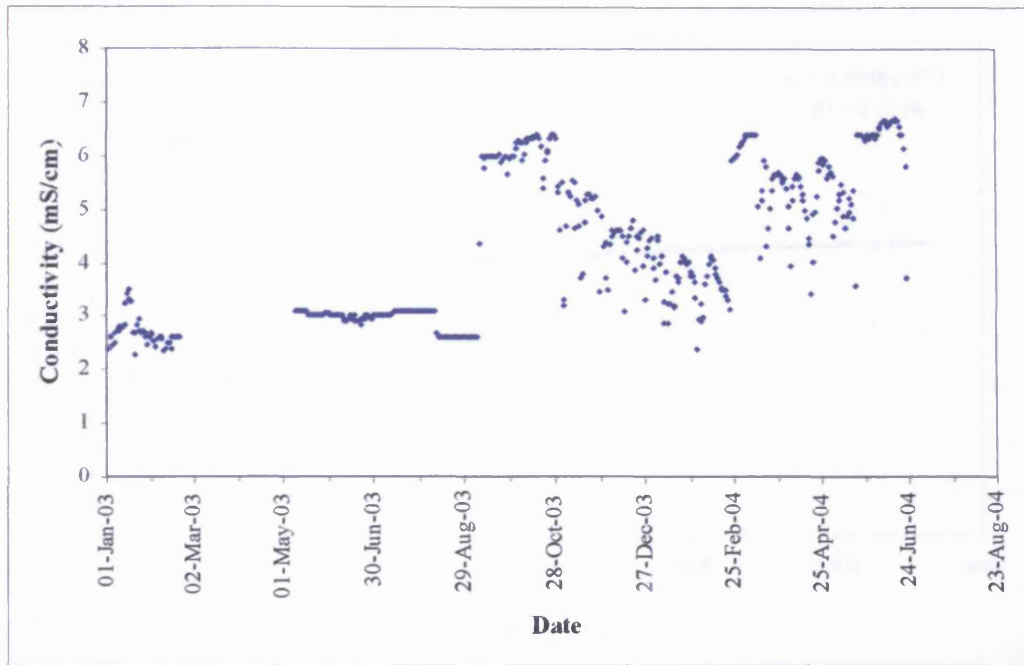


Figure 6.30 Graph showing how average daily conductivity varies for the Settlement Tank between January 2003 and June 2004.

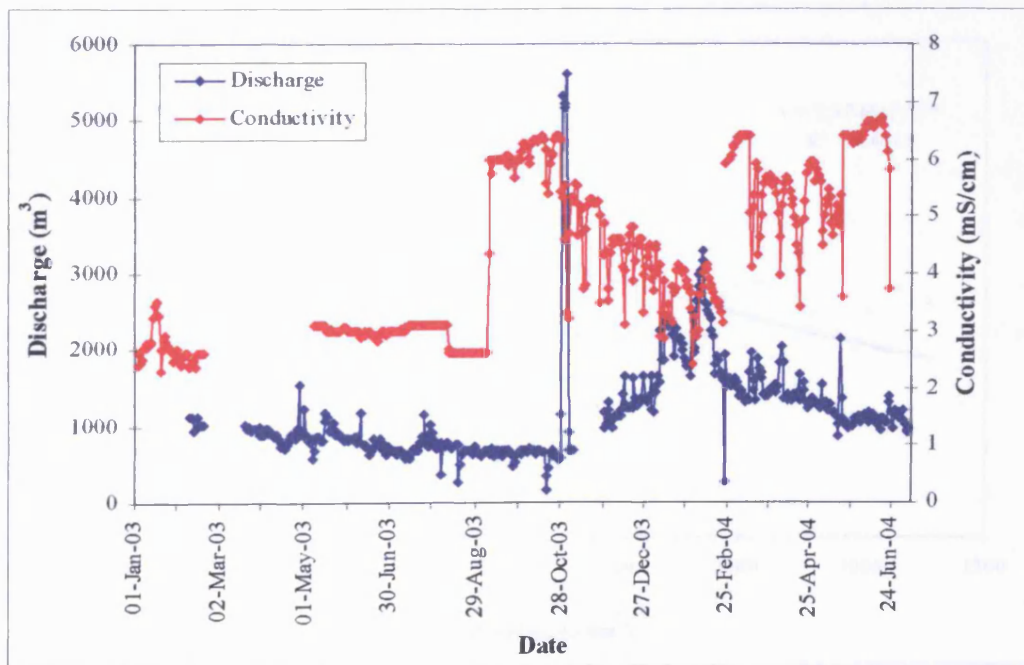


Figure 6.31 Graph showing average daily conductivity and discharge for the Settlement Tank between January 2003 and June 2004.

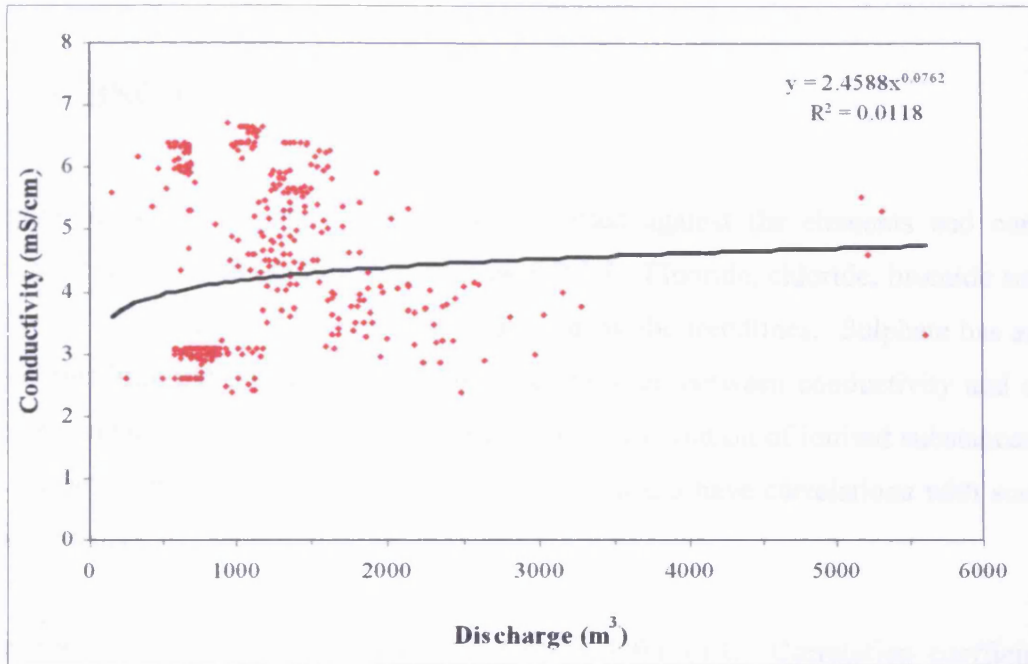


Figure 6.32 Graph showing discharge for the Settlement Tank against average daily conductivity between January 2003 and June 2004.

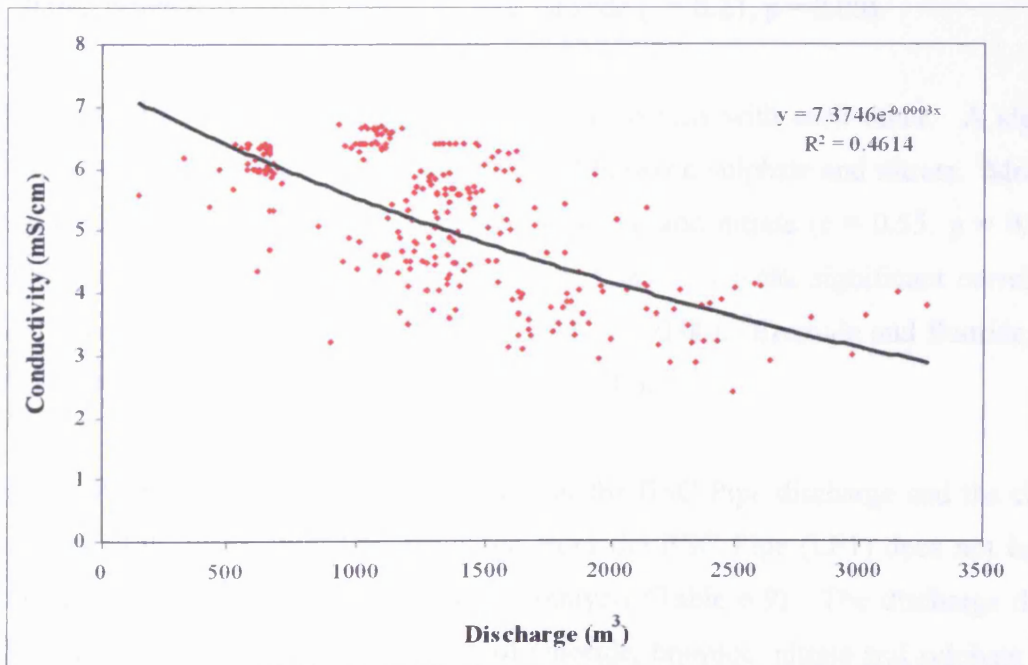


Figure 6.33 Graph showing discharge for the Settlement Tank against average daily conductivity between 8 September 2003 and June 2004.

6.4 ANALYSIS OF GEOCHEMICAL DATA

6.4.1 BSC PIPE (LP1)

Figures 6.34 to 6.38 show conductivity plotted against the elements and compounds analysed using IC and reported in Section 6.2.3.1. Fluoride, chloride, bromide and nitrate increase as conductivity increases as indicated by the trendlines. Sulphate has an almost level trendline indicating that there is no correlation between conductivity and sulphate. Since conductivity is related to the nature and concentration of ionised substances present in the solution, it is expected that conductivity would have correlations with some of its constituents.

Bivariate analysis results are given in table 6.9 for LP1. Correlation coefficients and significance for the discharge, conductivity and the chemical analysis are compared against each other.

The conductivity of LP1 shows significant weak correlations with chloride ($r = 0.28$, $p = 0.00$), bromide ($r = 0.25$, $p = 0.00$) and fluoride ($r = 0.23$, $p = 0.00$).

The chemical substances within LP1 show correlations with each other. A significant strong correlation ($r = 0.78$, $p = 0.00$) is found between sulphate and nitrate. Moderately significant correlations are found between chloride and nitrate ($r = 0.55$, $p = 0.00$) and between chloride and sulphate ($r = 0.55$, $p = 0.00$). A weak significant correlation is found between chloride and bromide ($r = 0.27$, $p = 0.00$). Bromide and fluoride show a significant very weak correlation ($r = 0.18$, $p = 0.00$).

Figure 6.39 shows that there are no trends for the BSC Pipe discharge and the chemical analysis of LP1 using IC. The discharge from the BSC Pipe (LP1) does not have any significant correlations with the chemical analysis (Table 6.9). The discharge does not influence the patterns of concentrations of chloride, bromide, nitrate and sulphate seen in Section 6.2.3.1.

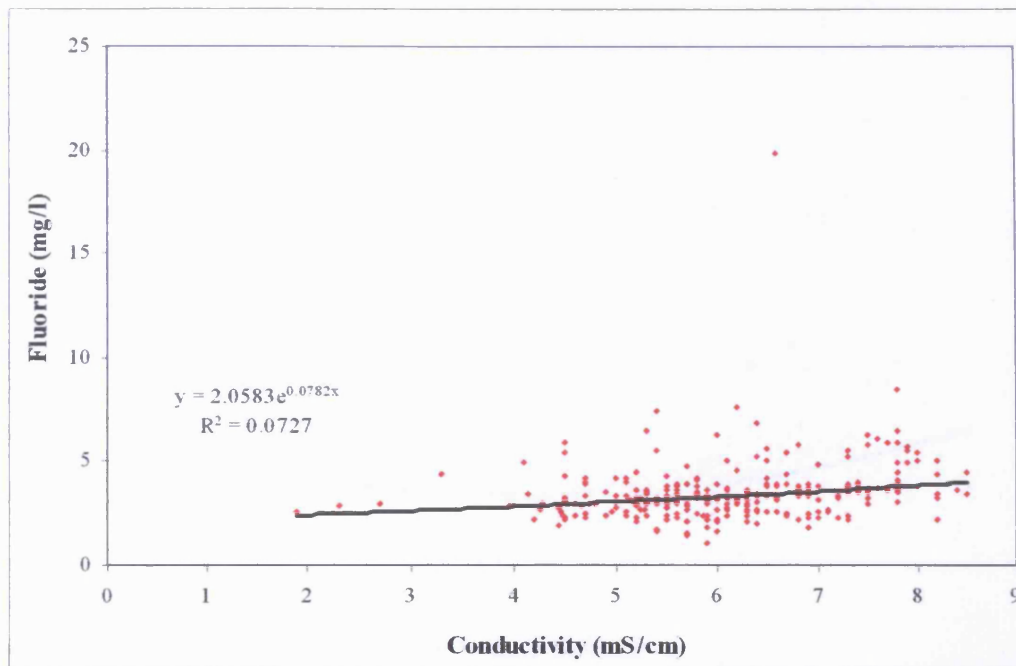


Figure 6.34 Graph showing fluoride concentration for the BSC Pipe (LP1) against average daily conductivity between January 2003 and June 2004.

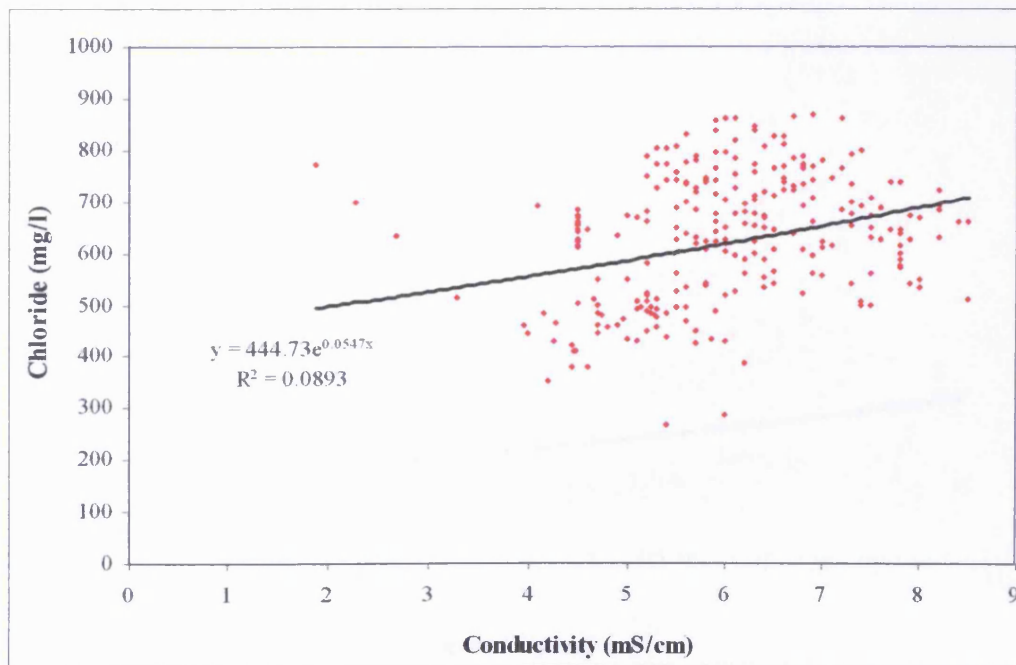


Figure 6.35 Graph showing chloride concentration for the BSC Pipe (LP1) against average daily conductivity between January 2003 and June 2004.

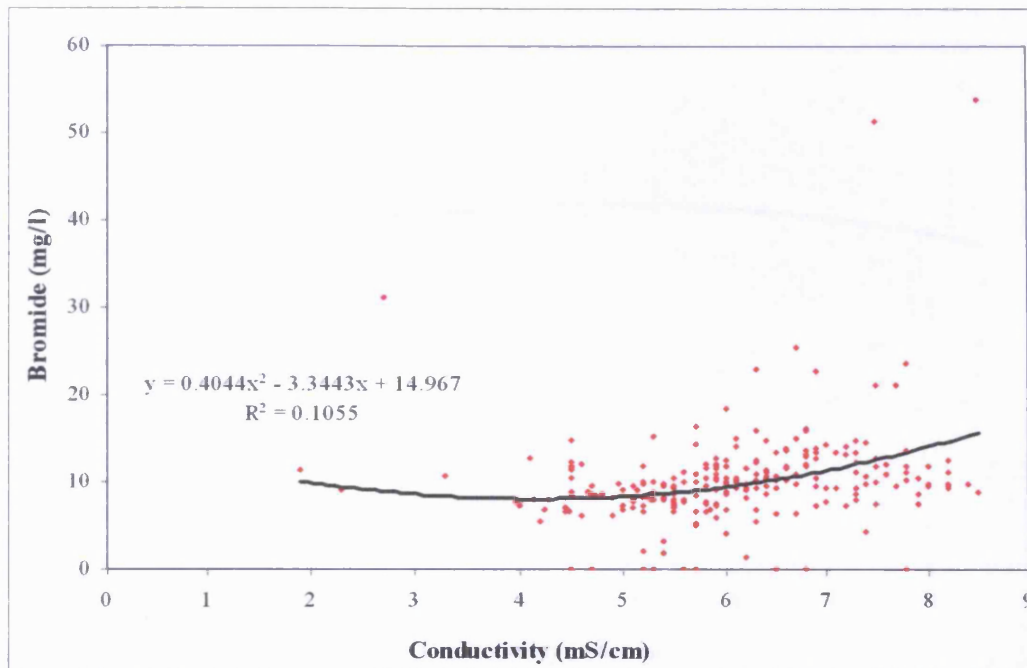


Figure 6.36 Graph showing bromide concentration for the BSC Pipe (LP1) against average daily conductivity between January 2003 and June 2004.

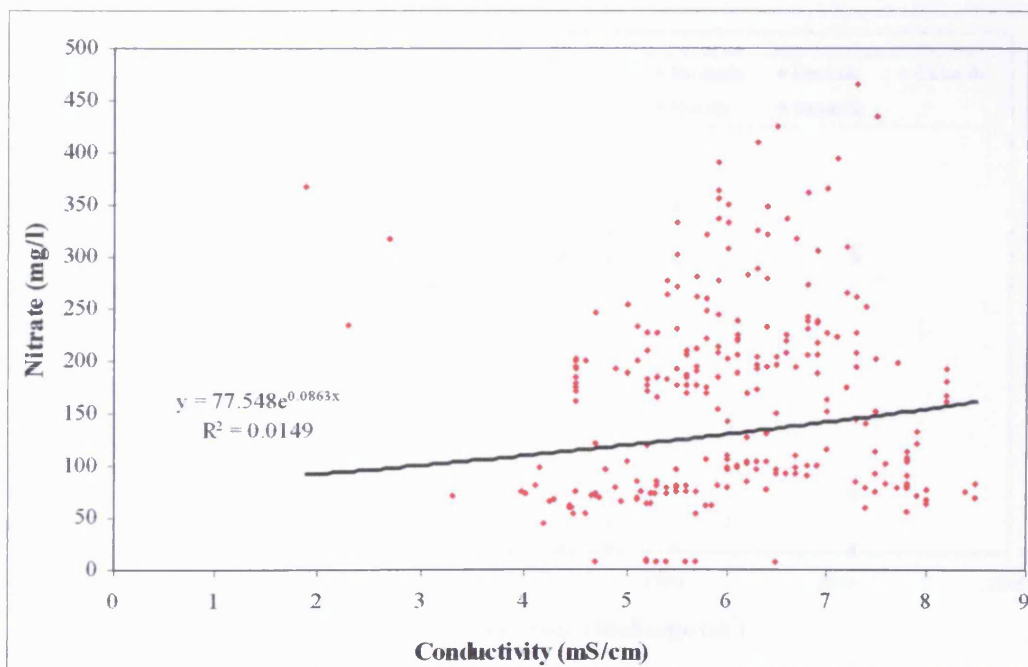


Figure 6.37 Graph showing nitrate concentration for the BSC Pipe (LP1) against average daily conductivity between January 2003 and June 2004.

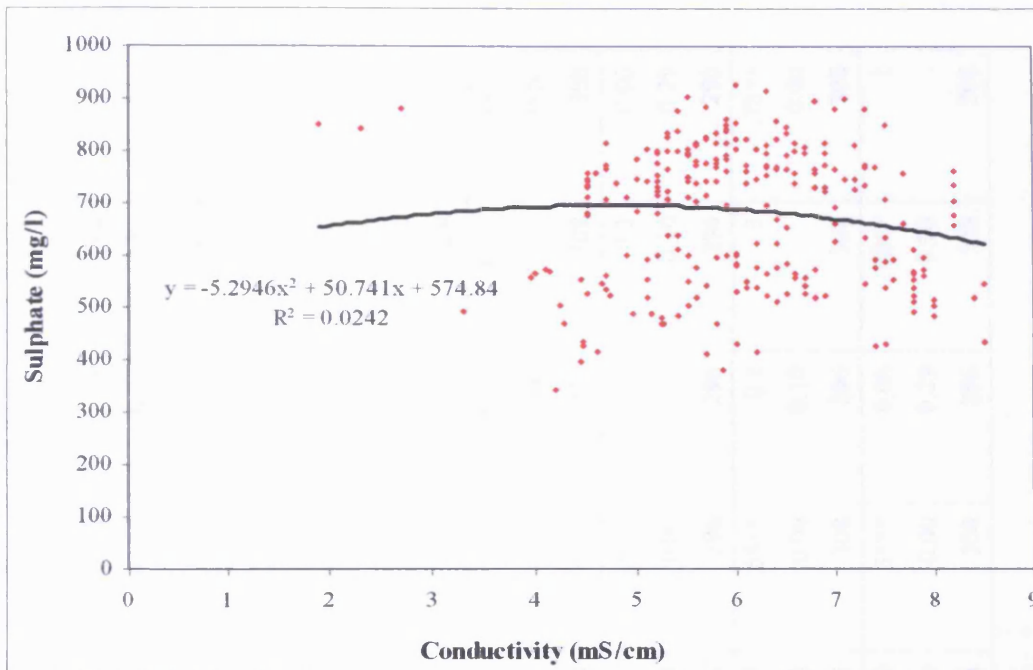


Figure 6.38 Graph showing sulphate concentration for the BSC Pipe (LP1) against average daily conductivity between January 2003 and June 2004.

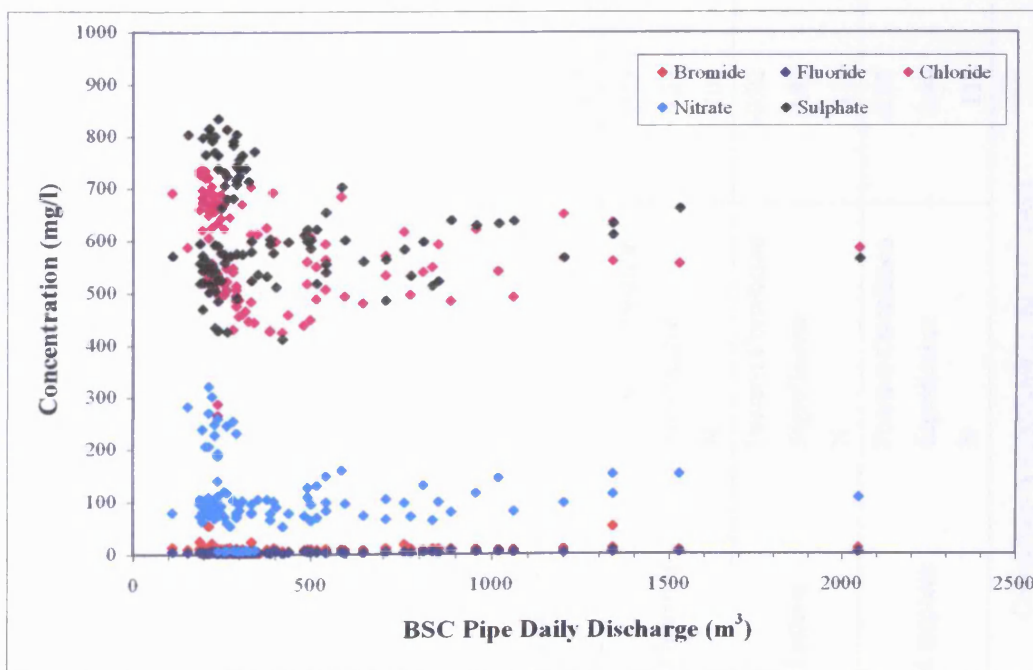


Figure 6.39 Graph showing discharge through the BSC Pipe (LP1) against the IC results.

		BSC Pipe discharge	LP1 Conductivity	LP1 fluoride	LP1 chloride	LP1 bromide	LP1 nitrate	LP1 sulphate
BSC Pipe discharge	Pearson Correlation	1	0.12	0.05	-0.12	0.1	-0.02	-0.08
	Significance	.	0.07	0.60	0.21	0.32	0.81	0.40
	N	472	223	113	113	102	113	113
LP1 Conductivity	Pearson Correlation	0.12	1	.23**	.28**	.25**	0.07	-0.07
	Significance	0.07	.	0.00	0.00	0.00	0.27	0.26
	N	223	475	256	256	244	256	256
LP1 fluoride	Pearson Correlation	0.05	.23**	1	0.09	.18**	-.12*	-0.09
	Significance	0.60	0.00	.	0.13	0.00	0.03	0.10
	N	113	256	308	308	296	308	308
LP1 chloride	Pearson Correlation	-0.12	.28**	0.09	1	.27**	.55**	.55**
	Significance	0.21	0.00	0.13	.	0.00	0.00	0.00
	N	113	256	308	308	296	308	308
LP1 bromide	Pearson Correlation	0.1	.25**	.18**	.27**	1	0.1	0.06
	Significance	0.32	0.00	0.00	0.00	.	0.10	0.29
	N	102	244	296	296	296	296	296
LP1 nitrate	Pearson Correlation	-0.02	0.07	-.12*	.55**	0.1	1	.78**
	Significance	0.81	0.27	0.03	0.00	0.10	.	0.00
	N	113	256	308	308	296	308	308
LP1 sulphate	Pearson Correlation	-0.08	-0.07	-0.09	.55**	0.06	.78**	1
	Significance	0.40	0.26	0.10	0.00	0.29	0.00	.
	N	113	256	308	308	296	308	308

** Correlation is significant at the 0.01 level

* Correlation is significant at the 0.05 level

Table 6.9 Table of correlations for the BSC Pipe (LP1) discharge and geochemical data.

6.4.2 SETTLEMENT TANK

As discussed in Section 6.3.2.2, it is possible that the conductivity readings for January to September 2003 are unreliable. In the following figures (6.40 to 6.44) the conductivity data has been split into data that is considered unreliable (3 January to 7 September 2003) and reliable (8 September 2003 to 23 June 2004). Trendlines given are for the data between 8 September 2003 and 23 June 2004.

Figures 6.40 to 6.44 show conductivity against the elements and compounds analysed in Section 6.2.3.2. Fluoride, chloride, bromide, nitrate and sulphate all increase as conductivity increases as indicated by the trendlines.

Bivariate analysis results are given in table 6.10 for the Settlement Tank. Correlation coefficients and significance for the discharge, conductivity and the chemical analysis are compared against each other. The conductivity has been divided into all the data (3 January to 23 June 2004) and data for 8 September 2003 to 23 June 2004.

The discharge from the Settlement Tank has a significant moderate correlation with conductivity for data between 8 September 2003 to 23 June 2004 ($r = -0.54$, $p = 0.00$). If all the conductivity data are included then there is no correlation between discharge and conductivity.

Taking all the conductivity data, significant weak correlations are found between conductivity and bromide ($r = 0.39$, $p = 0.00$) and chloride ($r = 0.25$, $p = 0.00$). Significant very weak correlations are found with nitrate ($r = 0.16$, $p = 0.01$) and fluoride ($r = 0.15$, $p = 0.02$).

The conductivity data between 8 September 2003 and 23 June 2004 gives higher correlations with the chemical data. A very strong significant correlation is found with chloride ($r = 0.85$, $p = 0.00$). Moderate correlations are found with bromide ($r = 0.51$, $p = 0.00$) and nitrate ($r = 0.40$, $p = 0.00$). Significant weak correlations are found with sulphate ($r = 0.35$, $p = 0.00$) and fluoride ($r = 0.33$, $p = 0.00$).

When considering the data between 8 September 2003 and 23 June 2004 instead of all the data, stronger correlations are obtained (Table 6.10), which supports the idea that conductivity data between 3 January and 7 September 2003 is unreliable.

Figure 6.45 and 6.46 shows how chloride, nitrate, sulphate and bromide show a decrease in concentration with an increase in discharge. This suggests a dilution effect. Significant correlations are obtained for the discharge and chloride ($r = -.56$, $p = 0.00$), nitrate ($r = -.56$, $p = 0.00$), sulphate ($r = -.49$, $p = 0.00$) and bromide ($r = -.16$, $p = 0.01$) (Table 6.10). It is possible that the discharge influences the patterns of concentrations of chloride, bromide, nitrate and sulphate seen in Section 6.2.3.2.

The chemical substances within the Settlement Tank show significant co-variation. A significant very strong correlation ($r = 0.81$, $p = 0.00$) is found between sulphate and nitrate. A strong significant correlation is found between chloride and sulphate ($r = 0.63$, $p = 0.00$). Moderate significant correlations are found between chloride and nitrate ($r = 0.53$, $p = 0.00$) and between chloride and bromide ($r = 0.41$, $p = 0.00$). Weak significant correlations are found between chloride and fluoride ($r = 0.29$, $p = 0.00$), sulphate and bromide ($r = 0.25$, $p = 0.00$), and nitrate and bromide ($r = 0.23$, $p = 0.00$).

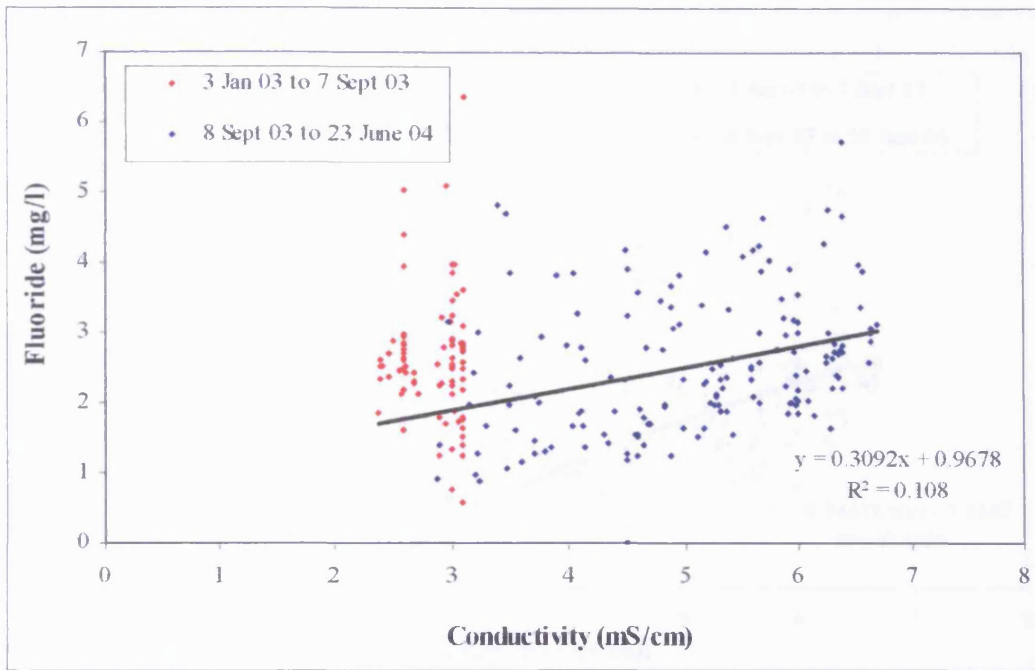


Figure 6.40 Graph showing fluoride concentration for the Settlement Tank against average daily conductivity between January 2003 and June 2004.

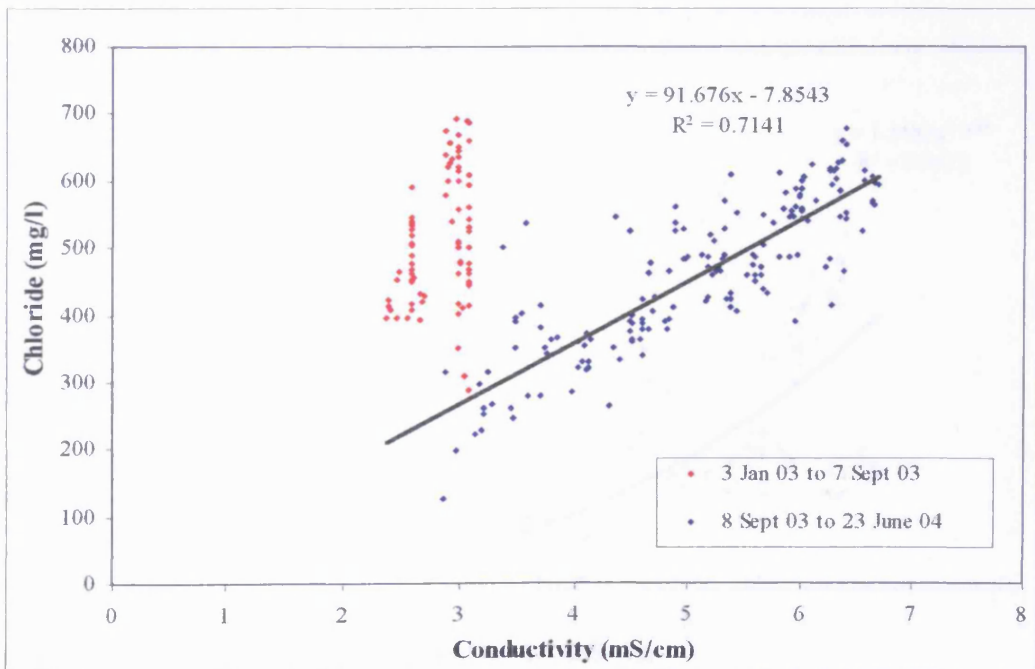


Figure 6.41 Graph showing chloride concentration for the Settlement Tank against average daily conductivity between January 2003 and June 2004.

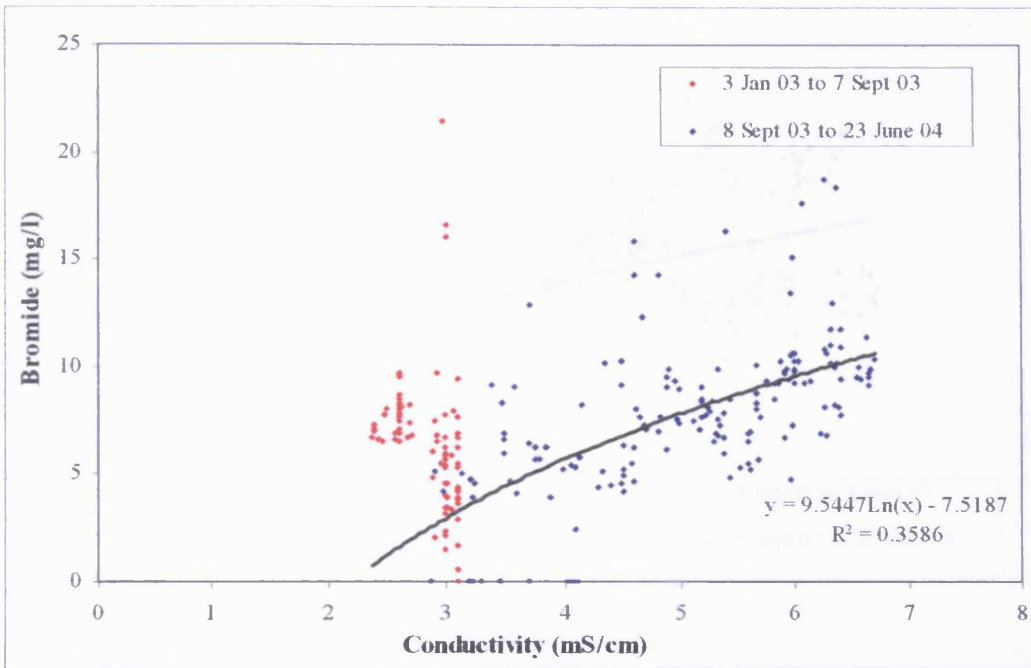


Figure 6.42 Graph showing bromide concentration for the Settlement Tank against average daily conductivity between January 2003 and June 2004.

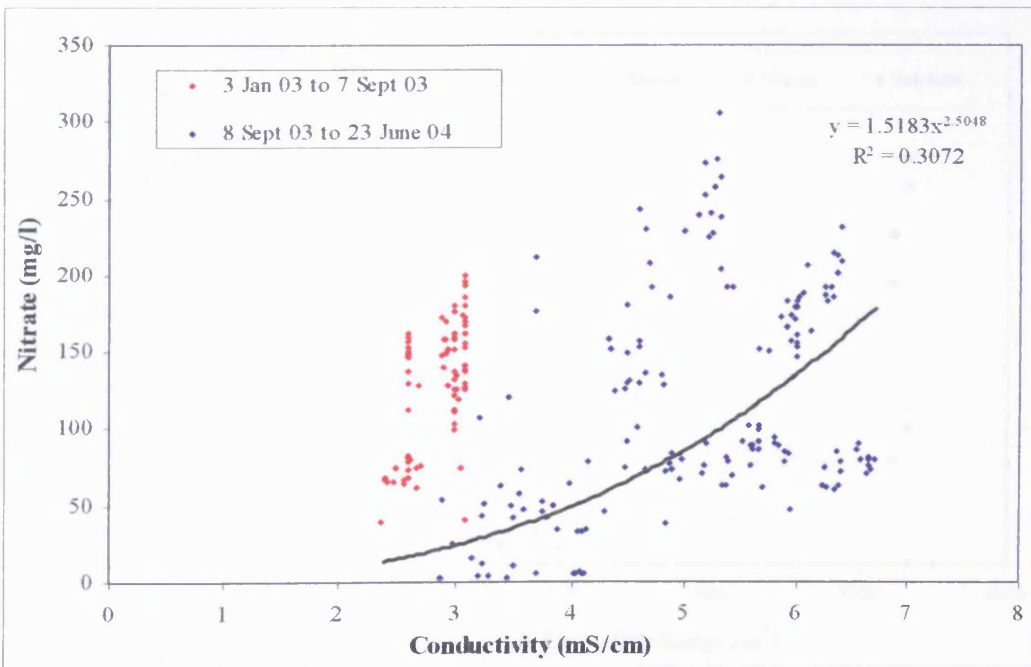


Figure 6.43 Graph showing nitrate concentration for the Settlement Tank against average daily conductivity between January 2003 and June 2004.

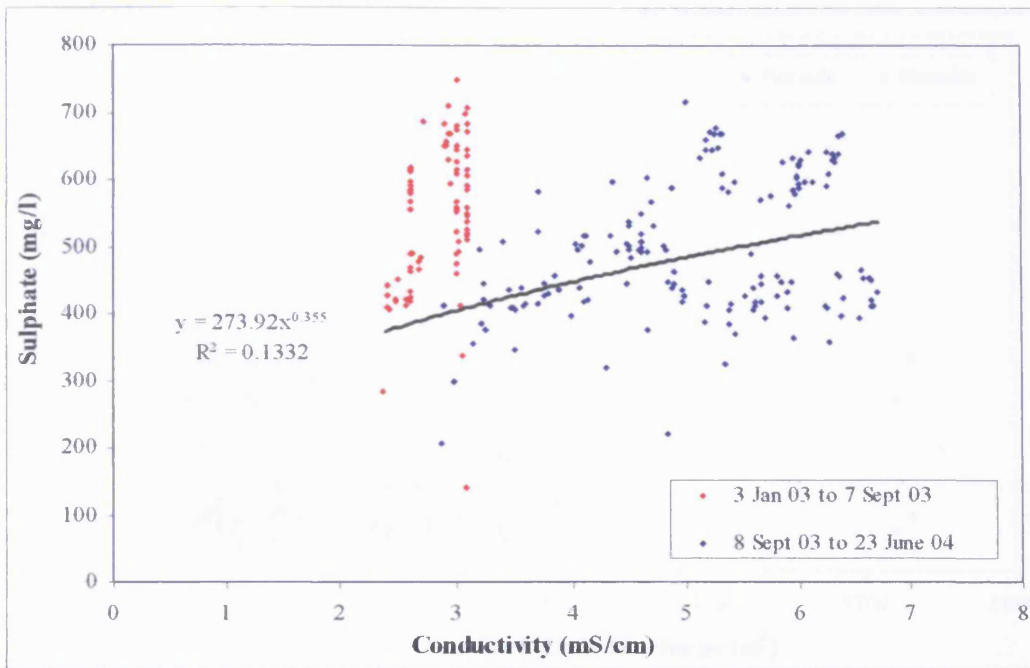


Figure 6.44 Graph showing sulphate concentration for the Settlement Tank against average daily conductivity between January 2003 and June 2004.

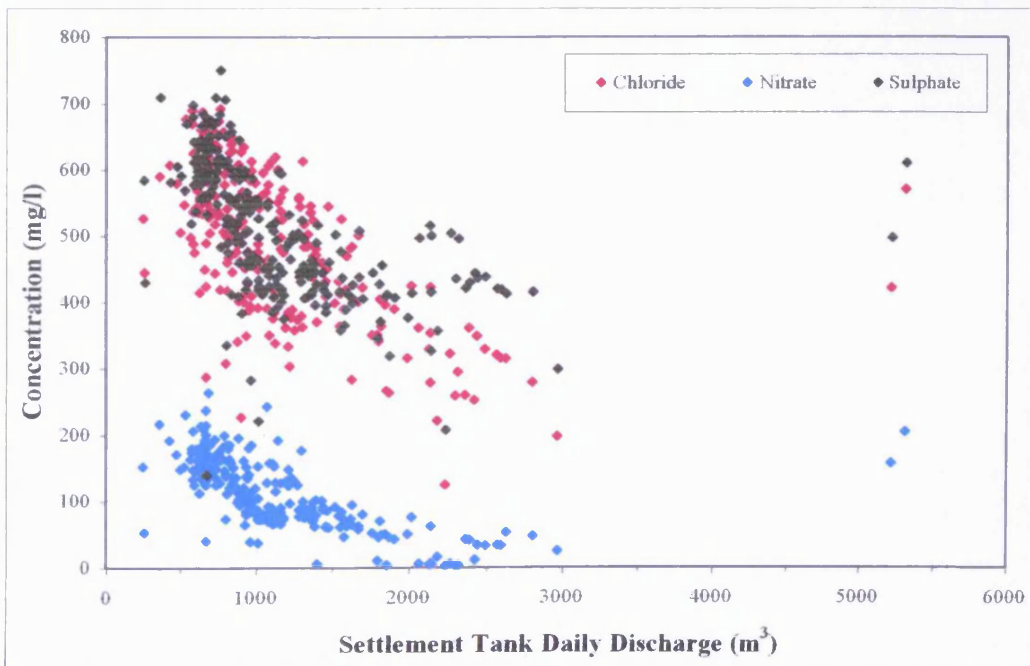


Figure 6.45 Graph showing discharge through the Settlement Tank against the chloride, nitrate and sulphate IC results.

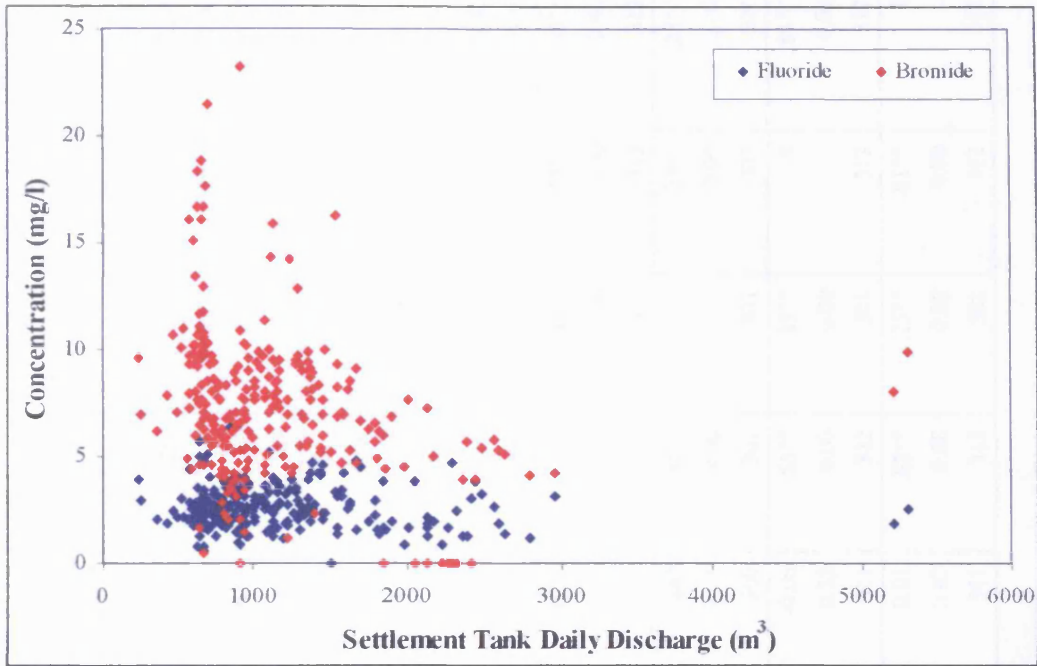


Figure 6.46 Graph showing discharge through the Settlement Tank against the fluoride and bromide IC results.

		Settlement Tank discharge	Settlement Tank Conductivity (Jan 03 to June 04)	Settlement Tank Conductivity (Sept 03 to June 04)	Settlement Tank fluoride	Settlement Tank chloride	Settlement Tank bromide	Settlement Tank nitrate	Settlement Tank sulphate
Settlement Tank discharge	Pearson Correlation	1	0.02	-.54**	-0.09	-.56**	-.16*	-.56**	-.49**
	Significance	.	0.70	0.00	0.17	0.00	0.01	0.00	0.00
	N	1044	400	267	264	265	254	265	265
Settlement Tank Conductivity (Jan 03 to June 04)	Pearson Correlation	0.02	1	1	.15*	.25**	.39**	.16**	-0.03
	Significance	0.70	.	.	0.02	0.00	0.00	0.01	0.64
	N	400	458	287	247	248	237	248	248
Settlement Tank Conductivity (Sept 03 to June 04)	Pearson Correlation	-0.54**	1	1	.33**	.85**	.51**	.40**	.35**
	Significance	0.00	.	.	0.00	0.00	0.00	0.00	0.00
	N	267	287	287	157	158	148	158	158
Settlement Tank fluoride	Pearson Correlation	-0.09	.15*	.33**	1	.29**	.14*	-0.06	0.01
	Significance	0.17	0.02	0.00	.	0.00	0.01	0.32	0.82
	N	264	247	157	311	311	300	311	311
Settlement Tank chloride	Pearson Correlation	-.56**	.25**	.85**	.29**	1	.41**	.53**	.63**
	Significance	0.00	0.00	0.00	0.00	.	0.00	0.00	0.00
	N	265	248	158	311	312	301	312	312
Settlement Tank bromide	Pearson Correlation	-.16*	.39**	.51**	.14*	.41**	1	.23**	.25**
	Significance	0.01	0.00	0.00	0.01	0.00	.	0.00	0.00
	N	254	237	148	300	301	301	301	301
Settlement Tank nitrate	Pearson Correlation	-.56**	.16**	.40**	-0.06	.53**	.23**	1	.81**
	Significance	0.00	0.01	0.00	0.32	0.00	0.00	.	0.00
	N	265	248	158	311	312	301	312	312
Settlement Tank sulphate	Pearson Correlation	-.49**	-0.03	.35**	0.01	.63**	.25**	.81**	1
	Significance	0.00	0.64	0.00	0.82	0.00	0.00	0.00	.
	N	265	248	158	311	312	301	312	312

** Correlation is significant at the 0.01 level

* Correlation is significant at the 0.05 level

Table 6.10 Table of correlations for the Settlement Tank discharge and geochemical data.

6.5 SUMMARY

The leachate produced at Silent Valley landfill site is a weak leachate. The majority of the constituents monitored are low in concentration when compared to the figures quoted by the DoE (1995) for large acetogenic (Table 2.5) and methanogenic (Table 2.6) landfill sites. The leachate from the BSC Pipe (LP1) is similar to the leachate recorded at valley landfills with groundwater ingress (Table 2.16). This fits, since Silent Valley landfill is a valley landfill with suspected groundwater ingress.

Nitrate and nitrite concentrations at Silent Valley landfill site are both relatively high; higher than those presented for large acetogenic (Table 2.5) and methanogenic (Table 2.6) landfill sites.

Analysis of the LP1 leachate from the Silent Valley landfill site reveals that, over the period for which results were available, some of the constituents monitored showed variations (Table 6.11). Conductivity and many of the metals show no trend between 1993 and the present. Sulphate, pH, the BOD/COD ratio and iron show a general decrease over the 11 years. Temperature, ammoniacal nitrogen, alkalinity, COD, BOD, TOC, sodium, potassium, manganese and chloride all show a general increase over the 11 years. It is likely that some of these trends will continue but it is unknown for how long. If the trends do continue then the leachate will become more contaminated overall and require more treatment.

With reference to table 6.12, the concentration of the leachate decreases as the age of the waste increases. The Silent Valley leachate has many of its constituents increasing suggesting that much of the leachate exiting through the BSC Pipe is generated from younger waste. Since the size of the landfill is increasing, there is always young waste being broken down.

Upward trend with time	Downward trend with time	No trend
Temperature	pH	Conductivity
Ammoniacal nitrogen	BOD/COD (slight)	Calcium
Alkalinity	Iron (slight)	Magnesium
COD	Sulphate	Copper
BOD (slight)		Zinc
TOC		Nickel
Sodium		Cadmium
Potassium (slight)		Lead
Manganese (slight)		Chromium
Chloride		

Table 6.11 Long-term trends for determinands measured in LP1.

Parameter	Age Category			
	0 to 5 years	5 to 10 years	10 to 20 years	>20 years
BOD	10000 - 25000	1000 - 4000	50 - 100	<50
COD	15000 - 40000	10000 - 20000	1000 - 5000	<1000
Total Kjeldahl nitrogen	1000 - 3000	400 - 600	75 - 300	<50
Ammonia nitrogen	50 - 1500	300 - 500	50 - 200	<30
Alkalinity	10000 - 15000	1000 - 6000	500 - 2000	<500
TDS	10000 - 25000	5000 - 10000	2000 - 5000	<1000
pH	5 - 6	6 - 7	7 - 7.5	7.5
Calcium	2000 - 4000	500 - 2000	300 - 500	<500
Sodium and Potassium	2000 - 4000	500 - 1500	100 - 500	<100
Magnesium and Iron	500 - 1500	500 - 1000	100 - 500	<100
Zinc and Aluminium	100 - 200	50 - 100	10 - 50	<10
Chloride	1000 - 3000	500 - 2000	100 - 500	<100
Sulphate	500 - 2000	200 - 1000	50 - 200	<50
Total phosphorus	100 - 300	10 - 100		<10

Units in mg/l except for pH

Table 6.12 Changes in concentration of leachate parameters with age of the waste. From Birks & Eyles (1997).

Readings from the conductivity sensors installed in LP1 and the Settlement Tank have been compared with discharge. A weak negative correlation ($R^2 = 0.0284$) is obtained for conductivity with the BSC Pipe (LP1) discharge. A strong negative correlation ($R^2 = 0.4614$) is obtained between conductivity and discharge from the Settlement Tank when only data considered reliable is used. An increase in discharge is associated with a decrease in conductivity, representing dilution.

Conductivity readings are compared with the IC analysis results for LP1 and the Settlement Tank. For LP1, fluoride, chloride, bromide and nitrate increase as conductivity increases, with sulphate remaining about the same. The conductivity of LP1 shows significant weak correlations with chloride ($r = 0.28$, $p = 0.00$), bromide ($r = 0.25$, $p = 0.00$) and fluoride ($r = 0.23$, $p = 0.00$).

For the Settlement Tank, fluoride, chloride, bromide, nitrate and sulphate all increase as conductivity increases. A very strong significant correlation is found for chloride with conductivity ($r = 0.85$, $p = 0.00$). Moderate significant correlations are found with bromide ($r = 0.51$, $p = 0.00$) and nitrate ($r = 0.40$, $p = 0.00$). Significant weak correlations are found with sulphate ($r = 0.35$, $p = 0.00$) and fluoride ($r = 0.33$, $p = 0.00$).

The chemical substances within LP1 and the Settlement Tank discharge show correlations with each other. Since conductivity is related to the nature and concentration of ionised substances present in the solution, it is expected that conductivity would be correlated with some of its constituents.

The discharge from the BSC Pipe (LP1) does not have any significant correlations with the IC analysis. For the Settlement Tank chloride, nitrate, sulphate and bromide show a decrease in concentration with an increase in discharge suggesting a dilution effect. Significant correlations are obtained for the discharge and chloride ($r = -.56$, $p = 0.00$), nitrate ($r = -.56$, $p = 0.00$), sulphate ($r = -.49$, $p = 0.00$) and bromide ($r = -.16$, $p = 0.01$).

Many of the observations of the Silent Valley leachate suggest the current phases of activity within the site. Some are consistent with Phase III, actogenic, conditions. These include decreasing sulphate, increasing alkalinity, and nitrate concentrations closest to

those reported for acetogenic sites. Other observations are consistent with Phase IV, methanogenic, conditions. These include slightly alkaline pH heading towards neutral, decreasing BOD/COD ratio, increasing ammoniacal nitrogen, and TOC, COD, BOD levels closest to those reported for methanogenic sites. As all stages of degradation may occur at different rates at any one time within a single site, it is not inconsistent to record indicators of both Phase III and Phase IV co-existing.

CHAPTER 7

THE USE OF ARTIFICIAL NEURAL NETWORKS TO PREDICT DISCHARGE AT SILENT VALLEY

The classic statistical approach to building models involves linear regression, which is sufficient to describe those systems that behave linearly or approximately linearly, or can be appropriately transformed to create a linear relationship. Linear models have advantages in that they can be understood and analysed in great detail, and they are easy to explain and implement. However, they may be totally inappropriate if the underlying mechanism is non-linear.

Artificial Neural Networks provide a computational or mathematical technique for modelling systems and can be used where the form of the relationship between the variables involved is unknown.

7.1 ARTIFICIAL NEURAL NETWORKS (ANN)

Artificial Neural Networks (ANNs) were originally developed to mimic basic biological neural systems, the human brain in particular. They are composed of a number of interconnected simple processing elements called neurons or nodes. Each node receives an input signal which is the total “information” from other nodes or external stimuli, processes it locally through an activation or transfer function and produces a transformed output signal to other nodes or external outputs. Although each individual neuron implements its function rather slowly and imperfectly, collectively a network can perform a surprising number of tasks quite efficiently. This information processing characteristic makes ANNs a powerful computational device and able to learn from examples and then to generalise to examples never before seen (Zhang *et al.*, 1998).

Artificial Neural Networks are able to learn from and generalise from experience. Currently, ANNs are being used for a wide variety of tasks in many different fields of business, industry and science. One major application area of ANNs is forecasting. There are several features that make ANNs valuable for forecasting tasks:

- They are data-driven self-adaptive methods that learn from examples and capture functional relationships among the data even if the underlying relationships are unknown or hard to describe.
- They can generalise. After learning the data presented to them (a sample), they can often correctly infer the unseen part of a population.
- They are universal functional approximators. A network can approximate any continuous function to any desired accuracy – traditional statistical forecasting models frequently have limitations in estimating underlying functions due to the complexity of real systems.
- They are non-linear. Real world systems are often non-linear, and ANNs are capable of performing non-linear modelling without a priori knowledge about the relationships between input and output variables (Zhang *et al.*, 1998).

7.1.1 THE MULTI-LAYER PERCEPTRONS (MLP)

Many different ANN models have been proposed with perhaps the most influential models being the multi-layer perceptrons (MLP), Hopfield networks, and Kohonen’s self organising networks. The multi-layer perceptrons are described here.

The MLP networks are used in a variety of problems especially in forecasting because of their inherent capability of arbitrary input–output mapping.

An MLP is typically composed of several layers of neurons or nodes (Fig. 7.1). The first layer is an input layer where external information is received. The last layer is an output layer where the problem solution is obtained. The input layer and output layer are separated by one or more intermediate layers called the hidden layers. The nodes in adjacent layers are usually fully connected by acyclic arcs between layers.

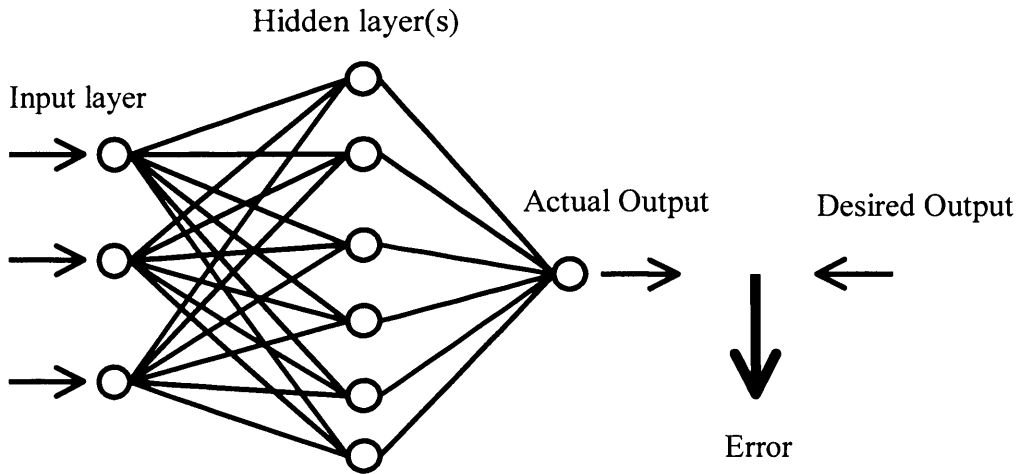


Figure 7.1 A simple Multi-Layered Perception network

The number of nodes in the input layer is equal to the number of independent variables while the output node represents the dependent variable. The weights associated with each processing node are adjusted using the error, which is obtained by comparing the actual output with the desired output.

Backpropagation (BP) neural networks, in addition to the processing neurons, contain a bias neuron connected to each processing unit in the hidden and output layers. The bias node has a value of +1 and serves a similar purpose as the intercept in regression models.

BP networks are a class of feedforward neural networks with supervised learning rules. Feedforward refers to the direction of information flow from the input to output layer. Inputs are passed through the neural network once to determine the output. Supervised learning is the process of comparing each of the network's forecasts with the known correct answer and adjusting the weights based on the resulting forecast error to minimise the error function (Kaastra & Boyd, 1996).

Before an ANN can be used to perform any desired task, it must be trained to do so. Basically, training is the process of determining the arc weights which are the key elements of an ANN. The knowledge learned by a network is stored in the arcs and nodes in the form of arc weights and node biases. It is through the linking arcs that an ANN can carry out complex non-linear mappings from its input nodes to its output nodes. An MLP training is a supervised one in that the desired response of the network (target value) for each input pattern (example) is always available (Zhang *et al.*, 1998).

Whatever the dimension, the input vector for a time series forecasting problem will be almost always composed of a moving window of fixed length along the series. The total available data are usually divided into a training set (in-sample data) and a test set (out-of-sample or hold-out sample). The training set is used for estimating the arc weights while the test set is used for measuring the generalisation ability of the network (Zhang *et al.*, 1998). Generalisation is the ability to draw conclusions about highly complex new situations by making associations with previous experience of similar situations (Stegemann & Buenfeld, 1999).

7.1.2 APPLICATIONS OF ANNS AS FORECASTING TOOLS

Artificial neural networks have been used extensively for financial applications. Many other forecasting problems have been solved by ANNs including airborne pollen, commodity prices, environmental temperature, helicopter component loads, international airline passenger traffic, macroeconomic indices, ozone, personnel inventory, rainfall, river flow, student grade point averages, tool life, total industrial production, trajectory, transportation, water demand, and wind pressure profile (Zhang *et al.*, 1998).

7.1.2.1 Rainfall-Runoff Modelling

Shamseldin (1997) looked at the application of a neural network technique in the context of rainfall-runoff modelling. The performance of the technique was compared with those of models that utilise similar input information, namely, the simple linear model (SLM), the seasonally based linear perturbation model (LPM) and the nearest neighbour linear perturbation model (NNLPM). The results suggested that the neural network shows considerable promise in the context of rainfall-runoff modelling.

Lange (1999) showed that an artificial neural network is able to represent the rainfall-runoff process of a catchment. After a phase of training the neural network is able to calculate the corresponding hydrograph for any precipitation distribution. Lange also produced a hydrograph similar to a unit hydrograph using the trained network.

Sajikumar & Thandaveswara (1999) used an artificial neural network paradigm, known as the temporal back propagation neural network (TBP-NN) for a monthly rainfall-runoff model. The performance of their model in a “scarce data” scenario (i.e., the effects of using reduced calibration periods on the performance) was compared with Volterratype Functional Series Models (FSM), utilising the data of the River Lee (in the UK) and the Thuthapuzha River (in Kerala, India). The results confirmed the TBP-NN model as being the most efficient of the black-box models tested for calibration periods as short as six years.

Ancil *et al.* (2004) studied the impact of the length of observed records on the performance of multiple-layer perceptrons (MLPs), and compared their results with those of a parsimonious conceptual model equipped with an updating scheme. The results revealed that MLP stream flow mapping was efficient as long as wet weather data were available for the training; the longer series implicitly guarantee that the data contain valuable information of the hydrological behaviour; the results were consistent with those reported for conceptual rainfall-runoff models. The physical knowledge in the conceptual models allowed them to make much better use of 1-year training sets than the MLPs. However, longer training sets were more beneficial to the MLPs than to the conceptual model. Both types shared best performance about evenly for 3- and 5-year training sets, but MLPs did better whenever the training set was dominated by wet weather. The MLPs continued to improve for input vectors of 9 years and more, which was not the case of the conceptual model.

7.1.2.2 River Flow Forecasting

Dibike & Solomatine (2001) investigated the applicability of ANNs for downstream flow forecasting in the Apure river basin (Venezuela). Two types of ANN architectures, namely multi-layer perceptron network (MLP) and a radial basis function network (RBF) were implemented. The performances of these networks were compared with a conceptual rainfall-runoff model and they were found to be slightly better for this river flow-forecasting problem.

7.1.2.3 Rainfall–Runoff Model for Real-Time Flash-Flood Forecasting

Toth *et al.* (2000) undertook a comparison of time-series analysis techniques for short-term rainfall forecasting to be used as input in a deterministic rainfall–runoff model for real-time flash-flood forecasting. Different structures of ARMA (linear stochastic autoregressive moving average) models, ANNs and nearest-neighbour approaches were

applied for forecasting storm rainfalls that occurred in the Sieve River basin, Italy, in the period 1992–1996.

The forecast performances of each technique were evaluated by comparing observed and predicted rainfall data and also by comparing the river discharge predictions provided by a conceptual rainfall–runoff model using observed and predicted rainfall as input. Their results indicate how the considered time-series analysis techniques, and especially those based on the use of ANN, provide a significant improvement in the flood forecasting accuracy in comparison to the use of simple rainfall prediction approaches of heuristic type, which are often applied in hydrological practice.

7.2 BUILDING A MODEL

Designing a neural network can be split into eight steps (Table 7.1). The procedure may require visiting previous steps especially between training and variable selection.

Step 1: Variable selection
Step 2: Data collection
Step 3: Data pre-processing
Step 4: Training, testing and validation sets
Step 5: Neural network paradigms
Number of input nodes
Number of hidden layers
Number of hidden nodes
Number of output nodes
Transfer functions
Step 6: Evaluation criteria
Step 7: Neural network training
Number of training iterations
Learning rate and momentum
Step 8: Implementation

Table 7.1 Steps in designing a neural network forecasting model. Adapted from Kaastra & Boyd (1996).

7.2.1 STEP 1: VARIABLE SELECTION

As in any prediction/forecasting model, the selection of appropriate model inputs is extremely important.

7.2.2 STEP 2: DATA COLLECTION

All data should be checked for errors by examining day to day changes, ranges, logical consistency and missing observations.

7.2.3 STEP 3: DATA PRE-PROCESSING

Data preprocessing refers to analysing and transforming the input and output variables to minimise noise, highlight important relationships, detect trends, and flatten the distribution of the variable to assist the neural network in learning the relevant patterns (Kaastra & Boyd, 1996). Data pre-processing can have a significant effect on model performance (Maier & Dandy, 2000).

Data normalisation is the process of standardising the possible numerical range that the input data vectors can take in order to ensure that all variables receive equal attention during the training process. It is particularly relevant in cases where input variables are of different range - without normalisation, the effects of a change in one can completely outweigh the effects of changes in other variables.

In addition, the variables have to be scaled in such a way as to be equated with the limits of the activation functions used in the output layer. Non-linear transfer functions will squash the possible output from a node into, typically, $[0,1]$ for logistic function and $[-1,1]$ for hyperbolic tangent function. For example, if the outputs of the logistic transfer function are between 0 and 1, the data are generally scaled in the range 0.1–0.9 or 0.2–0.8. This is based on the fact that the nonlinear activation functions usually have asymptotic limits (they reach the limits only for infinite input values) (Zhang *et al.*, 1998).

It should be noted that, as a result of normalising the target values, the observed output of the network will correspond to the normalised range. Thus, to interpret the results obtained from the network, the outputs must be rescaled to the original range and the

accuracy obtained by the ANNs should also be based on the rescaled data set (Zhang *et al.*, 1998).

7.2.4 STEP 4: TRAINING, TESTING AND VALIDATION SETS

It is common practice to split the available data into two or three sub-sets; a training set, a test set and sometimes an independent validation set. In the literature, the test set and validation set are sometimes interchanged. The test set is a set of data which the neural network has not previously seen, which is used to test how well the neural network has learned to generalise. The validation set is a set of data used to test the performance of the network during training, but not used for modifying the weights of the network (Stegemann & Buenfeld, 1999).

Typically, ANNs are unable to extrapolate beyond the range of the data used for training. Consequently, poor forecasts/predictions can be expected when the validation data contain values outside of the range of those used for training. It is also imperative that the training and validation sets are representative of the same population (Maier & Dandy, 2000).

7.2.5 STEP 5: NEURAL NETWORK PARADIGMS

7.2.5.1 Number of Input Nodes

Each independent variable is represented by its own input node. Too few or too many input nodes can affect either the learning or prediction capability of the network.

In a time series forecasting problem, the number of input nodes corresponds to the number of lagged observations used. A series of lagged observations (a window) is used, on the assumption that future values are related in some way to the series that precedes them.

Getting the number of input nodes right is extremely important, since it largely determines the subsequent network design and its ability to forecast. A network should have sufficient nodes to allow the learning of the features embedded in the data, without so large a number that its prediction capability is adversely affected – a network with a large number of inputs may be unable to generalise sufficiently to produce a meaningful prediction.

Zhang *et al.* (1998) express the opinion that “*the number of input nodes is probably the most critical decision variable for a time series forecasting problem since it contains the important information about the complex (linear and/or nonlinear) autocorrelation structure in the data*”.

7.2.5.2 Number of Hidden Layers

The hidden layer(s) provide the network with its ability to generalise. A network never needs more than two hidden layers to solve most problems including forecasting and one hidden layer may be enough for most forecasting problems. However, using two hidden layers may give better results for some specific problems, especially when one hidden layer network is overladen with too many hidden nodes to give satisfactory results (Zhang *et al.*, 1998).

Increasing the number of hidden layers increases computation time and the danger of overfitting which leads to poor out-of-sample forecasting performances (Kaastra & Boyd, 1996).

7.2.5.3 Number of Hidden Nodes

The issue of determining the optimal number of hidden nodes is a crucial yet complicated one. In general, networks with fewer hidden nodes are preferable as they usually have

better generalisation ability and less overfitting problem (construction of a network to fit the details of the training patterns rather than generalise well for new data). However, networks with too few hidden nodes may not have enough power to model and learn the data.

The most common way in determining the number of hidden nodes is via experiments or by trial-and-error.

7.2.5.4 Number of Output Nodes

The number of output nodes is relatively easy to specify as it is directly related to the problem under study. For a time series forecasting problem, the number of output nodes often corresponds to the forecasting horizon. There are two types of forecasting: one-step-ahead (which uses one output node) and multi-step-ahead forecasting (Zhang *et al.*, 1998). However, neural networks with multiple outputs, especially if these outputs are widely spaced, will produce inferior results as compared to a network with a single output (Kaastra & Boyd, 1996). The solution is to have the neural networks specialise by using separate networks for each forecast.

7.2.5.5 Transfer Functions

Transfer functions are mathematical formulas that determine the output of a processing node. They are also referred to as transformation, squashing, activation, or threshold functions. They determine the relationship between inputs and outputs of a node and a network. The purpose of a transfer function is to prevent outputs from reaching very large values that can ‘paralyse’ the neural network and thereby inhibit training. It also introduces a degree of nonlinearity that is valuable for most ANN applications.

7.2.6 STEP 6: EVALUATION CRITERIA

At the beginning of the model building process, it is important to clearly define the criteria by which the performance of the model will be judged, as they can have a significant impact on the model architecture and weight optimisation techniques chosen. In most applications, performance criteria include one or more of the following: prediction accuracy, training speed and the time delay between the presentation of inputs and the reception of outputs for a trained network.

7.2.7 STEP 7: NEURAL NETWORK TRAINING

Training a neural network to learn patterns in the data involves iteratively presenting it with examples of the correct known answers. The objective of training is to find the set of weights between the nodes that determine the global minimum of the error function. The BP network uses a gradient descent training algorithm which adjusts the weights to move down the steepest slope of an error surface (Kaastra & Boyd, 1996).

7.2.7.1 Number of Training Iterations

Kaastra & Boyd (1996) detail the two schools of thought regarding the point at which training should be stopped. Both methods agree that generalisation of the validation set is the ultimate goal and both use testing sets to evaluate a large number of networks.

The first says that the researcher should only stop training when there is no improvement in the error function. The point at which the network does not improve is called convergence. In this approach there is no such thing as overtraining only overfitting which is a symptom of a network that has too many weights. The solution is to reduce the

number of hidden nodes (or hidden layers if there is more than one) and/or increase the size of the training set.

The second view suggests a series of train-test interruptions. Training is stopped after a predetermined number of iterations and the network's ability to generalise on the validation set is evaluated then training is resumed. The problem with this is that the researcher has no way of knowing if additional training could improve the generalisation ability of the network. The test-train approach attempts to guard against overfitting by stopping training based on the ability of the network to generalise.

One method to determine a reasonable value of the maximum number of runs is to plot the sum of squared errors (or Root Mean Squared Error (RMSE)) for each iteration or at predetermined intervals up to the point where improvement is negligible.

7.2.7.2 Learning Rate and Momentum

The most popularly used training method is the backpropagation algorithm which is essentially a gradient steepest descent method, which follows the contours of the error surface by always moving down the steepest slope. For the gradient descent algorithm, a step size, called the learning rate, must be specified.

The learning rate is crucial for backpropagation learning algorithm since it determines the magnitude of weight changes. The learning rate is directly proportional to the size of the steps taken in weight space. Smaller learning rates tend to slow the learning process while larger learning rates may cause network oscillation in the weight space.

The momentum term suppresses side to side oscillations by filtering out high-frequency variations allowing larger learning rates to be used. Momentum values that are too great will prevent the algorithm from following the twists and turns in weight space. It should be noted that the momentum term must be less than 1.0 for convergence (Maier & Dandy, 2000).

7.2.8 STEP 8: IMPLEMENTATION

Although the implementation step is listed as the last one, it requires careful consideration before collecting data. There are a number of neural network software packages that provide a means by which trained networks can be implemented or a trained network can be created in a spreadsheet by knowing its architecture, transfer functions and weights.

7.3 SILENT VALLEY MODEL

The objective of using artificial neural networks for the Silent Valley data was to produce a forecasting system that could be used to predict the daily discharge from the Settlement Tank. Multiple ANN models were produced and the results averaged.

7.3.1 NETWORK ARCHITECTURE AND TRAINING

The Silent Valley model was constructed using a feedforward backpropagation neural network¹. The model was constructed using a single output node to produce a one-step-ahead prediction of daily discharge for the Settlement Tank.

The number of nodes in the hidden layers was arrived at using an initial series of experiments with trial networks. A two hidden layer architecture was used with the number of interconnections between the two layers lying in the range of 15 to 30 (with fewer than 15, the training error increased and the networks appeared to be unable to model the complexities of the relationships adequately; with more than 30, the networks appeared to be overfitting to the data and losing the ability to generalise).

The number of input nodes was determined by the data used in the training process.

The data were split into two sets, a training set and a testing set. The training process did not use a validation set, but was an extension of the first process described in Section 7.2.7.1. Training was stopped once a predetermined value of the error function (Gamma value) was reached or when there was no further improvement in the error function.

¹ Neural networks for Silent Valley landfill were built by Stuart Paris using data supplied by the author.

The Gamma (near neighbour) test is a data analysis algorithm that estimates the mean squared error (MSE) that can be achieved by a model constructed using a data set (Wilson *et al.*, 2002). The training process is stopped once the MSE reaches the Gamma value, as further reduction in the MSE is likely to be the result of overfitting to noise within the data.

7.3.2 THE DATA

The data used for constructing models were rainfall, temperature, wind speed and discharge. Whilst other measurements, for instance humidity, might also have been expected to influence the model, the data available was not considered to be reliable (Section 5.1.1.4). Effective Rainfall was not used, although it was shown to be significant (Table 5.16), because the available data only went back to April 2000 and were recorded as daily totals only. However, it is likely that evaporative loss will at least in part be captured by the temperature and wind speed data sets.

Rainfall, temperature and wind speed were shown to be significant by stepwise multiple regression analysis (Section 5.5.1.4.2.2).

Discharge was used both as an input and an output for the model. The rationale behind this was that using discharge as an input defines the initial conditions at the beginning of the forecasting period. The effect on discharge of rainfall entering a ‘wet’ system (high discharge) is likely to be different to that of rainfall entering a ‘dry’ system (low discharge). This was borne out by comparison between trial networks, some of which included discharge as an input and some of which excluded it.

Models were produced in which the values for discharge used were the initial measured values. A further series of models were produced in which the values for discharge were the detrended values. In the former series, it was necessary to include date as a specific variable in order to allow the network to determine the trend.

It was anticipated that the effects on the system would be cumulative rather than instantaneous. For instance, the effects of rainfall onto cold, wet ground (following a few cold rainy days) is likely to be different to that of rainfall onto warm, dry ground (following a few warm sunny days). For this reason, the networks were trained using a window of data from the preceding few days.

Two methods of utilising data from the preceding few days were adopted. One method was to incorporate a window of up to ten 24 hour average/cumulative values for each of the four variables. The other method was to incorporate a window of average/cumulative values covering periods of 24, 48, 72, 96, 120 and 168 hours for each of the variables. Both methods gave broadly similar results.

The data available for the site covered a period of approximately five and a half years (October 1998 to May 2004). However, because of equipment failures, the number of days for which a window of all four variables was available was considerably less than this (approximately 700 days). The data set was discontinuous.

The data were normalised (see Section 7.2.3) so that the values for each variable lay within the range +0.9 to -0.9.

The data set was partitioned to allow two different testing periods to be used. It was partitioned to provide test sets covering the period 5 August to 10 October 2001 and the period 12 April to 19 May 2004. These were chosen as continuous periods of data of reasonable length, representing different seasons and well spaced sections of the total data set. The whole of the remainder of the data set not included in each test set was used as the corresponding training set.

7.3.3 RESULTS

A number of network models were trained for both of the partitioned data sets. In each case the models were used to produce a forecast of daily discharge over the period covered by the test set. The data presented to the networks consisted of windows of the actual rainfall, temperature and wind speed. The initial discharge window consisted of actual values. Thereafter, the forecast for the daily discharge was incorporated in the input for the next prediction.

The models were trained until the target MSE (the Gamma value) was reached and then stopped. Figure 7.2 shows a typical graph for the training of a model. The horizontal red line represents the target MSE and the blue line represents the MSE as training progresses. The MSE on the graph is the MSE of the normalised flow data (i.e., the data reduced to the range +0.9 to -0.9), not the MSE of actual flow data. Cycles represent the number of times that the whole training dataset has been presented to the network (each cycle followed by error backpropagation).

Within the two series of models, the individual model predictions were averaged to provide a single forecast for each of the test periods. This approach was adopted as it was not possible to select the best model(s) without biasing the results of the experiments. If networks are tested using the test set and only those which perform well are used for forecasting, bias has occurred. The process has essentially used the test set as part of the training process (Masters, 1993).

Figure 7.3 shows the forecast of daily discharge for the period 2 August to 9 October 2001. Figure 7.4 shows the forecast for the period 11 April to 18 May 2004. The predicted discharge using simultaneous and stepwise regression analysis are also included for comparison.

Both graphs show reasonably close neural network forecasts compared to the actual, with many of the turning points captured. The forecast using neural networks gives a closer predicted flow to the actual compared with the simultaneous and stepwise regression

analysis. The Root Mean Squared Error (RMSE) for the neural network forecasts is lower than that for the simultaneous and stepwise regression analysis (Table 7.2).

Time Period	Prediction Method	Root Mean Squared Error (RMSE)
2 August to 9 October 2001 (Figure 1)	Neural network	185
	Simultaneous regression	260
	Stepwise regression	246
11 April to 18 May 2004 (Figure 2)	Neural network	188
	Simultaneous regression	325
	Stepwise regression	322

Table 7.2 Root Mean Square Errors for the predicted discharge over each period.

However, not all the features of the actual discharge have been forecast. Whilst we can not be certain that the actual flow recorded is completely accurate (examination of the quarter hour data shows a noisy series), the failure to predict these features suggests that there are other variables which have not been included in the models. The most obvious of these is humidity and solar radiation. Evapotranspiration is affected by the weather parameters solar radiation (amount of sunshine), wind speed, humidity and temperature. Wind speed and temperature have been incorporated into the model but there is no data available for humidity or solar radiation. When calculating the water balance over a landfill site, the monthly duration of sunlight (Section 5.6.2.1.4) was needed to estimate the potential evapotranspiration. Roderick & Farquhar (2002) also stress the importance of solar irradiance in pan evaporation.

The discontinuous nature of the data set may also have had an affect on the accuracy of the forecast; this particular set of circumstances may not have been represented in the training set. If the data at hand were found to be during dry years, it is expected that such trained ANN models would not perform well during wet years (Anctil *et al.*, 2004).

If further work is to be carried out at site involving neural network modelling, it would be worth installing a reliable humidity sensor and a solar radiation detector on site. Further work would also involve continued monitoring so that the network can be trained using a longer continuous set of data. A longer training set should improve the network's ability to generalise since it will have seen more data covering more situations. Anctil *et al.* (2004) found that for forecasting rainfall-runoff their MLPs continued to improve for input vectors of 9 years and more.

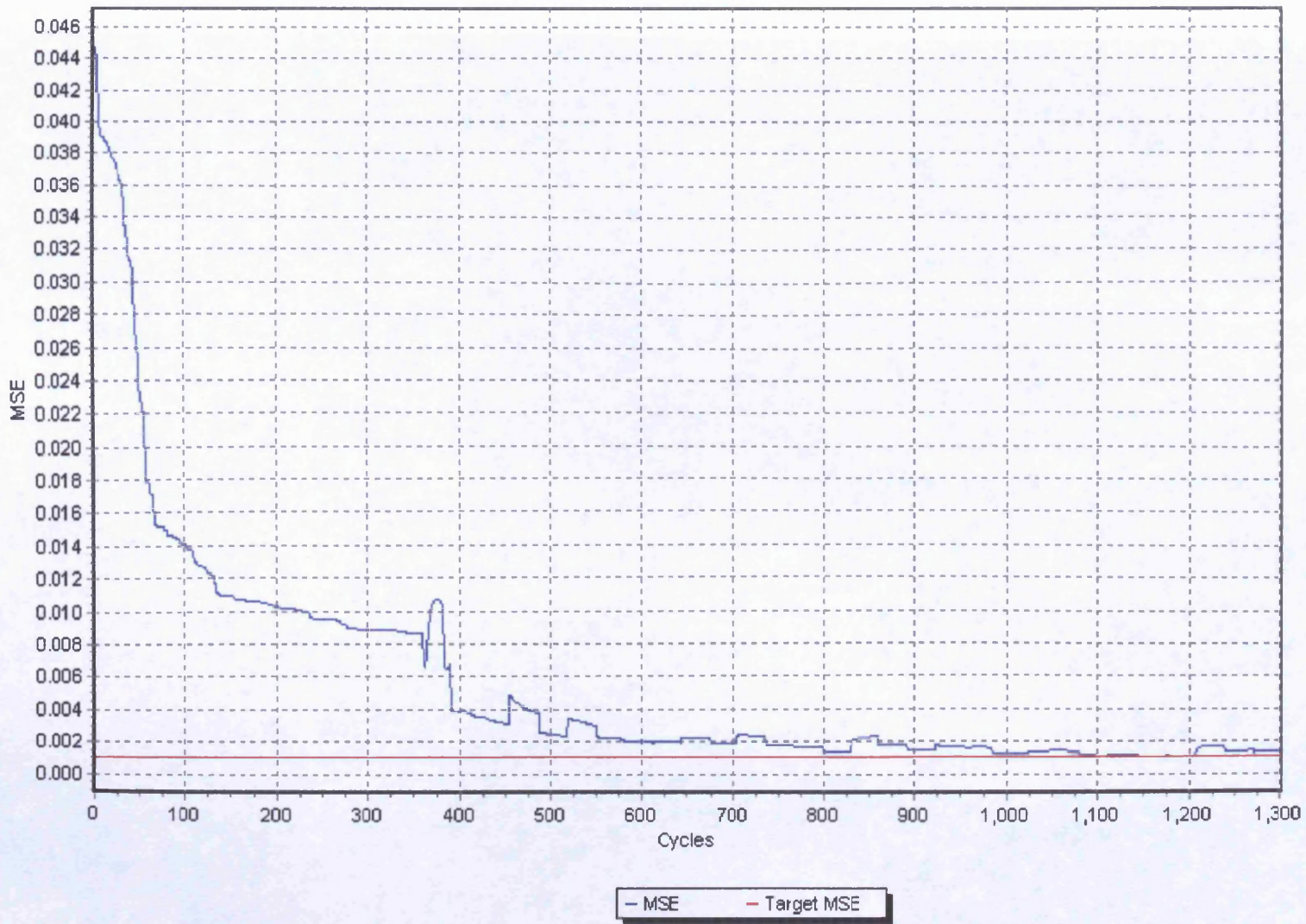


Figure 7.2 Graph showing the training Mean Squared Error of a model using the normalised data.

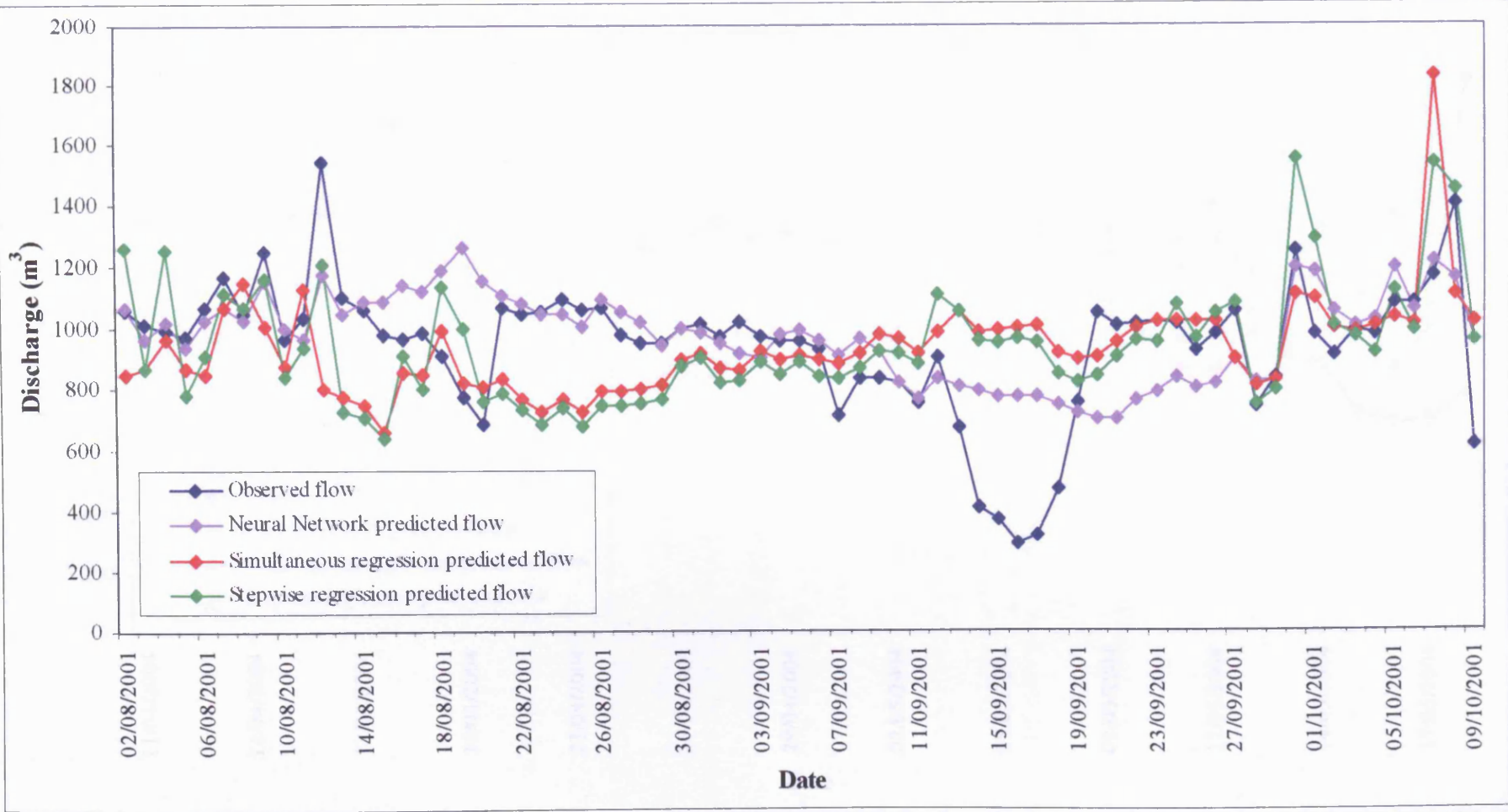


Figure 7.3 Graph showing the observed discharge in the Settlement Tank with predicted discharge using neural networks, simultaneous regression analysis and stepwise regression analysis between 2 August and 9 October 2001.

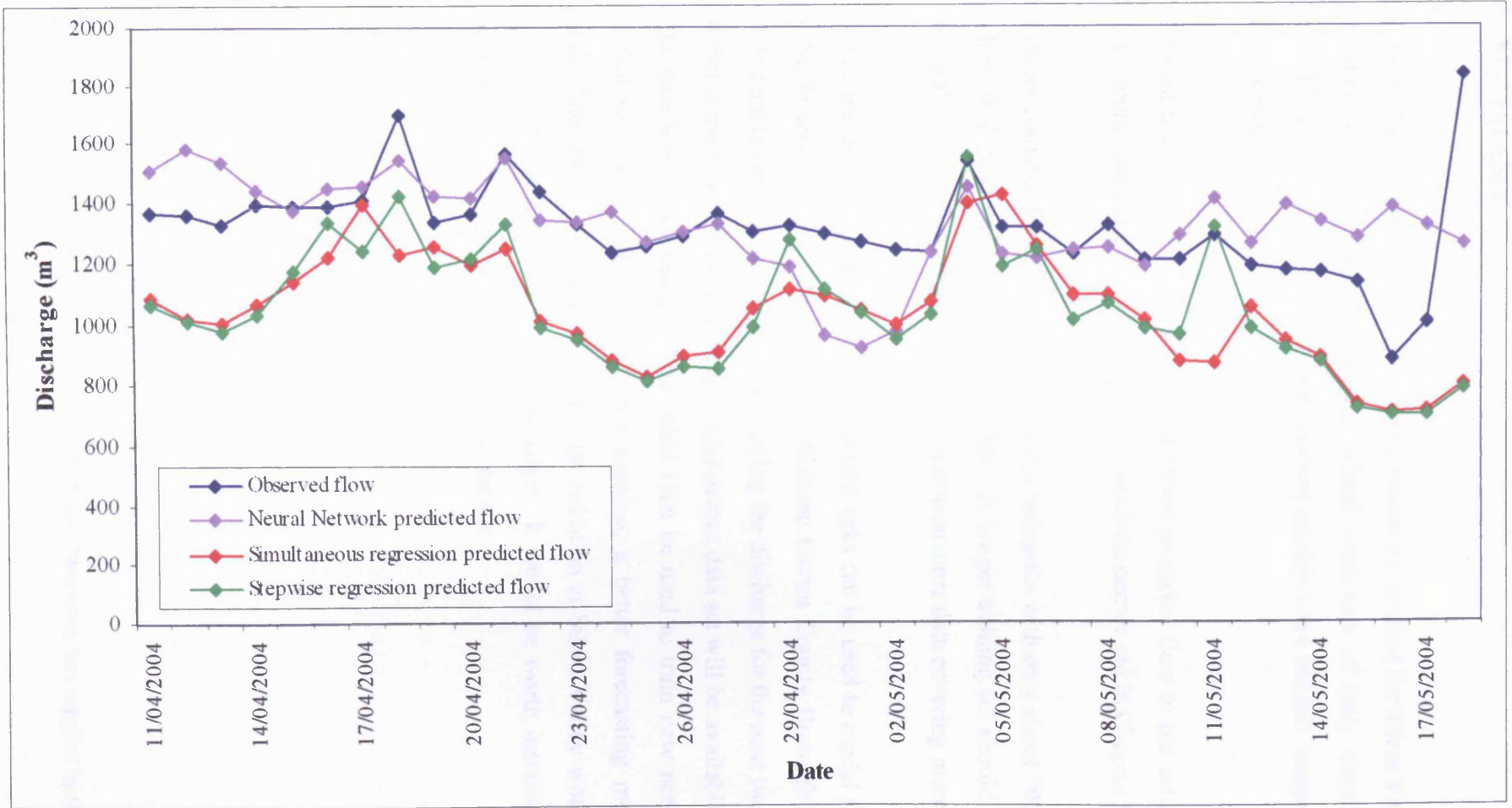


Figure 7.4 Graph showing the observed discharge in the Settlement Tank with predicted discharge using neural networks, simultaneous regression analysis and stepwise regression analysis between 11 April and 18 May 2004.

7.4 SUMMARY

Feedforward backpropagation neural networks were constructed for Silent Valley¹ using a single output node to produce a one-step-ahead prediction of daily discharge for the Settlement Tank. The data used for constructing models were rainfall, temperature, wind speed and discharge.

The forecast using neural networks gives a closer predicted flow to the actual compared with the simultaneous and stepwise regression analysis carries out in Chapter 5.

The data set available for Silent Valley was discontinuous with only about 700 days where a window of all four variables was available. A longer training set should improve the network's ability to generalise since it will have seen more data covering more situations.

This was a preliminary study of how neural networks can be used to model the discharge in the Settlement Tank at Silent Valley. Blaenau Gwent County Borough Council has agreed to fund the author to continue monitoring the discharge for the next two years. It is hoped that at the end of these two years a continuous data set will be available to combine with the data already available. This could then be used to train new networks. It is hoped that with more data available for training, a better forecasting model will be obtained. Information on humidity and solar radiation at Silent Valley would be useful since they are likely to influence the discharge. It would be worth installing a reliable humidity sensor and a solar radiation detector on site.

¹ Neural networks for Silent Valley landfill were built by Stuart Paris using data supplied by the author.

CHAPTER 8

DISCUSSION

8.1 INTRODUCTION

Silent Valley landfill is an active unlined landfill site that is evolving over time. The site works on a dilute and attenuate principal. The clay rich deposits covering the valley floor, which met the NRA guideline of $<1 \times 10^{-8}$ m/s for an acceptable lining material, act as a relatively impermeable layer.

Chapter 4 presented a Conceptual Site Model of Silent Valley landfill site (Section 4.3, Figures 4.27 to 4.30). The figures showed the original valley bottom, the area of slag and the area of landfill. Resistivity surveys confirmed the location of the slag and landfill, and have shown that the saturation of the landfill does not vary significantly over a year.

8.2 WATER BALANCE ANALYSIS

With reference to the drainage map of the site (Figure 3.33), it appears that the area within the drainage ditches is approximately 25 ha. Assuming a catchment size of 25 ha, the percentage of discharge accounted for by rainfall input is 88% and the percentage of discharge accounted for by Effective Rainfall input is 60%. This suggests that groundwater is entering the landfill site. For the data available, this equates to something between 46000 m³ and 156000 m³ a year entering the site as groundwater, representing between 12% and 40% of the discharge. The actual value is likely to be somewhere between the two values. Groundwater entering the site implies that the landfill will have less of an environmental impact on the surrounding area, since groundwater flows are likely to be towards the landfill rather than away from it (at least in the area lying up gradient with respect to piezometric head) but it also means that the landfill operator needs to dispose of a greater volume of leachate with higher costs.

Using monthly averages the water balance on the capped Southern Slope has been calculated. The actual evaporation calculated for the model (25%) compares well with the actual evaporation of the MORECS data for Cwm (23%) supplied by the Met Office. The average percolation over a year is 593 mm, which represents 33% of the precipitation. The percolation occurred over January, February, March, April, October, November and December. This corresponds with the increase in predicted leachate discharge obtained from the multiple regression models for both the BSC Pipe and the Settlement Tank.

8.3 BSC PIPE DISCHARGE

Analysis of the leachate data from the BSC Pipe showed that there is a weak correlation (0.22) between daily discharge and rainfall with a lag of 5 days. No significant correlation was found for daily discharge in the BSC Pipe with Effective Rainfall. Recharge of leachate, leachate storage, possibly flows from higher perched water tables to the main leachate water table in the base of the landfill, and groundwater entering the site would all attenuate the rainfall signal.

The strongest correlation with the discharge through the BSC Pipe was found with average daily temperature ($r = -0.26$, $p = 0.00$).

BSC Pipe discharge was considered as the dependant variable with meteorological data as the independent variables for multiple regression analysis. Both the simultaneous and the stepwise multiple regression analysis gave stronger correlations than the strongest single correlation. Using average daily temperature and daily rainfall (with the 5 day lag) the stepwise regression analysis had a correlation of 0.32 compared to 0.33 with the simultaneous regression analysis using all the variables (average daily temperature, average wind speed, daily rainfall (with the 5 day lag) and pressure). This shows the lack of predictive power of pressure and average wind speed.

The resulting models both show seasonal fluctuations in leachate discharge, with high flows in winter and low flows in summer. The predicted flows varied between around 500 m³/day in the winter to around 260 m³/day in the summer. The actual data shows significant short-term fluctuations that cannot be modelled using this simple multiple regression based approach. The multiple regression analysis has however highlighted average daily temperature as the strongest predictive variable for discharge for the BSC Pipe.

8.4 SETTLEMENT TANK DISCHARGE

The discharge from the Settlement Tank was shown to have a long-term upward trend (Section 5.4.2). Due to the gaps in the data it was not possible to say whether there is an overall increase in discharge or whether this increase simply reflects the available data. The rainfall data showed no significant trend suggesting that the trend in the flow data reflects other factors, for instance changes in the size of the landfill site itself.

The landfill operator has indicated that the Settlement Tank does not get full as frequently as it used to since the engineering works were carried out in 2001. This could be due to a lower flow rate exiting the Settlement Tank in the past (rate could have been altered when the flume was installed in July 2001) or these higher discharges (anecdotal evidence only) were not recorded accurately or at all by the flow monitoring equipment.

Assuming the long-term increasing trend in discharge is correct, discharges to the sewer have increased over the monitoring period. If this trend continues, then while the landfill is active and increasing in area, the discharge is likely to continue to increase. The discharge through the Settlement Tank between July 2003 and June 2004 was approximately 430000 m³. The regression line for the trend in discharge is $y = 0.1353x - 4054.5$, indicating that with each year the daily discharge increases by about 49 m³. Over a year the discharge would increase by approximately 18000 m³, which represents about 4% of the July 2003 to June 2004 discharge. If the trend were to continue for the next 5 years, based on the July 2003 to June 2004 discharge, the discharge in 5 years would be approximately 520000 m³ representing a 21% increase. When the landfill is restored the discharge will decrease, although if groundwater is still entering the site there will remain a significant discharge.

Chapter 5 (Sections 5.5.2.2, 5.5.2.3) illustrated the effect rainfall and Effective Rainfall have on the volumes of leachate at the site. Increases in discharge for the Settlement Tank correspond to rainfall events. There is a weak correlation (0.291) between daily discharge and rainfall with a lag of 0 days. Using data for every 30 minutes, the best correlation (0.189) of half hourly discharge and rainfall occurs with a lag of 3 intervals - one and a half hours. This implies that the discharge shows a rapid response to rainfall events. It is

likely that the rapid response is derived largely from surface runoff across the landfill that is collected by drainage ditches and enters the Settlement Tank.

Slightly stronger correlations are obtained for daily discharge through the Settlement Tank and daily Effective Rainfall for a lag of 1 day (0.307) and a lag of 0 days (0.294).

The strongest correlation with the unadjusted discharge through the Settlement Tank is with daily rainfall ($r = 0.29$, $p = 0.00$) and daily effective rainfall ($r = 0.29$, $p = 0.00$). Slightly higher correlations are obtained with all the meteorological data when using the discharge values with the long-term trend removed. This suggests that the trend observed is not driven by these external variables, but most probably reflects an increase in the catchment area supplying water to the settlement tank.

Settlement Tank discharge was considered as the dependant variable with meteorological data as the independent variables for multiple regression analysis. Analysis was performed on unadjusted discharge data and discharge data that had had the long-term trend removed. Both the simultaneous and the stepwise multiple regression analyses gave stronger correlations than the strongest single correlation. For both simultaneous and stepwise regression analysis, the results were slightly better when using the discharge data with the long-term trend removed.

The best regression method for the data was using stepwise regression on the discharge data with the trend removed, with the highest R (0.51) and R square values (0.26) and the lowest RMSE (448).

The resulting models show seasonal fluctuations in leachate discharge, with high flows in winter and low flows in summer. The predicted flows varied between around 1500 m³/day in the winter to around 900 m³/day in the summer. The actual data shows significant short-term fluctuations that cannot be modeled using this simple multiple regression based approach. The multiple regression analysis has however highlighted average daily temperature as the most important variable with the greatest predictive power in determining discharge for the Settlement Tank.

Settlement Tank discharge data in the winter (October to March) and summer (April to September) were analysed separately. Although higher correlations are obtained for simple regression of the summer data rather than all the data, when using multiple regression analysis the best correlations are obtained when using all the data set. This could be due to the increased size of the data set when using all the data.

8.5 BSC PIPE LEACHATE GEOCHEMISTRY

Data from the monitoring programmes of Blaenau Gwent County Borough Council and later Silent Valley Waste Services are available for the leachate exiting the BSC Pipe. These data are used together with the analysis results from this study.

Analysis of the LP1 leachate reveals that, over the period for which results were available, some of the constituents monitored showed variations. Conductivity and many of the metals show no trend between 1993 and the present. Sulphate, pH, the BOD/COD ratio and iron show a general decrease over the 11 years. Temperature, ammoniacal nitrogen, alkalinity, COD, BOD, TOC, sodium, potassium, manganese and chloride all show a general increase over the 11 years. It is likely that some of these trends will continue but it is unknown for how long. If the trends do continue then the leachate is going to become more contaminated overall and require more intensive treatment. Assuming that all of the trends continue unchanged, then the concentrations of some of the constituents of LP1 will change as indicated in table 8.1. Although sulphate has shown a decrease over time, the trend is levelling off, so there is not significant change in sulphate concentrations in 5 years. The rest of the constituents in the table show an increase.

Constituent	Approximate mid 2004 level	Predicted level 5 years on (mid 2009)	Percentage increase (%)
Temperature (°C)	35	50	42
Ammoniacal nitrogen (mg/l)	85	185	117
Alkalinity (mg/l)	1050	1800	71
BOD (mg/l)	8	12	50
COD (mg/l)	425	850	100
Chloride (mg/l)	560	575	3
Manganese (mg/l)	95	160	68
Potassium (mg/l)	375	580	55
Sodium (mg/l)	730	1230	68
Sulphate (mg/l)	750	750	0
TOC (mg/l)	110	210	91

Table 8.1 Table showing present and predicted levels of constituents within LP1 based on trends seen between 1993 and the present.

Readings from the conductivity sensors installed in LP1 were compared with the discharge. A weak negative correlation ($R^2 = 0.0284$) was obtained for conductivity with the BSC Pipe (LP1) discharge. Observed conductivity values ranged from 1.9 to 8.5 mS/cm.

Conductivity readings were compared with the IC analysis results. For LP1, fluoride, chloride, bromide and nitrate increase as conductivity increases, with sulphate remaining about the same. The conductivity of LP1 shows significant weak correlations with chloride ($r = 0.28$, $p = 0.00$), bromide ($r = 0.25$, $p = 0.00$) and fluoride ($r = 0.23$, $p = 0.00$).

The discharge from the BSC Pipe (LP1) does not have any significant correlations with the IC analysis.

Many of the observations of the Silent Valley leachate suggest the current phases of activity within the site. Some are consistent with Phase III, acetogenic, conditions. These include decreasing sulphate, increasing alkalinity, and nitrate concentrations closest to those reported for acetogenic sites. Other observations are consistent with Phase IV, methanogenic, conditions. These include slightly alkaline pH heading towards neutral, decreasing BOD/COD ratio, increasing ammoniacal nitrogen, and TOC, COD, BOD levels closest to those reported for methanogenic sites. As all stages of degradation may occur at different rates at any one time within a single site, it is not inconsistent to record indicators of both Phase III and Phase IV co-existing.

At this time there is no UK guidance on groundwater quality for the protection of human health, so the Dutch Intervention Values are commonly used in assessment. The Dutch guidelines (Table 8.2) consider toxicity effects on natural ecosystems. The 'Optimum' value is that below which the site can be considered to be uncontaminated. The 'Action' trigger level is the concentration above which the contamination is considered to be unacceptable and some form of further investigation and/or remedial works are necessary. Only those constituents of the guidelines for which comparison data are available for the Silent Valley site have been included in the table.

A comparison of the LP1 concentrations reveals that the mean values for chromium and mercury exceed the Dutch 'Action' trigger level. The maximum recorded values in LP1 of arsenic, chromium, lead, nickel and mercury lie above the 'Action' trigger level. The mean values for lead and zinc lie below the Dutch 'Optimum' level.

Contaminant	Dutch Standards ($\mu\text{g/l}$)		LP1 Values ($\mu\text{g/l}$)	
	Optimum	Action	Max	Mean
Arsenic	10	60	116.3	27.43*
Cadmium	0.4	6	2	0.41*
Chromium	1	30	264	39.95*
Copper	15	75	53	22.58*
Lead	15	75	174	8.47*
Nickel	15	75	90	43.27*
Mercury	0.05	0.3	21	18*
Zinc	65	800	328	50.62*

* <values not included in mean calculation

Table 8.2 Dutch guidelines on water standards compared with LP1. Dutch Standards adapted from Layla Resources Ltd (2001).

8.6 SETTLEMENT TANK LEACHATE GEOCHEMISTRY

A strong negative correlation ($R^2 = 0.4614$) was obtained between conductivity and discharge from the Settlement Tank when only data considered reliable was used. An increase in discharge was associated with a decrease in conductivity, representing dilution.

Conductivity readings were compared with the IC analysis results. For the Settlement Tank, fluoride, chloride, bromide, nitrate and sulphate all increase as conductivity increases. A very strong significant correlation was found for chloride with conductivity ($r = 0.85$, $p = 0.00$). Moderate significant correlations were found with bromide ($r = 0.51$, $p = 0.00$) and nitrate ($r = 0.40$, $p = 0.00$). Significant weak correlations were found with sulphate ($r = 0.35$, $p = 0.00$) and fluoride ($r = 0.33$, $p = 0.00$).

For the Settlement Tank chloride, nitrate, sulphate and bromide show a decrease in concentration with an increase in discharge suggesting a dilution effect. Significant correlations were obtained for the discharge and chloride ($r = -.56$, $p = 0.00$), nitrate ($r = -.56$, $p = 0.00$), sulphate ($r = -.49$, $p = 0.00$) and bromide ($r = -.16$, $p = 0.01$).

8.7 FORECASTING USING ANNS

Feedforward backpropagation neural networks were constructed for Silent Valley¹ to produce a one-step-ahead prediction of daily discharge for the Settlement Tank. The forecast using neural networks gave a closer predicted flow to the actual compared with the simultaneous and stepwise regression analysis. Root Mean Squared Error (RMSE) for the periods 2 August to 9 October 2001 and 11 April to 18 May 2004 were 185 and 188 respectively, which represent about 20% and 14% of the discharge. For the same time periods multiple regression analysis had RMSE representing about 27% and 25% of the discharge.

Not all the features of the actual discharge were forecast. Whilst we cannot be certain that the actual flow recorded is completely accurate (examination of the quarter hour data shows a noisy series), the failure to predict these features suggests that there are other variables which were not included in the models. The most obvious of these is humidity and solar radiation. The discontinuous nature of the data set may also have had an affect on the accuracy of the forecast; this particular set of circumstances may not have been represented in the training set. For instance it is unlikely that extreme rainfall events with recurrence intervals of hundreds of years are included in the training data set making it impossible for the ANN forecast to include system response to such extremes. Clearly there may be thresholds within the system that lead to a change in discharge response to extreme rainfall inputs. If events exceeding such thresholds are not included within the training data set then the model is unlikely to be able to predict resulting discharge with accuracy.

This preliminary study showed how neural networks can successfully be used to model the discharge in the Settlement Tank at Silent Valley. The forecasts are better than the results using multiple regression analysis. Once more data has been collected, new networks can be built that should be able to generalise better.

¹ Neural networks for Silent Valley landfill were built by Stuart Paris using data supplied by the author.

For the Settlement Tank, chloride, nitrate, sulphate and bromide showed a decrease in concentration with an increase in discharge. Trendlines of the data can be used to obtain regression equations. The discharge can be predicted using weather data (rainfall, temperature, wind speed and previous predicted discharge) that are fed through the neural networks. The predicted discharge can then be used to predict the concentrations of chloride, nitrate, sulphate and bromide (Fig. 8.1). The predicted chloride measurements are lower than the measured concentrations. Sulphate and nitrate predicted measurements are generally about the same or a bit higher than the measured concentrations. The measured bromide concentrations are close to the predicted measurements; within the limits of precision for the measured concentrations.

This research can be used as a management tool for Silent Valley. By monitoring the rainfall, temperature and wind speed, and knowing the discharge the day before, the discharge for the following days and weeks can be predicted, which can then in turn be used to predict the chloride, nitrate, sulphate and bromide concentrations.

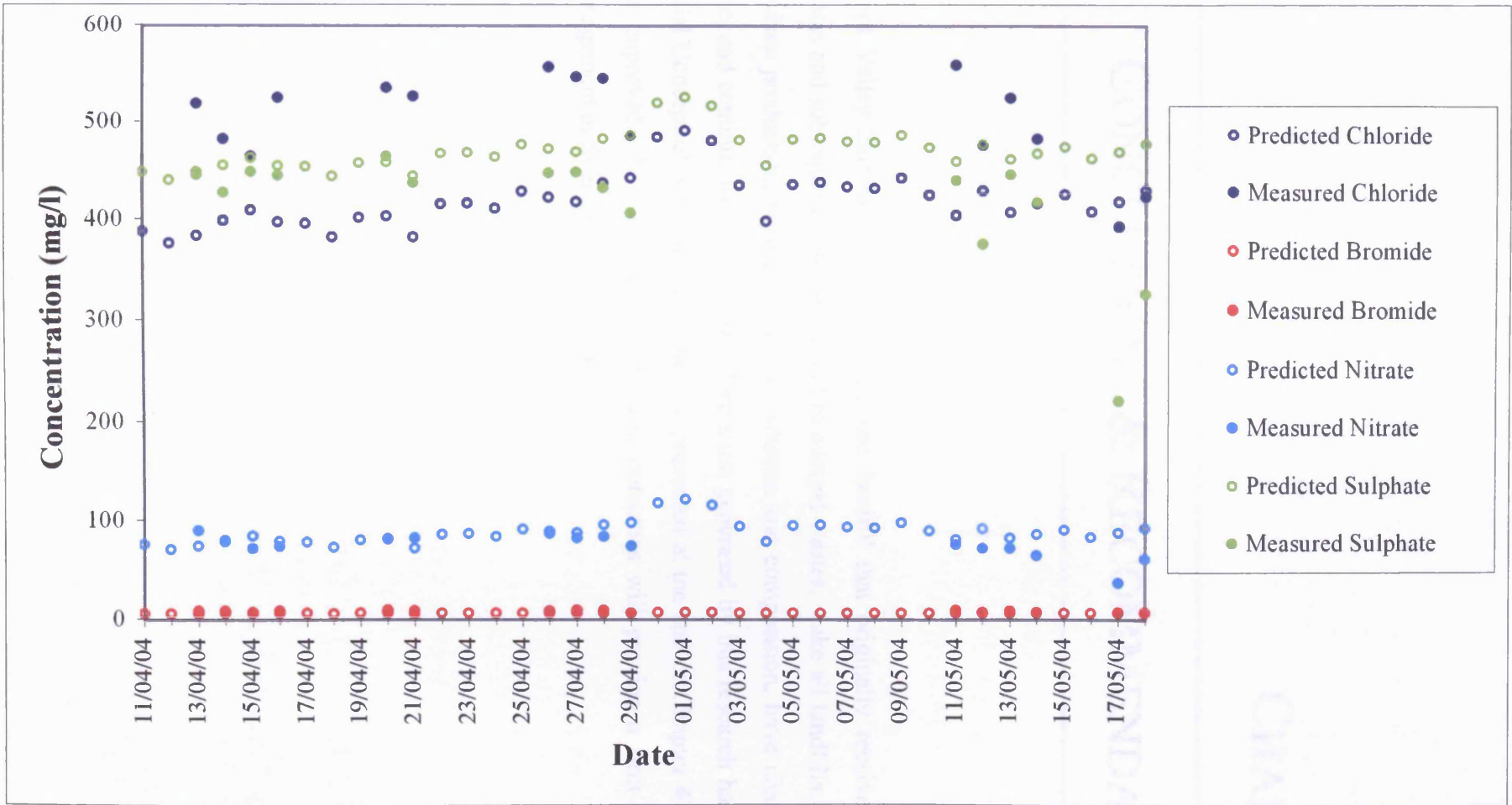


Figure 8.1 Graph showing the observed concentrations of chloride, bromide, nitrate and sulphate in the Settlement Tank with the predicted concentrations based on the predicted discharge using neural networks between 11 April and 18 May 2004.

CHAPTER 9

CONCLUSIONS & RECOMMENDATIONS

Silent Valley landfill is an active unlined landfill that originally received steelworks wastes and subsequently domestic and municipal wastes. Like all landfills, Silent Valley leachate production, both in terms of volumes and composition, have changed through time, and continue to do so. The information generated by this research has allowed the initial Conceptual Site Model of the site presented at the end of Chapter 4 to be refined and improved. It is hoped that research outcomes will provide a firm basis for the management of Silent Valley landfill site.

9.1 CONCLUSIONS

The major conclusions of the project will be presented sequentially, commencing with results of the hydrological assessment, then detailing the leachate chemical analysis and finally considering the interrelationships found between discharge and leachate composition.

Hydrology and Hydrogeology

- Water balance analysis has demonstrated that groundwater is entering the site since rainfall landing on the landfill site catchment (25 ha) does not account for all of the discharge. It is calculated that between 12% and 40% of the discharge recorded through the Settlement Tank is accounted for by groundwater input.
- The discharge through the Settlement Tank shows a rapid response to rainfall events. Regression analysis has indicated a lag of approximately 1 ½ hours. This rapid response is likely to be derived largely from surface runoff across the landfill that is collected by drainage ditches and enters the Settlement Tank.
- The strongest correlation between rainfall and discharge through the BSC Pipe was found to have a lag of 5 days.
- Discharges through the BSC Pipe and the Settlement Tank vary. Data recorded between October 1998 and July 2004 show that:
 - the minimum discharge recorded in 24 hours for the BSC Pipe was 109 m³, the maximum was 2589 m³ and the mean was 440 m³.
 - the minimum discharge recorded in 24 hours for the Settlement Tank was 51 m³, the maximum was 5604 m³ and the mean was 975 m³.
- The discharge from the Settlement Tank was shown to have a long-term upward trend. This upward long-term trend of Settlement Tank discharge is not mirrored by the rainfall recorded at the site. The trend was modelled through curve fitting to the

discharge data set from 1993 to the present day. The resulting model shows a linear regression curve with equation $y = 0.1353x - 4054.5$. Year on year the discharge would increase by approximately 18000 m^3 , which represents about 4% of the July 2003 to June 2004 discharge. In ten years a discharge increase of 42% could be expected if the trend continued unaltered.

- From the Settlement Tank discharge results it does not appear that there has been a significant reduction in leachate since the engineering works on the drainage ditches and southern slope were carried out in 2001.
- Regression analysis was performed on the discharge data and the meteorological data for the BSC Pipe and the Settlement Tank.
 - The strongest correlation ($r = -.26$, $p = 0.00$) for the BSC Pipe discharge was found with average daily temperature.
 - For the Settlement Tank discharge the strongest correlations were found with daily rainfall ($r = .29$, $p = 0.00$) and daily Effective Rainfall ($r = .29$, $p = 0.00$).
- Multiple regression analysis was used to model discharge on the basis of discontinuous data set from October 1998 to the present. Discharge was considered as the dependant variable with meteorological data as the independent variables.
- Multiple regression analysis for the BSC Pipe found that:
 - Using average daily temperature and daily rainfall (with the 5 day lag) the stepwise regression analysis had a correlation of 0.32 with the equation:
 $BSC' = 517.47 + -15.55(temp) + 4.14(rain)$
 - Simultaneous regression analysis using all the variables (average daily temperature, average wind speed, daily rainfall (with the 5 day lag) and pressure) had a correlation of 0.33 with the equation:
 $BSC' = -1230.71 + -14.42(temp) + 1.97(wind) + 4.42(rain) + 1.76(mb)$
 - The slight increase in correlation when using all the variables shows the lack of predictive power of pressure and average wind speed.

- The resulting models both show seasonal fluctuations in leachate discharge, with high flows in winter and low flows in summer. The predicted flows varied between around 500 m³/day in the winter to around 260 m³/day in the summer.
- Multiple regression analysis for the Settlement Tank was performed on unadjusted discharge data and on discharge data with the long-term trend removed. It was found that:
 - Simultaneous regression analysis for the unadjusted discharge, using all the variables (average daily temperature, average wind speed, daily Effective Rainfall and pressure) had a correlation of 0.47 with the equation:
$$ST' = 3129.38 + -41.08(temp) + -5.75 (wind) + -1.67(mb) + 13.80(ER)$$
 - Simultaneous regression analysis for the discharge with the long-term trend removed, using all the variables (average daily temperature, average wind speed, daily Effective Rainfall and pressure) had a correlation of 0.48 with the equation:
$$ST' = 6422.27 + -39.63(temp) + -5.87 (wind) + -4.96(mb) + 12.34(ER)$$
 - Stepwise regression analysis for the unadjusted discharge, using average daily temperature, daily rainfall and average wind speed had a correlation of 0.51 with the equation:
$$ST' = 1454.95 + -40.87(temp) + 23.82(rain) + -6.79(wind)$$
 - Stepwise regression analysis for the discharge with the long-term trend removed, using average daily temperature and daily rainfall had a correlation of 0.51 with the equation:
$$ST' = 1454.95 + -40.87(temp) + 23.82(rain)$$
 - The slight increase in correlation when using all the variables shows the lack of predictive power of pressure and average wind speed.
 - The resulting models show seasonal fluctuations in leachate discharge, with high flows in winter and low flows in summer. The predicted flows varied between around 1500 m³/day in the winter to around 900 m³/day in the summer.
- Multiple regression analysis for the BSC Pipe and the Settlement Tank show seasonal fluctuations in leachate discharge, with high flows in winter and low flows in summer. The actual data shows significant short-term fluctuations that cannot be modeled using this simple multiple regression based approach. The multiple

regression analysis has however highlighted average daily temperature as the strongest predictive variable for discharge.

- A preliminary study was undertaken to investigate the effectiveness of neural networks in modelling the discharge in the Settlement Tank. Feedforward backpropagation neural networks were constructed¹ to produce a one-step-ahead prediction of daily discharge for the Settlement Tank.
 - The input data used were rainfall, temperature, wind speed and previous days discharge (or predicted discharge after the first day).
 - The networks were trained using the majority of the available data (training set) between October 1998 and May 2004. The unseen data (testing set) between 2 August to 9 October 2001 and 11 April to 18 May 2004 were then used to evaluate the networks ability to generalise.
 - The forecast using neural networks gave closer predicted flow to the actual than simultaneous and stepwise regression analysis, with many of the turning points captured. However, not all the features of the actual discharge were forecast.

LEACHATE CHEMISTRY

- The leachate produced at Silent Valley landfill site is a weak leachate.
 - The majority of the constituents monitored are low in concentration when compared to the figures quoted by the DoE (1995). However, nitrate and nitrite concentrations are higher than those quoted.
- LP1, the leachate from the BSC Pipe shows variations in many of the constituents since monitoring began in 1993. The following are the main findings:
 - No trend in conductivity and concentration of many of the metals.
 - Decrease over time in sulphate, pH, the BOD/COD ratio and iron.

¹ Neural networks for Silent Valley landfill were built by Stuart Paris using data supplied by the author.

- Increase over time in temperature, ammoniacal nitrogen, alkalinity, COD, BOD, TOC, sodium, potassium, manganese and chloride.

It is concluded that these trends indicate increased significance of biodegradation of domestic waste in leachate production over the period for which data are available (1990 to 2004).

- Dilution effects can be seen in the Settlement Tank, indicated by a strong negative correlation ($R^2 = 0.4614$) between conductivity and discharge.
- Conductivity readings showed correlations with the leachate geochemistry.
 - For LP1, fluoride, chloride, bromide and nitrate increase as conductivity increases, with sulphate remaining about the same. The conductivity shows significant weak correlations with chloride ($r = 0.28$, $p = 0.00$), bromide ($r = 0.25$, $p = 0.00$) and fluoride ($r = 0.23$, $p = 0.00$).
 - For the Settlement Tank, fluoride, chloride, bromide, nitrate and sulphate all increase as conductivity increases. A very strong significant correlation was found for chloride with conductivity ($r = 0.85$, $p = 0.00$). Moderate significant correlations were found with bromide ($r = 0.51$, $p = 0.00$) and nitrate ($r = 0.40$, $p = 0.00$). Significant weak correlations were found with sulphate ($r = 0.35$, $p = 0.00$) and fluoride ($r = 0.33$, $p = 0.00$).
- The discharge from the BSC Pipe (LP1) does not have any significant correlations with the IC analysis.
- Significant correlations between discharge and the IC analysis were found for the Settlement Tank and suggest a dilution effect.
 - Significant correlations were obtained for the discharge and chloride ($r = -.56$, $p = 0.00$), nitrate ($r = -.56$, $p = 0.00$), sulphate ($r = -.49$, $p = 0.00$) and bromide ($r = -.16$, $p = 0.01$).
- If the long-term leachate concentration trends continue then the leachate will become more contaminated overall and require more intensive treatment. If the trends in concentration seen continue unchanged, then many of the constituents (ammoniacal

nitrogen, alkalinity, COD, BOD, TOC, sodium, potassium, manganese and chloride) will increase with time. In 5 years time it is possible that ammoniacal nitrogen, COD and TOC will be approximately twice the concentration that they are at the present.

- The cost of leachate treatment in the future is likely to increase since many of the leachate constituents are increasing in concentration with time and the discharge shows an upward trend.

RELEVANCE TO OTHER LANDFILL SITES

All unlined landfills are unique. This research has demonstrated the need for an accurate and detailed understanding of the site geology and hydrogeology. Landfills that have been active for decades will have seen changes in the waste stream. The fill will therefore vary through time as well as between landfills. At Silent Valley landfill for example there is a strong influence of steel works waste. Therefore understanding the leachate geochemistry of a site requires an equally detailed knowledge of the waste stream composition. The meteorological inputs will also vary between sites and these strongly influence leachate quality and quantity by controlling rainfall inputs and evaporative losses.

The approaches that have been developed in this research to model leachate generation on the basis of meteorological inputs provide a novel methodology that may be applied to other unlined landfills (active and closed) to provide a better understanding of leachate generation. The ANN methodology appears to offer a promising approach to landfill leachate modelling because given sufficient data it provides a more robust methodology than simple regression based modelling, which may be influenced by data characteristics. This project was of three years duration and data were available for a limited time period. Continued monitoring will provide larger data sets, improving the ANN training, and it is hoped will lead to significant improvements in the predictive capability of the model.

9.2 RECOMMENDATIONS

The results of the present project were limited by the three-year time period of the research and the discontinuous nature of the data available. It is therefore recommended that efforts should be made to:

- Continue to collect continuous data for the weather, flow and conductivity. Blaenau Gwent County Borough Council has agreed to fund the author to continue monitoring the discharge for the next two years. It is hoped that at the end of these two years a continuous data set will be available to combine with the data already available. This could then be used to train new neural networks. It is hoped that with more data available for training, a better forecasting model will be obtained.
- Install a reliable humidity sensor and a solar radiation detector on site. Information on humidity and solar radiation at Silent Valley would be useful in determining more accurately the effective rainfall term in water budget analysis.
- Undertake an analysis of rainfall depth-frequency-duration for the Silent Valley site. The parameters of the depth-duration-frequency model are provided on the Flood Estimation Handbook CD-ROM as a 1 km grid and as catchment average values. The CD-ROM includes software that allows estimates of design rainfall or event rarity to be calculated for any point on the grid or for any catchment that has a drainage area of at least 0.5 km².
- Undertake more detailed leachate sampling through observation boreholes across the site. This would enable in-situ leachate chemistry to be investigated, possible source areas for particular contaminants to be identified (e.g. steelworks slag) and the influence of groundwater ingress in leachate concentrations to be assessed.
- Perform ANN modelling at another landfill site with several years of continuous data for discharge and meteorological conditions.

REFERENCE LIST

- ANDREOTTOLA, G. & CANNAS, P. 1992. Chemical and Biological Characteristics of Landfill Leachate. IN: CHRISTENSEN, T.H., COSSU, R. & STEGMANN, R. (Eds). 1992. *Landfilling of Waste: Leachate*. Elsevier Applied Science.
- ANCTIL, F., PERRIN, C. & ANDRÉASSIAN, V. 2004. Impact of the length of observed records on the performance of ANN and of conceptual parsimonious rainfall-runoff forecasting models. *Environmental Modelling & Software*, **19**, 357–368.
- APPELO, C.A.J. & POSTMA, D. 1996. *Geochemistry, groundwater and pollution*. A.A. Balkema.
- BARCLAY, W.J. 1989. *Geology of the South Wales Coalfield, Part II, the country around Abergavenny, Third Edition*. British Geological Survey.
- BARLAZ, M.A. & HAM, R.K. Leachate and gas generation. IN: DANIEL, D.E. (ed). 1993. *Geotechnical Practice for Waste Disposal*. Chapman & Hall.
- BENDZ, D. & BENGTSSON, L. 1996. Evaporation from an active, uncovered landfill. *Journal of Hydrology*, **182**, 143-155.
- BERNSTONE, C. & DAHLIN, T. 1997. DC resistivity mapping of old landfills: two case studies. *European Journal of Environmental and Engineering Geophysics*, **2**, 121-136.
- BERNSTONE, C., DAHLIN, T., OHLSSON, T. & HOGLAND, W. 2000. DC-resistivity mapping of internal landfill structures: two pre-excitation surveys. *Environmental Geology*, **39**(3-4), 360-371.
- BINLEY, A. & DAILY, W. 2003. The Performance of Electrical Methods for Assessing the Integrity of Geomembrane Liners in Landfill Caps and Waste Storage Ponds. *Journal of Environmental & Engineering Geophysics*, **8**(4), 227-237.

- BIRKS, J. & EYLES, C.H. Leachate from Landfills along the Niagara Escarpment. IN: EYLES, N. (ed). 1997. *Environmental Geology of Urban Areas*. Geological Association of Canada.
- CAMPBELL, D.J.V. 1983. Understanding Water Balance in Landfill Sites. *Wastes Management*, **73**, 594-600.
- CANZIANI, R. & COSSU, R. 1989. Landfill Hydrology and Leachate Production. IN: CHRISTENSEN, T.H., COSSU, R. & STEGMANN, R. (Eds). 1989. *Sanitary Landfilling: Process, Technology and Environmental Impact*. Academic Press
- CELTIC TECHNOLOGIES. 1995. *Treatability Study for Oily Waste Disposal at Silent Valley Landfill*. Report No: 054/95/104.
- COSSU, R., ANDREOTTOLA, G. & MUNTONI, A. 1996 Modelling Landfill Gas Production. IN: CHRISTENSEN, T.H., COSSU, R. & STEGMANN, R. (Eds). 1996. *Landfilling of Waste: Biogas*. E & FN Spon.
- DEPARTMENT OF THE ENVIRONMENT. 1986. *Landfilling Wastes Waste Management Paper No 26, A Technical Memorandum for the Disposal of Wastes on Landfill Sites*. HMSO.
- DEPARTMENT OF THE ENVIRONMENT. 1991. *Landfill Gas: a technical memorandum providing guidance on the monitoring and control of landfill gas. Waste Management Paper No. 27*. HSMO.
- DEPARTMENT OF THE ENVIRONMENT. 1995. *Landfill Design, Construction and Operational Practice. Waste Management Paper 26B*. HMSO.
- DEPARTMENT OF THE ENVIRONMENT. 2000. *Waste Strategy 2000, for England and Wales. Part 1 & 2*. The Stationary Office Limited.
- DEUTSCH, W.J. 1997. *Groundwater Geochemistry: fundamentals and applications to contamination*. CRC Press LLC.
- DIBIKE, Y.B. & SOLOMATINE, D.P. 2001. River Flow Forecasting Using Artificial Neural Networks. *Phys. Chem. Earth (B)*, **26(1)**, 1-7.
- DIONEX CORPORATION. 2001. *DX-80 Analyzer Operator's Manual*. Document No. 031675.
- EHRIG, H-J. 1996 Prediction of Gas Production from Laboratory-Scale Tests. IN: CHRISTENSEN, T.H., COSSU, R. & STEGMANN, R. (Eds). 1996. *Landfilling of Waste: Biogas*. E & FN Spon.
- EL-FADEL, M., FINDIKAKIS, A.N. & LECKIE, J.O. 1996a. Numerical Modelling of Generation and Transport of Gas and Heat in Sanitary Landfills I. Model Formulation. *Waste Management & Research*, **14**, 483-504.

- EL-FADEL, M., FINDIKAKIS, A.N. & LECKIE, J.O. 1996b. Numerical Modelling of Generation and Transport of Gas and Heat in Sanitary Landfills II. Model Application. *Waste Management & Research*, **14**, 537-551.
- EL-FADEL, M., FINDIKAKIS, A.N. & LECKIE, J.O. 1997. Numerical Modelling of Generation and Transport of Gas and Heat in Sanitary Landfills III. Sensitivity Analysis. *Waste Management & Research*, **15**, 87-102.
- ENVIRONMENT AGENCY. 2000. *Strategic Waste Management Assessment – Wales*.
- ENVIRONMENT AGENCY. 2001. *Monitoring of Landfill Sites: Guidance on Monitoring of Landfill Leachate, Groundwater and Surface Water*.
- ENVIRONMENTAL PROTECTION AGENCY. 1996. *Turning a Liability into an Asset: A Landfill Gas-to-Energy Project Development Handbook*.
- ENVIRONMENTAL PROTECTION AGENCY. 2003. *Example Moisture Mass Balance Calculations for Bioreactor Landfills*. Report No: EPA-456/R-03-007
- EXPLORATION ASSOCIATES. 1996. *Factual Report on Ground Investigation*. Report No: 155184.
- FETTER, C.W. 2001. *Applied hydrogeology, Forth Edition*. Prentice Hall.
- GEORGE, A. 2004. *Goelectrical Monitoring of Sub-Surface Characteristics at Nantygwyddon Landfill Site, Rhondda*. Cardiff University. Report number NYG-GEO 1, November 2004.
- GEOTOMO SOFTWARE. 2002. RES2DINV ver. 3.50 for Windows 98/Me/2000/NT/XP Manual. Rapid 2D Resistivity & IP inversion using least-squares method.
- GOLDER ASSOCIATES. 1993a. *Site Characerisation of Materials, Silent Valley Landfill, Phase II (Proposed)*. Report No: 92523088.
- GOLDER ASSOCIATES. 1993b. *Assessment of Hydrogeology in Silent Valley*. Report No: 92523088.
- GOLDER ASSOCIATES. 1993c. *Proposed Site Investigation into Underlying Clay, Silent Valley Landfill, Phase 1A*. Report No: 93523120.
- GOLDER ASSOCIATES. 1993d. *Site Investigation, Silent Valley Landfill, Phase 1A*. Report No: 93523120.
- GOLDER ASSOCIATES. 1994. *Probabilistic Assessment of Stability at Silent Valley Landfill*. Report No: 94523174.
- GOLDER ASSOCIATES. 2004. *Section D, Landfill Gas Generation & Risk Assessment, Silent Valley Landfill Site*. Report No: 04529441.500.

- GWENT CONSULTANCY. 2000. *Silent Valley Leachate Volume Reduction, Summary Report*.
- INSTITUTE OF GEOLOGICAL SCIENCES. 1980. *South Wales Coalfield Landslip Survey*. Report No: EG 80/4.
- KAASTRA, I. & BOYD, M. 1996. Designing a neural network for forecasting financial and economic time series. *Neurocomputing*, **10**, 215-236.
- KARLIK, G. & KAYA, M.A. 2001. Investigation of groundwater contamination using electric and electromagnetic methods at an open waste-disposal site: a case study from Isparta, Turkey. *Environmental Geology*, **40**(6), 725-731.
- KEAREY, P. & BROOKS, M. 1991. *An Introduction to Geophysical Exploration, Second Edition*. Blackwell Science.
- KINNEAR P.R. & GRAY C.D. 2000. *SPSS for Windows Made Simple, Release 10*. Psychology Press Ltd.
- KOERNER, R.M. & DANIEL, D.E. 1997. *Final covers for solid waste landfills and abandoned dumps*. American Society of Civil Engineers.
- KNOX ASSOCIATES. 1995. *Silent Valley Landfill Site Leachate Management Plan*.
- LANGE, N.T. 1999. New Mathematical Approaches in Hydrological Modeling - An Application of Artificial Neural Networks. *Phys. Chem. Earth (B)*, **24**(1-2), 31-35.
- LAYLA RESOURCES LTD. 2001. The New Dutchlist.
<http://www.ContaminatedLand.co.uk/std-guid/dutch-1.htm>. Last Page Update: 15 July 2001.
- LOKE, M.H. 1999a. *Electrical imaging surveys for environmental and engineering studies - A practical guide to 2-D and 3-D surveys*.
- LOKE, M.H. 1999b. *Time lapse resistivity imaging inversion*. Proceedings of the 5th Meeting of the EEGS European Section, Em1.
- LOPES, M.A.F. 2000. *Geophysical Characterisation of Silent Valley Landfill*. MSc thesis, unpublished. Cardiff University.
- MAIER, H.R. & DANDY, G.C. 2000. Neural networks for the prediction and forecasting of water resources variables: a review of modelling issues and applications. *Environmental Modelling & Software*, **15**, 101-124.
- MASTERS, T. 1993. *Practical Neural Network Recipes in C++*. Academic Press.
- MCDUGALL, J. R., SARSBY, R. W. & HILL, N. J. 1996. A numerical investigation of landfill hydraulics using variably saturated flow theory. *Geotechnique*, **46**(2), 329-341.

- MURPHY, S. 2002. General Information on Alkalinity.
<http://bcn.boulder.co.us/basin/data/NUTRIENTS/info/Alk.html> Last Page Update - June 15, 2002.
- NORTH WEST WASTE DISPOSAL OFFICERS. 1991. *Leachate Management Report*.
- OGILVY, R., MELDRUM, P., CHAMBERS, J. & WILLIAMS, G. 2002. The Use of 3D Electrical Resistivity Tomography to Characterise Waste and Leachate Distribution within a Closed Landfill, Thriplow, UK. *Journal of Environmental and Engineering Geophysics*, 7(1), 11–18.
- OVE ARUP & PARTNERS. 1995. *Review of Probabilistic Assessment of Stability*.
- OVE ARUP & PARTNERS. 1996a. *Slope Stability Report (Phase 2)*. Report No: 96/3144.
- OVE ARUP & PARTNERS. 1996b. *Phase 1A Stability Review*. Report No: 96/3162.
- OVE ARUP & PARTNERS. 1997. *Remediation of Land associated with British Steel Deposits – Leachate Treatment Proposals, Draft for Discussion*. Report No: 97/3380.
- OVE ARUP & PARTNERS. 1999. *Proposal for Leachate Volume Reduction*. Report No: 99/4004.
- PARRA, J.O. 1988. Electrical response of a leak in a geomembrane liner. *Geophysics*, 53(11), 1445-1452.
- PARIS, E.C. 2000. *Geochemical Aspects of the Leachate at Silent Valley Landfill Site, South Wales*. MSc thesis, unpublished. Cardiff University.
- QIAN, X., KOERNER, R.M. & GRAY, D.H. 2002. *Geotechnical Aspects of Landfill Design and Construction*. Prentice-Hall
- REYNOLDS, J.M. 1997. *An Introduction to Applied and Environmental Geophysics*. Wiley.
- RODERICK, M.L. & FARQUHAR, G.D. 2002. The Cause of Decreased Pan Evaporation over the Past 50 Years. *Science*, 298(5597), 1410-1411.
- SAJIKUMAR, N. & THANDAVESWARA, B.S. 1999. A non-linear rainfall–runoff model using an artificial neural network. *Journal of Hydrology*, 216, 32–55.
- SHAMSELDIN, A.Y. 1997. Application of a neural network technique to rainfall-runoff modelling. *Journal of Hydrology*, 199, 272-294.
- SHARMA, P.V. 1997. *Environmental and engineering geophysics*. Cambridge University Press.

- STEGEMANN, J.A. & BUENFELD, N.R. 1999. A Glossary of Basic Neural Network Terminology for Regression Problems. *Neural Computing & Applications* **8**, 290–296.
- TOTH, E., BRATH, A. & MONTANARI, A. 2000. Comparison of short-term rainfall prediction models for real-time flood forecasting. *Journal of Hydrology*, **239**, 132–147.
- WARWICKSHIRE ENVIRONMENTAL PROTECTION COUNCIL. 1995. *Landfill gas from closed sites in Coventry and Warwickshire*.
- WASTE MANAGEMENT INFORMATION BUREAU. 1995. *The Technical Aspects of Controlled Waste Management: A review of the composition of leachates from domestic wastes in landfill sites*. Report No. CWM/072/95.
- WESTLAKE, K. 1995. *Landfill Waste Pollution and Control*. Albion Publishing.
- WILSON, I.D., PARIS, S.D., WARE, J.A. & JENKINS, D.H. 2002. Residential property price time series forecasting with neural networks. *Knowledge-Based Systems*, **15**, 335–341.
- ZHANG, G., PATUWO, E. & HU, M.Y. 1998. Forecasting with artificial neural networks: The state of the art. *International Journal of Forecasting*, **14**, 35–62.

MAPS

- BRITISH GEOLOGICAL SURVEY. Solid and Drift Geology. England and Wales Sheet 232, Abergavenny. 1:50,000
- BRITISH GEOLOGICAL SURVEY. Hydrogeological Map of South Wales. 1:125,000.
- ENVIRONMENT AGENCY. Groundwater Vulnerability of Gwent, South & Mid Glamorgan. Sheet 36. 1:100,000
- INSTITUTE OF GEOLOGICAL SCIENCES, NATURAL ENVIRONMENT RESEARCH COUNCIL. 1979. Geological Survey of Great Britain (England and Wales). Sheet SO 10 NE, Monmouthshire. 1:10,560
- ORDNANCE SURVEY. 1880. 1:2500 Monmouthshire map.
- ORDNANCE SURVEY. 1901. 1:10,560 Monmouthshire map.
- ORDNANCE SURVEY. 1920. 1:2500 Monmouthshire map.
- ORDNANCE SURVEY. 1969. Sheet SO 10 NE, Monmouthshire. 1:10,560
- ORDNANCE SURVEY. Landranger Series 161, Abergavenny & the Black Mountains. 1:50,000

APPENDICES

	Page
Appendix A Mean possible monthly duration of sunlight in the Northern Hemisphere	504
Appendix B Resistivity Sections	506
Appendix C Pearson's level of significance	529
Appendix D Discharge Data	CD
Appendix E Weather Data	CD
Appendix F Leachate Data	CD

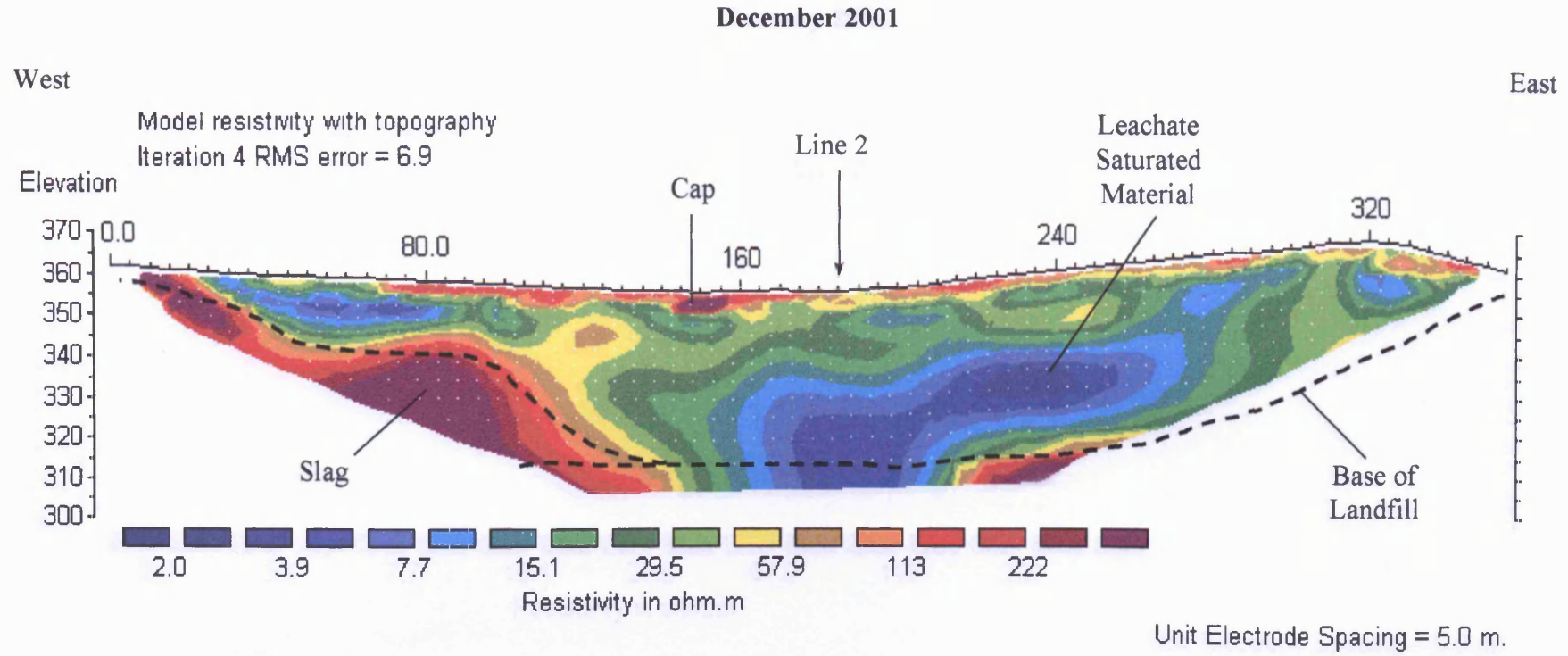
Appendix A - Mean possible monthly duration of sunlight in the Northern Hemisphere.

Mean possible monthly duration of sunlight in the Northern Hemisphere. Expressed in units of 12 hours. From Koerner & Daniel, 1997 (who took it from Thornthwaite & Mather, 1957).

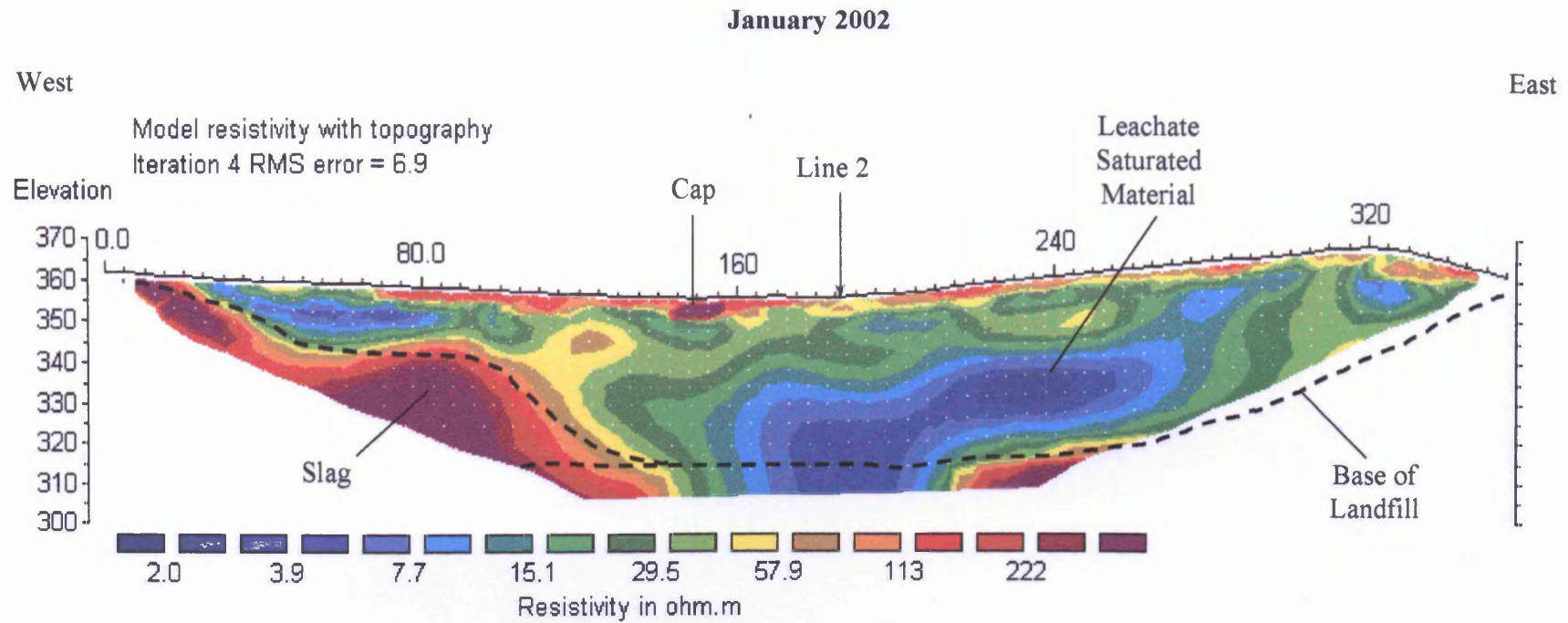
Degrees	J	F	M	A	M	J	J	A	S	O	N	D
0	31.2	28.2	31.2	30.3	31.2	30.3	31.2	31.2	30.3	31.2	30.3	31.2
1	31.2	28.2	31.2	30.3	31.2	30.3	31.2	31.2	30.3	31.2	30.3	31.2
2	31.2	28.2	31.2	30.3	31.5	30.6	31.2	31.2	30.3	31.2	30.0	30.9
3	30.9	28.2	30.9	30.3	31.5	30.6	31.2	31.2	30.3	31.2	30.0	30.9
4	30.9	27.9	30.9	30.6	31.8	30.9	31.5	31.5	30.3	30.9	30.0	30.6
5	30.6	27.9	30.9	30.6	31.8	30.9	31.8	31.5	30.3	30.9	29.7	30.6
6	30.6	27.9	30.9	30.6	31.8	31.2	31.8	31.5	30.3	30.9	29.7	30.3
7	30.3	27.6	30.9	30.6	32.1	31.2	32.1	31.8	30.3	30.9	29.7	30.3
8	30.3	27.6	30.9	30.9	32.1	31.5	32.1	31.8	30.6	30.6	29.4	30.0
9	30.0	27.6	30.9	30.9	32.4	31.5	32.4	31.8	30.6	30.6	29.4	30.0
10	30.0	27.3	30.9	30.9	32.4	31.8	32.4	32.1	30.6	30.6	29.4	29.7
11	29.7	27.3	30.9	30.9	32.7	31.8	32.7	32.1	30.6	30.6	29.1	29.7
12	29.7	27.3	30.9	31.2	32.7	32.1	33.0	32.1	30.6	30.3	29.1	29.4
13	29.4	27.3	30.9	31.2	33.0	32.1	33.0	32.4	30.6	30.3	28.8	29.4
14	29.4	27.3	30.9	31.2	33.0	32.4	33.3	32.4	30.6	30.3	28.8	29.1
15	29.1	27.3	30.9	31.2	33.3	32.4	33.6	32.4	30.6	30.3	28.5	29.1
16	29.1	27.3	30.9	31.2	33.3	32.7	33.6	32.7	30.6	30.3	28.5	28.8
17	28.8	27.3	30.9	31.5	33.6	32.7	33.9	32.7	30.6	30.0	28.2	28.8
18	28.8	27.0	30.9	31.5	33.6	33.0	33.9	33.0	30.6	30.0	28.2	28.5
19	28.5	27.0	30.9	31.5	33.9	33.0	34.2	33.0	30.6	30.0	27.9	28.5
20	28.5	27.0	30.9	31.5	33.9	33.3	34.2	33.3	30.6	30.0	27.9	28.2
21	28.2	27.0	30.9	31.5	33.9	33.3	34.5	33.3	30.6	30.0	27.6	28.2
22	28.2	26.7	30.9	31.8	34.2	33.6	34.5	33.3	30.6	29.7	27.6	27.9
23	27.9	26.7	30.9	31.8	34.2	33.9	34.8	33.6	30.6	29.7	27.6	27.6
24	27.9	26.7	30.9	31.8	34.5	34.2	34.8	33.6	30.6	29.7	27.3	27.6
25	27.9	26.7	30.9	31.8	34.5	34.2	35.1	33.6	30.6	29.7	27.3	27.3
26	27.6	26.4	30.9	32.1	34.8	34.5	35.1	33.6	30.6	29.7	27.3	27.3
27	27.6	26.4	30.9	32.1	34.8	34.5	35.4	33.9	30.6	29.7	27.0	27.0
28	27.3	26.4	30.9	32.1	35.1	34.8	35.4	33.9	30.9	29.4	27.0	27.0
29	27.3	26.1	30.9	32.1	35.1	34.8	35.7	33.9	30.9	29.4	26.7	26.7
30	27.0	26.1	30.9	32.4	35.4	35.1	36.0	34.2	30.9	29.4	26.7	26.4
31	27.0	26.1	30.9	32.4	35.4	35.1	36.0	34.2	30.9	29.4	26.4	26.4
32	26.7	25.8	30.9	32.4	35.7	35.4	36.3	34.5	30.9	29.4	26.4	26.1

Appendix A - Mean possible monthly duration of sunlight in the Northern Hemisphere.

33	26.4	25.8	30.9	32.7	35.7	35.7	36.3	34.5	30.9	29.1	26.1	25.8
34	26.4	25.8	30.9	32.7	36.0	36.0	36.6	34.8	30.9	29.1	26.1	25.8
35	26.1	25.5	30.9	32.7	36.3	36.3	36.9	34.8	30.9	29.1	25.8	25.5
36	26.1	25.5	30.9	33.0	36.3	36.6	37.2	34.8	30.9	19.1	25.8	25.2
37	25.8	25.5	30.9	33.0	36.6	36.9	37.5	35.1	30.9	29.1	25.5	24.9
38	25.5	25.2	30.9	33.0	36.9	37.2	37.5	35.1	31.2	28.8	25.2	24.9
39	25.5	25.2	30.9	33.3	36.9	37.2	37.8	35.4	31.2	28.8	25.2	24.6
40	25.2	21.9	30.9	33.3	37.2	37.5	38.1	35.4	31.2	28.8	24.9	24.3
41	24.9	24.9	30.9	33.3	37.2	37.8	38.1	35.7	31.2	28.8	24.6	24.0
42	24.6	24.6	30.9	33.6	37.8	38.1	38.4	35.7	31.2	28.5	24.6	23.7
43	24.3	24.6	30.6	33.6	37.8	38.4	38.7	36.0	31.2	28.5	24.3	23.1
44	24.3	24.3	30.6	33.6	38.1	38.7	39.0	36.0	31.2	28.5	24.0	22.8
45	24.0	24.3	30.6	33.9	38.4	38.7	39.3	36.3	31.2	28.2	23.7	22.5
46	23.7	24.0	30.6	33.9	38.7	39.0	39.6	36.6	31.2	28.2	23.7	22.2
47	23.1	24.0	30.6	34.2	39.0	39.6	39.9	36.6	31.5	27.9	23.1	21.6
48	22.8	23.7	30.6	34.2	39.3	39.9	40.2	36.9	31.5	27.9	23.1	21.6
49	22.5	23.7	30.6	34.5	39.6	40.2	40.5	37.2	31.5	27.6	22.8	21.3
50	22.2	23.4	30.6	34.5	39.9	40.8	41.1	37.5	31.8	27.6	22.8	21.0

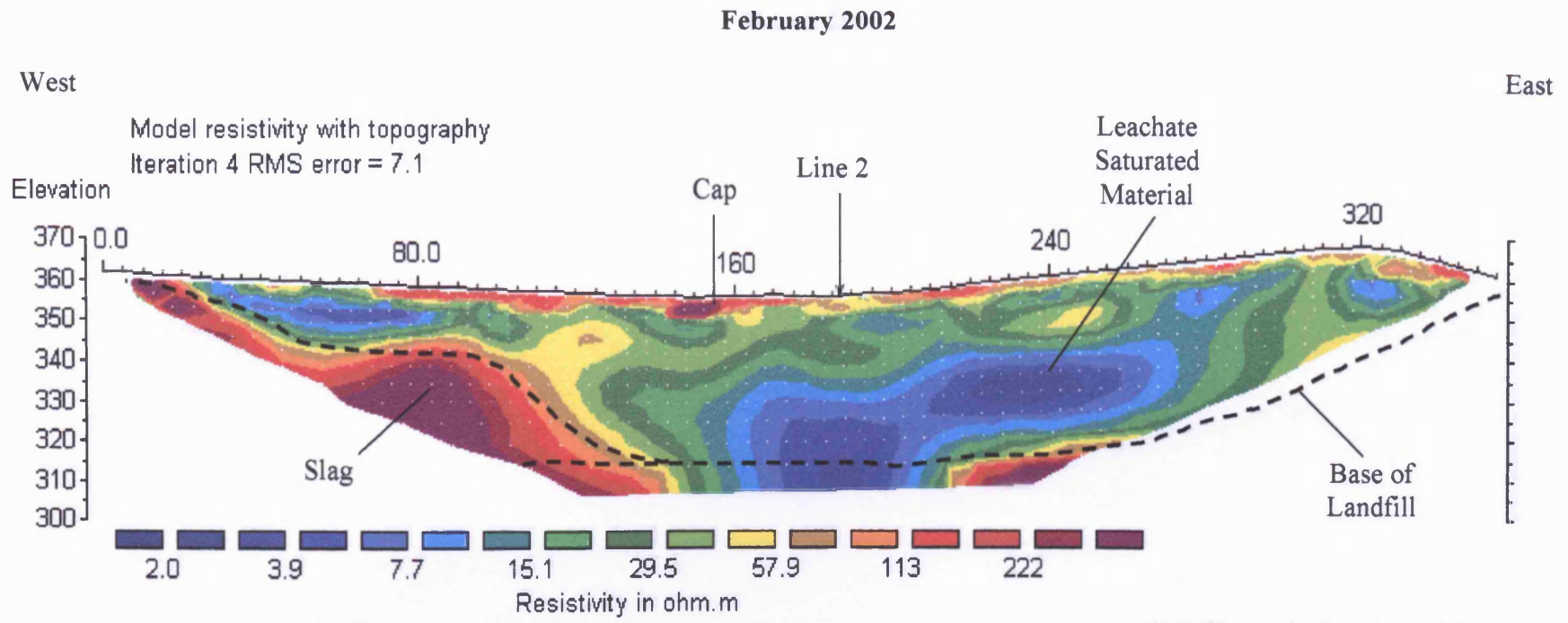


Horizontal scale is 10.28 pixels per unit spacing
Vertical exaggeration in model section display = 1.00
First electrode is located at 0.0 m.
Last electrode is located at 355.0 m.



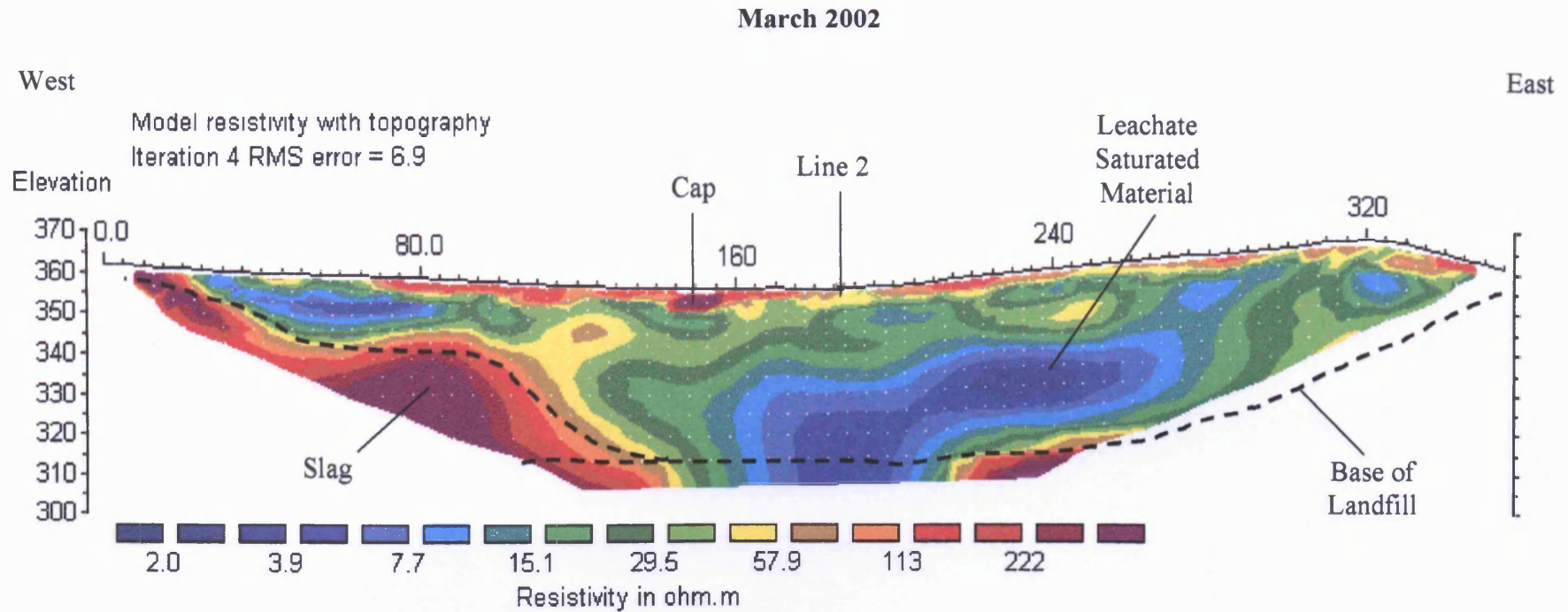
Unit Electrode Spacing = 5.0 m.

Horizontal scale is 10.28 pixels per unit spacing
 Vertical exaggeration in model section display = 1.00
 First electrode is located at 0.0 m.
 Last electrode is located at 355.0 m.



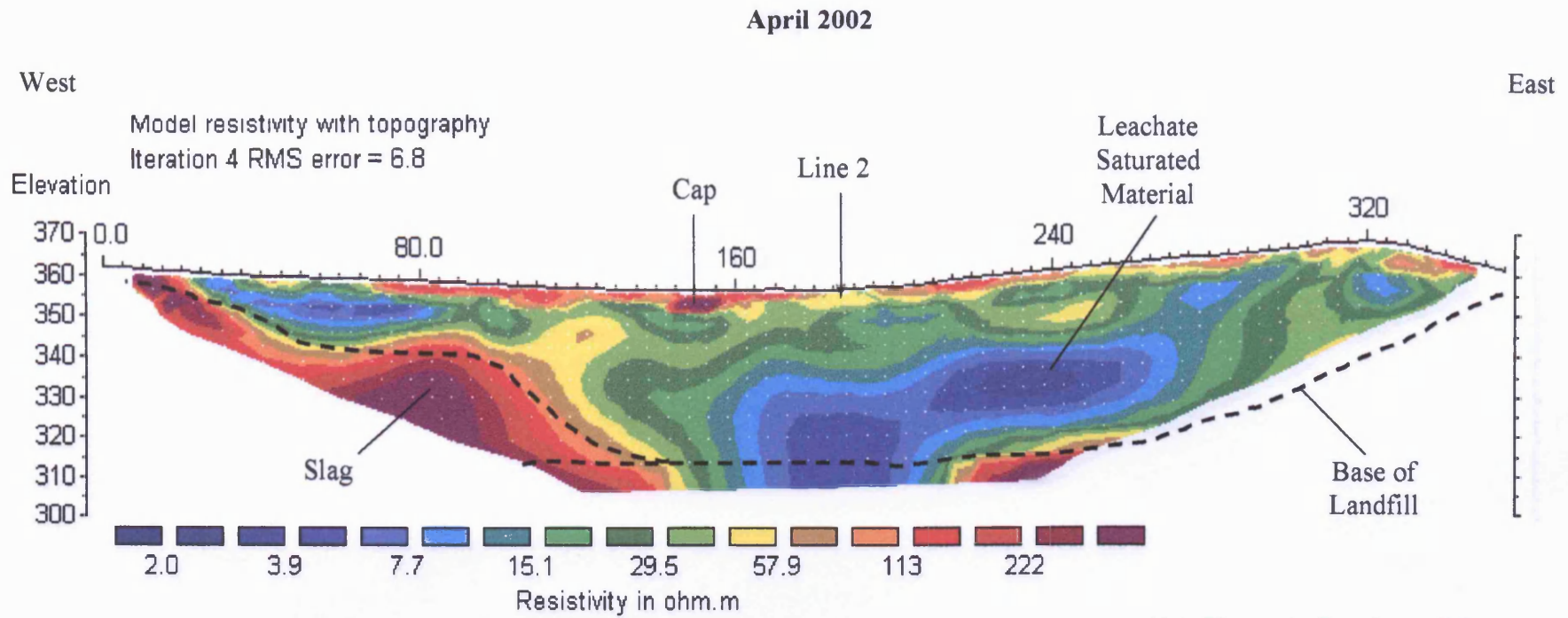
Unit Electrode Spacing = 5.0 m.

Horizontal scale is 10.28 pixels per unit spacing
Vertical exaggeration in model section display = 1.00
First electrode is located at 0.0 m.
Last electrode is located at 355.0 m.



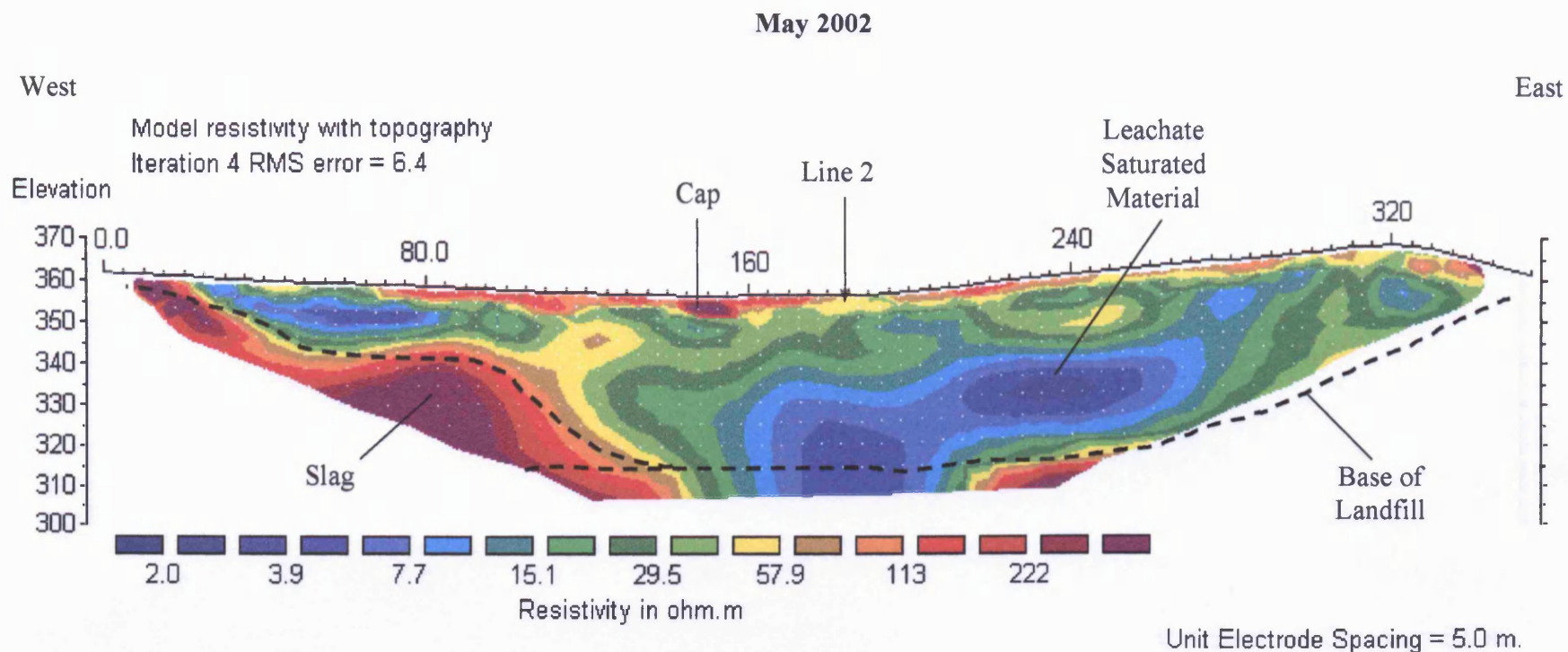
Unit Electrode Spacing = 5.0 m.

Horizontal scale is 10.28 pixels per unit spacing
Vertical exaggeration in model section display = 1.00
First electrode is located at 0.0 m.
Last electrode is located at 355.0 m.

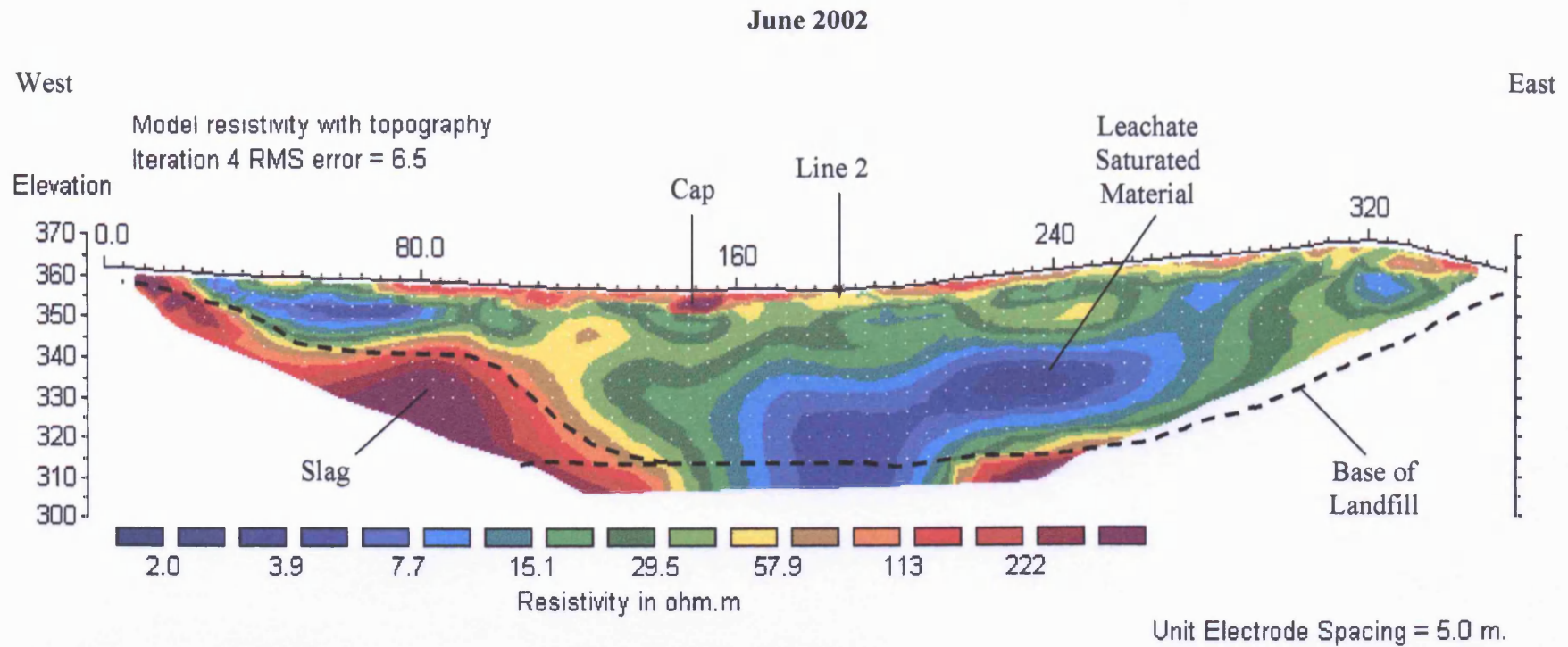


Unit Electrode Spacing = 5.0 m.

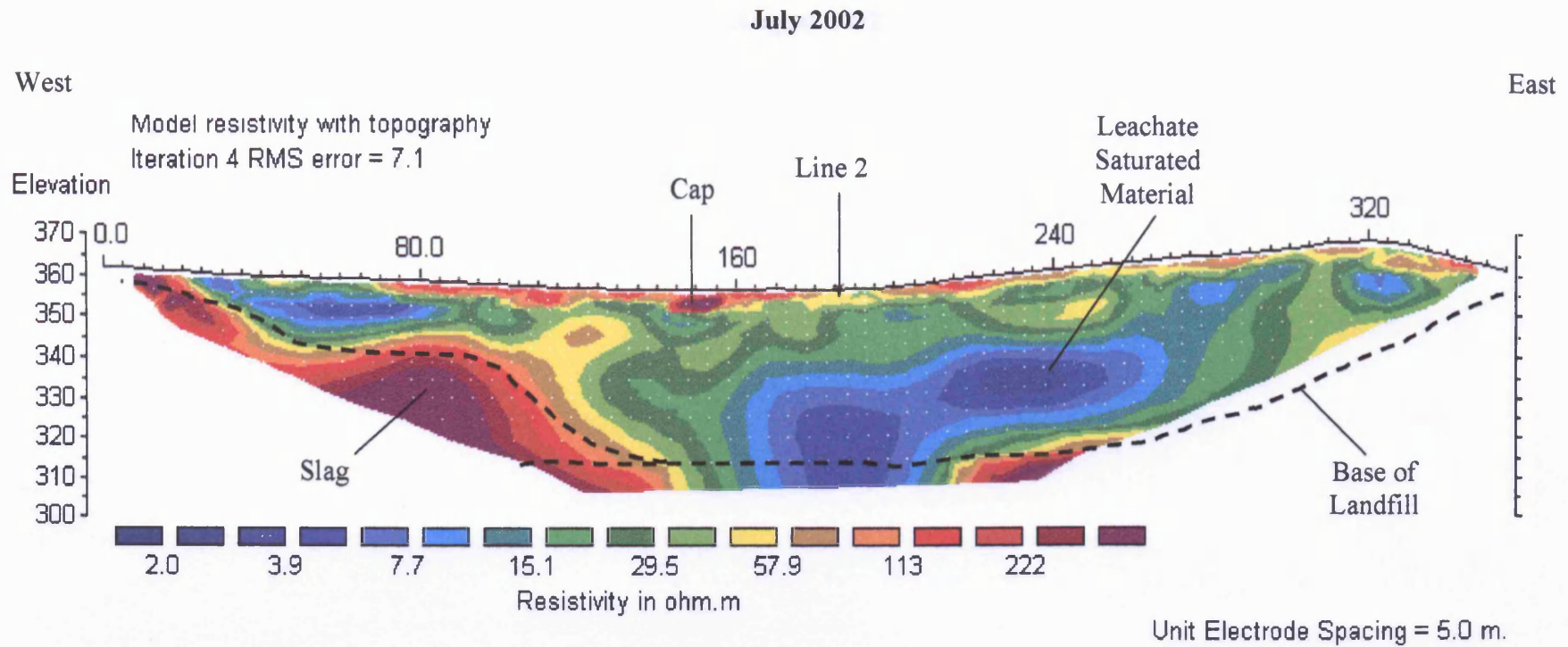
Horizontal scale is 10.28 pixels per unit spacing
Vertical exaggeration in model section display = 1.00
First electrode is located at 0.0 m.
Last electrode is located at 355.0 m.



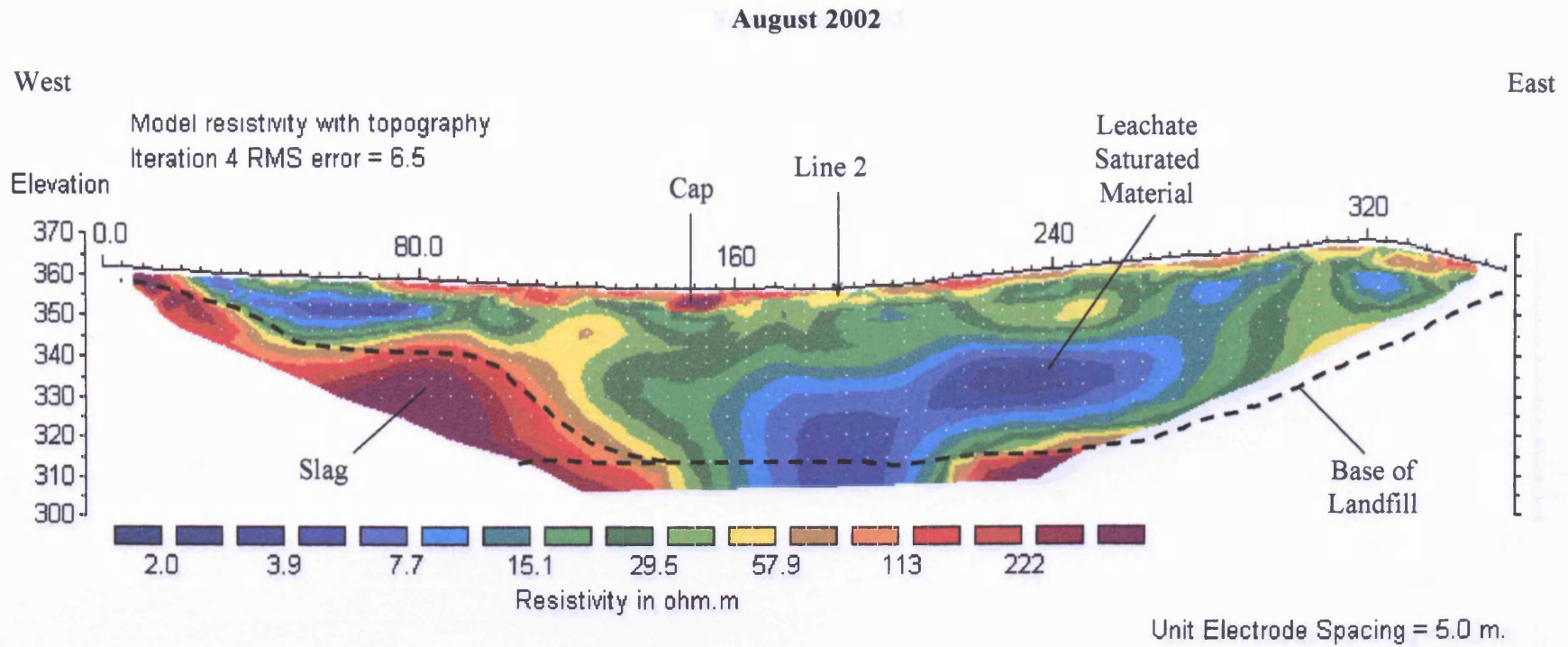
Horizontal scale is 10.43 pixels per unit spacing
Vertical exaggeration in model section display = 1.00
First electrode is located at 0.0 m.
Last electrode is located at 350.0 m.



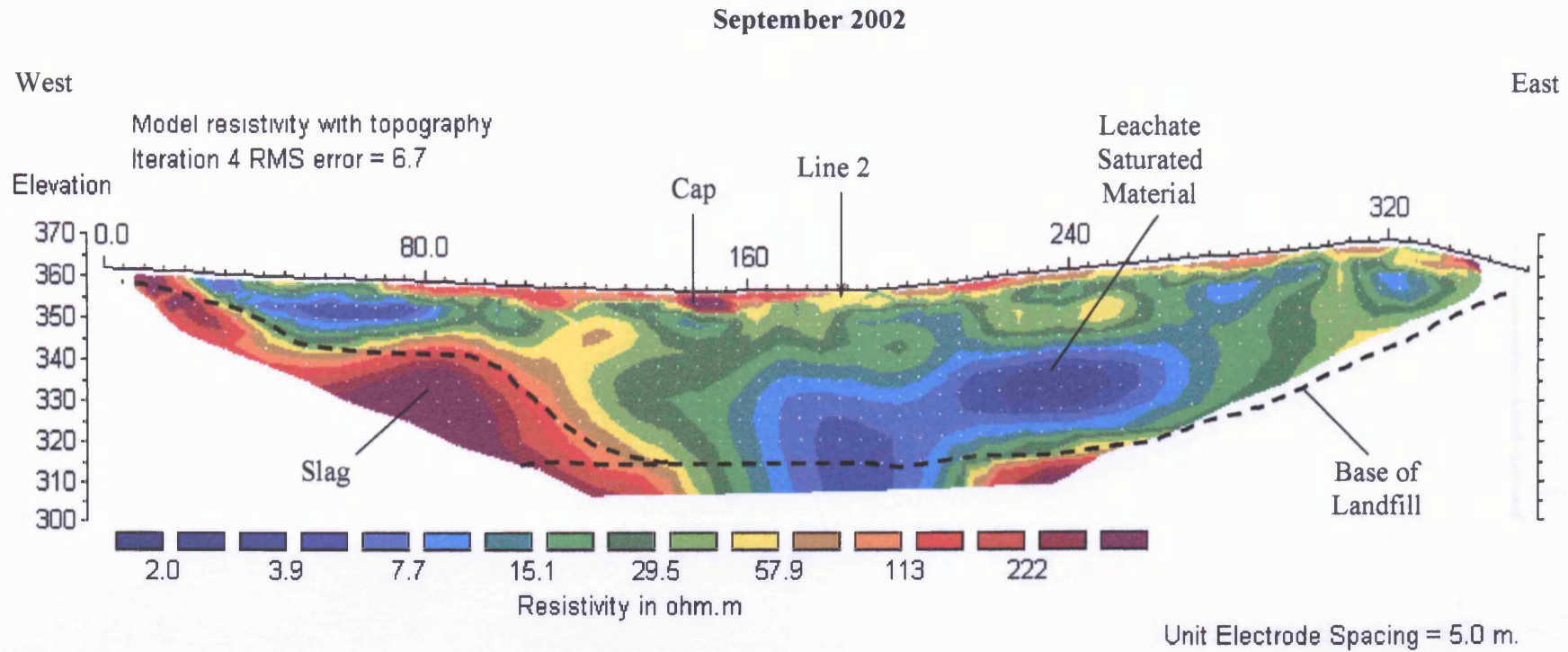
Horizontal scale is 10.28 pixels per unit spacing
Vertical exaggration in model section display = 1.00
First electrode is located at 0.0 m.
Last electrode is located at 355.0 m.



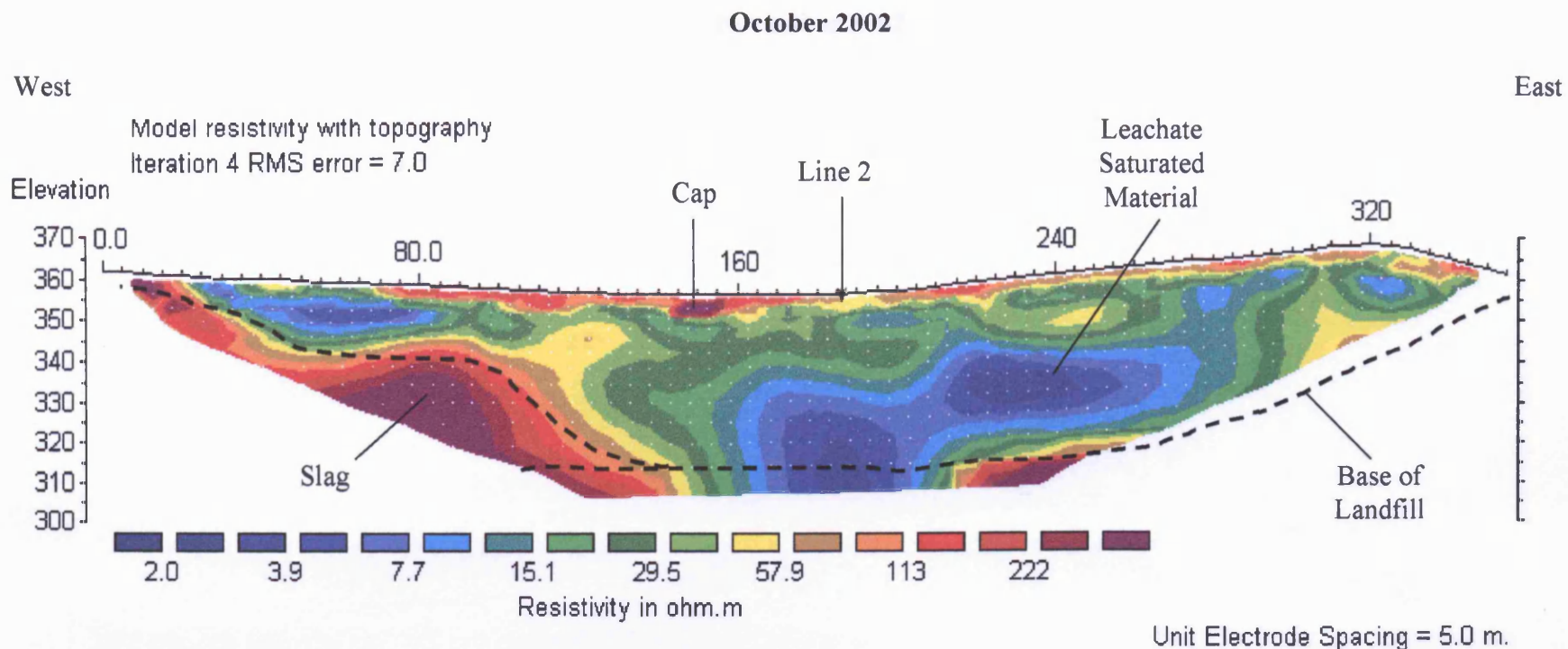
Horizontal scale is 10.28 pixels per unit spacing
Vertical exaggeration in model section display = 1.00
First electrode is located at 0.0 m.
Last electrode is located at 355.0 m.



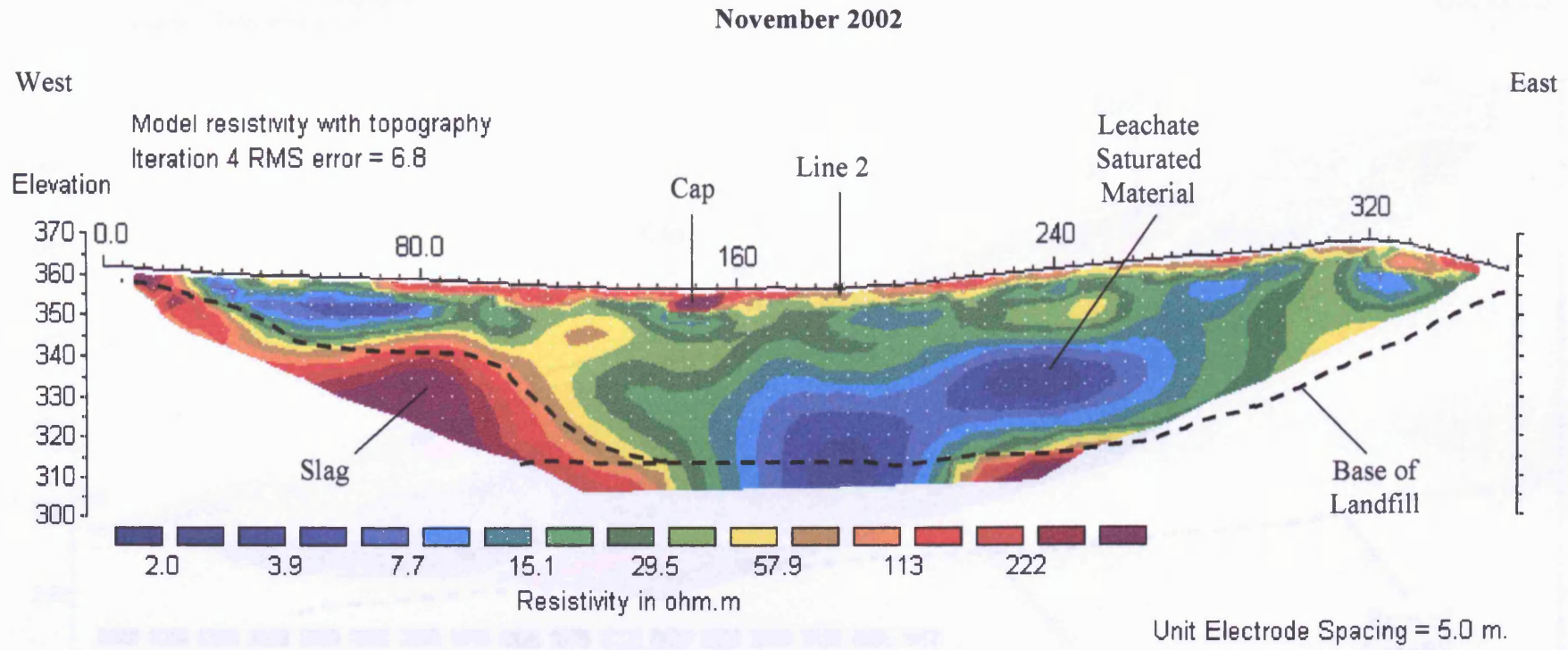
Horizontal scale is 10.28 pixels per unit spacing
Vertical exaggeration in model section display = 1.00
First electrode is located at 0.0 m.
Last electrode is located at 355.0 m.



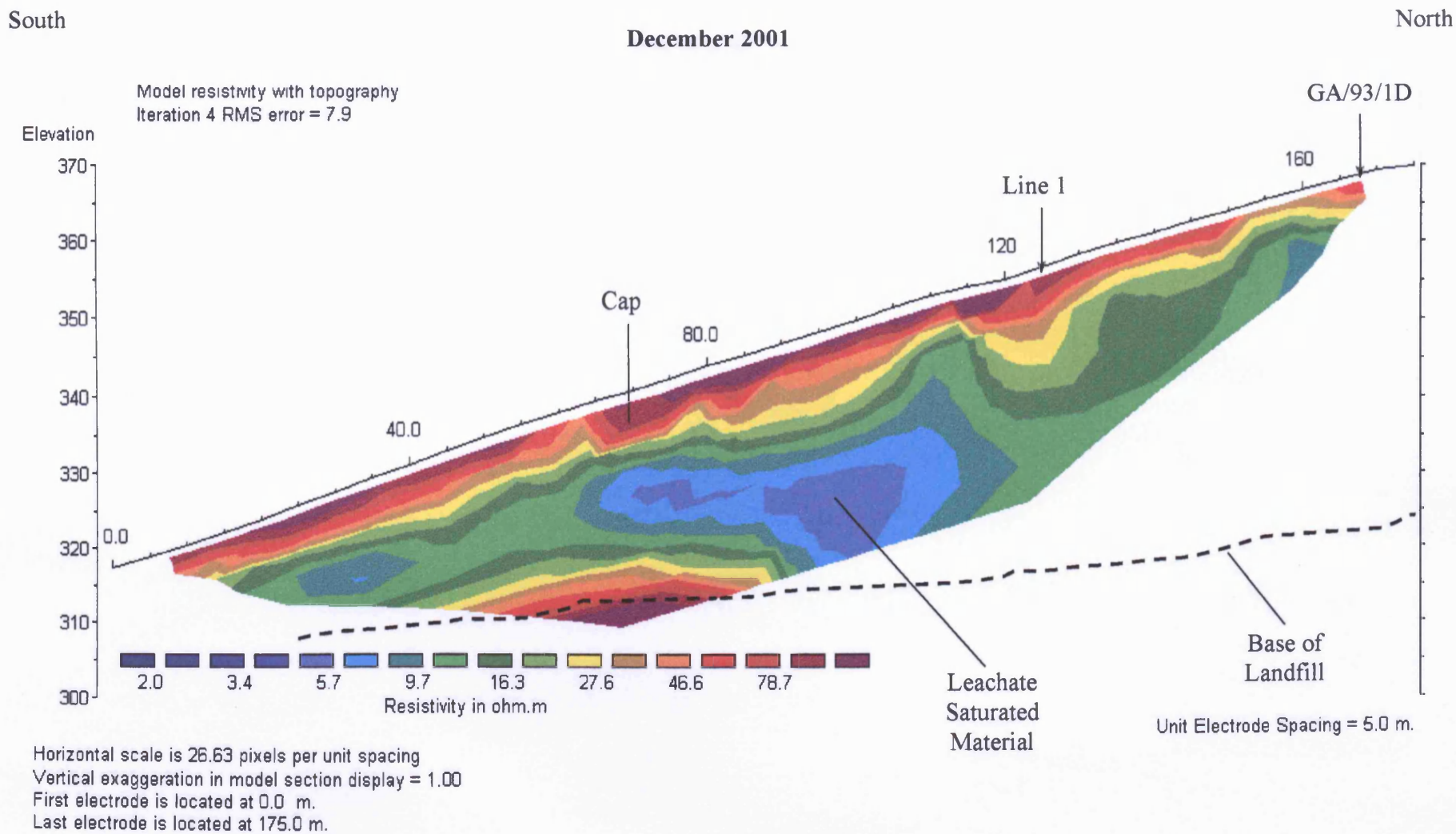
Horizontal scale is 10.43 pixels per unit spacing
Vertical exaggeration in model section display = 1.00
First electrode is located at 0.0 m.
Last electrode is located at 350.0 m.

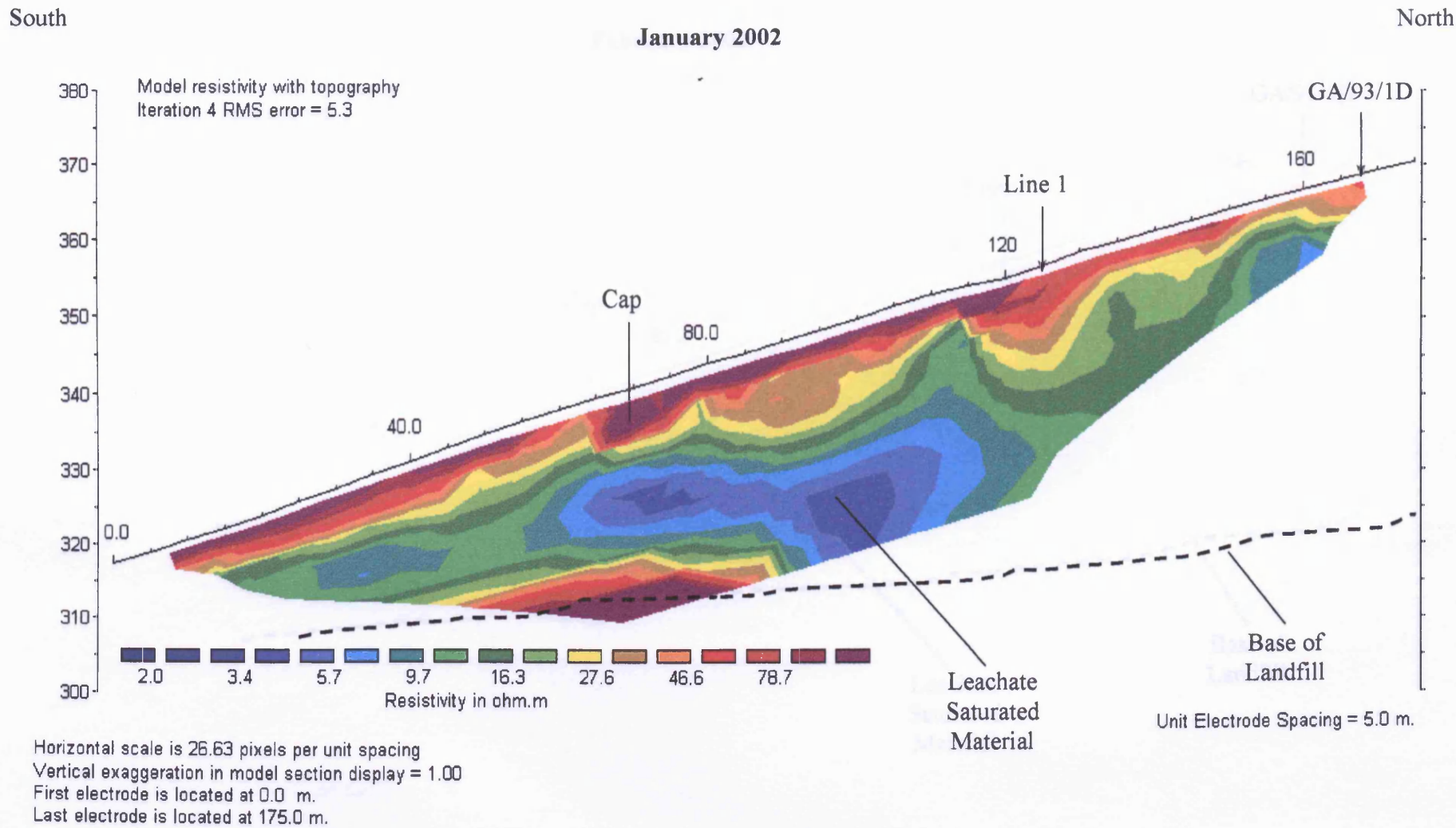


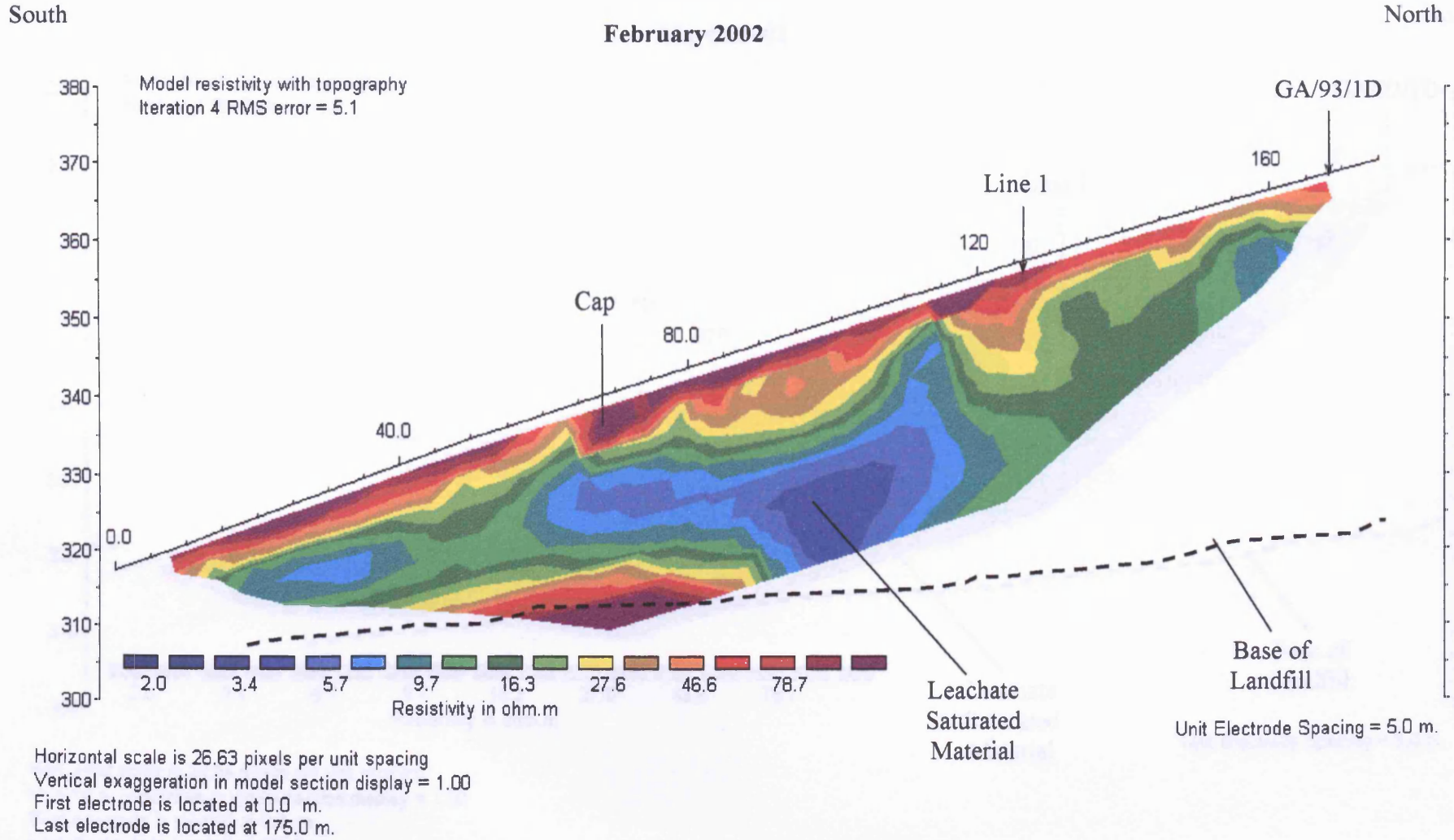
Horizontal scale is 10.28 pixels per unit spacing
 Vertical exaggeration in model section display = 1.00
 First electrode is located at 0.0 m.
 Last electrode is located at 355.0 m.

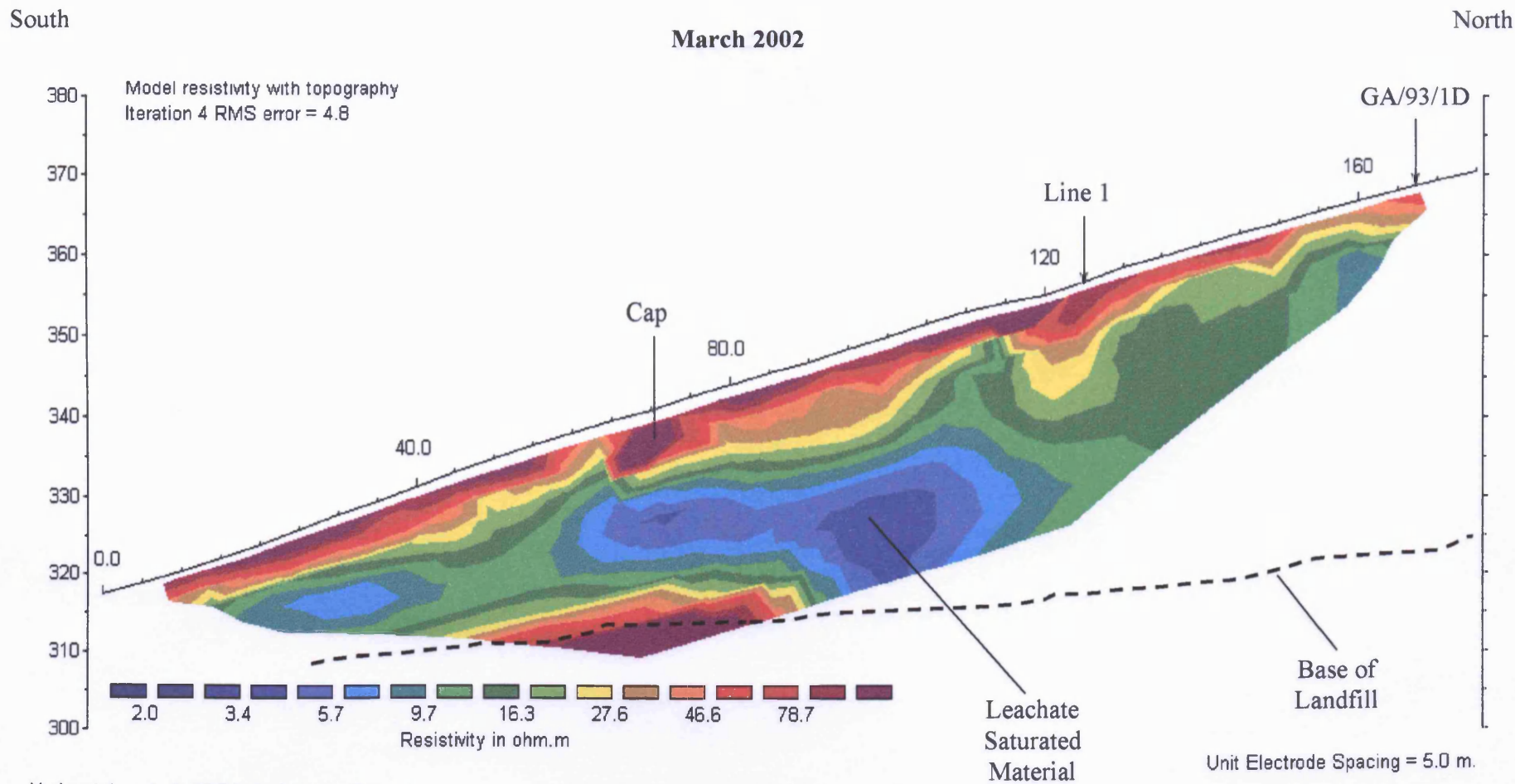


Horizontal scale is 10.28 pixels per unit spacing
Vertical exaggration in model section display = 1.00
First electrode is located at 0.0 m.
Last electrode is located at 355.0 m.

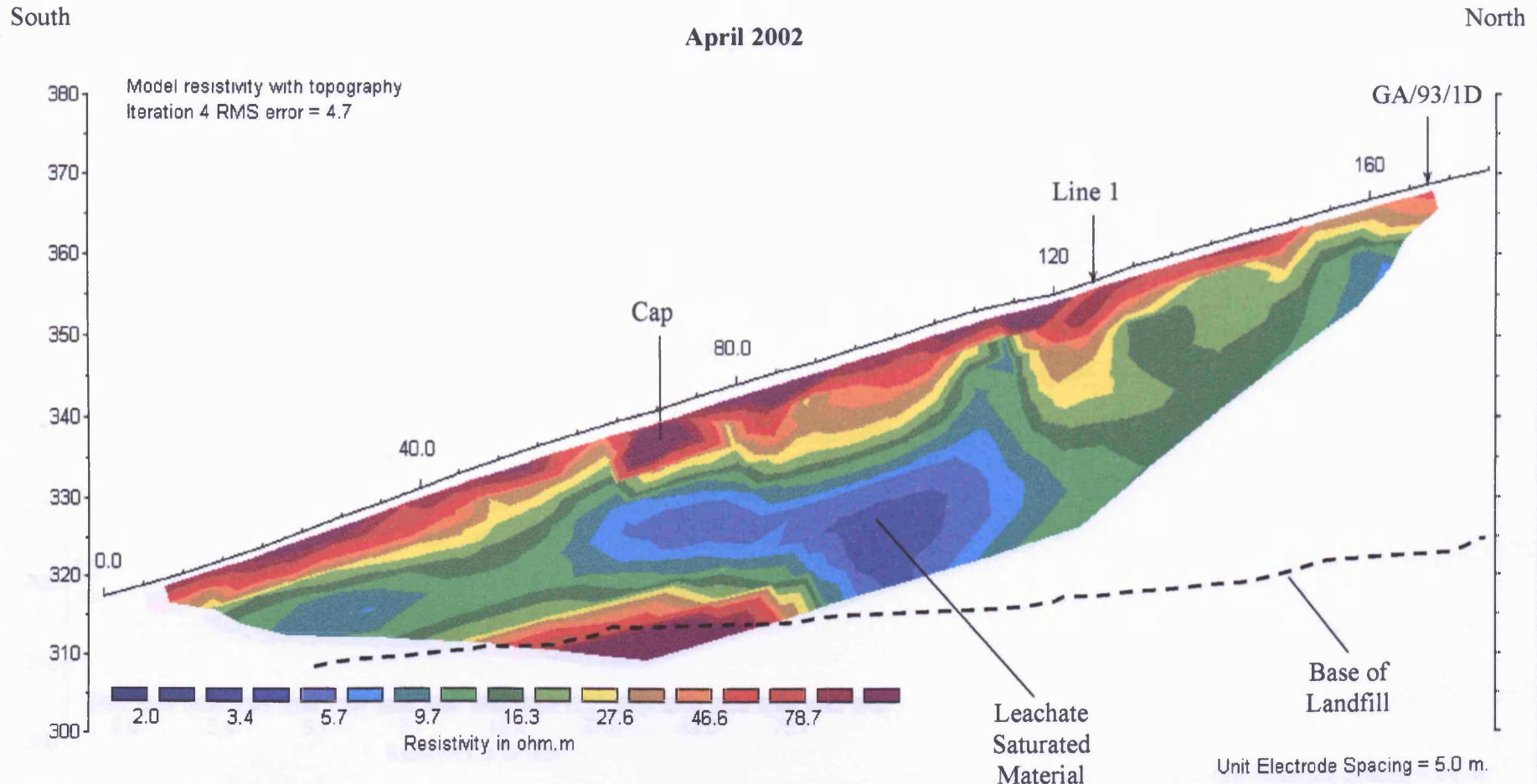




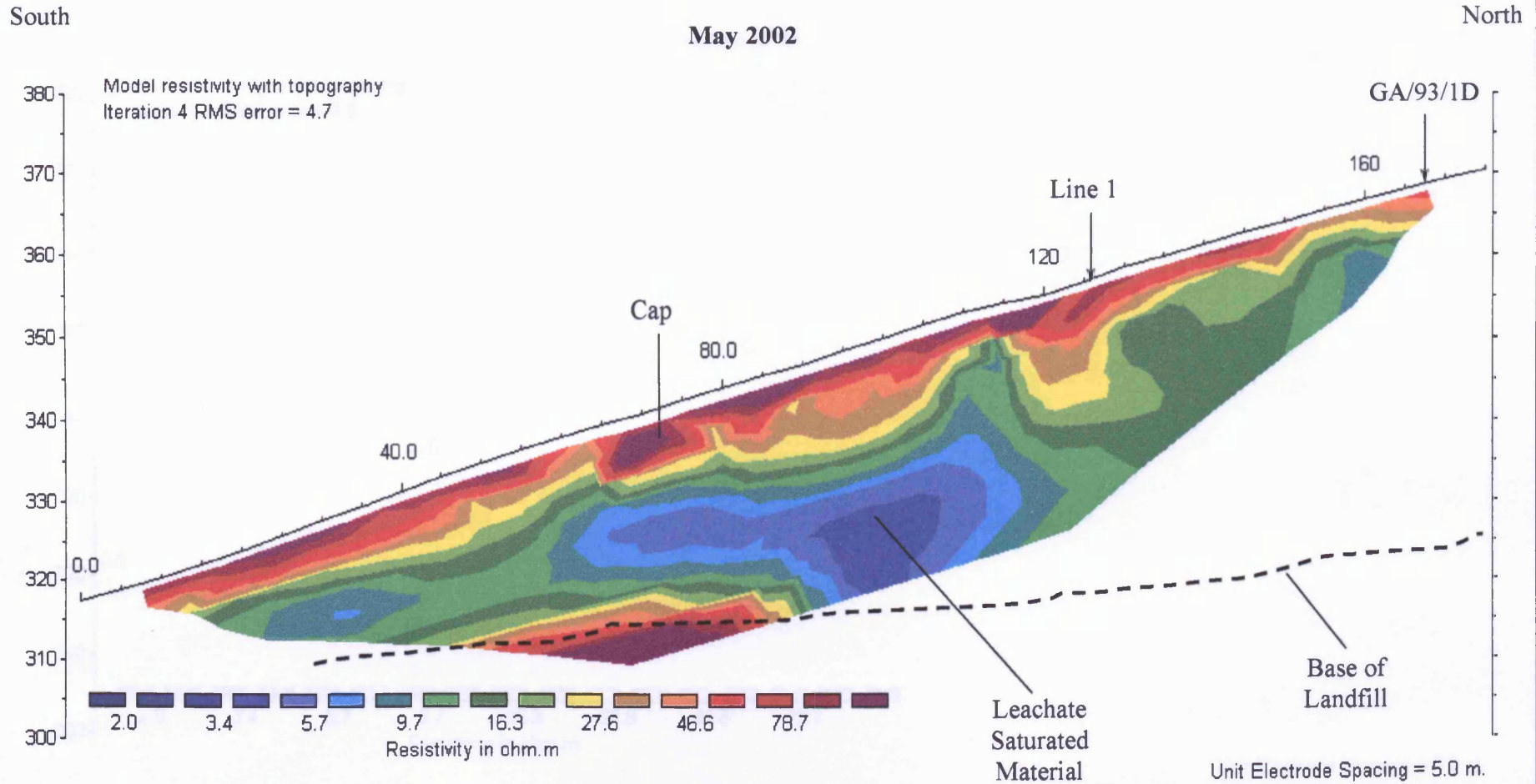




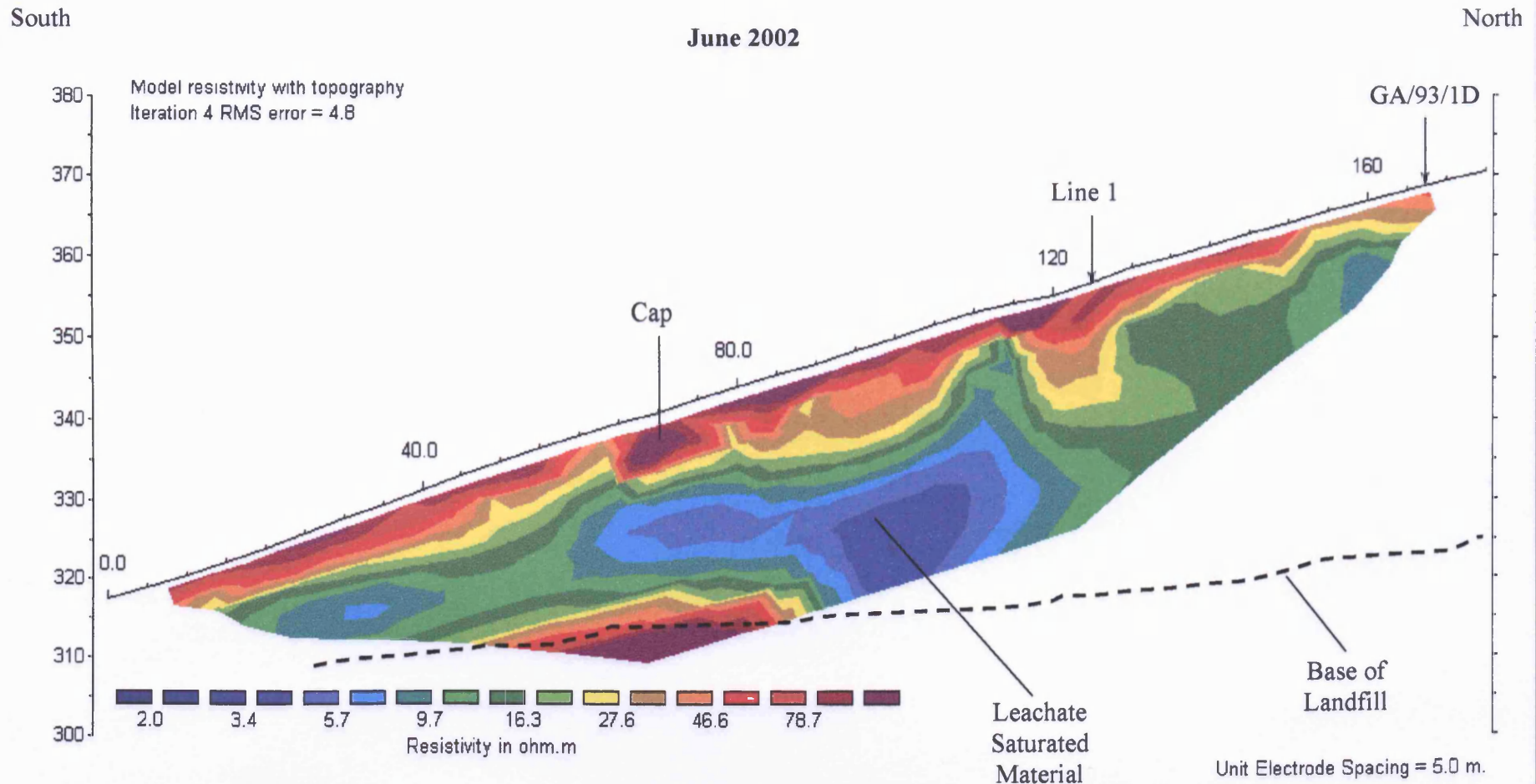
Horizontal scale is 26.94 pixels per unit spacing
Vertical exaggeration in model section display = 1.00
First electrode is located at 0.0 m.
Last electrode is located at 175.0 m.



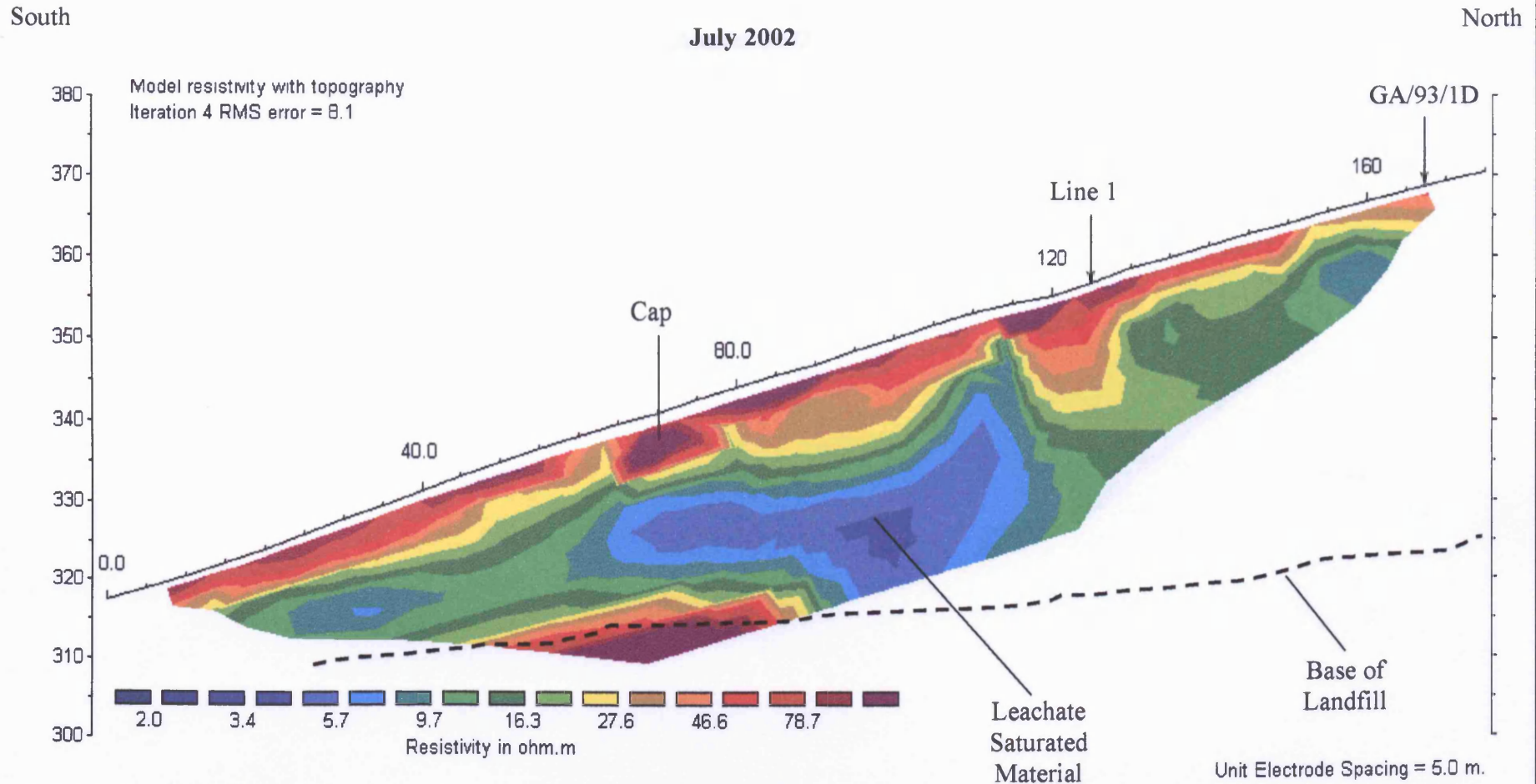
Horizontal scale is 26.94 pixels per unit spacing
Vertical exaggeration in model section display = 1.00
First electrode is located at 0.0 m.
Last electrode is located at 175.0 m.



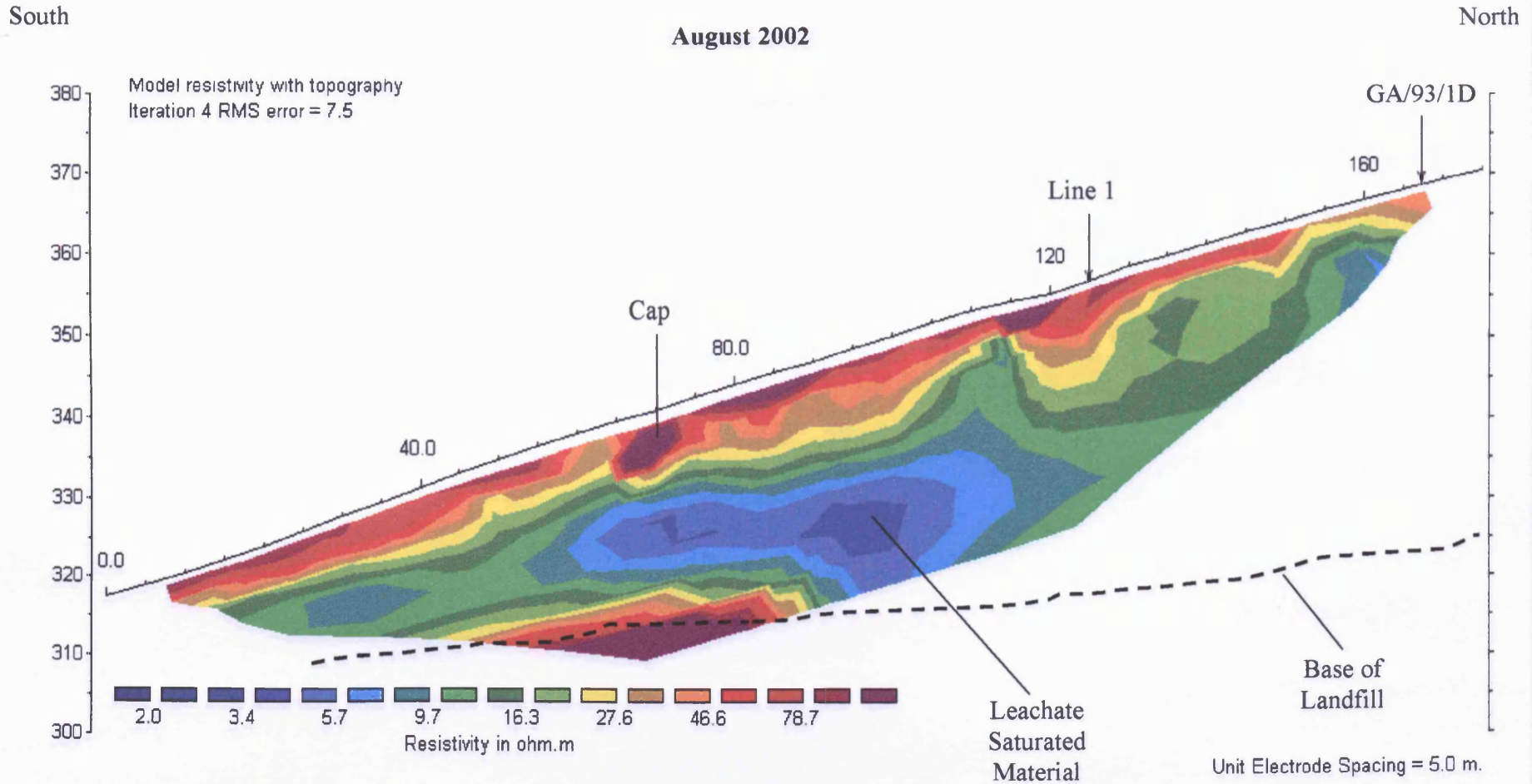
Horizontal scale is 26.94 pixels per unit spacing
Vertical exaggeration in model section display = 1.00
First electrode is located at 0.0 m.
Last electrode is located at 175.0 m.



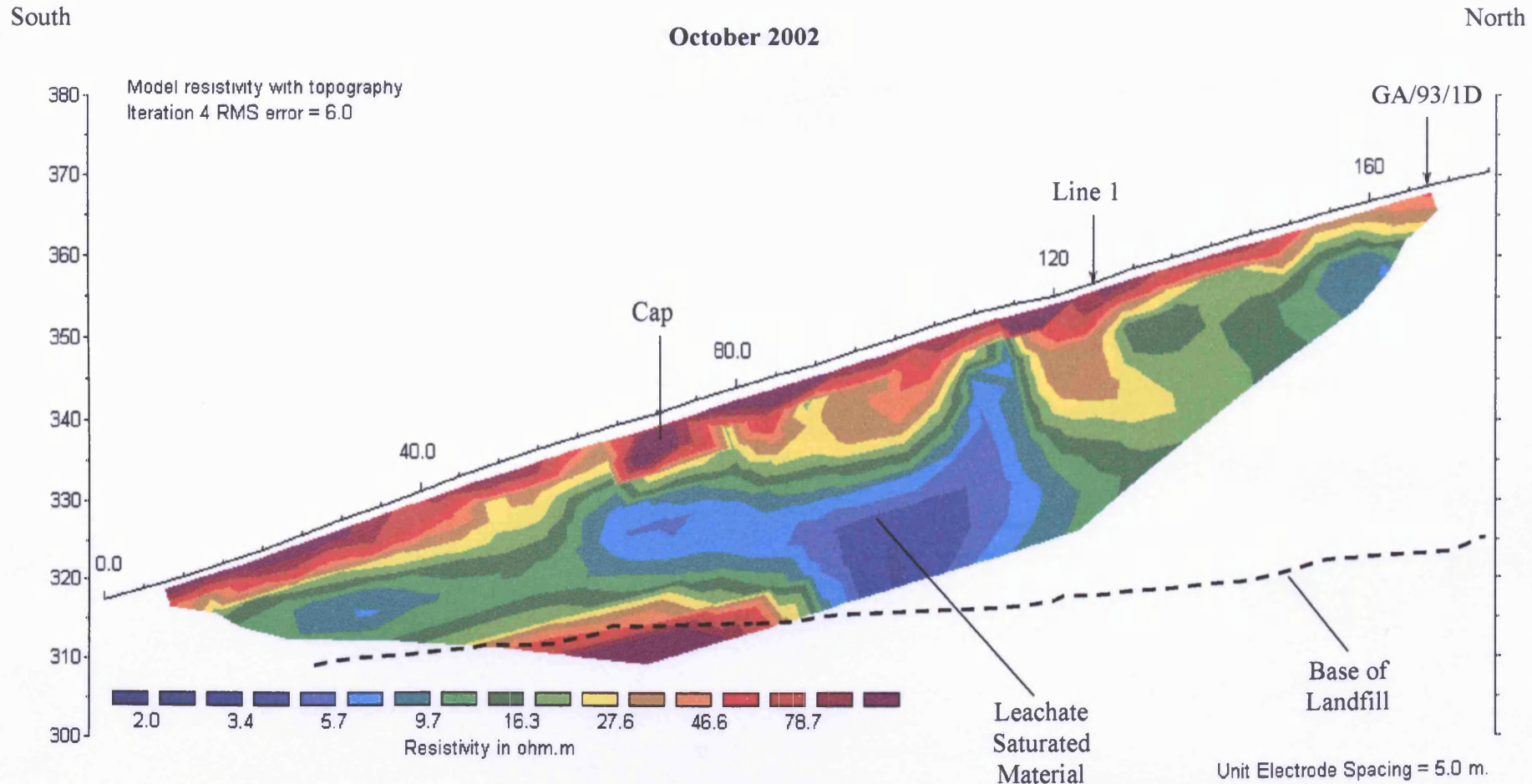
Horizontal scale is 26.94 pixels per unit spacing
Vertical exaggeration in model section display = 1.00
First electrode is located at 0.0 m.
Last electrode is located at 175.0 m.



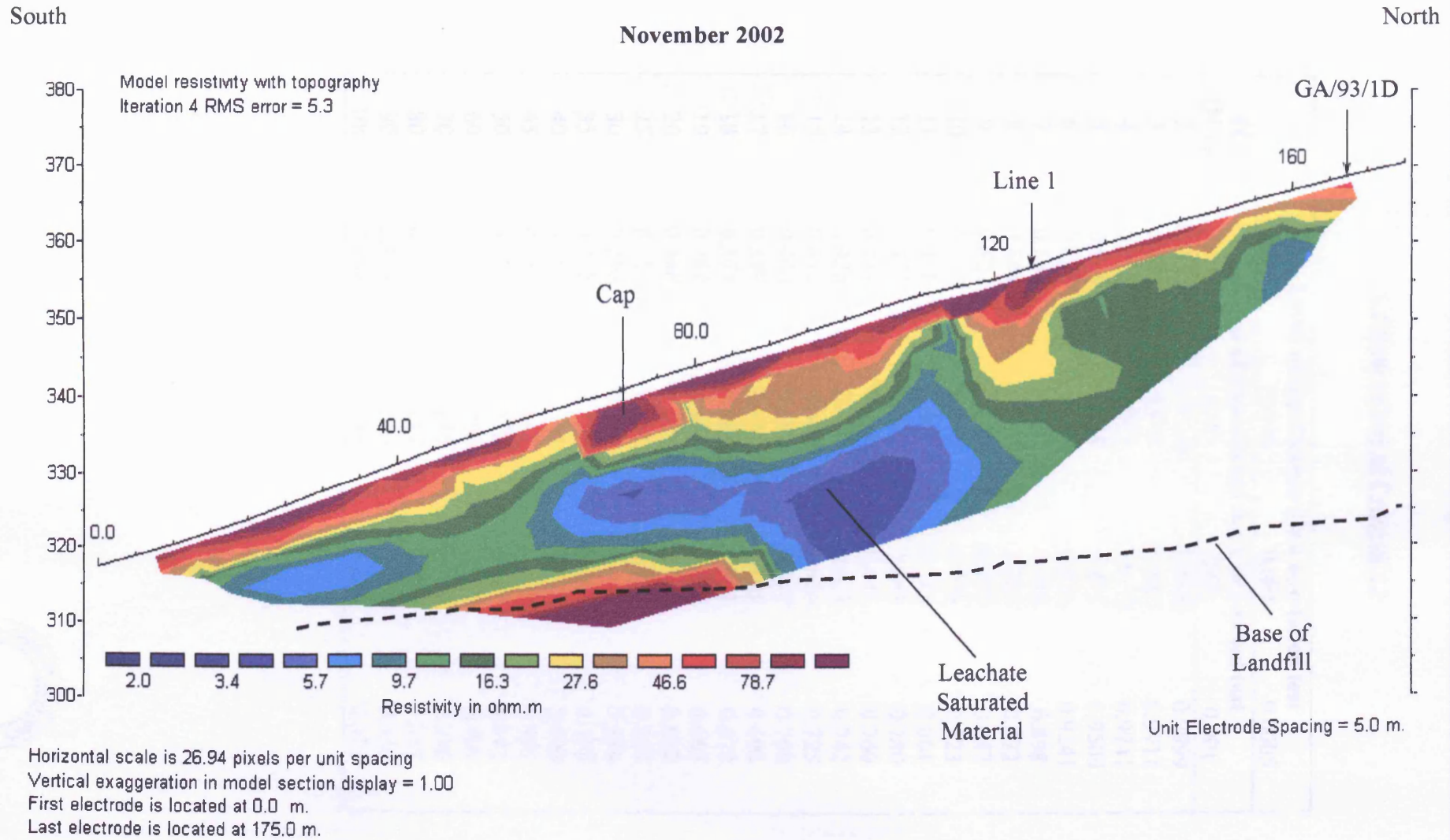
Horizontal scale is 26.94 pixels per unit spacing
Vertical exaggeration in model section display = 1.00
First electrode is located at 0.0 m.
Last electrode is located at 175.0 m.



Horizontal scale is 26.94 pixels per unit spacing
Vertical exaggeration in model section display = 1.00
First electrode is located at 0.0 m.
Last electrode is located at 175.0 m.



Horizontal scale is 26.94 pixels per unit spacing
Vertical exaggeration in model section display = 1.00
First electrode is located at 0.0 m.
Last electrode is located at 175.0 m.



Critical values of Pearson's r

df (N-2)	Level of significance for a one-tailed test			
	0.05	0.025	0.005	0.0005
	Level of significance for a two-tailed test			
	0.10	0.05	0.01	0.001
2	0.9000	0.9500	0.9900	0.9999
3	0.805	0.878	0.9587	0.9911
4	0.729	0.811	0.9172	0.9741
5	0.669	0.754	0.875	0.9509
6	0.621	0.707	0.834	0.9241
7	0.582	0.666	0.798	0.898
8	0.549	0.632	0.765	0.872
9	0.521	0.602	0.735	0.847
10	0.497	0.576	0.708	0.823
11	0.476	0.553	0.684	0.801
12	0.475	0.532	0.661	0.780
13	0.441	0.514	0.641	0.760
14	0.426	0.497	0.623	0.742
15	0.412	0.482	0.606	0.725
16	0.400	0.468	0.590	0.708
17	0.389	0.456	0.575	0.693
18	0.378	0.444	0.561	0.679
19	0.369	0.433	0.549	0.665
20	0.360	0.423	0.537	0.652
25	0.323	0.381	0.487	0.597
30	0.296	0.349	0.449	0.554
35	0.275	0.325	0.418	0.519
40	0.257	0.304	0.393	0.490
45	0.243	0.288	0.372	0.465
50	0.231	0.273	0.354	0.443
60	0.211	0.250	0.325	0.408
70	0.195	0.232	0.302	0.380
80	0.183	0.217	0.283	0.357
90	0.173	0.205	0.267	0.338
100	0.164	0.195	0.254	0.321

